Canadian Journal of Research

Issued by THE NATIONAL RESEARCH COUNCIL OF CANADA

VOL. 19, SEC. A. JANUARY, 1941 NUMBER 1

THE EFFECTS OF TROPOSPHERIC AND STRATOSPHERIC ADVECTION ON PRESSURE AND TEMPERATURE VARIATIONS[1]

By C. M. PENNER[2]

Abstract

Pressure and temperature variations at Sault Ste. Marie during 1938–39 for all levels up to 20 km. have been studied. The pressure extremes are progressively retarded at higher levels in the troposphere, while in the stratosphere the retardation decreases so that the phase becomes more nearly that of the surface pressure. The temperature extremes at greater altitudes in the troposphere are advanced with respect to the surface values. In the stratosphere the temperature variation reverses phase. Pressure and temperature anomalies are discussed in their relation to advection. High surface pressures are accompanied by a warm troposphere and a cold stratosphere. The opposite is true of low surface pressures. Seasonal differences in pressure and temperature variations are discussed.

Introduction

One of the fundamental problems of synopt [illegible] ieteorology is the determination of the causes of press [illegible] ations and the discovery of the underlying physical p [illegible] easing use of aerological observations for daily forec [illegible] nding of the interactions between the different atn [illegible] strata is becoming more and more valuable.

Correlation studies of upper air data were first made by W. H. Dines (3, p. 271) and A. Schedler (8). From an investigation of interdiurnal pressure and temperature variations, Schedler (9) concluded that the stratosphere is of major importance as compared to the troposphere in bringing about surface pressure variations. Later results (4) indicated that the troposphere is, at least, equally effective in causing surface pressure variations. Further studies of interdiurnal variations of the pressure and temperature (4, 5, 6, 9) showed that the extreme values of the pressure take place in the rear of lows and highs at greater altitudes up to 8 km. The extreme values of the temperature are displaced forward, at higher levels in the troposphere, with respect to the surface values. It is the purpose of the present investigation to extend these studies to greater heights, well up into the stratosphere.

To this end, the radiosonde observations taken at Sault Ste. Marie, Mich., during 1938–39 are analyzed. The data are arranged in six groups according to the position of Sault Ste. Marie, relative to surface pressure systems (i.e.,

[1] *Manuscript received in original form, August 9, 1940, and as revised, October 29, 1940.*
Contribution from the Meteorological Division, Air Services Branch, Department of Transport.

[2] *At the time, holder of a Bursary under the National Research Council of Canada. At present, Meteorologist, Meteorological Division, Air Services Branch, Department of Transport.*

highs and lows). Sault Ste. Marie must be situated in one of the following six areas:—

Lf—front or east side of a low.
Lc—centre of a low.
Lr—rear or west side of a low.
Hf—front or east side of a high.
Hc—centre of a high.
Hr—rear or west side of a high.

Since almost all pressure systems move from west to east, the east side can be called the front and the west side the rear. To decide into which area Sault Ste. Marie belonged at a given time, the daily weather maps of the Canadian Meteorological Service were used. The position of the station is, naturally, somewhat arbitrary since no fixed rules can be given as to what should constitute the boundaries of the above areas. The term centre has been applied, generally, to the innermost two or three isobars, but as the horizontal extent of the pressure systems is extremely variable, each case must be considered individually without any attempt to apply general rules.

Mean values of the pressures and temperature in each area have been found for every 2 km. level from the surface to 20 km. The values are plotted, arranging the six areas, into which the highs and lows have been divided, on an idealized time axis in the sequence given above. The curves are fairly regular. They were therefore subjected to a harmonic analysis. Further, the observations have been divided according to seasons, summer and winter, and the mean values have been calculated separately for each season.

Variations of Pressure and Temperature at the Different Levels during the Passage of Highs and Lows at the Surface

Harmonic Analysis; Pressure and Temperature Variations.

The number of observations at some of the levels and in each area is given in Table I. The number is sufficient to form a fairly reliable statistical mean at all heights except 20 km., where much fewer observations are available than at 18 km.

TABLE I

NUMBER OF OBSERVATIONS IN THE DIFFERENT AREAS AND AT EACH LEVEL

Height, km.	0	10	18	Height, km.	0	10	18
Area				Area			
Lf	61	53	25	*Hc*	70	67	25
Lc	42	36	11	*Hr*	53	48	22
Lr	60	48	15				
Hf	74	68	17	Total	360	320	115

In Table II are found the mean values of P_z and T_z, the pressure and temperature at a level z, the height of the tropopause H, and the pressure P_H and the temperature T_H at the tropopause, for all data.

The mean values of P_z, T_z, P_H, and T_H for all the data at every level in each area have been plotted in Figs. 1 and 2. Since the curves are quite regular, they have been expressed by a trigonometric series of the form $A_1\cos(t-\alpha_1) + A_2\cos(2t-\alpha_2)$. For the purpose of the harmonic analysis

TABLE II

MEAN VALUES OF P_z, T_z, P_H, T_H, AND H FOR ALL DATA

P_0 = 987.0 mb.	T_0 = + 3.3° C.	P_{12} = 194.8 mb.	T_{12} = −54.1° C.
P_2 = 791.9	T_2 = − 0.8	P_{14} = 142.8	T_{14} = −56.7
P_4 = 613.7	T_4 = −10.8	P_{16} = 104.3	T_{16} = −59.2
P_6 = 470.3	T_6 = −23.1	P_{18} = 76.7	T_{18} = −59.4
P_8 = 355.1	T_8 = −36.8	P_{20} = 55.1	T_{20} = −58.4
P_{10} = 264.3	T_{10} = −48.1	P_H = 229.2	T_H = −57.6
	H = 11.15 km.		

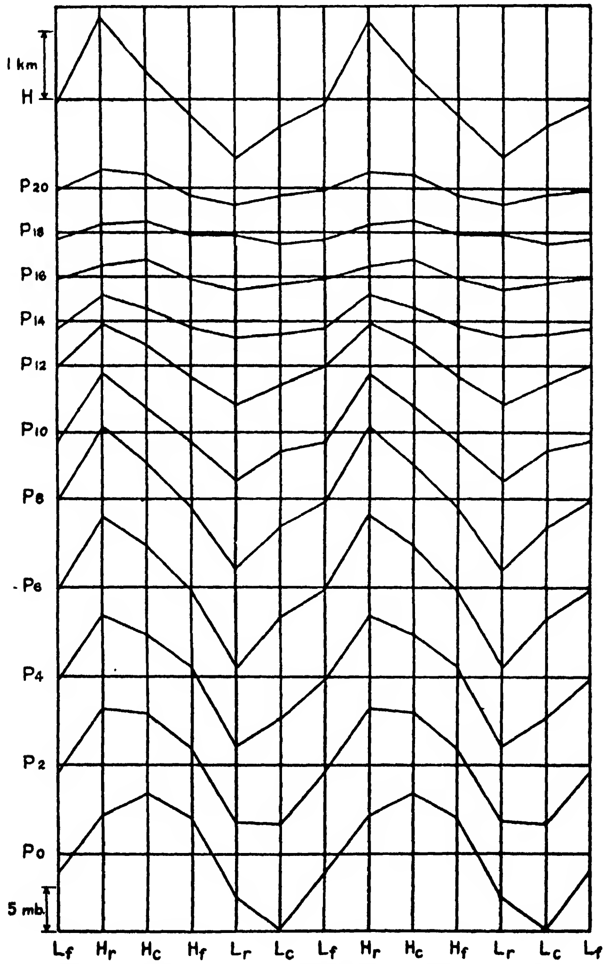

FIG. 1. *Variation of the pressure and of the height of the tropopause with the passage of surface highs and lows; yearly mean.*

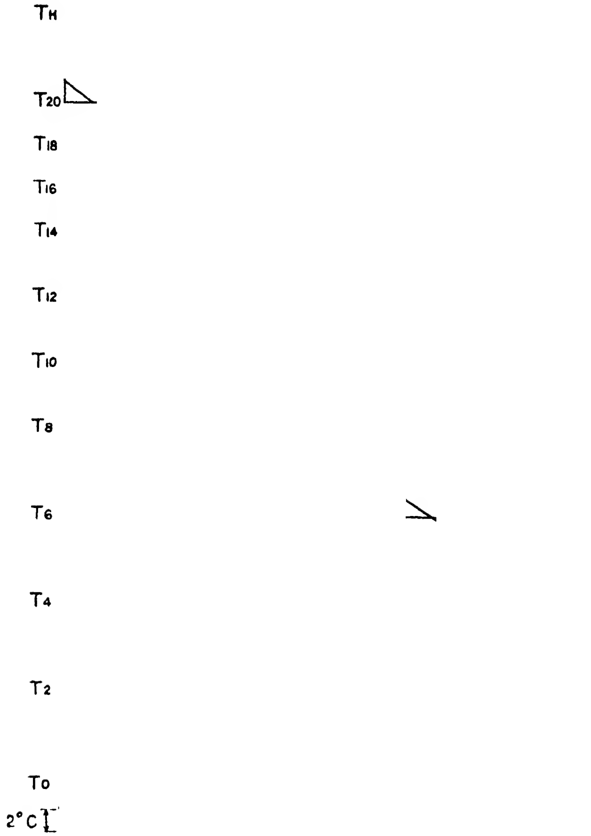

FIG. 2. *Variation of the temperature with the passage of surface highs and lows; yearly mean.*

it was assumed that the six pressure areas are equidistant and that one cycle comprises the time from one passage to the next of a certain region (*Lf* . . . . *Hr*, *Lf*). The first two terms of the harmonic series are given in Table III.

The behaviour of the pressure and temperature variations at different levels during the passage of surface highs and lows is shown in Figs. 1 and 2 and is clearly brought out by the harmonic analysis (Table III). Considering the first harmonic component of the pressure variation (the second component is generally much smaller), it can be seen that the amplitude decreases only slightly in the first 4 km. and shows a second maximum at 6 km. Above 6 km. the amplitude decreases strongly throughout the troposphere and the stratosphere. The phase angle increases in the troposphere, showing the progressive retardation of the pressure extremes. Above 12 km. (in the stratosphere) the retardation decreases and at 18 km. the phase is again nearly equal to that of the surface pressure. This shows that the retardation

TABLE III

HARMONIC COMPONENTS OF THE PRESSURES AND TEMPERATURES DURING THE PASSAGE OF SURFACE HIGHS AND LOWS—YEARLY MEAN

—	A_1, mb.	α_1,°	A_2, mb.	α_2,°
P_0	7.8	247	1.1	343
P_2	7.4	264	0.3	332
P_4	7.0	274	0.6	33
P_6	7.4	281	0.7	105
P_8	6.9	284	0.6	165
P_{10}	5.0	284	1.0	190
P_{12}	4.1	287	0.6	180
P_{14}	2.2	277	0.8	204
P_{16}	1.5	269	0.4	132
P_{18}	1.1	249	0.5	210
P_{20}	1.8	283	0.5	153
H	0.88 km.	288	0.19 km.	212
T_0	2.1° C.	356	0.6° C.	153
T_2	3.8	313	0.6	134
T_4	3.9	300	0.7	132
T_6	3.5	294	0.7	143
T_8	2.5	289	1.2	196
T_{10}	0.4	64	1.5	230
T_{12}	2.8	111	0.2	232
T_{14}	2.6	104	0.3	125
T_{16}	1.5	126	0.4	133
T_{18}	1.4	155	0.4	0
T_{20}	0.4	283	1.3	11
T_H	4.0	113	0.6	263

of the pressure extremes continues only in the troposphere and that the retardation decreases in the stratosphere.

From the first harmonic component of the temperature series, it is seen that the amplitude of the temperature variation increases from 0 to 4 km.; then it decreases rapidly as the tropopause is approached. At 10 km., which is roughly the height of the tropopause, the amplitude of the second harmonic component of the temperature variation is about four times as great as the amplitude of the first harmonic. Thus the temperature variation at 10 km. during the passage of highs and lows does not resemble a simple but rather a double sine curve, as can also be seen from Fig. 2. This anomalous behaviour of the temperature variation in the neighbourhood of the tropopause probably takes place because the temperature variation at 10 km. sometimes is under the influence of stratospheric and at other times of tropospheric advection of air. Above the tropopause the amplitude A_1 increases somewhat, at first, but then it decreases rapidly with height. Thus the maximum temperature variation occurs in the troposphere from 2 to 6 km. and in the lower stratosphere from 12 to 14 km. The phase angle decreases in the troposphere, indicating that the temperature extremes at greater altitudes are advanced with respect to the surface values. Above 10 km. (in the stratosphere) the temperature series have almost exactly the opposite phase. This change in phase of the temperature variation at the tropopause can be explained by

assuming simultaneous advection in the troposphere and in the stratosphere from the same direction. In the troposphere the temperature decreases from S to N, while in the stratosphere the temperature increases from S to N. Hence, advection from the south, for example, would make the troposphere warmer and the stratosphere colder. Thus, where the warmest temperatures occur in the troposphere (i.e., where advection has taken place from the south), the coldest temperatures will be found in the stratosphere. Investigations of aerological ascents in individual cases (7) have shown that when advection from the south takes place (i.e., tropical air replaces polar air) the troposphere becomes warmer and the stratosphere becomes colder and vice versa.

The change in phase of the temperature variation at the tropopause could also be explained by vertical motions, if the assumption is made that where descending currents are found in the stratosphere there are ascending currents in the troposphere, since air is warmed by descent and cooled by ascent. Previous investigations have produced some evidence in support of this theory (7). We shall return to this question later (p. 12).

Two different theories account equally well for the retardation of the pressure extremes in the troposphere. One advanced by Stüve (10) assumes that the surface pressure centres are steered by the pressure distribution aloft. It is known as the theory of "stratospheric steering". The other, the polar front theory, advanced by V. Bjerknes and others (1), considers the lower layers as the primary cause of surface pressure variations and the influence of the upper layers as producing more secondary effects. A brief discussion of both theories is given by Haurwitz and Haurwitz (6).

The retardation of the pressure extremes follows partly as a result of the advance of the temperature extremes, according to the barometric formula. At the surface, the highest pressure and lowest temperature occur over *Hc*. At higher levels in the troposphere the temperature extremes are advanced, the highest temperature occurring over *Hr* and the lowest over *Lr*. Therefore the decrease in pressure with height will be less over *Hr* than over *Hc*, for instance. Thus, at higher levels in the troposphere, the highest pressure will tend to occur over *Hr* rather than over *Hc*, that is, the pressure extremes will be retarded with respect to the surface values. In the stratosphere, however, the temperature has the opposite phase; the coldest temperatures now are found over *Hr* and the warmest over *Lr*. Hence the decrease in pressure with height will now be greater over *Hr* than over *Hf* or *Hc* since the colder air is found over *Hr*. Consequently, the maximum pressure will again tend to occur over *Hc*, that is, in the stratosphere the retardation of the pressure extremes becomes less. Similar considerations apply, of course, to minimum pressures.

The forward displacement of the temperature extremes with altitude in the troposphere can probably be explained by higher wind velocities aloft. The increase in wind velocity with height is greatest in the lowest layers. This

agrees with the result that the phase advance is largest in the lowest levels, being 43° in the first 2 km. and 13° from 2 to 4 km. (Table III).

Similar series have been found for the height of the tropopause H, and its temperature T_H. The results confirm previous investigations. The tropopause is lowest in the rear of a surface low and highest in the rear of surface high. A low tropopause is accompanied by a warm stratosphere, a high tropopause by a cold stratosphere.

Temperature and Pressure Anomalies

When the mean temperature for each level and in each area is subtracted from the mean temperature for all data at each level given in Table II, temperature anomalies are obtained. By drawing lines of equal temperature anomaly, the regions of air warmer (positive temperature anomaly) and the regions of air colder (negative temperature anomaly) than normal are indicated. This diagram is shown in Fig. 3. The heavy line is the tropopause. Temperatures lower than normal in the troposphere, in general, are accompanied by temperatures higher than normal in the stratosphere and vice versa. The greatest deviations from the normal occur in the rear of surface highs and lows both in the stratosphere and in the troposphere, temperatures being lower than normal in the rear of a low and higher than normal in the rear of a high in the troposphere. In the stratosphere, temperatures are lower than normal in the rear of a high and higher than normal in the rear of a low. It can be seen that, on the average, advection in the troposphere and the stratosphere from the same direction must produce opposite effects on the surface pressure variation. According to the geostrophic law, the wind blows from a southerly direction on the west side of a high and on the east side of a low. In the rear of a high the air has come from the most southerly latitude, owing to the greater horizontal extent of highs; hence in the troposphere the warmest temperatures and the greatest temperature anomalies would be found over *Hr*, except in the lowest levels where the effect of the cyclonic warm sector causes the warmest temperatures to be found over *Lc*. In the stratosphere, advection from the south brings colder air, so that the coldest temperatures and the greatest negative temperature anomaly would be found over *Hr*. The coldest temperatures in the troposphere occur over *Lr* following the influx of polar air behind the cold front and before the descending currents found in highs have resulted in the consequent warming of the tropospheric air.

A similar attempt was made to draw lines of equal pressure anomaly. Because of the rapid decrease of the pressure with height, the pressure anomalies at different altitudes are not directly comparable with one another. The pressure at a height z is given by

$$P_o = P_z e^{\frac{+gz}{RT}},$$

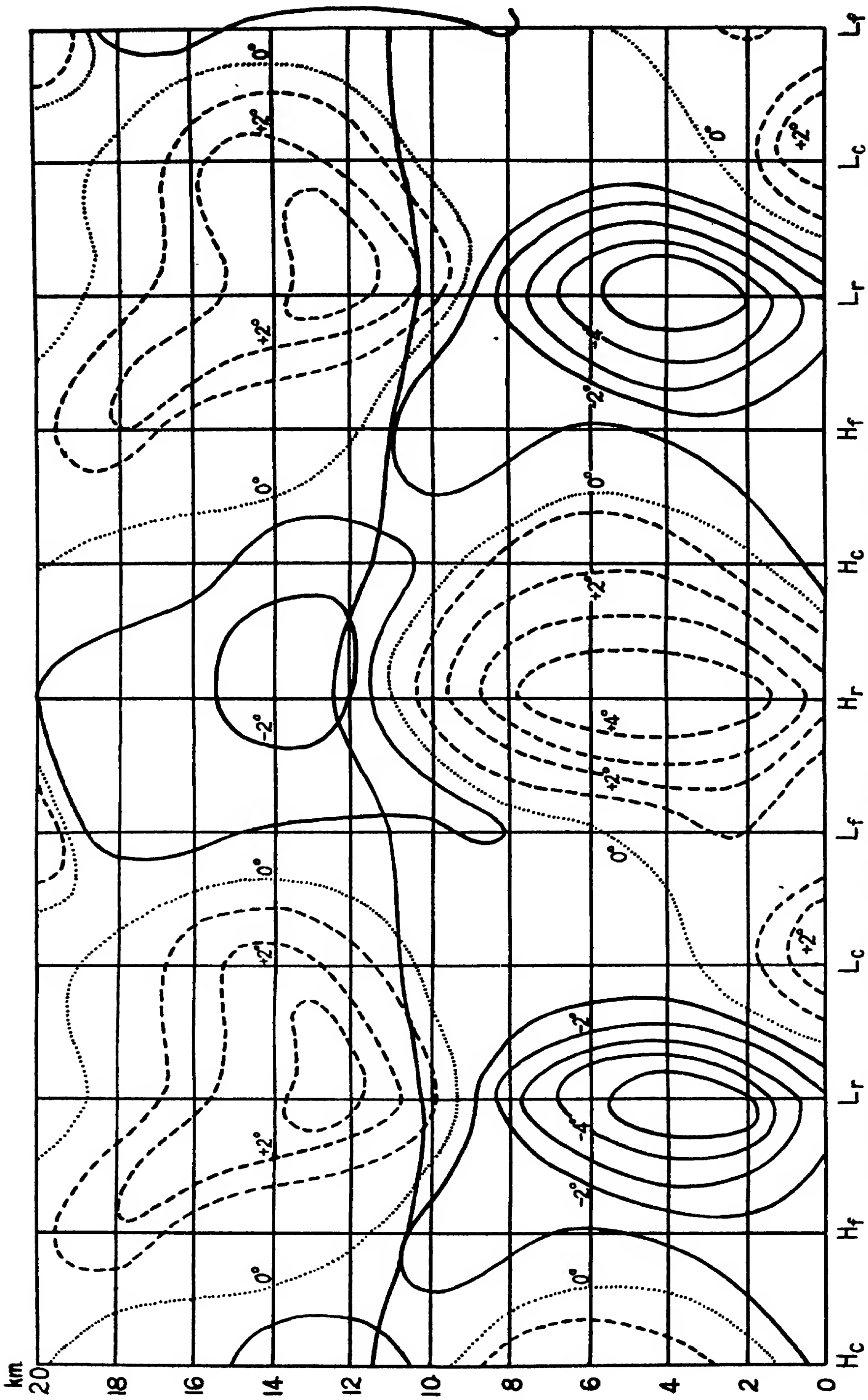

FIG. 3. *Temperature anomalies with the passage of surface highs and lows; yearly mean. Heavy curve: Tropopause.*

where P_o is the pressure at the surface, g the acceleration of gravity, R the gas constant, and T the mean temperature of the air column. It follows that

$$\frac{dP_o}{P_o} = \frac{dP_z}{P_z} - \frac{gzdT}{RT^2}.$$

Assuming that the temperature of the intermediate layers does not change

$$dP_o = \frac{P_o}{P_z} \times dP_z\,.$$

Thus, a change dP_o in the surface pressure is P_o/P_z times as large as the pressure change dP_z at a level z. This does not imply, however, that a change dP_z at a level z causes a change P_o/P_z times as great at the surface, since no account has been taken of the compressibility and the possible temperature changes of the air column. For example, if the total advection takes place above the level z, dP_z will represent the mass added above the level z, while dP_o will represent the total mass added to the air column. It would seem, at first, that these two values should be equal. However, if the mass is added above z, the air column below z will be compressed, so that part of the air previously above z will now be below it. dP_z will then represent the total mass of the air added less the mass of the air that sinks below z. dP_o, which represents the total mass added, must be larger than dP_z. Therefore, to make the pressure anomalies more comparable to one another they were multiplied by the factor P_o/P_z. Fig. 4 shows the lines of equal pressure anomaly treated in this manner. The heavy line in the diagram is the position of the tropopause. At the surface the maximum pressure anomalies occur, of course, in the centre of lows and highs. Above 2 km., the largest pressure anomalies are

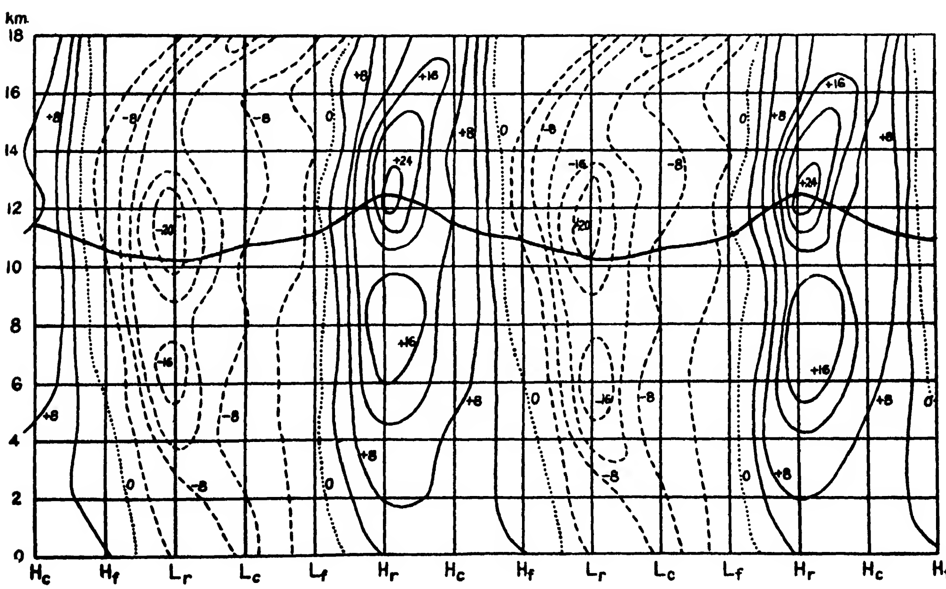

FIG. 4. *Reduced pressure anomalies with the passage of surface highs and lows; yearly mean. Heavy curve: Tropopause.*

found over the rear of surface lows and highs, with a maximum between 4 and 8 km. altitude and a second maximum in the stratosphere from 10 to 14 km. Above 14 km., the maximum pressure anomalies occur more nearly over *Lc* and *Hc*, indicating that the retardation of the pressure extremes becomes less in the stratosphere. In the troposphere, regions where the pressure is below normal are also regions where the temperature is below normal except in the first 3 or 4 km. over *Lc* where the temperature is above normal. This is the region of the cyclonic warm sector, which does not seem to extend above 4 km. on the average. In the stratosphere, regions where the pressure is below normal are regions where the temperature is above normal.

Advective Changes of Mass

The difference in pressure between any two levels is a measure of the mass between those two levels. In Fig. 5 are plotted the pressure differences for the layer 0–4 km., 4–8 km., 8–12 km., and above 12 km. for each of the six areas of highs and lows. The amplitudes of these curves indicate the amount

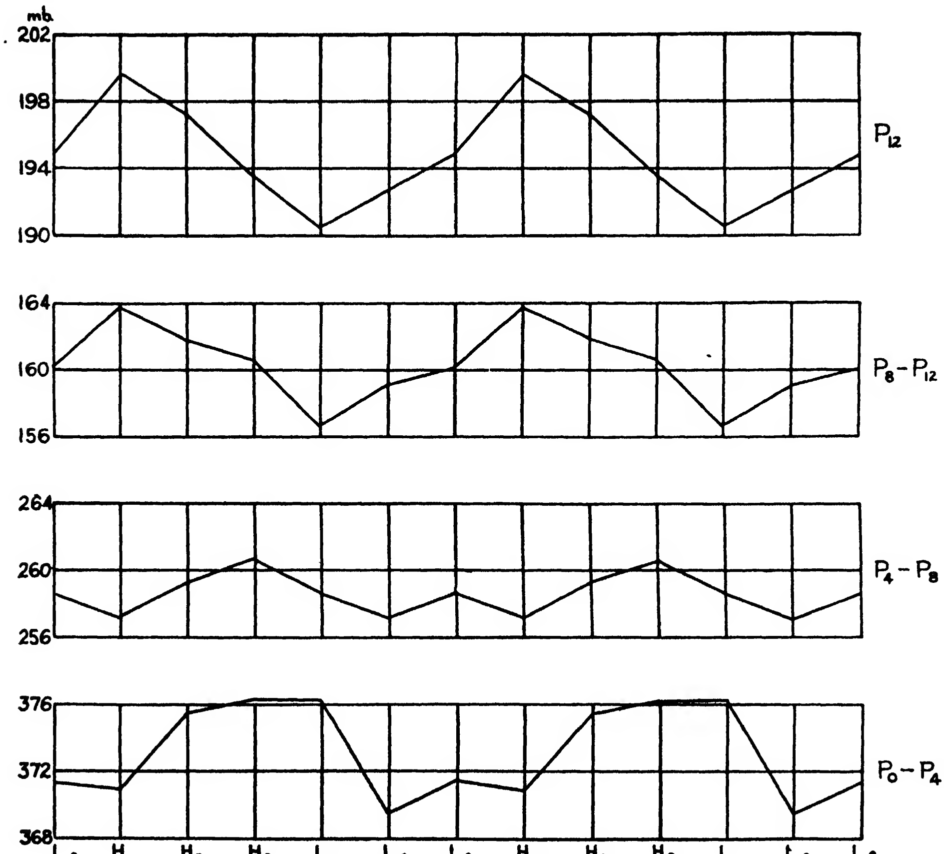

FIG. 5. *Variation of mass in different atmospheric layers with the passage of surface highs and lows; yearly mean.*

of advective change of mass during the passage of surface highs and lows. Thus, it can be seen that the advective change of mass is greatest in the layer 0–4 km. Here the amplitude is 4.5 mb. In the intermediate layer, 4–8 km. (the upper troposphere), the amplitude is much less, being only 1.8 mb., while in the neighbourhood of the tropopause and in the lower stratosphere (8–12 km.) the amplitude of the advective change of mass is again considerably larger, having increased to 3.5 mb. The amplitude of the advective change of mass at all levels above 12 km. is 4.1 mb. Thus since the surface pressure change is a measure of the total mass added in the atmosphere, it can be seen that the layers in the lower troposphere and in the lower stratosphere are the most important in causing surface pressure variations, while the intermediate layer (the upper troposphere) is much less effective. Previous investigations (6) have shown that the greatest advective changes of mass occur near the surface and near the tropopause. In the lowest layer (0–4 km.) the most pronounced advective change occurs from *Lc* to *Lr*, namely, with the passage of the cold front. In the higher layers the advective changes from one region to the next are approximately of the same order of magnitude for all regions. In the layer 0–4 km. the greatest mass is found over *Lr* and *Hf* where advection from the N has occurred. The smallest mass is found over *Lc* owing to the effect of the cyclonic warm sector. In the layer 4–8 km. the greatest mass occurs over *Hf*, while the least is found over *Hr* and *Lc*, with a secondary maximum over *Lf*. In the layers 8–12 km. and above 12 km. the greatest mass is found over *Hr* and the least over *Lr*. This is nearly opposite to the distribution of mass in the lower layers, thus showing the opposite effects of advection in the troposphere and in the stratosphere.

Potential Temperatures

The next element that was considered is the potential temperature. The potential temperatures were calculated from Poisson's adiabatic equation,

$$\frac{T}{\theta} = \left(\frac{P}{1000}\right)^{.288}$$

where T is the temperature at a pressure P (in millibars), and θ is the potential temperature. Lines of equal potential temperature are shown in Fig. 6. The dotted line represents the tropopause. At any particular level in the tropopause the minimum potential temperature is found in the rear of a surface low, while the maximum occurs in the rear of a surface high. A secondary maximum is found in the centre of a low, in the lower levels; this might be due to the condensation of water vapour in the ascending currents in the low pressure area (7). Since the axes of highs and lows lean backwards, it can be said, in general, that the potential temperature is higher over regions of high pressure than over regions of low pressure. Between 8 and 10 km. the equipotential temperature lines are nearly horizontal. In the stratosphere the variation of the potential temperatures is reversed. The higher potential temperatures are in the rear of surface lows and the lower potential

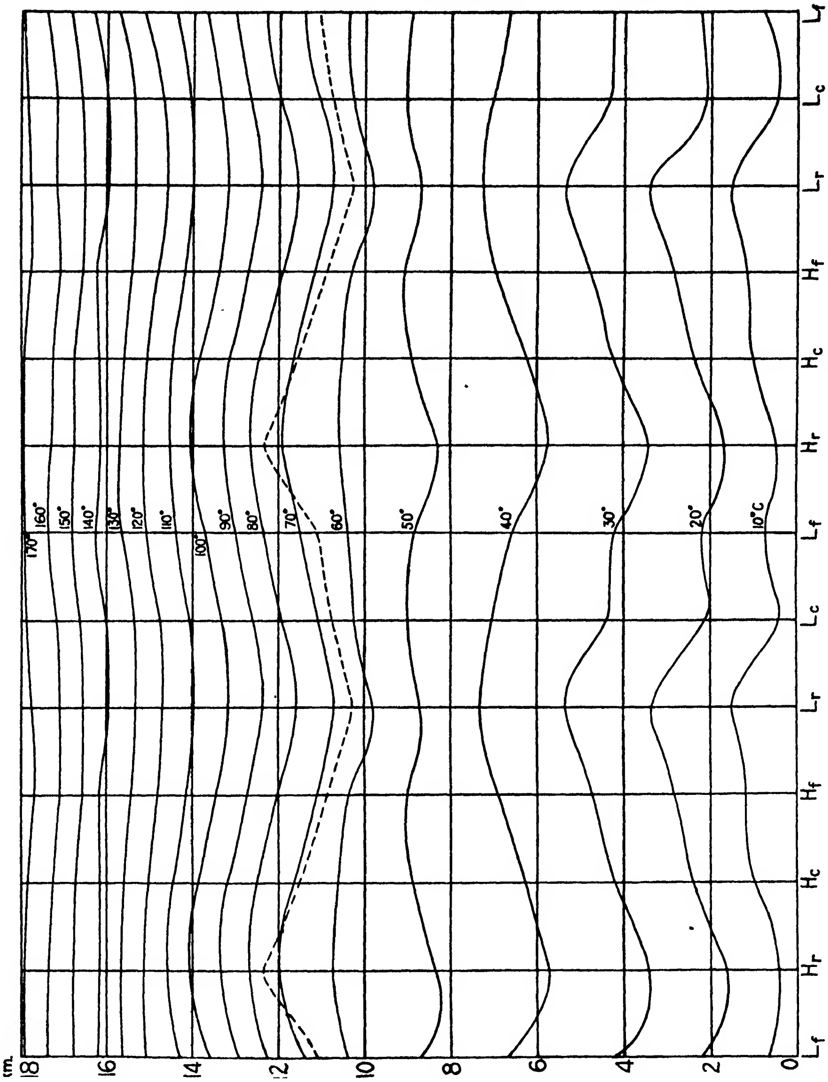

FIG. 6. *Variation of the potential temperature with the passage of surface highs and lows; yearly mean. Broken curve: Tropopause.*

temperatures are in the rear of surface highs. The amplitude of the variation decreases rapidly with height.

Palmén (7) arrived at a similar distribution of equipotential temperature lines in an investigation of cyclones and anticyclones. By choosing all his aerological observations in polar air masses and by arranging them so that each group contained ascents where the wind direction was from the N and from the S, he attempted to eliminate advection and to consider only vertical motions. He concluded that descending currents occur in the stratosphere where ascending currents are found in the troposphere. This would account for the fact that the minimum potential temperature in the troposphere is located over the same place as the maximum potential temperature in the stratosphere. However, this distribution of the potential temperature can

also be explained by horizontal advection in the same manner as the distribution of the temperatures. The method of attack used in this investigation stresses the effects of advection by dividing the ascents into six areas of highs and lows. Thus, only ascents with advection from approximately the same directions are grouped together. The effects of advection are not separated from those of vertical motion. Nevertheless, the same results for the distribution of equipotential temperatures are obtained as in Palmén's investigation. It seems plausible then to attribute this observed distribution of potential temperature to advection, at least in part, even though vertical motions may also be a contributing factor. Moreover, it seems doubtful that Palmén eliminated advection effects completely by his method of selecting the material. In particular it appears unlikely that advection effects in the stratosphere would also be eliminated in view of the large changes of the wind and temperature observed in passing from lower to higher layers. It may therefore be assumed that Palmén's results indicate not only the effects of vertical motion but also of horizontal advection.

Seasonal Means

To study seasonal differences that might show themselves in the distribution of pressure and temperature variations, the data were grouped according to two seasons, summer (June, July, August), and winter (December, January, February). The results are plotted in Figs. 7 to 10 and the components of the harmonic series are shown in Tables IV and V. Comparing the first

TABLE IV

HARMONIC COMPONENTS OF THE PRESSURES AND TEMPERATURES DURING THE PASSAGE OF SURFACE HIGHS AND LOWS—SUMMER

—	A_1, mb.	α_1, °	A_2, mb.	α_2, °
P_0	5.2	250	0.2	344
P_2	4.5	257	0.8	304
P_4	3.5	277	0.9	316
P_6	3.4	288	1.1	358
P_8	3.1	297	0.9	321
P_{10}	3.3	312	1.5	335
P_{12}	2.1	309	1.1	329
P_{14}	1.1	303	1.0	286
P_{16}	1.4	301	0.8	46
P_{18}	0.6	263	0.1	270
H	0.63 km.	324	0.35 km.	342
T_0	2.1° C.	35	0.9° C.	352
T_2	1.9	350	0.9	297
T_4	1.3	335	0.4	300
T_6	1.7	321	0.7	2
T_8	2.0	332	0.6	300
T_{10}	1.3	348	0.9	339
T_{12}	1.6	122	1.3	333
T_{14}	1.9	126	0.1	210
T_{16}	1.3	150	0.7	125
T_{18}	0.9	88	1.0	148
T_H	2.7	133	0.7	7

TABLE V

HARMONIC COMPONENTS OF THE PRESSURE AND TEMPERATURES DURING THE PASSAGE OF SURFACE HIGHS AND LOWS—WINTER

—	A_1, mb.	α_1, °	A_2, mb.	α_2, °
P_0	9.7	243	1.3	295
P_2	6.6	273	0.8	253
P_4	6.3	292	1.5	208
P_6	6.8	297	1.8	190
P_8	6.7	304	1.8	192
P_{10}	4.7	315	2.2	194
P_{12}	3.8	333	0.9	203
P_{14}	1.6	319	1.4	185
P_{16}	1.0	331	1.1	160
H	0.91 km.	300	0.28 km.	206
T_0	5.4° C.	32	1.4° C.	187
T_2	4.1	340	1.9	155
T_4	4.5	329	1.6	178
T_6	3.0	328	1.4	209
T_8	1.4	320	1.8	216
T_{10}	2.9	98	1.6	246
T_{12}	4.1	116	0.3	155
T_{14}	3.2	95	0.3	60
T_{16}	2.2	67	0.9	112
T_H	4.4	95	1.2	333

harmonic components of the pressure variation (Table IV—summer, and Table V—winter), we see that the amplitude of the pressure variation is about twice as large in winter as in summer. In summer the amplitude decreases rapidly in the first 4 km. but it remains fairly constant in the upper troposphere. In winter the amplitude decreases very rapidly in the first 2 km. so that above 2 km. the amplitude is even somewhat less than for the yearly mean values but still larger than the summer amplitudes for the corresponding heights. The phase retardation of the pressure extremes is larger in winter than in summer. This is to be expected because the temperature variation is much greater in winter than in summer. As a result, the difference in the decrease of pressure with height over *Hc* and *Hr* will be greater in winter than in summer, that is, the decrease in pressure with height over *Hc* is much more rapid relative to the decrease over *Hr* in winter than in summer because the temperature difference between *Hc* and *Hr* is so much greater in winter, *Hr* being the warmer. It follows that the maximum pressure will occur over *Hr* at a lower level in winter than in summer, in other words the retardation of the pressure extremes is greater in winter.

The phase advance of the temperature extremes is somewhat larger in winter than in summer; this presumably might be due to the higher wind velocities in the troposphere in winter. The temperature variation changes phase above 8 km. in winter and at 12 km. in summer, indicating the higher position of the tropopause in summer. In both summer and winter the amplitude of the temperature variation increases as soon as the phase reverses, i.e., there is a strong secondary maximum of temperature variation in the

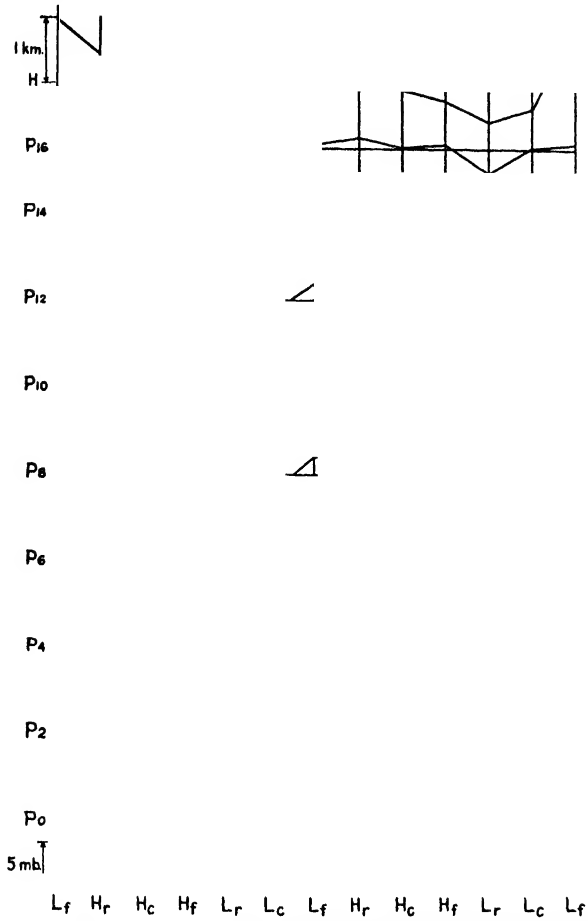

FIG. 7. *Variation of the pressure and of the height of the tropopause with the passage of surface highs and lows; summer mean.*

lower stratosphere in the neighbourhood of the tropopause (8 to 11 km. in winter and 12 to 13.5 in summer). Thus, the layers in the lower stratosphere are at least as effective in causing surface pressure variations as the layers in the upper troposphere, although the increase in temperature variation above the tropopause is partly offset by the decrease in the density of air with altitude. This is also in agreement with the fact that the greatest advective changes of mass occur near the surface and near the tropopause (6). The increase in the amplitude of the temperature variation, however, need not necessarily be an advective phenomenon, but could be due, at least, in part, to large vertical motions near the tropopause.

Special Case. Jan. 8–14, 1939

An attempt has been made to amplify the preceding statistical results by the presentation of individual synoptic situations. To do this, aerological observations are needed in the six areas of highs and lows. Since aerological

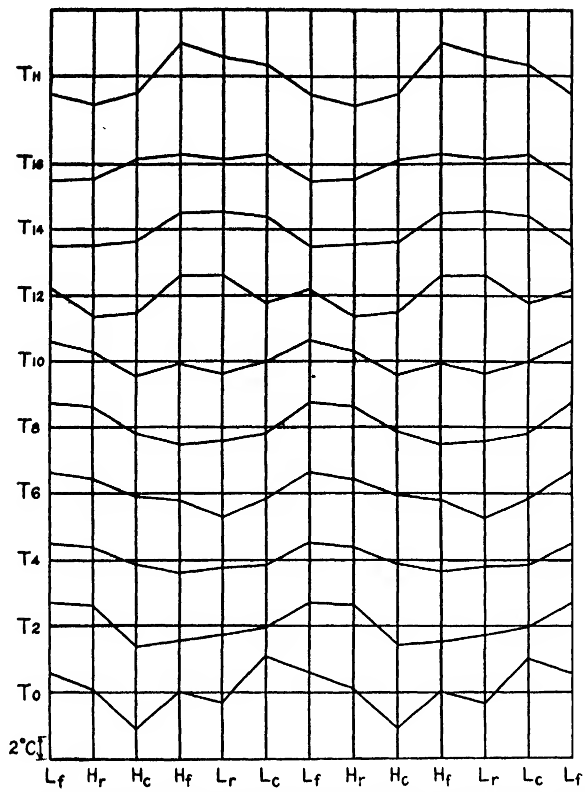

FIG. 8. *Variation of the temperature with the passage of surface highs and lows; summer mean.*

observations are taken only once a day, it was difficult to find a situation in which sufficient aerological material was available. Many cases failed to yield any satisfactory results, owing mainly to the fact that a time scale unit of one day is too large to reveal these effects. J. Bjerknes and E. Palmén (2) have constructed barograms at the different levels for European stations for which enough aerial ascents were available in a selected cyclone. These barograms show the retardation of the pressure extremes. In the barogram for Sealand (Fig. 21 in the reference), for example, the lowest pressure occurred between 16 and 17 h. (Feb. 16, 1935), while from 4 to 8 km. the lowest pressure is found from 19 to 20 h. Taking three to six days as a reasonable time interval from one passage to the next of a certain region (which represents 360° in the above harmonic analysis), the retardation between 0 and 8 km. (37°) for the yearly mean would be 8 to 15 hr. For the special case of Bjerknes and Palmén, the retardation between the surface and 8 km. is only about four hours, much less than the yearly mean value of 8 to 15 hr. However the above value of four hours holds for an individual European cyclone that may have had characteristics different from those of the cyclones generally found over North America. Also, polar front theory indicates that the

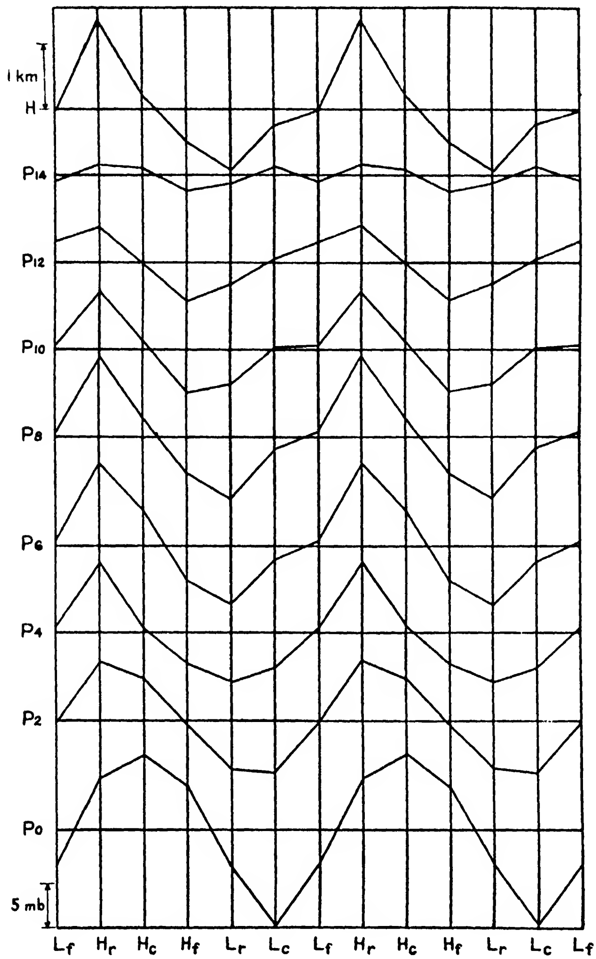

FIG. 9. *Variation of the pressure and of the height of the tropopause with the passage of surface highs and lows; winter mean.*

lag should be greater for younger cyclones than for older ones. Either of the above factors may contribute to the explanation of the greater time lag of the yearly mean values than of this special case.

One of the cases in this investigation for which sufficient data was available is described below.

On Jan. 8, 1939, a low, which subsequently moved NE, was developing in the southwestern United States. On Jan. 9 it was centred N of Omaha while Sault Ste. Marie was situated in the area between *Hr* of the preceding high and *Lf* of this low. On Jan. 10, Sault Ste. Marie was in the centre of the low. On Jan. 11 this slow moving low had passed over the station, leaving it in *Lr*. On Jan. 12 to 14 a polar Canadian anticyclone following the cold front associated with the low passed over Sault Ste. Marie. In Figs. 11 and

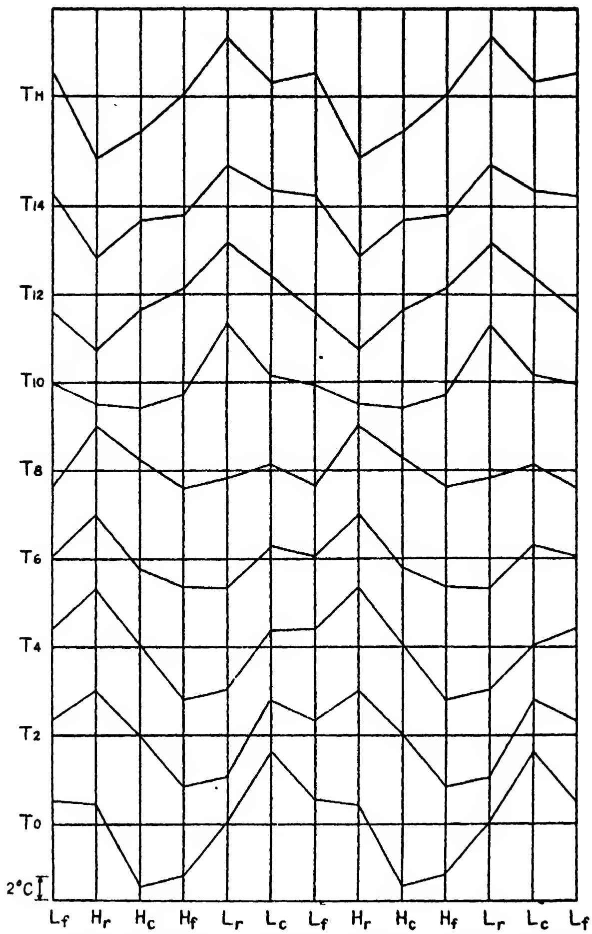

FIG. 10. *Variation of the temperature with the passage of surface highs and lows; winter mean.*

12 are plotted the pressures and temperatures by days. According to the diagrams the lowest pressure occurred on Jan. 10 at the surface and on Jan. 11 at higher levels. The highest temperature was observed on the 10th at the surface and on the 9th at higher levels, thus showing the retardation of the pressure extremes and the forward displacement of the temperature extremes for the low. Above the tropopause the temperature changes phase. The preceding high also shows the retardation of the pressure extremes, since the pressure at the surface was higher on Jan. 8 than on Jan. 9, while at 2 km. and above, the highest pressure was found on the Jan. 9. The high that followed the low, however, does not show the retardation of the pressure extremes.

An attempt was also made to use the aerological material from different stations to obtain a cross-section through a low. The distance between the

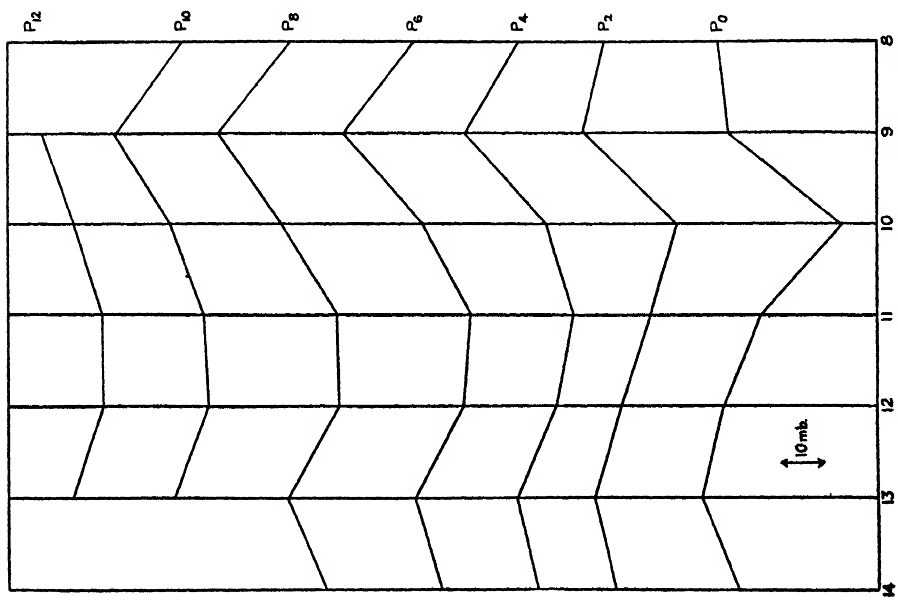

FIG. 11. *Pressure variation from Jan. 8–14, 1939.*

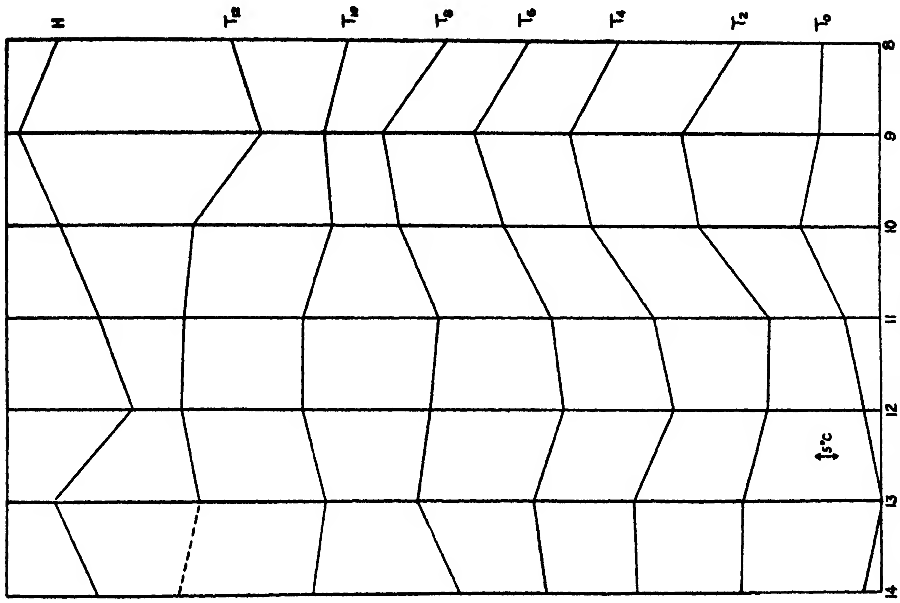

FIG. 12. *Temperature variation from Jan. 8–14, 1939.*

stations at present available is too large to show the displacement of pressure and temperature extremes aloft, although considerable use can be made of such cross-sections for other purposes (11).

It is to be expected that there are considerable regional differences depending on the latitude of the station and the predominating type of air mass found there. The writer intends to make a further study of the problem by investigating the aerological material at a station in a more southerly latitude.

Acknowledgments

The writer wishes to express his gratitude to the U.S. Weather Bureau for supplying the data; to Mr. J. Patterson, Controller of the Meteorological Service of Canada, for obtaining the data and for permission to use the facilities of the Meteorological Office; and to Dr. B. Haurwitz for numerous valuable suggestions and helpful advice during the course of the investigation.

References

1. Bjerknes, V., Bjerknes, J., Solberg, H., and Bergeron, T. Physikalische Hydrodynamik, J. Springer, Berlin. 1933.
2. Bjerknes, J. and Palmén, E. Geofys. Pub. Oslo, 12 (2). 1937.
3. Dines, W. H. Coll. Sci. Papers. 1931.
4. Haurwitz, B. Veröffentl. Geophys. Inst. Leipzig. ser. 2. 3 : 267–336. 1927.
5. Haurwitz, B. and Turnbull, W. E. Can. Meteor. Memoirs, 1 (3) : 67-92. 1938.
6. Haurwitz, B. and Haurwitz, E. Harvard Meteor. Studies No. 3. 1939.
7. Palmén, E. Beitr. Physik frei. Atm. 19 : 55-70. 1932.
8. Schedler, A. Beitr. Physik frei. Atm. 7 : 88-101. 1915.
9. Schedler, A. Beitr. Physik frei. Atm. 9 : 181-201. 1921.
10. Stüve, G. Beitr. Physik frei. Atm. 13 : 23-36. 1926.
11. Willett, H. C. Mass. Inst. Tech. Papers in physical oceanography and meteorology. 4 (2). 1935.
12. Van Mieghem, J. Ciel et Terre, Bruxelles, No. 1. 1940.

Canadian Journal of Research

Issued by THE NATIONAL RESEARCH COUNCIL OF CANADA

VOL. 19, SEC. A FEBRUARY, 1941 NUMBER 2

A NEW IONIZATION AMPLIFIER[1]

BY H. LE CAINE[2] AND J. H. WAGHORNE[3]

Abstract

A new type of instrument for measuring ionization currents is described. Whenever a charge is placed upon the electrode of the ionization chamber, an alternating voltage is obtained by electrostatic translation of the motion of a reed. The alternating voltage is amplified in an amplifier containing only standard radio parts and used to measure the ionization current by a condenser balance method. An instrument tested in the laboratory measured a quantity of 1.5×10^{-12} coulombs with about the same accuracy as a DuBridge and Brown instrument. The readings were recorded automatically and could be taken as rapidly as every three seconds with no linearity correction.

Introduction

In linear amplifiers used with an ionization chamber for measuring ionization currents, it is customary to connect the control grid of a tube directly to the electrode of the ionization chamber. A special tube is required in which the grid current from all sources has been reduced to the smallest practicable value. Such a tube is necessarily fragile and expensive. The associated circuit must be constructed with a view to obtaining the greatest stability possible. Circuits that provide a satisfactory degree of stability are cumbersome and are not ideally suited for further amplification of the output to permit the use of rugged recording mechanisms.

If the principle of the generating voltmeter is applied to convert the d-c. signal into an alternating voltage before amplification, important improvements in the operating characteristics of the circuit are obtained. The basic circuit is shown in Fig. 1. When a small quantity of charge is added to the system at A, the steady state conditions at B are unaltered as long as C_1 and C_2 are fixed. If either C_1 or C_2 is a periodic function of time, the alternating voltage appearing at B is changed by the addition of charge at A. The alternating voltage at B is proportional to the voltage at A and may be used to measure the voltage at A. Three points are of especial interest. The internal impedance of the device is inversely proportional to the modulation frequency and may be made sufficiently low that special precautions to raise the input resistance of the first tube are unnecessary. The fluctuations in

[1] *Manuscript received in original form September 9, 1940, and as revised, November 7, 1940. Contribution from the Department of Physics, Queen's University, Kingston, Ont.*

[2] *Holder of a Studentship under the National Research Council of Canada.*

[3] *At the time, holder of a Bursary under the National Research Council of Canada. Present address, National Research Laboratories, Ottawa.*

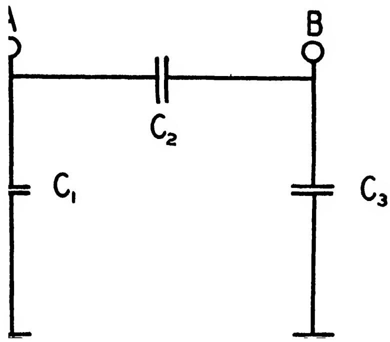

FIG. 1. *Generating voltmeter.*

output arising in the amplifier itself are now due to a band of frequencies from which the low frequencies may be excluded. For fairly narrow band widths, the random voltage is inversely proportional to the band width and has a lower limit depending upon the rapidity of action required of the device. The great decrease in noise level obtainable when a restricted frequency response may be introduced into a system has been widely used elsewhere. Finally, the usual values of input tube and ionization chamber capacity are such that it is not difficult to give to C_1 or C_2 values that result in a reasonable fraction of the maximum voltage obtainable. The maximum peak voltage is half the direct voltage developed at the input of a direct coupled amplifier when the input capacity is the same in both cases.

The principle of electrostatic translation has been used for some years in microphones, musical instruments, and voltmeters for measuring high voltages. In 1932 Hull (2) suggested the use of a vibrating reed as one electrode of a condenser for modulating a small direct voltage, but apparently the idea was not used. In the same year Gunn (1) and Kirkpatrick (3) published articles of a somehwat similar nature.

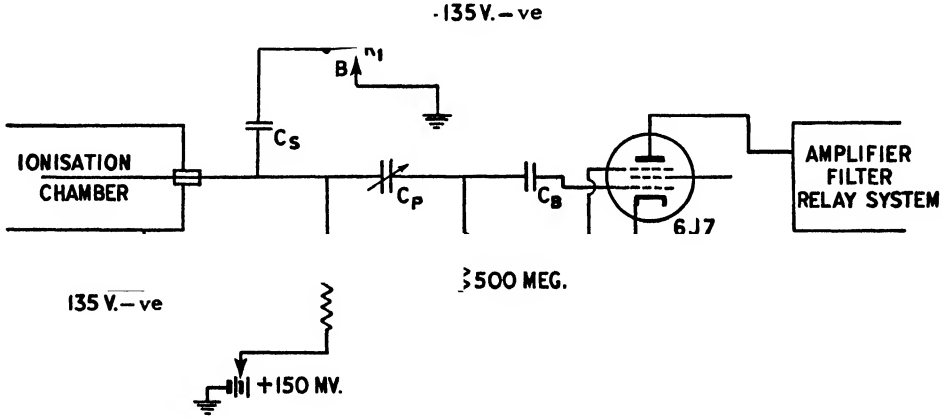

FIG. 2. *Input circuit.*

Experimental Amplifier

Fig. 2 shows an instrument tested in this laboratory. The ionization chamber electrode is connected directly to a stationary plate of a small air condenser C_p; the other plate of the condenser is a steel reed set vibrating at 120 cycle.sec^{-1} by means of an electromagnet supplied with 60 cycle current. The reed is tuned to 120 cycles by adjusting its length. The spacing between the reed and the stationary plate is only about 1/32 in., and the amplitude of vibration is of the same order. The cushioning effect of the air between the two surfaces of the condenser serves as an effective amplitude control for the reed. The reed is connected through a 500 megohm resistor to ground.

A circuit diagram including the amplifier is given in Fig. 3.

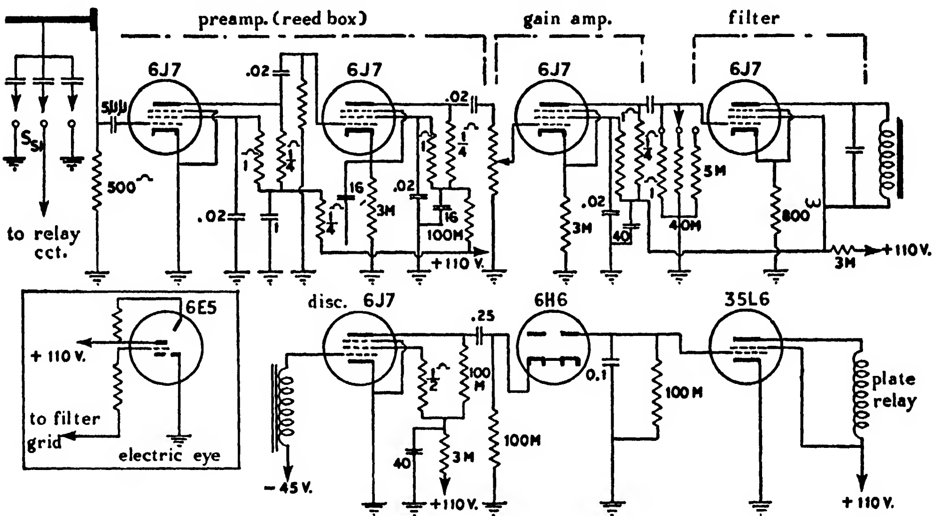

FIG. 3. *Amplifier.*

The mechanical construction of the periodic condenser and electrode system is shown in Fig. 4. The parts indicated are:—

A—cylinder that forms the outer electrode of one of the balance condensers;

B—condenser. The capacity between B and electrode is adjusted to be $\frac{1}{10}$ that between cylinder A to electrode.

C—not used (permanently grounded);

D—condenser. The capacity between *D* and electrode is adjusted to be $\frac{1}{100}$ that between A and electrode.

E—grounding key solenoid;

F—coil supplying a-c. energy to reed;

G—end of the electrode facing reed—$\frac{5}{8}$ in. diameter, faced with the same steel used in the reed;

H—reed of $\frac{5}{8}$ in. clock spring;

L—condenser composed of $\frac{1}{32}$ in. ebonite next to the reed and $\frac{1}{32}$ in. brass;

M—bracket for supporting two 6J7 tubes of preamplifier.

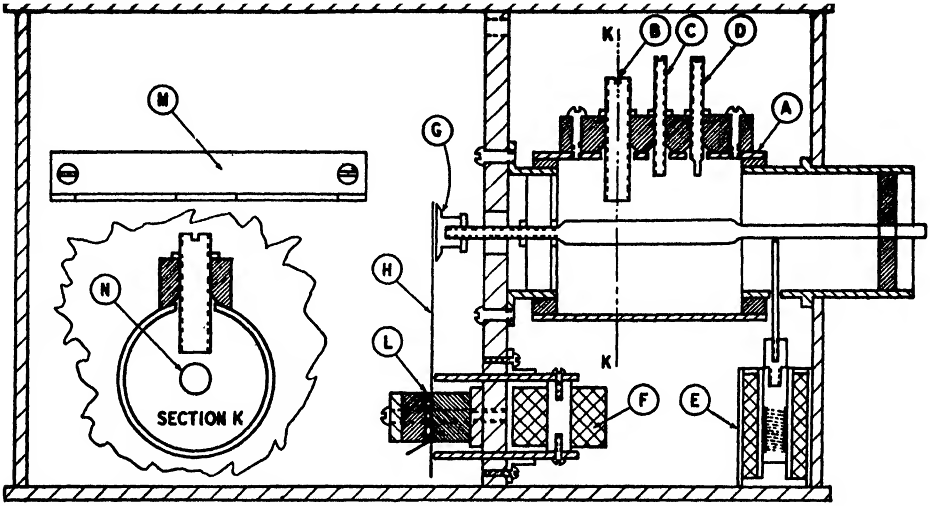

FIG. 4. *Periodic condenser and balance condenser.*

This unit, which is approximately 2 by 6 by 9 in., is connected to a second unit of approximately 6 by 9 by 12 in. by means of a flexible cable. The second unit contains the remainder of the amplifying and timing circuit together with four 45 volt portable *B* batteries used to provide standard voltages and a polarisizing voltage for the ionization chamber.

The relay system used is shown in Fig. 5. L_1 represents the plate relay coil, and S_1 the contacts on this relay. Contacts marked S_2 are controlled by the coil L_2. A bond indicates the position taken by a set of contacts when the corresponding coil is not energized.

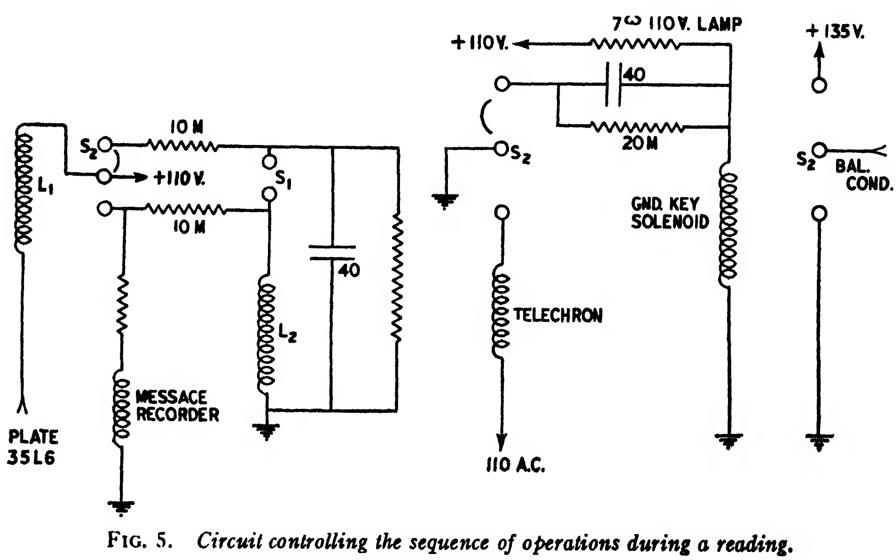

FIG. 5. *Circuit controlling the sequence of operations during a reading.*

The system is used as an electrometer, and currents are obtained by a modified balance method. The electrode voltage over a complete cycle is shown in Fig. 6. With K_1 in position D (Fig. 2) a polarizing voltage is set on the grounding key which is then released giving a signal of amplitude M. Owing to the flow of current in the ionization chamber the signal decreases to a minimum value A and the relay system operates to start a telechron timer and to switch K_1 to the position B, so that a definite charge is added to the electrode system, thus increasing the signal to the value P. Since the volt-ampere characteristic of the electrode system is linear, it is permissible to add all the balancing charge at once. The signal again decreases to the value A, at which time the relay system operates to stop the telechron, return K_1 to D and reconnect the grounding key momentarily, so that a new cycle is started automatically. A message recorder is connected to record the number of readings taken. The time measured by the telechron is the time required for the chamber electrode to collect a known charge, and enables the average current to be calculated.

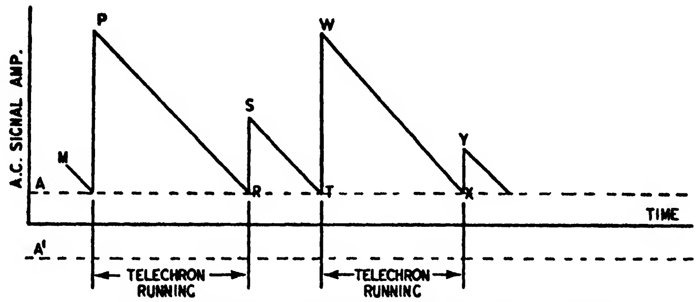

FIG. 6. *Variation of electrode voltage over two readings.*

Characteristics of the Device

The limit to the useful sensitivity is at present set by the insulation of the supports for the electrode assembly. The inclusion of the two 6J7 amplifier tubes in the same case as the reed assembly has proved unfortunate as it has been established that the temperature rise thus produced has a pronounced effect on this insulation. Sulphur has been found superior to ebonite in this respect.

An improvement in the timing circuit would result if the change of phase of the signal as it passes through zero amplitude were used to operate the relay system. It would then be impossible for the signal to pass through its minimum value too rapidly to allow the relay contacts to close. In a model tested, one side of the periodic capacity was grounded. A second stationary electrode was placed on the opposite side of the reed to the one already in use and a constant d-c. potential applied to it through a resistor. the a-c. signal produced was used as a standard with which to compare the phase of the original signal.

The instrument as constructed has a sensitivity range of 10^4 and requires about 1.5×10^{-12} coulombs for a full scale deflection. It will take readings every three seconds with no linearity correction. It should find application wherever a sensitive and rugged d-c. amplifier of very high input impedance is required. Small currents such as those arising in dielectric material may be observed under the most favourable conditions because the electrode assembly may be made as large or as small as desired. Surface conditions of the electrode faces of the periodic condenser had a pronounced effect on the polarizing voltage required for zero signal. This suggests a possible use in the study of surface voltages.

Acknowledgments

The writers would like to thank Dr. J. A. Gray and Dr. J. S. Marshall for their helpful interest in this work.

References

1. HULL, A. W. Physics, 2 : 409-431. 1932.
2. KIRKPATRICK, P. Rev. Sci. Instruments, 3 : 430-438. 1932.
3. ROSS, G. Phys. Rev. 40 : 307-312. 1932.

NEW ELECTRONIC TRANSITIONS OF THE BH MOLECULE[1]

By A. E. Douglas[2]

Abstract

In a discharge in helium with a trace of boron trichloride and hydrogen three new bands are found at 3415 Å, 3396 Å, and 3099 Å. Measurements of these bands show that they are due to two new electronic transitions of the BH molecule. The upper states of both transitions are previously unknown $^1\Sigma^+$ states. The lower state of both transitions is the same and is a known $^1\Pi$ state. The rotational constants of both new states have been determined and their electron configuration is suggested.

Introduction

The spectrum of the BH molecule has been studied by several investigators. A complete record of all the known bands can be found in the papers of Thunberg (6) and of Almy and Horsfall (1). The only singlet band system of the BH molecule recorded by these investigators occurs around 4330 Å and is due to a $^1\Pi - {}^1\Sigma^+$ transition. The $^1\Sigma^+$ state is the ground state of the molecule. In what follows, the observation and analysis of three new singlet bands of BH, which involve two new electronic states, will be described.

Experimental

The spectrum was excited in an uncondensed discharge through a tube of the type described by Douglas and Herzberg in a previous paper (2). The tube was filled with helium to about 15 mm. pressure and sufficient hydrogen was added that H_α and the adjacent red helium line had about the same intensity. This is an extremely small amount of hydrogen, and usually the hydrogen occurring as an impurity in the tube was sufficient. To this mixture a small amount of boron trichloride was added and the discharge tube was then operated in the manner described in the previous paper (2).

Under these conditions the well known BH band at 4330 Å appeared with an intensity so great that it could be photographed in the third order of the 21 ft. grating spectrograph in a few minutes. At the same time three new, much weaker bands, which had their Q heads at 3415 Å, 3396 Å, and 3099 Å, were observed. They were photographed in the second order of the grating spectrograph with a dispersion of about 1.4 Å/mm. The exposure time was about 20 min. The wide structure of the bands indicated immediately that they are hydride bands, and the analysis confirms the assumption (suggested by the conditions of excitation) that they are due to BH.

[1] *Manuscript received November 16, 1940.*
Contribution from the Department of Physics, University of Saskatchewan, Saskatoon, Sask., with financial assistance from the National Research Council of Canada.

[2] *At the time graduate student, holder of a Bursary (1939–1940) under the National Research Council of Canada. At present at the University of Minnesota.*

Analysis of the Bands at 3415Å and 3396Å

The two bands at 3415 and 3396 Å, which obviously belong together, were relatively free from other overlapping bands (BCl, AlCl, etc.) and could therefore be accurately measured. Each of them consists of a P, a Q, and an R branch. In consequence of the open structure of the bands the branches could be picked out and the quantum numbers assigned by inspection.

The first three columns of Table I show the wave numbers of the lines in the band at 3415 Å (0−0 band). Though lines due to the $B^{10}H$ molecule could be seen they were not measured. All lines are single, showing that the band represents a singlet transition. Since the first line of the P branch $P(1)$ is present and the first line of the R branch $R(0)$ is missing, the bands must be due to a $^1\Sigma - {}^1\Pi$ transition. The fourth column of Table I gives the values

TABLE I

WAVE NUMBERS OF THE LINES AND COMBINATION DIFFERENCES IN THE BH BAND AT 3415 Å (0−0 BAND OF $^1\Sigma^+ - {}^1\Pi$ SYSTEM)

$\nu_0 = 29272.78$ cm.$^{-1}$

J	$R(J)$	$Q(J)$	$P(J)$	$\Delta_2F''(J) = R(J-1) - P(J+1)$	$\Delta_2F'(J)$ for band 4330 Å after Thunberg
0					
1	29321.44	29273.24	29248.89		
2	346.21	74.05	225.49	119.02	119.10
3	371.09	75.22	202.42	166.46	166.34
4	396.31	76.86	179.75	213.51	213.54
5	421.68	78.88	157.58	260.39	260.37
6	447.19	81.32	135.92	306.85	306.76
7	472.92	84.26	114.83	352.82	352.79
8	498.80	87.68	094.37	398.33	398.31
9	524.83	91.60	074.59	443.19	443.02
10	551.03	96.01	055.61	487.42	487.45
11		29301.00	037.41	530.88	531.01
12		06.56	020.04		
13		12.73			
14					

of $\Delta_2F''(J) = R(J-1) - P(J+1)$ calculated from the measurements of the new band, while the fifth column gives the values of $\Delta_2F'(J) = R(J) - P(J)$ calculated from the data given by Thunberg for the 0−0 band of the $^1\Pi - {}^1\Sigma$ transition of BH. The agreement of corresponding values in the two columns shows definitely that the two electronic transitions have the $^1\Pi$ state in common. The good agreement also establishes the fact that the upper state for the new bands is a $^1\Sigma^+$ state. If it were a $^1\Sigma^-$ state the Λ type doubling of the $^1\Pi$ state would prevent such an agreement.

In Table II are given the wave numbers of the lines in the band at 3396 Å. It can be shown by means of the agreement of the combination differences that the lower state for this band is the upper state for the 1−1 band of the $^1\Pi - {}^1\Sigma$ system around 4330 Å. This establishes the fact that the bands at 3415 Å and 3396 Å are the 0−0 and 1−1 bands of the same system.

Since only the $0-0$ and $1-1$ bands have been observed, the vibrational constants of the new $^1\Sigma^+$ state can not be determined directly. A rough value can be obtained by using the formulae $\omega_e^2 = \frac{4B_e^3}{D_e}$ and $\omega_e x_e = \frac{0.7\alpha\omega_e}{B_e}$ [see (6)]. The vibrational constants so determined are listed together with the rotational constants for the new state in Table III. Since the constants for the $^1\Pi$ state have been determined by several investigators they have not been evaluated from the new data. The agreement of the values of $\Delta_2F(J)$ for the $^1\Pi$ state calculated from the present data and from the data given by Thunberg shows that any re-evaluation of the constants would not lead to a significant change.

TABLE II

WAVE NUMBERS OF THE LINES OF THE BH BAND AT 3396 Å
($1-1$ BAND OF $^1\Sigma-{}^1\Pi$ SYSTEM)

$\nu_0 = 29433.75$ cm.$^{-1}$

J	$R(J)$	$Q(J)$	$P(J)$
0	—	—	—
1	29480.59	29434.71	29411.57
2	504.86	36.10	389.95
3	529.62	38.33	368.98
4	555.03	41.25	348.84
5	581.01	44.90	329.48
6	607.48	49.43	310.98
7	634.42	54.76	293.58
8	661.72	60.94	Covered
9		68.08	261.90
10		76.24	247.89
11		85.40	235.19
12		95.79	223.99
13			214.35

TABLE III

CONSTANTS FOR THE UPPER $^1\Sigma$ STATE OF THE BANDS AROUND 3415 Å

B_0, cm.$^{-1}$	B_1, cm.$^{-1}$	α, cm.$^{-1}$	B_e, cm.$^{-1}$	r_e, 10^{-8}cm.	D_e, cm.$^{-1}$	ω_e, cm.$^{-1}$	$\omega_e x_e$, cm.$^{-1}$
12.083	11.512	0.571	12.368	1.215	0.00134	2400	65

Analysis of the Band at 3099 Å

The BH band at 3099 Å has a structure very similar to the one at 3415 Å, but it is not as intense. Since a strong group of aluminium atomic lines falls on this band, a discharge tube with iron electrodes had to be used. Though this removed the troublesome aluminium lines the BH band was still overlapped by a band of SiCl, which was obviously formed by the action of the active chlorine (formed by the decomposition of boron trichloride in the discharge) on the glass walls. Owing to the small intensity and the overlapping SiCl band only the P and Q branches of the BH band at 3099Å

could be measured. The wave numbers of the measured lines are given in Table IV.

TABLE IV

WAVE NUMBERS OF THE LINES AND COMBINATION DIFFERENCES IN THE BH BANDS AT 3099 Å

$\nu_0 = 32260.04$ cm.$^{-1}$

J	$P(J)$	$Q(J)$	$\Delta_1 F'(J)$
0			24.57
1	32235.88	32260.52	48.83
2	212.66	61.69	73.15
3	189.98	63.53	97.32
4	168.07	66.06	121.62
5	146.60	69.23	145.55
6	126.15	73.11	169.26
7	106.55	77.69	192.74
8	087.74	82.91	216.18
9	069.84	89.05	
10		96.03	

Since the first line of the P branch is present in this band the upper state is also a $^1\Sigma^+$ state. It is found that the values of $Q(J) - P(J+1)$ calculated from the measurements of this band are equal to the values of $R(J) - Q(J)$ calculated from Thunberg's data for the 0–0 band of the $^1\Pi - {}^1\Sigma^+$ transition at 4330 Å. The lower state for the new band must therefore be the known $^1\Pi$ state, just as for the bands 3415 and 3396 Å. The agreement also establishes the fact that the upper state is $^1\Sigma^+$, not a $^1\Sigma^-$ state.

In order to obtain the constants for the $^1\Sigma^+$ state, $\Delta_1 F'(J)$ was calculated by subtracting the Λ doubling of the $J+1$ level of the $^1\Pi$ state from the value of $Q(J+1) - P(J+1)$ calculated from the new band. The Λ doubling of the $^1\Pi$ state was taken from Thunberg's data. The values of $\Delta_1 F'(J)$ are shown in the last column of Table IV. The constants of the upper state of the new band are found to be:

$$B_0 = 12.23 \text{ cm.}^{-1}, \quad D_0 = 0.00148 \text{ cm.}^{-1}, \quad r_0 = 1.222.10^{-8} \text{ cm.},$$

$$\omega_0 = \sqrt{\frac{4B_0^3}{D_0}} = 2230 \text{ cm.}^{-1}.$$

Electronic Structure of the BH Molecule

In Table V the known electronic states of AlH and BH are compared. The data for AlH are from Sponer (5, vol. 1). It is interesting to note that with the two new $^1\Sigma^+$ states of BH found here there is a complete analogy between the electronic states of BH and AlH.

The six electronic states of BH can easily be accounted for by the following four electron configurations:

$(1s\sigma)^2(2s\sigma)^2(2p\sigma)^2$	$^1\Sigma^+$
$(1s\sigma)^2(2s\sigma)^2 2p\sigma 2p\pi$	$^3\Pi\ {}^1\Pi$
$(1s\sigma)^2(2s\sigma)^2\ (2p\pi)^2$	$^3\Sigma^-\ {}^1\Sigma^+({}^1\Delta)$
$(1s\sigma)^2 2s\sigma 2p\sigma(2p\pi)^2$	$^1\Sigma^+({}^1\Delta\ {}^3\Sigma^-\ {}^5\Sigma^-\ {}^3\Sigma^-\ {}^1\Sigma^-\ {}^3\Delta\ {}^3\Sigma^+)$

TABLE V

EXCITATION ENERGIES OF THE KNOWN ELECTRONIC STATES OF BH AND AlH

State	Excitation energy	
	BH	AlH
$A^1\Sigma^+$	0	0
$a^3\Pi$	x	y
$B^1\Pi$	23073.8	23470.9
$b^3\Sigma$	$x + 27056.7$	$y + 26100$
$C^1\Sigma^+$	52346.6	44597.1
$D^1\Sigma^+$	55333.6	49288

While the first two have been assumed previously to account for the two lowest singlet states (5, vol. 1) the two others seem to be the most likely configurations for the newly found states (as well as for the $^3\Sigma$ state). It is probable that the electron configurations for the corresponding states of AlH may be obtained simply by changing the principal quantum number 2 to 3 and adding the complete L shell of Al. However, one difficulty is that the observed transitions $C^1\Sigma^+ \rightarrow A^1\Sigma^+$ and $D^1\Sigma^+ \rightarrow A^1\Sigma^+$ of AlH (not observed for BH) would involve simultaneous jumps of two electrons.

Acknowledgments

This investigation was made possible by a grant from the Penrose Fund of the American Philosophical Society and also a grant for research to Professor Herzberg from the National Research Council of Canada. Finally the author is greatly indebted to Dr. G. Herzberg for giving much valuable advice and help during the course of this work.

References

1. ALMY, G. M. and HORSFALL, R. B. Jr. Phys. Rev. 51 : 491-500. 1937.
2. DOUGLAS, A. E. and HERZBERG, G. Can. J. Research, A, 18 : 165-174. 1940.
3. DOUGLAS, A. E. and HERZBERG, G. Can. J. Research, A, 18 : 179-185. 1940.
4. HERZBERG, G. Molecular spectra and molecular structure. Prentice-Hall, Inc., New York. 1939.
5. SPONER, H. Molekülspektren. Julius Springer, Berlin. 1935.
6. THUNBERG, S. F. Z. Physik, 100 : 471-478. 1936.

Canadian Journal of Research

Issued by THE NATIONAL RESEARCH COUNCIL OF CANADA

VOL. 19, SEC. A. MARCH, 1941 NUMBER 3

THE CAPTURE CROSS-SECTION FOR THERMAL NEUTRONS OF CADMIUM, LITHIUM^6, BORON^{10}, BARIUM, MERCURY AND HYDROGEN[1]

BY E. L. HARRINGTON[2] AND J. L. STEWART[3]

Abstract

A comparison method of measuring, by using solutions, the capture cross-sections for thermal neutrons is described. The chief advantages are directness, simplicity, and freedom from uncertainties as to direction of path, or as to the magnitude of the scattering effect. The method is best suited to nuclei of large cross-sections. Assuming the well checked value for the cadmium nucleus to be correct, the capture cross-sections of certain other nuclei were determined. The results for barium and for hydrogen differ widely from values previously published.

Most determinations of the cross-sections for capture of thermal neutrons by various nuclei have been made by the use of materials in sheet form. Amaldi and Fermi (1, 2) employed absorbers placed near the sources of neutrons. Dunning and his co-workers (4) used arrangements that provided for greater distances between the source and the detectors, and hence reduced considerably the uncertainties as to the direction of the incident neutrons. In all such determinations two difficulties are inherent. It cannot be determined accurately how much of an observed absorption is due to the scattering of the neutrons and how much to their capture, nor is there any certainty as to the paths travelled by the neutrons through the absorber, since generally a large number of scattering impacts are suffered by a neutron before the final impact that results in its capture. The extent to which such factors affect the results also varies from element to element, since the thickness chosen for any absorber must depend on the total cross-section of its nuclei if the magnitudes of the absorption effects are to be kept within suitable ranges. Because of the uncertainties involved, the errors may range up to 10 or even 25% in the case of strong absorbers (4, p. 277).

The solution method of comparing capture cross-sections of nuclei offers many advantages and has been proposed or used along two or more lines. Furry (6) in 1936 suggested the principle involved. In 1938, Frisch, Halban, and Koch (5) and also Knauer (7) published results obtained by using solutions of the absorbing element. It is believed that the method, employed in the investigation herein reported, and which is due in part to Professor Goudsmit, involves certain additional modifications of importance.

[1] *Manuscript received November 20, 1940.*
Contribution from the Department of Physics, University of Saskatchewan, Saskatoon, Sask.
[2] *Professor of Physics, University of Saskatchewan.*
[3] *Research Student and Technician for Radon Plant, Saskatchewan Cancer Commission, Saskatoon, Sask.*

Theory of Experiment

When fast neutrons move through a hydrogenous material like paraffin or water their speeds are rapidly reduced to those corresponding to thermal conditions (1, 2). However a thermal neutron may make many additional elastic impacts without further change in energy before making the inelastic impact that results in a deuteron. This means that in a hydrogenous medium subject to the bombardment of fast neutrons there accumulates a certain concentration of thermal neutrons, which may be represented by c, where c is the number per cubic centimetre.

The value of $\frac{dc}{dt}$ will depend mainly on three factors: (i) the gain in neutrons due to the diffusion of thermal neutrons from adjacent space, (ii) the gain due to the slowing down of fast neutrons entering the space, and (iii) the loss due to captures by hydrogen or other nuclei. A general differential equation covering these factors may be written as follows:

$$\frac{dc}{dt} = D\left[\frac{d^2c}{dx^2} + \frac{d^2c}{dy^2} + \frac{d^2c}{dz^2}\right] + KS - Bc,$$

where D is the diffusion constant for thermal neutrons, KS the rate at which the unit volume acquires thermal neutrons through the slowing down of fast neutrons from a source of strength S, and B is a constant such that Bc gives the rate of capture.

For a steady state $dc/dt = 0$. Also, if the experimental arrangements are such as to eliminate or at least greatly reduce any effect of diffusion, as is the case for the twin sources employed in the work herein described, then the equation simplifies to $KS = Bc$ or $\frac{1}{c} = \frac{B}{KS}$.

The probability of capture, B, must depend on the total capture cross-section present in the unit volume, and may be written $\Sigma N_i\sigma_i$, where N_i is the number of nuclei of substance i per cubic centimetre, each having a capture cross-section of σ_i. In a pure water medium N_H would be taken as the number of hydrogen nuclei, the oxygen nuclei being neglected because of the very small value of σ_o. In a water solution, say of cadmium, B becomes $N_H\sigma_H + N_{Cd}\sigma_{Cd}$. For additional substances in solution additional terms must be added. Experimentally the relative values of c were determined by introducing into the solution a detector, whose induced radioactivity, a, due to exposure for a fixed time, may be taken as proportional to c. If a be the numerical value of the activity measured in any convenient empirical units, and if S is constant, then for a given series of observations obtained by changing the concentration of a solution of cadmium,

$$\frac{1}{a} = K'(N_H\sigma_H + N_{Cd}\sigma_{Cd}),$$

where K' is a new constant of proportionality. Since $N_H\sigma_H$ and σ_{Cd} are constant it follows that $1/a$ plotted against N_{Cd} should give a straight line

such as PM in Fig. 1. When $1/a$ is zero, $\sigma_H = \frac{-N_{Cd(H)}}{N_H} \sigma_{Cd}$, where $N_{Cd(H)}$ is the value of N_{Cd} that would effect the same capture as the hydrogen of the water. $N_{Cd(H)}$ may be read from OP. N_H is known from Avogadro's number. Hence, assuming the published value (7) of σ_{Cd} to be correct, the value of σ_H may be directly computed provided that all losses in neutrons in pure water are due to captures by hydrogen nuclei. Actually the plateau of uniform concentration is finite and there must be some diffusion losses. Any such will tend to give σ_H an apparent value higher than its true value.

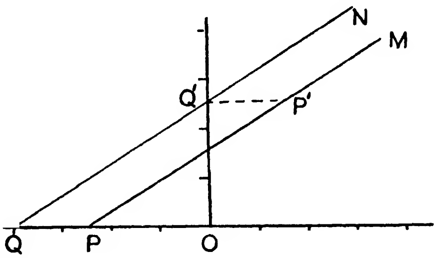

FIG. 1. *Graphical method of comparing capture cross-sections.*

The method may be applied also to the determination of the value of the capture cross-section of the atomic nucleus of an element J by employing initially a solution of J of known concentration in place of the pure water. This should give a new line parallel to PM, as QN. The increase in the intercept PQ (or $P'Q'$) gives directly the value $N_{Cd(J)}$ of N_{Cd} that would offer the same total capture cross-section as N_J of the J atoms that were placed in a unit volume of the solution. From this it follows that $\sigma_J = \frac{-N_{Cd(J)}}{N_J} \sigma_{Cd}$. In a similar way a σ_K might be obtained, and as a cross check, $\sigma_J + \sigma_K$. The uncertainty mentioned in the paragraph next above will not enter here since only the difference in intercept is involved.

Apparatus

The two principal items of the equipment were an Edelmann electrometer, with its connected ionization chamber, and an exposure tank with its accessories and the sources. The former was practically equivalent to that described by Amaldi and Fermi (1, 2). The more essential features of the latter are represented by Fig. 2.

The two beryllium-radon sources S_1 and S_2 are mounted at such a distance apart that the concentration of neutrons throughout the region of the silver detector D is substantially constant, as required by the theory of the experiment. The glass jar surrounding these contained the test solutions and could be drained readily by lifting the ground glass plug P. This and the fixed guides for the detector support rod were mounted within a water tank on suitable supports as shown. No metal other than the detector was included with the inner jar, as any change in the concentration of the solution through

ion replacement must be prevented. The detector had a diameter of 50 and a thickness of 0.15 mm.; a thin coat of Duco was applied to it. S_1 and S_2 contained substantially equal quantities of beryllium granules and also like quantities of radon (about 150 m.c. each at the beginning of a series). An electric timing system subject to dual control was available. Ample protective shielding was provided for the observers and the electrometer system.

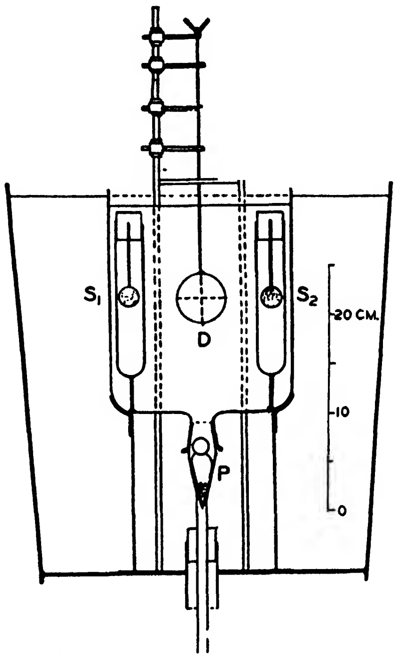

FIG. 2. *Diagrammatic representation of the arrangement of the equipment, sources, and solutions used in exposing detectors to the neutronic radiation.*

Experimental Procedure

Briefly stated, the essential steps in any measurement of the relative concentration of thermal neutrons included merely the exposure of D and the subsequent measurement of its relative activity. The steps were carried out in a manner very much like that reported by Amaldi and Fermi, and need not be described in detail. These involved the exposure of D in the position shown in Fig. 2 for exactly 120 sec., followed 16 sec. later (the time found necessary in practice to remove, dry, and then transport the detector to the somewhat distant electrometer system) by an observation of the rate of deflection of the electrometer fibre due to the induced radioactivity of D. For each determination a number of check runs (usually six) were made. This was followed by a set of measurements similar except that D was shielded on each side by a disk of cadmium sufficiently thick to absorb the thermal neutrons. From this set it could be ascertained how much of the activity first observed was due to fast neutrons. The difference in the two rates of deflection gave a measure of the radioactivity, a, acquired by D due to the

slow neutrons alone, and therefore of their concentration (see Refs. 1, 2). The sensitivity of the electrometer was constantly checked by means of a Ra D standard and due allowance made for the decay of the radon.

Since these comparisons of capture cross-sections of nuclei hinge on an accurate knowledge of their numbers per unit volume, great care was required in the preparation of the solutions employed. Trial runs showed that cadmium solutions ranging up to say 20×10^{18} nuclei per cubic centimetre gave absorptions of suitable magnitude. The concentrations of the subsequently added ions of lithium, boron, etc., were so adjusted as to give effects of the same order of magnitude as that due to the cadmium solutions, hence were varied roughly inversely as their corresponding capture cross-sections.

Attention should be called to certain practical difficulties with respect to the preparation of solutions. Each metal should be introduced into the solution in the form of one of its soluble salts and the salt most suitable is the one having the acid radicle of lowest cross-section for the capture of thermal neutrons. The nitrates and bromides are particularly suitable since bromine, nitrogen, and oxygen nuclei have negligible capture cross-sections for thermal neutrons. Unfortunately the nitrates and bromides needed in this investigation are so highly deliquescent that the accurate weighings needed to determine numbers of nuclei could not be made. This difficulty was overcome by using carbonates that could be obtained pure as well as dry, and, after weighings were completed, by converting the carbonates into bromides. Also, in certain cases the elements used included isotopes of unequal but known abundance ratios, the large absorption for thermal neutrons being due to one particular isotope. In such cases due allowance for the abundance ratios were made, and the capture cross-sections were assigned to the particular isotope known to be responsible. The question of purity of the salts used is also of great inportance, as a mere trace of an element having a large capture cross-section would seriously affect the results. Actually the usefulness of the solution method is practically limited to the study of nuclei having capture cross-sections that are large compared to those of their associated acid radicles or of the constituents of water itself, and to the use of salts either pure or known to include no trace of an element possessing a large nuclear capture cross-section. In dealing with the problems mentioned in this paragraph the authors found the table prepared by Bethe (3) most useful.

Results

The final determinations of relative capture cross-sections may be made analytically, or graphically as outlined above in the discussion of the theory. The graphical method was employed and involved plotting $1/a$ against N_{Cd} first for aqueous solutions containing cadmium only. Fig. 3 represents a typical series of measurements and shows that the resulting curve is a straight line, as predicted from the theory, and also gives the ranges of concentrations found most suitable. Each point shown represents the result of a group of measurements. A repetition of the series of measurements say on the fol-

lowing day would give likewise a straight line—see dotted line—but with a greater slope due to the decay of the radon. Whatever the strength of the source, such lines should pass through the point P, since OP represents the concentration of cadmium nuclei that offers the same total capture cross-section as the water itself, assuming no other losses. The mean value of OP, obtained from a number of series of observations, was -12.02×10^{18}/cc.

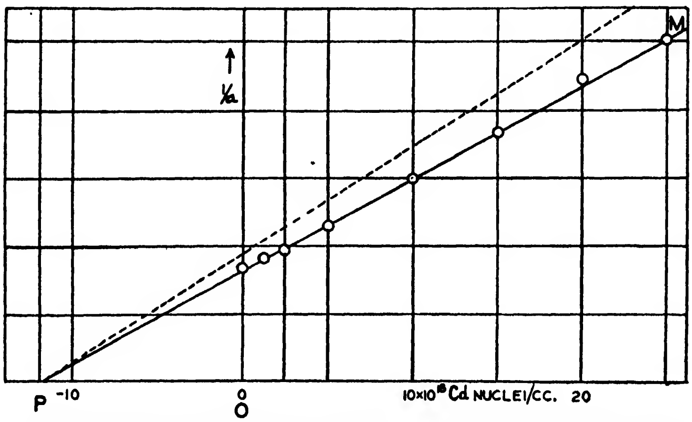

FIG. 3. *Curve showing relation between activity of detector and concentration of cadmium nuclei.*

The capture cross-section for thermal neutrons of a cadmium nucleus given by Bethe (3) was assumed as correct and to have the value of 2600×10^{-24}cm.². Since the number of hydrogen nuclei per cubic centimetre is 0.673×10^{23}, the capture cross-section for thermal neutrons for hydrogen may be directly computed on the basis of these values by means of the relation:

$$\sigma_H = \frac{-N_{Cd(H)}\,\sigma_{Cd}}{N_H}\ .$$

The result is 0.464×10^{-24}cm.². In this it is assumed that any captures by oxygen nuclei and diffusion effects may be neglected. The value obtained is much higher than the value 0.33×10^{-24}cm.², which was given by Knauer. It is not easy to account for such a large discrepancy on the basis of diffusion losses, since the use of twin sources in the present experiments must have very greatly reduced such losses. Certainly the value obtained must mark the upper limit for σ_H. The uses of stronger sources in the present investigation and an ionization chamber in place of a Geiger counter were other very distinct advantages as thereby the uncertainties due to the background count were reduced. The close agreement in the results of the independent trials herein reported would seem to be significant.

At this point it may be well to report that an experimental check on the existence of the plateau of concentration was made by exposing the silver detector at a series of positions on a line joining the two sources, first without, then with cadmium shields. The resulting activations indicated the plateau effect both for thermal and for fast neutrons. The latter is important since

the mean free path for thermal neutrons is only about 1 cm. and the "diffusion length" about 3.5 cm. (7). The concentration of thermal neutrons on the plateau then hinges on the conversion of fast neutrons in the plateau region, hence the one plateau follows from the other. Also it was found experimentally that the concentration of fast neutrons in the plateau region was inappreciably affected by the nature of the solution. This experimental fact greatly supports the theory of this method.

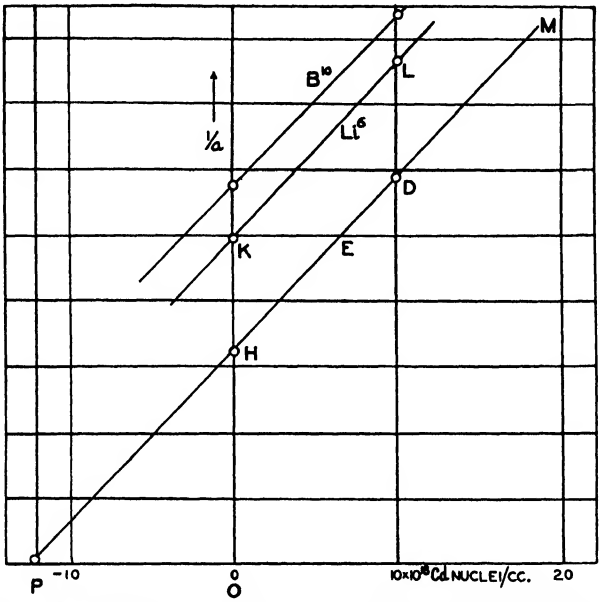

FIG. 4. *Curves showing effects of adding other absorbing nuclei to solutions containing cadmium nuclei on the induced radioactivity of the detector.*

The method employed in the determination of the capture cross-sections for thermal neutrons for other nuclei may be readily understood from the curves shown in Fig. 4. PM represents the line passing through the point -12.02×10^{18} and points H and D which were obtained respectively with water alone and with a cadmium solution containing 10×10^{18}Cd nuclei per cc. Points K and L represent values obtained when to the water and to this cadmium solution enough lithium bromide was added to give each a Li^6 nuclei concentration of 21.22×10^{18}. This required a total of 268.6×10^{18} ordinary lithium nuclei per cc. since the abundance ratio of Li^6 is 7.9% (8). It is seen that the addition of the lithium has increased the intercept by an amount equivalent to KE. This was found to have a mean value of 6.91×10^{18}. Since the capture of slow neutrons by the lithium nuclei has been found due to the Li^6 isotope, the value of σ_{Li^6} is given by the relation:

$$\sigma_{Li^6} = \frac{-N_{Cd(Li^6)}\sigma_{Cd}}{N_{Li^6}}.$$

A substitution of the above values leads to 846×10^{-24}cm.^{2} as the value of σ_{Li^6}.

In a similar manner other capture cross-sections were measured. Table I gives the values obtained, together with the values listed by Bethe (3) in his summary.

TABLE I

VALUES OF $\sigma_{capture}$ OBSERVED, AND VALUES PREVIOUSLY PUBLISHED

Nucleus	$\sigma_{capture}$ (Observed)	$\sigma_{capture}$ (Bethe)
Cd	2600×10^{-24}cm.^{2} (assumed)	2600×10^{-24}cm.^{2}
B^{10}	2760×10^{-24}cm.^{2}	3000×10^{-24}cm.^{2}
Li^6	846×10^{-24}cm.^{2}	900×10^{-24}cm.^{2}
Hg	323×10^{-24}cm.^{2}	440×10^{-24}cm.^{2}
Ba	Less than 21.4×10^{-24}cm.^{2} (See below)	140×10^{-24}cm.^{2}

It is of interest to note that the agreement with published values is reasonably close in each case, except that of barium, if the uncertainties involved in the experimental methods employed previously are considered. It is generally believed that the absorption by cadmium nuclei is due entirely to capture, hence the cadmium nucleus was a suitable one to take as a standard. Since each other value for $\sigma_{capt.}$ falls below the corresponding value in Bethe's table, it might be suspected that the value given for cadmium itself is too low.

The experimental work in the cases of Li^6, B^{10}, and Hg involve a statistical error of the order of 2%. The extent to which the results may be affected by any absorption due to bromine nuclei must be small. Any uncertainties as to whether, when water alone is used, there may be losses of neutrons other than through captures by hydrogen nuclei as mentioned above, are not involved here, as water is present in each of these cases, and such effects would be constant. Certainly the method is simple and the comparisons direct. Should the value of σ_{Cd} assumed correct in this investigation be found later to require revision, the values herein listed would be affected accordingly.

These results with barium were quite unexpected and interesting. Neglecting the absorption of the associated bromine nuclei and following the same technique as for the other nuclei, the capture cross-section was found to be 21.4×10^{-24}cm.^{2}, in strong disagreement with the previously published value of 140×10^{-24}cm.^{2}. In view of this result a new determination using barium from a different stock was carried out, but the result obtained was in excellent agreement with that of the first determination. If the value given by Bethe for the bromine nucleus is accepted, then the two bromine nuclei associated with the barium atom would fully account for the observed captures, and it might well be concluded that the barium nucleus has a negligible capture cross-section for thermal neutrons.

While the above report was in the hands of a referee, a paper reporting the same type of work was published by Lapointe and Rasetti (see Phys. Review, 58, 554. 1940). While the experimental approach and the elements tested were for the most part different, it is interesting to note that these observers,

too, found the capture cross-section of the barium nucleus to be very small. They, like the present authors, experimentally proved that the density of the fast neutrons in the region of the detector is inappreciably affected by the nature of the solution.

Acknowledgment

The authors are grateful to the Saskatchewan Cancer Commission for the radon used in this investigation. Having the plant located at the University was highly advantageous in the preparation of the sources.

References

1. AMALDI, E., D'AGOSTINO, O., FERMI, E., PONTECORVO, B., RASETTI, F., and SEGRE, E. Proc. Roy. Soc. (London), A. 149 : 522-558. 1935.
2. AMALDI, E. and FERMI, E. Phys. Rev. 50 : 899-928. 1936.
3. BETHE, H. A. Rev. Modern Phys. 9(2) : 69-244. 1937.
4. DUNNING, J. R., PEGRAM, G. B., FINK, G. A., and MITCHELL, D. P. Phys. Rev. 48 : 265-280. 1935.
5. FRISCH, O. R., HALBAN, H. JR., and KOCH, J. Kkl. Danske Videnskab. Selakab. Math.-fys. Medd. 15(10). 1938.
6. FURRY, W. H. Phys. Rev. 50 : 381. 1936.
7. KNAUER, F. Z. Physik, 108 : 153-161. 1938.
8. RASETTI, F. Elements of Nuclear Physics, Prentice-Hall, Inc., New York.

THE DIFFUSION OF WATER VAPOUR THROUGH A SLIT IN AN IMPERMEABLE MEMBRANE[1]

By J. D. Babbitt[2]

Abstract

Starting with the elementary equation for the diffusion of a vapour, an equation is developed giving the relation between the amount of vapour diffusing through a slit in an impermeable membrane and the width of the slit. The results given by this equation are compared with experimental values and a satisfactory agreement is obtained.

Introduction

In order to prevent the condensation of moisture in the walls of buildings it has become standard practice to provide in the wall a membrane of some material having vapour barrier qualities. This vapour barrier is placed at such a position that the vapour cannot reach those cold parts of the wall where condensation might occur. Methods have been developed by means of which the value of various materials as vapour barriers can be measured, and data have been obtained on the merits of the different types of construction. It is difficult however to evaluate the effects of cracks or joints in such a vapour barrier membrane, and, since in most cases the vapour barrier cannot be applied to the wall in one unbroken sheet but must be built up from a number of small sections or panels, this is important.

In the majority of constructions some sort of a building paper is used as the vapour barrier. In this case the joints can easily be overlapped, and, if an especially tight seal is desired, asphalt or some other sealing compound can be used to seal the overlap. In constructions of this nature the effect of the cracks can be neglected; in other cases, however, it is impossible to obtain an overlapped joint, and then the cost of obtaining a satisfactory seal is prohibitive. Under these conditions a small slit or crack remains in the otherwise vapour proof membrane and it is important to estimate how this slit will affect the vapour barrier qualities of the construction.

Such a problem was presented to the National Research Laboratories in the course of its work on vapour barriers. In certain types of construction an aluminium-backed building board is used as a plaster base. The aluminium foil not only serves as a vapour barrier but also adds a certain amount to the insulation of the wall. With the increased attention that is being given to vapour barriers, the point was raised that in such a construction it was not practical to seal the cracks between the boards, and the resulting flow of vapour might lead to condensation in the wall. It was, therefore, imperative to determine the amount of vapour diffusing into the wall in this manner

[1] *Manuscript received December 31, 1940.*

Contribution from the Division of Physics and Electrical Engineering, National Research Laboratories, Ottawa, Canada. Issued as N.R.C. No. 979.

[2] *Physicist.*

in order to compute whether the wall as a whole could be considered as adequately protected from condensation.

In order to attack this problem a series of measurements were made to determine the amount of water vapour diffusing through cracks of different widths under standard conditions. At first sight it might be expected that the amount of water vapour would be directly proportional to the area of the crack. However, preliminary results obtained from the measurements immediately showed that this viewpoint was much too superficial, and that the diffusion through narrow cracks was proportionally much greater than that through wide ones. This follows naturally if it is considered that the lines of flow are not straight lines perpendicular to the crack and that the vapour diffuses in from the side. There is, therefore, a greater flow through the edges of the slit than through the centre. Thus the narrow slits will transmit proportionally a greater amount of vapour than the wide ones.

The importance of this fact from a practical standpoint was such that it warranted a more thorough investigation of the problem. In this paper the theory underlying the diffusion of water vapour through such a crack is developed, and the resulting equation is shown to agree with experimental measurements.

Development of Theory

The theory underlying the diffusion of a vapour was first developed by Stefan (4) who was primarily interested in the evaporation from a circular beaker. He pointed out the essential difference between the evaporation or condensation of a vapour and the inter-diffusion of two non-condensing gases. In the case of the two non-condensing gases, the fluxes of partial pressure across any plane perpendicular to the direction of diffusion are opposite and equal for the two gases. This follows from the fact that the total pressure must everywhere be equal so that if Gas A is diffusing in one direction there must be a corresponding diffusion of Gas B in the opposite direction in order that no inequalities of pressure will be built up. In a case such as this the fundamental equations are (3, p. 370).

$$\rho_1 u_1 = -\frac{k_1 k_2}{CP}\frac{d\rho_1}{dx} \quad \text{and} \quad \rho_2 u_2 = -\frac{k_1 k_2}{CP}\frac{d\rho_2}{dx}, \tag{1}$$

where ρ = density of the gas,

u = velocity of the gas,

$k = \dfrac{RT}{M}$ = a constant at constant temperature

P = total pressure = $p_1 + p_2$, where p_1 and p_2 are the partial pressures,

and C = coefficient of resistance.

The subscripts 1 and 2 refer to Gas A and Gas B respectively. According to Equations (1) the diffusion coefficient, D, is equal to $\frac{k_1 k_2}{CP}$ and is proportional to the reciprocal of the total pressure.

In the case of the condensation or evaporation of a vapour, the condition of equality of the fluxes of partial pressure does not hold, because the fact that the vapour is condensing or evaporating assures that the total pressure remains constant without any movement of the second gas. There is, then, in this case the movement of one gas alone. As Stefan has shown, the equation governing this movement is:

$$\rho_1 u_1 = -\frac{k_1 k_2}{C(P - p_1)} \frac{d\rho_1}{dx}, \tag{2}$$

which differs from Equations (1) in that the denominator contains $(P - p_1)$ instead of P. Now since $p_1 = k_1 \rho_1$, we can write

$$\rho_1 u_1 = -\frac{k_2 \, .}{C(P - p_1)} \frac{dp_1}{dx}$$

In this case let is be assumed, after Stefan, that the coefficient of diffusion $D = \frac{k_2}{C}$, so that

$$\rho_1 u_1 = -\frac{D}{(P - p_1)} \frac{dp_1}{dx}$$

$$= D \frac{d}{dx} [\log (P - p_1)] \tag{3}$$

Put

$$V \equiv \log (P - p_1).$$

Then

$$\rho_1 u_1 = D \frac{dV}{dx} \, . \tag{4}$$

Now, this equation is similar in form to that giving the relation between the charge on the surface of a conductor and the field at that point ($4\pi\sigma = -D \frac{dV}{dn}$, where σ is the charge per unit area and D is the dielectric constant) and to the equation governing the flow of heat in a solid body ($Q = C \frac{dt}{dx}$, where Q is the amount of heat transmitted across unit area when the temperature gradient is $\frac{dt}{dx}$. C is the coefficient of thermal conductivity). The mathematical theory developed in those cases can be applied to diffusion. It is obvious then that diffusion in three dimensions can be represented by Laplace's equation in the form:

$$\frac{\partial^2 V}{\partial x^2} + \frac{\partial^2 V}{\partial y^2} + \frac{\partial^2 V}{\partial z^2} = 0 \tag{5}$$

This is the fundamental equation governing the diffusion of a vapour. It is essential to note that V, the potential function, has the form $\log (P - p_1)$.

It remains now to solve Laplace's equation in this form subject to the boundary conditions pertaining to the problem. It is required to find how the amount of water vapour diffusing through a slit of infinite length in an impermeable material varies with the width of the slit. Since the length of

the slit can be considered infinite, it is only necessary to consider a section of unit length, so that the problem may be reduced to one of two dimensions. Laplace's equation can therefore be used in the form.

$$\frac{\partial^2 V}{\partial x^2} + \frac{\partial^2 V}{\partial y^2} = 0\,. \tag{6}$$

In order to obtain a solution of this equation it is necessary to use the method of conjugate functions*.

Put

$$z = x + iy \qquad \text{and} \qquad W = U + iV, \tag{7}$$

where z and W are complex imaginaries that are connected by the relation $z = \phi(W)$, where $\phi(W)$ is some function of W. Let it be assumed that

$$\phi(W) = f\cos W,$$

where f is a constant whose significance will be determined later. Then

$$\begin{aligned} z &= f\cos W \\ &= f\cos(U + iV) \\ &= f(\cos U\cos iV - \sin U\sin iV) \\ &= f(\cos U\cosh V + i\sin U\sinh V) \end{aligned}$$

By comparing this with Equation (7) the following parametric equations for x and y are obtained:

$$x = f\cos U\cosh V \qquad \text{and} \qquad y = f\sin U\sinh V \tag{8}$$

Elimination of U and V respectively from these equations gives the relations

$$\frac{x^2}{f^2\cosh^2 V} + \frac{y^2}{f^2\sinh^2 V} = 1 \tag{9}$$

and

$$\frac{x^2}{f^2\cos^2 U} - \frac{y^2}{f^2\sin^2 U} = 1 \tag{10}$$

Equation (9) is the equation of a family of confocal ellipses whose semi-axes are $f\cosh V$ and $f\sinh V$ respectively, while Equation (10) is the equation of a family of confocal hyperbolas of semi-axes $f\cos U$ and $f\sin U$. f is thus the focal distance in both cases. These curves have been plotted in Fig. 1. It is obvious now from the theory of conjugate functions that V given by Equation (9) can be considered as satisfying the conditions of a potential in Equation (6) and that the confocal ellipses are the equipotential surfaces. On this viewpoint the confocal hyperbolas are the lines of flow at right angles to the equipotential surfaces. When $V = 0$ is substituted in Equation (9), the confocal ellipse becomes a line joining the two foci. This is the case in which we are interested as this line may be considered as a slit through which the vapour is diffusing. We are concerned in finding how the amount of vapour flowing through the slit varies with the width of the slit, that is, with the focal distance.

* *See, for instance: J. H. Jeans, "Electricity and Magnetism", Cambridge Press, 1927, p. 270; Handbuch der Physik, Band XII, p. 472; Clerk Maxwell, "Electricity and Magnetism", Oxford Press, 3rd ed. 1901, Vol. 1, p. 296.*

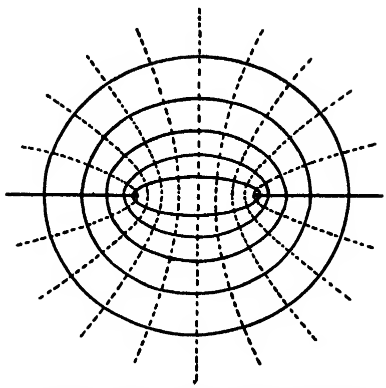

FIG. 1. *Potential surfaces and lines of flow through slit.*

In order to proceed with this it simplifies matters if the corresponding electrostatic problem is considered. This would be the case of an infinite strip of conducting material embedded in a non-conducting medium. The non-conducting medium will be considered to be a vacuum, so that the dielectric constant will be equal to unity. Then

$$4\pi\sigma = -\frac{\partial U}{\partial s} \tag{11}$$

where σ is the charge per unit area and ∂s is a small element of surface.

Now in this system of confocal ellipses

$$ds^2 = dx^2 + dy^2 = f^2 (\cosh^2 V - \cos^2 U)(dU^2 + dV^2).$$

From this it follows that, on the equipotential surfaces where V = constant,

$$\frac{dU}{ds} = \frac{1}{f\sqrt{\cosh^2 V - \cos^2 U}} = -4\pi\sigma. \tag{12}$$

But the general equation for the charge σ on the surface of an ellipsoid is given by*

$$\sigma = \frac{q}{4\pi abc} \frac{1}{\sqrt{\frac{x^2}{a^4} + \frac{y^2}{b^4} + \frac{z^2}{c^4}}}, \tag{13}$$

where a, b and c are the axes of the ellipsoid and q is the total charge. In the case of our system of elliptical cylinders, where c is infinite we can write $\frac{q}{2c} = e$, where e is the charge per unit length. Then

$$4\pi\sigma = \frac{2e}{ab} \frac{1}{\sqrt{\frac{x^2}{a^4} + \frac{y^2}{b^4}}}$$

and substituting for x and y from Equation (8) and remembering that $a = f\cosh V$ and $b = f\sinh V$ we obtain

$$4\pi\sigma = \frac{2e}{f^2\sqrt{\cosh^2 V - \cos^2 U}} \tag{14}$$

* *cf. Handbuch der Physik, vol. XII, p. 459.*

Comparison of this with Equation (12) shows that the charge per unit length of the cylinder is given by

$$e = -\tfrac{1}{2} \tag{15}$$

This is to say, that the charge on each of the cylinders is equal to $-\frac{1}{2}$. It is essential to realize that this charge distribution is that which is required to build up the potential distribution from which we obtained the equations for the equipotential surfaces. From the derivation it follows that the potential was zero on the line joining the foci and from there it increased to infinity at an infinite distance. Now it is obvious that any of the equipotential surfaces may be raised to any potential desired. In that case the charge e will change accordingly. The invariable quantity connected with the cylinders is the capacity. The capacity can be calculated from the specific case that was used to obtain the equations for the cylinders and then this value of the capacity may be used to calculate the charge that will be necessary to raise the cylinder to the desired potential.

From the above, it is known that $e = \frac{1}{2}$ for any cylinder that may be defined by the relation $\sinh V = \frac{b}{f}$, where b is the minor axis. For the capacity of this cylinder, therefore,

$$\begin{aligned} C = \frac{e}{V} = \frac{1}{2V} &= \frac{1}{2\sinh^{-1}\frac{b}{f}} \\ &= \frac{1}{2\log\frac{a+b}{f}} \\ &= \frac{1}{\log\frac{a+b}{a-b}}\,. \end{aligned} \tag{16}$$

This equation gives the capacity of any of the equipotential cylinders and this depends only on the major and minor axes of the cylinder. Let us see now how we can apply this solution to our specific problem.

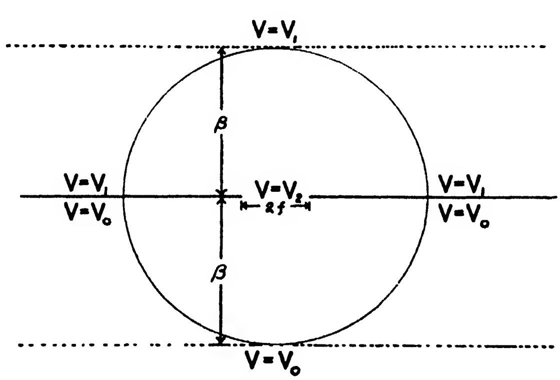

FIG. 2.

At some particular distance β from the slit (see Fig. 2) there is a potential $V = V_1$ [corresponding to $V_1 = \log (P - p_1)$], while at the slit there is a potential $V = V_2$ [corresponding to $V_2 = \log (P - p_2)$, where p_2 is the vapour pressure at the slit]. Also it can be assumed that at a distance β on the other side of the slit the pressure is p_0, so that $V = V_0 = \log (P - p_0)$. For the time being conditions on the under side of the slit can be neglected, since it is obvious that these will be the exact converse of those on the upper side.

We are interested then in the capacity of a system composed of an elliptical cylinder of minor axis β and the line joining its foci. Employing the same reasoning that was used to obtain Equation (16), we find the capacity of the two confocal elliptical cylinders to be

$$C = \frac{e}{V_1 - V_2} = \frac{1}{2 \log \dfrac{a_1 + b_1}{a_2 + b_2}} . \tag{17}$$

In the case of the two cylinders in which we are interested,

$$b_1 = \beta$$

$$a_1 = \sqrt{\beta^2 + f^2}$$

$$b_2 = 0$$

and

$$a_2 = f.$$

Thus the capacity of the system is given by

$$C = \frac{1}{2 \log \dfrac{\sqrt{\beta^2 + f^2} + \beta}{f}} . \tag{18}$$

This refers to the complete cylinder. For the present we are interested in only the upper half so that the capacity would be one-half of the above. Thus

$$C = \frac{1}{4 \log \dfrac{\sqrt{\beta^2 + f^2} + \beta}{f}} . \tag{19}$$

It is necessary now to find how the diffusion case is related to the electrostatic. In the latter,

$$4\pi\sigma = -\frac{dV}{dn} , \tag{20}$$

while for the former we have developed the equation

$$\rho_1 u_1 = D\frac{dV}{dn} . \tag{21}$$

It is then obvious that

$$\rho_1 u_1 = - 4\pi D\sigma, \tag{22}$$

and that the mass diffusing through the slit is proportional to the charge in the corresponding electrostatic problem. It is obvious that the mass diffusing through unit length would be proportional to the charge per unit length.

The charge per unit length in the system composed of elliptical cylinder and the line joining the foci is

$$
\begin{aligned}
e' &= C(V_1 - V_2) \\
&= \frac{V_1 - V_2}{4 \log \dfrac{\sqrt{\beta^2 + f^2} + \beta}{f}}, \qquad (23)
\end{aligned}
$$

and thus from Equation (22) the mass W diffusing through unit length of the slit would be

$$
\begin{aligned}
W &= \int \rho_1 u_1 ds \cdot = -4\pi D \int \sigma ds = 4\pi D e' \\
&= -\pi D \frac{V_1 - V_2}{\log \dfrac{\sqrt{\beta^2 + f^2} + \beta}{f}} \qquad (24)
\end{aligned}
$$

and since

$$V_1 = \log(P - p_1) \quad \text{and} \quad V_2 = \log(P - p_2)$$

$$W = -\pi D \cdot \frac{\log \dfrac{P - p_1}{P - p_2}}{\log \dfrac{\sqrt{\beta^2 + f^2} + \beta}{f}}. \qquad (25)$$

This then gives the essential equation relating the mass of vapour diffusing through the slit with the half-width of the slit f.

There are two simplifications that can be made in this formula. In the first place β is, by hypothesis, large compared with f, so that f^2 may be neglected in comparison with β^2. Secondly in order to apply the formula it is generally simpler to consider the vapour as diffusing from a vapour pressure p_1 at a distance β above the slit to a pressure p_0 at the distance β below the slit. From a consideration of symmetry the potential at the slit will be half-way between the potential at β and $-\beta$. Thus

$$
\begin{aligned}
V_1 - V_2 &= \tfrac{1}{2}(V_1 - V_0) \\
&= \tfrac{1}{2}[\log(P - p_1) - \log(P - p_0)] \\
&= \tfrac{1}{2} \log \frac{P - p_1}{P - p_0}. \qquad (26)
\end{aligned}
$$

Hence

$$W = -\frac{\pi D}{2} \frac{\log \dfrac{P - p_1}{P - p_0}}{\log \dfrac{2\beta}{f}}. \qquad (27)$$

This is the equation relating the mass diffusing through the slit with the half-width f.

Comparison with Experiment

In order to test Equation (27) two sets of experiments were carried out. In both cases aluminium foil was used as the impermeable membrane. In the first set of experiments this foil was placed between two pieces of plaster-

board each $\frac{3}{8}$ in. thick; in the second set the plasterboard was replaced with two pieces of $\frac{1}{2}$ in. fibreboard. This experimental arrangement was used in preference to a membrane in air alone as it was felt that in the latter case convection currents and currents caused by the fan in the humidity chamber would disturb the potential distribution. The specimens constructed in this way were mounted in glass crystallizing dishes, and the amount of water vapour diffusing through the slit was measured by the method used to obtain the permeability of building materials.

TABLE I

ALUMINIUM FOIL BETWEEN TWO PIECES OF PLASTERBOARD

Width of slit $2f$, cm.	Transmission, gm./24 hr./cm.	Width of slit $2f$, cm.	Transmission, gm./24 hr./cm.
0.022	3.64×10^{-2}	0.182	6.14×10^{-2}
0.042	4.36	0.260	7.97
0.072	5.00	0.374	7.43
0.113	5.54		

TABLE II

ALUMINIUM FOIL BETWEEN TWO PIECES OF FIBREBOARD

Sample	Width of slit = $2f$, cm.	Transmission, gm./24 hr./cm.	Sample	Width of slit = $2f$, cm.	Transmission, gm./24 hr./cm.
I	0.009	5.24×10^{-2}	II	0.075	7.37×10^{-2}
I	0.048	7.01	II	0.106	7.44
I	0.086	7.34	II	0.153	7.89
I	0.115	7.26	II	0.208	8.55
I	0.142	7.40	II	0.315	10.72
I	0.166	8.41	II	0.382	9.35
I	0.219	9.28	III	0.024	5.42
I	0.305	9.08	III	0.130	6.90
I	0.394	12.02	IV	0.018	5.14
II	0.047	6.84			

The results of the measurements are given in Tables I and II. In these experiments the temperature was 89.8° F. and the external relative humidity was maintained at 75%. Hence the vapour pressure difference across the samples was 26.6 mm. of mercury.

Now consider Equation (27)

$$W = -\frac{\pi D}{2} \frac{\log \dfrac{P - p_1}{P - p_0}}{\log \dfrac{2\beta}{f}} .$$

Since in all the measurements the vapour pressures were the same, $\log \dfrac{P - p_1}{P - p_0}$ can be considered as constant and the equation can be written in the form

$$W = \frac{C_1}{C_2 - \log 2f}, \tag{28}$$

where

$$C_1 = -\frac{\pi D}{2} \log \frac{P - p_1}{P - p_0}$$

and

$$C_2 = \log 2\beta + \log 2 .$$

If, therefore, log $2f$ is plotted against $\frac{1}{W}$ the resulting curve will be a straight line. The slope of this line will give the constant C_1, from which D can be determined since $\log \frac{P - p_1}{P - p_0}$ can be evaluated. C_2 and hence β can be determined from the fact that the intercept on the $\frac{1}{W}$-axis is equal to C_2/C_1.

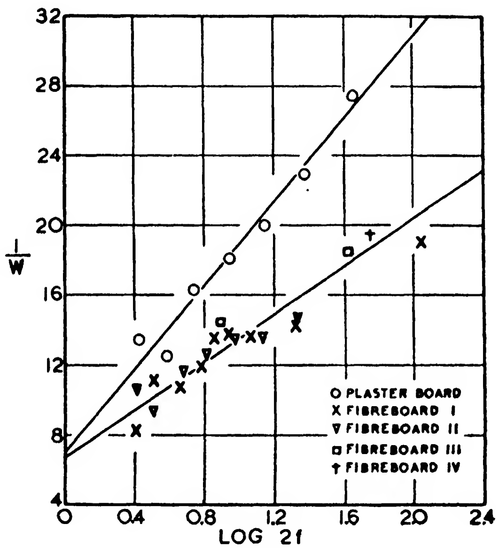

FIG. 3. *Relation between* $\frac{1}{W}$ *and log* $2f$.

In Fig. 3, $\frac{1}{W}$ has been plotted against log $2f$ for the two sets of samples. From these curves the following data are obtained for the plasterboard and fibreboard samples respectively:

(1) *Plasterboard:*

$$C_2/C_1 = 7.00$$

$$C_1 = 0.0837,$$

thus

$$C_2 = 0.586.$$

From this it is found that D = 3.44 gm./24 hr./sq. cm./unit change in log $(P - p_1)$ and

$$\beta = 0.96 \text{ cm.}$$

It is interesting to compare these values with those obtained from other measurements. In the ordinary measurement of diffusion coefficients (1, 2) the less accurate formula

$$W = -d\frac{dp}{dx}$$

is used. This corresponds to Equation (1). Comparing this with Equation (3) it is seen that

$$d = \frac{D}{P - p_1}.$$

The error involved in using this simpler formula instead of the more accurate log formula is small for the range of pressures involved in our work. Therefore by changing D to the usual unit used in permeability measurements it is found that

$$D = 46.9 \text{ gm./24 hr./sq. m./}\frac{\text{mm. Hg}}{\text{cm.}}$$

The value found previously (1) for the diffusance of a plasterboard sample of thickness 0.94 cm. was 22.8. Although a plasterboard of this nature cannot be considered as homogeneous, being faced on each surface with paper, a rough value for D is obtained by multiplying the diffusance by the thickness. In this way the value 21.4 gm./24 hr./sq. m./$\frac{\text{mm. Hg}}{\text{cm.}}$ is obtained. In a more recent publication (2) it has been found that in measuring the permeability of materials such as this there is an appreciable end effect, so that one should expect the true permeability to be larger than the value obtained from a sample only 0.94 cm. thick. When it is considered also that there would be a small air film between the two pieces of plasterboard since no effort was made to cement them together, the value obtained for D from these measurements may be considered to be in good agreement with previous work.

The value obtained for β is also very interesting. Theoretically β is that distance from the slit at which the pressure becomes equal to the exterior pressure. It would be assumed from the experimental set-up that this would approximate to the thickness of the plasterboard. The actual thickness of the latter is 1.05 cm. The fact that β comes out as 0.96 cm. is very satisfactory.

(2) *Fibreboard*

$$C_2/C_1 = 6.75$$

$$C_1 = 0.146,$$

thus

$$C_2 = 0.988$$

From these values it is found that $D = 6.014$ gm./24 hr./sq. cm./unit change in log $(P - p_1)$ per cm.

$$\beta = 2.43 \text{ cm.}$$

If D is changed to the other units as for the plasterboard

$$D = 82.0 \text{ gm./24 hr./sq. m./}\frac{\text{mm. Hg}}{\text{cm.}}.$$

A representative value for D taken from the data in (2) would be in the neighbourhood of 50.0. While this is not good agreement, it is of the right order, and the difference could easily be accounted for by the experimental set-up and errors of observation. The thickness of the fibreboard used was 1.3 cm., so that the agreement with β is not so good as was the case with the plasterboard.

In Fig. 4 the curves obtained by substituting the above values for C_1 and C_2 in Formula (28) have been plotted. The experimental values from Tables I and II are also given, and the agreement between the curve and the experimental points is quite satisfactory.

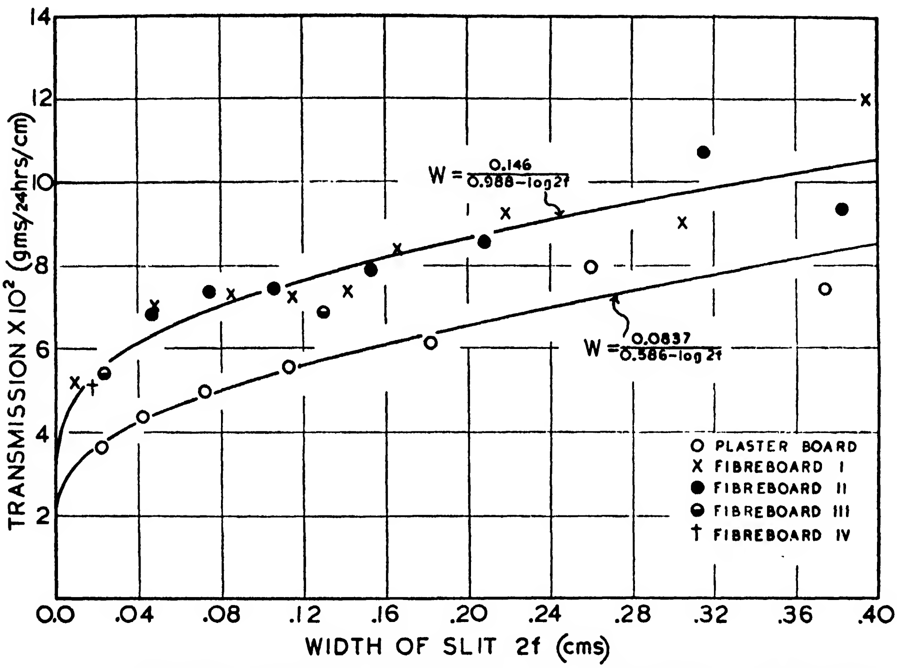

FIG. 4. *Transmission of water vapour through a slit cut in aluminium foil enclosed on both surfaces.*

Finally, in Fig. 5 are given the results obtained from the original measurements on foil-backed plasterboard. In making these measurements, the plasterboard was placed over the mouth of the cell with the aluminium foil facing outwards. The foil and hence the slit were left exposed to the air in the humidity chamber, which was circulating fairly rapidly owing to the circulating fan. Under these circumstances, it is difficult to say just what D and β mean, but it is obvious from the figure that the experimental results can be explained by an equation such as (27). Measurements were carried out on samples of both the plain aluminium-backed plasterboard samples and on samples that were plastered with $\frac{3}{8}$ in. rough base and $\frac{1}{16}$ in. finishing coat. The values of D and β that are used to plot the curves in Fig. 5 are as follows:

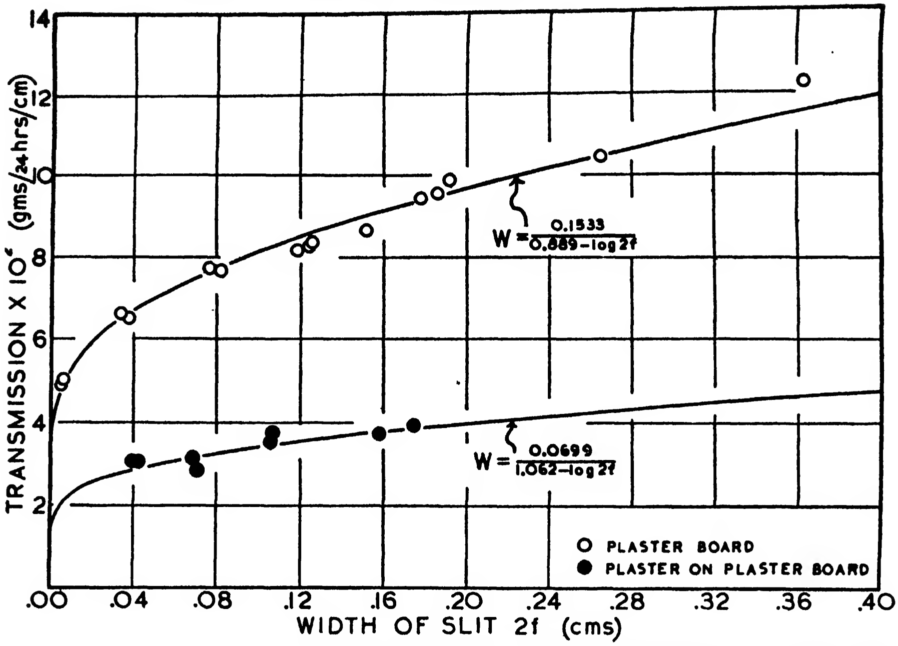

FIG. 5. *Transmission of water vapour through a slit cut in aluminium foil backed with plasterboard on one surface only.*

(1) *Aluminium-backed plasterboard:*

D = 6.175 gm./24 hr./sq. cm. unit change in log $(P - p_1)$ per cm.

= 84.3 gm./24 hr./sq. m./ $\dfrac{\text{mm. Hg}}{\text{cm.}}$

β = 1.94 cm.

(2) *Plaster on foil-backed plasterboard:*

D = 3.370 gm./24 hr./sq. cm./ unit change in log $(P - p_1)$ per cm.

= 45.7 gm./24 hr./sq. m./ $\dfrac{\text{mm. Hg}}{\text{cm.}}$

β = 2.88 cm.

These results have been given in order that they may be available for calculations involving the amount of vapour diffusing through such cracks in actual construction. It is essential therefore to state that the vapour pressure differences in the two sets of experiments were 27.1 and 22.8 mm. of mercury for the plasterboard and the plastered plasterboard respectively. Therefore in order to obtain the amount of vapour diffusing through the slit per unit vapour pressure, the transmissions obtained from the curves must be divided by 732.9 and 737.2 respectively. The results will then be given in grams per 24 hours per millimetre of mercury per centimetre length of crack.

Acknowledgment

The author wishes to express his appreciation of the work of W. A. Rowe, laboratory helper at the National Research Laboratories, who carried out the numerous weighings involved in the measurement of the vapour transmissions. He also wishes to acknowledge the suggestions which he gained from Dr. C. D. Niven in many discussions of this problem.

References

1. Babbitt, J. D. Can. J. Research, A, 17 : 15-32. 1939.
2. Babbitt, J. D. Can. J. Research, A, 18 : 105-121. 1940.
3. Enclyclopedia Britannica. 14th Ed., Vol. 7.
4. Stefan, J. Sitzber. Akad. Wiss. Wien, Math.-naturw. Klasse. Abt. IIa : 83. 1881.

Canadian Journal of Research

Issued by THE NATIONAL RESEARCH COUNCIL OF CANADA

VOL. 19, SEC. A. APRIL, 1941 NUMBER 4

THE CHINOOK WIND EAST OF THE CANADIAN ROCKIES[1]

BY H. L. OSMOND[2]

Abstract

The phenomenon known as the Chinook wind, which occurs in the foothills of the Canadian Rockies, has been investigated. A number of salient features of the Chinook have been established. The most important one is that of the pressure distribution associated with a Chinook. This involves the establishment of a pressure trough between two anticyclones, one on each side of the Rocky Mountain ridge. The location of this trough relative to the ridge is extremely important. In order that a strong Chinook occur, the trough must lie in the lee of the Rockies. It has been shown also that the region of the Chinook is in southern Alberta, extending a short distance east from the mountains.

Introduction

The Chinook wind is a meteorological phenomenon associated with the Rocky Mountains along the west coast of North America. The name itself is merely one of many local names applied throughout the world to a warm, dry wind deriving its properties from adiabatic changes. Argentina has its 'Zonda'; Sumatra its 'Bohorak'; southern California its 'Santa Ana' (4); and the Alpine countries their 'Foehns'.

The origin of the name 'Chinook' as used in North America has been accounted for by C. F. Talman in "Why the Weather". He quotes J. Neilson Barry, Secretary of the Trail Seekers' Council of Orgeon, as follows, "The name was given first of all neither to the dry wind east of the Rockies nor to the 'wet Chinook' of the coast, but to a dry northwesterly wind experienced in summer at Astoria, Oregon." This wind came from the direction of the Chinook Indian villages on the opposite shore of the Columbia River, between Point Ellice and Cape Disappointment. According to Mr. Barry the name 'Chinook' was applied as a joke about 1840 by Mr. Birnie, a Hudson's Bay factor.

The 'Three Characteristics' method of identification of Chinook winds was used by the author in his investigation. This method considers the direction of the wind, temperature changes, and the humidity of the air. As the Chinook wind is considered to result from the movement of air across or down a range of mountains (2, pp. 63-65), it always comes from a westerly direction in Alberta. To be a Chinook, a westerly wind must introduce a warmer air mass that is comparatively dry.

[1] *Manuscript received in original form October 8, 1940, and as revised, January 24, 1941.*

[2] *At the time, holder of a Bursary under the National Research Council of Canada, at the University of Toronto, Toronto, Ont. At present, Meteorologist, Stevenson Field Airport, Winnipeg, Man.*

According to Ekhart (3) this method allows too many summer occurrences of the wind to pass unnoticed. In particular, at Funsbruck in the Austrian Alps many days of Foehn occur when not all three characteristics are present. In place of the characteristics method, Ekhart adopts a slightly different set of criteria. According to him a wind from the right direction (depending on the locality) and showing a pronounced gustiness should be classified as a Chinook. However, Ekhart admits that there is the possibility of false identification by the 'gustiness' method. In the winter, there is no danger that Foehn occurrences pass unnoticed when the "three characteristics" method is used. Since only winter cases are studied here, the latter method will be used.

Results

The present writer, with the permission of Mr. J. Patterson, Controller, Meteorological Service of Canada, and under the supervision of Mr. Andrew Thomson, Assistant Controller, Meteorological Service of Canada, has investigated the occurrence during February and March, 1939, of the Chinook along the eastern foothills of the Canadian Rockies.

The following facts with respect to the Chinook wind have been established:

1. Each Chinook began after anticyclonic circulations had been established simultaneously on both sides of the mountains.

2. Before the Chinook is evident at Lethbridge and Calgary, there is a line of temperature discontinuity along the leeward side of the mountains.

3. The Chinook may begin as a gentle breeze or as a fresh wind.

4. The Chinook is generally stronger and steadier at Lethbridge than at Calgary.

5. The temperature at Calgary undergoes a greater and more sudden change at the beginning of the Chinook than that at Lethbridge.

6. The Chinook may begin at any time of day.

7. The direction from which the Chinook blows varies from the southwest through to the northwest.

8. Swift Current and Saskatoon are approximately the eastern limits to which the Chinook is still a drying wind.

9. The pressure does not increase during the Chinook period. During Chinooks lasting for days, the small diurnal pressure variation is present.

10. The advance of a Pacific air mass across the mountains into Alberta may be marked at the surface by frontal characteristics such as high humidity, low clouds, and precipitation in the north, and Chinook properties, namely, warmth and dryness, in the south. Further east, the Chinook properties diminish or disappear, and the mass may continue eastward with merely a warm front at the surface marking its progress. In these cases, a cyclonic centre develops in eastern Saskatchewan and western Manitoba.

The Typical Pressure Distribution

The first point, namely, that anticyclonic circulations must be established simultaneously on both sides of the Rockies, is most important. Math (5), in an investigation on the Chinook of Havre, Montana, stated that the pressure distribution typical for a Chinook situation was an intense low centered off the north Pacific coast and reaching inland to Alberta, with a centre of high pressure over the north Plateau* region. Ward (6, pp. 413-414), also, has

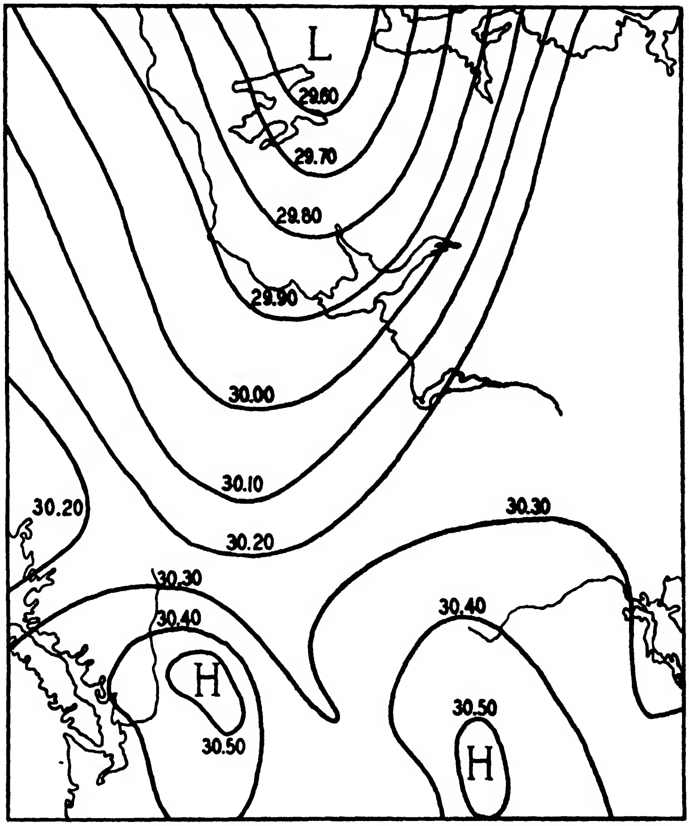

FIG. 1. *Pressure distribution (pressures in millibars) over Western Canada at 1130 hr. M.S.T., March 17, 1939. Centres of high pressure are located on both sides of the Rockies with a trough extending southward from a centre of low pressure centered in northern Canada. This is typical of the pressure distribution found to exist just before a Chinook period.*

described such a pressure distribution as being typical of a Chinook period. However, in the present investigation it was found that for each of the Chinook periods examined there were two anticyclonic centres—one on each side of the Rockies. Generally, one area of high pressure moved in off the Pacific and the other moved south from the Arctic. At the beginning of the Chinooks the Pacific high was centered over northern Oregon and southern British Columbia, near the International Boundary, while the Arctic high was

* *This is the flat plateau between the Cascades and the Rockies.*

centered just east of the foothills over the Prairies and near the boundary. Fig. 1, which shows the pressure distribution at 1130 hr. M.S.T. on March 17, 1939, illustrates conditions typical of the periods examined. With the anticyclones located in these positions, it was possible for a well defined trough to form between them on the east side of the Rockies—extending southward from the Aleutian low centered in the Bay of Alaska or from a low moving across northern Canada. On other occasions when the high pressure centres were shifted to the west, the trough formed on the windward side of the mountains, and no Chinook was observed. Also, at times the Arctic high moved southward in the neighbourhood of Hudson Bay. This gave a very broad, shallow trough extending across the prairies, with no accompanying Chinook effect, or, at most, with a very mild one. Fig. 2 shows the position

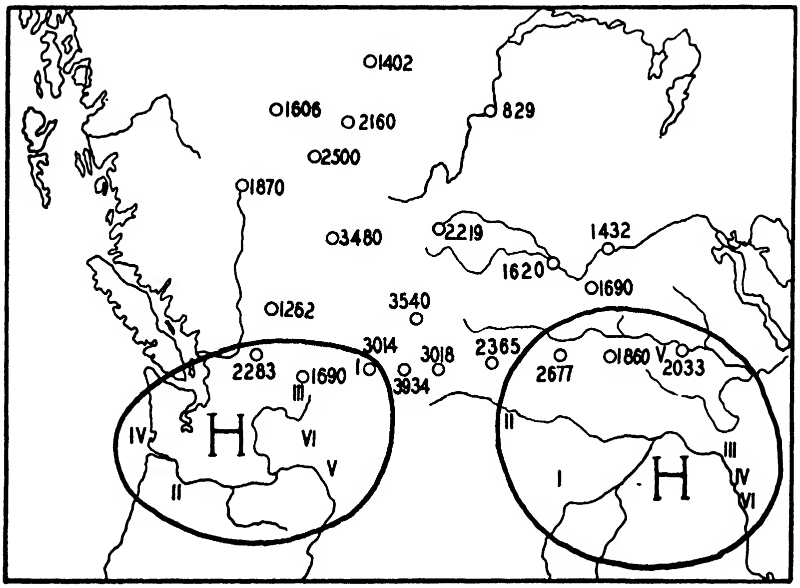

FIG. 2. *Typical locations of the centres of high pressure on both sides of the Rockies preceding a Chinook. The Arabic figures give the elevation of the terrain in feet above sea level. The Roman numerals give the location of pairs of centres of high pressure for six of the Chinook periods studied. The heavy bounding lines mark the general position of the high pressure areas—one on each side of the mountain ridge.*

of the anticyclonic centres for the six Chinook periods briefly summarized in Table I. It might be added that in checking back on pressure maps for periods discussed by previous writers (1, 5) this same distribution was found to exist.

The Line of Temperature Discontinuity Between Air Masses

The circulations about the two pressure centres result in the line of temperature discontinuity that is found to exist along the leeward side of the Rockies preceding a Chinook. The centre to the west brings in Pacific air which, although modified to a certain extent by its trajectory across land, is still moist and comparatively warm. This air mass lies on the windward side of the mountains. On the leeward side, there is the Polar Continental air

TABLE I

Date 1939	Station	Time M.S.T.	Wind From	Wind To	Temperature change	Humidity* change	Sky** condition	Eastern limits of the chinook effect***	Pressure tendency	Pressure distribution	Following weather
Feb. 10	Lethbridge	12 hr.	S5 Vel. increased to 55 m.p.h. by 17 hr.	SW6	18° rise in 2 hours	R.H.—15%	Clr.	Medicine Hat	Rate of decrease accelerated	Centres of high pressure at Cranbrook, B.C., and northeast of Billings, Montana. Both moved southward rapidly	Polar front passed late on the 11th bringing light snow and fog until the middle of Feb. 12
	Calgary	15 hr.	S5	SW10	10° rise in few minutes	Dropped sharply	Clr.		Falling steadily before and after		
Feb. 16	Lethbridge	01 hr.	S16 Vel. increased steadily	SW10	Diurnal decrease checked. At 03 hr. rose 10° in 1 hour	R.H.—20%	Ovc. Ac.	Medicine Hat	Falling steadily before and after	High pressure centres at Portland, Oregon, and Havre, Montana on the 2330 hr. chart of Feb. 15. Western high continued southward; coastal centre did not move until Feb. 17	Polar front moved slowly southward during the 17th and 18th. Snow showers reducing visibility and ceiling until the afternoon of Feb. 21
	Calgary	01 hr.	SW5 Vel. 19 m.p.h. next hr.	W8	9° rise in 1 hour	R.H.—30%	Ovc. Ac.				
Feb. 21	Lethbridge	20 hr.	SE3	SW9	4° rise in 1 hour	R.H.—30% in 2 hours	Hi. sctd.	Medicine Hat	Falling steadily before—steady for 7 hours, then falling again	High pressure centres at Grand Forks, B.C. and north of Bismarck, N.D. The N.D. high moved south rapidly, but a high was maintained west of the Rockies	Polar front followed by light snow and fog which limited visibility and ceiling during Feb. 23 and morning of Feb. 24
	Calgary	23 hr.	NW1	W2	22° rise in 2 hours	R.H.—18%	Hi. sctd.		Falling steadily before and after		
Feb 24	Lethbridge	0830	S17	SW8	5° rise in 1 hour	R.H.—9% w, 0.1 gm.	Hi. sctd.	Medicine Hat	Began to fall before the Chinook and continued until the wind shifted to the northwest at both stations	Anticyclones centred at Bismarck, N.D., and off the mid-Pacific coast	Polar air advanced. Snow reduced ceiling and visibility on Feb. 25
	Calgary	1930	SW4	W11	8° rise in 1 hour	R.H.—25%	Hi. sctd.				
Mar. 10	Lethbridge	02 hr.	NE6	W10	No diurnal decrease	R.H.—10%	Clr.	Medicine Hat	Slow decline until 10 hr. Rapid fall next 6 hours, then steady	Centres of high pressure southeast of Spokane and east of Regina. Spokane centre moved south and Regina centre moved east at about the same time	Occluded system moved in off the Pacific behind the Chinook. Then the Polar front moved south bringing light snow and fog during March 12 and 13
	Calgary	1830	W2	W14	6° rise in 1 hour	R.H.—20%	Clr.		Falling steadily until 19 hr. then steady for 7 hours before falling again		
Mar. 17	Lethbridge	1125	S4	SW7	7° rise in 1 hour	R.H.—15% w, 0.2 gm.	Hi. sctd.	Swift Current	Falling steadily before and after	High centres at Spokane and Bismarck at 1730 hr. on March 17. Bismarck high moved southeast; Spokane high remained until March 24	Warm Chinook continued until March 24, then the Polar air advanced
	Calgary	19 hr.	S6	W21	12° rise in 1 hour	R.H.—15% w, 0 6 gm.	Hi. sctd.		Falling rapidly except for steady period from 19 to 21 hr.		

** The change in moisture content of the air at the station is given in terms of the relative humidity (ratio of actual vapour pressure to the saturation value as a percentage). The values of 'w' when given indicate the grams of water per kilogram of air. **Abbreviations used: clr.—clear; ovc.—overcast; ac.—altocumulus clouds; hi.—high; sctd.—scattered. ***The air mass frequently moves farther east but loses the fundamental Chinook property—dryness.*

brought in by the Arctic high. The P_C air remains but slightly modified, as the terrain over which it has been brought is very similar to that found in its source region during the winter months. As a result, the air mass on the leeward side of the mountains is stable, dry, and cool. Thus, the originally homogeneous air mass is modified in an entirely different way on either side of the mountains—with the ridge of land acting, as it were, like a bulwark separating them.

The establishment of the well defined trough between the anticyclones finally breaks down the imaginary wall separating the two masses. It was observed that, while the trough existed, the Pacific high remained stationary, whereas the Arctic centre moved southeastward. At the same time the Chinook made its appearance.

The Direction from which the Chinook Blows

There seems to be very little regularity in the Chinook winds—except in direction. In the periods examined they were evident at Lethbridge earlier than at Calgary. The wind began as a gentle breeze or as a fresh wind, sometimes attaining velocities of 40 to 50 m.p.h. At Lethbridge, the records show that the Chinook blows from the southwest or west and is strikingly persistent for its duration. The most marked example of this was the period March 18 to 24, 1939, when the wind blew constantly from the southwest or west (with the exception of 10 hr. when it was temporarily halted) with an average velocity of 26.3 m.p.h. At Calgary the Chinook wind comes from the west but is not nearly as steady as at Lethbridge. The velocity is generally somewhat less at Calgary. These consistencies and inconsistencies are related to the topographical locations of these two stations. Lethbridge is situated at the mouth of a valley running in an east-west direction, whereas Calgary is exposed on an open slope. The duration of the Chinook varies from a few hours to a few days, as shown in Table II.

TABLE II

DURATION (IN HOURS) OF CHINOOK WINDS BEGINNING ON THE GIVEN DATES

	February				March		
	10	16	21	24	10	17	19
Duration at Lethbridge	29	61	25	20	36	35	142
Calgary	21	57	3	4	13	21	

It has been mentioned that from March 19 to 24 Lethbridge experienced very consistent westerly winds. Although the temperature, humidity, and pressure curves for Calgary are very similar to those given for Lethbridge for the period March 18 to 24, the winds at Calgary were not nearly as consistent as those at Lethbridge. The winds at Calgary had a velocity generally less

than 10 m.p.h.; they came from all directions but were predominantly westerly. Table III gives the number of miles of wind from the various directions recorded at Calgary from March 20 to 23, inclusive.

TABLE III

MILES OF WIND RECORDED AT CALGARY, MARCH 20 TO 23, 1939

Blowing from	N	E	SE	S	SW	W	NW
Miles of wind	45	3	47	83	114	193	84

Variability of the Chinook

The Chinook wind may begin at any time of the day. Table I shows that, in these few examples, at Lethbridge the first effect of the Chinook was felt at noon, in the evening, at midnight, and in the morning. The same is true for Calgary, but here the first effects are felt generally later than at Lethbridge. Frequently, it was noticed that when Lethbridge was experiencing the Chinook, at Calgary the temperature rose and the humidity declined with a south wind. The changes at Calgary were due to the "side-tracking" of the Chinook air from the vicinity of Lethbridge by the prevailing anticyclonic circulation. When the wind at Calgary veered to the west and the real Chinook began to blow, the changes in temperature and humidity were accentuated.

The temperature change accompanying a Chinook is generally more marked at Calgary than at Lethbridge. When the wind began blowing at night it was observed that at Lethbridge merely the normal diurnal cooling was checked while there was a definite warming at Calgary. When the Chinook makes its initial appearance during the day, there is at Lethbridge an accelerated temperature increase but at Calgary there is a definite jump in the temperature. A good example is that of March 17, 1939, when the Chinook began in the heat of the day at 1125 hr. at Lethbridge, accompanied by a temperature increase of 7° F. within an hour; while at Calgary it began at the beginning of the cooling period—at 1900 hr.—and was marked by a 12° F. rise within the next hour.

Air Mass Changes at Edmonton

Red Deer and Edmonton, which are 80 and 170 miles respectively north of Calgary, seldom experience the true Chinook wind. When the southern stations are under the influence of the drying wind, the northern stations often experience a westerly wind that is warm but moist. This difference in the air properties is probably related to the fact that the mountains recede to the northwest, leaving a wide flat region between them and the northern stations. Also the mountains are considerably lower in the northern section. However, there are times when a west wind at Edmonton is a Chinook, exhibiting the property of relative dryness. These winds are generally of shorter duration than those in the southern part of Alberta. Usually, a Chinook in the southern section is accompanied by an advance of warm

moist air from the Pacific to Edmonton, provided that the Polar front lies to the north of it. It was seldom that upper air data were available for the Alberta region. However, data taken by observers in airplanes were obtained from March 17 to 22, 1939. The graphs in Fig. 3 show that between March 17 and 18 the structure of the air above Edmonton was altered completely. On March 17, there was a surface inversion of 16° C. up to the 0.55 km. level. Above that, the air column was isothermal up to 3.9 km. at least. On March 18, the air was much warmer and the lapse rate in the layer from 0.9 km. up to 3.2 km. was about 2.5° C. per 1000 ft. There was an inversion of 11.5° C. up to the 0.9 km. level. The mixing ratio had increased five- to ninefold and the relative humidity was much higher except for the surface levels. It is quite evident that between 0647 hr. on March 17 and 0648 hr. on March 18, moist Pacific air replaced the cooler and drier Polar air.

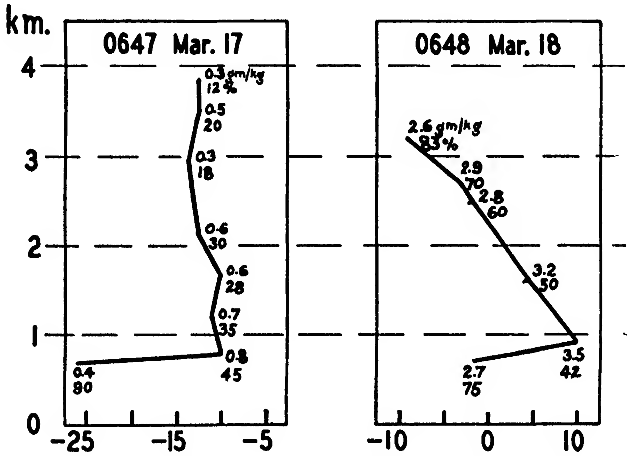

FIG. 3. *Ascent graphs for Edmonton, showing the moisture and temperature variations with height at the same time for two consecutive days, March 17 and 18, 1939. Temperature in degrees centigrade is plotted against height in kilometres. The moisture content at different levels is expressed in two forms—specific humidity (grams of water per kilogram of air) and relative humidity (ratio of actual vapour pressure to the saturation value as a percentage). The graphs show that the air mass over Edmonton was much warmer and more moist on the second day. At the same time a strong Chinook was blowing in southern Alberta.*

Change in Humidity as the Chinook Air Moves Eastward

The passage eastward of the Chinook air is accompanied by a rapid change in its relative humidity. The air has an increased relative humidity at Medicine Hat which is only 100 miles east of Lethbridge. By the time it reaches Regina the air can no longer be said to be dry. In the periods examined it was found that the specific humidity of the surface layer did not change noticeably as the air moved east. Thus the increase in the relative humidity of the lower level may be due to the decrease in temperature resulting from the cooling effect of the surface traversed, rather than to the picking up of moisture. On the other hand, the upper levels of the air mass may have become more moist by the rising of moisture from below. Then the heat of evaporation required to maintain the moisture content at the

surface would account for decreasing temperatures, and, thus, increasing relative humidity. Closely related to this problem is the question whether the Chinook phenomenon is merely a surface effect or one involving a considerable thickness of the atmosphere. If only the surface layer is involved, there would be a temperature inversion in the lower levels. This, in turn, would eliminate the possibility of the rise of moisture to the higher levels On the other hand, if the whole air mass is involved there would be a lapse rate approaching the dry adiabatic—on the assumption that the air has moved down the mountain slope. Such a condition might conceivably favour the rise of moisture. The winds aloft in southern Alberta which were observed to be from the west and of increased intensity during a Chinook, and the complete air mass change at Edmonton as shown by Fig. 3, would seem to favour the second possibility. This can be checked only when additional upper air data are available. A further factor indicative of such a process is the gradual increase of cloudiness from west to east during a Chinook period.

The Appearance of Warm Frontal Characteristics

Under certain circumstances the original Chinook air continues eastward as a warm front at the surface. This was found to be so when cyclonic centres originating in the Aleutian low advanced east along the boundary of the Northwest Territories to Saskatchewan and then southeast to the Great Lakes. A series of cyclonic centres formed and moved across northern Canada during the period March 18 to 24. These systems developed in the trough, which extended in a southeasterly direction from the low centered in the Gulf of Alaska. The first centre to form in the trough was observed on the 0530 hr. chart of March 18, and was located near McMurray (240 miles north of Edmonton), where the pressure was reported to be 29.54 in. at that time. The low advanced southeast from McMurray, reaching Winnipeg by the time of the 2330 hr. chart on the same day. At this point the warm air, which was the original dry Chinook air in the foothills of Alberta, took on distinctive frontal properties. Precipitation was reported at Winnipeg at 1730 hr. on March 18, and preceded the front as it advanced eastward across the Great Lakes and out onto the Atlantic.

The Advance of the Polar Front

From March 20 to 24, four centres of low pressure that followed the McMurray low moved eastward just along the 55th parallel until finally there was a broad band of low pressure extending from the Alaskan low across the northern part of the prairies and along the west shore of Hudson Bay. When the high pressure west of the Rockies began to weaken, the polar front lying in the band of low pressure advanced south, finally passing Lethbridge on March 25.

The termination of a Chinook is generally brought about by a wind shift to a northerly direction, marking the advance of the Polar Continental air. Math (5) spoke of the battle between the Chinook and the P_C air masses.

In the March 18 to 24 period it was noted that the Chinook was temporarily halted on March 19. This coincides with the southeastward movement of the low from near McMurray to Winnipeg. The cyclonic circulation about this centre brought fresh P_C air from the north into the Chinook region. But the plateau high remained in position. Thus, with the development of another high just east of the Rockies, resulting in a new trough formation, the Chinook was restored. Later, on March 24, the band of low pressure advanced southward, bringing in polar air behind it. This time the plateau high dissipated and the Chinook period was brought to a close.

The warm sunny period of the Chinook is followed by unsettled weather, bringing cloudy skies, chilly winds, snow storms, and generally foggy conditions in the foothills. On rare occasions an occluded front moves in from the Pacific with the withdrawal of the western high. The advance of the P_C air is then delayed until the passage of this front.

Conclusion

From the results of this investigation the writer believes that a Chinook may be safely expected in the region from Lethbridge north to Calgary when anticyclonic circulations are established on both sides of the Rockies so as to allow the formation of a trough in the lee of the mountains. Warm, moist air may at the same time be brought across the mountains further north. The distance that this air mass moves east will depend on its own energy and the strength of the cooler air being displaced. The drying property of the Chinook air soon disappears as it moves east. If a cyclonic centre develops in the north and moves southeast, a warm front will develop and move across the Great Lakes region. The Chinook is generally terminated by the advance of polar air following the removal of the high pressure areas.

References

1. BROOKS, C. F. Bull. Am. Met. Soc. 12 : 51-52. 1931.
2. BRUNT, D. Physical and dynamical meteorology. Cambridge University Press, MacMillan Company, Toronto. 1939.
3. EKHART, E. Met. Z. 49 : 452-459. 1932.
4. KRICK, I. P. Gerl. Beitr. Geophys. 39 : 399–407. 1933.
5. MATH, F. A. Monthly Weather Rev. 62 : 54-57. 1934.
6. WARD, D. C. Climates of the United States. Ginn and Company, Boston. 1925.

Canadian Journal of Research

Issued by The National Research Council of Canada

VOL. 19, SEC. A | MAY, 1941 | NUMBER 5

RECOMPRESSION PHENOMENA IN STEAM NOZZLES[1]

PART I[1]

By Charles Alexander Robb[2]

Abstract

The purpose of the investigation was to find when and how recompression occurs in the flow of steam through a nozzle, its causes and effects, how the results can be predicted, and what losses are caused by these phenomena. Four types of recompression were observed: equilibrium, latent, vena contracta, and shock recompression.

It is shown that steam in flowing through a nozzle of varying cross-section responds to the changes of area within certain limits and recompression phenomena may be expected. The Venturi effect has been observed in single nozzles, and in both parts of a composite nozzle.

The behaviour of steam in equilibrium recompression in convergent-divergent nozzles can be predicted by means of an equation from which a value is obtained for the pressure p_r at which overexpansion ends and an increase in pressure begins; the pressure p_r depends on the inlet pressure to the nozzle and on the difference in pressure at inlet and outlet.

The recompression due to the contraction of the section can be controlled and avoided by suitable provision in the design. The compression following a change of state of a flowing fluid can be controlled by adjusting the rate of expansion of the fluid in specified pressure ranges. Novel evidence of latent recompression is found in a break or notch in the pressure expansion curve plotted from search tube observations.

The experiments were carried out at inlet pressures within the range at which turbine-condition curves may cross the saturation line between the superheat and wet regions on the Mollier diagram, and the effects of recompression to be expected under varying load conditions can be interpreted for particular nozzle designs.

Comparative studies of the effect of the nozzle shape on recompression phenomena and the losses resulting therefrom have indicated that the conditions for favourable efficiency require a larger inlet radius at the throat and a length shorter than the lengths commonly found in practice.

I. Introduction

Recompression is the name given to certain secondary effects in steam flowing through a nozzle. Four types of recompression may occur in steam nozzles. The terms equilibrium, latent, vena contracta, and shock recompression, which characterize the respective phenomena, have been adopted. Examples of each of these types are to be found in the tests under review.

In *equilibrium recompression* the steam reaches its lowest pressure in the nozzle for fixed values of inlet and outlet pressure. Equilibrium exists between

[1] *Manuscript received March 12, 1941.*

Condensed from a thesis presented to the School of Engineering, The Johns Hopkins University, in partial fulfilment of the requirements for the degree of Doctor of Engineering, 1937.

[2] *Professor of Mechanical Engineering, University of Alberta, Edmonton, Alta. At present on leave of absence, serving as Power Consultant, Munitions Production Branch, Department of Munitions and Supply, Ottawa, Canada.*

the kinetic energy and the heat energy of the steam. As expansion proceeds in the steam flowing through the nozzle, the pressure falls, and the velocity V increases; the specific volume increases; consequently, the average density d decreases. It is found that the product of d and V at first increases and then decreases. The maximum product dV occurs at the section of the nozzle where the pressure bears a ratio of about 0.58 to the initial pressure. Up to this section, dV increases, and A, the area of cross-section, is made to diminish by making this portion of the nozzle convergent.

Supposing the nozzle to end at this section and the steam to be discharged direct from it into the exhaust chamber, the pressure in the exhaust chamber should be about 0.58 of the initial pressure for saturated steam and 0.54 for superheated steam, i.e., the same as that at the terminal section of the nozzle. Should the pressure in the exhaust chamber be less than this value, the pressure in the terminal section of the nozzle would be the same as before, but expansion of the steam would be completed by lateral spreading after discharge from the nozzle. To secure further expansion in the nozzle to a pressure lower than 0.58 of the initial pressure, the nozzle should be extended beyond the throat section. As the product dV is now diminishing, the area of the section must be increasing, hence the nozzle diverges in the portion beyond the throat, forming a diverging section. This portion is made conical in circular nozzles, the angle of the cone being about 10°. The cone must not diverge so rapidly that there is risk of the steam becoming separated from the sides of the nozzle. At all except the lowest exhaust pressures it is found that after expansion to some minimum pressure p_2, or recompression pressure to be discussed later, the process of reconversion of the kinetic energy to pressure energy takes place and the steam begins to recompress, discharging at approximately the exhaust pressure. When the pressure at exit from a nozzle is greater than the external pressure, the expansion is incomplete, and the nozzle is said to "underexpand" the steam. In this case the exit is too small. When the exit area is too large or the nozzle is lengthened, the steam expands below the pressure p_0 inside the nozzle and then rises to this value again at exit, that is, there is recompression. In this case the steam is said to be overexpanded. Equilibrium recompression is satisfactorily produced in each of the forms of nozzle used in the final series of tests.

Latent recompression follows undercooling or supersaturation. This is dependent upon the change of state of the water drops and the heat of vaporization or latent heat. It is regional and may be expected in the zone between the saturation and the 4% wetness line of the Mollier diagram. The steam is supercooled during expansion from the saturation line on the Mollier diagram down to the Wilson line, and a large number of drops of small size may be expected to form quickly at that point. The heat of vaporization from the condensation of the drops immediately becomes available, and tends to increase the temperature of the mixture of steam and drops, to decrease the density of the mass, and to speed up the velocity and hence the flow.

Vena contracta recompression occurs as the steam recovers from the effect of too quick a change of area at the throat or too small a radius in the converging portion of the nozzle. This effect gives the vena contracta at the throat of the nozzle and results in the jet leaving the wall in much the same way as a jet of water is reduced in cross-section as it leaves a sharp-edged orifice. As the recovery or recompression takes place, the jet refills the nozzle section. The effect may be expected in a nozzle having a very rapid reduction of area in the converging portion, or a short approach curve. There is an increase of pressure when the jet hits the wall after the vena contracta.

Shock recompression follows a sudden overexpansion due to shock or other disturbance to the flow. Such a disturbance may be caused by a slight roughness in the surface of the nozzle.

Certain of the above types of recompression may occur simultaneously, as, for example, latent recompression and vena contracta recompression.

In order to provide reliable information on recompression effects when using steam nozzles, it was decided to carry out a thorough experimental investigation in order to determine *(a)* when and how recompression occurs in the flow of steam through a nozzle, *(b)* its causes and effects, *(c)* whether and to what extent recompression can be predicted, and *(d)* what losses occur through recompression. The work was performed in 1931–32 at The Johns Hopkins University.

II. Description of Test Apparatus

(a) General Arrangement of Apparatus

Figs. 1, 2, and 3 show the main features of the apparatus. Fig. 1 shows the general arrangement of the apparatus; Fig. 2, the details of the search tube; Fig. 3, the details of the first nozzle form. Steam from the boiler was passed through the superheater S_1 (Fig. 1). This superheater was constructed of steel pipe, flanged and fitted with a spiral bronze coil. The core of the coil was sealed by means of a smaller pipe, plugged at the ends. High pressure steam entered the spiral coil through the valve V_3 and the condensate was discharged to the sewer through the trap T. This coil served to dry and superheat the steam supplied to the nozzle. The pressure of the steam supply to the nozzle was reduced by the main valve V_1 or by the by-pass valve V_2, or by both.

Steam at about 60 lb. per sq. in. absolute and 330° F. (30 degrees of superheat) was made to pass to the receiver R and the nozzle N, the pressure and temperature of the steam being observed by means of the supply gauge G_1 and the thermometer t_1. This arrangement of valves and superheater gave satisfactory pressure and temperature control of the initial conditions at the nozzle. Most of the steam supply to the nozzle was admitted through the main valve V_1, and the final adjustment of pressure was made by means of the small ($\frac{1}{2}$ in.) by-pass valve V_2.

The spiral path of the steam supply to the nozzle insured good contact with the superheater coil, and the temperature variation during an individual test was small. The receiver R was provided with a drip V_4 to clear the system of water during the warming up period.

The nozzle N was clamped between the flange of the receiver, which consisted of an extra heavy 2 in. tee, and the flange of the exhaust chamber H, which was also a 2 in. tee, by means of the studs Q, Fig. 2. The thimble T_3 was used as a distance piece since the over-all length of the nozzle assembly varied. Retaining grooves for the packing were cut in the ends of the thimble.

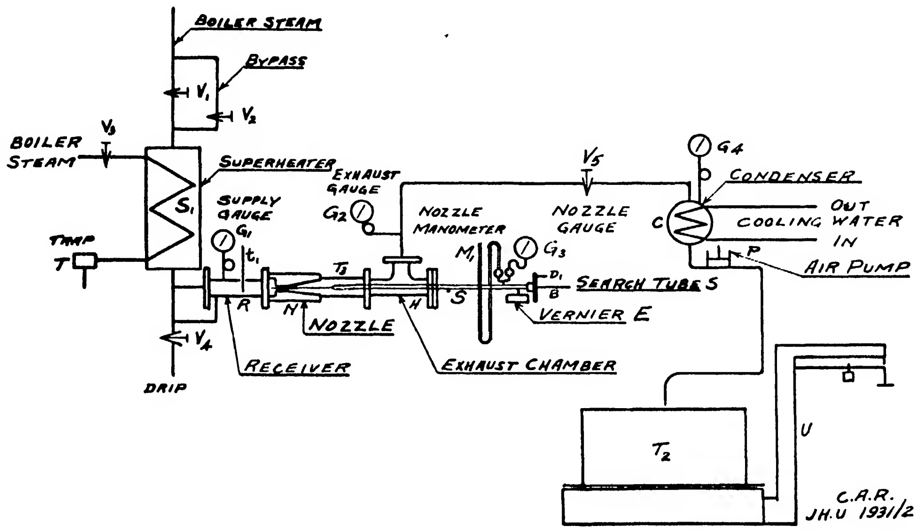

FIG. 1. *Arrangement of apparatus for the study of recompression of steam.*

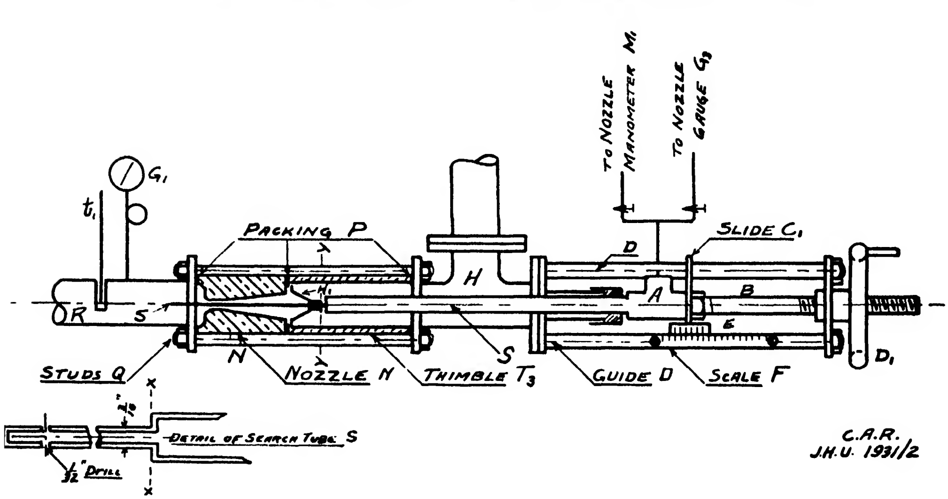

FIG. 2. *Construction of search tube.*

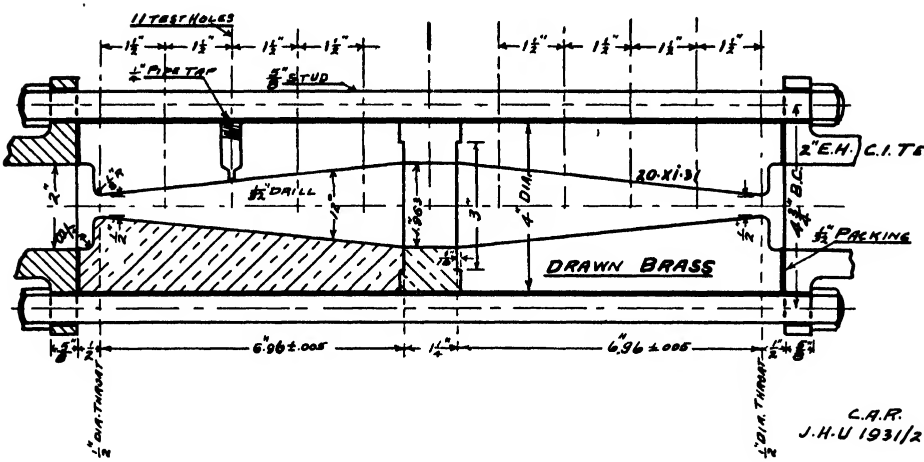

FIG. 3. *Convergent-divergent nozzle No. 1.*

(*b*) *Measurement of Pressures*

The *search tube S*, Fig. 2, consisted of a steel tube about $\frac{3}{16}$ in. outside diameter with a copper tube inside the steel tube. The copper tube had a bore of about $\frac{1}{32}$ in. A hole, $\frac{1}{32}$ in. diameter, was drilled diametrically in the tube. The outer end of the tube was sealed. This tube was brazed to the end of a $\frac{1}{2}$ in. o.d. brass pipe that served as a guide for the tube and as a means of transmitting the steam gauge pressure through the tee A to the nozzle manometer or to the nozzle gauge. The tee A was screwed on a solid threaded steel rod B, and a motion of translation was given to the search tube S by means of the handwheel D_1, the slide C_1, and the guides DD. The slide C_1 carried the Vernier E and this, in combination with the scale F, determined the position of the exploring hole in the search tube relative to the nozzle. The search tube S was supported concentrically at the nozzle by the spider H_1, which was fastened by means of screws to the nozzle. This arrangement provided a metal-to-metal contact between the spider H_1 and nozzle N as follows,—the plane of contact XX of the search tube S and the brass pipe was made to coincide with the plane YY of the spider H_1 (Fig. 2) and served as a datum from which the relative locations of the exploring hole, the outlet face of the nozzle, and the scale reading could be measured.

The pressure in the exhaust chamber H was controlled by means of the valve V_5, Fig. 1, and the pressure was observed by means of the exhaust gauge G_2. The steam from this chamber passed to the condenser C, Fig. 1, and the condensate was led to the tank T_2 on the platform scale U. When the exhaust chamber was to have subatmospheric pressures, the air pump P was used and gauge G_4 recorded the pressure in the condenser. The test instruments generally shown in Fig. 1 consisted of a barometer of the mercurial observatory type equipped with adjustment and thermometer, and pressure gauges G_1, G_2, G_3, and G_4 of the Bourdon single spring type. These were calibrated periodically during the whole program and immediately following

the final series of tests by means of a dead weight type of gauge tester. The manometer M_1 was used to record the lower pressures of the search tube. The condensation of vapour and heating of the mercury in the exposed leg of the manometer made it necessary to observe the initial and final difference of head at each new pressure reading and to apply corrections.

(c) Nozzles

Sketches of all the nozzles tested are shown in Figs. 4 to 13. All nozzles were circular in cross-section. The *nozzle forms* shown in Figs. 10 to 13, being those used in the final series of tests, were all cut from a single block of metal, and in such a way that the diverging part and the diameter of the throat remained unchanged for the set of nozzles Nos. 8 to 11 and similarly for the set Nos. 12 to 15. The radius of the approach was $\frac{1}{4}$ in. for nozzles Nos. 8, 12, and 11, 15, Figs. 10 and 13, and $\frac{1}{2}$ in. for nozzles Nos. 9, 13, and 10, 14, Figs. 11 and 12. The diameter of the throat was $\frac{1}{2}$ in. throughout and the length of throat was $\frac{3}{4}$ in. in nozzles Nos. 8 and 12, $\frac{1}{2}$ in. in nozzles Nos. 9 and 13, and nil in nozzles Nos. 10, 14, and 11, 15. The diverging portion was the same throughout each set of nozzles, i.e., Nos. 8 to 11 and Nos. 12 to 15, and was conical in form. The total angle of the cone was 6 degrees, each diverging side making an angle of 3 degrees with the axis. The length of the diverging part was 2.83 in., Fig. 10.

(d) Method of Operation

The superheating arrangements proved to be adequate. The warming up was quick and the inlet temperature, during a test, was nearly constant. The by-pass valve V_2 provided a sensitive adjustment for the inlet pressure to the nozzle. This arrangement made it easy to hold the inlet pressure at a constant value within the capacity of the Schaeffer and Budenberg single spring Bourdon gauge to indicate variations.

The steam supply pipe was insulated by means of asbestos covering, and, after the initial warming up period, a short time interval was sufficient for conditions to become steady.

The Vernier on the search tube was graduated to read in hundredths of an inch. The search tube was checked against a metallic stop after each test, as described above. This stop served as a reference point to the throat of each nozzle. The range of the search tube was $5\frac{1}{2}$ in., extending from the inlet to about $1\frac{1}{2}$ in. clear of the nozzle outlet. A constant inlet pressure of 59.2 psi abs., or about $44\frac{1}{2}$ psi (gauge) was chosen. The temperature range was from 300 to 315° F. in the series or about 30° F. above saturation temperature. The temperature variation during a test amounted to 1 to $2\frac{1}{2}$° F. from the average. Back pressures of 4, 14, 24, 34, 39, and 43 psi gauge, and a vacuum of 25 in. of mercury were adopted for the search tube experiments. A series of seven tests was carried out on each nozzle at constant inlet pressure and supplementary tests at an inlet pressure of 30 psi gauge and a back pressure of 14 psi, also at an inlet pressure of 15 psi gauge and 5 psi gauge back pressure.

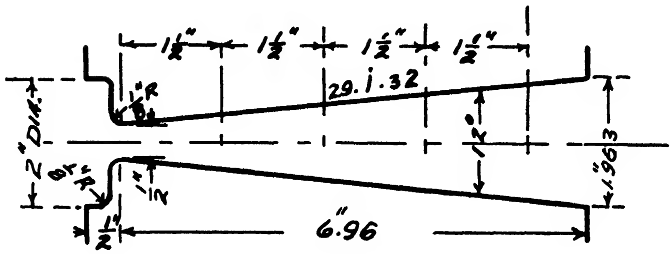

FIG 4 NO. 2

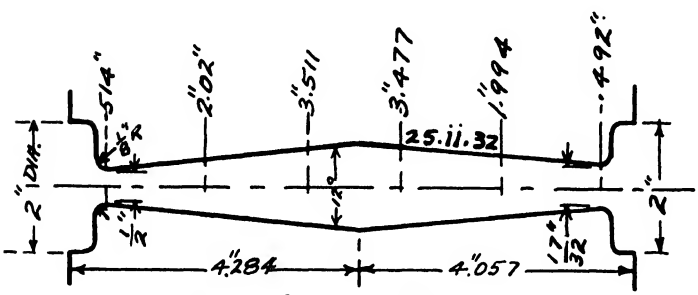

FIG. 5 NO. 3

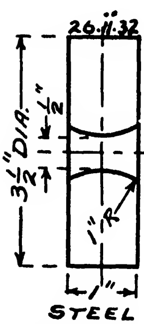

FIG. 6 NO. 4

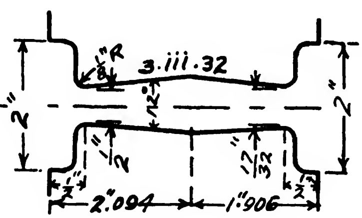

FIG. 7 NO. 5

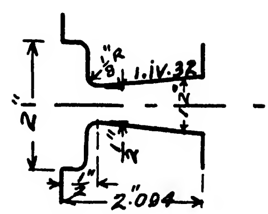

FIG. 8 NO. 6

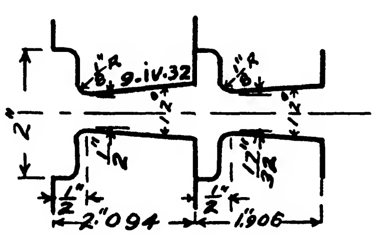

FIG. 9 NO. 7

C.A.R.
J.H.U. 1931/2.

FIGS. 4 – 9. *Nozzle forms. Axial cross-sections of nozzles No. 2 to No. 7, for the study of the flow of steam.*

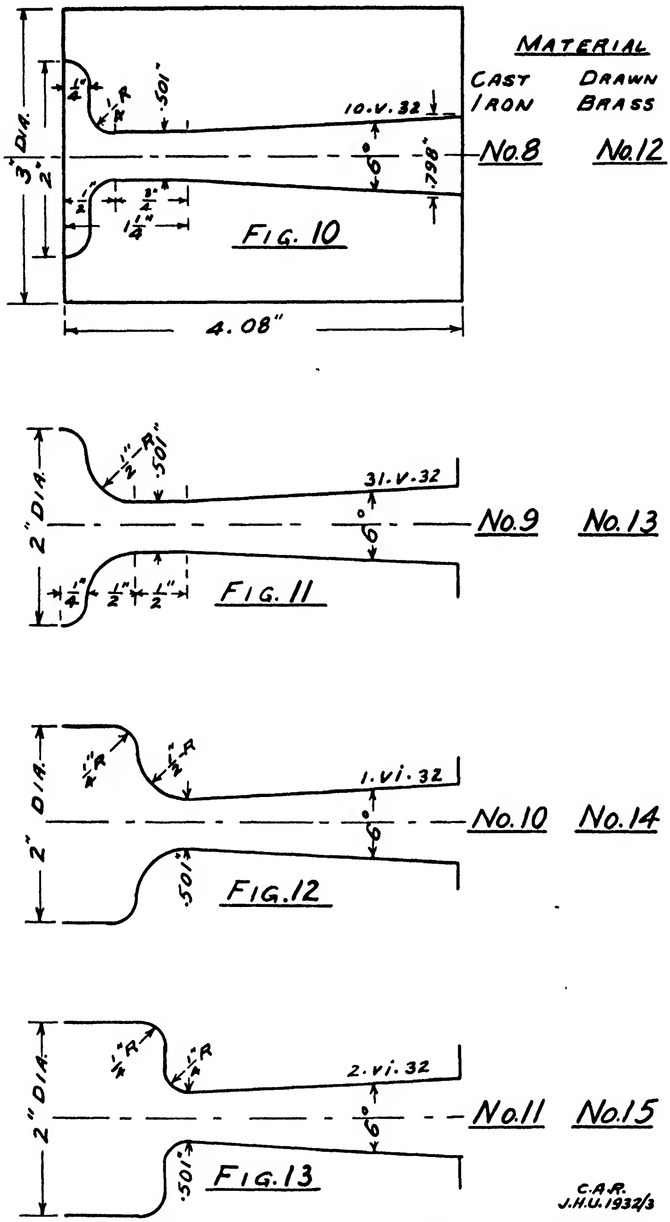

FIGS. 10 – 13. *Nozzle forms No. 8 to No. 15 designed for the final series of tests.*

Pressure readings to the nearest 0.25 psi gauge or 0.1 in. of mercury (manometer) were taken at intervals of from 0.01 to 0.25 in. along the axis of the nozzle, the distance depending upon the importance of the region. The manometer was used for the low inlet and back pressures and for vacua. In changing from one instrument to the other, simultaneous readings were taken, thus providing a continuous check on the gauge.

The maladjustment of the mercury manometer due to thermal changes, condensation, and other influences was compensated at the beginning of each set of readings. At any indication of a break in the continuity of the observations, suggesting lack of stability in the static pressure, the search tube was backed up and the previous readings were checked.

The time, to the nearest second, at which the beam of the weight scale lifted clear was noted at the beginning and end of the test, and the net weight of the condensate was observed. An intermediate reading of time and weight was taken at about half-time, or a separate test was carried out. The duration of the test was governed by the capacity of the measuring tank at maximum flow. The duration of the other tests approximately correspond. Following the experiments, all gauges were checked by means of a dead weight gauge tester and the necessary corrections were made. The observed pressures, as ordinates, were plotted against the distance along the axis of the nozzle, as abscissae, after each test and before the remodelling of the nozzle for the next series.

At all points where a break, notch, or irregularity in the pressure expansion or recompression occurred, the pressure readings were observed a second time, confirmed for the doubtful interval, and so recorded. This notch, the author's observation of which was reported by Professor Christie (2), was the subject of very careful consideration throughout the whole investigation. Roughness of the surface of the nozzle was suspected as a possible cause for certain irregularities in the pressure readings, but it was found to persist even when the surface of the drawn brass nozzles was proved to be smooth.

In these nozzle experiments, a notch in the pressure-drop curve has been present in many of the pressure expansion and recompression curves. The inclination at first was to consider the notch as due to an error in observation, to a break in the continuity due to a surface irregularity, or to a lack of stability in the state of the steam. Even after what was expected to be the final series of tests had been carried out with cast-iron nozzles, the nozzle was cut in halves along the axis for inspection, and when it was found to have been pitted, the notch was the factor that led to a decision to repeat the whole series of tests with a new set of polished drawn brass nozzles.

Inspection of the cast-iron nozzle showed a faulty casting, and the pits and roughness were due to the combined effects of blow holes, oxidation, and erosion by the steam. None of these troubles developed with the drawn brass nozzles. The smoother surface of the drawn brass nozzles had the effect of permitting a greater overexpansion and of delaying equilibrium recompression. The effect was noted in the case of expansion curves for the outlet pressures 24 and 34 in Fig. 24 for nozzle No. 11. At a scale reading of 4.5 to 5 in. the two curves merged. The curves in Fig. 25 show the persistence of the notch in the curves obtained with the brass nozzles. The total weight of condensate observed in the tests of these nozzles amounted to 50 to 150 lb., according to the pressure drop. The duration of the test was from 364 to 1407 sec., and the rate of flow ranged from 0.0942 to 0.1496 lb. per sec.

III. Experimental Data

(a) Tests with Composite Nozzles

A question arose whether a specified recompression effect could be secured in certain apparatus. The question was:—"Following expansion of steam in a nozzle of conventional form (as in steam turbines), is an additional nozzle necessary to carry out a process of recompression, or would the addition, as the reverse of a Venturi meter, make the whole assembly constitute a simple chamber with no particular characteristics? Is it like adding two equal quantities, one negative and one positive?"

In order to study this question, it was decided to adopt the design of converging-diverging nozzle shown in Fig. 3, to provide two nozzles, and to insert a short cylindrical or parallel section between them. Test holes were drilled and tapped to receive gauges at the ½ in. throat of each nozzle and at the centre as noted. These, with the pressures at the inlet and discharge chambers, gave five static pressure values along the axis. A series of observations was taken at inlet or supply pressures of 45, 30, 15 psi gauge and at various discharge pressures. For the 45 psi series the discharge pressures were 4, 14, 24, 34, 39, and 44 psi gauge. The pressure observations showed the effect on the static pressure of the variable cross-section. The pressure dropped at the first throat, increased as the cross-section increased, dropped again at the second throat and continued to expand to the receiver pressure. The limit of the pressure drop at the second throat was reached at a pressure in the outlet receiver of about 14 psi. Similar effects were found at the lower inlet pressures of 30 and 15 psi gauge.

The observations indicated that this combination of nozzles would serve to show the characteristics of a channel of varying cross-section; cocks were installed at points along the nozzle, and connected by a pipe manifold to a gauge and manometer. Pressure-flow tests were made with various inlet pressures (100, 45, 30, or 15 psi) and different discharge pressures. Evidence of a limiting critical pressure was found at the throats. In the case of the lower back pressure there was a striking disposition for the recompression pressure to reach a similar limiting value at a point 1½ in. from the throats. The variation in pressure in the major central section was small.

(b) Tests with Single Nozzles

To investigate the behaviour of a single nozzle, the nozzle, which we shall call the recompression nozzle, at the right of Fig. 3, and the cylindrical distance

TABLE I

PRESSURE SCHEDULE, PSI GAUGE, FOR NOZZLE No. 2

Inlet	Discharge
45	37, 18, 5; vac., 10 in. of mercury
30	24, 10, 5; vac., 14 in. of mercury
15	11.5, 1.5, 0; vac., 24 in. of mercury

piece were replaced by a short section of 2 in. E. H. steel pipe, the ends of which were grooved to retain the packing.

The schedule of the pressure-flow tests is given in Table I. Similar schedules were followed with all the nozzles.

FIG. 14. *Recompression in the single nozzle No. 2.*

The pressure observations from the 45 lb. inlet pressure series are plotted in Fig. 14. All the curves except the curve for the highest back pressure show expansion at the throat to 7 to 7.5 psi gauge (21.6 to 22.1 abs.). The recompression is definite and regular. The single nozzle is providing recompression. This series of tests showed that the throat pressure p_t can be rendered unstable by a small change in the outlet or back pressure, as, for example, 37 psi gauge (51.6 abs.) when p_t is above the critical. It was observed that an increase of 1 psi in the back pressure raised the pressure at the throat by 4.5 psi.

Since the expansion is generally completed at from 1 in. to 2 in. from the throat, it would appear that the angle of divergence of the nozzle is excessive for the conditions under review.

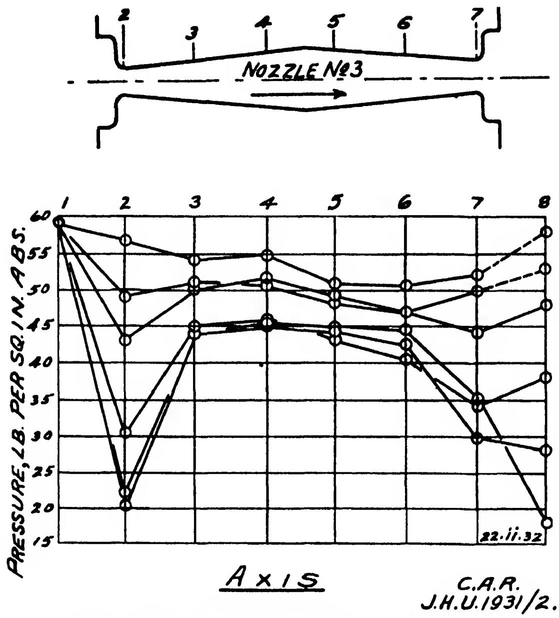

FIG. 15. *Effect of nozzle length on recompression. Inlet pressure 45, discharge pressure 44, 39, 34, 24, 14, 4 psi gauge.*

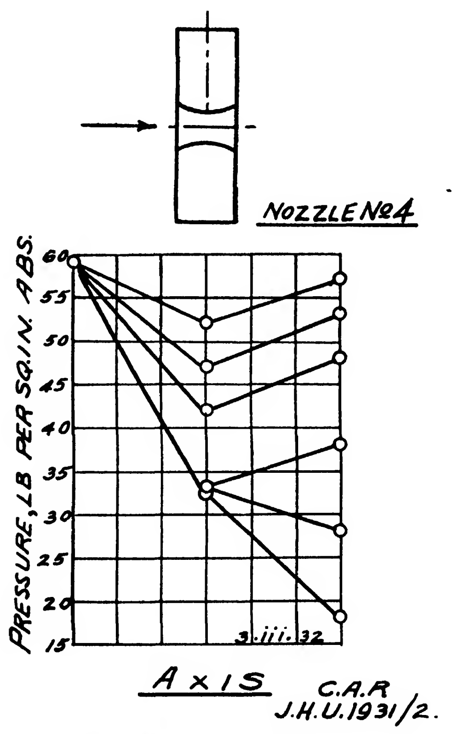

FIG. 16. *The Venturi effect in nozzle No. 4. Inlet and outlet pressures as in Fig. 15.*

In order to compensate for the losses in the nozzles, the throat of the recompression nozzle, shown at the right in Fig. 3, was opened out approximately 20% to $\frac{17}{32}$ in. diameter. The length of the nozzles was reduced, the distance piece or ring was omitted, and the nozzles reassembled as nozzle No. 3, shown in Fig. 5.

The pressure observations for the 45 lb. series are plotted, as ordinates, against the distance along the axis, as abscissae, in Fig. 15.

The need for the search tube, to permit pressure observations throughout the length of the nozzle assembly, became apparent at this stage. The construction of the search tube is shown in Fig. 2.

In order to study the behaviour of a single nozzle having easy converging and diverging sections, nozzle No. 4, shown in Fig. 6, was constructed of steel and erected with a distance piece consisting of 2 in. pipe.

The static pressure was read at the inlet, throat, and outlet only. The results are plotted in Fig. 16, which shows the effect of critical pressure.

The characteristics of nozzles No. 1, 2, 3, and 4 and the effect of nozzle form in producing recompression at various back pressures are shown in Fig. 17. The ordinates represent flow in pounds per second and the abscissae represent recompression pressures expressed in percentage of the inlet pressure $= \frac{p_0}{p_1} \times 100$.

It may be noted that the form of nozzle No. 2 is well adapted to a wide range of recompression with a minimum variation of the flow, as compared with nozzles No. 1, 3, and 4. Curve No. 2, Fig. 17, shows a recompression range of from 17 to 87%, the flow ranging from 0.172 to 0.167 lb. per sec.

The tests on nozzle No. 3, shown in Fig. 15, indicate that both the expansion and recompression nozzles are still longer than necessary for the pressure ranges under consideration, and the length was reduced to approximately 4 in. from throat to throat.

Nozzle No. 5, as remodelled, is shown in Fig. 7. Pressure-flow tests with the search tube were carried out at inlet pressures of 45 and 30 psi and a series of outlet pressures.

The pressures for the 45 psi inlet and 4 psi outlet condition are plotted in Fig. 18.

TABLE II

Pressure schedule, psi gauge, for nozzles Nos. 6 to 15

Inlet	Discharge
45	43, 39, 34, 24, 14, 4; vac., 7¾ in. of mercury
30	28, 25, 20, 14, 10, 5; vac., 12¾ in. of mercury
15	13, 10, 5; vac., 16 in. of mercury

These tests demonstrate that the process of overexpansion and recompression can be carried out on one nozzle only, and a series of tests was carried out on nozzle No. 6, a single converging-diverging nozzle.

The schedule of conditions is shown in Table II.

The pressures for the 45 psi gauge inlet and various discharge pressures are plotted in Fig. 19.

The two portions of nozzle No. 5 were placed in series, shown as nozzle No. 7 in Fig. 9 and the pressure-expansion curve, Fig. 20, indicates a repeated Venturi effect. The schedule of tests for this nozzle No. 7 and nozzles Nos. 8

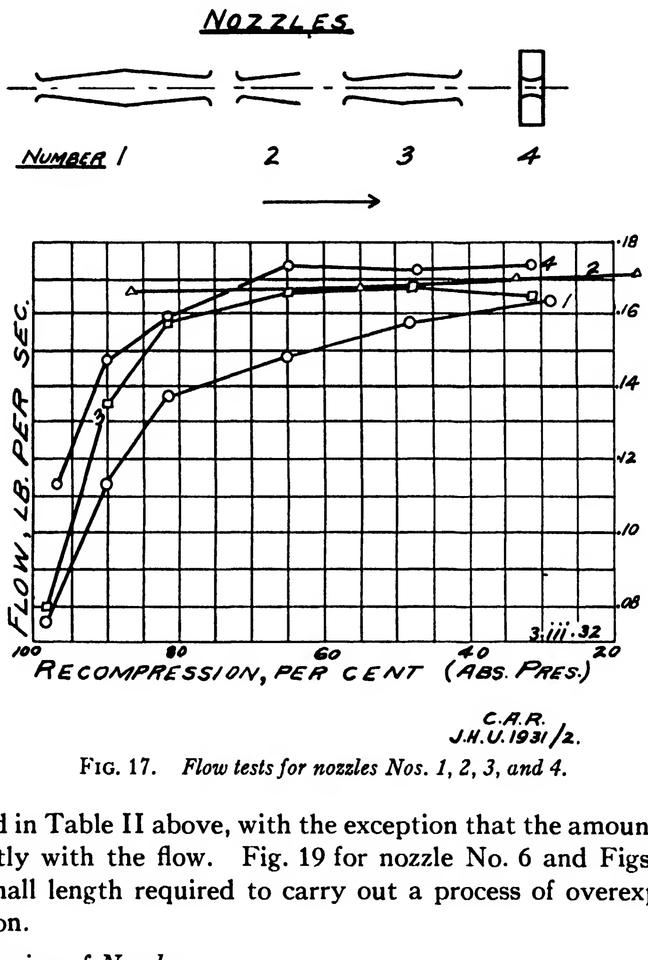

FIG. 17. *Flow tests for nozzles Nos. 1, 2, 3, and 4.*

to 15 is listed in Table II above, with the exception that the amount of vacuum varied slightly with the flow. Fig. 19 for nozzle No. 6 and Figs. 18 and 20 show the small length required to carry out a process of overexpansion and recompression.

(c) Final Design of Nozzles

An examination of the performance of the above nozzle forms was carried out with a view to the design of a final series of nozzles in which expansion and recompression processes could be controlled. For this purpose the nozzle is considered to consist of three parts, the converging, throat, and diverging portions, the form and functions of which will be considered separately.

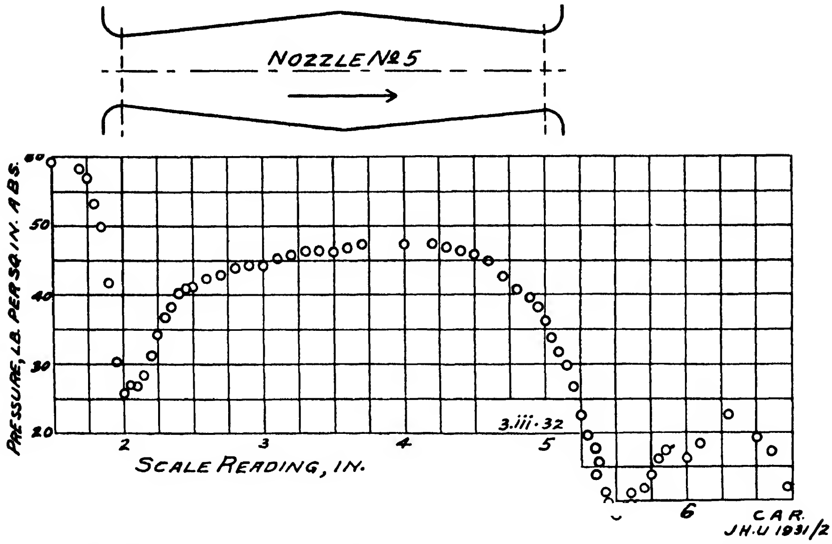

FIG. 18. *Recompression in composite nozzle of reduced length (No. 5). Inlet pressure 45, discharge pressure 4 psi gauge.*

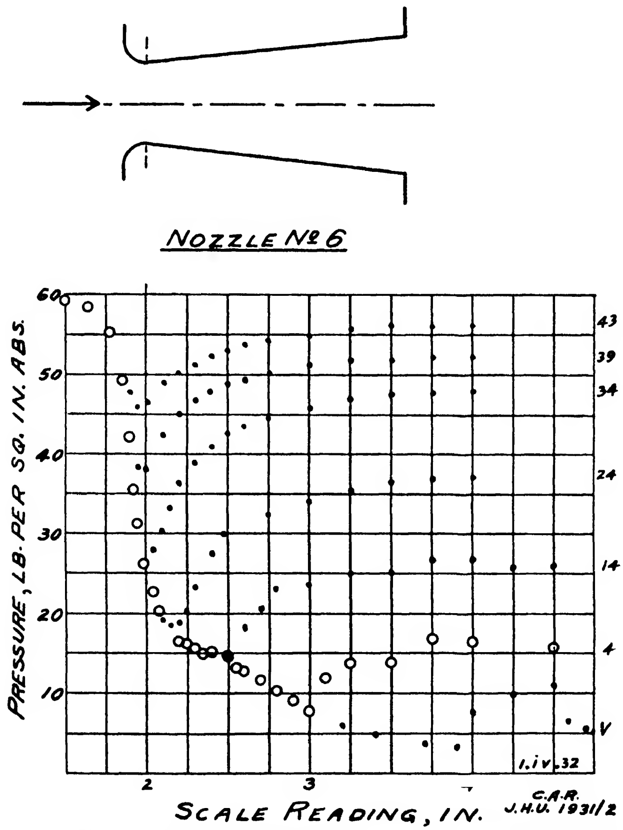

FIG. 19. *Recompression in single converging-diverging nozzle (No. 6). Discharge conditions are indicated in Table II.*

In the nozzles described above, preliminary expansion is rapid and the small inlet radius of $\frac{1}{8}$ in. rendered observation of a sufficient number of pressure values difficult. Radii of $\frac{1}{4}$ in. and $\frac{1}{2}$ in. were adopted, the smaller offering a satisfactory minimum and the larger radius serving to avoid the sharp edge or vena contracta effect, and to reduce the rate of expansion of the steam.

Further control of the rate of expansion and convenience of observation is obtained by the introduction of a parallel or extended throat section. This section provides a convenient location for suitable devices in case it is desired to separate the drops that form in the steam as it condenses.

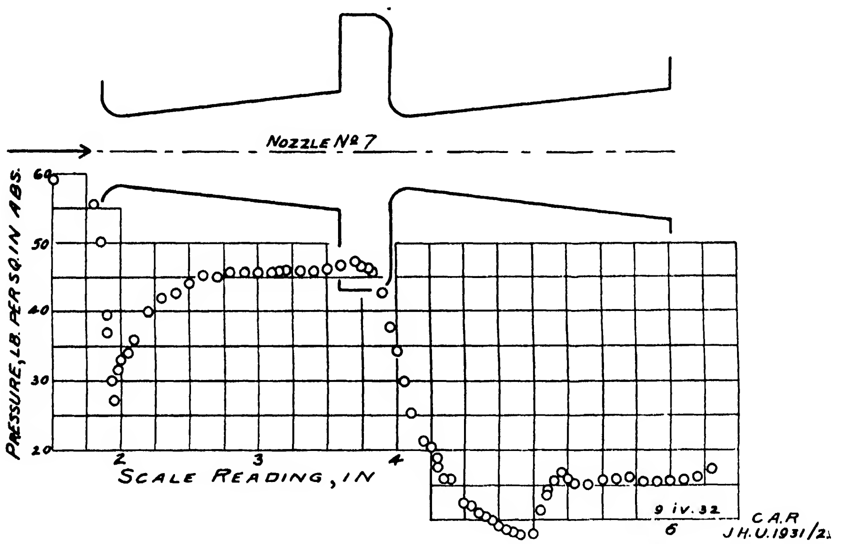

FIG. 20. *Pressure conditions in channel formed of the two portions of No. 5 in series (Nozzle No. 7).*

In order to obtain a more gradual recompression, the angle of the cone of revolution of the diverging section was reduced from a total angle of 12 degrees in the earlier designs to 6 degrees.

The cutting of the nozzles Nos. 8 to 11, constructed of cast iron, and of Nos. 12 to 15, of drawn brass, from a single piece of material, was executed in such a way that the original diverging section was retained in each of the succeeding models. The nozzle forms Nos. 8 to 15 are shown in Figs. 10 to 13 and specimen curves for each nozzle are shown in Figs 21 to 28. Nozzle No. 9 superseded No. 8 in order to remove the vena contracta effect noted at the point A in Fig. 21 due to the combination of the small entrance radius and to the parallel section. The notch in the expansion curve, an example of latent recompression, which is shown at B in Fig. 21, and which appears in each of the subsequent expansion curves, Figs. 22 to 24, occurs in the region of the Wilson line on the Mollier diagram, as indicated by the constant pressure line p_2 in Fig. 32. The parallel section or extended throat is omitted in

nozzles Nos. 10 and 11. The reduction in the rate of expansion at entrance, due to the larger (½ in.) radius and the parallel or extended throat, can be seen in Fig. 22 as compared with the smaller (¼ in.) radius and more rapid expansion shown in Fig. 24. The cast-iron nozzles, Nos. 8 to 11, were found to have an unsatisfactory internal surface when split and inspected after

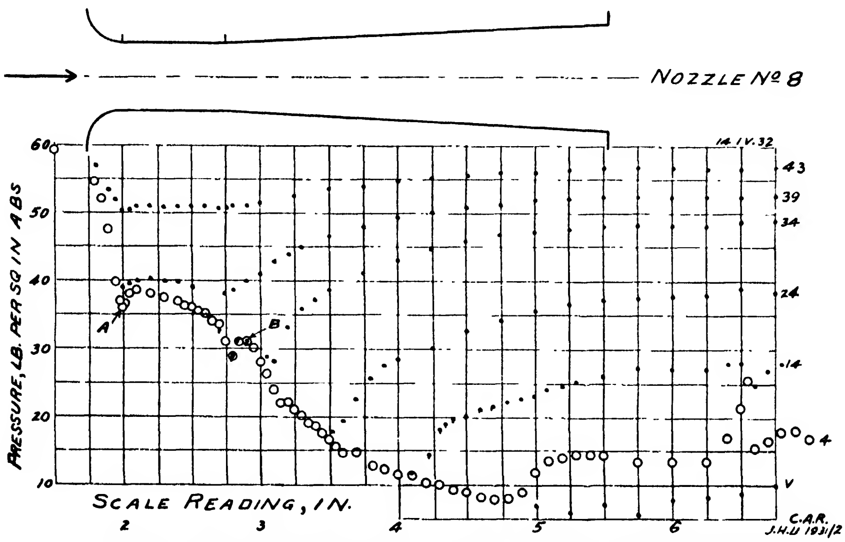

FIG. 21. *Vena contracta recompression at A in the single convergent-divergent cast-iron nozzle No. 8.*

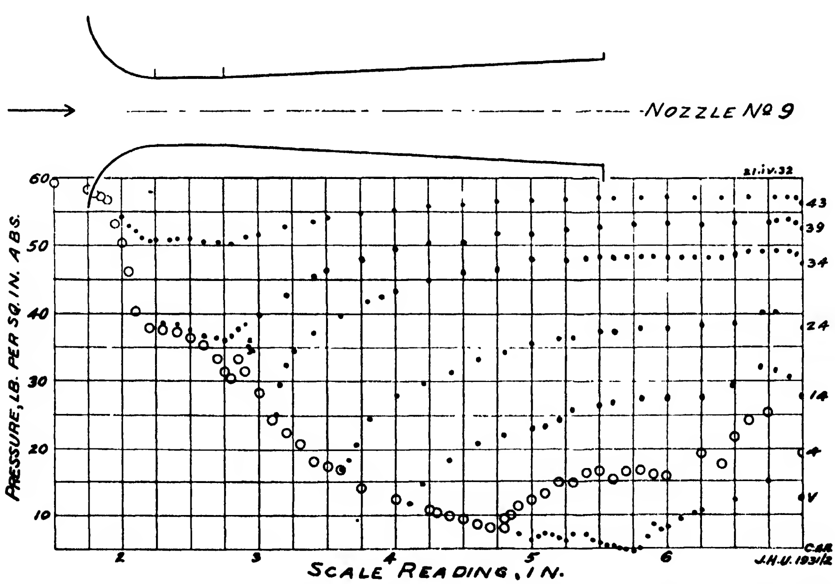

FIG. 22. *Equilibrium recompression in cast-iron nozzle No. 9 with increased inlet radius.*

the tests, and were superseded by drawn brass nozzles, Nos. 12 to 15, of the same design. Pressure expansion curves for nozzles Nos. 12 to 15 are shown in Figs. 25 to 28 respectively.

The effect of harmonic vibrations on the pressure expansion curves is shown in Fig. 19, Curve *V*, for nozzle No. 6, in Fig. 21, Curve 4, for nozzle No. 8, and in subsequent pressure expansion curves.

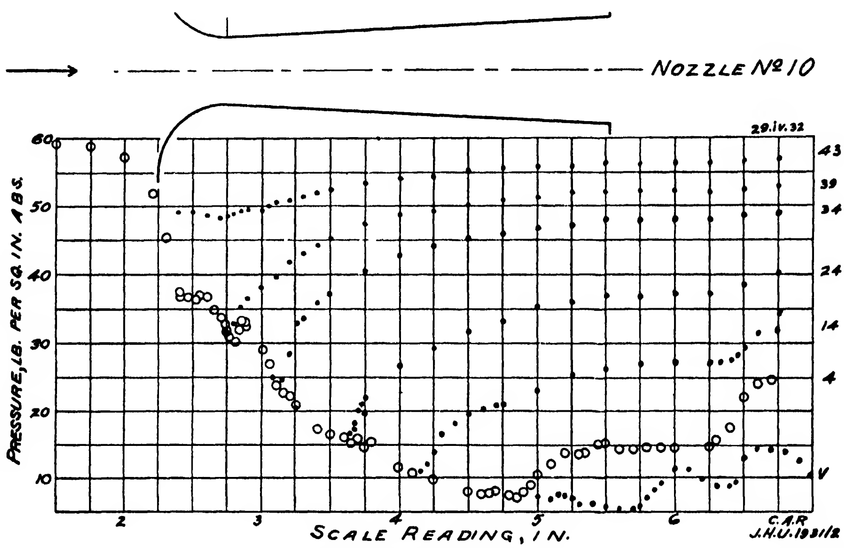

FIG. 23. *Example of shock recompression in the flow of steam for discharge pressures 14, 4, and V.*

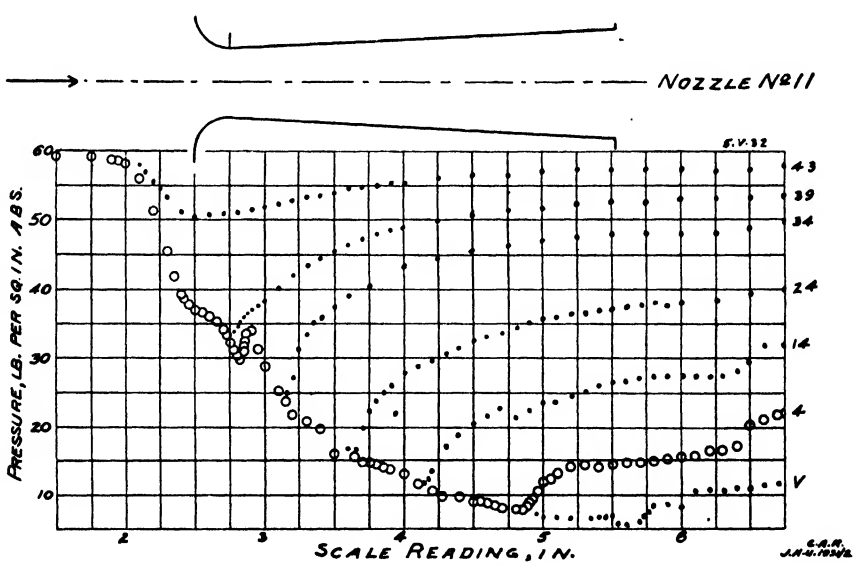

FIG. 24. *Latent recompression in cast-iron nozzle No. 11.*

The question formulated at the beginning of the section can be considered as answered, at least in part, by the tests on nozzle No. 1; i.e., the addition of the reverse of a Venturi meter does not make the assembly constitute a simple chamber with no particular characteristics. The pressure expansion curves show that the steam expands and recompresses in such a way as to indicate a direct relation, within certain limits, between the expansion and the cross-sectional area of the nozzle. The limits are fairly defined by Figs. 15 and 18 in which the lengths of the composite nozzles Nos. 3 and 5 are reduced as compared with nozzle No. 1.

(Part II will appear in the June issue.)

Canadian Journal of Research

Issued by THE NATIONAL RESEARCH COUNCIL OF CANADA

VOL. 19, SEC. A. JUNE, 1941 NUMBER 6

RECOMPRESSION PHENOMENA IN STEAM NOZZLES

PART II[1]

BY CHARLES ALEXANDER ROBB

IV. Discussion of Experimental Data

(a) Types of Recompression in the Final Series of Tests

The objective at this point in the program was to find what laws, if any, govern recompression. Mellanby and Kerr, in their paper on pressure flow in steam nozzles (7, p. 125), say of recompression, "It would appear that a recompression may be either of wave form or continuous; and such alternatives, taken in conjunction with the almost invariable pressure fluctuations that exist might seem to indicate that a recompression follows no laws but those of chance."

Inspection of the expansion curves for nozzle No. 8 (Fig. 21) shows a dip marked *A* at scale reading 2 in. due to the vena contracta effect, and the recovery or contracta recompression amounts to $2\frac{1}{2}$ psi. The vena contracta appears in some degree at each of the back pressures including the 43 psi gauge. It was proposed to eliminate the dip *A* by adjusting the inlet radius of the nozzle to reduce the necking down of the jet. The results are shown for nozzle No. 9 in Fig. 22 and for nozzle No. 10 in Fig. 23 in which the dip has almost entirely disappeared.

With the same nozzle, No. 8, an additional break or notch is noted at *B* in Fig. 21 at scale reading 2.8 in. This notch appears in the region where supersaturation, as described by Stodola (11), Goudie (3), Powell (9), and others (1, 10, 12-14), may be expected. Considering the process to be isentropic, the notch occurs in the wet region of the Mollier diagram, below the saturation line and in the region of the Wilson line or zone. The observation of this notch and consideration of the latent recompression that characterizes the pressure disturbance was at the time of these experiments (1931–2) a novel contribution of this investigation, and further reference will be made to this interesting phenomenon.

When the notch was first noted, the author was disposed to attribute it to a roughness in the surface of the nozzle. The persistence of the notch in the same region in various nozzles that were known to be free from rough spots, and at various inlet pressures, made it necessary to look elsewhere for the cause. Later experiments, by other investigators (1, 10, 12–14) using a modified technique, have proved the notch of the author's pressure expansion

[1] *Part I appeared in the May issue.*

curves to be due to change of state of the steam. The latent heat, being suddenly released as the supersaturated steam condenses, becomes available to accelerate the stream or jet. The formation of the drops tends to obstruct the flow since the drops will tend to lag behind the stream, and, failing accelera-

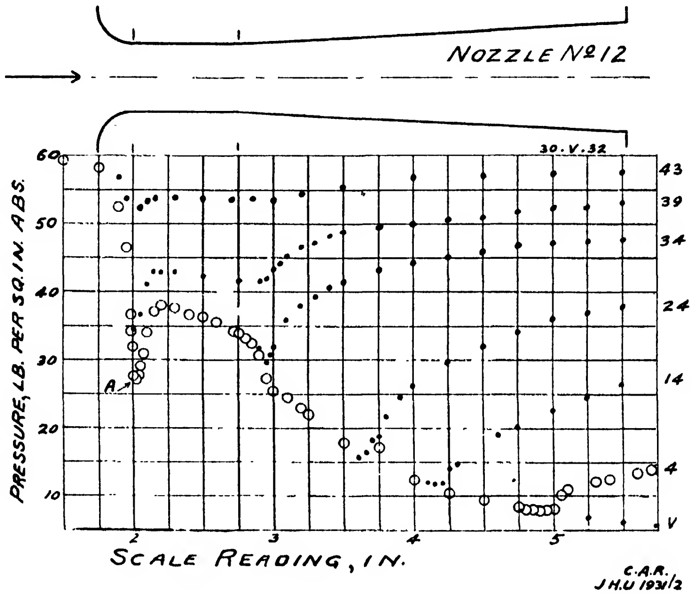

FIG. 25. *Vena contracta recompression in brass nozzle No. 12.*

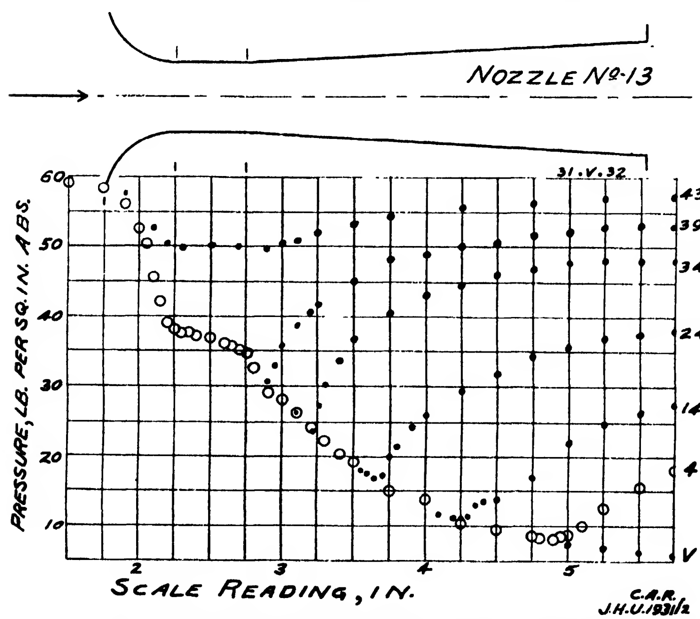

FIG. 26. *Equilibrium recompression in brass nozzle No. 13.*

tion of the jet, the heat will tend to expand the steam. This change in volume is resisted by the nozzle walls, with the result that the static pressure builds up, and this increase of pressure, or what is described above as latent recompression, occurs. The amount of the pressure increase was observed by

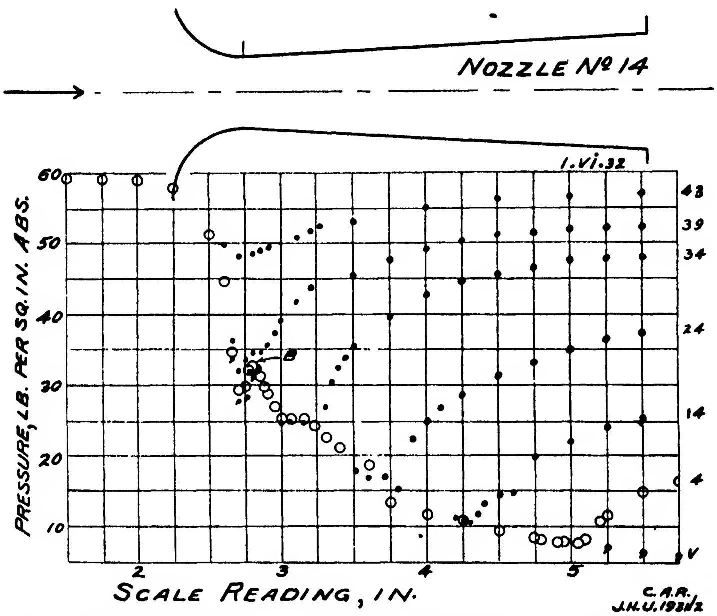

FIG. 27. *The "notch" at B, due to latent recompression in brass nozzle No. 14.*

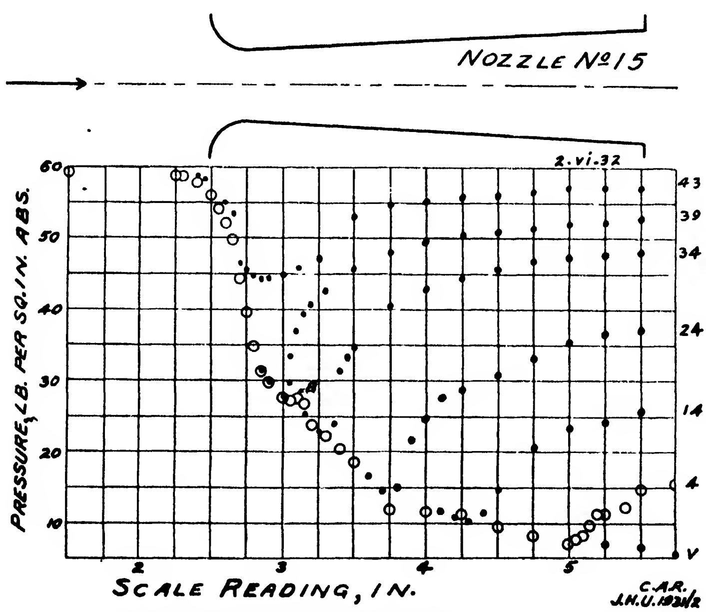

FIG. 28. *Latent recompression in brass nozzle No. 15 at scale reading 3.*

means of the search tube and pressure gauge. The notch is repeated in the various expansion curves of Fig. 21 for nozzle No. 8 and the coincidence of the 14 psi gauge back pressure observations with the 4 psi curve is recorded.

The effect of changing the inlet radius and the length of the parallel section or throat on the rate of expansion can be observed in the slope of the pressure expansion curves for the nozzles Nos. 8 to 11 (Figs. 21 to 24). The slope progressively increases as the throat is shortened and the radius reduced.

In the final series of tests, which were made on the polished drawn brass nozzles Nos. 12, 13, 14, and 15, the dip indicating vena contracta recompression is noted at *A* in Fig. 25 for nozzle No. 12. The notch marked *B*, indicating latent recompression, appears in Fig. 27 for nozzle No. 14 and in the other curves for nozzle No. 14 at inlet pressures of 15 and 30 psi gauge and back pressures of 5 and 14 psi respectively. The dip occurs in the low inlet pressure curves of No. 12. The curves resulting from the tests on Nos. 12 to 15, Figs. 25 to 28, can be superimposed on one another in such a way that they show the effects of the changes in nozzle form on the rate of expansion, change of state, and recompression.

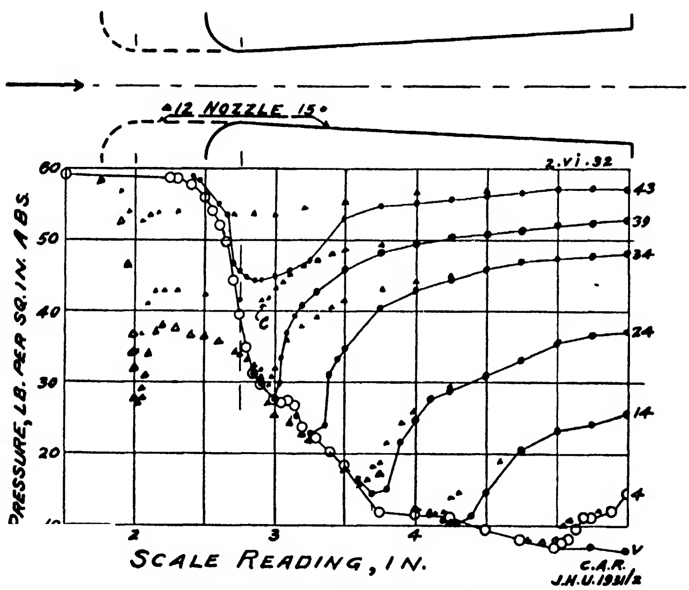

FIG. 29. *Elimination of vena contracta "dip" by shortening of throat (No. 15) despite small inlet radius (¼ in.).*

The curves for Nos. 12 and 15 are combined in Fig. 29. They show the effect of the parallel part or throat ¾ in. in length, other dimensions being the same for both nozzles. The inlet radius is ¼ in. The vena contracta effect and vena contracta recompression occur in nozzle No. 12 with the long throat only. Equilibrium recompression occurs earlier in No. 12 but the recompression pressure, p_r, is higher; that is to say, the steam does not expand to

such a low pressure in nozzle No. 12. The difference in p_r is greater at pressures above the critical, as for example at C in Fig. 29. The symbol p_r is used here to indicate the lowest static pressure attained by the steam in the nozzle as shown by the pressure expansion curve. With particular reference to recompression phenomena, p_r indicates the base of the cusp in the whole pressure expansion curve at which the pressure changes from a decreasing to an increasing value, that is to say, the steam ceases to expand and begins to recompress. The recompression curves occur earlier or the recompression pressures, p_r, are reached earlier in the case of nozzle No. 12, although ultimately the expansion curves coincide, with no apparent loss of pressure.

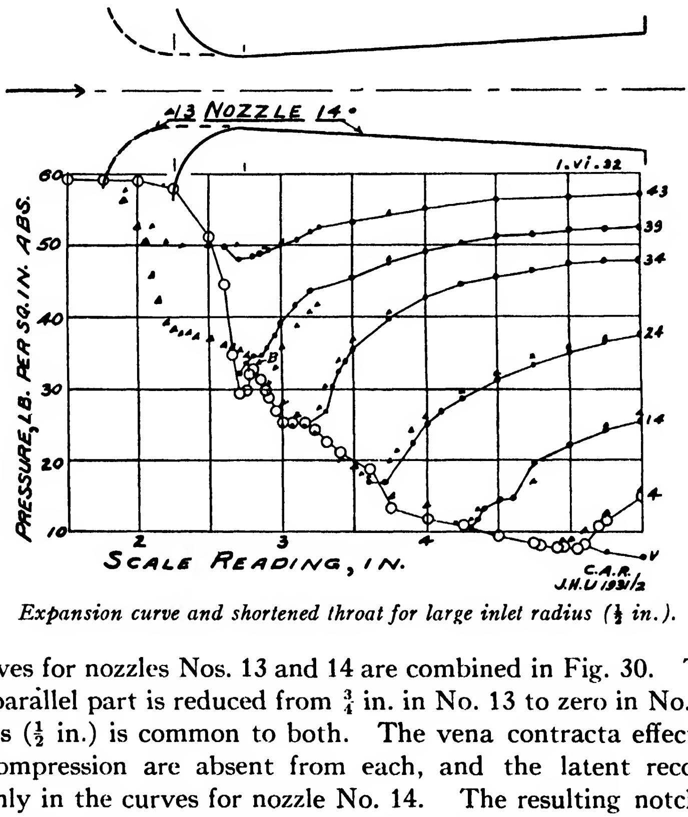

FIG. 30. *Expansion curve and shortened throat for large inlet radius (½ in.).*

The curves for nozzles Nos. 13 and 14 are combined in Fig. 30. The throat length or parallel part is reduced from ¾ in. in No. 13 to zero in No. 14. The inlet radius (½ in.) is common to both. The vena contracta effect and contracta recompression are absent from each, and the latent recompression survives only in the curves for nozzle No. 14. The resulting notch is shown at B. An important difference in the rate of expansion is noted, the curve being steeper and the expansion more rapid in the curves for nozzle No. 14 than in those for No. 13. Similarly the curves for nozzle No. 15 are steeper and show a more rapid expansion than those for No. 12 (Fig. 29). In Fig. 30 the equilibrium recompression occurs earlier for No. 13, the nozzle with the ¾ in. parallel section, than it does for No. 14, with the exception of the 39 lb. curve. In the latter case the situation is reversed, the expansion in nozzle No. 14 is earlier, and the value of the recompression pressure p_r is slightly higher. The point of equilibrium recompression coincides approximately with the point of latent recompression, that is, the notch.

When the expansion curves for nozzle No. 14 (Fig. 27) are superimposed on those for No. 15 (Fig. 28), the inlet radius contributes the only change in the nozzle form. The equilibrium recompression in nozzle No. 14 is consistently earlier than in No. 15. Equilibrium recompression on the 39 psi curve for nozzle No. 14 coincides with the notch, and the recompression pressure p_r of nozzle No. 14 is higher, showing less complete expansion than No. 15.

It is noted that the notch appears in each of the curves for nozzles Nos. 8 to 11 shown in Figs. 21 to 24, whereas in the final series with nozzles Nos. 12 to 15 the step appears only in the case of nozzle No. 14, Fig. 27, and No. 15, Fig. 28. The notch and dip appear at a scale reading of approximately 2.75 in. and 3 in. respectively.

Examples of the peculiar forms of expansion curves due to harmonic vibrations can be seen in Fig. 23 for nozzle No. 10. The wave-like vibrations occur in the jets having the higher velocities such as Curves 14, 4, and V, and only after the jet has passed the nozzle mouth. The frequency of the vibrations increases with the speed of the jet. In test No. 10—45/V, Fig. 23, the amplitude of the vibration is approximately 0.7 in.

The phenomenon of latent recompression results in the notch referred to above and is marked *B* in the expansion curves for nozzle No. 14, Fig. 27, and No. 15, Fig. 28. The amount of recompression involved in the notch of No. 14 is 3½ psi.

The possibility that erosion of the jet surface might disturb the continuity of the expansion curves received special consideration in connection with the tests of the cast-iron nozzles, Nos. 8 to 11. Following the tests, nozzle No. 11 was cut through the centre for inspection, and evidence of both blow holes and erosion was found. Considering the short time that the nozzles were in service, the erosion appeared severe. It resembled cavitation resulting from a continued bombardment of collapsing bubbles or drops. The erosion was most severe in the region where the jet left the throat and entered the diverging part of the nozzle. A comparison of the curves for nozzles Nos. 8 to 11 with those of Nos. 12 to 15 would suggest that since the notch appears in all the curves for the cast-iron channels, Nos. 8 to 11 (Figs. 21 to 24) but in the case of the brass nozzles it appears in the curves of No. 14 and No. 15 only, possibly the notch in the curves of nozzles Nos. 8 and 9 is due to shock recompression resulting from the erosion or pitting.

In connection with the phenomenon of latent recompression and the notch in the pressure expansion curve which was observed at this time and has been described, it should be noted that these tests are the first of a series. At the time of the tests, certain facts were obscure, and they were investigated by means of a modified technique, of which the parallel or extended throat used in these tests formed a part. Later work by other investigators made clear certain factors such as the growth of the water drops (10, 13).

(b) Recompression Effects and Angle of Flare

A comparison of these effects in nozzles having small and large angles of flare can be made by means of the tests of nozzles Nos. 14 and 15 (Figs. 27 and 28) and nozzle No. 6 (Fig. 19). In the latter the flare or nozzle angle is 12°, and the expansion to about atmospheric pressure takes place with great rapidity. The equilibrium recompression is almost as rapid and results in a sharp cusp in the expansion curves for the higher back pressures. The small radius of the inlet or converging section contributes to the rapid expansion, which for moderate pressure ranges demands a short nozzle only, and the combination of the small inlet radius and large angle of flare tends to limit the freedom of control for experimental work in the region where phenomena involving change of state, and recompression, occur. The larger inlet radius of ½ in. in the case of nozzle No. 14, Fig. 27, and ¼ in. in No. 15, Fig. 28, in combination with the parallel section or throat and the smaller angle of flare of 6 degrees, tends to slow down the rate of expansion and makes it possible to observe pressure values at measurable intervals along the axis, as shown in the curves of Figs. 25 to 31.

(c) Prevention of Recompression

To avoid recompression, the design of the nozzle and operating conditions must be considered with a view to avoiding each specific type of recompression.

Equilibrium recompression must be expected wherever the nozzle takes the converging-diverging form and the outlet or back pressure is raised above a specified minimum; the behaviour of this type of recompression will depend upon the angle of flare of the diverging section. The effect of the angle of flare is shown also by a comparison of the curves for nozzle No. 6, Fig. 19, with those for nozzle No. 13, Fig. 26.

Latent recompression has been avoided by reducing the rate of expansion of the steam in the nozzle as in No. 13. Flow tests summarized in Table V and later experiments by other investigators (10) have shown that the means described of reducing the rate of expansion are undesirable. The later experiments have shown that preliminary condensation with rapid growth of drop size occurs when the rate of expansion is decreased. Large drops cause blade erosion. Hence this cure for latent recompression is not satisfactory. It would seem better to allow it to occur, as supersaturation persists.

Vena contracta recompression can be avoided by the use of a liberal inlet radius, with or without a short throat in which the length is from zero to not more than the throat diameter. Examples in which this type of recompression has been eliminated are to be found in nozzles Nos. 13 to 15, for which the pressure expansion curves are shown in Figs. 26 to 28. The later tests referred to above have shown that no length of straight throat is desirable or necessary (10).

Recompression due to roughness of the nozzle surface has been avoided in the case of the cast-iron nozzle No. 9 by substituting the polished drawn

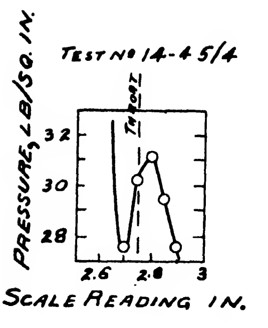

FIG. 31. *Notch produced by latent recompression in No. 14.*

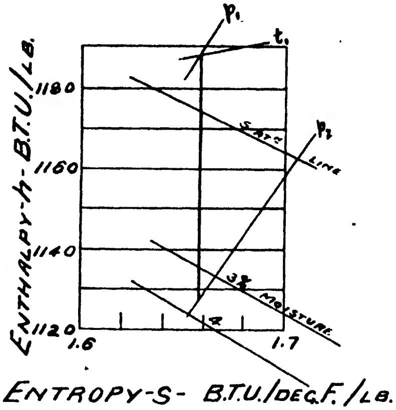

FIG. 32. *Saturation and supersaturation lines in the Mollier diagram.*

brass nozzle No. 13, as will be seen by comparing the respective curves of Figs. 22 and 26.

The notch in the expansion curve representing the test with nozzle No. 14—45/4, as shown at *B*, in Fig. 27, is reproduced on a large scale in Fig. 31. Its position corresponds to a region near the throat of the nozzle. The valley of the expansion curve is reached immediately before the stream enters, and the following recompression immediately after it leaves the throat. In dealing with the quality of the steam and the change of state, the assumption is made that the expansion through the throat is isentropic. There are losses, but those due to wall friction, eddy currents, and the like, occur mainly after the throat has been passed. The operating conditions for test No. 14—45/4 are shown in the Mollier diagram, Fig. 32. The valley of the notch is seen to be between the 3 and 4% constant moisture lines.

V. Calculation of the Recompression Pressure in a Converging-diverging Nozzle

Some deductions may now be drawn from the results obtained in these experiments. The observed notch and the amount of latent recompression resulting is shown in Fig. 31 for test No. 14—45/4. The effect of the inlet pressure on latent recompression is indicated in Fig. 33, i.e., the latent recompression pressure or height of notch from valley to crest at typical back pressures of tests on nozzle No. 14 (Fig. 27) are plotted as ordinates, and the corresponding inlet pressures, as abscissae. At constant inlet pressure, the lower back pressures on the nozzle tend to a slightly higher latent recompression or notch. For an initial pressure of 59.2 psi abs. recompression at the notch is $3\frac{1}{2}$, $3\frac{1}{4}$, 3, and 3 psi respectively for the back pressures of vacuum, 4, 14, and 24 psi gauge.

The possibility of predicting values of the pressure at which equilibrium recompression will occur in a conventional type of convergent-divergent nozzle

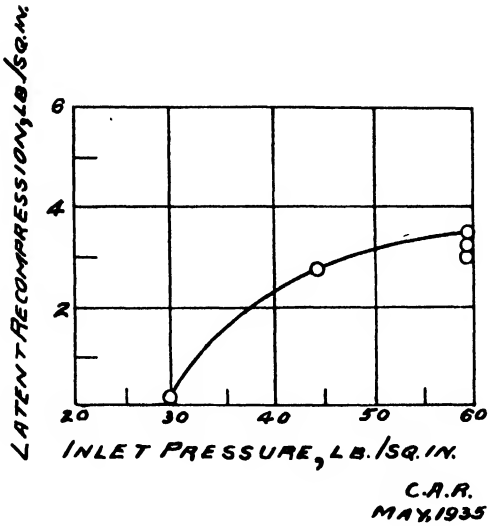

FIG. 33. *Height of notch.*

will now be discussed. Referring to the curves for nozzles Nos. 14 and 15 (Figs. 27 and 28), it will be seen that as the outlet or back pressure is decreased, the steam continues to expand and Curve V, for example, represents a continuous expansion with the notch as the only disturbing element in the continuity. As the outlet pressure is raised, however, there is a halt in the expansion curve and the pressure, which has been decreasing, begins to increase. For example, at a back pressure of 4 psi gauge, the expansion stops and the pressure begins to increase, or equilibrium recompression begins at a scale reading of 5 in. Similarly at a back pressure of 14 psi, recompression begins at a scale reading of 4.25 in., and for 24 psi, at 3.75 in., and so on. It is understood, of course, that the diverging portion of the nozzle must have sufficient length to permit the complete expansion of the steam at the lowest back pressure to which it is proposed to subject the nozzle. It may be useful, in studying the behaviour of a nozzle of this type, to be able to predict the point in the nozzle at which this reversal of pressure or equilibrium recompression will take place, or, since the fundamental Curve 4 can be drawn with a fair degree of accuracy from steam table data for steam in equilibrium with the moisture that it contains, it will be sufficient if one is able to predict the pressure at which the expansion will halt and equilibrium recompression will begin. This pressure, p_r, at which equilibrium recompression begins, will be called simply the recompression pressure in what follows.

The procedure adopted was to investigate the value of p_r relative to $p_1 - p_0$, the difference between the inlet and outlet pressures for various values of p_0 and in the same general type of nozzle. Values of $p_1 - p_0$ for the various tests on nozzles Nos. 12, 13, 14, and 15 were plotted as ordinates against observed values of p_r as abscissae. A curve to approximate all these values was drawn, in view of the possibility that this curve might serve to predict

the value of the recompression pressure, p_r, to be expected in steam nozzles of the convergent-divergent type when the inlet and discharge pressures were known and for variations in the operating conditions in any particular nozzle of this type. The curve is shown in Fig. 34 in conjunction with the observed values of p_r, for nozzles Nos. 12, 13, 14, and 15, including the various pressure conditions of the tests listed in Table II for each nozzle. The approximation is fairly satisfactory, and it would appear that the recompression pressure, p_r, is a function of $p_1 - p_0$. To express the relation between p_r and $p_1 - p_0$ the following equation was computed, from the observed data, by the method of Legendre (5)

$$p_r = \frac{p_1}{59.2}\sqrt{\left(\frac{476}{p_1 - p_0}\right)^3}.$$

where p_r = recompression pressure,
p_1 = inlet pressure,
p_0 = outlet pressure,
$p_1 - p_0$ may be considered to represent the driving force or potential of the flow.

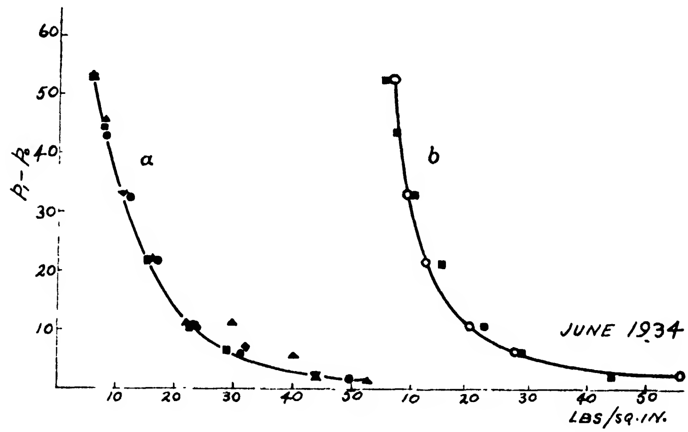

FIG. 34. *(a) Recompression pressures and pressure differences (Nozzle No. 12, ▲; No. 13, ▼; No. 14, ●; No. 15, ■).*
(b) Comparison of the equation for recompression pressures (○, computed points; ■, observed values for No. 15).

Applying the formula to the conditions in nozzle No. 12 operating at an inlet pressure of 59.2 psi abs. and a back pressure of 24 psi gauge, $p_1 - p_2 = 59.2 - (24 + 14.7) = 20.5$. The formula gives a value $p_r = 15.6$ psi abs., which agrees with the observed value. The observed value of p_r from test No. 14—45/24 (Fig. 27) is 15 psi abs., which is the largest variation from the curve for all four nozzles Nos. 12, 13, 14, and 15, operating at a back pressure of 24 psi abs. The value of p_r for the various back pressures in the test on nozzle No. 15 are plotted in Fig. 34, in which the curve is repeated, and the agreement between the estimated and observed values is seen to be good.

In order to test the efficiency of the curve and equation, the method has been applied to published data for convergent-divergent steam nozzles tested by

other investigators, and the following comparison is given of the observed recompression pressure, p_r, and the author's estimated value for p_r.

Mellanby and Kerr (7, p. 125) present a series of pressure expansion curves for various outlet pressures, the initial conditions being 76 psi abs. and 250° F. Table III shows the outlet pressures and the observed and estimated values of p_r.

TABLE III

COMPARISON OF OBSERVED AND ESTIMATED VALUES OF RECOMPRESSION PRESSURE, p_r. INLET PRESSURE, 76 PSI

Outlet pressure psi abs.	Observed recompression pressure, p_r, psi abs., Mellanby and Kerr	Estimated value of p_r, Robb	Difference in per cent of inlet pressure (76 psi)
16.4	15.2	9	8.2
32.7	17.5	13.2	5.7
44.1	21.3	17.9	4.5
54.7	25.8	24	2.4

Stodola (11, p. 83) presents a similar series of pressure expansion curves for which the inlet conditions are 147 psi abs. and 381 to 392° F. Table IV shows a comparison similar to that given above.

TABLE IV

COMPARISON OF OBSERVED AND ESTIMATED VALUES OF RECOMPRESSION, p_r

Outlet pressure	Observed recompression pressure, p_r, psi abs. Stodola	Estimated value of p_r, Robb	Difference in per cent of inlet pressure (147 psi)
144	131	134	2
139	105	102	2
129	66	67	0.7
107	45	47.1	1.4
91	37	37.2	0.13
65	21	27.3	4.3
44	15	20.6	3.8
27	9	16.4	5
12	5	12.7	5.2
8	4	11.9	5.4

The average difference, in percentage of the inlet pressure, between the observed values of the recompression pressure, p_r, and the values estimated by means of the curve and equation, is just more than 5% for the data considered in Table III and 3% for that of Table IV. The examples are taken at random from the reports of representative investigators and would seem

to indicate a fair degree of accuracy for purposes of estimation, and they set limits for the method. The application of the method has been limited to the convergent-divergent type of steam nozzle.

VI. Losses in Nozzles

The ideal expansion of steam in a nozzle is adiabatic and free from losses. The application of the conventional theory for calculating the losses in the actual flow through a convergent-divergent nozzle of the type considered presents certain difficulties. The theory of what is described as the "losses method" of calculating nozzle efficiency has been presented by Goudie (4, p. 643). The pressure p_1, quality x_1, and total heat h_1 of the steam arriving at the nozzle, and the weight w of the steam flowing per second, are known from the tests. From the readings of the search tube, at any section A_2, the pressure is p_2. At this cross-section the steam is wet but with an unknown quality x_2 since expansion is not perfectly adiabatic. Let V_1 be the small velocity of the steam arriving at the nozzle. If the unknown velocity V_2, at Section 2, is uniform and axial, or nearly so, for all particles, and if y is the friction loss in the nozzle, then the following equation based on the conservation of energy is true (11, p. 68):

$$\frac{V_2^2}{2gJ} = (h_1 - h_2)(1 - y) .$$

The symbol J denotes the mechanical equivalent of heat (1 B.t.u. = 778 ft.-lb.), and h_2 is the total heat in the steam after it has expanded adiabatically to p_2.

The volume discharged at any pressure equals the weight discharged per second multiplied by the specific volume of the steam. The law of steady flow requires that the volume discharged per second equal the area of the section multiplied by the velocity per second. Hence

$$wx_2v_2 = \frac{A_2V_2}{144} .$$

At cross-section A_2 the heat h_2 in the steam is

$$h_2 = x_2h_{fg_2} + h_{f_2}$$

Then the velocity equation becomes

$$V_2 = 173.97 - \left[\frac{A_2h_{fg_2}}{wv_2} + \sqrt{\left(\frac{A_2h_{fg_2}}{wv_2}\right)^2 + 1.6554\,(h_1 - h_{f_2})}\right].$$

In reality, V_2 may not be uniform or axial, x_2v_2 may vary, the amount of variation depending on the distribution of the water drops, and the section may not be filled if the steam leaves the walls. Notwithstanding these difficulties it was expedient to calculate the losses in the brass nozzles Nos. 12, 13, 14, and 15, with a view to comparing the behaviour of the steam in the various forms of nozzle and to account at least in part for the effects of certain recompression phenomena that have been observed.

Nozzle No. 12 will first be considered, and, on the assumption of an ideal expansion in which the process is adiabatic, the velocity, V_m, after expansion to absolute pressure p_m is calculated on the basis of the observed pressures and plotted as an ordinate in Fig. 35 against the distance along the axis corresponding in area to the point at which the nozzle would just be filled by the stream in accordance with the continuity equation. Twelve points in the divergent section of the nozzle are considered and a best fitting curve is drawn through the calculated points. Values of the actual velocity V_2 were calculated by means of the velocity equation on the basis of observed pressures and flow tests. These are plotted as ordinates in Fig. 35 at points along the nozzle axis corresponding to the actual area A_2 of the nozzle. The calculations were extended to include the test conditions listed in Table II for back pressures up to and including 24 psi gauge. Similar calculations were carried out for nozzles Nos. 13, 14, and 15.

The results are summarized in Table V, which gives the calculated velocity, V_m, after an assumed adiabatic expansion to absolute pressure p_m, the actual velocity V_2 based on observed pressures and flow tests, and the loss, y, in percentage.

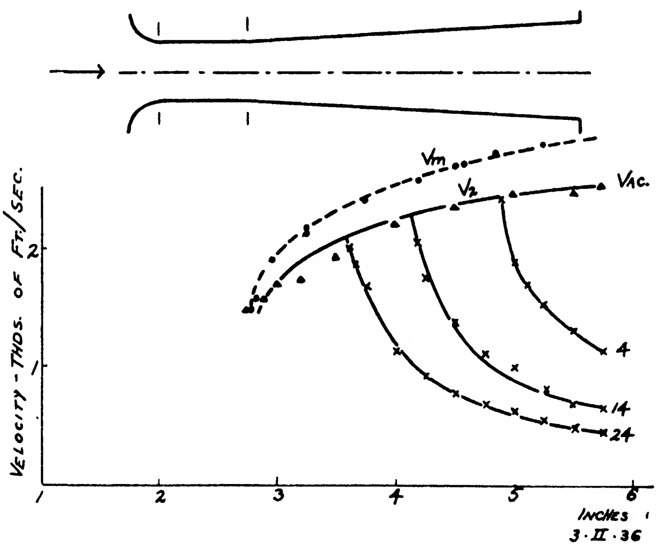

FIG. 35. *Losses in velocity for nozzle No. 12.*

The effect of the nozzle form and its relation to losses and recompression phenomena can now be considered. The greatest loss, 26.6%, is found in nozzle No. 15. This nozzle is characterized by a small ($\frac{1}{4}$ in.) radius of approach, producing a very quick expansion of the steam to throat pressure and a steep pressure expansion curve. The relatively sharp corner of the nozzle, around which the stream must pass, delays the recompression cusp in the curves for the higher back pressures, as, for example, in test No. 14—45/39

TABLE V

CALCULATED VELOCITIES AND LOSSES IN NOZZLES NOS. 12, 13, 14, AND 15

Nozzle No.	V_m Velocity after adiabatic expansion	V_1 Actual velocity	y = loss in per cent of heat drop
12	2940	2530	26
13	2940	2530	26
14	2925	2530	25.2
15	3000	2570	26.6

shown in Fig. 30. A slightly lower recompression pressure, p_r, is produced than in nozzle No. 14 for the same back pressure. The recompression curve following the minimum value p_r is considerably steeper; this denotes a quicker recompression once the process of recompression had begun. The small radius of approach and the sharp corner have produced conditions definitely unfavourable to high efficiency as compared with the larger ($\frac{1}{2}$ in.) radius of approach, more gradual expansion, and best efficiency of nozzle No. 14. The loss in percentage is 26.6 for nozzle No. 15 and 25.2 for nozzle No. 14.

It would appear from the above that, in design, the trend should be toward a larger inlet radius on turbine nozzles than has been the common practice. The introduction of the parallel or extended throat has affected the efficiency adversely both in nozzle Nos. 12 and 13. The parallel throat, in view of later work, is undesirable as it permits growth of water drops, which increase losses. The larger inlet radius of No. 13 has produced a less disturbed pressure expansion curve, Fig. 26, than the small radius of nozzle No. 12, in which the vena contracta recompression is excessive, as shown at point A in Fig. 25. It is concluded that, at this point A, the jet has left the wall of the nozzle. In cases in which it is desired to utilize the nozzle for processing of the jet, such as the introduction at the throat of other fluids at a slightly higher and regulated pressure for mixture with the jet, or the extracting of liquid drops from a vapour jet with a view to improving the quality of the jet, the parallel or extended throat offers advantages both as regards the relatively steady pressure throughout the throat, as noted for nozzle No. 13 in Fig. 26, and the space that may be required for the injection and extraction operations. These advantages may, in such cases, offset the loss of efficiency.

Acknowledgments

The author wishes to acknowledge his indebtedness to Professor A. G. Christie and Associate Professor J. C. Smallwood of the Johns Hopkins University, for their advice and helpful criticism.

References

1. Binnie, A. M. and Woods, M. W. Inst. Mech. Eng. Proc. 138 : 229-266; Discussion, 138 : 284-308. 1938.
2. Christie, A. G. See (12) pp. 427-430. 1934.
3. Goudie, W. J. Steam Turbines. London. 1922.
4. Goudie, W. J. Ripper's Steam Engine. London. 1932.
5. Legendre, A. M. Nouvelles méthodes pour la détermination des orbites des comètes. Paris. 1806.
6. Martin, H. M. Engineering, 95 : 37-38. 1913.
7. Mellanby, A. L. and Kerr, W. J. Roy. Tech. Coll. 1 (Part 2): 123-143. 1925.
8. Mellanby, A. L. and Kerr, W. Trans. Inst. Engrs. & Shipbuilders in Scot. 64. Dec., 1920.
9. Powell, C. F. Engineering, 127 : 711-713, 779-780. 1927.
10. Retalliata, J. T. Am. Soc. Mech. Eng. Trans. 58 : 599-605. 1936.
11. Stodola, A. Steam and Gas Turbines. McGraw-Hill Book Co., New York. 1927.
12. Yellott, John I. Am Soc. Mech. Eng. Trans. 56 : 411-427. Discussion, 427-430. 1934. Or, Engineering, 137 : 303-305, 333-335. 1934.
13. Yellott, John I. and Holland, C. K. Engineering, 143 : 647-649. 703-705. 1937.
14. Zerban, A. H. and Johnston, R. M. Combustion, 7 : 23-24. 1935.

Canadian Journal of Research

Issued by THE NATIONAL RESEARCH COUNCIL OF CANADA

VOL. 19, SEC. A | JULY, 1941 | NUMBER 7

A DIRECT READING MICROPHOTOMETER[1]

BY G. O. LANGSTROTH[2], K. B. NEWBOUND[3], AND W. W. BROWN[3]

Abstract

A direct reading photoelectric microphotometer, designed for use in spectrographic analysis, is described.

The speed and convenience of a spectrographic method of analysis depend largely on the character of the equipment employed. The refinement of apparatus intended for such use therefore appears to be desirable. This article describes a direct reading photoelectric microphotometer that has been constructed at a relatively low cost. The instrument has the advantages of speed and convenience of operation with minimum fatigue to the operator. These qualities are attained through the arrangement of the optical system and controls, the design of the plate movement, and the method of making the observations.

1. General Design

The general features of the design may be seen from Figs. 1 and 2. The optical train is a modification of that used in most microphotometers. It is so arranged that the photographic plate, the observation screen containing the slit which admits light to the photocell, and the galvanometer scale are grouped together in a row vertically, and are in approximately the same plane with respect to the operator's eye. This grouping of the parts that must be under constant observation has been made with a view to minimizing the fatigue inherent in the continuous use of a microphotometer over an appreciable period of time. With the same aim, the various controls have been grouped in convenient positions, as indicated in the illustrations.

The galvanometer is situated below and behind the instrument. Light from its mirror is focused on a ground glass scale set into the top of an inclined drawing board and contiguous with a 9 by 10 in. glass plate also set into the board. A sheet of semilogarithmic graph paper placed on the plate with the linear scale lying along the galvanometer scale is illuminated from the back with red light. This arrangement provides excellent illumination for observing the graph co-ordinates, and minimizes the amount of scattered light

[1] *Manuscript received June 2, 1941.*
Contribution from the Department of Physics, the University of Manitoba, Winnipeg, Man.

[2] *Associate Professor of Physics.*
[3] *Holders of Bursaries under the National Research Council of Canada.*

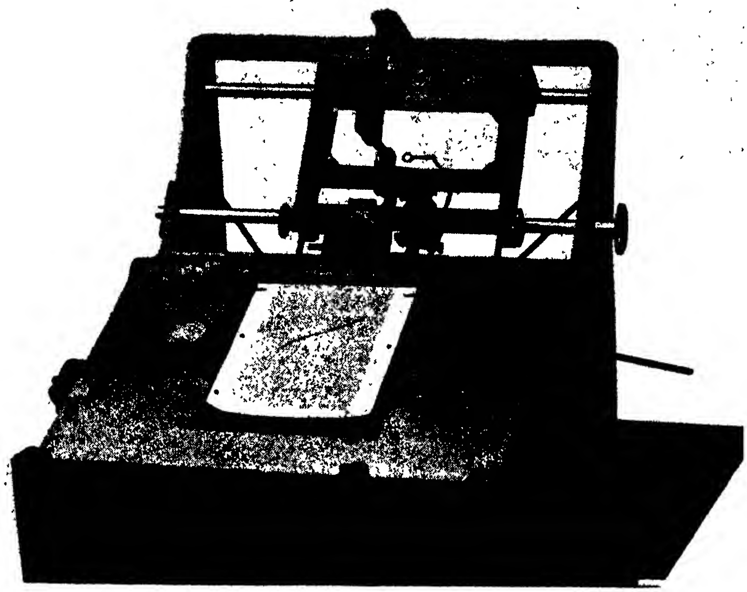

FIG. 1. *The microphotometer.*

in the microphotometer room. As will appear later, determination of relative intensities is made without reading off numerical values for the galvanometer deflections and calculating the transmission value for each spectral line.

The plate holder is of sufficient size to permit the investigation of all parts of a standard 4 by 10 in. plate without readjustment in the holder. It is mounted on friction bearings, which facilitate rapid rough adjustment lengthwise, combined with a micrometer adjustment for accurate setting on the desired spectral line. Further details are given below.

2. Details

The Mounting

All parts of the optical system, including the photocell, are mounted on a framework of $\frac{5}{16}$ in. boiler plate. Three inch channel iron and $1\frac{1}{2}$ in. angle irons screwed respectively to the base and side plates ensure the necessary rigidity. The angle iron extending across the top of the framework is reinforced with $1\frac{1}{2}$ in. pipe. The framework is securely fastened to a cabinet of $1\frac{1}{4}$ in. maple.

The Optical System

The light source consists of a six volt 32 cp. automobile lamp operated from a storage battery. The current through it is controlled by a one ohm "Ohmite" variable resistance; the potential drop across it is indicated by the voltmeter, *V* (Fig. 2). The lamp housing carries a slit, behind which is fixed an *f:* 3.5, 3.5 cm. focal length lens. This unit is adjusted to form an image of the lamp filament approximately in the plane of the condensing objective. The con-

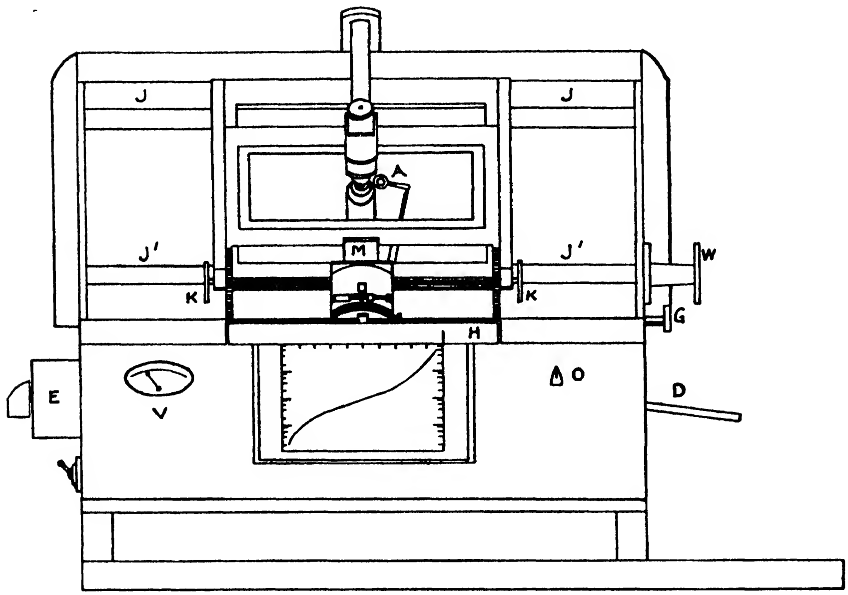

(a)

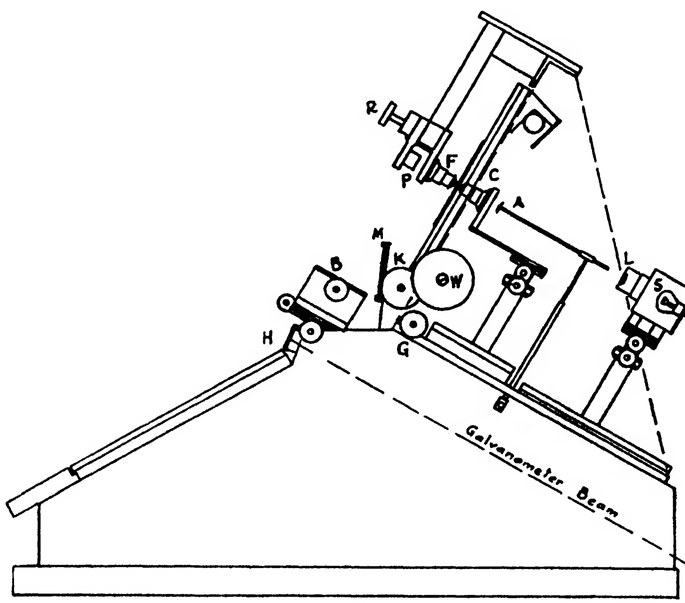

(b)

FIG. 2. *Front and side elevations of the microphotometer. The symbols have the following significance. S, light source; L, lens and slit unit; A, auxiliary lens; C, condensing objective; F, focusing objective; P, reflecting prism; B, observation screen and photocell mount; M, mirror for viewing the screen; H, galvanometer scale; R, adjustment for the focusing objective; G, adjustment for the condensing objective; K, adjustment for vertical plate motion; W, adjustment for horizontal plate motion; J, J', rods on which the plate holder slides; E, rheostat controlling the lamp current; V, voltmeter connected across the lamp terminals; O, control for varying the resistance of the galvanometer circuit; D, lever control for the auxiliary lens.*

densing objective forms an image of the slit on the emulsion of the photographic plate, which in turn is focused by the focusing objective on a white observation screen containing an adjustable photocell slit. Magnifications of 0.1 and 10, respectively, are used. Both objectives are achromats of 16 mm. equivalent focal length and 0.25 numerical aperture. The photometer beam is directed to the observation screen by a fixed reflecting prism mounted about 3 cm. behind the focusing objective. The image on the screen may be conveniently observed by the operator in the plane mirror *M*.

Micrometer screws are provided for the axial adjustment of the objectives. Each optical part, with the exception of the focusing objective unit, has cross and vertical movements, and the observation screen has cross and rotational movements. Adjustment of the reflecting prism is made by means of three grub screws.

An auxiliary lens, *A*, is provided. It may be swung into the photometer beam by means of the lever shown in the illustration. It permits observation of an appreciable range of the spectrum on the screen, and is used in the usual manner to obtain critical focus for the objective, *F*.

The Photocell Circuit

A Weston Photronic cell is used as a detecting unit. It is connected in series with a 2000 ohm variable resistance and a Leeds and Northrup galvanometer (sensitivity 3×10^{-9} amps per mm.; period 2.6 sec.). Under ordinary conditions the changes made in the circuit resistance during operation are not sufficiently great to affect detectably the critical damping of the instrument.

The Plate Holder and Plate Movement

The metal plate-holder, which accommodates a 4 by 10 in. plate, is fitted in ways attached to a larger rectangular frame. Vertical plate motion is

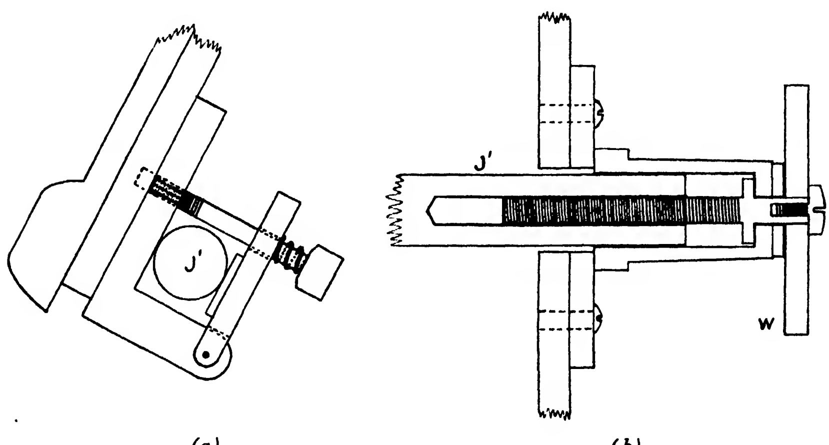

FIG. 3. *(a) Detail diagram of the friction bearings of the plate holder, and (b) detail diagram of the micrometer adjustment for horizontal plate motion.*

accomplished by means of a rack and pinion at each side of the plate holder. The frame is hung from the upper bearing rod *J* (Fig. 2) by means of right-angle bronze bearings, and is held against the outer surface of the lower rod by friction bearings (Fig. 3*a*). The lower rod may be moved endwise by means of a micrometer screw operated by a 3 in. wheel (*W*, Fig. 3*b*). This arrangement allows rapid manual movement of the plate holder endwise, and at the same time makes provision for fine adjustment of the motion by means of the micrometer screw.

It is essential that the emulsion of the photographic plate should remain in the focal plane of the objectives over the entire range of the plate motion. This condition was fulfilled by the following procedure. *(a)* The bearing rods of $\frac{3}{4}$ in. cold rolled steel shafting were adjusted accurately parallel. *(b)* The movable bearing rod was keyed to prevent rotational motion, thus eliminating the possibility that some eccentricity in the rod might throw the emulsion out of the focal plane of the objectives. *(c)* The bearings, and also the surface of the plate holder, were fitted by trial, using the critical focus of the emulsion on the observation screen as the criterion to be satisfied.

Method of Making Observations

The method used in determining relative intensities of spectral lines is a modification of that described by Langstroth and McRae (1). As previously stated, a sheet of semilogarithmic graph paper is placed with the linear scale lying along the galvanometer scale. It is adjusted so that the co-ordinate zero coincides with the galvanometer zero. The 'clear plate' deflection is adjusted to read 1.0 (10 large co-ordinate divisions) by means of the series resistance, *O* (Fig. 2). In plotting the calibration curve for the plate, the calibration marks are introduced successively into the photometer beam; a point is plotted opposite each position of the galvanometer spot at the appropriate intensity value on the logarithmic scale. On subsequent introduction of a spectral line into the beam, the relative intensity is read off directly from the curve as that value on the logarithmic scale corresponding to the point on the calibration curve opposite the position of the galvanometer spot on the linear scale. This procedure obviates the reading of numerical values for the galvanometer deflections and the calculation of transmission ratios.

3. Remarks

The microphotometer described in this article has been in constant use for the past six months, and has been found to be time saving and convenient. In addition, the method of making the observations goes far toward the avoidance of arithmetical mistakes, which sometimes occur when galvanometer deflections are recorded and transmission values calculated. The precision of measurement is comparable with that of other direct reading instruments.

Constant use has suggested that the instrument might be improved at a reasonable cost by substitution of a shorter period galvanometer. Furthermore, the micrometer wheel *W* controlling the plate motion might, with some advantage, be placed on the left-hand side of the instrument.

4. Acknowledgments

The authors are grateful to Dr. M. W. Johns of Brandon College, to Mr. R. Bird of the University workshop, and to Mr. R. M. Smith, for aid in the construction of the apparatus.

Reference

1. Langstroth, G. O. and McRae, D. R. J. Optical Soc. Am. 28:440. 1938.

Canadian Journal of Research

Issued by THE NATIONAL RESEARCH COUNCIL OF CANADA

VOL. 19, SEC. A. AUGUST, 1941 NUMBER 8

EDITOR'S NOTE

Material scheduled for publication in this issue will appear later. This title page is included for purposes of record.

Canadian Journal of Research

Issued by The National Research Council of Canada

VOL. 19, SEC. A. SEPTEMBER, 1941 NUMBER 9

RESONANCE METHOD OF MEASURING THE RATIO OF THE SPECIFIC HEATS OF A GAS, C_p/C_v. PART III.[1]

SULPHUR DIOXIDE AND NITROUS OXIDE

By A. L. Clark[2] and L. Katz[3]

Abstract

This paper is a continuation of work published in the Canadian Journal of Research in 1940. The results for nitrous oxide and sulphur dioxide are now shown. A paper now in preparation will deal with some theoretical matters and will contain additional results for some of the gases already discussed.

In previously published papers (3) the authors developed the theory of a resonance method for measuring the ratio of the specific heats of gases, γ, and gave the results for a number of the gases at pressures up to 25 atm. at room temperature.

The resonance method is particularly suitable for measuring the variation of γ with pressure at constant temperature. Such measurements were carried out on helium, argon, nitrogen, hydrogen, and carbon dioxide. The values of γ at zero pressure were found by extrapolation and were listed in Table XV of Part II. Later examination showed these values to agree with those calculated from spectroscopic data to better than 0.1% with the exception of the value for carbon dioxide which was found to be 0.49% too large. Since this was the only triatomic gas investigated at that time, it was felt advisable to examine other triatomic gases. With this purpose in mind sulphur dioxide and nitrous oxide were investigated.

Sulphur Dioxide

This gas was obtained from the Ohio Chemical Company who gave its purity as better than 99.5%. For this reason the gas was used without any further purification.

To calculate the correction factors G and Λ it was necessary to have experimental $Pv - P$ data or an equation of state capable of yielding the derivative $(\partial v/\partial P)_T$ with a fair degree of accuracy. There are surprisingly few pressure-volume data on sulphur dioxide to be found in the literature. One paper,

[1] *Manuscript received July 3, 1941.*
Contribution from the Department of Physics, Queen's University, Kingston, Ont.
[2] *Dean of the Faculty of Applied Science, Queen's University.*
[3] *Teaching Fellow, California Institute of Technology, Pasadena, California, U.S.A.*

by W. Cawood and H. S. Patterson (2) lists the first virial coefficient as a function of temperature for a number of gases, that is, values of A in the empirical equation,

$$Pv = RT(1 - Ap), \tag{1}$$

from which

$$G = -P/v \,.\, (\partial v/\partial p)_T = 1 + \frac{ART}{v} = \frac{1}{1 - AP} \,. \tag{2}$$

In the case of sulphur dioxide, we find $A = 0.0173$ at 25.1° C. The correction factor Λ is given by the equation

$$\Lambda = \frac{m + m_g}{m} = \left(1 + \frac{104.02}{143.69v}\right), \tag{3}$$

where v is the specific volume of the gas in cubic centimetres per gram, obtained from Equation (1).

For comparison we may use Wohl's equation of state, which seems to be suitable for this gas over a wide range of temperatures and pressures with a fair degree of accuracy (6). This equation may be written in the form

$$P = \frac{RT}{v - b} - \frac{a}{Tv(v - b)} + \frac{c}{T^{4/3}v^3}, \tag{4}$$

with

$$a = \frac{32}{75} \cdot \frac{R^2T_k^3}{p_k} \qquad b = \frac{RT_k}{15p_k} \qquad c = 0.07585\,\frac{R^3T^{13/3}}{p_k^2},$$

where T_k = critical temperature, p_k = critical pressure. The equation for G follows directly, and is

$$\frac{1}{G} = 1 + \left(RTb - \frac{a}{T}\right)\frac{1}{P(v - b)^2} + \frac{2c}{PT^{4/3}v^3} \tag{5}$$

For sulphur dioxide at 25.1° C., this reduces to

$$\frac{1}{G} = 1 - \frac{2299.8}{P(v - b)^2} + \frac{7077.5}{Pv^3}, \tag{6}$$

with

$$P = \left(394.83 - \frac{2486.4}{v}\right)\frac{1}{v - b} + \frac{3538.8}{v^3}\,. \tag{7}$$

As before, the factor Λ is calculated by means of Equation (3) with v obtained from Equation (6).

Table I gives the corresponding resonance frequencies and correction factors for sulphur dioxide at various pressures. The factors Λ and G were calculated from the data of Cawood and Patterson. In Part II a quantity $\Delta\gamma$ was added to γ to correct for the fact that the compressions are not strictly adiabatic. The equation for $\Delta\gamma$ was derived by an approximation method. A more accurate analysis gives a correction factor that may be expressed in terms of $\Delta\gamma$ as

$$\Gamma = 1 + 0.83\frac{\Delta\gamma}{\sqrt{\gamma}} + 0.69\,\frac{(\Delta\gamma)^2}{\gamma}$$

The complete derivation of Γ and its effect on previously published values will be given in Part IV of this series of articles. In the meantime it is used in the present calculations and values of Γ are listed in Table I. The final corrected values of γ are listed in Column 6. A second degree curve was fitted to these values by the method of least squares and was found to be

$$\gamma = 1.2642 + 0.0169P + 0.0026P^2. \tag{8}$$

TABLE I

SULPHUR DIOXIDE (25.1° C.)

Press., atm.	Frequency at resonance	Λ	G	Γ	γ	$\gamma_{calc.}$	$(\gamma - \gamma_{calc.}) \times 10^{-3}$
0 9970	26 032	1.00192	1 0175	1.0039	1.283_3	1 2836	−0.3
2 241	29.070	1 00440	1.0403	1 0022	1.315_4	1.3152	0
2.8705	44 269	1.00570	1 0523	1.0020	$1\ 335_4$	1.3341	+1
3.641	49.914	1.00733	1.0670	1.0018	1.359_4	1.3602	−1

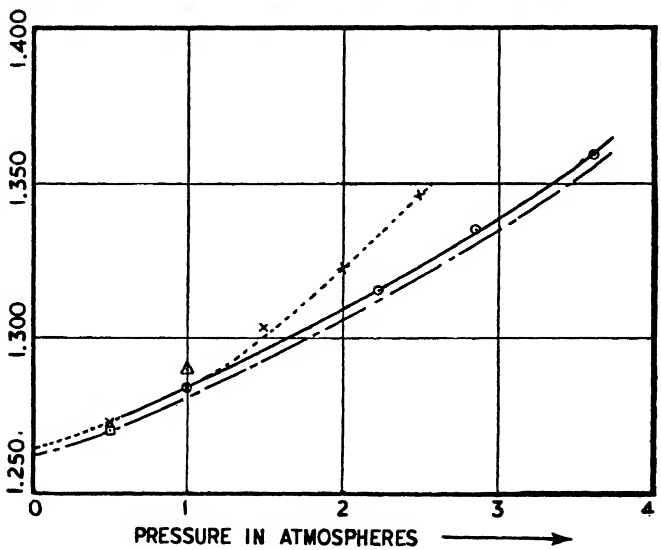

FIG. 1. *Sulphur dioxide—γ as a function of pressure at 25.1° C. $\gamma = 1.2642 + 0.0169P + 0.00260P^2$. ———Curve using Cawood and Patterson Pv — P data to calculate Λ and G. — — — -- Using Wohl equation of state to calculate Λ and G. ⊙, Clark and Katz. ×, Scholer (20° C.). ⊡, Capstick. △, I.C.T. (15° C.) also Partington and Cant (20° C.).*

Values of γ calculated from Equation (8) are given in Column 7 and are compared with the corrected values in Column 8. Both are plotted in Fig. 1. If the Wohl equation is used, the correction factors are altered sufficiently to lower all the values of γ by about 0.2% as shown by the broken-line curve in Fig. 1. The equation for this curve by the method of least squares is

$$\gamma = 1.2620 + 0.0165P + 0.00265P^2.$$

The authors feel that the results obtained by use of the data of Cawood and Patterson are the more reliable. The friction factor χ was found to be very close to unity ($\chi < 1.00002$) and was neglected.

A few experimental values found in the literature are also shown in Fig. 1. The values of Scholer (5) were given at 20° C. and are plotted without change. They would be altered only slightly (about 0.2% in the lower pressure range) when corrected to 25.1° C. His values for pressures of ½ and 1 atm. are in good agreement with those of the authors, but those at the higher pressures are larger. A single value by Capstick (1) at ½ atm. pressure and another by Partington (4) at 1 atm. and 20° C. are also shown.

Nitrous Oxide

This gas was obtained from the same company as the sulphur dioxide and its purity was given as 98%. As in the case of sulphur dioxide, the only $Pv - P$ data found in the literature for calculating the correction factors were those of Cawood and Patterson (2), and even these are given only for pressures up to 5 atm. For higher pressures the Wohl equation was again used, and it was reassuring to note that within the common pressure range up to 5 atm. the values of γ calculated by the two methods agreed to within less than 0.1%. For nitrous oxide at 25.1° C. the Wohl equation reduces to

$$P = \left(538.85 - \frac{1933.6}{v}\right)\frac{1}{(v-b)} + \frac{2515.1}{v^3}, \tag{9}$$

giving

$$\frac{1}{G} = 1 - \frac{1635.8}{P(v-b)^2} + \frac{5030.2}{Pv^3}. \tag{10}$$

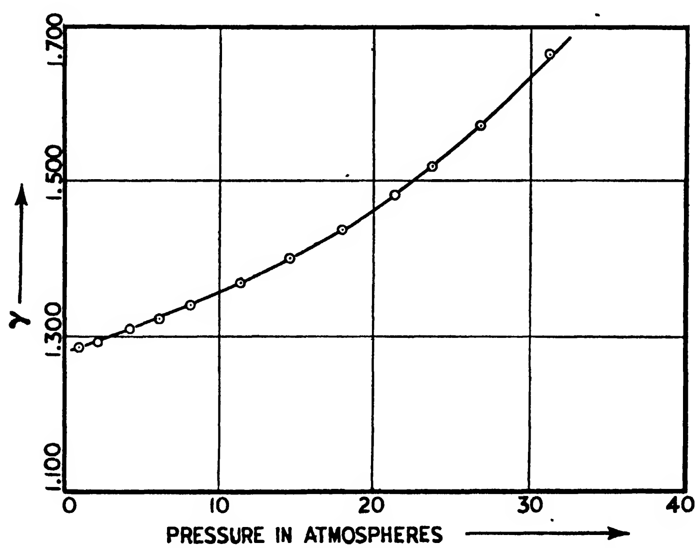

FIG. 2. *Nitrous oxide*—γ *as a function of pressure at 25.1° C.* $\gamma = 1.2783 + 6.320 \times 10^{-3} P + 1.22 \times 10^{-4} P^2 + 6.80 \times 10^{-8} P^4$.

As before, Λ is calculated from Equation (3) with the values of v for particular pressures given by Equation (10).

Table II summarizes the authors' work on this gas. A fourth degree curve fitted to the corrected values of γ as listed in Column 6 was found to be

$$\gamma = 1.2783 + 6.320 \times 10^{-3}P + 1.22 \times 10^{-4}P^2 + 6.80 \times 10^{-8}P^4. \quad (11)$$

Values of γ calculated from this equation are given in Column 7 and are compared to the corrected values in Column 8. The corrected values are plotted as a function of the pressure in Fig. 2. The full line drawn through these values is given by the Least Square Equation (11).

TABLE II

NITROUS OXIDE (25.1° C.)

Press., atm.	Frequency at resonance	Λ	G	Γ	γ	$\gamma_{calc.}$	$(\gamma - \gamma_{calc.}) \times 10^{-3}$
0.9987	26.211	1.00135	1.0057	1 0054	1.2847	1 2847	0
2.224	39.106	1.00303	1.0129	1.0031	1 292	1.2930	−1
4 334	51 568	1.00597	1 0259	1 0019	1.308	1 3080	0
6.157	64.870	1.00858	1 0379	1 0015	1.322	1.3220	0
8.208	74.782	1.01158	1.0519	1.0013	1 339	1.3407	−2
11.439	88.030	1.01648	1 0754	1.0011	1 368	1.3678	0
14.641	99.206	1.02169	1 1043	1 0010	1 400	1.4001	0
17 952	109.560	1.02707	1.1341	1 0009	1.438	1.4382	0
21.384	119.156	1 03312	1.1710	1 0009	1.483	1.4836	−1
23.769	125.304	1.03756	1.2001	1.0008	1 519	1.5189	0
26.942	133.008	1.04376	1.2441	1.0008	1.574	1 5731	+1
31.354	142.645	1.05315	1.3193	1.0008	1.664	1 6621	+2

Analysis of Results

Since the equations fitted to the experimental data give equal weight to all the measurements made on each gas, it is felt that the values given by these equations are relatively free of accidental errors, and are more accurate than the experimental values themselves. These results will be analysed in Part IV of these articles, which the authors hope to publish at an early date. It will be shown that the zero pressure value of γ for sulphur dioxide agrees perfectly with that calculated spectroscopically but that the nitrous oxide value is 0.38% too large.

References

1. CAPSTICK, J. W. Trans. Roy. Soc. (London), A(1), 186 : 567-592. 1895.
2. CAWOOD, W. and PATTERSON, H. S. J. Chem. Soc., 619-624. 1933.
3. CLARK, A. L. and KATZ, L. Can. J. Research, A, 18 : 23-63. 1940.
4. PARTINGTON, J. R. and CANT, H. J. Phil. Mag. (Ser. 6) 43 : 369-380. 1922.
5. SCHÖLER, K. Ann. Physik (Ser. 4), 45 : 913-928. 1914.
6. WOHL, K. Z. Physik. Chem. 133 : 305-349. 1928.

Canadian Journal of Research

Issued by THE NATIONAL RESEARCH COUNCIL OF CANADA

VOL. 19, SEC. A. OCTOBER, 1941 NUMBER 10

ABSORPTION OF LIGHT AND HEAT RADIATION BY SMALL SPHERICAL PARTICLES

I. ABSORPTION OF LIGHT BY CARBON PARTICLES[1]

BY R. RUEDY[2]

Abstract

From Mie's classical theory of the action of small spherical particles on plane waves of light, the expression giving the loss of light due to absorption and scattering is reduced to the formula involving only Bessel functions of orders given by half integral values. The result is used for calculating the absorption by small carbon particles whose diameter is comparable with the wave-length of the incident light, particles that can be measured only by interference methods. When the diameter is less than 0.2 μ the coefficient of absorption decreases toward the red end of the spectrum. The reverse is true for 0.3 and 0.4 μ particles.

Propagation of a Plane Wave of Light past a Spherical Particle

When a small spherical particle is placed in the path of a plane wave of light, a fraction of the radiation striking the particle is returned along different directions into the outer medium, either before or after penetration of the boundary surface; the rest of the radiation is absorbed by electric conduction currents in the particle. On the boundary surface separating the particle from the surroundings, the electric and magnetic forces in the outer medium merge into the components produced by the wave inside the sphere.

The disturbance caused by the particle depends in the first place on the ratio $2a/\lambda$ between the diameter of the particle and the wave-length of light, and in the second place on the optical properties of each medium. When the diameter of the particle is large in comparison with the wave-length, the vibrations transmitted along a given direction from various points of the particle surface may possess appreciable phase differences, so that patterns with alternate dark and bright zones are produced around the obstacle. The phase difference between the vibration transmitted directly through the centre of the sphere and the vibrations transmitted, for instance, from the two poles at the end of a diameter perpendicular to the direction of propagation of the wave, may be such that behind the particle the light is either strengthened or extinguished. On very small particles, on the other hand, the vibrations of all the points on the surface are approximately in phase, even

[1] *Manuscript received June 24, 1941.*

Contribution from the Research Plans and Publications Section, National Research Laboratories, Ottawa, Canada. Issued as N.R.C. No. 1015.

[2] *Research Investigator.*

after more than one complete passage through the particle, and the main result is radiation of light in all directions rather than the formation of distinct beams of light. Close to the direction of propagation large phase differences are then found only at points so remote from the small sphere that the intensity has become negligible.

The main complication with respect to the better known diffraction observed near sharp edges or behind small opaque discs is that in the case of spherical particles the phase differences and amplitudes depend not only on the path traversed but on the nature of the particle, that is, whether it consists of a dielectric or a conductor. When the sphere is formed of an ideal conductor the small dimensions prevent it from acting as an impenetrable barrier or sink submerged in the light. Neither does the particle behave as a multitude of elementary sources of light, all vibrating in phase and allowing the resultant effect to be obtained by drawing the spherical wavelets according to Huygen's principle.

But whether the particle is opaque or transparent, in so far as the vibration observed along a given direction is the resultant of the vibrations propagated from points inside and outside the sphere, the diffraction due to large particles and the scattering by particles with a diameter smaller than the wave-length of light in the surrounding medium are both subject to the laws expressed by Maxwell's equation of the electromagnetic field (2).

In the calculation of the amplitudes for the diffracted or scattered wave that reaches a given point, the spherical particle is placed at the origin of a system of co-ordinates consisting of three axes (x, y, z) at right angles (Fig. 1). The position of any point is expressed by its distance ρ from the centre, or better by the much enlarged distance $r = 2\pi\rho m/\lambda$, where m, the square root of the dielectric constant, is the refractive index at that distance (m_n inside the particle, m_0 outside the particle), and λ is the wave-length measured in the medium concerned (5). All over the surface of the particle, r assumes the two distinct values $\alpha = 2\pi a m_0/\lambda$ or $\beta = 2\pi a m_n/\lambda$; the first value holds when the point is considered to belong to the inner medium, and the second, when to the outer medium. The azimuth, θ, or co-latitude, of the point, measured between the vertical axis x and the line joining the point to the origin, and the longitude ϕ, counted from axis y in the plane (y, z), serve as the second and third co-ordinates of the point. A plane wave of light of frequency f is assumed

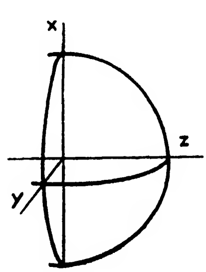

FIG. 1. *System of co-ordinates x, y, z, chosen for the small sphere.*

to advance toward the centre along the axis z through a medium in which the wave-length is λ/m_0 and the magnetic permeability μ. If the electric vibrations of this incident wave take place parallel to axis x in the plane (x, z), the equations of the components along the three axes (x, y, z) are

$$e_x = \epsilon^{2\pi i f t + 2\pi i m_0 z/\lambda} \qquad h_x = 0$$
$$e_y = 0 \qquad h_y = -\sqrt{\frac{k}{\mu}}\,\epsilon^{2\pi i f t + 2\pi i m_0 z/\lambda}$$
$$e_z = 0 \qquad h_z = 0$$

The amplitude of the incident vibration is taken as unity.

When applied to alternating currents represented by $E\epsilon^{2\pi i f t}$ and $H\epsilon^{2\pi i f t}$ Maxwell's equation for the amplitude of the electrical vibrations along the directions (r, θ, ϕ) becomes

$$E_r r^2 \sin\theta = \frac{\partial(r\sin\theta M_\phi)}{\partial\theta} - \frac{\partial(rM_\theta)}{\partial\phi}$$

$$E_\theta r\sin\theta = \frac{\partial M_r}{\partial\phi} - \frac{\partial(M_\phi r\sin\theta)}{\partial r}$$

$$rE_\phi = \frac{\partial(rM_\theta)}{\partial r} - \frac{\partial M_r}{\partial\theta}$$

The expression

$$M = -\frac{if\mu\lambda H}{m}$$

is used in place of the component H of the magnetic field.

A second similar group of equations is valid for the amplitudes of the components of the magnetic field M_r along the radius, M_θ along a meridian circle, and M_ϕ along a circle of latitude. Elimination of the other variables leads to the equation

$$\frac{\partial^2(r^2E_r)}{\partial r^2} + \frac{1}{\sin\theta}\,\frac{\partial}{\partial\theta}\left(\sin\theta\,\frac{\partial E_r}{\partial\theta}\right) + \frac{1}{\sin^2\theta}\,\frac{\partial^2E_r}{\partial\phi^2} + r^2E_r = 0$$

and to a perfectly similar equation in which M_r replaces E_r. It is assumed that a solution for E_r, and consequently also for E_θ and E_ϕ, exists in the form of a product, or rather an infinite series of products of two functions, the first one a function of the distance r only, the second a function of the angles θ and ϕ,

$$E_r = \frac{K_\nu(r)}{r^2}\,P_\nu(\theta, \phi),$$

where the subscript ν is any whole number different from zero. Substitution of this expression for E_r in the differential equation furnishes two separate relations for K and P, with the solution

$$i^\nu K_\nu(r) = C_\nu(r) - iS_\nu(r)$$

for all points outside the particle, whereas for points inside the particle there remains the solution

$$K_\nu(r) = S_\nu(r)$$

The functions S and C are simple Bessel functions for which the order is half an odd integer:

$$S_\nu(r) = \sqrt{\frac{\pi r}{2}}\, J_{\nu+½}(r) \qquad \text{and} \qquad C_\nu(r) = (-1)^\nu \sqrt{\frac{\pi r}{2}}\, J_{-\nu-½}(r).$$

The equation for $P(\theta, \phi)$ is identical with the differential equation valid for the functions known as spherical surface harmonics or Laplace functions used in certain solutions of the wave equation. Since

$$\epsilon^{2\pi i m s/\lambda} = \epsilon^{ir\cos\theta} = \sum_1^\infty (2\nu + 1) i^{\nu-1} \frac{S_\nu(r)}{r^2}\, \Pi_\nu(\cos\theta)$$

where

$$\Pi_\nu(\cos\theta) = \frac{P_\nu(\theta,\phi)}{\cos\theta},$$

the incident plane wave also can be considered as composed of an infinite number of waves of varying amplitudes expressed by products of the same kind of Bessel functions of r, and Laplace functions of θ and ϕ, for instance,

$$E_r = \sum_1^\infty (2\nu + 1) i^{\nu-1} \frac{S_\nu}{r^2} P_\nu$$

All the components have the same frequency and must not be confused with natural partial waves.

The electric and magnetic amplitudes that the incoming plane wave of unit amplitude excites along the axes of co-ordinates add themselves to the similar amplitudes, proportional to a_ν and p_ν, set up by vibrations returning from the particle but involving the functions $E_\nu = C_\nu - iS_\nu$. In the interior of the particle the amplitudes are proportional to b_ν and q_ν. According to the equations of continuity for the boundary surface, at the distance $\rho = a$, the following relations hold at any time for each of the ν vibrations:

$$\begin{aligned}
-(2\nu + 1)S_\nu'(\alpha) + a_\nu E_\nu'(\alpha) &= (-1)^\nu \alpha/\beta\, b_\nu S_\nu'(\beta) \\
-(2\nu + 1)S_\nu(\alpha) + a_\nu E_\nu(\alpha) &= (-1)^\nu b_\nu S_\nu(\beta) \\
(2\nu + 1)S_\nu(\alpha) + p_\nu E_\nu(\alpha) &= (-1)^\nu \alpha/\beta\, q_\nu S_\nu(\beta) \\
(2\nu + 1)S_\nu'(\alpha) + p_\nu E_\nu'(\alpha) &= (-1)^\nu q_\nu S_\nu'(\beta)
\end{aligned}$$

Therefore the amplitudes of electrical vibrations issuing from the particle must be equal to

$$a_\nu = (2\nu + 1)(-1)^\nu \frac{\beta S_\nu'(\alpha)S_\nu(\beta) - \alpha S_\nu(\alpha)S_\nu'(\beta)}{\beta E_\nu'(\alpha)S_\nu(\beta) - \alpha E_\nu(\alpha)S_\nu'(\beta)}$$

the amplitudes of the magnetic vibrations leaving the particle are

$$p_\nu = -(2\nu + 1)(-1)^\nu \frac{\beta S_\nu(\alpha)S_\nu'(\beta) - \alpha S_\nu'(\alpha)S_\nu(\beta)}{\beta E_\nu(\alpha)S_\nu'(\beta) - \alpha E_\nu'(\alpha)S_\nu(\beta)}.$$

With the aid of these amplitudes it is possible to express the components E_r, E_θ, and E_ϕ of the electric wave at any point given by the modified distance r, the co-latitude θ, and the longitude ϕ.

When the actual distance from which the particles are observed (or if they are too small to be seen, the effects produced by them), measures thousands

of wave-lengths, the amplitudes in the medium at the point r, θ, ϕ outside the particles become

$$E_\theta = iM_\phi = -\frac{i}{r}\epsilon^{-ir}\Sigma\left(\frac{a_\nu}{\nu(\nu+1)}\Pi_\nu + \frac{p_\nu}{\nu(\nu+1)}(\cos\theta\Pi_\nu - (1-\cos^2\theta)\Pi_\nu')\right)$$

$$E_\phi = -iM_\theta = -\frac{i}{r}\epsilon^{-ir}\Sigma\left(\frac{a_\nu}{\nu(\nu+1)}(\cos\theta\Pi_\nu - \Pi_\nu'\cdot\sin^2\theta) + \frac{p_\nu}{\nu(\nu+1)}\Pi_\nu\right)$$

$$E_r = 0.$$

These formulas are valid on the assumption that with the electrical vibrations parallel to axis x, the amplitude of the plane wave of light that arrives along axis z is taken as unit amplitude. In practice the directions along which the particle is observed will be so chosen that they lie either in the plane of the equator (y, z), while the wave advances along z, and for these directions $\theta = \pi/2$, or in the plane (x, z) containing the electric oscillations, and for these directions $\phi = \pm\pi/2$. The electrical component E_ϕ along the circles of latitude vanishes for these special values; only the component E_θ along the meridian remains. It will be designated as E_1 when the particle is viewed from a point in the plane (y, z), and as E_2 when the optical effects are observed from a point lying in the plane (x, z). When the electrical oscillations in the incident wave are perpendicular, instead of parallel, to axis x in the plane (x, z), the designations E_1 and E_2 have to be interchanged. Unpolarized light is resolved into two components, one of them parallel, the other perpendicular to axis x.

The intensity of the light received in a direction is proportional to the square of the amplitude. The amplitude of the incoming plane wave was assumed to be unity. If the actual intensity is integrated around the particle for the duration of one second over the entire surface of a sphere whose area is very large compared to unity, the result contains positive and negative terms. The negative quantity represents the power withdrawn by the obstacle from the wave of unit amplitude and intensity; if there is one particle per unit volume, k represents therefore the power lost per unit length of path by scattering or diffraction, and at the same time the loss due to electrical convection currents excited in the particle. If there is one particle in unit volume, the total loss per unit path is equal to the real portion in the expression

$$k = \frac{-i}{2\pi}\frac{\lambda^2}{m^2}\Sigma(-1)^\nu(a_\nu - p_\nu).$$

The positive term

$$k_s = \frac{1}{2\pi}\frac{\lambda^2}{m^2}\sum_1^\infty\frac{|a_\nu|^2 + |p_\nu|^2}{2\nu+1}$$

represents the intensity of the radiation emitted by the particle. The difference ($k - k_s$) must be considered as the component of the radiation dissipated as heat.

Size of Carbon Black Particles

Enormous quantities of fine carbon particles are produced in the manufacture of carbon black, an industry that has acquired considerable importance during the last 30 years (4). The annual output amounts at present to about 250,000 tons, produced almost entirely in the United States. The principle of manufacture is the simple method according to which, in the absence of better protection for the eyes, soot is deposited from a luminous flame on a piece of glass intended for viewing the sun or other bright source of light. The finest particles obtained on a commercial scale are produced by the combustion of natural gas in a regulated supply of air, followed by rapid cooling of the flame gases. Thousands of flames in rows and groups impinge on the flat lower surface of a metal channel that is drawn slowly back and forth, catching the carbon particles in the rising flame before they have time to grow into very coarse grains. For the manufacture of special types of carbon black, discs and rollers have been used on occasion as depositing surfaces.

In another method the gas is burned in large flames, the clouds of smoke are collected in water, the powder is allowed to settle, and afterwards it is filtered, pressed, and dried. Electrostatic precipitation is also resorted to for gathering the particles. Carbon produced by such methods is known commercially as lamp black. The so-called thermatomic black is obtained by heating the hydrocarbon gases to temperatures at which they dissociate. Not all available supplies of natural gas are suited to the manufacture of carbon black. Gases rich in methane but poor in ethane give a hard graphitic grade of carbon black. Production methods in which the carbon is deposited on a moving surface, whether it be channel or roller, give the finest particles. In any case, however, the average particles produced by any of these methods are too small to be seen under the microscope, so that a study of the light they diffract or scatter is of interest.

In one of the earliest accurate and direct determinations of the size of carbon particles Mie's theory of scattering was used and the value of 175 mμ was obtained for the diameter of the carbon grains in a luminous flame fed by amyl acetate (7). This dimension must be considered as an average for lamp black and as an upper limit for gas black, because the size of the grains was limited only by the natural draught set up by the burner. Studies on carbon blacks with the aid of the ultra-microscope, or the study of sedimentation, or of carbon black diaphragms, and of precipitation in an electric field, gave diameters between about 50 and 60 mμ. In a recent investigation the electron microscope was applied to the problem; in another the rate of settling in a centrifuge was measured (3, 6). Both studies lead to the same mean value of the diameter, namely, 30 mμ for typical samples of channel black. Despite this small size, corresponding to a mass of 2.3×10^{-17} gm. if the specific weight is assumed to be equal to 7/4, each particle still contains about one million carbon atoms. The particles are not pure carbon, however, but contain slight traces of mineral and organic compounds. The fact that with these small spheres the time of grinding of Portland cement is reduced and the fineness enhanced suggests

that they are solid particles for which the optical constants obtained for arc carbons can be used (8). The study with the electron microscope led moreover to the conclusion that the preponderating form of the ultimate particles is spherical and that these fine grains may be treated as sensibly isotropic (3).

The refractive index of amorphous carbon, measured on electrodes of high purity is equal to $m = n(1 - i\kappa)$, where n may be taken with sufficient accuracy as equal to 2, and $n\kappa$, the absorption index, is equal to 2/3. When a plane wave has travelled a distance λ through a solid piece of carbon, its amplitude drops therefore to the fraction (exp.) $- 2\pi\kappa n$ or 0.015, the length λ being measured in air. The optical properties of this substance may be considered as constant throughout the visible spectrum.

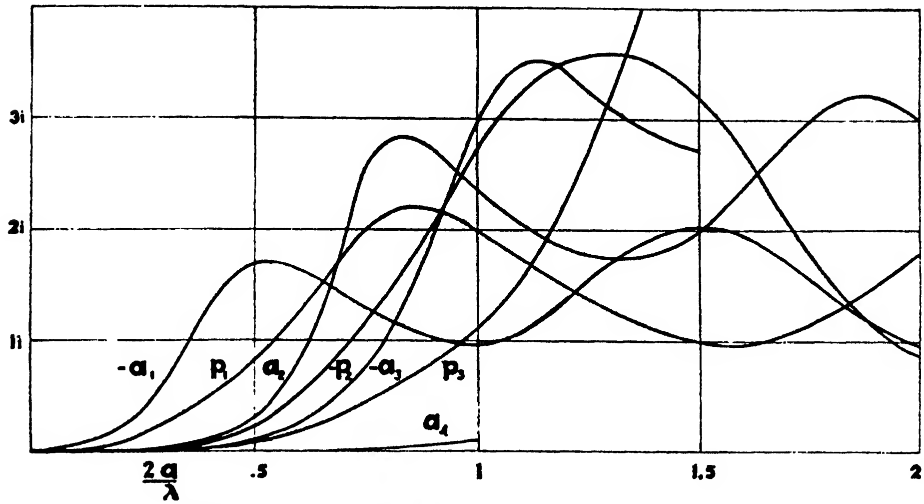

FIG. 2. *Amplitudes a_ν and p_ν of the electric and magnetic components of the oscillations issuing from the spherical obstacle and interfering in the outer medium with the oscillations of the incoming plane wave of unit amplitude.*

The absorption obtained in the presence of one carbon particle per unit volume is too small to be measured, since it is proportional to the product of λ^2 and a small number. However, as long as the number of particles per unit volume is not sufficient to cause overlapping, the coefficient of absorption k of the suspension of particles is proportional to the number of particles. It may be assumed that when the concentration of the carbon grains is such that they are unable to cover 1 sq. cm. after having been collected from 1 cu. cm. and placed side by side, there is no danger of serious overlapping. With particles 200 mμ in diameter there is room for 2.5×10^9 particles per unit area; with particles 20 mμ in diameter this number increases one hundredfold. Even with the larger particles it is therefore safe to compute the absorption coefficients for small multiples of 10^9 particles per unit volume. With concentrations greater than 10^{12} particles per cc., it becomes necessary to consider the finite free path of the light between particles.

The formula for the absorption coefficient may be written

$$k = -iN\frac{\lambda^2}{2\pi m_0^2}\sum_1^\infty(-1)^\nu(a_\nu - p_\nu) = -2i\frac{\pi a^2 N}{\alpha^2}\sum_1^\infty(-1)^\nu(a_\nu - p_\nu)$$

and it is valid so long as $N\pi a^2$, the total area of cross-section of the particles, is smaller than unity. On introducing the Bessel functions of half-integral order, the terms a_ν and p_ν are given by the simple formulae.

$$\frac{(-1)^\nu(2\nu+1)}{a_\nu} = -i + (-1)^\nu\frac{J_{-\nu-\frac{1}{2}}(\alpha)}{J_{\nu+\frac{1}{2}}(\alpha)}\,\frac{\dfrac{\beta}{\alpha}\dfrac{J'_{-\nu-\frac{1}{2}}(\alpha)}{J_{-\nu-\frac{1}{2}}(\alpha)} - \dfrac{J'_{\nu+\frac{1}{2}}(\beta)}{J_{\nu+\frac{1}{2}}(\beta)}}{\dfrac{\beta}{\alpha}\dfrac{J'_{\nu+\frac{1}{2}}(\alpha)}{J_{\nu+\frac{1}{2}}(\alpha)} - \dfrac{J'_{\nu+\frac{1}{2}}(\beta)}{J_{\nu+\frac{1}{2}}(\beta)}}$$

$$-\frac{(-1)^\nu(2\nu+1)}{p_\nu} = -i + (-1)^\nu\frac{J_{-\nu-\frac{1}{2}}(\alpha)}{J_{\nu+\frac{1}{2}}(\alpha)}\,\frac{\dfrac{\beta}{\alpha}\dfrac{J'_{\nu+\frac{1}{2}}(\beta)}{J_{\nu+\frac{1}{2}}(\beta)} - \dfrac{J'_{-\nu-\frac{1}{2}}(\alpha)}{J_{-\nu-\frac{1}{2}}(\alpha)}}{\dfrac{\beta}{\alpha}\dfrac{J'_{\nu+\frac{1}{2}}(\beta)}{J_{\nu+\frac{1}{2}}(\beta)} - \dfrac{J'_{\nu+\frac{1}{2}}(\alpha)}{J_{\nu+\frac{1}{2}}(\alpha)}}$$

where

$$J'_{\nu+\frac{1}{2}}(\alpha) = J_{\nu-\frac{1}{2}} - \frac{2\nu+1}{2\alpha}J_{\nu+\frac{1}{2}}$$

$$J'_{-\nu-\frac{1}{2}}(\alpha) = -J_{-\nu+\frac{1}{2}} - \frac{2\nu+1}{2\alpha}J_{-\nu-\frac{1}{2}}$$

Fig. 2 shows the values of the first terms a_1, a_2, and p_1, p_2 when the ratio $2a/\lambda$ increases from 0 to 2.

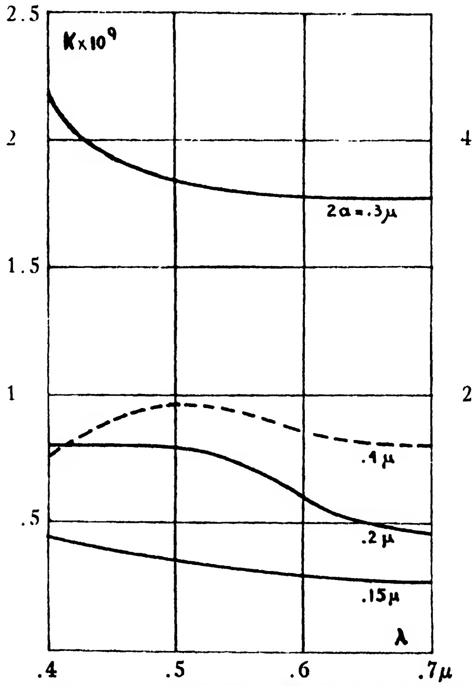

FIG. 3. *Coefficient of absorption for different particle sizes (radius a = 0.075 to 0.2μ) at various ratios $2a/\lambda$. (The scale for 4 μ is on the right.)*

A glance at the expressions for a_ν and p_ν shows that they are functions of the ratio $2a/\lambda$, not of a and λ separately (1). The dimensions enter only through the product $N\pi a^2$, the total area of cross-section in unit volume, with which the sum of the differences has to be multiplied in order to obtain the coefficient of absorption. Were there no diffraction or scattering, the carbon particles would behave as simple geometrical screens, and the absorption coefficient would be proportional to $N\pi a^2$. The coefficient tends toward this value for the larger particles, but possesses higher values for small ratios $2a/\lambda$; moreover it varies markedly with the wave-length despite the fact that the optical constants of a solid block of carbon, which show no difference between wave-lengths in the visible spectrum, have been assumed to be valid. The coefficient of absorption (Fig. 3) increases toward the blue when the particles have a diameter of 0.1 to 0.2 μ, the increase amounting to more than 40% between 700 mμ and 500 mμ. A cloud of such particles will appear red by transmitted light, and blue in scattered light, an effect well known from the observation of columns of smoke. An opposite effect is obtained for the larger particles of 0.3 and 0.4 μ, but the percentage change is small, and the particles assume more and more the properties of the gray body represented by amorphous carbon.

Acknowledgment

The results of this study were computed in 1931 at the request of Dr. D. F. Stedman, Chemistry Division, National Research Laboratories. The author is indebted to him for having called his attention to this problem.

References

1. Blumer, H. Z. Physik, 38 : 304-329, 920-947. 1926.
2. Bromwich, T. J. I'A. Trans. Roy. Soc. (London) A. 220 : 175-206. 1920.
3. Columbian Carbon Research Laboratories. Rubber Chem. Tech., 14 : 52-84. 1941.
4. Drogin, I. Chem. & Met. Eng. 43 : 139-142. 1936.
5. Mie, G. Ann. Physik, (4) 25 : 377-445. 1908.
6. Parkinson, D. Rubber Chem. Tech. 14 : 98-112. 1941.
7. Senftleben, H. and Benedict, E. Ann. Physik, 60 : 297-323. 1919.
8. Sweitzer, C. W. and Craig, A. E. Ind. Eng. Chem. 32 : 751-756. 1940.

Canadian Journal of Research

Issued by THE NATIONAL RESEARCH COUNCIL OF CANADA

VOL. 19, SEC. A. NOVEMBER, 1941 NUMBER 11

BAND SPECTRUM AND STRUCTURE OF THE BCl MOLECULE[1]

BY G. HERZBERG[2] AND W. HUSHLEY[3]

Abstract

The $^1\Pi - {}^1\Sigma^+$ system of the BCl molecule has been photographed in the sixth order of a 20 ft. grating. The previous interpretation of the vibrational structure by Miescher (5) is slightly modified. The new formula for the Q heads of the $B^{11}Cl^{35}$ molecule is

$$\nu = 36750.92 + 849.04(v'+\tfrac{1}{2}) - 11.37(v'+\tfrac{1}{2})^2 - 0.100(v'+\tfrac{1}{2})^3 - 0.0271\,(v'+\tfrac{1}{2})^4 - [839.12(v''+\tfrac{1}{2}) - 5.11(v''+\tfrac{1}{2})^2]$$

The fine structure of a number of bands has been measured and analysed, leading to the following accurate values for the rotational constants: $B_e' = 0.7054$ cm.$^{-1}$, $\alpha_e' = 0.00820$ cm.$^{-1}$, $B_e'' = 0.6838$ cm.$^{-1}$, $\alpha_e'' = 0.00646$ cm.$^{-1}$. The internuclear distance in the ground state is $r_e'' = 1.716 . 10^{-8}$ cm. The molecular constants of BCl are compared with those of the iso-electronic molecules CS, PN, and SiO as well as with those of BBr, BCl_3, and BBr_3.

A. Introduction

Jevons (4) in 1924 discovered a band system of BCl in the region 2600 to 2900Å in a discharge through boron trichloride vapour. The vibrational structure of this system was analysed in 1935 by Miescher (5). While investigating the band spectra of the molecules B_2 and BN we found it possible to obtain the BCl spectrum with sufficiently high dispersion to make possible a rotational analysis. In the course of the investigation it turned out that Miescher's interpretation of the vibrational structure had to be changed somewhat. An accurate knowledge of the vibrational and rotational constants of BCl obtained here should be of interest particularly for a comparison with other diatomic molecules and with certain polyatomic molecules.

B. Experimental

The BCl spectrum was excited in an ordinary uncondensed discharge through helium to which a small amount of boron trichloride vapour had been added. Such a discharge is preferable to one through boron trichloride vapour alone, since, in the latter, higher rotational levels are excited which give rise to a much greater complexity of the spectrum.

[1] *Manuscript received September 23, 1941.*

Contribution from the Department of Physics, University of Saskatchewan, Saskatoon, Sask., with financial assistance from the National Research Council of Canada.

[2] *Research Professor of Physics.*

[3] *Graduate Student, holder of a Bursary (1940-41) under the National Research Council of Canada.*

The spectrum was taken in the sixth order of the Saskatoon 20 ft. grating. The exposure times were 3 to 15 hr. Figs. 1 and 2 give enlargements of the spectra obtained. The band lines were measured against iron lines of the fifth and sixth orders by means of a Gaertner comparator.

C. Vibrational Analysis

The ultra-violet BCl bands represent a band system with well developed sequences (see Fig. 1). The vibrational analysis would therefore be very simple if it were not for the facts that four isotopic species, $B^{11}Cl^{35}$, $B^{10}Cl^{35}$, $B^{11}Cl^{37}$, $B^{10}Cl^{37}$ exist, whose spectra overlap, that the bands are not all shaded in the same direction, and that in general each one has two heads. At first sight the analysis given by Miescher (5) would appear to be correct. But there are two points in the vibrational structure that cannot be explained on its basis: (1) The two bands 37580.39 and 37552.45 cm.$^{-1}$ are assigned by Miescher as 1–0 bands of $B^{10}Cl^{35}$ and $B^{11}Cl^{35}$ respectively in spite of the fact that their intensity ratio 8 : 7 (as given by Miescher and confirmed by our plates, Fig. 1) disagrees radically with the abundance ratio 1 : 4 (approximately) of the two isotopic species. Very artificial assumptions would be necessary to explain this unless one assumes that the two bands are the 1–0 and 2–1 bands of $B^{11}Cl^{35}$ and increases the numbering of the succeeding bands correspondingly. Indeed, on our plates two further weaker bands appear at 37610.41 and 37605.17 (see Fig. 1), which are naturally explained as 1–0 bands of $B^{10}Cl^{35}$ and $B^{10}Cl^{37}$. These bands have not been found by Miescher apparently because they were hidden by the rotational structure of the preceding bands which extend in his source much further than in ours. (2) In the $\Delta v=0$ sequence the strong band head 36751.10 has not been assigned by Miescher although it is given by him. The only possible explanation on the basis of Miescher's analysis is that it is the $B^{10}Cl^{35}$ isotopic band belonging to the main band 36754.22 which Miescher considers as 0–0. However, the isotope shift would then be far too large (4.1 cm.$^{-1}$ against a value of 0.33 cm.$^{-1}$ calculated from Miescher's formula). The only reasonable explanation seems to be that the band 36751.10 is the 1–1 of $B^{11}Cl^{35}$, and that the 0–0 and 1–1 bands of $B^{10}Cl^{35}$ are not separated from the corresponding $B^{11}Cl^{35}$ bands. On this assumption the numbering of the succeeding bands in this sequence has of course to be raised by one unit. In fact, a reasonable variation in the $\Delta G'$ and $\Delta G''$ values can be obtained only by raising the numbering in all sequences simultaneously.

Table I gives the Deslandres table for the Q heads of $B^{11}Cl^{35}$ and $B^{10}Cl^{35}$ with the new assignment. Wherever available our new wave numbers obtained under high dispersion are given while for the bands that we could not measure Miescher's values are used. The former are given with one more decimal place.

Please cut on dotted line and attach lower part of this gummed strip to page 215, Section B, Canadian Journal of Research, Volume 19 (9), September, 1941.

ERRATUM

Page 215, Fig. 3, for "Wt. % Pb" read "Wt. % Al", and for "Wt. % Al" read "Wt. % Pb".

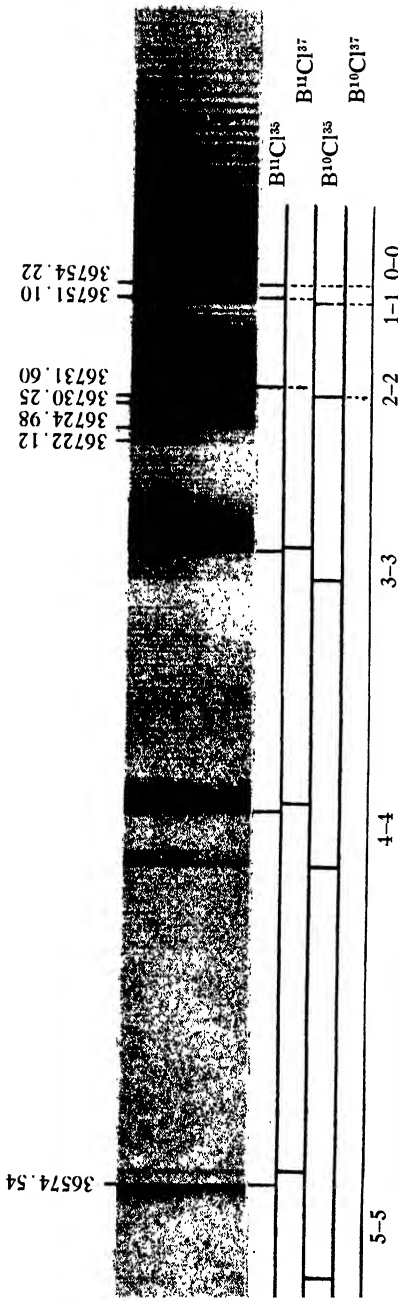

36754.22
36751.10
36731.60
36730.25
36724.98
36722.12
36574.54
$B^{11}Cl^{35}$
$B^{11}Cl^{37}$
$B^{10}Cl^{35}$
$B^{10}Cl^{37}$
0–0
1–1
2–2
3–3
4–4
5–5

FIG 1*a*.

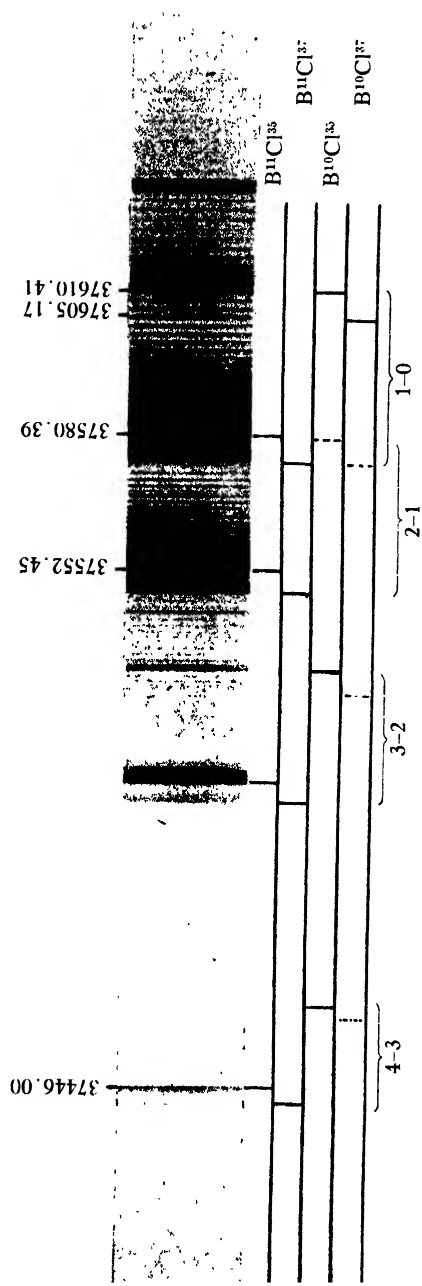

37610.41
37605.17
37580.39
37552.45
37446.00
$B^{11}Cl^{35}$
$B^{11}Cl^{37}$
$B^{10}Cl^{35}$
$B^{10}Cl^{37}$
1–0
2–1
3–2
4–3

FIG. 1*b*.

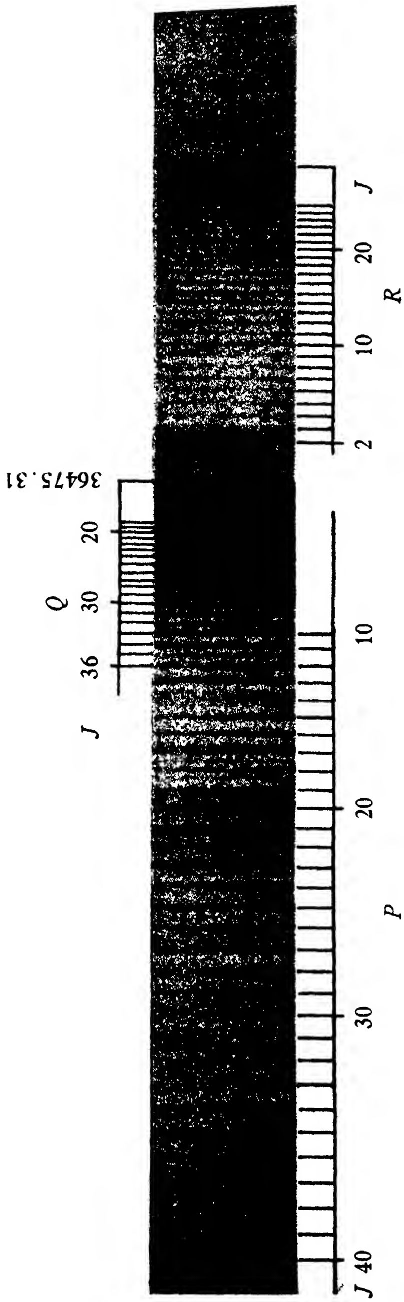

FIG. 2.

TABLE I

Deslandres table of the ultra-violet BCl bands

The upper figure for a given v' and v'' is the wave number of the Q head of $B^{11}Cl^{35}$, the lower figure that of the Q head of $B^{10}Cl^{35}$. Overlapped bands are in square brackets. The figures in parentheses are the deviations from Formulae (1) and (2) respectively.

v' \ v''	0	1	2	3	4	5	6	7	8
0	36754.22(−.08) [36754.2](−.2)	[35925.2](−.2) 35895.0(−.1)							
1	37580.39(+.25) 37610.41(+.45)	36751.10(−.14) 36750.10(−.56)	35931.9(−.7)						
2	38381.5(−.1) 38439.0(−.2)	37552.45(−.21) [37580.4](+.5)	36733.92(−.08)	[35925.2](−.3)					
3			37508.70(−.38) 37531.71(−.55)	36700.48(−.14) 36694.81(− 16)	35903.3(+ 9) 35870.4(+1.7)				
4				37446.00(−.85) 37462 81(−1.33)	36648.44(−.17) 36637.63(+.22)	35860 4(−.2) 35823.0(+.4)	35082.8(0 0)		
5				38158.7(−2.3)	37362 4(−.4) 37370.0(−1.8)	36574.54(−.21) 36556.33(−.24)	35796 5(−.5) 35753.8(+1.5)	35029.3(−.1)	
6					38041.1(+.1)	37253.4(+.4)	36475.31(+ 12)	35707.7(+.1)	
7						37890.8(0.0)		36345.0(−.4)	
8									36180.0(−.3)

TABLE II

WAVE NUMBERS OF BAND LINES

J	0–0 Band			1–0 Band			3–3 Band		4–3 Band	
	$R(J)$	$Q(J)$	$P(J)$	$R(J)$	$Q(J)$	$P(J)$	$R(J)$	$P(J)$	$R(J)$	$P(J)$
6		36754 91	36747 13				36710 16	36692 69		37438 19
7	36766 44	55 24	45 93			37571.29	11 64	91.44	37456 61	36 67
8	68.12	55 56	44 77	37693.54		70 10	13 18	90.28	57.81	35.40
9	69.89	55 94	43.56	95.05		68 95	14 77	89.15	59 12	34.07
10	71.76	56 41	42 42	96.80		67 77	16 11	87 96	60.38	32.62
11	73.63	56.83	41 45	98 39		66.69	17.65	86 89	61.60	31 35
12	75.53	57 32	40.51	37700.08		65 53	19 27	85.75	62.81	29 94
13	77.53	57 87	39.66	01.76	37582 41	64.45	20 59	84 75	64 11	28 61
14	79.45	58 46	38.87	03 52	82.71	63 36		83.66	65 37	27 22
15	81.52	59.13	38 07	05 17	83.04	62.34		82.55	66 63	25 81
16	83.59	59 82	37.22	06.89	83 41	61 36	25 67	81 48	67.79	24.42
17	85.75	60.49	36 71	08.61	83.79	60 20	27 25	80.46	68.97	23 00
18	87.88	61.29	36.05	10 41	84.21	59.29	29 04	79 51	70 28	21 63
19	90 03	62.06	35 44	12 21	84 65	58.40	30.89	78.52	71.48	20 17
20	92.29	62.97	34.91	14 05	85 09	57 38	32 50	77 55	72.64	18 81
21	94.59	63 76	34 42	15 93	85 54	56.56	34.42	76 62	73.84	17 43
22	96 90	64.66	33 89	17 74	86.05	55 67	36 05	75 73	75 02	15 91
23	99.25	65 65	33 45	19 64	86 55	54 79	37 62	74 80	76 18	14 50
24	36801.65	66.66	33 05	21.51	87 07	53 94	39 66	73 92	77 30	13.04
25	04.09	67.65	32.77	23 48	87 60	53 15	41 45	73 10	78.39	11.61
26	06 57	68.75	32 50	25.43	88.19	52 45		72 19	79 43	10.07
27	09.08	69 89	32 24	27.39	88.85	51 65		71 34	80 59	08 62
28	11.64	71.12		29 37	89.39	50 81		70.47	81 78	07.08
29	14 24	72 35		31 30	90.00	50 03		69 77		05 62
30	16.87	73.63			90.57	49 32		68.93		
31	19.55	74.90		35 38	91 33	48.65		68.23		
32	22.39	76 24		37 41	92.05	47 92		67.44		
33	25.02	77.53		39 52	92.68	47 34		66.77		
34	27 82	79.08		41 61	93.54	46 78		66 01		
35	30.65	80 47		43 70	94 22	46 07		65 29		
36	33 46	81.97		45 81				64 59		
37	36.40	83.59		48 05				63 91		
38	39.36	85.07		50 11						
39	42.35	86.67		52.18						
40	45.34	88.32								
41	48.37	90.03								
42	51.51	91.79								
43	54.62	93 51								
44	57.77	95.26								
45	61.00	97.15								
46	64 22	99.25								
47		36801 02								
48		03.01								

The $B^{11}Cl^{35}$ Q heads, which are essentially the zero lines, can be represented by the formula

$$(1)\quad \nu(B^{11}Cl^{35}) = 36750.92 + [849.04(v'+\tfrac{1}{2}) - 11.37(v'+\tfrac{1}{2})^2 - 0.100(v'+\tfrac{1}{2})^3 - 0.0271(v'+\tfrac{1}{2})^4] - [839.12(v''+\tfrac{1}{2}) - 5.11(v''+\tfrac{1}{2})^2].$$

The deviations (observed minus calculated) from this formula are given in parentheses after each wave number in Table I. On the basis of the above formula also a few band heads unidentified by Miescher could be assigned.

According to the elementary theory of the isotope effect [see Herzberg (3)] the formula that should hold for the other isotopic species can be easily

TABLE II—*concluded*

WAVE NUMBERS OF BAND LINES—*concluded*

J	4–4 Band		5–5 Band		6–6 Band		
	$R(J)$	$P(J)$	$R(J)$	$P(J)$	$R(J)$	$Q(J)$	$P(J)$
2			36578.51		36479.03		
3			79.75		80.21		
4			81.02		81.39		
5			82.26	36568.17	82.56		
6			83.54	66.74	83.67		
7			84.80	65.47	84.79		
8	36660.49		86.06	64.12	85.85		
9	61.85	36636.88	87.30	62.81	86.89		36462.97
10	63.19	35.65	88.50	61.46	87.94		61.51
11	64.59	34.40	89.72	60.08	88.92	36473.84	60.02
12	66.01	33.22	90.93	58.74	89.94	73.54	58.42
13	67.44	32.01	92.17	57.34	90.90	73.26	56.91
14	68.93	30.77	93.34	56.02	91.83	72.92	55.31
15	70.47	29.57	94.53	54.63	92.70	72.55	53.66
16		28.39	95.72	53.23	93.58	72.14	52.18
17	73.10	27.20	96.86	51.85	94.44	71.77	50.42
18	74.80	25.97	98.02	50.43	95.26	71.35	48.76
19	76.10	24.74	99.20	49.02	96.03	70.89	47.05
20	77.55	23.73	36600.34	47.63	96.80	70.43	45.28
21	78.94	22.54	01.46	46.20	97.46	69.94	43.54
22	80.46	21.43	02.61	44.77	98.23	69.34	41.76
23	81.86	20.27	03.68	43.31	98.93	68.76	39.93
24	83.45	19.16	04.78	41.87	99.55	68.19	38.09
25	84.75	18.04	05.85	40.39	36500.05	67.53	36.22
26	86.29	16.85	06.87	38.99	00.73	66.84	34.30
27	87.78	15.81	07.99	37.45	01.22	66.16	32.40
28	89.15	14.62	09.07	35.98	01.70	65.41	30.42
29	90.70	13.51	10.15	34.43	02.17	64.66	28.46
30	92.11	12.40	11.28	32.94	02.57	63.84	26.39
31	93.62	11.28	11.99	31.42	02.96	62.97	24.35
32		10.15	12.95	29.90	03.33	62.11	22.21
33		09.07	13.95	28.36		61.17	20.08
34			14.85	26.68		60.25	17.91
35			15.81	25.14		59.30	15.68
36				23.48		58.42	13.43
37				21.92			11.10
38				20.27			08.83
39				18.57			06.41
40				16.89			04.02
41				15.11			

obtained from Equation (1). For $B^{10}Cl^{35}$ we found using $\rho = \sqrt{\frac{\mu}{\mu^i}} = 1.03715$ (μ and μ^i are the reduced masses of $B^{11}Cl^{35}$ and $B^{10}Cl^{35}$ respectively).

$$(2)\ \nu(B^{10}Cl^{35}) = 36750.92 + [880.58(v'+\tfrac{1}{2}) - 12.23(v'+\tfrac{1}{2})^2 - 0.1116(v'+\tfrac{1}{2})^3 - 0.0313(v'+\tfrac{1}{2})^4] - [870.29(v''+\tfrac{1}{2}) - 5.50(v''+\tfrac{1}{2})^2].$$

The deviations of the observed $B^{10}Cl^{35}$ bands from this formula are also given in parentheses in Table I. It is seen that the agreement is very satisfactory. This is another confirmation of the new vibrational analysis since Miescher in his analysis found deviations between observed and calculated isotope shifts up to 6 cm.$^{-1}$.

A further important confirmation of the new vibrational assignment comes from the rotational analysis (see below).

It should be noted that the strong head at 36731.60 cm.$^{-1}$ which was considered as Q head of the 1–1 band by Miescher is actually the P head of the 0–0 band of $B^{11}Cl^{35}$. This is shown by the fact that it occurs at exactly the place where it is expected from the analysis of the rotational structure (see below) and that, if considered as 2–2 band in our numbering, it would give a deviation of 2.4 cm.$^{-1}$ from the formula, which is much greater than the accuracy of the measurements. The actual 2–2 band can just be recognized at 36733.92 cm.$^{-1}$ under the stronger P head of the 0–0 band. The head at 36730.25 is obviously the corresponding P head of the 0–0 band of $B^{10}Cl^{35}$, which no longer coincides with that of $B^{11}Cl^{35}$ on account of the rotational isotope shift. Similarly, the heads at 36724.98 and 36722.12 cm.$^{-1}$, which were considered as P heads of the 0–0 band by Miescher, must be interpreted as P heads of the 1–1 band of $B^{11}Cl^{35}$ and $B^{10}Cl^{35}$ respectively.

D. Rotational Analysis

As an illustration Fig. 2 gives a greatly enlarged reproduction of the fine structure of the 6–6 band. In spite of the slight overlapping by the isotopic bands the three branches P, Q, and R can be easily recognized; this confirms Miescher's conclusion that the band system represents a $^1\Pi - {}^1\Sigma$ transition. The numbering in the branches of the 6–6 band was obtained by systematic trial until the relation $R(J) - Q(J) = Q(J+1) - P(J+1)$ was fulfilled for all J values. This numbering also agrees with that obtained directly from the spectrogram for the R branch if it is assumed that the head of the Q branch is at ν_0 (see Fig. 2). In a similar way the 0–0 and 1–0 bands were analysed. For them the correctness of the numbering is further confirmed by the exact agreement of the Δ_2F'' values which at the same time confirms the vibrational analysis. For the other bands measured, the Q branch was not or not as well resolved. But for them the numbering could be obtained from the position of the Q head or the agreement of combination differences in two bands of the same v' or the same v''.

Table II gives the wave numbers of the band lines in all the analysed bands. In order to save space we refrain from giving all the combination differences but illustrate only in Table III the kind of agreement obtained by the values of $\Delta_2F''(J) = R(J-1) - P(J+1)$ of the 0–0 and 1–0 bands as far as they can be formed for both bands. The excellent agreement of the two columns supplies the final proof for our new vibrational numbering. According to Miescher's analysis the two bands are the 0–0 band of $B^{11}Cl^{35}$ and the 1–0 band of $B^{10}Cl^{35}$ and therefore the Δ_2F'' should be quite different.

From the combination differences the rotational constants B_v and D_v were obtained in the usual way [see Herzberg (3)]. As far as possible Δ_2F values were used but in those cases in which the P or the R branch was not measurable Δ_1F values had to be used. The latter procedure is open to objection only

TABLE III

COMBINATION DIFFERENCES $\Delta_2F''(J)$ FOR THE 0–0 AND 1–0 BANDS

J	0–0 Band	1–0 Band	J	0–0 Band	1–0 Band
9	25.70	25.77	18	50.31	50.21
10	28.44	28.36	19	52.97	53.03
11	31.25	31.27	20	55.61	55.65
12	33.97	33.94	21	58.40	58.38
13	36.66	36.72	22	61.14	61.14
14	39.46	39.42	23	63.85	63.80
15	42.23	42.16	24	66.48	66.49
16	44.81	44.97	25	69.15	69.09
17	47.54	47.60	26	71.85	71.83

when there is an appreciable Λ-type doubling in the $^1\Pi$ state. Actually for the bands in which all three branches could be measured no combination defect between $R(J) - Q(J)$ and $Q(J+1) - P(J+1)$, which would indicate a Λ-type doubling, was found. Also an independent determination of B_0'' from the Δ_2F'' values of the 1–0 band and from the Δ_1F'' values of the 0–0 band gave exact agreement.

TABLE IV

ROTATIONAL CONSTANTS OF $B^{11}Cl^{35}$

v	Upper state, $^1\Pi$		Lower state, $^1\Sigma^+$	
	B_v', cm.$^{-1}$	D_v', cm.$^{-1}$	B_v'', cm.$^{-1}$	D_v'', cm.$^{-1}$
0	0.7013	$1.80\cdot10^{-6}$	0.6806	$1.75\cdot10^{-6}$
1	0.6919	$1.92\cdot10^{-6}$		
2				
3	0.6704	$(2.46\cdot10^{-6})$*	0.6612	$1.92\cdot10^{-6}$
4	0.6586	$2.70\cdot10^{-6}$	0.6549	$2.15\cdot10^{-6}$
5	0.6454	$3.05\cdot10^{-6}$	0.6483	$2.10\cdot10^{-6}$
6	0.6308	$3.45\cdot10^{-6}$	0.6419	$2.19\cdot10^{-6}$

**This value was obtained by interpolation between the other D_v' values.*

The resulting values of B_v and D_v for the upper and lower states are listed in Table IV. The B_v values are also plotted against v in Fig. 3. It is seen that B_v'' is very closely a linear function of v'', while B_v' is decidedly curved. The values of B_e, α_e, γ_e in

(3) $$B_v = B_e - \alpha_e(v+\tfrac{1}{2}) + \gamma_e(v+\tfrac{1}{2})^2$$

are given in Table V below.

The intersection of the B_v curves of the upper and lower states (Fig. 3) accounts for the fact that the direction of shading changes from violet to red in each sequence of the BCl bands. As previously noted by Miescher, for the bands nearest to the reversal of the shading, a reversal even within the band takes place, that is, one branch may have two heads or there may be a head in both the P and R branch. Fig. 1*b* shows clearly two opposing

heads in the Q branch of the 4–4 band of $B^{10}Cl^{35}$ and, not quite so clearly, for the corresponding band of $B^{11}Cl^{35}$. This effect is due to the term $DJ^2(J+1)^2$ in the energy formula [see Herzberg (3)]. In Fig. 4, Δ_1F' and Δ_1F''

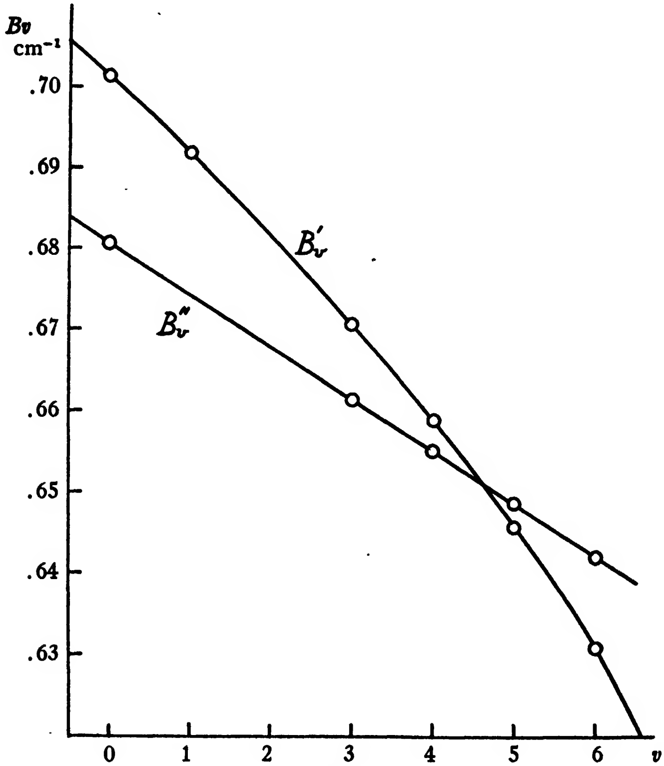

FIG. 3

TABLE V

MOLECULAR CONSTANTS OF $B^{11}Cl^{35}$

——	Upper state, $^1\Pi$	Lower state, $^1\Sigma^+$
B_e, cm.$^{-1}$	0.7054	0.6838
B_0, cm.$^{-1}$	0.7012	0.6806
α_e, cm.$^{-1}$	0.00820	0.00646
γ_e, cm.$^{-1}$	0.00050	
D_e, cm.$^{-1}$	$1.60\cdot10^{-6}$	$1.72\cdot10^{-6}$
β_e, cm.$^{-1}$	$0.27\cdot10^{-6}$	$0.07\cdot10^{-6}$
r_0, cm.	$1.694\cdot10^{-8}$	$1.720\cdot10^{-8}$
r_e, cm.	$1.689\cdot10^{-8}$	$1.716\cdot10^{-8}$
I_e, gm.-cm.^{2}	$39.68\cdot10^{-40}$	$40.94\cdot10^{-40}$
ω_e, cm.$^{-1}$	849.04	839.12
ω_ex_e, cm.$^{-1}$	11.37	5.11
ω_ey_e, cm.$^{-1}$	−0.100	
ω_ez_e, cm.$^{-1}$	−0.0271	
ν_e, cm.$^{-1}$	36750.92	

are plotted for the 4–4 band of $B^{11}Cl^{35}$ after subtracting $1.26(J+1)$. Where these two curves intersect, a head must occur since for those J values an increase of J does not change the position of the Q lines (since the change of energy is the same in the upper and lower state). It is seen that in addition to the ordinary Q head corresponding to $J = -1$ a second head is to be expected for $J=57$ because of the different curvature of the Δ_1F curves (that is, different D values). Substituting into the formula for the Q branch, the wave number of the second head is predicted to be at 36654.66 cm.$^{-1}$ while the (not very accurate) observed value is 36654.3 cm.$^{-1}$.

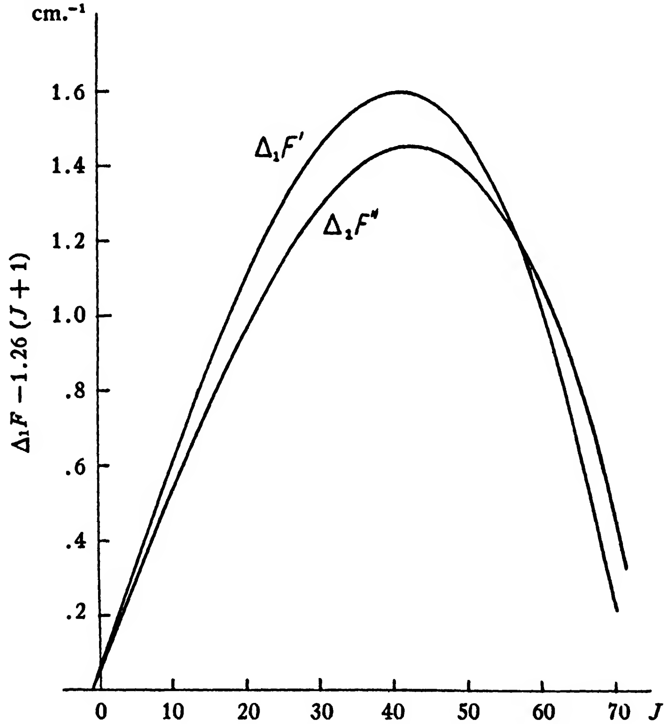

FIG. 4

It is clear from Fig. 4 that such an additional head can occur only when B' and B'' are very nearly equal (as for bands near the point of reversal of shading in a sequence) and when in addition D' is rather different from D'' and $D'-D''$ has the same sign as $B'-B''$.

E. Molecular Constants and Comparisons with Other Molecules

In Table V are listed the rotational as well as the vibrational constants of the $B^{11}Cl^{35}$ molecule that follow from the above analysis. The values for the internuclear distances and moments of inertia are based on the atomic constants used by Herzberg (3). $^1\Pi-^1\Sigma^+$ band systems very similar to the one investigated here for BCl have been observed to be the strongest transitions of the isoelectronic molecules CS, PN, and SiO. Since in the case of PN

TABLE VI

MOLECULAR CONSTANTS OF MOLECULES WITH 22 ELECTRONS ($^1\Pi$–$^1\Sigma^+$ TRANSITIONS)

Molecule	BCl	CS	PN	SiO
r_e''(10^{-8} cm.)	1.716	1.536	1.491	1.510
r_e'(10^{-8} cm.)	1.689	1.563	1.547	1.621
ω_e''(cm.$^{-1}$)	839.12	1285.1	1337.24	1242.03
ω_e'(cm.$^{-1}$)	849.04	1072.3	1103.09	851.51
ν_e(cm.$^{-1}$)	36750.92	38912.15	39805.66	42835.3
Reference	This paper	(1)	(2)	(7)

and SiO these $^1\Pi$–$^1\Sigma^+$ transitions have also been observed in absorption it may be concluded that for all four molecules the lower $^1\Sigma^+$ state is the ground state. Thus the data in the last column of Table V refer to the ground state of $B^{11}Cl^{35}$.

It is interesting to compare the molecular constants of the four isoelectronic molecules BCl, CS, PN, and SiO in the upper and lower states of their $^1\Pi$–$^1\Sigma^+$ transitions. Table VI gives the necessary data. As is to be expected the r_e values in both upper and lower states have a minimum, the ω_e values a maximum value for PN. However, it is rather unexpected that the value of the excitation energy ν_e increases from BCl to SiO (that is, with increasing atomic number of the lighter atom). Unfortunately, data for the next molecule in this series AlF are not available. But they could be predicted roughly on the basis of Table VI: the r_e and ω_e values should be similar to those of BCl, while the electronic excitation is probably even higher than that of SiO.* Relations very similar to those for BCl, CS, PN, SiO exist for the molecules BBr, CSe, AsN, and GeO.

Another interesting comparison can be made between the diatomic molecules BCl and BBr, on the one hand, and the four-atomic molecules BCl_3 and BBr_3, on the other. Table VII gives the boron-halogen internuclear distances r_0 and force constants k for these molecules. The r_0 values for the trihalides are electron diffraction values [taken from Pauling (6)], which have a much smaller accuracy than the spectroscopic values for the diatomic molecules. But within this accuracy (± 0.02) the boron-halogen distance is the same in the diatomic radical and the saturated polyatomic molecule. The force constants for the trihalides are those given by Wu (8) as obtained from the observed fundamental vibrations of these molecules. In order to give comparable values for the diatomic radicals their force constants have been evaluated from the $\Delta G''_{\frac{1}{2}}$ values not from ω_e or ω_0. Again the values agree

* *Note added in proof: In stating that no data for AlF are available, we overlooked, unfortunately, a paper by G. D. Rochester (Phys. Rev. 56 : 305-307. 1939) in which the absorption spectrum of AlF has been studied. The constants ω_e'', ω_e' and ν_e were found by Rochester to have respectively the values of 814.5, 822.9, and 43935 cm.$^{-1}$ and are thus in good agreement with the predictions made above.*

TABLE VII

B–Cl AND B–Br DISTANCES AND FORCE CONSTANTS IN BCl, BBr, BCl_3, AND BBr_3

—	in BX	in BX_3
r_0(B−Cl) (10^{-8} cm.)	1.720	1.74 } X = Cl
k (B−Cl) (10^5 dynes/cm.)	3.391	3.30 } X = Cl
r_0(B−Br) (10^{-8} cm.)	1.89	1.87 } X = Br
k (B−Br) (10^5 dynes/cm.)	2.612	2.50 } X = Br

in the diatomic radical and the corresponding saturated molecule within the accuracy of the latter values. It may be mentioned that differences *greater* than ± 0.02Å in r_0 and $\pm 0.1 \cdot 10^5$ dynes/cm. in k are found when the C–H distances and force constants in free CH, in C_2H_2, CH_4, and C_2H_4 are compared while, on the other hand, the observed differences of the OH and SH distances and force constants in free OH and SH, and in H_2O and H_2S respectively are smaller than the limits given, as is the case for the boron halides. It is to be expected that with the more precise measurements for the four-atomic halides small differences of the same order as actually observed for OH–H_2O, SH–H_2S will be found.

Acknowledgment

The authors are greatly indebted to the American Philosophical Society for a grant from the Penrose Fund through which the grating spectrograph was provided.

References

1. Crawford, F. H. and Shurcliff, W. A. Phys. Rev. (Ser. 2) 45(12) : 860-870. 1934.
2. Curry, J., Herzberg, L., and Herzberg, G. Z. Physik, 86 : 348-366. 1933.
3. Herzberg, G. Molecular spectra and molecular structure. I. Diatomic molecules. Prentice-Hall, Inc., New York. 1939.
4. Jevons, W. Proc. Roy. Soc. (London) A, 106 : 174-194. 1924.
5. Miescher, E. Helv. Phys. Acta, 8 : 279-308. 1935.
6. Pauling, L. C. The nature of the chemical bond and the structure of molecules and crystals. Cornell University Press, Ithaca, N.Y. 1939.
7. Saper, P. G. Phys. Rev. (Ser. 2) 42(4) : 498-508. 1932.
8. Wu, T.-Y. Vibrational spectra and structure of polyatomic molecules. National University of Peking, Peking. 1939.

Canadian Journal of Research

Issued by THE NATIONAL RESEARCH COUNCIL OF CANADA

VOL. 19, SEC. A. DECEMBER, 1941 NUMBER 12

SOME PROPERTIES OF A COMPOSITE, BIVARIATE DISTRIBUTION IN WHICH THE MEANS OF THE COMPONENT NORMAL DISTRIBUTIONS ARE LINEARLY RELATED[1]

BY F. CHARNLEY[2]

Abstract

Equations relating the statistics of a linear, composite, bivariate, normal distribution with those of the component distributions are derived for two types of data; first, for the special (ideal) case when the means represented by the samples correspond to the points of the linear continuum, and the proportions of the component populations remain constant and, second, for the practical case when the point set representing the means of the component distributions from which the samples have been drawn differs from the linear continuum, and the proportions or densities of the component populations vary along the line of relation. The results show that, if the component populations are normal and the variances and correlation coefficient in the component populations are constant, we can calculate at most only two of the parameters of the component populations from the composite data. We can, however, always calculate the values of the slope of the line of relation and the vertical variance around this line irrespective of the functional forms of the component populations, providing the means of the latter are collinear and provided also that the data can be separated into subgroups corresponding to single populations. The use of the equations is illustrated by means of a composite distribution constructed from a known component distribution.

Introduction

As is well known, the use of a regression equation to describe a relation between two variates is legitimate only if one of the variates is free from any appreciable error. This requirement is easily met in many of the problems arising in biometry, but in applications of the physical sciences to industrial problems both variates are usually subject to error and the relation required is not a regression line but the line relating the means of the two variates.

Composite distributions of this type are frequently related through time series. In the simple case when the variates are normally distributed around their respective lines of trend and the variances remain constant, the usual procedure is to fit the trends with arbitrary power series and to deduce the partial correlation between the two variates by eliminating powers of t (4). This procedure, however, is open to several serious objections. One of these is that the fitting of time series with arbitrary power series introduces a sub-

[1] *Manuscript received in original form July 9, 1941, and as revised, August 25, 1941.*
Contribution from the Canned Salmon Inspection Laboratory, Department of Fisheries, Vancouver, B.C.

[2] *Chief Chemist.*

jective element that runs through all subsequent calculations and may lead to quite erroneous results. Second, the procedure involves arduous and time-consuming computations, and, third, the result gives no information regarding the nature of the relation connecting the means of the two variates.

The values of the variances and the functional forms of the two variates may, of course, be readily deduced without introducing any assumption regarding the nature of the trends, other than that the means of the two variates remain substantially constant over small intervals of time, by dividing the total interval, over which the time series extend, into a number of arbitrarily small intervals (1). This procedure, however, like the method of fitting trends, yields no information regarding the nature of the relation connecting the means of the two variates, since we can deduce this relation only from the table of corresponding values of the variates.

As far as the writer is aware, the equations connecting the parameters of the composite distribution with those of the component distributions, that are needed in deducing the relation between the means of the two variates, are not yet available in the literature, even in the simple case of linearly related normal distributions in which the respective variances and correlation coefficients remain constant. The object of this paper, therefore, was to deduce these equations for the latter simple case.

Evidently, in the composite distributions encountered in practical work, the point set representing the means of the component distributions from which the samples have been drawn will, in general, differ from the linear continuum. Furthermore, the densities or proportions of the component distributions along the line of relation will, in most instances, vary over the point set representing the individual means. For purposes of comparison, however, it will be of value first to deduce the required equations for the ideal case when the means represented by the samples correspond to the points of the linear continuum and the densities remain constant over the interval.

Assuming that we have obtained estimates of the values of the variances and the correlation coefficient r in the component populations, our principal problem is to determine the position of the line of relation, that is, to determine (i) a point on this line and (ii) the slope m of the line. In certain cases, even when we know the equation of the line of relation, we may wish to calculate one of the parameters of the component populations from the composite data. A convenient method of deducing this value is by means of the variance of the composite distribution around the line of relation.

Variance Around Line of Relation

Let AC in Fig. 1 be the series of normally correlated populations whose means are linearly related. For convenience, the individual populations may be represented by means of single probability contours (ellipses). Also, let us suppose that the populations are distributed in the interval AC, as described in the ideal case. Let B be the midpoint of AC, l the projection

of AC on the X-axis, X a deviation from the origin B, x a deviation from the mean of a single population, $P(x,y)$ the probability law of a single population, and $P(x)$, $P(y)$ the corresponding probability laws of the single variates.

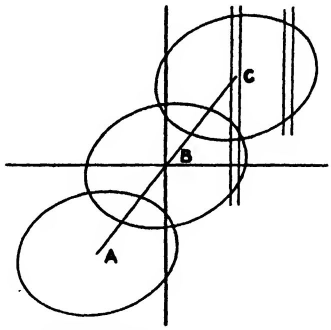

FIG. 1. *Diagrammatic representation of linear, composite, bivariate, normal distribution.*

Then the number of frequencies in the strip dX centred at B will be

$$\mu_{OB} = \int_{-l/2}^{l/2} \int_{-\infty}^{\infty} P(x,y)dydx,$$

the number of frequencies in the strip at C will be

$$\mu_{OC} = \int_{0}^{l} \int_{-\infty}^{\infty} P(x,y)dydx,$$

and the number of frequencies in a strip at X, whether the strip be within or outside the interval AC, will be

$$\mu_{OX} = \int_{X-l/2}^{X+l/2} \int_{-\infty}^{\infty} P(x,y)dydx.$$

Consider a strip at C. The vertical distance of a measure in this strip from the line of relation due to the population at C is y, and the vertical distance from the line of relation of a measure in this strip due to a population centred x units distant from C is $y - mx$. If X is the abscissa of the strip, the distance of any measure in the strip from the X-axis is therefore $y - mx + mX$.

Since the centre B is a point of symmetry, the line of best fit must clearly pass through B. Let M be the slope of any line through B (not necessarily the line of relation) and A the angle that this line makes with the X-axis. Then in a strip centred at X, the vertical distance of a measure from the line of slope M is $y - mx + (m - M)X$ and the perpendicular distance from this line is $[y - mx + (m - M)X] \cos A$.

Accordingly, in any strip at a distance X from the origin, that is, from B, the sum of the squares of the distances from the line M is

$$\Sigma \Delta_X^2 = \cos^2 A \int_{X-l/2}^{X+l/2} \int_{-\infty}^{\infty} [y - mx + (m - M)X]^2 P(x,y)dydx.$$

To integrate

$$I = \int_{-\infty}^{\infty} [y - mx + (m - M)X]^2 P(x,y)dy$$

let $k = -mx + (m - M)X$ and (2) let

$$P(x,y) = \frac{\sqrt{ac - b^2}}{2\pi} e^{-\frac{1}{2}(ax^2 + 2bxy + cy^2)},$$

where

$$\frac{ac - b^2}{c} = \frac{1}{\sigma_x^2}, \frac{b}{c} = -\frac{r\sigma_y}{\sigma_x}, \frac{ac - b^2}{a} = \frac{1}{\sigma_y^2}.$$

Then

$$I = \int_{-\infty}^{\infty} y^2 \frac{\sqrt{ac - b^2}}{2\pi} e^{-\frac{1}{2}(ax^2 + 2bxy + cy^2)} dy + \left(2k \cdot \frac{r\sigma_y}{\sigma_x} x + k^2\right) \frac{e^{-\frac{x^2}{2\sigma_x^2}}}{\sigma_x\sqrt{2\pi}}.$$

The integral in the right member of this last expression is readily obtained by writing it in the well known form

$$G = e^{-\frac{1}{2}\left(a - \frac{b^2}{c}\right)x^2} \cdot \frac{\sqrt{ac - b^2}}{2\pi} \int_{-\infty}^{\infty} y^2 e^{-\frac{1}{2}c\left(y + \frac{b}{c}x\right)^2} dy = \left[\sigma_y^2(1 - r^2) + r^2 \frac{\sigma_y^2}{\sigma_x^2} x^2\right]. P(x).$$

Consequently,

$$I = \left[k^2 + 2kr\frac{\sigma_y}{\sigma_x} x + \sigma_y^2(1 - r^2) + \frac{r^2\sigma_y^2 x^2}{\sigma_x^2}\right] P(x).$$

On substituting the value of k we thus obtain

$$I = \left[\left(m^2 - 2mr\frac{\sigma_y}{\sigma_x} + r^2\frac{\sigma_y^2}{\sigma_x^2}\right) x^2 + \left(\frac{r\sigma_y}{\sigma_x} - m\right) 2hXx \right.$$
$$\left. + h^2X^2 + \sigma_y^2(1 - r^2)\right] P(x)$$
$$= [Ax^2 + BXx + CX^2 + D] P(x),$$

where A, B, C, and D are constants determined by the values of m, σ_x, σ_y, r, and $h = m - M$. Accordingly,

$$\frac{\Sigma\Delta_X^2}{\cos^2 A} = \int_{X - l/2}^{X + l/2} (Ax^2 + BXx + CX^2 + D)P(x)dx,$$

so that on integrating and collecting terms we have

$$\frac{\Sigma\Delta_X^2}{\cos^2 A} = -[(A + B)X + Al/2]\sigma_x^2 P(X + l/2)$$
$$+ [(A + B)X - Al/2]\sigma_x^2 P(X - l/2)$$
$$+ (A\sigma_x^2 + CX^2 + D)\int_{X - l/2}^{X + l/2} P(x)dx.$$

Hence for all the strips, that is, on integrating with respect to X between the limits $-\infty$ and $+\infty$, we obtain

$$\frac{\Sigma\Sigma\Delta_X^2}{\cos^2 A} = Bl\sigma_x^2 + \int_{-\infty}^{\infty} (A\sigma_x^2 + CX^2 + D)\int_{X - l/2}^{X + l/2} P(x)dxdX.$$

If n is the number of populations per unit of l, the total number of measures is nl. The right member of the last equation therefore becomes

$$Bnl\sigma_x^2 + Anl\sigma_x^2 + Dnl + CnlS_X^2,$$

or, if S^2 is the perpendicular variance around the line of slope M,

$$\frac{S^2}{\cos^2 A} = (A + B)\sigma_x^2 + D + CS_X^2,$$

where S_X is the variance of the composite distribution around the Y-axis. Substituting the values of A, B, C, and D, we accordingly find

$$\frac{S^2}{\cos^2 A} = (h - m)2r\sigma_x\sigma_y + \sigma_x^2(m^2 - 2hm) + \sigma_y^2 + h^2S_X^2,$$

where $h = m - M$.

The last equation gives several interesting results. Putting $\cos^2 A = 1$ and $m = M$, that is $h = 0$, in this equation we find that the variance of the Y-variate around the line of relation is

$$S_{YL}^2 = m^2\sigma_x^2 - 2rm\sigma_x\sigma_y + \sigma_y^2.$$

Similarly, putting $\cos^2 A = 1$ and $M = 0$, we obtain the variance of the Y-variate around the origin, namely,

$$S_Y^2 = \sigma_y^2 - m^2\sigma_x^2 + m^2S_X^2.$$

But

$$nlS_X^2 = \int_{-l/2}^{l/2} n(\sigma_x^2 + X^2)dX.$$

Hence,

$$S_X^2 = \sigma_x^2 + \frac{l^2}{12}$$

and consequently,

$$S_Y^2 = \sigma_y^2 + m^2\frac{l^2}{12} = \sigma_y^2 + \frac{l'^2}{12},$$

which is the corresponding formula relating the variances of the Y-variate.

To find the slope of the line of best fit we write $\frac{\partial S^2}{\partial M} = 0$. Since $\cos^2 A = \frac{1}{1 + \tan^2 A} = \frac{1}{1 + M^2}$, the equation giving the required slope is

$$0 = \frac{1}{1 + M^2}[- 2r\sigma_x\sigma_y + 2m\sigma_x^2 - 2hS_X^2]$$
$$- \frac{2M}{(1 + M^2)^2}[- 2r\sigma_x\sigma_y M + \sigma_x^2(m^2 - 2hm) + \sigma_y^2 + h^2S_X^2].$$

From this equation and the relations $h = m - M$, $S_X^2 = \sigma_x^2 + \frac{l^2}{12}$, and $S_Y^2 = \sigma_y^2 + \frac{l'^2}{12}$, we find on collecting terms that the slope of the line of best fit is given by the equation

$$(M^2 - 1)\left(r\sigma_x\sigma_y + \frac{ll'}{12}\right) + M(S_X^2 - S_Y^2) = 0.$$

Using the result deduced in the section on the apparent correlation that, for $N = 1$, $\Sigma XY = r\sigma_x\sigma_y + \frac{ll'}{12}$, we thus see that this is merely the well

known formula for calculating the slope of the line of best fit, namely,

$$M^2 - 1 - \frac{S_Y^2 - S_X^2}{\Sigma XY} \cdot M = 0.$$

The condition that the line of relation should coincide with the line of best fit is obtained by substituting $h = 0$ in the equation resulting from putting $\frac{\partial S^2}{\partial M} = 0$. The required condition is found to be

$$- r\sigma_x\sigma_y + m^2 r\sigma_x\sigma_y + m(\sigma_x^2 - \sigma_y^2) = 0,$$

whence

$$m^2 - 1 - \frac{\sigma_y^2 - \sigma_x^2}{r\sigma_x\sigma_y} m = 0.$$

The line of relation therefore coincides with the line of best fit, if, and only if, the line of relation coincides with the line of best fit of a single population.

Finally, it should be noted that we obtain precisely similar formulae for the second variate by writing y, Y, l', m', and M' in the above equations in place of x, X, l, m, and M.

Apparent Correlation

To find the equation connecting the apparent correlation R of the composite distribution with the parameters of the component distributions we note that, in any strip at X, the vertical distance of a measure from the centre of the whole distribution is, putting $M = 0$, $y - mx + mX$. Consequently, the partial product of this strip is

$$p_{XY} = X\int_{X-l/2}^{X+l/2}\int_{-\infty}^{\infty}(y - mx + mX)P(x,y)dydx,$$

and for all the strips we thus have

$$\Sigma p_{XY} = \int_{-\infty}^{\infty} X\int_{X-l/2}^{X+l/2}\int_{-\infty}^{\infty}(y - mx + mX)P(x,y)dydxdX.$$

On integration this last equation gives

$$\Sigma p_{XY} = lr\sigma_x\sigma_y - lm\sigma_x^2 + \int_{-\infty}^{\infty} mX^2\int_{X-l/2}^{X+l/2} P(x)dxdX,$$

that is,

$$\Sigma p_{XY} = lr\sigma_x\sigma_y - lm\sigma_x^2 + mNS_X^2,$$

where N is the total number of measures. The formula corresponding to this, obtained on integrating over the Y-variate, is

$$\Sigma p_{XY} = l'r\sigma_x\sigma_y - l'm'\sigma_y^2 + m'NS_Y^2,$$

in which $l' = ml$ and $m' = 1/m$.

To harmonize the two equations giving the values of Σp_{XY} we must evidently choose the units to satisfy the condition that their right members are equal. In the simple case when $m = 0$, the number of frequencies due to one com-

ponent population at a distance x from the centre of this population, which is centred at, say, X units from the origin, is

$$\int_{-\infty}^{\infty} P(x,y)dy = P(x)dX,$$

and the total number of frequencies due to this population is 1. In the derivation of the equations giving the values of Σp_{XY} we have thus assumed one component population per unit of the variate in each case.

Let n and n' be the numbers of populations per unit lengths of X and Y. The above equations then become

$$\Sigma p_{XY} = nlr\sigma_x\sigma_y - nlm\sigma_x^2 + mNS_X^2$$
$$\Sigma p_{XY} = n'l'r\sigma_x\sigma_y - n'l'm'\sigma_y^2 + m'NS_Y^2.$$

Writing the total number of measures equal to 1 we therefore find, since $N = nl = n'l'$,

$$\Sigma p_{XY} = r\sigma_x\sigma_y - m\sigma_x^2 + mS_X^2$$

and

$$\Sigma p_{XY} = r\sigma_x\sigma_y - m'\sigma_y^2 + m'S_Y^2.$$

Also, we have

$$nlS_X^2 = \int_{-l/2}^{l/2} n(\sigma_x^2 + X^2)dX,$$

so that

$$S_X^2 = \sigma_x^2 + \frac{l^2}{12}\text{, and, similarly, } S_Y^2 = \sigma_y^2 + \frac{l'^2}{12}\,.$$

Remembering that $l' = ml$ and $l = m'l'$ we thus finally have

$$\Sigma p_{XY} = r\sigma_x\sigma_y + \frac{ll'}{12},$$

and

$$R = \frac{r\sigma_x\sigma_y + \frac{ll'}{12}}{\sqrt{\sigma_x^2 + \frac{l^2}{12}}\sqrt{\sigma_y^2 + \frac{l'^2}{12}}} = \frac{\Sigma XY}{NS_XS_Y}\,.$$

Experimental Distributions

As mentioned above, the composite distributions obtained experimentally will in general differ from the ideal case, and, in fact, will very rarely, if ever, accurately fulfil the conditions of this case. That is to say, the point set representing the means of the component distributions from which the samples have been drawn will almost always differ appreciably from the linear continuum, while, at the same time, the densities of the component distributions along the line of relation will vary from point to point. If the equations are to be of service in practical computations, they must therefore be modified so as to be rigidly applicable to the non-ideal case also.

The required equations may be readily deduced from the equations giving the moments from an arbitrary origin in terms of moments from the mean (5),

or they may be derived from the characteristic function by taking successive derivatives of the latter with respect to the variables u and v and substituting $u = 0$ and $v = 0$ in the results. Following the second method, we have for the characteristic function of a single component distribution

$$\phi(u,v) = p_1 e^{\frac{1}{2}(\sigma_x^2 u^2 + 2r\sigma_x\sigma_y uv + \sigma_y^2 v^2 + 2a_1 u + 2b_1 v)},$$

where a_1, b_1 are the means of the independent and dependent variates respectively, and p_1 is the proportion of this component in the composite distribution. Consequently,

$$(\phi)_0 = p_1 ,$$

$$\left(\frac{\partial\phi}{\partial u}\right)_0 = p_1 a_1 ,$$

$$\left(\frac{\partial^2\phi}{\partial u^2}\right)_0 = p_1\sigma_x^2 + p_1 a_1^2 ,$$

$$\left(\frac{\partial^2\phi}{\partial v\partial u}\right)_0 = p_1 r\sigma_x\sigma_y + p_1 a_1 b_1 ,$$

$$\left(\frac{\partial^3\phi}{\partial u^3}\right)_0 = 3p_1\sigma_x^2 a_1 + p_1 a_1^3 ,$$

$$\left(\frac{\partial^4\phi}{\partial u^4}\right)_0 = 3p_1\sigma_x^4 + 6p_1 a_1^2\sigma_x^2 + p_1 a_1^4 .$$

On adjusting the origin to the means of the composite distribution and summing these equations with respect to the means of the component distributions we accordingly find

$$\mu_0 = \Sigma p_i = 1,$$

$$\mu_1 = \Sigma p_i a_i = \lambda_1 = 0; \; \mu_1' = \lambda_1' = 0 ,$$

$$\mu_2 = \sigma_x^2 + \Sigma p_i a_i^2 = \sigma_x^2 + \lambda_2^2 ; \; \mu_2' = \sigma_y^2 + m^2\lambda_2^2 ,$$

$$\mu_{12} = r\sigma_x\sigma_y + \Sigma p_i m a_i^2 = r\sigma_x\sigma_y + m\lambda_2^2 = r\sigma_x\sigma_y + \lambda_2\lambda_2' ,$$

$$\mu_3 = 3\sigma_x^2\Sigma p_i a_i + \Sigma p_i a_i^3 = 3\sigma_x^2\lambda_1 + \lambda_3^3 = \lambda_3^3 ; \; \mu_3' = m^3\lambda_3^3 ,$$

$$\mu_4 = 3\sigma_x^4 + 6\sigma_x^2\Sigma p_i a_i^2 + \Sigma p_i a_i^4 = 3\sigma_x^4 + 6\sigma_x^2\lambda_2^2 + \lambda_4^4 ,$$

$$\mu_4' = 3\sigma_y^4 + 6\sigma_y^2 m^2\lambda_2^2 + m^4\lambda_4^4 ,$$

in which the λ's and $m\lambda$'s are the moments of the means of the component distributions around the means of the composite distribution.

The required equations are now easily deduced. Multiplying the equation in μ_2 by m^2, that in μ_{12} by $2m$, and subtracting the latter from the sum of the equations giving the values of $m^2\mu_2$ and μ_2', we obtain

$$\mu_2' - 2m\mu_{12} + m^2\mu_2 = \sigma_y^2 - 2mr\sigma_x\sigma_y + m^2\sigma_x^2 = S_{YL}^2 ,$$

as in the ideal case. Also we have

$$\mu_2' - \sigma_y^2 = m^2\mu_2 - m^2\sigma_x^2 = m\mu_{12} - mr\sigma_x\sigma_y ,$$

and the apparent correlation is

$$R = \frac{r\sigma_x\sigma_y + \lambda\lambda'}{\sqrt{\sigma_x^2 + \lambda_2^2}\sqrt{\sigma_y^2 + \lambda_2'^2}} ,$$

in which $\lambda' = m\lambda$.

The third moments will be zero whenever the composite distribution is symmetrical. Furthermore, since these moments will usually consist of relatively small positive or negative differences, they will not, in general, give reliable estimates of m.

Under certain conditions the value of m, however, can be calculated from the composite data if we make use of the fourth moments, for, the elimination of λ_4^4 from the two equations giving the values of μ_4 and μ_4' and application of the equations in μ_2 and μ_2' give the equation,

$$\mu_4' - m^4\mu_4 = 3(\mu_2')^2 - 3m^4(\mu_2)^2.$$

As might be expected, there is an analogous relation between the sixth, fourth, and second moments, namely,

$$\mu_6' - m^6\mu_6 = 15\mu_2'(\mu_4' - 2\mu_2'^2) - 15m^6\mu_2(\mu_4 - 2\mu_2^2).$$

Hence, while theoretically we can, under certain conditions, determine m from the composite data, we can calculate at most only two of the parameters of the component distributions from the composite data. In other words, in order to determine all the parameters of the composite distribution we must know the value of at least one of the quantities σ_x, σ_y, and r.

The properties of the various particular cases that arise when one or more of the parameters of the composite distribution have the value zero easily follow from the above equations. For example, when $\sigma_x = 0$, $S_{YL}^2 = \sigma_y^2$, and the line of relation becomes a linear regression line with regression coefficient m. Similarly, when the length of the interval approaches zero in both variates, the composite distribution becomes a normal distribution. The value of m is then indeterminate, since under the latter conditions $S_X^4 = 3S_X^2$, $S_X^6 = 15S_X^2$, and similar equations hold for the second variate.

The special case when $m = 0$ reveals at once a simple method of testing the hypothesis regarding the linearity of the relation between the means of the component distributions, providing it is known that the parameters σ_x, σ_y, and r remain constant over the interval and we are in possession of a means of separating the data into subgroups such that each subgroup may, with reasonable accuracy, be considered to have been drawn from a single component population. To test for linearity under these conditions we plot the means of the Y-variate against the corresponding means of the X-variate in the individual subgroups and apply the sampling limits $\pm \dfrac{t\sigma_y}{\sqrt{n}}$, when $m = 0$, while for $m \neq 0$ we apply the limits $b_i \pm \dfrac{tS_{YL}}{\sqrt{n}}$, where n is the number of measures in the subgroup.

The probabilities to be associated with the latter limits are those of a normal distribution, since the distribution of the composite population around the line of relation is normal. To demonstrate this we need only consider the moments of a single population around the line of relation. These are

$$(\mu_{YL})_n = \int_{-\infty}^{\infty}\int_{-\infty}^{\infty} (y - mx)^n P(x,y)dydx,$$

where $P(x,y)$ is the normal correlation surface in two variables. Integrating the right member of this equation for the values $n = 1, 2, 3$, etc., we find that $\mu_1 = \mu_3 = \mu_5 = 0$, $\mu_2 = \sigma_y^2 - 2mr\sigma_x\sigma_y + m^2\sigma_x^2$, $\mu_4 = 3(\sigma_y^2 - 2mr\sigma_x\sigma_y + m^2\sigma_x^2)^2$, and so on for higher moments, thus proving the statement.

Instead of plotting corresponding means we may also test the relation by comparing calculated and experimental values of one of the variances or the correlation coefficient in the component populations. The comparison of values of the correlation coefficient, however, is unsuitable for practical work, because the experimental determination of this parameter usually entails greatly increased tabulations and computations.

Lastly, we may note that the equations giving the values of m, the slope of the line of relation, and S_{YL}^2, the vertical variance around this line, are applicable to any linear, composite, bivariate distribution, so that we can always calculate the values of these two parameters irrespective of the nature of the functional forms of the component populations, provided the means of the latter are collinear.

To show that the equations

$$\frac{S_Y^2 - \sigma_y^2}{S_X^2 - \sigma_x^2} = \frac{\lambda'^2}{\lambda^2} = m^2$$

hold for any linear, composite, bivariate distribution it is necessary only to show that the relations $S_Y^2 - \sigma_y^2 = \lambda'^2$ and $S_X^2 - \sigma_x^2 = \lambda^2$ are true for any distribution of this type. Let s_p^2 be the variance, $\bar{y}_p$ the mean, and n_p the number of measures in a single population. Then the contribution of a single population to the sum of the squares of the composite distribution around the mean of the Y-variate is $n_p s_p^2 + n_p \bar{y}_p^2$. Hence, if there are k component populations and the total number of measures is N, we have

$$NS_Y^2 = \sum_{p=1}^{k} n_p s_p^2 + \sum_{p=1}^{k} n \bar{y}_p^2,$$

that is, $S_Y^2 = \sigma_y^2 + \lambda'^2$, and similarly, $S_X^2 = \sigma_x^2 + \lambda^2$. But, by hypothesis, the means are collinear. Consequently, $\bar{y}_p = m\bar{x}_p$ or $\lambda'^2 = m^2\lambda^2$, and the equations giving the value of m are true for any linear, composite, bivariate distribution.

To prove that the relation

$$S_{YL}^2 = S_Y^2 - 2mp_{XY} + m^2 S_X^2$$

is true for any linear, composite, bivariate distribution we proceed in a similar manner. In a single population the vertical distance of any measure from the line of relation is $y - mx$. The contribution of a single population to the sum of the squares of the deviations of the Y-variate from the line of relation is therefore

$$\begin{aligned} n_p s^2{}_{YL} &= \sum_1^{n_p} (y - mx)^2 \\ &= \sum_1^{n_p} \{ Y - \bar{Y}_p - m(X - \bar{X}_p)\}^2 \end{aligned}$$

in terms of deviations from the means of the composite distribution. But $\bar{Y}_p = m\bar{X}_p$. Hence

$$n_p s^2_{YL} = \sum_1^{n_p} (Y - mX)^2 .$$

Summing with respect to the k component populations we obtain the equation giving the value of S^2_{YL}.

Numerical Example

Examples of experimental linear, composite, normal distributions will be found in other communications. In order to illustrate the simplicity of the numerical calculations, however, we shall conclude this paper by applying the preceding equations to a composite distribution that has been constructed from a known component distribution, that is, a component distribution for which we know the frequencies corresponding to given values of x and y.

In the example given below, a component distribution having the parameters $\sigma_x = \sigma_y = 1$, $r = 0.80$ was chosen, since for this value of r, four cell frequencies in each of two quadrants were immediately available in Table XXX of Pearson's "Tables for Statisticians and Biometricians" (6). The cell frequencies in the two remaining quadrants, together with those in the cells along the boundaries of the quadrants and those for values x (or y) $= 3$, were calculated by the method described by Everitt (3). In order to reduce the labour of the calculations, however, intervals of 0.5 and Simpson's Rule 1 were employed in these computations. This abridged calculation gives less accurate results than those obtained from Everitt's table, but the approximation is sufficiently close for practical purposes. For example, Everitt's table gives the value 0.1272 as the frequency in the block centred at $x = 1$, $y = 1$ on unit base, while the abridged calculation gives 0.1277. Similarly, for the block centred at $x = 2$, $y = 2$, the corresponding frequencies are 0.0260 and 0.0265 respectively. The resulting component population is shown in Table I.

Composite distributions corresponding to given values of m and given spacings may be constructed from a component population either geometrically

TABLE I

CELL FREQUENCIES IN COMPONENT NORMAL DISTRIBUTION IN WHICH $\sigma_x = \sigma_y = 1$ and $r = 0.80$

y	x							
	−3	−2	−1	0	1	2	3	Total
3					0.001	0.003	0.002	0.006
2				0.004	0.028	0.026	0.003	0.061
1			0.006	0.079	0.127	0.028	0.001	0.241
0		0.004	0.079	0.217	0.079	0.004		0.383
−1	0.001	0.028	0.127	0.079	0.006			0.241
−2	0.003	0.026	0.028	0.004				0.061
−3	0.002	0.003	0.001					0.006
Total	0.006	0.061	0.241	0.383	0.241	0.061	0.006	0.999

by summing frequencies along diagonals, or analytically, as illustrated in Table II. Table III shows a linear composite distribution derived by the latter method from the component distribution given in Table I. As will be observed from Table III, this linear composite distribution consists of three components centred on a line of slope $m = 2$.

TABLE II

DETAILS OF ANALYTIC METHOD OF CALCULATING THE FREQUENCIES IN THE ARRAY $X = 0$ OF THE COMPOSITE DISTRIBUTION CONSISTING OF THE COMPONENTS CENTRED AT (i) $X_1 = -1$, $Y_1 = -2$; (ii) $X_2 = 0$, $Y_2 = 0$; (iii) $X_3 = 1$, $Y_3 = 2$, EACH IDENTICAL WITH THE DISTRIBUTION IN TABLE I

Y	(i) $x = X + 1 = 1$, $y = Y + 2$	(ii) $x = X = 0$, $y = Y$	(iii) $x = X - 1 = -1$, $y = Y - 2$	f (From Table I)
3			1	0.006
2		2	0	0.083
1	3	1	−1	0.207
0	2	0	−2	0.273
−1	1	−1	−3	0.207
−2	0	−2		0.083
−3	−1			0.006

TABLE III

COMPOSITE DISTRIBUTION CONSISTING OF THREE COMPONENTS, $\sigma_x = \sigma_y = 1$, $r = 0.80$ CENTRED AT $X_1 = -1$, $Y_1 = -2$; $X_2 = Y_2 = 0$; $X_3 = 1$, $Y_3 = 2$, RESPECTIVELY

Y	X: −4	−3	−2	−1	0	1	2	3	4	f	$\bar{X}$
5							0.001	0.003	0.002	0.006	3.17
4						0.004	0.028	0.026	0.003	0.061	2.46
3					0.006	0.080	0.130	0.030	0.001	0.247	1.76
2				0.004	0.083	0.245	0.105	0.007		0.444	1.06
1			0.001	0.034	0.207	0.209	0.036	0.001		0.488	0.51
0			0.007	0.109	0.273	0.109	0.007			0.505	0.00
−1		0.001	0.036	0.209	0.207	0.034	0.001			0.488	−0.51
−2		0.007	0.105	0.245	0.083	0.004				0.444	−1.06
−3	0.001	0.030	0.130	0.080	0.006					0.247	−1.76
−4	0.003	0.026	0.028	0.004						0.061	−2.46
−5	0.002	0.003	0.001							0.006	−3.17
f	0.006	0.067	0.308	0.685	0.865	0.685	0.308	0.067	0.006		
$\bar{Y}$	−4.17	−3.34	−2.44	−1.33	0.00	1.33	2.44	3.34	4.17		

Table IV shows values of certain statistics of the distribution listed in Table III. These were calculated (i) directly from the combined distribution and (ii) from the component distributions by means of the formulae derived in the preceding sections. In computing the second series of figures the

value of $m = 2$ was employed, and Sheppard's corrections were added to the variances of the component distribution, since the measures in the latter were grouped prior to setting up the composite distribution. The results, it will be observed, agree, for the most part, to three significant figures, the limit of accuracy of the data.

TABLE IV

COMPARISON OF OBSERVED AND CALCULATED VALUES OF STATISTICS DERIVED FROM THE COMPOSITE DISTRIBUTION OF TABLE III. (i) OBSERVED; (ii) CALCULATED

$\Sigma f = 2.997$; $\Sigma fX = \Sigma fY = 0$; $\Sigma fX^2 = 5.232$; $\Sigma fY^2 = 11.226$; $\Sigma fX^4 = 25.152$; $\Sigma fY^4 = 93.930$; $\lambda^2 = 0.667$; $\lambda'^2 = 2.667$; $\Sigma f(XY)/N$, (i) 2.128, (ii) 2.133; S_X^2, (i) 1.746, (ii) 1.750; S_Y^2, (i) 3.746, (ii) 3.750; S_{YL}^2, (i) 2.215, (ii) 2.217; R, (i) 0.832, (ii) 0.833; m, (i) 1.97, (ii) 2.00

References

1. CHARNLEY, F. and HARCUS, L. M. Can. J. Research, D, 18 : 410-422. 1940.
2. DARMOIS, G. Statistique mathématique. Gaston Doin et Cie, Paris. 1928.
3. EVERITT, P. F. Biometrika, 8 (3 and 4) : 385–395. 1912.
4. FISHER, R. A. Statistical methods for research workers. 5th ed. rev. and enl. Oliver and Boyd, Ltd., Edinburgh and London. 1934.
5. KELLEY, T. L. Statistical method. The Macmillan Company, New York. 1923.
6. PEARSON, K. Tables for statisticians and biometricians. 3rd ed. Part I. Cambridge University Press, London. 1930.

INDEX

CANADIAN JOURNAL OF RESEARCH

VOLUME 19
1941
SECTION A

Published by the
NATIONAL RESEARCH COUNCIL *of* CANADA

SECTION A

INDEX TO VOLUME 19

Authors

SECTION A

INDEX TO VOLUME 19

Subjects

CANADIAN JOURNAL OF RESEARCH

VOLUME 19
1941
SECTION B

CANADA

Published by the
NATIONAL RESEARCH COUNCIL *of* CANADA

Canadian Journal of Research

Issued by THE NATIONAL RESEARCH COUNCIL OF CANADA

VOL. 19, SEC. B. JANUARY, 1941 NUMBER 1

THE MECHANISM OF THE ALKALINE DELIGNIFICATION OF WOOD[1]

BY G. L. LAROCQUE[2] AND O. MAASS[3]

Abstract

Measurement was made of the rate of delignification of sprucewood with lithium, barium, sodium, potassium, and tetra-ethyl ammonium hydroxides under closely controlled conditions of temperature and concentration. The reaction rates were compared with the ionic mobilities and adsorption coefficients of the different alkalis. Methanol, ethanol, and glycerol were used as solvents.

From these results a mechanism is suggested, according to which adsorption of alkali at the reaction interface is the determining factor in setting the rate of delignification. The rate is also dependent on the specific nature of the alkali cation and varies with the temperature in accordance with the general theory of thermal activation.

Introduction

The alkaline digestion of wood for the production of paper pulp is a common industrial process that has been in use for more than 50 years. Notwithstanding the commercial importance of this process, the methods employed are largely empirical and little is known of the actual physical-chemical mechanism. The present investigation is an attempt to determine the exact nature of this cooking process, which consists essentially in the treatment of wood with an alkaline liquor and heat in a pressure resisting vessel. The cooking liquor extracts most of the lignin, pentosan, and other non-cellulosic materials, leaving the desired cellulose, the yield and purity of which depend on the conditions of the pulping.

The mechanism of the process is by no means a simple one. The wood substance is not a homogenous material, but a mixture of α-cellulose, hemi-celluloses, pentosan, lignin, and small amounts of extractives; and these substances vary decidedly in their chemical behaviour toward alkali. Since, however, the lignin is the most resistant of the incrusting materials present, the rate of its solution in alkali is the governing factor in the purification of the cellulose.

There are a number of secondary factors, such as the shape and size of the chip, and the density and moisture content of the wood, that may influence the delignification process. Most of these secondary factors have now been

[1] *Manuscript received July 16, 1940.*
Contribution from the Division of Physical Chemistry, McGill University, Montreal, Que.
[2] *Graduate student in Physical Chemistry and holder of a Bursary under the National Research Council of Canada.*
[3] *Macdonald Professor of Physical Chemistry, McGill University; Director, Canadian Pulp and Paper Institute, Montreal.*

investigated. Thus, Larocque and Maass (4) have shown that with spruce wood and aqueous alkali, the rate of delignification was the same irrespective of the size of the sample from a wood meal of 0.0005 mm. particle size up to a limiting chip thickness of about 10 mm.

Furthermore, the density of the wood had no influence on the delignification other than that which would be expected from the higher original lignin content of the denser wood. Also, the presence of moisture in the chips was without effect other than that of diluting the liquor, and the addition of wetting agents for facilitating the penetration rate was without significant effect.

It was the purpose of the present investigation to examine some of the remaining factors capable of affecting the rate of reaction, with a view to determining what are the qualities of an alkaline liquor that render it most suitable for delignification, and in this manner to gain a new insight into the mechanism of the alkaline delignification of wood.

The experimental sequence was the following. A study of the rate of reaction indicated that it was of the apparent monomolecular type, having a definite velocity constant for each set of experimental conditions. The effect of different experimental conditions on the velocity constant was then examined, in order to ascertain the factors that really controlled the reaction rate. The variables investigated were as follows:—

The ionic properties of the alkali cation, the concentration of the hydroxyl ion, the solubility of the alkali in the solvent used, the absorption of the alkali at the reaction interface, and the influence of the temperature on the rate of reaction. From a consideration of these factors, a tentative theory has been submitted concerning the mechanism of the delignification reaction.

Experimental Procedure and Results

The experimental method used was that previously described in detail by Lusby and Maass (6). Essentially it consists in digesting for a definite time interval 10 gm. of spruce wood chips in a steel pressure-resisting cell of 80 cc. capacity. The sample having been saturated with cold liquor, the cell was immersed in a thermostatically controlled oil bath preheated to the desired temperature. A stream of caustic liquor of the desired concentration was sent through the cell at a steady rate during the digestion period, with the double object of removing the waste products of the reaction and maintaining constant the alkali concentration.

The reaction was stopped when desired by quenching the cell in water. The pulp was then removed and dried at 105° C. to determine the yield. The amount of unchanged lignin remaining in the pulp was determined by the method of Ross and Potter (12). The yield of carbohydrate was obtained by subtracting the value obtained from the yield of pulp, all yields being expressed as a percentage of the original oven dried wood. In some of the experiments, a constant flow was not considered to be necessary and a 200 cc. capacity closed bomb, containing 10 gm. of chips was used instead.

Unless otherwise indicated, the standard procedure was to employ 2.0 *N* aqueous alkali, and to allow it to digest for three hours at 160° C.

I. The Time-rate of Delignification

The first step towards a better understanding of the mechanism of the soda-delignification process was to determine the manner in which the reaction rate varied with time. It was then possible to calculate whether the reaction was proceeding in accordance with an apparent monomolecular, bimolecular, or other regular law governing chemical action.

Cooking experiments were performed in which wood samples of three different densities were cooked under identical experimental conditions for periods up to $6\frac{3}{4}$ hr. Details are given in Table I.

TABLE I

THE TIME-RATE OF DELIGNIFICATION

Runs 46, 53. Bombs: Cast-iron, 200 cc. capacity, no liquor circulation. Wood: black spruce, 20 by 10 by 2 mm. chips, 10 gm. per bomb—wood density and lignin content as indicated. Liquor: aqueous sodium hydroxide, 2.0 *M*, 165 cc. per bomb. Temp.: 160 C.

Time, hr.	Density = 0.45		Density = 0.35		Density = 0.406	
	Lignin res.	Carbohydrate yield	Lignin res.	Carbohydrate yield	Lignin res.	Carbohydrate yield
0.00	32.0	68.0	30.3	69 7	—	—
0.75	19.2	49.6	17.25	49.5	—	—
1.33	11.4	47.3	10.68	47.0	—	—
2.25	6.0	43.3	5.62	43.6	—	—
3.33	2.67	41.1	2.67	40.7	—	—
4.50	2.02	40 2	1.73	38.8	1.80	41.9
6.75	—	—	—	—	1.18	38.5

The lignin percentage remaining in the pulp as given in Table I, is shown plotted on a logarithmic scale against time in Fig. 1. A linear relation is seen to hold during the solution of all but the last 2% or so of lignin. This was first noticed by Svante Arrhenius (1), and indicates that for the most part the delignification reaction is a first order or apparent monomolecular reaction, that is, *the amount of lignin going into solution at any time is proportional to the amount of undissolved lignin still remaining in the wood at that time.*

The behaviour is that given by the relation:

$$- dL/dt = k(L_0 - L), \tag{1}$$

which can also be written:

$$k = 1/t \log_e L_0/L, \tag{2}$$

where L_0 is the original lignin content of the wood, L is the lignin remaining after a time t hours. k is the velocity constant, and is a measure of the velocity with which the reaction is proceeding for any one set of experimental conditions.

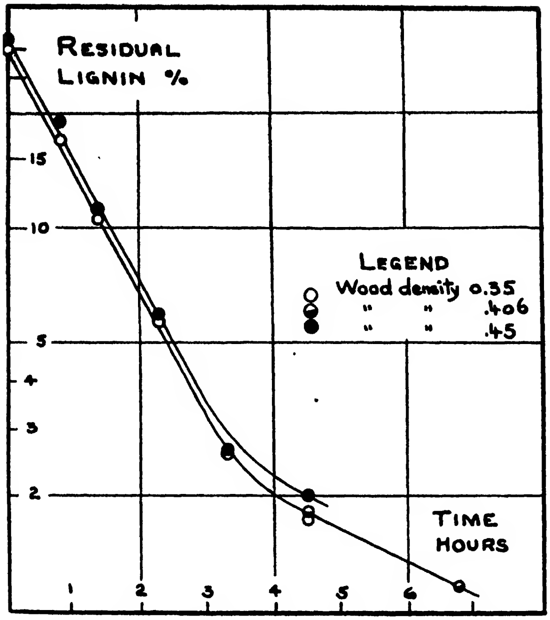

FIG. 1. *Rate of delignification—2.0 M sodium hydroxide, 160° C.*

The last 2% or so of lignin does not follow the monomolecular law, but dissolves at about one-quarter the rate of the bulk of the lignin. The difficulty of accurately measuring these small lignin values is not a sufficient explanation for this behaviour, since Corey and Maass (2) have shown that in the case of sulphite cooking the monomolecular relation still holds good for these low lignin values.

This behaviour has been noticed before, and the explanation offered by Mitchell and Yorston (7) is that this part of the lignin is held in the interior of the cell wall and that its outward diffusion is hindered by its relatively large particle size. It follows that velocity constants should be used only for comparing rates of delignification when these have been determined for residual lignin values greater than 2% or so.

The parallelism of the two curves also indicates that the lignin in the wood of higher density dissolves at the same rate as the lignin in the more porous wood. This confirms a previous observation by Larocque and Maass (4) that notwithstanding the greater resistance of dense wood to diffusion, wood density has no influence on delignification other than that which would be expected from the higher original lignin content of denser wood.

The conclusion to be drawn is that all the lignin in the wood seems to be equally accessible to the cooking liquor. Either the cooking liquor completely permeates the lignin substance, or more probably the area of the reaction interface between the liquor and the solid phase at any one time is proportional to the amount of lignin present in the wood.

II. The Nature of the Alkali

The second step towards the elucidation of the mechanism of soda-pulping was to determine the influence of alkalis other than sodium hydroxide, on the reaction rate, in order to find out what relation existed between the rate of delignification and the ionic properties: degree of ionization, ionic mobility, degree of hydration, coefficients of diffusion, etc., of the particular alkali used. From the manner in which the rate of delignification varied with the properties of the alkali employed, it should then be possible to put forth a theory describing the mechanism of the reaction.

Pulping was therefore carried out using the strong inorganic bases lithium, barium, sodium, and potassium hydroxides, and the strong organic base tetraethyl ammonium hydroxide. The procedure followed and the results obtained are given in Tables II and III.

TABLE II

DELIGNIFICATION BY STRONG INORGANIC BASES

Run No. 45. Bombs: Cast-iron, 200 cc. capacity, no liquor circulation. Wood: black spruce, density 0.406, 20 by 10 by 2 mm. chips, 10 gm. per bomb. Liquor: Aqueous lithium, barium, sodium, and potassium hydroxides—165 cc. per bomb. Temp.: from 100 to 160° C. for one hour, then at 160° for three hours.

	LiOH	$Ba(OH)_2$*	NaOH	KOH
Carbohydrate yield, %	45.5	27.4	41.3	41.6
Lignin yield, %	6.6	3.8	2.5	1.83
Velocity constant	0.51	0.69	0.83	0.94

* *With the barium hydroxide liquor, the barium alkali-lignin compound formed during the reaction is insoluble in the cooking liquor and remained adhering to the pulp. Consequently, this pulp was extracted with 5% hydrochloric acid to free it from barium, then with 1% sodium hydroxide to dissolve the changed lignin. The small residue of uncooked lignin remaining in the pulp was then determined in the usual manner.*

TABLE III

DELIGNIFICATION BY A STRONG ORGANIC BASE

Run 69. Same procedure as in Run 45 except that only 150 cc. of 0.70 *M* tetra-ethyl ammonium hydroxide was used per bomb. Sodium hydroxide was also used for purposes of comparison.

	NaOH	$(C_2H_5)_4NOH$
Carbohydrate yield, %	46.5	46.0
Lignin yield, %	14.8	5.52
Velocity constant	0.241	0.57

The values obtained for the velocity constants rank the alkalis in the following order of increasing reactivity: lithium hydroxide, barium hydroxide, sodium hydroxide, potassium hydroxide tetra-ethylammonium hydroxide. The observed differences in reaction rate must necessarily have depended on some differences in the properties of the alkaline ions involved, and may have been due to:

(1) Differences in their degree of dissociation,

(2) Differences in ionic mobility caused by hydration of the ions,

(3) Differences in the degree to which they are absorbed by the lignin, on the assumption that absorption of alkali is a necessary prerequisite to reaction,

(4) Variation in the chemical affinity which the lignin substance has for the different alkalis.

These four possibilities are considered separately:

The degree of dissociation of these alkalis at 160° C. is not on record. Conductivity and viscosity data do exist, however, which makes it possible to calculate the dissociation of lithium hydroxide, sodium hydroxide, and potassium hydroxide relative to one another with a fair degree of accuracy. The values obtained were 1.00, 1.11, and 1.19 respectively for each of these alkalis, and are too much alike to account for the marked differences in their rates of delignification.

The presence of a sufficient hydroxyl ion concentration, corresponding to a pH value of 12 or 13, is necessary in the alkaline delignification of wood, but the above considerations indicate that the reaction rate is also dependent on some special property of the cation employed, other than its degree of dissociation.

Differences in the mobility of the cations might account for the different rates of delignification. In Table IV are given the relative velocity constants and ionic mobilities of the four strong inorganic alkalis, based on unity for lithium hydroxide.

TABLE IV

IONIC MOBILITIES AND VELOCITY CONSTANTS

Alkali	LiOH	$Ba(OH)_2$	NaOH	KOH
Velocity constant	1.00	1.35	1.62	1.84
Ionic mobility	1.00	1.67	1.31	1.94

Although there is a rough analogy between the ionic mobility and the velocity of delignification, diffusion cannot be the main factor governing the reaction velocity since it has been shown (13) that the temperature coefficient of diffusion of aqueous sodium and potassium hydroxide solutions is 1.2 for a 10° rise in temperature, whereas the observed temperature coefficient is materially greater, namely, from 1.7 to 2.7 at 160°, the exact value depending upon the particular concentration and the alkali used. In such a case where

the observed temperature coefficient of the reaction velocity is greater than the coefficient of diffusion, it follows (11) that the observed reaction velocity is the true chemical velocity constant *k* independent of viscosity considerations.

TABLE V

YIELDS OF CARBOHYDRATE AND LIGNIN IN THE ALKALINE DELIGNIFICATION OF SPRUCEWOOD

Concentration, *M*	Time, hr.	Carbohydrate, %	Lignin, %
Lithium hydroxide			
1.38	1.0	42.2	17.2
*2.0	3.0	44.5	6.9
2.89	1.0	47 3	15.4
*4.5	1.0	46.0	13.0
Sodium hydroxide			
1.4	0.5	44.8	32.6
	1.0	42.4	32.1
	1.5	42.0	23.5
	2.0	41.5	20.3
	3.0	39.0	15.3
2.0	3.0	42.0	3.6
2.9	0.5	44.7	30.6
	1.0	41.0	22.1
	1.5	40.7	15.6
	2.0	37.5	9.7
	3.0	32.7	7.0
4.5	0.5	49.7	29.6
	1.0	42.0	17.9
	1.25	39.4	13.8
	2.0	33.0	5.1
	3.0	28.2	4.3
6.2	1.0	38.5	6.4
8.1	1.0	39.1	5.4
	3.0	27.0	1.5
9.74	1.0	38.3	6.8
	3.0	28.7	0.8
Potassium hydroxide			
1.4	1.0	45.3	15.0
*2.0	3.0	39.1	0.9
2.9	1.0	42.6	19.5
	1.5	41.9	15.0
4.56	0.5	48.4	22.4
	1.0	39.9	15.3
6.26	1.0	44.0	3.4
9.6	1.0	45.0	1.6
14.2	1.0	41.5	0.6

III. The Effect of Concentration

The next step was to investigate how the velocity constant varied with the concentration. Three alkalis, namely: lithium, sodium and potassium hydroxides were used at concentrations of from 1.4 to 14 *M*. The experiments were carried out at 160° C. according to the previously described standard procedure. The results obtained are reported in Table V. Those values preceded by an asterisk have been experimentally determined in the present investigation. The remainder of the data has been calculated from the results of Lusby and Maass (6).

The residual lignin values follow the monomolecular law in that they tend to fall on a straight line when plotted logarithmically.

From the slopes of these curves mean values have been calculated for the velocity constant at every concentration. The values are reported in Table VI.

TABLE VI

VELOCITY CONSTANTS AND CONCENTRATION OF ALKALI IN THE DELIGNIFICATION OF WOOD

Molarity	*k*	Molarity	*k*
Lithium hydroxide			
1.38	0.53	2.89	0.66
1.97	.59	4.5	.80
Sodium hydroxide			
1.4	0.65	6.2	1.55
2.0	.84	8.1	1.71
2.9	1.06	14.2	2.77
4.5	1.40		
Potassium hydroxide			
1.4	0.71	6.2	2.19
2.0	1.16	9.6	2.95
2.9	1.28	14.2	3.92
4.5	1.89		

The velocity constants for the three alkalis calculated in this manner have been plotted on a concentration basis in Fig. 2. The curves obtained indicate the manner in which the reaction velocity increases with the concentration for each of these alkalis.

The resemblance of these curves to Freundlich's absorption isotherms suggests that the rate of reaction might depend on the absorption of alkali at the liquor-lignin interface. This would be a necessary prerequisite to chemical action and for any one alkali the rate of reaction would depend on the concentration of the absorbed alkali. Further evidence is available from direct measurements of absorption and from pulping experiments in alcoholic solutions.

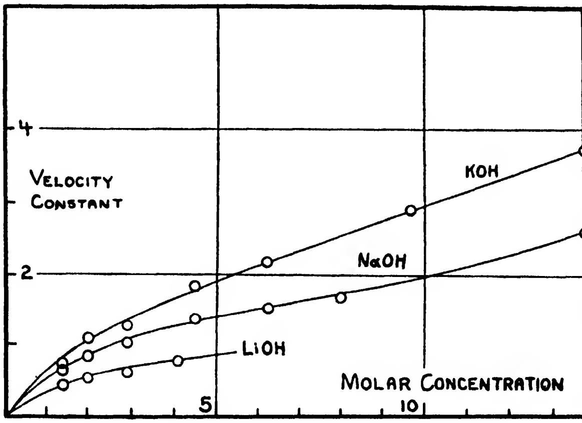

FIG. 2. *Reaction velocity and concentration.*

IV. The Absorption of Alkali

Lusby and Maass (5) have shown that the sorption of alkali on spruce wood at any concentration is proportional to the sorption on cotton at that concentration. The cotton sorption values of Dehnert and König (3) can, therefore, be legitimately compared to the velocity constants obtained previously, as shown in Table VII.

TABLE VII

THE SORPTION OF ALKALI BY COTTON AND THE VELOCITY OF DELIGNIFICATION OF SPRUCEWOOD

Molarity	Sorption at 20° C.	k at 160° C.	Adsorption/k
Sodium hydroxide			
1.4	0.30	0.648	0.442
2.0	.38	.845	.450
2.9	.45	1.06	.424
4.5	.52	1.40	.371
6.2	.52	1.56	.334
8.1	.88	1.71	.513
Potassium hydroxide			
1.4	0.26	0.708	0.367
2.9	.41	1.28	.321
4.5	.51	1.84	.277
6.2	.52	2.19	.237
9.6	.57	2.95	.193

For any one alkali the values for the velocity constant of delignification are seen to be only roughly proportional to the cotton sorption values, as would be expected from the differences in temperature of the sorption and cooking processes, but nevertheless they suggest a certain relation between the two.

On the other hand, when the action of different alkalis on wood is considered, the observed differences in velocity constant are not in any way proportional to the extent to which the individual alkalis are absorbed, as indicated in Table VIII. The wood sorption values were determined according to the titration method described by Richardson and Maass (10, p. 3069).

TABLE VIII

THE ABSORPTION OF ALKALI BY WOOD AND COTTON, AND THE VELOCITY OF DELIGNIFICATION

Alkali	Adsorption at 20° C.		k at 160° C.	Absorption/k
	On cellulose	On wood		
2.0 M LiOH	0.48		0.59	0.81
2.0 M NaOH	0.38		0.845	0.45
2.0 M KOH	0.32		1.16	0.28
0.7 M $(C_2H_5)_4NOH$		0.70	0.57	1.23
0.7 M NaOH		0.63	0.24	2.62
0.7 M NH_4OH		0.30	Negligible	—

This evidence is sufficient to conclude that differences in the magnitude of sorption of different alkalis will not account for differences in their reaction rate. Experiments with different solvents will add further evidence, however, that for any one alkali, the reaction velocity is proportional to the extent of the sorption.

V. The Effect of the Solvent

Instead of using aqueous solutions, delignifications were carried out with methyl and ethyl alcohols since they are good solvents for sodium hydroxide and are in many respects similar to water. Both technical-95% alcohol and alcohol freed from water by twice distilling over lime were used. The methyl alcohol was a technical grade and over 99.5% pure. The results obtained are given in Table IX.

TABLE IX

THE EFFECT OF THE SOLVENT ON THE DELIGNIFICATION OF WOOD

Solvent	Time	Carbohydrate, %	Lignin, %
Water	3 hr.	41.3	2.5
	1½ hr.	47.0	11.5
Absolute ethyl alcohol	3 hr.	20.7	.2
Technical ethyl alcohol	3 hr.	30.6	.2
	1½ hr.	35.1	1.4
	55 min.	41.4	2.1
	30 min.	49.5	3.7
Methyl alcohol	1½ hr.	41.3	3.2

The lignin values indicate that alcoholic solutions of sodium hydroxide are considerably more effective for delignification than aqueous solutions of the same concentration. The yield of carbohydrate is also lower and it was found that a considerable fraction of the lignin originally present in the wood is completely disintegrated and cannot be accounted for in the waste liquor. This is an indication of the greater chemical activity that sodium hydroxide possesses in alcoholic solutions.

This increased rate of delignification can be explained on the basis of the partition law (9) and lends considerable support to the previously mentioned "adsorption" theory of delignification.

The solubility at 20° C. of sodium hydroxide in each of the solvents used was found to be:

Solvent	*Solubility*
Water	20.1 moles per litre
Methyl alcohol	5.6
Ethyl alcohol	3.57

Since each of these saturated solutions is in equilibrium with solid sodium hydroxide, the partition law applied to such a case states that the "escaping tendency" of the sodium hydroxide, that is, its tendency to leave the saturated solution and enter another phase will be the same for each of the solutions. If however, with any particular solvent the concentration is less than saturation, it follows that the escaping tendency will be given by the fractional value that the observed concentration will bear to the saturation concentration for that solvent.

The magnitude of this escaping tendency is a measure of the extent to which the dissolved substance tends to pass off as a gas, to dissolve in a second non-miscible fluid phase, or to become sorbed on a solid surface.

The escaping tendency of sodium hydroxide in 2.0 M aqueous or alcoholic solutions is then calculated by dividing the saturated solubility by the molarity, as indicated in Table X.

TABLE X

THE ESCAPING TENDENCY OF 2.0 M SODIUM HYDROXIDE IN ALCOHOLS AND WATER

Solvent	Escaping tendency
Water	2.0/20.1 = 0.100
Methyl alcohol	2.0/5.6 = 0.357
Ethyl alcohol	2.0/3.57 = 0.56

A certain parallelism is found to exist between the escaping tendency and the absorption of alkali in alcoholic solutions as determined by Vieweg (14).

TABLE XI

THE RELATION OF THE VELOCITY OF DELIGNIFICATION TO THE ESCAPING TENDENCY AND THE SORPTION OF ALKALI FOR THREE SOLVENTS

Solvent	Escaping tendency	Sorption	*k*	Escaping tendency/*k*
Water	0.100	1.00	0.84	0.12
Methyl alcohol	0.357	8.8	1.79	0.19
Ethyl alcohol	0.560	9.8	3.74	0.15

The explanation offered for this increased delignification is that owing to the greater escaping tendency of sodium hydroxide in these solvents, the sodium hydroxide has an increased affinity for the solid phase, which results in a greater absorption of alkali at the reaction interface and in a correspondingly greater reaction velocity.

This increased reaction velocity cannot be ascribed to an increase in the degree of dissociation of the sodium hydroxide since it is known that it is the reverse phenomenon that takes place. Nor can it be due to differences in viscosity since the viscosities of water, methyl alcohol, and ethyl alcohol at 30° C. are respectively 0.008, 0.005, and 0 01 in C.G.S. units.

It was interesting to determine whether a solvent of high viscosity would retard the rate of delignification of wood. Glycerol was selected since it is an alcohol and is similar in some respects to water, and to ethyl and methyl alcohols. It is a fairly good solvent for sodium hydroxide and has a viscosity 600 times that of water and 500 times that of ethyl alcohol.

In Table XII are given the yields of lignin and carbohydrate of two cooks made under comparable conditions with water and glycerol as solvents.

TABLE XII

GLYCEROL AS A SOLVENT

Solvent	Carbohydrate, %	Lignin, %
Water	47.0	11.5
Glycerol	53.4	14.9

The solubility of sodium hydroxide is less in glycerol than in water, so that the different escaping tendency of 2.0 *M* sodium hydroxide in glycerol cannot be considered as a reason for the lesser delignification observed.

It is probable that, in this case, the high viscosity of the solvent hinders the submicroscopic diffusion of the alkali into the lignin gel-structure, resulting in a lower rate of diffusion than would otherwise occur. Thus, under extreme conditions, viscosity of the medium can be a factor influencing the reaction rate.

A cooking experiment was carried out using 2.0 *M* sodium ethylate dissolved in absolute alcohol, in order to ascertain whether delignification would take place in the absence of hydroxyl ions.

Only a slight amount of pulping took part in the outside of the chips. The interior was hard, light in colour, and completely uncooked.

Sodium ethylate, $Na^+OC_2H_5^-$, is therefore not a pulping agent. The slight amount of pulping that did take place was very likely due to the action of sodium hydroxide, formed in small amount from the sodium ethylate by traces of moisture still present in the wood or in the liquor.

The presence of a sufficient hydroxyl ion concentration, in addition to a suitable alkali cation is therefore necessary for the delignification process.

VI. The Influence of Temperature on the Reaction Rate

No experimental work on the influence of temperature was performed in the present research. However, the object of the investigation, namely, the elucidation of the mechanism of alkaline pulping, required that the temperature data of other investigations should be examined and reinterpreted in the light of the Arrhenius equation and the general theory of chemical activation (8).

Arrhenius observed that the variation with temperature of the velocity constant for a number of chemical reactions could be represented by an equation of the type:

$$\ln k = B - A/T,$$

in which *A* and *B* are specific constants for each reaction. Recognizing the similarity of this equation with the van't Hoff isochore, which connects the equilibrium constant, *K*, of a chemical reaction with the increase in internal energy, *U*,

$$\ln K = \text{const} - U/RT,$$

he suggested by analogy the existence of an equilibrium between "passive" molecules of the reacting species and "active" molecules formed from normal molecules by absorption of energy.

Of the total number of molecules, only that small fraction that is "active" at any instant during the reaction can react. The result is that the chemical reaction is not instantaneous, but occurs at a measurable rate, since the special distribution of energy that is required takes a finite time. The general correctness of this view has received overwhelming confirmation.

Putting $B = \ln Z$ and $A = E/R$, the above relation can be written:

$$\ln k = \ln Z - E/RT$$

or,

$$k = Ze^{-E/RT},$$

where *Z* and *E* are the new specific constants, and *R* is the gas constant.

The fraction $e^{-E/RT}$, according to the Maxwell-Boltzmann distribution law, is proportional to the number of molecules possessing an energy content *E*. *E* is termed the critical energy and is determined experimentally by plotting the logarithm of the velocity constant against the reciprocal of the absolute

temperature. The slope of the line multiplied by the gas constant R (1.985 cal. per degree) gives the value of E in calories per gram-mole.

Applying this theory to some results obtained by Lusby, and calculating the values of k from the relation: $k = 1/t \ln L_0/L$, we obtain the data in Table XIII.

TABLE XIII

THE INFLUENCE OF TEMPERATURE ON THE REACTION VELOCITY

Temp., °C.	2.9 M NaOH		14.3 M NaOH		14.3 M KOH	
	L_r	k	L_r	k	L_r	k
120	—	—	24.1	0.184	23.6	0.205
140	23.2	0.223	11.7	0.91	4.6	1.84
160	10.4	1.026	1.9	5.03	0.6	6.18

These results are shown plotted in Fig. 3 and indicate that, taking into consideration the accuracy with which k can be determined, the straight line relation between ln k and $1/T$ is closely obeyed. We may then conclude that:

(i) In alkali-pulping, with sodium or potassium hydroxide, at both high and low alkali concentrations, this increase in the rate of delignification with increase in temperature takes place in the manner predicted by the activation theory of Arrhenius.

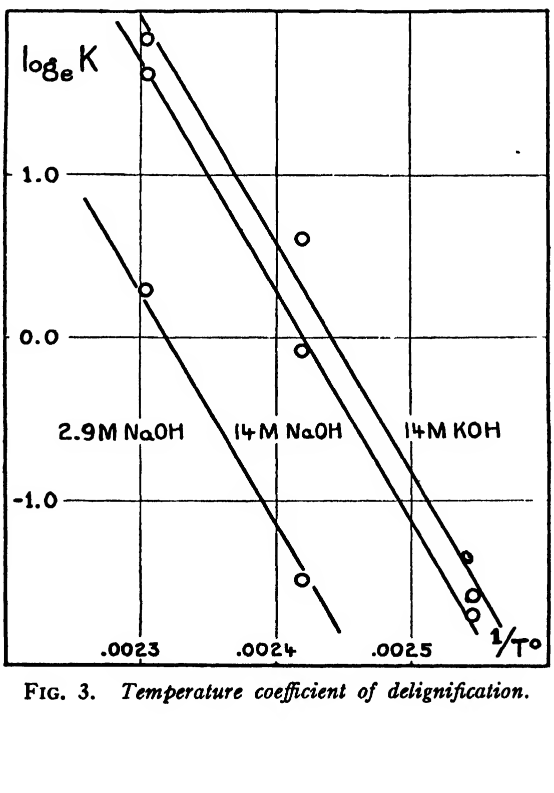

FIG. 3. *Temperature coefficient of delignification.*

(ii) The value of the energy of activation is found to be 32,000 cal. per gram-molecule, or 5.3×10^{-20} cal. per molecule.

(iii) The same activation energy is obtained whether 2.9 *M* sodium hydroxide, 14.3 molar sodium hydroxide, or 14.3 molar potassium hydroxide is used.

(iv) The calculated values for Z are:

2.9 *M* NaOH : 1.5×10^{16} per hr.
14.3 *M* NaOH : 7.0×10^{16} per hr.
14.3 *M* KOH : 8.8×10^{16} per hr.

Conclusion

The writers have given some evidence suggesting that absorption of alkali at the reaction interface was the determining factor in setting the rate of delignification. Let us consider the molecular phenomena that are taking place at a point on the solid lignin surface.

There are three separate stages to the reaction. (i) The acidic phenolic groups in the lignin complex bring about absorption of alkali at the interface. There is no hindrance to this absorption. The interface is at all times in saturated equilibrium with the alkali in the liquid phase, since we have seen previously that the diffusion of alkali to the solid-liquid interface is always sufficiently rapid so as not to influence the reaction rate. The amount of alkali present depends on the escaping tendency of the solution. (ii) Either immediately following absorption, or after a certain interval of time, chemical combination takes place between the lignin and the absorbed alkali. (iii) There then follows a chemical hydrolysis and the separation of one alkali-lignin complex from the lignin surface, and its solution in the liquor.

We have no method of distinguishing the "combination" reaction from the "solution" reaction. We do not know whether they take place simultaneously or whether one is slower than the other and governs the reaction rate. But since the variation of the velocity of the complete reaction with temperature takes place in accordance with the Arrhenius equation, some intermediate complex must be formed between the absorbed alkali and part of the lignin, and this molecular complex requires a certain minimum energy of activation for further reaction. The energy that must be concentrated at a point of the lignin structure, in order to bring into solution one alkali-lignin complex (and incidental by-products), has been calculated to be of the order of 5.3×10^{-20} cal.

At the interface between the lignin and the absorbed alkali the complicated molecular orientations brought about by valence forces are being constantly disturbed and changed by forces of thermal agitation. By analogy with homogeneous bimolecular reactions, the constant will be the number of "favourable orientations" of the lignin-alkali complex occurring per second, any one of which, if suitably activated by an energy E, will result in the solution of one alkali-lignin particle.

With increase in concentration, the observed increase in the value of velocity constant k and in the value of Z, would be due to the greater number of favourable orientations rendered possible by the higher concentration of absorbed alkali at the lignin interface. Similarly, the increase in the value of k with the nature of the alkali in the order lithium hydroxide, sodium hydroxide, potassium hydroxide, would be due to the greater number of favourable orientations possible with the smaller potassium ions than with the more highly hydrated lithium and sodium ions.

References

1. Arrhenius, S. and Schmidt-Neilsen. Svensk Pappers Tid. May 31, 1924.
2. Corey, A. J. and Maass, O. Can. J. Research, B, 14 : 336-345. 1936.
3. Dehnert, F. and König, W. Cellulosechemie, 5 : 107-112. 1924. 6 : 1-10. 1925.
4. Larocque, G. L. and Maass, O. Can. J. Research, B, 15 : 89-97. 1937.
5. Lusby, G. R. and Maass, O. Can. J. Research, B, 10 : 180-189. 1934.
6. Lusby, G. R. and Maass, O. Can. J. Research, B, 15 : 536-544. 1937.
7. Mitchell, C. R. and Yorkston, F. H. Forest Products Lab. Can. Quart. Rev. 18 : 6-16. 1934.
8. Moelwyn-Hughes, E. A. The kinetics of reactions in solution. The Clarendon Press, Oxford. 1933.
9. Nernst, W. Theoretical chemistry from the standpoint of Avogadro's rule and thermodynamics. The Macmillan Company, New York. 1923.
10. Richardson, R. and Maass, O. J. Phys. Chem. 36 : 3064-3073. 1932.
11. Roller, P. S. J. Phys. Chem. 39 : 221-237. 1935.
12. Ross, J. H. and Potter, J. G. Pulp Paper Mag. Can. 29 : 569-571. 1930.
13. Taylor, H. S. Treatise on physical chemistry. D. Van Nostrand Company, New York. 1924.
14. Vieweg, W. Ber. 40 : 3876-3883. 1907.

STUDIES ON ANTIOXIDANT ACTIVITY

I. ESTIMATION OF ANTIOXIDANT ACTIVITY IN STABILIZING VITAMIN A IN OILS[1]

By W. E. Parker[2], A.C. Neish,[3] and W. D. McFarlane[4]

Abstract

The efficiency of wheat-germ oil in stabilizing vitamin A against the destructive action of ultra-violet radiations was investigated. A rapid and convenient method of estimating antioxidant potency is described which is based on ultra-violet irradiation of mixtures of halibut liver oil and antioxidant in chloroform solution and estimation of vitamin A by the direct application of the antimony trichloride reaction employing photoelectric colorimetry.

Introduction

The destruction of vitamin A in rancid oils was first noted by Fridericia (3) and Powick (14) in 1925, and confirmed by Mattill (12) two years later. Whipple (16) and Lowen, Anderson, and Harrison (11) have shown that in oils undergoing oxidation the decrease in vitamin A is paralleled by an increase in peroxide value. Extensive experiments by Lease *et al* (10) indicated that rancid fats destroyed vitamin A in the stomachs of test animals and that high peroxide values in oil supplements decreased the amount of vitamin stored in the liver. The similarity between the oxidation of fat and the destruction of vitamin A is indicated by the fact that both processes are accelerated by the presence of metallic ions, by ultra-violet light, and by increased temperature, and are retarded by antioxidants.

Various procedures for measuring the susceptibility of fats to oxidative changes and the efficiency of antioxidants have been described in the literature (9). Most of these are based on manometric measurements of the uptake of oxygen by the oil or on the time required for its content of peroxide oxygen to reach an arbitrary value. Greenbank and Holm (4) have described a photoelectric method of measuring the length of the induction period, based on the reduction of methylene blue by the oxidizing oil. Acceleration of the oxidation of the oil by heat is commonly employed to reduce the time necessary for carrying out determinations; ultra-violet light (15) and metallic catalysts (7, 15) have been used to a limited extent for the same purpose. Even under these conditions the procedures are too long to permit their general use as routine methods of analysis. No systematic investigation of the effect of antioxidants on the stability of vitamin A in oils has yet been reported, although hydroquinone (5, 6), lecithin (5), and ground cereals (11) have been shown to protect the vitamin in varying degrees.

[1] *Manuscript received July 31, 1940.*

Contribution from the Faculty of Agriculture of McGill University, Macdonald College, Que. Macdonald College Journal Series 144.

[2] *Senior Demonstrator, Department of Chemistry, Macdonald College.*

[3] *Graduate Research Assistant. Present Address: Division of Industrial and Cellulose Chemistry, McGill University.*

[4] *Professor of Chemistry, Macdonald College.*

The comparatively rapid decomposition of vitamin A by ultra-violet radiations (2, 13) suggested to the writers the possibility of measuring the antioxidant potency of different substances by comparing the protection they afforded to vitamin A in oils exposed to ultra-violet irradiation.

Experimental

The vitamin A content of the oils was determined by the Dann and Evelyn (1) modification of the Carr-Price antimony trichloride reaction. Wilkie's (17) procedure for saponification was employed where a non-saponifiable residue was required. Peroxide oxygen was determined by the method of C. H. Lea (8).

To avoid the time-consuming saponification procedure if at all possible, a number of oils from different sources were tested to determine whether the values obtained for vitamin A on an oil directly agreed with those obtained on its non-saponifiable residue. The results, summarized in Table I, show that there is some substance present in cod liver oil that inhibits the full development of the blue colour. This fact is well known, but it will be noted that the inhibiting substance is not present in halibut liver oil or in pilchardene. Measurements of the rate of fading of the blue colour showed that there was little difference in this respect when the oil, or its non-saponifiable fraction, was used for the test. As a result of these experiments either halibut liver oil or pilchardene was used in all subsequent experiments.

For the first tests of antioxidant activity a sample of wheat-germ oil prepared by a solvent-extraction process was employed. Although this oil contained relatively large quantities of carotinoid pigments (75 micrograms per 100 gm. of oil) it was found that an equivalent amount of carotene added

TABLE I

THE EFFECT OF SAPONIFICATION ON THE VITAMIN A VALUE OF OILS AS DETERMINED BY THE ANTIMONY TRICHLORIDE METHOD

Sample	Vitamin A, International units per gram of oil	
	With saponification	Without saponification
Cod liver oil No. 1	1180	795
No. 2	2415	1425
No. 3	546	360
Clo-trate (Cod liver oil)	2250	1950
Pilchardene No. 1	735	735
No. 2	1980	1980
No. 3	2025	2170
Halibut liver oil No. 1	54500	53100
No. 2	89250	89250

to pilchardene did not significantly affect the results of the vitamin A determinations. The values for vitamin A obtained with mixtures of pilchardene and wheat-germ oil were slightly higher than calculated, but this was due to a slight cloudiness that developed on the addition of the antimony trichloride reagent, rather than to an enhanced blue colour.

A. *Direct Irradiation of Oil Mixtures*

Portions (10 ml.) of mixtures of pilchardene with wheat-germ oil were irradiated simultaneously in 30 ml. beakers placed directly beneath a Hanovia

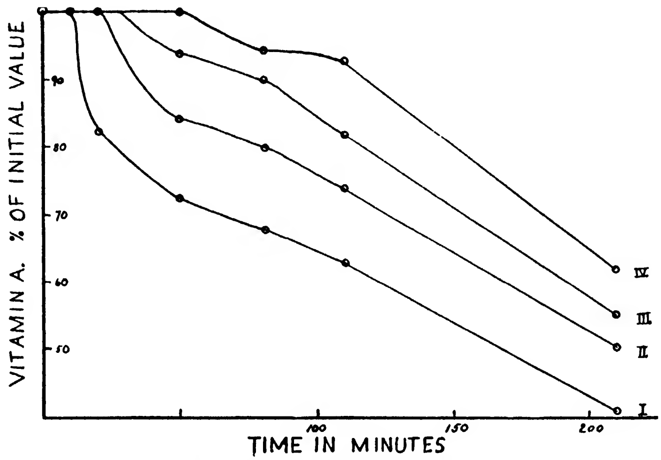

FIG. 1. *The destruction of vitamin A in pilchardene and mixtures of pilchardene with wheat-germ oil by irradiation with a quartz mercury arc.*

I. *100% pilchardene.*
II. *95% pilchardene + 5% wheat-germ oil.*
III. *80% pilchardene + 20% wheat-germ oil.*
IV. *50% pilchardene + 50% wheat-germ oil.*

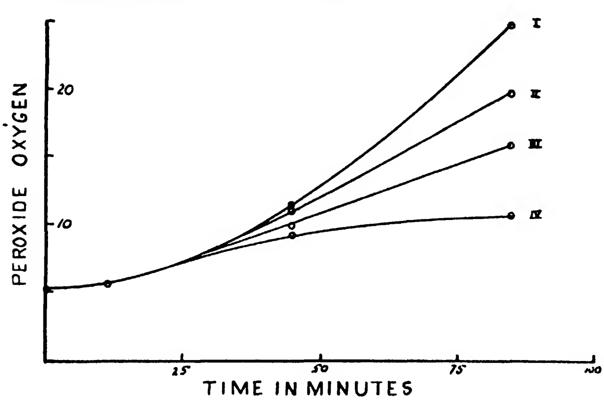

FIG. 2. *The increase in peroxide oxygen in pilchardene and mixtures of pilchardene with wheat-germ oil, by irradiation with a quartz mercury lamp. The peroxide oxygen is expressed in terms of 0.002 N thiosulphate per ml. of oil.*

I. *100% pilchardene.*
II. *95% pilchardene + 5% wheat-germ oil.*
III. *80% pilchardene + 20% wheat-germ oil.*
IV. *50% pilchardene + 50% wheat-germ oil.*

quartz mercury arc 17 cm. from the surface of the oil. At intervals, 1 ml. aliquots were removed, dissolved in chloroform, and their vitamin content determined. The results, shown graphically in Fig. 1, indicated a definite inhibition of the decomposition of the vitamin by the wheat-germ oil, and an increased induction period. Irradiation also increased the peroxide values of the irradiated oil mixtures (Fig. 2).

There was a possibility that the results were affected by the difference in concentration of vitamin A in the mixtures. To test this, fresh mixtures were prepared in which the concentration of vitamin was kept constant by the addition of petrolatum as a diluent. The mixtures were irradiated, and the vitamin A and peroxide contents determined as before. The results did not differ significantly from those obtained in the first experiment, and indicated that the rate of decomposition of the vitamin was independent of its concentration.

Although this method of testing antioxidant activity was comparatively rapid, the results were not entirely satisfactory. Oil mixtures of identical composition did not give good agreement in duplicate experiments, the viscous oils were difficult to pipette accurately, and the heating from the mercury arc was not controlled in any way.

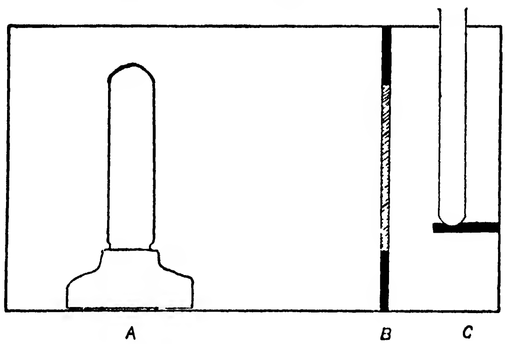

FIG. 3. *Apparatus used for the irradiation of oils in chloroform solution A. General Electric Type H3 mercury lamp. B. Corning Filter No. 986. C. Rack and test tubes.*

Irradiation of the oil in a suitable solvent appeared to offer the best means of overcoming the difficulty of removing aliquots for analysis, and of the various fat solvents, chloroform appeared to be the most suitable. Vitamin A is known to be relatively unstable in this solvent (2, 13) and its use would permit antimony trichloride tests to be carried out directly without the necessity of evaporating any solvent. Preliminary experiments showed that sufficient ultra-violet light passed through the walls of Pyrex test-tubes to decompose the vitamin at a reasonably rapid rate.

B. *Irradiation in Chloroform Solution*

For more extensive tests the apparatus illustrated in Fig. 3 was constructed. The light source (A) was a General Electric Type H3 mercury lamp, and was placed at a distance of 8 in. from a rack (C), which held three 16 by 150 mm.

Pyrex test-tubes. A No. 986 Corning filter (B) placed between the light source and the tubes protected the latter from excessive heat and from visible light, but transmitted 90% of the ultra-violet radiation at 3300 Å. The entire apparatus was enclosed in a well ventilated box.

With this apparatus very consistent results were obtained for the rate of decomposition of vitamin A. Irradiation of a chloroform solution of halibut liver oil for one hour reduced its vitamin A content to 42% of its original value, and this result could be closely duplicated with different concentrations of the oil. The addition of wheat-germ oil reduced the rate of decomposition of the vitamin, and slightly increased the induction period (Fig. 4).

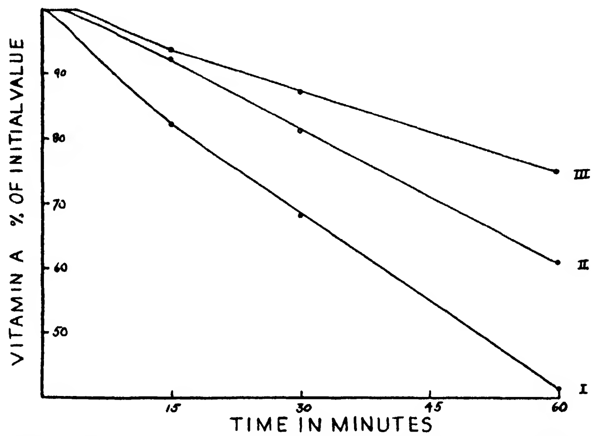

FIG. 4. *The destruction of vitamin A in halibut liver oil, and mixtures of halibut liver oil with wheat-germ oil, by ultra-violet irradiation in chloroform solution.*

I. *Halibut liver oil.*
II. *Halibut liver oil + 4% expressed wheat-germ oil.*
III. *Halibut liver oil + 4% extracted wheat-germ oil.*

In carrying out tests of antioxidant activity with this apparatus, the following technique was adopted. Three tubes containing halibut liver oil in chloroform in the same concentration were irradiated simultaneously. In addition to the halibut liver oil one contained 4% of wheat-germ oil which was adopted as a standard; the second contained a known weight of the oil being tested. No addition was made to the third tube, which served as a control. At the end of 15, 30 and 60 min. intervals, 1 ml. aliquots were removed and analyzed immediately for vitamin A. Typical decomposition curves (Fig. 4) are very similar to those obtained by Holmes (5) who used heat to accelerate the decomposition of the vitamin.

In order to obtain a numerical comparison of the antioxidant efficiencies of different oils as determined by this method the writers propose to employ the term "protection factor" for the ratio defined by the following equation.

$$\text{Protection factor} = \frac{x-y}{x},$$

where x = the percentage of vitamin A destroyed by irradiation for one hour

in chloroform solution in the absence of antioxidant, and y = the percentage of vitamin A destroyed under the same conditions in the presence of an antioxidant.

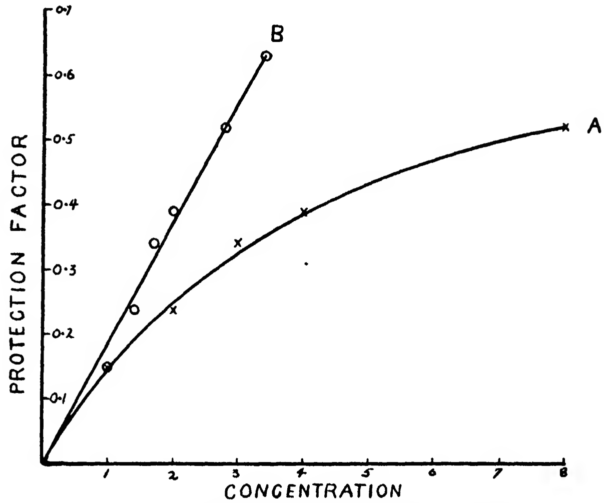

FIG. 5. *Protection factors plotted against—(A) the concentration of wheat-germ oil, (B) the square root of the concentration of wheat-germ oil.*

Protection factors have been calculated from the experimental results for different oils, and for different concentrations of the same oil. The protection factor does not appear to vary directly with the concentration of the oil, but the points obtained by plotting the square root of the concentration against protection factors fall approximately on a straight line passing through the origin (Fig. 5).

TABLE II

THE REPRODUCIBILITY OF RESULTS ON REPEATED IRRADIATION OF HALIBUT LIVER OIL WITH AND WITHOUT WHEAT-GERM OIL

Antioxidant	Strength, %	Number of determinations	% Vitamin A destroyed in one hour	Protection factor
None	–	18	58.5 ± 0.5	–
Oil No. 1	2	3	35.2 ± 0.6	0.40
Oil No. 1	4	3	27.8 ± 0.4	0.52
Oil No 2	4	15	35.4 ± 0.3	0.39

Table II illustrates the reproducibility of the results that have been obtained by the method. Protection factors, calculated as described above, are also included. The consistency with which the results could be duplicated with solutions of identical composition leads to the belief that it might be possible to dispense with control solutions. However, they have always been included as a precautionary measure against marked fluctuations in line voltage.

Different samples of wheat-germ oil, fractions obtained from wheat-germ oil by different methods of treatment, and pure substances reported to possess antioxidant activity have been tested by this method. The results of these investigations will be published in the second paper of this series.

Acknowledgment

This work was supported in part by a grant to one of the writers (A.C.N.) from the Ogilvie Flour Mills Co. Limited, Montreal, who also supplied us with the wheat-germ oil.

References

1. Dann, J. W. and Evelyn, K. A. Biochem. J. 32 : 1008-1017. 1938.
2. De, N. K. Indian J. Med. Research, 24 : 737-749. 1937.
3. Fridericia, L. S. J. Biol. Chem. 62 : 471-485. 1925.
4. Greenbank, G. R. and Holm, G. E. Ind. Eng. Chem. (Anal. Ed.) 2 : 9-10. 1930.
5. Holmes, H. N., Corbett, R. E., and Hartzler, E. R. Ind. Eng. Chem. 28 : 133-135. 1936.
6. Huston, R. C., Lightbody, H. D., and Ball, C. D. J. Biol. Chem. 79 : 507-518. 1928.
7. King, A. E., Roschen, H. L., and Irwin, W. H. Oil and Soap, 10 : 105-109. 1933.
8. Lea, C. H. Proc. Roy. Soc. London, B, 108 : 175-189. 1931.
9. Lea, C. H. Rancidity in edible fats. Chemical Pub. Co., N.Y. 1939.
10. Lease, E. J., Lease, J. G., Weber, J., and Steenbock, H. J. Nutrition, 16 : 571-583. 1938.
11. Lowen, E. J., Anderson, D., and Harrison, R. W. Ind. Eng. Chem. 29 : 151-156. 1937.
12. Mattill, H. A. J. Am. Med. Assoc. 89 : 1505-1508. 1927.
13. McFarlane, W. D. and Sutherland, A. J. Can. J. Research, B, 16 : 421-433. 1938.
14. Powick, W. C. J. Agr. Research, 31 : 1017-1026. 1925.
15. Royce, H. D. Oil and Soap, 10 : 123-125. 1933.
16. Whipple, D. V. Oil and Soap, 13 : 231-232. 1936.
17. Wilkie, J. B. J. Assoc. Official Agr. Chem. 20 : 206-208. 1937.

SYNTHESIS OF VERATROYL ACETALDEHYDE AND INFLUENCE OF A HYDROXYL GROUP ON THE REACTIVITY OF THE PARA-CARBONYL GROUP[1]

By Leo Brickman[2], W. Lincoln Hawkins[3], and Harold Hibbert[4]

Abstract

Attempts, by three independent methods of synthesis, to prepare vanilloyl acetaldehyde are described. In each case it has been shown that the presence of a para phenolic hydroxyl group either prevents or alters the normal course of the reactions. The synthesis of veratroyl acetaldehyde has been accomplished, and this product is described. A theoretical explanation for the mutual interrelationship of the carbonyl and para phenolic hydroxyl group is suggested.

Introduction

Recent studies on the structure of lignin have resulted in the isolation of a large variety of compounds containing the guaiacyl and syringyl nuclei, in which a carbonyl group occupies a position para to the free phenolic hydroxyl group. Vanillin (22), guaiacol (13), and acetovanillone (5) have been isolated from the alkaline degradation products of lignin sulphonic acids obtained from soft woods, while similarly, from hard woods, these same products, along with their syringyl analogues, syringaldehyde (9), syringol (14), and acetosyringone (15), have been isolated.

Recently, a new series of lignin degradation products has been obtained from a variety of woods by the ethanolysis process (4, 6, 11). This method of converting lignin into simple building units consists in refluxing the resin-free wood meal with ethanolic hydrogen chloride in an inert atmosphere. The residual pulp is filtered off, and the solution, after concentration, poured into a large volume of water, from which the amorphous-ethanol lignin precipitates out.

For many years the latter process was employed solely for the preparation of water-insoluble ethanol lignin, any soluble oils being entirely overlooked. A recent careful examination of the aqueous-ethanol filtrate from maple and other hard woods revealed the presence of an appreciable quantity of volatile oils (25 to 30%, based on the Klason lignin originally present). These crude oils were then separated into bisulphite-soluble, bicarbonate-soluble, alkali-soluble, and neutral fractions. In the case of spruce wood the yields were lower (10%), α-ethoxypropiovanillone (6) being isolated from the alkali fraction, and vanilloyl methyl ketone, along with vanillin, from the bisulphite

[1] *Manuscript received in original form July 23, 1940, and, as revised, October 29, 1940.*

Contribution from the Division of Industrial and Cellulose Chemistry, McGill University, Montreal, Que., with financial assistance from the Spruce Falls Power and Paper Company and the Canada Paper Company. Abstracted from a thesis submitted by Leo Brickman to the Faculty of Graduate Studies and Research, McGill University, in partial fulfilment of the requirements for the Degree of Doctor of Philosophy, May, 1940.

[2] *Postgraduate student.*

[3] *Sessional Lecturer in Chemistry.*

[4] *Professor of Industrial and Cellulose Chemistry.*

fraction (3). Again, a chemical distinction between soft and hard woods was observed, hard woods yielding a mixture of the corresponding syringyl and guaiacyl derivatives. Thus, both α-ethoxypropiosyringone (11) and α-ethoxypropiovanillone were found to be components of the alkali fraction of maple, while syringaldehyde (20) and syringoyl methyl ketone (3), along with their guaiacyl analogues, were isolated from the bisulphite fraction.

Investigations in these laboratories, extending over several years, have resulted in a comprehensive study of this type of compound in which a carbonyl group occupies a position on the benzene nucleus para to a free hydroxyl group. The series of compounds that has been isolated from lignin offers a wide variety of such examples and includes aldehydes, methyl ketones, benzoins, and benzils. In every case, these lignin degradation products have been found to possess certain abnormal properties due, in general, to the presence of the free phenolic hydroxyl group. Thus vanillin, in contrast to a normal aromatic aldehyde, does not undergo the Cannizzaro reaction with alkalis, but on the contrary is stable for several hours to 8 *N* sodium hydroxide at 100° C. Furthermore, it has been observed that this abnormal stability disappears on replacement of the hydroxyl by an alkali-stable group such as methoxyl.

In the course of synthesizing several of these derivatives for identification purposes, further examples of this class of compound have been encountered. The presence of this free phenolic hydroxyl group in the para position to a carbonyl group has been found to influence both the rate and course of a variety of synthetic processes. In a study of the influence of solvents on the reactions of carbonyl compounds with the Grignard reagent, Lieff, Wright, and Hibbert (16) report the abnormal behaviour of vanillin and acetovanillone towards this reagent. In both cases, an apparent hindrance to normal addition at the carbonyl group was observed.

These preliminary observations indicated a mutual inhibiting effect on the reactivity of the carbonyl and phenolic hydroxyl groups when in the para position. In the present investigation, several attempts were made to synthesize vanilloyl acetaldehyde in order to compare its properties with those

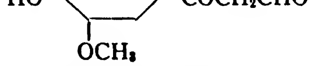

Vanilloyl acetaldehyde

of one of the components of the ethanolysis bisulphite fraction from spruce and maple woods. All attempts to synthesize this substance were unsuccessful however, a fact attributable to the presence of the para phenolic hydroxyl in the various intermediates. It was therefore necessary to abandon this synthesis and to prepare the methylated derivative, veratroyl acetaldehyde, the synthesis of which proceeded smoothly and in good yield.

Discussion

The preparation of vanilloyl acetaldehyde was attempted by three independent methods of synthesis.

Synthesis (A).

This was attempted by the action of allyl magnesium bromide on vanillin and its derivatives, the proposed synthesis involving the following steps:

$$\underset{\text{I}}{\text{RCHO} + \text{CH}_2\text{=CH—CH}_2\text{MgBr}} \longrightarrow \underset{\text{II}}{\text{RCHOH—CH}_2\text{—CH=CH}_2} \xrightarrow{\text{Cr}_2\text{O}_3}$$

$$\underset{\text{III}}{\text{RCO—CH}_2\text{—CH=CH}_2} \xrightarrow{\text{O}_3} \underset{\text{IV}}{\text{RCO—CH}_2\text{—CHO}}$$

R = Guaiacyl

With vanillin, the product obtained in the first step was an uncrystallizable yellow oil, the methoxyl analysis of which corresponded to the conjugated system, RCH=CH—CH=CH_2, presumably formed from the carbinol (II) by loss of water. To determine whether this secondary reaction was due to the influence of the free hydroxyl group, the methoxymethyl ether of vanillin was then treated similarly and a low yield of carbinol was obtained. Veratraldehyde, however, in which the phenolic hydroxyl is blocked by a more stable group, reacted smoothly to give a good yield of II which could be oxidized to III but not carried beyond this stage to give veratroyl acetaldehyde. This was probably due to the extreme sensitivity of veratroyl acetaldehyde to the reagents used to decompose the intermediary ozonide.

Synthesis (B).

This method involved bromination of acetovanillone, conversion of the bromide to the nitrile, followed by a Stephen reduction (21) to give vanilloyl acetaldehyde.

$$\text{R—CO—CH}_3 \xrightarrow{\text{Br}_2} \text{R—CO—CH}_2\text{Br} \xrightarrow{\text{KCN}} \text{R—CO—CH}_2\text{—CN} \xrightarrow[\text{reduction}]{\text{Stephen}}$$

$$\text{R—CO—CH}_2\text{—CH=NH . HCl} \xrightarrow{\text{H}_2\text{O}} \text{R—CO—CH}_2\text{—CHO}$$

R = Guaiacyl

With acetovanillone acetate as starting material, bromination was effected successfully and the resulting bromide converted to the nitrile. All attempts to reduce the nitrile by Stephen's method were unsuccessful.

Synthesis (C).

This procedure involved a Claisen-Schmidt condensation of both acetovanillone and several of its derivatives with ethyl formate under the conditions used by Auwers (1, 2) to prepare benzoyl acetaldehyde.

$$R{-}CO{-}CH_3 + H{-}\overset{\overset{\displaystyle O}{\|}}{C}{-}OC_2H_5 \xrightarrow{Na} R{-}CO{-}CH{=}CHONa \xrightarrow{H} R{-}CO{-}CH_2{-}CHO$$

$$R = \text{Guaiacyl}$$

The influence of the para phenolic hydroxyl on the carbonyl group was apparent when acetovanillone was employed as the starting material. Condensation with ethyl formate, which depends on activation of the hydrogen atoms by the carbonyl group, did not take place in this case, acetovanillone being recovered unchanged. An attempt was then made to offset the influence of the phenolic hydroxyl by converting it to the acetate. The ester, however, proved to be unstable to the conditions of the reaction, and again acetovanillone was recovered unchanged.

Since methoxymethyl ethers have been shown to be relatively stable to alkali, the condensation was next attempted using the methoxymethyl ether of acetovanillone. In this instance a condensation was effected, but instead of the expected methoxymethyl ether of vanilloyl acetaldehyde a final reaction product that corresponded, in analysis and properties, to the methoxymethyl ether of α-guaiacyl acrylic acid (V) was obtained. It was possibly formed as indicated below:

$$R{-}CO{-}CH_3 + H{-}\overset{\overset{\displaystyle O}{\|}}{C}{-}OC_2H_5 \xrightarrow{Na} R{-}\underset{\underset{\displaystyle OH}{|}}{\overset{\overset{\displaystyle CH_3}{|}}{C}}{-}\overset{\overset{\displaystyle O}{\|}}{C}{-}OC_2H_5 \xrightarrow[-H_2O]{Na}$$

$$R{-}\overset{\overset{\displaystyle CH_2}{\|}}{C}{-}COONa \xrightarrow{H_2O} R{-}\overset{\overset{\displaystyle CH_2}{\|}}{C}{-}\overset{\overset{\displaystyle O}{\|}}{C}{-}OH$$

V

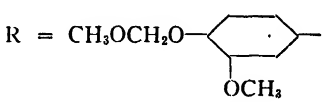

When, however, acetoveratrone was used in this condensation, a 90% yield of veratroyl acetaldehyde was obtained, indicating clearly the remarkable effect resulting from replacement of the para hydroxyl by a methoxyl group.

It is thus apparent that the para phenolic hydroxyl affects the reactivity of the carbonyl group directly and also influences the activation of other atoms in the molecule, rendering difficult the course of any reaction involving the para carbonyl group. Esterification seems to diminish the reactivity of the latter, or its ineffectiveness may be due to the ease of removal of the ester group under the conditions of the reaction. Etherification normalizes the behaviour of the carbonyl group, the methoxyl group, in this respect, having a greater effect than the methoxymethyl group. This fact is in agreement with the observations of Hunter, Cramer, and Hibbert (11), who, while unable to brominate propiosyringone directly, found this reaction took place normally with the methyl ether.

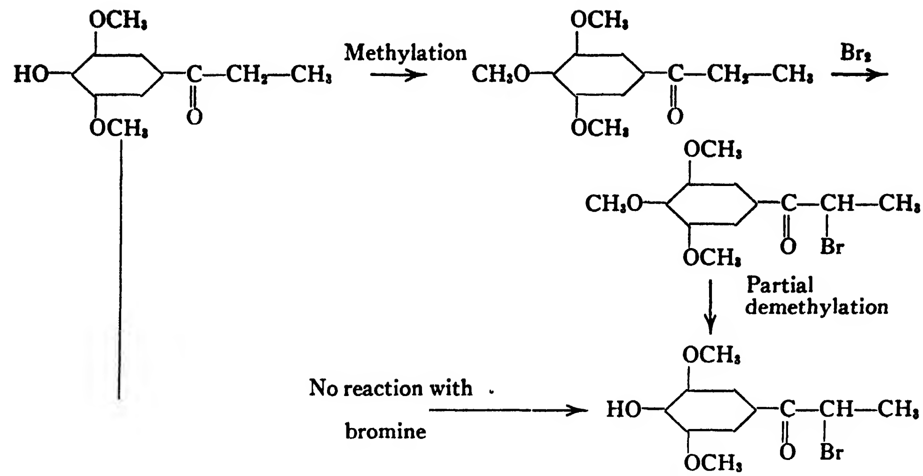

On the other hand, a number of observations have been made on the pronounced influence exerted by the carbonyl group on the reactions of a para phenolic hydroxyl group. Hunter and Hibbert (12) have shown that, whereas syringaldehyde, α-hydroxypropiosyringone, α-acetoxypropiosyringone and α-bromopropiosyringone, as well as propiosyringone, form a potassium salt with potassium acetate in ethanol solution, 3,5-dimethoxy-4-hydroxyphenyl propane (in which there is no carbonyl group) is completely unreactive towards this reagent, formation of the potassium salt apparently being dependent on the activating effect of the carbonyl group. Lock (17, 18) has also pointed out such interrelationships between 1,4-hydroxycarbinol groups in the benzene nucleus.

It is possible to account for many of the abnormal reactions of this class of 1,4-hydroxycarbonyl compounds on the assumption that a dynamic equilibrium exists between two resonating forms, this equilibrium shifting under the influence of reactants. This might be set up by the wandering of a hydrogen ion (proton) with resulting rearrangement of the electron system:

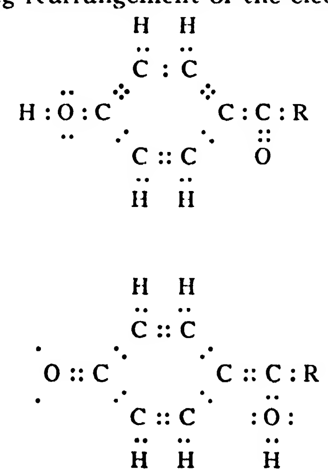

R = H, CH_3, $CHOHCH_3$, etc.

In this way it is possible to visualize a mutual interrelationship between the carbonyl and phenolic hydroxyl groups and to explain the resulting loss of activity in certain reactions, an explanation which, however, for the moment is a purely theoretical one.

Experimental

Attempted Synthesis of Vanilloyl Acetaldehyde

Synthesis A. Action of Allyl Magnesium Bromide

(I) On Vanillin

Allyl magnesium bromide was prepared according to the method of Gilman and McGlumphey (8). Vanillin (5 gm.) in anhydrous ether (70 cc.) was added to the Grignard reagent (2.5 moles) over a period of 30 min. with vigorous stirring. The mixture was allowed to stand overnight, decomposed with ice and dilute sulphuric acid, and then extracted with ether. The ethereal solution was extracted first with sodium bisulphite (20%) and then with sodium hydroxide (5%). The following fractions were obtained: *(a)* Bisulphite-soluble (vanillin), yield 2.88 gm.; *(b)* Alkali-soluble, yield, 1.7 gm.; *(c)* Residue, yield, 0.3 gm. The alkali-soluble fraction was a yellow oil distilling at a bath temperature of 160 to 220° C. at 0 01 mm. Found: OCH_3, 17.7%. Calc. for $C_{11}H_{14}O_3$: OCH_3, 16.0%.

(II) On Vanillin Benzoate

Vanillin benzoate (5 gm.) prepared by the method of Anderson (10) was treated with a slight excess of allyl magnesium bromide and the reaction mixture worked up as described under (I). There was recovered unchanged vanillin benzoate (2.1 gm.) and alkali-soluble material, presumably vanillin, (0.7 gm.). The experiment was repeated under varying conditions of time, temperature, and solvent but in all cases most of the original material was recovered unchanged.

(III) On Methoxymethyl Vanillin

This derivative was prepared according to the directions of Pauly and Wäscher (19). Methoxymethyl vanillin (25 gm.) was added to Grignard reagent (39.5 gm.) and the reaction mixture worked up in the usual manner. There was obtained α-allyl methoxymethyl vanillyl carbinol which was recrystallized from petroleum ether (b.p. 60 to 70° C.). Yield, 3.3 gm. (10%); m.p. 70 to 71° C.* Found: C, 65.2; H, 7.83; OCH_3, 25.6%. Calc. for $C_{13}H_{18}O_4$: C, 65.5; H, 7.57; OCH_3, 26.0%.

A portion of the product (1 gm.) was dissolved in acetone (5 cc.) and this solution added to potassium dichromate (0.5 gm.) dissolved in water (10 cc.) containing concentrated sulphuric acid (1 cc.). The temperature rose spontaneously to 70° C., the mixture at this point being very dark. After standing for 10 min., it was cooled and extracted with ether. Removal of the latter left 0.4 gm. of a brown resinous material that could not be crystallized nor distilled.

* *All melting points are uncorrected.*

(IV) On Veratric Aldehyde

Treatment of veratric aldehyde with allyl magnesium bromide gave α-allyl veratryl carbinol. Yield, 80%; m.p. 80.5 to 81.5° C. Found: C, 69.0; H, 7.5; OCH_3, 29.9%. Calc. for $C_{12}H_{16}O_3$: C, 69.3; H, 7.7; OCH_3, 29.8%.

Oxidation with chromic acid gave α-vinyl acetoveratrone which was recrystallized from ethanol-water followed by petroleum-ether (b.p. 60 to 70° C.). Yield, 50%; m.p. 58° C. Found: C, 69.7; H, 6.43; OCH_3, 29.9%. Calc. for $C_{12}H_{14}O_3$: C, 69.8; H, 6.78; OCH_3, 30.0%. The semicarbazone of the ketone was prepared and recrystallized from hot water; m.p., 140 to 142° C. Found: C, 59.2; H, 6 62; N, 16.2; OCH_3, 23.5%. Calc. for $C_{13}H_{17}O_3N_3$: C, 59.3; H, 6.46; N, 16.0; OCH_3, 23.6%.

Ozonization. α-Vinyl acetoveratrone (2 0 gm.), dissolved in glacial acetic acid (3 cc.), was cooled to 0° C. and ozone passed in until it was no longer absorbed. Calculation showed that this was a little in excess of theoretical. The ozonide was decomposed by the addition of ether (12 cc.) followed by zinc dust (1 gm.) and water (0.5 cc.). When the reaction had ceased, the solution was filtered, extracted with ether and the ethereal solution extracted first with bicarbonate and then with bisulphite, nothing dissolving in the latter. The ether residue was taken to dryness leaving a brown amorphous product no longer ether-soluble. A repetition with ethyl acetate as solvent gave the same result.

SYNTHESIS B. STEPHEN REDUCTION

(I) Of α-Cyanacetovanillone Acetate.

Preparation of α-Bromoacetovanillone Acetate. Acetovanillone acetate (10 gm.) was dissolved in anhydrous chloroform (75 cc.) and placed in a flask fitted with a stirrer, dropping funnel and reflux condenser. Bromine (7.8 gm.) in chloroform (25 cc.) was added slowly over a period of one and a half hours and the mixture then stirred for an additional hour. The chloroform solution was washed with water and bicarbonate, dried over sodium sulphate, and the solvent was removed under reduced pressure. A water-white liquid remained which solidified to colourless crystals on standing; yield, 12 gm. (87%). Recrystallization from ethanol gave a product melting at 86 to 87.5° C. Found: C, 46 0; H, 3.69; Br, 28.2; OCH_3, 10 8%. Calc. for $C_{11}H_{11}O_4Br$: C, 46 0; H, 3 84; Br, 27.9; OCH_3, 10 8%.

Preparation of α-Cyanacetovanillone Acetate. The procedure employed was that used by Gabriel (7) to synthesize α-cyanacetophenone. To a solution of 5 gm. of bromoacetovanillone acetate in ethanol (15 cc.) was added potassium cyanide (5 gm.) dissolved in water (15 cc.). The mixture was cooled, allowed to stand for 30 min., diluted with water (two volumes), and acidified with dilute hydrochloric acid. The heavy brown precipitate which separated out was removed by filtration and recrystallized from ethanol; yield, 1.3 gm. (32%); m.p. 191 to 192° C. Found: C, 62.0; H, 4.80; N, 6.2; OCH_3, 13.2%. Calc. for $C_{12}H_{11}O_4N$: C, 61.8; H, 4 72; N, 6.0; OCH_3, 13.3%.

Stephen Reduction of α-Cyanacetovanillone Acetate. Anhydrous stannous chloride (1.2 gm.) was placed in a flask with anhydrous ether (25 cc.) and saturated with anhydrous hydrogen chloride. The nitrile (0.97 gm.), which was insoluble in ether and chloroform, was suspended in chloroform and added to the ether solution with vigorous shaking. After shaking for two hours, the reaction mixture was filtered, and 0.9 gm. of unchanged α-cyanacetovanillone acetate recovered.

(II) Of α-Cyanacetovanillone

Deacetylation of α-Bromoacetovanillone Acetate. α-Bromoacetovanillone acetate (10 gm.) was dissolved in methanol (100 cc.) containing concentrated hydrochloric acid (10 cc.). The solution was heated to boiling point, allowed to stand three hours and then cooled to −10° C. A crop of colourless crystals melting at 102 to 103° C. was obtained; yield, 7.0 gm. (88%). Analysis showed that not only had the acetate group been removed but that bromine had been replaced by chlorine. Found: C, 53.8; H, 4.61; Cl, 17.9; OCH_3, 15.3%. Calc. for $C_9H_9O_3Cl$: C, 53.8; H, 4.48; Cl, 17.7; OCH_3, 15.5%.

Preparation of α-Cyanacetovanillone. This derivative was prepared directly by bromination of acetovanillone acetate followed by treatment of the deacetylated bromide with potassium cyanide. Yield, 23%; m.p. 152 to 153° C. Found: C, 62.9; H, 4.66; N, 7.05; OCH_3, 16.2%. Calc. for $C_{10}H_9O_3N$: C, 62.8; H, 4.71; N, 7.33; OCH_3, 16.2%. Several attempts were made to reduce this compound in the manner already described, but were unsuccessful. Removal of the acetyl group did not increase the solubility of the nitrile in cold organic solvents.

Synthesis C. Claisen-Schmidt Condensation

(I) Condensation of Acetovanillone Acetate with Ethyl Formate.

A mixture of acetovanillone acetate (2.2 gm.) and ethyl formate (1.32 gm.), dissolved in benzene (3 cc.), was added to sodium wire (0.28 gm.) suspended in anhydrous benzene (7 cc.). A vigorous reaction ensued which slowed down as the sodium became coated with the reaction product. After standing 12 hr., the precipitate was filtered off, washed with ether and dried in the air; yield 0.95 gm. The product was dissolved in water (5 cc.), acidified with dilute sulphuric acid, extracted with ether, and the ether removed. The solid residue was recrystallized from water; it melted at 112 to 114° C. A mixed melting point with acetovanillone showed no depression.

(II) Condensation of Methoxymethyl Acetovanillone with Ethyl Formate.

Preparation of Methoxymethyl Acetovanillone. This was prepared in the same way as the corresponding ether of vanillin, except that the time of shaking was cut to 30 min. The product was recrystallized from petroleum ether (b.p. 60 to 70° C.); yield, 52%; m.p. 52 to 53° C. Found: C, 62.4; H, 6.34; OCH_3, 29.4%. Calc. for $C_{11}H_{14}O_4$: C, 62.9; H, 6.66; OCH_3, 29.5%.

Claisen-Schmidt Condensation. This was carried out in the manner already described. The reaction product was recrystallized from petroleum ether (b.p. 60 to 70° C.); m.p. 58 to 59° C. It gave no reaction with semicarbazide acetate or 2,4-dinitrophenyl hydrazine hydrochloride, indicating the absence of a carbonyl group. It decolorized bromine in carbon tetrachloride and permanganate in acetone, proving the presence of an unsaturated bond. It did not react with *p*-nitrobenzoyl chloride, showing the absence of a free hydroxyl group. Finally, it dissolved in bicarbonate with the evolution of carbon dioxide, indicating the presence of a carboxyl group. These properties, coupled with the analytical data, correspond with those of the methoxymethyl ether of α-guaiacyl acrylic acid. Found: C, 60.3; H, 5.82; OCH_3, 25.9%. Calc. for $C_{12}H_{14}O_5$: C, 60.5; H; 5.88; OCH_3, 26.0%.

(III) Condensation of Acetoveratrone with Ethyl Formate

Synthesis of Veratroyl Acetaldehyde. A mixture of acetoveratrone (12 gm., prepared by methylating acetovanillone with dimethyl sulphate) and ethyl formate (7.5 gm.) was added to sodium wire (1.5 gm.) in benzene (40 cc.). After standing 12 hr., the reaction product was filtered off and dried in the air; yield 12 gm. (90% calculated as veratroyl acetaldehyde).

A portion of this sodium salt (4 gm.) was dissolved in water (10 cc.), acidified with dilute sulphuric acid, and extracted with ether. Removal of the solvent left a reddish oil (3 gm.) which on distillation (bath temperature 180 to 230° C. at 0.1 mm.) gave a clear yellow oil; yield, 0.9 gm. Most of the aldehyde polymerized during the distillation. Found: C, 63.6; H, 5.84; OCH_3, 30.1%. Calc. for $C_{11}H_{12}O_4$: C, 63.5; H, 5.76; OCH_3, 29.8%.

Preparation of the Copper Salt. Veratroyl acetaldehyde (0.15 gm.) was dissolved in a small amount of ether and shaken with a saturated aqueous solution of copper acetate. A green crystalline precipitate immediately settled out; it was filtered, washed with ether and water, and dried; yield, 0.12 gm. Found: C, 55.0; H, 4.79; OCH_3, 25.9%. Calc. for $C_{22}H_{22}O_8Cu$: C, 55.25; H, 4.60; OCH_3, 25.35%.

Preparation of the Semicarbazone. The sodium salt of veratroyl acetaldehyde was treated with semicarbazide hydrochloride in water, and the precipitate formed was filtered off and recrystallized from ethanol; m.p. 181 to 182° C. Found: C, 54.2; H, 5.94; N, 15.9; OCH_3, 23.5%. Calc. for $C_{12}H_{15}O_4N_3$: C, 54.35; H, 5.66; N, 15.8; OCH_3, 23.4%.

Preparation of the 2,4-Dinitrophenylhydrazone. To the free aldehyde dissolved in water was added an excess of 0.4% of 2,4-dinitrophenylhydrazine hydrochloride in water. The precipitate which formed was filtered off and recrystallized from chloroform-petroleum ether (b.p. 30 to 50° C.) and then dioxane-petroleum ether (b.p. 30 to 50° C.); m.p. 189 to 190° C. Found: C, 52.3; H, 4.4; N, 14.4; OCH_3, 16.05%. Calc. for $C_{17}H_{16}O_7N_4$: C, 52.5; H, 4.12; N. 14.4; OCH_3, 15.95%.

References

1. Auwers, K. v. and Schmidt, W. Ber. 58 : 528-543. 1925.
2. Auwers, K. v. and Ottens, B. Ber. 58 : 2072-2080. 1925.
3. Brickman, L., Hawkins, W. L., and Hibbert, H. J. Am. Chem. Soc. 62 : 986. 1940.
4. Brickman, L., Pyle, J. J., McCarthy, J. L., and Hibbert, H. J. Am. Chem. Soc. 61 : 868-869. 1939.
5. Buckland, I. K., Tomlinson, G. H., and Hibbert, H. Can. J. Research, B, 16 : 54-56. 1938.
6. Cramer, A. B., Hunter, M. J., and Hibbert, H. J. Am. Chem. Soc. 61 : 509-516. 1939.
7. Gabriel, S. and Eschenbach, G. Ber. 30 : 1126-1141. 1897.
8. Gilman, H. and McGlumphey, J. H. Rec. trav. chim. 47 : 418-422. 1928.
9. Hawkins, W. L., Wright, G. F., and Hibbert, H. J. Am. Chem. Soc. 59 : 2447-2448. 1937.
10. Howells, H. P., Little, B. H., and Anderson, H. P. J. Am. Chem. Soc. 52 : 4076-4082. 1930.
11. Hunter, M. J., Cramer, A. B., and Hibbert, H. J. Am. Chem. Soc. 61 : 516-520. 1939.
12. Hunter, M. J. and Hibbert, H. J. Am. Chem. Soc. 61 : 2190-2194. 1939.
13. Leger, F. J. and Hibbert, H. Can. J. Research, B, 16 : 68. 1938.
14. Leger, F. J., and Hibbert, H. Can. J. Research, B, 16 : 151. 1938.
15. Leger, F. J. and Hibbert, H. J. Am. Chem. Soc. 60 : 565-567. 1938.
16. Lieff, M., Wright, G. F., and Hibbert, H. J. Am. Chem. Soc. 61 : 865-867. 1939.
17. Lock, G. Ber. 61 : 2234-2240. 1928.
18. Lock, G., Ber. 62 : 1177-1188. 1929.
19. Pauly, H. and Wäscher, K., Ber. 56 : 603-610. 1923.
20. Pyle, J. J., Brickman, L., and Hibbert, H. J. Am. Chem. Soc. 61 : 2198-2203. 1939.
21. Stephen, H., J. Chem. Soc. 127 : 1874-1877. 1925.
22. Tomlinson, G. H. and Hibbert, H. J. Am. Chem. Soc. 58 : 345-348. 1936.

A NEW SOURCE OF COCOSITOL[1]

BY RICHARD H. F. MANSKE[2]

Abstract

The leaves of *Calycanthus floridus* and of *C. glaucus* have been shown to contain a polyhydric alcohol, $C_6H_{12}O_6$, which has been identified as cocositol.

The name cocositol was given by Müller (1) to a polyhydric alcohol that he isolated from the leaves of two plants belonging to the natural family Arecaceae (Palmaceae), namely, *Cocos nucifera* and *C. plumosa*. Analytical figures and molecular weight data pointed unmistakably to the simple formula, $C_6H_{12}O_6$, and this was confirmed by the preparation of a normal hexa-acetate. That it was an optical isomer of inositol seemed highly probable because the nitric acid oxidation product yielded a pink coloured compound with calcium chloride (Scherer reaction). Müller pointed out that his cocositol was probably identical with a substance, quercin, obtained by Vincent and Delachanal (2) from some quercitol mother liquors prepared from acorns.

The author has obtained a substance from the leaves of *Calycanthus floridus* and from *C. glaucus* (Calycanthaceae) that has proved to be identical with cocositol in all respects save one. Müller records that cocositol is optically inactive. The substance now isolated is slightly but measurably dextro-rotatory, namely $[\alpha]^{24}_{D} + 1.6°$ ($c = 0.4$ in. water). Cocositol as now obtained melts sharply and without decomposition at 367° C.* The melt on slight cooling recrystallizes immediately. If a specimen is heated cautiously over a free flame on a platinum spatula it melts to a colourless liquid that crystallizes at once when withdrawn from the heat. Müller had considerable difficulty in determining such a high melting point and records 345 to 350° C. uncorrected. On the author's uncorrected thermometer it melted at 354° C. The hexa-acetate was recrystallized from boiling acetic anhydride, and it melted sharply at 302° C. with no trace of discoloration or decomposition. When cooled to 301° C. it crystallized again. This melting and cooling was repeated some ten times without changing the melting point. Müller records 300° C. (corr.) for the melting point of the acetate.

Cocositol (as also the author's compound) dissolves in warm sulphuric acid without coloration and it crystallizes unchanged from hot concentrated nitric acid. The inositol colour reaction depending on nitric acid oxidation

1 *Manuscript received July 19, 1940.*
Contribution from the Division of Chemistry, National Research Laboratories, Ottawa, Canada. Issued as N.R.C. No. 975.

2 *Chemist.*

**All melting points are corrected.*

is therefore difficult to get with cocositol, but repeated evaporation with nitric acid ultimately yields enough croconic acid to give a colour with calcium chloride. With lead sub-acetate it yields a heavy precipitate.

Inasmuch as an authentic specimen of cocositol was not available for direct comparison, Prof. J. E. Hawley of the Department of Mineralogy, Queen's University, Kingston, Ontario, has kindly carried out a crystallographic study of the author's compound and its acetate. Müller records such a study as carried out by Prof. T. V. Barker and the following table completely confirms the identity of the two pairs of substances.

Polyhydric Alcohol—Submitted by R. H. F. Manske

Crystallography	J.E.H.	Barker
Crystals—	Monoclinic, slightly distorted	Monoclinic
		Mean
	$m : m$ — $110 \wedge \bar{1}10 = 64° 9'$ (2-circle goniometer measurement)	$110 \wedge \bar{1}10 = 64° 18' - 64° 9'$
	Measured with Contact Goniometer on one large crystal	
	$\beta = 117°+$	$\beta = 117° 12'$
	$110 \wedge \bar{1}11 = 58° \pm$	$110 \wedge \bar{1}11 = 57° 56'$
	$\bar{1}10 \wedge \bar{1}11 = 60° \pm$	$\bar{1}10 \wedge \bar{1}11 = 59° 56'$
	Forms present-prisms (110)	110
	hemi-pyramids ($\bar{1}11$)	$\bar{1}11$
	hemi-orthodome ($\bar{2}01$)	$\bar{2}01$
	Basal pinacoid (001)	001
	Crystal habit similar to drawings by Barker	

	J.E.H.	Barker
Optical Properties—	Biaxial, Positive (+)	
	Extinction on 110 = 34° (average).................	33°
	Maximum extinction measured against elongation = 38°	
	Indices of refraction	
	α or N_p = 1.550 ± .002	
	β or N_m = 1.560 ± .002	
	γ or N_g = 1.615 ± .002	
	Birefringence ± .06 Extreme	Strong (but not measured quantitatively)
	Optic plane ⊥ to 010 at 92° 42′ to (001)c	One of mean lines (x, y, or z) is almost perpendicular to c(001)
	Trace of optic plane ∧ (001)c, measured on prismatic section = 92° 42′	
	No marked dispersion of optic axes	

Acetate of Polyhydric Alcohol or Cocositol

Crystallography	J.E.H.	Barker
	Probably monoclinic, positive data not obtained on account small-sized crystals	Monoclinic
	Forms on crystallites [110] [001]	[110] [001] forms as illustrated
	Additional form on larger crystals is probably a hemi-orthodome	Not described
	Angles measured on petrographic microscope	Goniometer
	CM : $001 \wedge 110 = 84° 18' \pm$	$001 \wedge 110 = 84° 26'$
	$\beta = 98° \pm$	$\beta = 97° 33'$
	Habit—near cubic	Habit—near cubic
	No cleavage	No cleavage

Optical Properties—Biaxial—negative (−)		
	Extinction on m = 29° −35°	33°
	Maximum extinction measured against elongation = 44°	
	Prism faces (m) give near centered optic axis figure	Prism faces (m) give near centered optic axis figure
	Indices of refraction $\alpha = 1.48 \pm .003$ $\beta = 1.51 \pm .003$ $\gamma > 1.51$ (not obtainable from grains)	
	Birefringence $\pm$ .04 (medium)	Medium
	No marked dispersion of optic axes	
	$(Y$ or $N_m)$ Elongation on prism section = 16° −17°	

It may be added that a flavone-like compound of undetermined identity was also obtained from the leaves.

Experimental

The leaves of *Calycanthus floridus* and of *Calycanthus glaucus* were collected, in the autumn when the vegetative period was virtually complete, from shrubs growing in the Arboretum, Central Experimental Farm, Ottawa. The author is indebted to Mr. John Adams for permission to collect them.

The dried and ground materials were separately extracted with hot methanol during which extraction a sparingly soluble substance separated in crystalline form from the extract. After several weeks the extract was filtered and the crystals washed with methanol and then with acetone. The insoluble portion was next extracted with hot water and the filtered solution evaporated to dryness on a steam bath. The resulting residue was recrystallized twice from hot water with the aid of charcoal and then washed with methanol. The brilliant colourless prisms thus obtained melted sharply and without decomposition at 367° C. The yield of purified cocositol from either source was slightly more than 0.5%. Calc. for $C_6H_{12}O_6$; C, 40.00; H, 6.67%. Found: C, 40.00, 40.00; H, 6.84, 6.79%. The optical activity was found to be $[\alpha]^{24}_{D} + 1.6°$ ($c = 0.4$ in. water).

Cocositol Hexa-acetate

The purified cocositol was suspended in 100 times its weight of acetic anhydride containing a little pyridine and an equal weight of anhydrous sodium acetate. The mixture was boiled under reflux until the solid had completely dissolved (24 to 48 hr.). On cooling the mixture, cocositol hexa-acetate crystallized in large colourless prisms that were filtered off and washed with water and then with methanol. It then melted at 301 to 302° C. It was redissolved in boiling acetic anhydride (75 cc. of solvent per gram of substance) and the solution filtered through a crucible with a sintered glass plate heated by being suspended in the vapour of boiling acetic anhydride. The filtered solution was evaporated until crystallization began in the boiling liquid. After cooling, the brilliant colourless crystals were filtered off and washed with methanol, water, and methanol in the order named. The

substance then melted sharply and without discoloration or decomposition at 302° C., the melt crystallizing when it was allowed to cool to 301° C. Calc. for $C_{18}H_{24}O_{12}$; C, 50.00; H, 5.56%. Found: C, 50.10, 50.12; H, 5.76, 5.73%.

Isolation of a Flavone (?)

The methanolic filtrate from which the cocositol had crystallized was evaporated to a thick syrup, diluted with hot dilute hydrochloric acid, and the remainder of the methanol boiled out. After several days the mixture was filtered and the clear filtrate extracted repeatedly with ether. The residue from the combined ether extracts was triturated with water and the crystalline substance thus obtained filtered and washed with water. It was recrystallized twice from methanol-water (70 : 30) and obtained in pale yellow fine needles melting at 296° C. Calc. for $C_{15}H_{10}O_6.H_2O$; C, 59.21; H, 3.95%. Found: C, 58.90, 58.91; H 3.92, 3.94%. Methoxyl was absent.

References

1. MÜLLER, H. J. Chem. Soc. 91 : 1767-1780 1907.
2. VINCENT, C. and DELACHANAL. Compt. rend. 104 : 1885. 1887.

Canadian Journal of Research

Issued by The National Research Council of Canada

VOL. 19, SEC. B. FEBRUARY, 1941 NUMBER 2

THE REDUCTION OF RESAZURIN IN MILK AND AQUEOUS SOLUTIONS[1]

By H. R. Thornton[2], F. McClure[3], and R. B. Sandin[4]

Abstract

The action of resazurin in milk is complex and not as yet clearly understood. The various resazurin tests have been proposed as practical tests for estimating bacterial populations in milk before they have emerged from the experimental stage. A significant proportion of results cannot at present be interpreted with the reasonable certainty necessary to justify widespread use of these tests by the dairy industry.

The colour changes undergone by resazurin in milk have been proposed over a period of eleven years as the basis for a test, or number of tests, to supplant the methylene blue reduction test as a measure of bacterial populations in raw milks. Yet Johns and Howson (13) are the first to publish E_h-time curves of resazurin. Their work serves to bring into sharp focus some of the exaggerated claims for resazurin, particularly for the one-hour test.

The purpose of the present communication is to set forth further and confirmatory evidence and to evaluate some of the proposed resazurin tests in the light of that evidence.

Methods

For the E_h measurements in milk, 0.1 ml. of a 0.05% solution of resazurin was added to 10 ml. of milk. Three preparations of resazurin, two American* and one European, were studied. The new standard methylene blue thiocyanate tablets were used, resulting in a concentration of 1 part of dye to 300,000 parts of milk. Oxidation-reduction potentials were measured by means of the usual electrometric set-up, the potentiometer** being a Leeds and Northrup type K2.

[1] *Manuscript received August 19, 1940.*

Contribution from the Departments of Dairying and Chemistry, University of Alberta, Edmonton, Alta.

[2] *Professor of Dairying.*

[3] *Graduate Student in Chemistry.*

[4] *Associate Professor of Chemistry.*

* *The American resazurin was manufactured by The National Anilin and Chemical Co. Part of the dye was supplied through the courtesy of this company and Dr. H. J. Conn, Chairman, Commission on Standardization of Biological Stains. It is not known whether the two samples were from the same dye batch.*

** *The potentiometer was purchased with funds obtained from the National Research Council of Canada, Ottawa.*

Preliminary Chemical Studies

The available information regarding the chemistry of resazurin is very meagre, indeed (see Neitzki *et al.* (15).). Gunderson and Templeton (8), on treating an aqueous solution of resazurin with carbon dioxide, obtained a purple-black precipitate and a red supernatant liquid. When the precipitate was dissolved in dilute alkali, "the resulting blue solution behaved in the normal manner". On the concentration of the supernatant red liquid with simultaneous removal of the carbon dioxide, a reddish-blue solution was obtained which was thought to be resazurin. The addition of carbon dioxide to milk accelerated the first colour change of added resazurin.

It is common experience that some samples of commercial resazurin are unfit for use in a reduction test in milk. Manufacturers report to the writers that resazurin is a difficult chemical to prepare, that large and varying quantities of resorufin are synthesized along with the resazurin, attempts to remove which are probably not wholly successful, and that another substance of unknown constitution is thought to be synthesized during the manufacture of the resazurin.

In a preliminary study of the chemistry of resazurin the present authors were unable to obtain a titration curve with the European dye in aqueous solution. The American dye gave a perfect two-step titration curve at approximately pH 1, and dye reduction was completely reversible at this pH. At pH 7 reproducible potentials were unobtainable, decomposition of the dye presumably having taken place, and reversibility of reduction was not complete. Preliminary attempts to purify the dye or to synthesize resazurin in a pure state failed. Although more extensive trials might prove successful, the experiments indicate that considerably more information on the chemistry of resazurin is necessary before satisfactory standards for a reduction test in milk can be evolved.

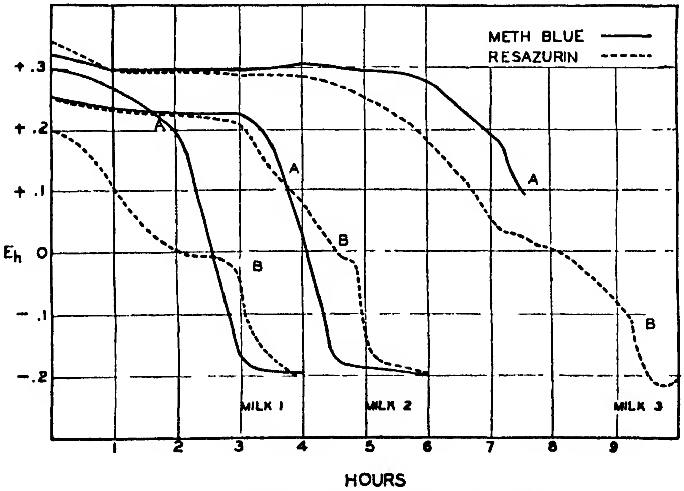

FIG. 1. *E_h-time curves of three milks containing methylene blue and resazurin.*

The Reduction of Resazurin in Milk

In Fig. 1 are shown E_h-time curves of methylene blue and resazurin milk mixtures for three samples of milk. The methylene blue milks had reduced at the points marked *A*, while the resazurin tubes were white at the points marked *B*. In the methylene blue tube of Milk 3 the electrode was inadvertently broken shortly after reduction of the dye but the essential part of the curve is not affected. It is included here because Milk 1 is Milk 3 after 24 hours' incubation at room temperature, unincubated milks of high bacterial content not being available in this city. There is a good deal of similarity between these curves and those reported by Johns and Howson.

It will be noted that the resazurin curves followed the methylene blue curves for the first two to three hours in Milks 2 and 3. Then the resazurin milks became measurably negatively poised until reduction to the white compound had taken place, when the poising effect was lost. In Milk 1, in which the inherent poising capacity of the milk was largely decreased by bacterial action, the milk was immediately overpoised by the resazurin. It is apparent from these curves that the red-white reaction, or a component of it, strongly poised the milk electronegatively, the overpoising effect becoming apparent as the initial poising of the milk was lessened through bacterial action. Therefore, the time required to reach either the pink or white end-point was a function not only of bacterial influences but also of the comparative poising capacities of the milk and dye systems.

Vat milk from a pasteurizing plant was used for this work because it was thought likely to be more uniform and less subject to irregularities than individual milks. Notwithstanding this precaution an interesting exception was observed and Fig. 2 is presented because it represents a time-potential curve of methylene blue in milk which deviates materially from the classical shape

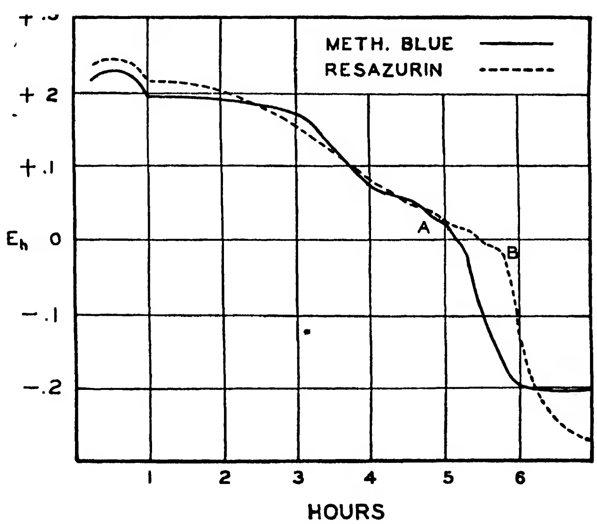

FIG. 2. *E_h-time curves of a milk containing methylene blue and resazurin.*

of curve as represented in Fig. 1. The milk used for the two dye milk mixtures was a vat sample that was discovered to have been run through a centrifugal clarifier. Suspecting that clarification might account for the unusual shape of the methylene blue milk curve, samples of a mixed vat milk before and after clarification were mixed with methylene blue in standard concentration and the potential changes followed as shown in Fig. 3. There is no evidence that clarification influenced the poising properties of this milk. Therefore, no explanation is attempted for the unusual results with the milk used for Fig. 2.

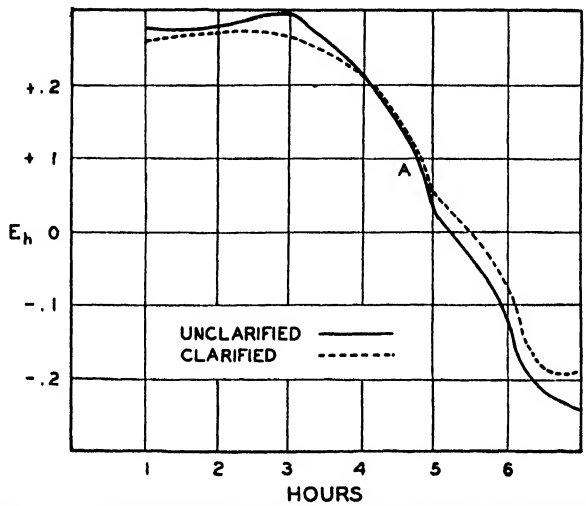

FIG. 3. *E_h-time curves of a milk before and after clarification.*

All attempts to reproduce the blue colour in milk by oxidation of the reduced resazurin failed. It would appear that the reduction of resazurin in milk is not a reversible reaction. The strong poising influence of the red-white reaction and its loss on complete reduction shows that at least one step in the reducing process is reversible.

The Pink End-point Test

The original resazurin test proposed by Pesch and Simmert (17) carried reduction only to the pink end-point. This first step in the reduction of resazurin is thought to be irreversible, and, in consequence, the test was believed by these authors to be insensitive to the presence of dissolved oxygen, janus green being cited as another such insensitive dye. Thornton and Hastings (19) pointed out the error of this assumption in regard to janus green B and the same reasoning holds for resazurin, a view substantiated by the recent interesting Vermont bulletin (6).

Collins *et al.* (2) and Johns (11) favour the resazurin-to-pink test, the advantage claimed being that the pink end-point is reached before methylene blue is reduced and time is thereby saved. To off-set this, however, it should be recognized that this end-point is subject to the same disadvantage as was

found in the case of janus green B by Thornton and Hastings, i.e., indefiniteness caused by (i) a mixing of the colours blue, red, and white, and (ii) the acceleration or retardation of E_h changes in milk overpoised by the red-white reaction. No exact and reproducible colour standard for determining this end-point has as yet been proposed, but the use of such a standard would not compensate for the differences in the slopes of the E_h-time curves of different milks. A further complicating factor is the colour sensitivity of resazurin to H-ion concentration, even yellow being reported as one of the possible colours.

Anomalies

When working with resazurin one quickly observes puzzling anomalies. Thus in the present study the colour changes were not always consistent at different temperatures; the extreme sensitivity to light reported by others was not observed by the writers; some milks with long methylene blue reduction times reduced resazurin quickly, and for this there was no apparent explanation; it was not unusual for the pink colour to remain in some milks for a surprisingly long time; the European sample of resazurin did not give the usual colour when added to milk and was unsatisfactory as an E_h indicator for this test.

Johns (12), Nelson (16), and Davis (4) report that some samples of resazurin are unsatisfactory as indicators in a reduction test. Keenan *et al.* (14) found that, of 200 milks reducing methylene blue in not less than five hours, 6% reduced resazurin to the white compound in not more than one hour and more than 50% of 163 samples which were vivid pink in the resazurin test at the end of one hour did not reduce methylene blue in less than five hours. Davies *et al.* (3) found that 11% of the samples reducing resazurin to purple pink in one hour failed to reduce methylene blue in seven hours. Some of Frayer's (6) resazurin-to-white reduction times were shorter than the methylene blue reduction times.

According to Collins *et al.* the reduction of resazurin to pink requires an average of 50% of the methylene blue reduction time. Johns and Howson on the other hand obtained a ratio of 3 : 4 between the resazurin-to-pink and methylene blue average reduction times. They attribute this discrepancy to their own use of the shaking technique or to end-point differences. Since Johns and Howson used the modified technique with both dyes and Collins *et al.* used the standard technique with both dyes, this difference in procedures remains an inadequate explanation. Difficulties of end-point determination are serious in any of the reduction tests and are particularly impressive to an operator using the resazurin pink end-point.

Any attempted explanation of these anomalies at the present time would constitute mere conjecture. However, the possibilities of the overpoising effects and decomposition of resazurin in some milks would seem to deserve further attention if this test is to be used in practice.

Shortening the Reduction Time

Clark, Cohen, and Gibbs (1) expressed the desirability of shortening the time of the methylene blue reduction test. Thornton and Hastings recognized some of the difficulties in such shortening. Ramsdell *et al.* (18) criticized the view expressed by Thornton and Hastings, considering that the behaviour of resazurin in milk justifies the assumption of a sound and interpretable decrease of reduction time. Johns (personal communication) believes that "the shortening of the reduction time is due chiefly to the poising effect of resazurin coming into play after the original poising of the milk has been partially overcome by bacterial growth." Davis (4) stated that, because resazurin is electropositive to methylene blue and both are electronegative to fresh milk, "It will be evident, therefore, that very weak reducing systems in milk, irrespective of their nature of origin, will affect resazurin much more than methylene blue." The same view was earlier expressed by Ramsdell *et al.* The E_h curves of Johns and Howson and those contained herein do not bear out this contention and show that the difference in the E_0 values of the two dyes exerts but slight, if any, influence on reduction times, the time saved in the resazurin test being largely the result of the overpoising effect of the red-white reaction.

The possibility of shortening the reduction test by overpoising the milk with a dye system was suggested to one of the present authors (T) fifteen years ago by Dr. Barnett Cohen. According to present theories this appears to be feasible only if milks do not vary in their inherent reducing intensities and capacities. Hobbs (9) considered that milks do not vary in reducing capacities (poising). On the other hand, Greenbank (7) contended that milks do so vary and presented good evidence in substantiation of his contention. The variation in reducing intensity of different milks is too well known to require comment. Some abnormal milks, such as many mastitis milks, behave in a manner very suggestive, indeed, of enhanced poising properties. Since market milks are dilutions of abnormal with normal milks, it is not unreasonable at present to assume varying poising in market milks. Until more is known of the nature of poising inherent in milk, interpretations of the behavior in milk of such strongly poised systems as resazurin should be tempered with caution.

Another possible mechanism for shortening the reduction test is the removal of a portion of the dissolved oxygen from the milk by non-poised chemical agents, leaving less oxygen for bacterial consumption. This procedure depends on the generally accepted theory that the bacteria play an oxygen-consuming role in the reduction test. This theory has recently been questioned by Hobbs (9) who found no relation between the time of reduction of methylene blue in milk by pure cultures of certain bacteria and their rate of oxygen consumption in the Barcroft apparatus. Miss Hobbs' belief does not find apparent substantiation in the common and simple observation that shaking a reduced tube of milk with oxygen oxidizes the methylene white, or that evacuation of the tube shortens the reduction time. Neither does it permit interpretation

of Jackson's findings (10) that exposure of anaerobically drawn milk to minute amounts of atmosphere immediately poises the milk at the usual E_h levels of fresh aerobically drawn milk. It may be that the rate of oxygen fixation by bacteria in a moving vessel partly filled with milk is not necessarily representative of oxygen removal from unagitated milk sealed by a butterfat layer. The more recently advanced evidence of Frayer (6) leaves little doubt that the reduction of dyes and the oxygen content of the milk are intimately related. However, the development of a reduction test shortened by the partial removal of oxygen by non-poised chemical agents is at present attended by difficulties and is a matter for the future.

Discussion

When a reversibly reducible system, such as methylene blue, is added to milk, the milk dye mixture comes to an E_h equilibrium at which point the dye exists partly in the oxidized and partly in the reduced form. The proportion of the two forms present is a function of the E_h value of the equilibrium. There are reasons for believing that milks differ in the initial E_h value at which they are poised and in the E_h value of the equilibrium they attain with an added dye system. There is evidence (10) indicative of lapsed time before such an equilibrium is reached in fresh milk of low bacterial content, and that this time factor may be an hour or even longer. Thus, when methylene blue is added to milks variable proportions of the dye change in variable periods of time to methylene white. This phenomenon escapes notice because the reductant is colourless.

It is probable that the one-hour resazurin test, when applied to normal milk of low bacterial content, merely measures the E_h value of the equilibrium reached by the milk dye mixture in one hour, since the oxidant in this case is blue while the reductants are red and colourless. This situation is made even more extreme by the strong poising action of the red-white reaction. Such a view receives support, not only in the general poor correlation between the resazurin and methylene blue tests as found by Frayer (5), but also in the data presented by Ramsdell *et al.* (18). Fig. 4 is a scatter-graph prepared by the present authors from the one-hour resazurin numbers and the methylene blue reduction times of 78 milks reported by Ramsdell *et al.* The lack of correlation, especially in the case of the good milks, is quite apparent.

Thornton and Hastings drew attention to the difficulty of interpreting milk reduction of indicators more electropositive than methylene blue, and the startling recent claims for the one-hour resazurin test seem to justify their view. Ramsdell *et al.* consider that the reduction even of methylene blue may be misleading because visual reduction in some milks may be effected at E_h levels as positive as the initial values of other milks. Attempts to explain the varying E_h ranges over which methylene blue reduces in milk have not been entirely satisfactory. Since methylene blue reduces in milk after bacterial action has assumed control of the E_h, i.e., after the potential has attained

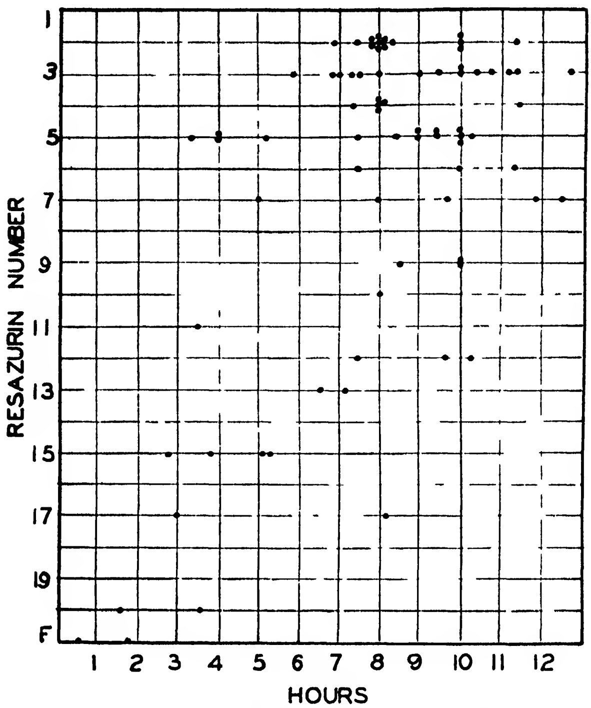

FIG. 4. *Scattergraph of the one-hour resazurin numbers and the methylene blue reduction times of 78 milks reported by Ramsdell et al.*

a steady negative drift and the upper break in the potential-time curve is discernible, it is probable that the reduction of methylene blue is not misleading in the manner suggested by Ramsdell *et al.*

The writers have seen no evidence, either in the literature or in their own experiments, that the resazurin test is sensitive to bacterial action during the first hour of incubation of a normal milk of low bacterial content. They are not acquainted with any theory that opens the possibility of a redox indicator being more sensitive to bacterial action than the O-R potential itself. On the other hand, when the bacteria begins to influence the O-R potential of the milk, resazurin may indicate the potential change more quickly than will methylene blue. This is illustrated in Fig. 1, Milk 1. Therefore, the one-hour resazurin test shows promise in indicating milks that will reduce methylene blue in periods up to about two hours.

The one-hour resazurin test seems to permit the separation of milks into two classes—those of very high bacterial content and those of low bacterial content. This picture, however, is complicated by the fact that some milks of low bacterial content, presumably abnormal, are rather strongly poised at E_h levels negative to the usual values of fresh milk. The one-hour resazurin test of some of these milks would, therefore, be independent of bacterial

action and, as a strictly bacteriological test, difficult of interpretation. Again further possible complications arise because of the behaviour of resazurin as a pH indicator.

Conclusions

The following conclusions are drawn from a potentiometric study of the behaviour of resazurin in milk and aqueous solutions:—

1. A European preparation labelled resazurin did not behave in the expected manner, was probably not resazurin, and was unsuitable as an indicator of reduction in milk.

2. Resazurin exhibiting the frequently described colour changes in milk is a redox indicator, at least at pH1. At pH7 the evidence is not yet clear.

3. The chemistry involved in these changes is probably as yet undetermined.

4. The blue-red reaction is electropositive and the red-white reaction is electronegative to the methylene-blue–methylene-white reaction.

5. In long time reducing milks as measured by methylene blue, the resazurin time-potential curve follows the methylene blue curve for the first two to three hours. The mixture then becomes strongly poised by the red-white reaction, this poising influence being rather sharply lost when reduction to the white compound is complete.

6. In milks reducing methylene blue in periods up to two to three hours, the time-potential curve of resazurin resembles the later stages of the resazurin time-potential curve in good milk.

7. The colour attained at the end of one hour by resazurin in milk of low bacterial content depends on the E_h value of the equilibrium set up by the mixing of the reducing systems of the dye and milk, and no evidence was forthcoming that it is related to the number of bacteria in such milk.

8. The one-hour resazurin test shows some promise as a means of segregating milks that will reduce methylene blue in periods up to two to three hours, but is complicated by the strong poising influence of the red-white reaction.

9. Intelligent interpretation of the one-hour resazurin test was not found to be always possible in the present state of knowledge.

10. The authors believe that the resazurin test has been placed in the hands of the dairy industry before it has emerged sufficiently from the experimental stage.

References

1. Clark, W. M., Cohen, B., and Gibbs, H. D. U.S. Pub. Health Service. Pub. Health Repts. Reprint No. 1017. 1925.
2. Collins, M. A., White, L. M., Chilson, W. H., Turner, H. G., and Rice, J. R. Assoc. Bull. Intern. Assoc. Milk Dealers, 31 : 104-119. 1939.
3. Davies, J., Thomas, B. F., and Thomas, S. B. Welsh J. Agr. 15 : 181-189. 1939. *From* Dairy Sci. Abstracts 1 : 266. 1939.
4. Davis, J. G. Food Manuf. 6 : 196-198. 1939.
5. Frayer, J. M. Vermont Agr. Expt. Sta. Bull. 435. 1938.

6. FRAYER, J. M. Vermont Agr. Expt. Sta. Bull. 461. 1940.
7. GREENBANK, G. R. Proc. Intern. Assoc. Milk Dealers, 29th Ann. Conv. Lab. Sect. 101–116. 1936.
8. GUNDERSON, M. F. and TEMPLETON, H. L. J. Bact. 38 : 483-484. 1939.
9. HOBBS, B. C. J. Dairy Research, 10 : 35-58. 1939.
10. JACKSON, C. J. J. Dairy Research, 7 : 31-40. 1936.
11. JOHNS, C. K. Am. J. Pub. Health, 29 : 239-247. 1939.
12. JOHNS, C. K. Can. Dairy Ice Cream J. 18 : 27-28, 47. 1939.
13. JOHNS, C. K. and HOWSON, R. K. J. Dairy Sci. 23 : 295-302. 1940.
14. KEENAN, J. A., BARRETT, W. D., and RUTAN, H. J. Milk Tech. 1 : 22-25. 1937.
15. NEITSKI, R., DIETZE, A., and MAECKLER, H. Ber. 22 : 3020-3038. 1889.
16. NELSON, F. E. J. Dairy Sci. 22 : 335-336. 1939.
17. PESCH, K. L. and SIMMERT, H. Reprint from Süddeutsch Molkereiz. Sept. 20, 1928.
18. RAMSDELL, G. A., JOHNSON, W. T. JR., and EVANS, F. R. J. Dairy Sci., 18 : 705-717. 1935.
19. THORNTON, H. R. and HASTINGS, E. G. J. Bact. 18 : 319-332. 1929.

THERMAL STUDIES ON ASBESTOS

I. EFFECT OF TEMPERATURE AND TIME OF HEATING ON LOSS IN WEIGHT AND RESORPTION OF MOISTURE[1]

By D. Wolochow[2] and W. Harold White[3]

Abstract

Heating a chrysotile asbestos mill fibre has shown that in the approximate temperature range of 500 to 700° C. the loss in weight depends on both the time and temperature. At other temperatures the loss is practically independent of the time.

Prolonged heating at about 490° C. expelled about 25%, and at 510° C. about 50%, of the combined water. Complete dehydration occurred on prolonged heating at about 580° C., but only above 700° C. was the loss in weight rapid.

On the basis of the data obtained on the resorption of moisture it is suggested that heating for half an hour at 215° C. would be a more accurate and rapid method for determining free moisture than that commonly employed.

Introduction

Previous published studies on the thermal treatment of asbestiform minerals have been limited to the effect of temperature on physical properties, such as tensile strength (4, 6) and the accompanying chemical changes (3, 5, 7, 9). The effect of time of heating has not been studied. The purpose of the present investigation was to obtain as complete information as possible on the effect of both temperature and time of heating on the loss in weight of chrysotile asbestos fibre, and on the subsequent sorption of moisture by the heated fibre.

Methods and Materials

A quantity of a Canadian mill fibre* (Quebec Standard Test: 1.7–9.3–4.0–1.0) was conditioned at 65% relative humidity and 70° F. Ten-gram samples were loosely packed into large crucibles and heated in an electric furnace with automatic temperature control (±8° C.), at temperatures up to 904° C. and for periods up to 20 hr. After heating, the samples were cooled in a desiccator and weighed. They were then replaced in the conditioning room, and the regain in weight, due to water resorption, determined.

Because of the importance of the time of heating between 493 to 555° C., heat treatments in this temperature range were made for periods up to almost 300 hr.

To determine the effect of repeated heating, a condition to which asbestos is exposed in normal use, loss determinations were made on one sample heated at all temperatures studied in this investigation.

[1] *Manuscript received September 16, 1940.*

Contribution from the Division of Chemistry, National Research Laboratories, Ottawa, Canada. Issued as N.R.C. No. 969.

[2] *Chemist, Division of Chemistry.*

[3] *Biochemist, Food Storage and Transport Investigation, Division of Biology and Agriculture. Formerly, Chemist, Division of Chemistry.*

* *Percentage composition of the dry fibre (loss at 110° C. = 1.4%): SiO_2, 40.2; Al_2O_3, 3.4; FeO, 1.9; Fe_2O_3, 0.7; MgO, 40.3; CaO, 0.48; CO_2, 0.20; ignition loss, 13.3.*

TABLE I

PERCENTAGE LOSS IN WEIGHT ON HEATING SAMPLES OF CANADIAN CHRYSOTILE ASBESTOS (MILL FIBRE) AT VARIOUS TEMPERATURES AND PERIODS OF TIME

Temp. of heating, °C.	Period of heating, hr.				
	0.25	0.50	1	2	20
110	1.27	1.33	1.40	1.38	1.40
160		1.61	1.52	1.52	1.61
216	1.72	1.79	1.80	1.85	1.94
271	1.96	2.06	1.95	2.00	2.18
327	2.14	2.17	2.29	2.34	2.52
382	2.35	2.40	2.82	2.79	3.05
438	3.16	3.13	3.23	3.21	3.29
493	3.36	3.34	3.46	3.51	3.72
555	4.12	4.41	4.92	5.30	*10.15
582	4.45	4.81	5.17	8.16	*13.31
604	4.84	4.76	6.27	10.32	*13.50
632	6.21	7.67	11.15	13.27	14.00
671	8.87	12.93	13.89	14.00	14.14
704	13.18	13.99	14.21	14.22	14.28
804	14.42	14.45	14.54	14.60	14.83
904	14.66	14.75	14.79	14.60	14.86

	555	582	604° C.
* 6 hr.	7.8	10.1	13.1

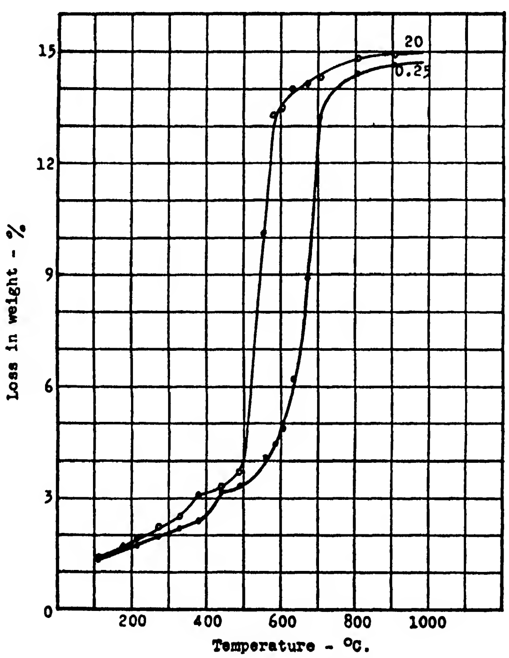

FIG. 1. *Weight lost by Canadian chrysotile asbestos (mill fibre) on heating for 0.25 hr. and 20 hr.*

Results and Discussion

The data obtained for the loss in weight after heating are given in Table I. In Fig. 1, the loss on heating for 0.25 hr. and 20 hr. has been plotted against the temperature of heating. From these it may be seen that, independently of the time of heating, a certain critical temperature must be reached before complete dehydration will occur. From Fig. 2, in which the loss at various temperatures has been plotted against time of heating, it is evident that at temperatures below 493° C. the loss in weight is practically independent of the time of heating. However, at temperatures between 493 and 704° C., the loss in weight is considerably affected by the time of heating, increasing markedly with increase of time. At and above the latter temperature the loss is again practically independent of the time of heating.

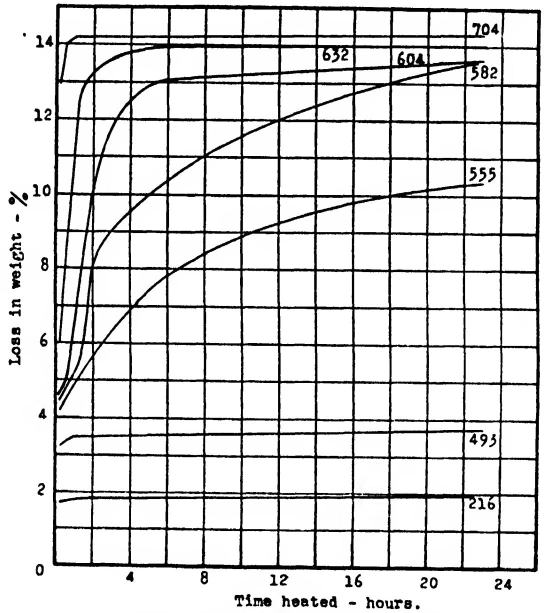

FIG. 2. *Weight lost by Canadian chrysotile asbestos (mill fibre) on heating at indicated temperatures (°C.).*

The data obtained from the more detailed examination of the effect of time and temperature of heating in the range 493 to 555° C. are graphically presented in Fig. 3. The points representing the loss in weight after heating for various time intervals at 510, 516, and 527° C. have been joined with broken lines because it is doubtful whether these are significant, except in so far as they indicate that in this temperature range the fibre is very sensitive to small changes in temperature. To definitely establish the course of dehydration in this temperature zone would require very precise control of temperature and other factors, over long periods of heating.

Taking into account the content of moisture, carbonates and ferrous iron, the maximum loss in weight of 4.8% at 493° C. corresponds approximately to

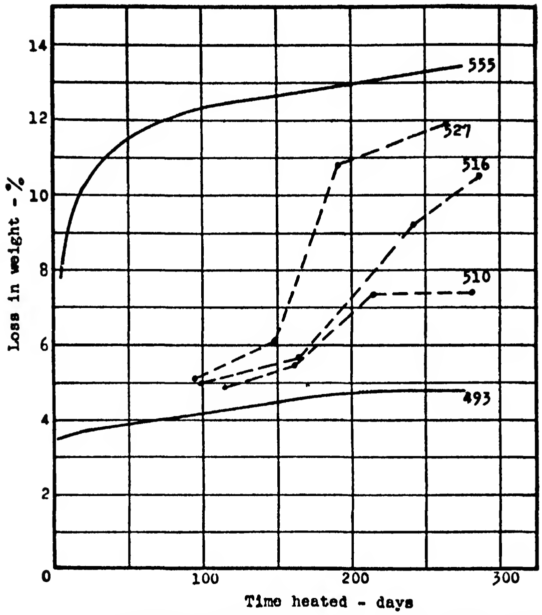

FIG. 3. *Weight lost by Canadian chrysotile asbestos (mill fibre) on prolonged heating at indicated temperatures (°C.).*

one-quarter of the combined water in the chrysotile molecule. This is in agreement with the data obtained by Warren and Bragg (8) who, as the result of X-ray studies, have proposed the formula $(OH)_6Mg_6Si_4O_{11} . H_2O$, a structure that suggests that one-quarter of the water present is less firmly held than the remainder. The data indicate further that not more than about one-half of the combined water is driven off on prolonged heating at 510° C. Complete dehydration may possibly result on heating for very long periods at temperatures slightly above 516° C., but only when the fibre is heated at 704° C. will complete dehydration take place in less than one hour.

The minor inflections in the curves noted at temperatures of 400 to 450° C. (Figs. 1 and 3) seem to confirm an observation made by previous investigators

TABLE II

PERCENTAGE LOSS IN WEIGHT UPON HEATING A SAMPLE OF CANADIAN CHRYSOTILE ASBESTOS (MILL FIBRE) AT ALL TEMPERATURES AND PERIODS OF TIME (REPEATED HEATING)

Temp. of heating, °C.	Period of heating, hr.			
	0.50	1.5	3.5	21
555	4.58	5.05	5.75	10.55
582	10.55	11.17	11.47	13.33
604	13.73	13.51	13.53	13.84
632	13.95	13.97	14.10	14.11
671	14.12	14.13	14.14	14.29
704	14.30	14.33	14.32	14.43
904	14.78	14.85	14.80	15.01

(1, 2), who suggest that this may be due to the decomposition of brucite, present in the chrysotile as an impurity. There is, however, reasonable doubt regarding the validity of such a conclusion.

The results obtained by the repeated heating of the same sample of fibre are essentially the same as those of the single heating method, up to 555° C. Above this temperature and up to 704° C. (Table II) the loss in weight was different, as was to be expected from a consideration of the results in Table I. Comparable results for a heating period of 0.50 hr. are shown graphically in Fig. 4.

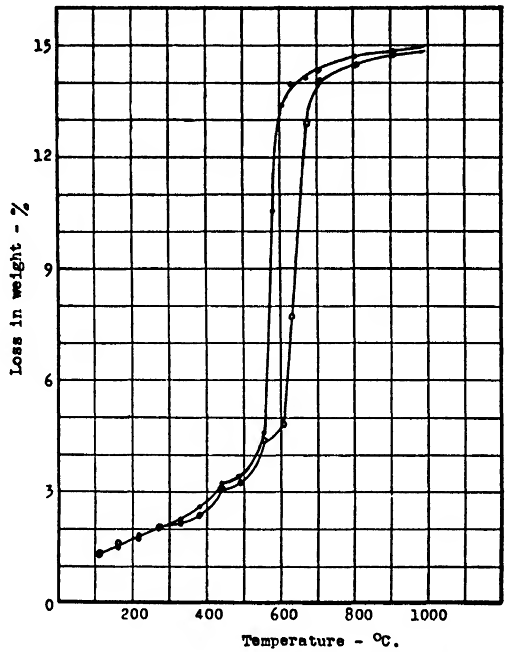

FIG. 4. *Weight lost by Canadian chrysotile asbestos (mill fibre) on heating for 0.50 hr.* o *Separate samples (i.e., single heating).* • *Same sample (i.e., repeated heating).*

The recovery of weight by the heated samples, when exposed in the conditioning room, is shown in Table III, in which the resorbed water is expressed as a percentage of the weight lost during heating. The results indicate that dehydration of the chrysostile molecule, that is, the loss of combined water, does not begin until the fibre has been heated at 216° C., for at least an hour. This would suggest that the present accepted method of determining sorbed moisture by drying to constant weight at 105 to 110° C.* gives low results. It would appear that a more accurate and more rapid procedure would be to dry for 0.50 hr. at approximately 215° C.

The amounts of water resorbed by the heated fibre, expressed as a percentage of the weight of the heated fibre, are given in Table IV, and graphically illustrated for the fibre heated for 0.25 hr. and 20 hr., in Fig. 5. These results

* *A.S.T.M. Standards on Textile Materials, 1939, page 50.*

TABLE III

PERCENTAGE RECOVERY OF WEIGHT LOST BY CANADIAN CHRYSOTILE ASBESTOS (MILL FIBRE) HEATED AT VARIOUS TEMPERATURES AND PERIODS

Temperature of heating, °C.	Period of heating, hr.				
	0.25	0.50	1	2	20
160		100	100	98	100
216	99	100	99	96	93
271	89	89	88	87	81
327	84	82	83	83	80
382	82	81	78	79	74
438	74	77	72	72	69
493	71	70	69	66	55
555	62	62	48	45	40
604	47	47	40	39	34
632	40	39	36	36	28
671	46	44	40	39	16
704	41	38	35	33	11
804	13	12	10	10	9
904	10	9	9	8	6

indicate that the observed loss in weight, caused by heating, is at the higher temperatures accompanied by chemical or physical changes, or by both, in the fibre.

The presence of the sorption maximum is of theoretical and possibly of practical interest. Haraldsen, as a result of his studies (3) concluded that serpentine decomposes to give olivine and silica, and that these products recombine at still higher temperatures to form enstatite. If such changes occur when serpentine is heated, it might reasonably be expected that similar

TABLE IV

PERCENTAGE WATER RESORBED BY CANADIAN CHRYSOTILE ASBESTOS (MILL FIBRE) AFTER HEATING AT VARIOUS TEMPERATURES AND PERIODS*

Temperature of heating, °C.	Period of heating, hr.				
	0.25	0.50	1	2	20
160		1.65	1.55	1.51	1.66
216	1.74	1.82	1.82	1.82	1.83
271	1.79	1.88	1.74	1.77	1.80
327	1.82	1.80	1.95	1.98	2.05
382	1.94	2.00	2.28	2.26	2.34
438	2.43	2.48	2.47	2.40	2.36
493	2.48	2.44	2.48	2.45	2.12
555	2.42	2.44	2.06	2.01	2.14
604	2.38	2.37	2.71	3.42	5.29
632	2.70	3.26	4.52	5.54	4.49
671	4.51	6.56	6.38	6.33	2.67
704	6.30	6.18	5.87	5.55	1.83
804	2.25	2.11	1.74	1.79	1.56
904	1.66	1.63	1.57	1.41	1.09

* *Calculated on basis of the weight after heating.*

reactions take place in the thermal decomposition of chrysotile. The sorption maxima observed may then be due to the transitory presence of silica, and not merely to surface effects.

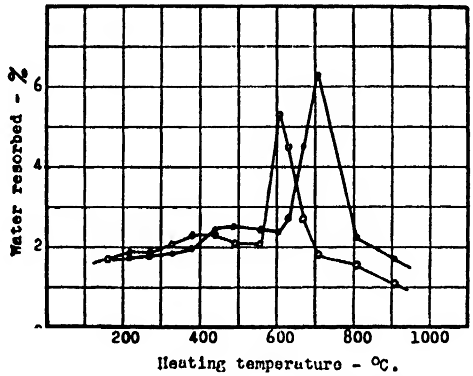

FIG. 5. *Resorption of water by Canadian chrysotile asbestos (mill fibre) after heating.* • *0.25 hr.* ○ *20 hr.*

References

1. CAILLÈRE, S. Comptes rendu. 196 : 628-630. 1933.
2. GILL, A. F. Can. J. Research, 10 : 703-12. 1934.
3. HARALDSEN, H. Centr. Mineral. Geol. A : 297-315. 1928.
4. JOSEPH, H. Mellon Institute Repts. 1923.
5. NUTTING, P. G. J. Wash. Acad. Sci. 18 : 81-89. 1928.
6. SOMNER, H. Gummi-Ztg. 47 : 940. 1933.
7. SUIROMYATNIKOV, F. V. Bull. Soc. Nat. Moscow, Sect. Geol. 12 : 137-149. 1934.
8. WARREN, B. E. and BRAGG, W. L. Z. Krist. 76 : 201-210. 1930.
9. ZAMBONI, F. Groth's Z. Krist. 79 : 73-79. 1911.

THERMAL STUDIES ON ASBESTOS

II. EFFECT OF HEAT ON THE BREAKING STRENGTH OF ASBESTOS TAPE AND GLASS FIBRE TAPE[1]

By D. Wolochow[2]

Abstract

The first result of heating pure chrysotile asbestos tape, crocidolite (blue) asbestos tape, and glass fibre tape to drive off the adsorbed moisture is an increase in breaking strength.

Pure chrysotile tape does not lose strength till a temperature of 370° C. is exceeded. Prolonged heating at 430° C. causes a loss in strength of about 20%, at 480° C. of about 40%. Heating at 540° C. causes a rapid loss in strength.

Crocidolite asbestos tape loses strength more rapidly than chrysotile asbestos tape.

Glass fibre tape, though initially stronger than chrysotile tape, is considerably less resistant to heat, beginning to lose strength rapidly at about 250° C., whereas chrysotile asbestos tape does not suffer any appreciable decrease in strength till a temperature of 400° C. is exceeded.

The literature (1, p. 56; 2; 3) contains little information on the effect of the temperature and the time of heating on the breaking strength of absestos textiles.

Most of the tests described below were made on pure (Grade AAAA) chrysotile asbestos tapes, but the results of some tests on underwriters' grade chrysotile asbestos, on crocidolite (blue) asbestos, and on glass fibre tapes are also reported.

Test Method

The samples were cut into 6-in. strips and conditioned at 65% relative humidity and 70° F. Twenty strips were taken for each test, in which the strips were heated in an electric furnace having automatic temperature control (±8° C.), cooled in a desiccator, and then broken in a standard pendulum type of testing machine. The loss in weight was also determined.

Test Results

The pure chrysotile asbestos tapes were all of the same nominal dimensions (1 in. wide and $\frac{1}{16}$in. thick), but because of various factors there were considerable differences in the breaking strength. These differences were of interest in another connection, but they do not affect the present study, which is primarily concerned with changes in breaking strength due to heating, rather than with actual breaking strengths. The breaking strength after heating was therefore in each case expressed as a percentage of the initial breaking strength, and the relative strengths were then averaged. These average relative breaking strengths have been plotted in Figs. 1, 2, and 3.

[1] *Manuscript received September 16, 1940.*

Contribution from Division of Chemistry, National Research Laboratories, Ottawa, Canada. Issued as N.R.C. No. 970.

[2] *Chemist.*

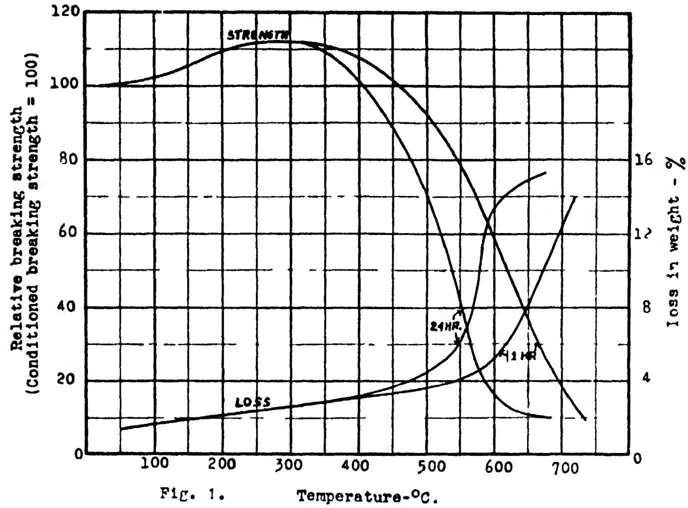

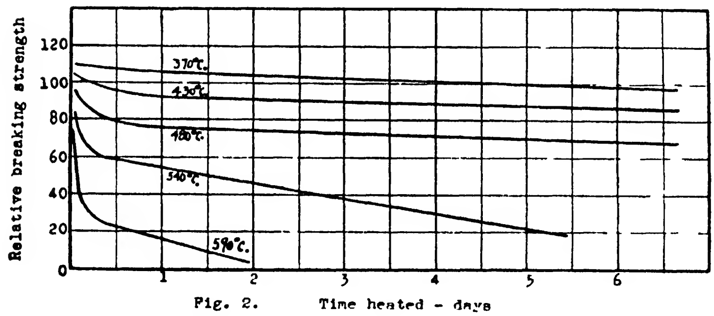

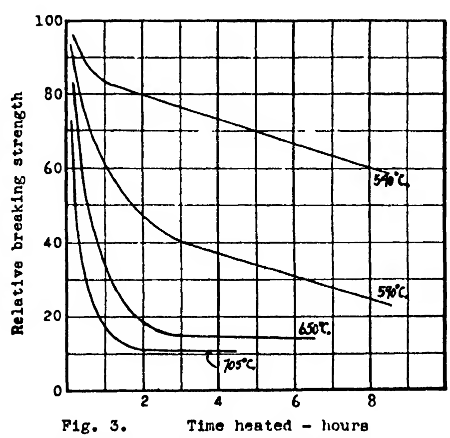

FIG. 1. *Relative breaking strength and loss in weight of pure chrysotile asbestos tape heated for 1 and 24-hr. periods.*

FIG. 2. *Relative breaking strength of pure chrysotile asbestos tape after prolonged heating at 370 to 590° C. (700 to 1100° F.).*

FIG. 3. *Relative breaking strength of pure chrysotile asbestos tape heated at 540 to 705° C.*

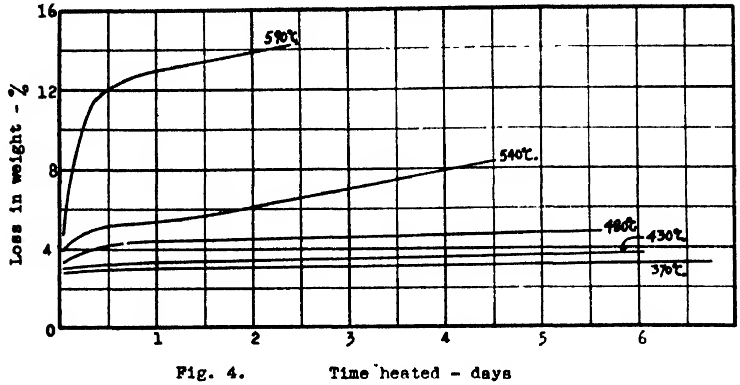

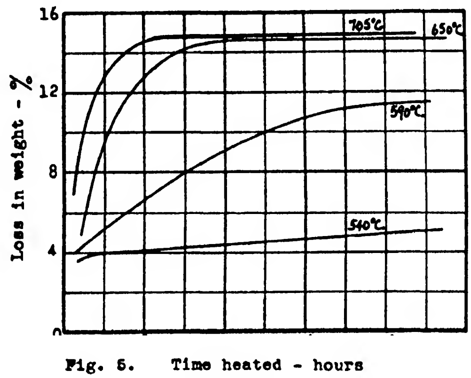

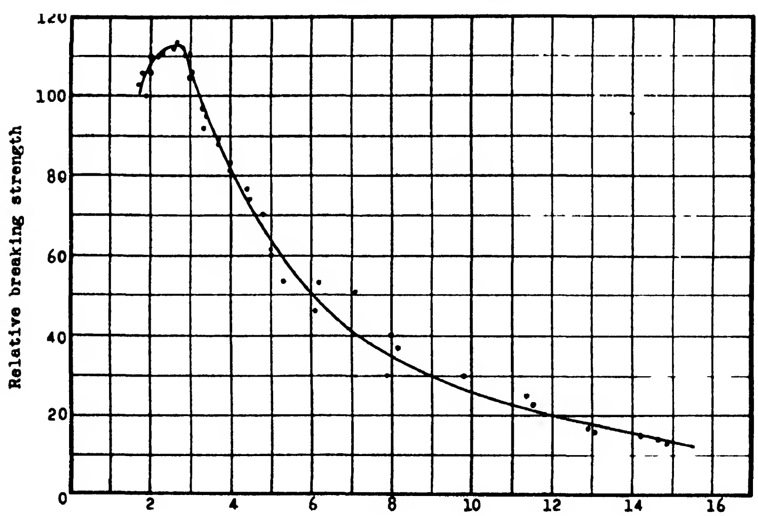

FIG. 4. *Loss in weight of pure chrysotile asbestos tape after prolonged heating at 370 to 590° C.*

FIG. 5. *Loss in weight of pure chrysotile asbestos tape heated at 540 to 705° C.*

FIG. 6. *Relation between relative breaking strength and loss in weight on heating.*

The weight losses were also averaged and the values have been plotted in Figs. 1, 4, and 5.

The relation between relative breaking strength after heating and loss in weight (average values for all pure chrysotile tapes tested) is shown in Fig. 6.

The extent of the variations in actual breaking strength and in the effect of heating, as illustrated by the curves for four samples of pure chrysotile tape, is shown in Fig. 7.

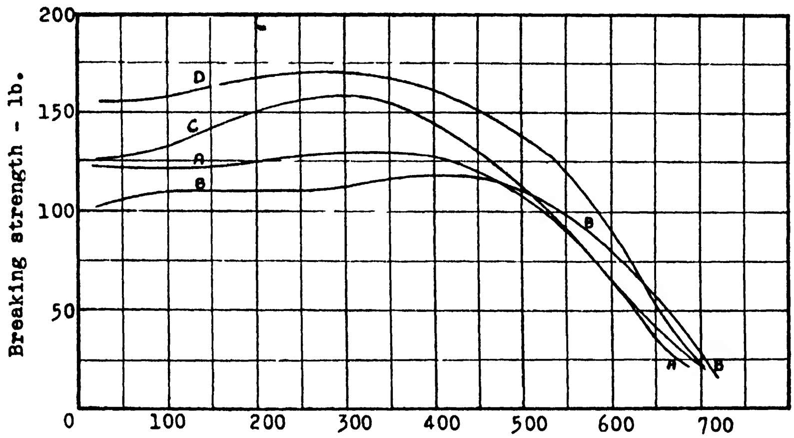

Fig. 7.

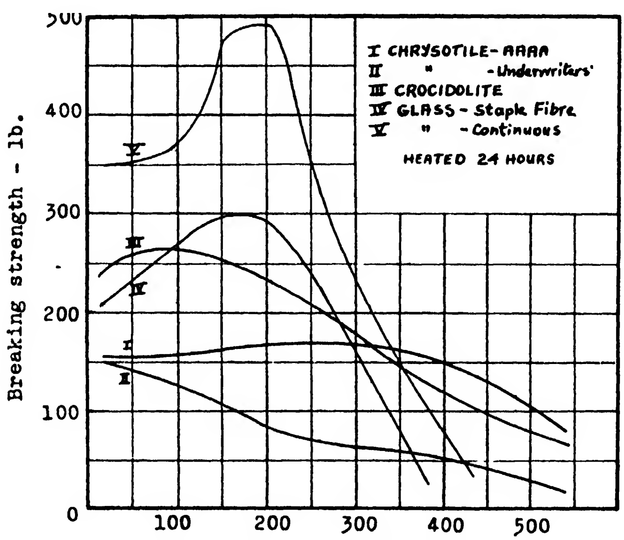

Fig. 8.

FIG. 7. *Variations in the breaking strength of pure chrysotile asbestos tapes heated one hour.*

FIG. 8. *Effect of heat on the breaking strength of chrysotile, crocidolite, and glass fibre tapes.*

The effects of heat on a pure chrysotile tape, an underwriters' grade tape, a crocidolite (blue) tape, and two glass fibre tapes, one made from the staple, the other from the continuous filament type of glass fibre, are shown in Fig. 8.

The maximum loss in weight of the crocidolite tape (0.0975 in. thick) was about 2%, of the staple fibre glass tape (0.015 in. thick) about 4%, and of the continuous filament glass tape (0.010 in. thick) about 4.5%.

Discussion of Results

The first noticeable effect of heating is an increase in the relative breaking strength of pure asbestos tape, amounting to an average of 12% at about 300° C., up to which temperature the effect of heating seems to be practically independent of the length of time the heating is continued. This increase in strength is most probably due to the removal of adsorbed moisture. If the heating is continued after the adsorbed moisture has been driven off, the tapes begin to lose strength, but the strength does not drop below the initial value, no matter how long the heating is continued, at any temperature below 370° C. Above this temperature, the strength begins to drop, decreasing to the initial value after one hour at 460° C. or after 24 hr. at 405° C. It is only above 480° C. that a rapid loss in breaking strength takes place.

It is evident that pure chrysotile asbestos tape retains its original breaking strength over a wide temperature range. Initially, the particular sample tested was not nearly as strong as the glass fibre tape (see Fig. 8), but after heating for 24 hr. at 400° C. it had retained all its initial breaking strength, whereas the glass fibre had retained only a fraction of its breaking strength and had only half the strength of the asbestos.

The crocidolite tape showed a small increase in breaking strength, followed by a decrease, which is much more rapid than in the case of the chrysotile asbestos.

The underwriters' grade of asbestos tape begins to lose strength as soon as heat is applied. This is of course due to the presence of cotton in the tape.

References

1. A.S.T.M. Standards on Textile Materials. 1939.
2. Atkinson, F. W. Elec. Eng. 58 : 277-286. 1939.
3. Joseph, H. Mellon Institute Repts. 1923.

PECTIC SUBSTANCES IN COTTON[1]

By Frank Leger[2] and P. Larose[3]

Abstract

The quantitative distribution of pectic substances* in raw cotton has been studied. A new method for the removal of cuticle pectin has been utilized. A combination of this method with analysis for α-cellulose has shown that the non-cellulosic material in undamaged cotton appears to be present in the form of pectin.

In direct support of recent work carried out by Harris and co-workers (5, 6), and in contrast to that published by Farr (3), it has been found that reduction of pectin content from 1.18 to 0.12% resulted in a change of fluidity from 1.93 to 2 08, whereas treatment with hydrochloric acid raised the fluidity to 25 8.

It is suggested that there is no essential chemical difference between pectin in the cuticle surrounding the fibre and that distributed throughout the fibre.

Introduction

This paper reports results of work carried out during the past few months in connection with an investigation of the degradation of cellulose. Besides presenting some new facts, it corroborates recent work published by Whistler, Martin, and Harris.

It was felt that the method employed by Farr (3, 4) for the removal of pectic substances, viz., the use of hydrochloric acid solutions, was too drastic and resulted not only in the removal of pectin but also in a degradation of cellulose. This was shown to be the case by determinations of α-cellulose and of fluidities. Moreover, Harris (6) has pointed out that the method removes only a part of the original pectin.

There is considerable danger of degradation of cellulose in any method utilizing solutions of strong acids or bases for the removal of pectic material from cotton. With this in mind, it was thought that the use of a dilute solution of a mild base, such as sodium carbonate, would be preferable. That this assumption was justified is shown by the results that follow.

Methods

An American raw cotton was dewaxed by extraction in a Soxhlet with neutral chloroform for a 24 hr. period, followed by several extractions with boiling water. The residual cotton was then air dried.

[1] *Manuscript received in original form August 2, 1940, and as revised, September 22, 1940.*
Contribution from the Division of Chemistry, National Research Laboratories, Ottawa, Canada. Issued as N.R.C. No. 968.

[2] *Research Assistant.*

[3] *Chemist.*

* ***Pectin or pectic substance is used to designate those carbohydrate materials that contain galacturonic acid units, as determined by the rate of evolution of carbon dioxide on treatment with boiling 12.8% hydrochloric acid.***

In order to remove pectic material, this cotton was boiled for eight hours with an aqueous 1% solution of sodium carbonate (the ratio of cotton to solution was 1 : 30). A further similar extraction was carried out with fresh carbonate solution. During the first eight hour extraction, samples of cotton were removed at one hour intervals, acidified with 0.5% acetic acid, washed free of acid, and dried. These samples were used for a microscopic examination of fibres stained with a solution of ruthenium red and for the microscopic observation of their behaviour on treatment with cuprammonium solution. At the end of the eight hour treatment, the cuticle was apparently completely removed.

Since removal of pectin was not complete after the eight hour extraction, the cotton was further treated with a 0.5% aqueous solution of ammonium oxalate for eight hours at 75° C., followed by a 24 hr. extraction with the same solution at room temperature.

Isolation of the sodium-carbonate–soluble pectin was accomplished as follows: The carbonate solution was acidified with dilute hydrochloric acid (10%), whereupon a flocculent precipitate settled out. This was filtered off and washed with 95% ethanol. The residue was dissolved in a minimum quantity of 0.5% ammonium oxalate solution at 75° C., the solution was cooled to 10° C., acidified to pH 2.6, and to it was added two volumes of ethanol. The resulting gel was removed by filtration, dried under reduced pressure at 40° C., and purified by repeated solution in boiling water, cooling, and adding two volumes of ethanol. The final gel was dried as above.

The α-cellulose was determined by means of the standard method (2). Fluidities were determined in cuprammonium hydroxide solution containing 15 $\pm$ 0.1 gm. of copper, 200 $\pm$ 10 gm. of ammonia, and less than 0.5% of nitrite. The concentration of the cellulose in the cuprammonium solution was 0.5%. X Type B.C.I.R.A. viscometers were used for the fluidity measurements.

Pectin was determined from the rate of evolution of carbon dioxide on boiling a sample with 12.8% hydrochloric acid solution. The apparatus was that of Dickson, Otterson and Link (1) so modified as to permit its application to semi-micro determinations. A further change was made in that the evolved carbon dioxide was carried to the absorption tower in a stream of carbon-dioxide–free nitrogen instead of by the application of a vacuum. A barium hydroxide solution (0.02 N) was used in the absorption tower, and the excess of alkali was determined by back titration with hydrochloric acid (0.02 N). Phenolphthalein was used as an indicator and carbon-dioxide–free solutions were used throughout. A constant correction was applied for carbon dioxide evolved from the cellulose itself (6, 7). The value used was 0.45 mg. of carbon dioxide from 1 gm. of cellulose in 2.5 hr. At an oil bath temperature of 150° C., 2.5 hr. was found to be sufficient time for complete removal and absorption of pectin carbon dioxide, and was the time used in all these experiments. The pectin content was calculated by multiplying the amount of pectin carbon dioxide by 4.8 (6, 7).

TABLE I

CHANGE IN PECTIN CONTENT AND IN FLUIDITIES OF COTTON AFTER VARIOUS TREATMENTS

Sample No.	1	2	3	4
α-cellulose, %	99.0	99.1	99.5	99.7
Pectin in α-cellulose, %	0.21	0.21	0.10	0.07
Pectin, % of whole fibre	1.18	0.99	0.30	0.12
Fluidity, rhes.	1.93	2.03	2.00	2.08

Sample 1—dewaxed cotton.
Sample 2—as for Sample 1, extracted with aqueous sodium carbonate (1 0%) at 100° C. for eight hours.
Sample 3—as for Sample 2, extracted with ammonium oxalate (0.5%) at 75° C. for eight hours.
Sample 4—as for Sample 3, extracted with the same ammonium oxalate 24 hr. at 25° C.

Discussion of Results

Table I summarizes some of the results obtained.

A microscopic examination of Sample 2, stained with ruthenium red and dissolved in cuprammonium hydroxide, indicated that the cuticle had been entirely removed after the eight hour treatment with 1.0% sodium carbonate solution. Complete removal of the cuticle resulted in a loss of only 16% of the pectin originally present in the cotton, as shown by a comparison of the results obtained with Samples 1 and 2.

However, the results given in Table II, show that further treatment with 1% sodium carbonate solution extracts more pectin, until at the end of 24 hr. practically all the pectin has been removed. It would thus seem that there is no essential chemical difference in cuticle and fibre pectin, although the latter is removed more slowly, probably owing to the slow rate of diffusion of the sodium carbonate solution into the fibre. Since complete removal of the cuticle results in elimination of only 16% of the pectin, corresponding to 0.2% of the dewaxed cotton, this would represent a maximum value for the cuticle pectin.

TABLE II

EFFECT OF TIME OF EXTRACTION BY SODIUM CARBONATE SOLUTION ON PECTIN CONTENT OF COTTON

Sample	Original	1	2
Pectin, % of whole fibre	1.18	0.17	0.17

Original—dewaxed cotton.
1—original extracted for 24 hr. at 100° C. with 1% sodium carbonate.
2—As for Sample 1, but extracted for 48 hr.

The amounts of pectin originally present in the dewaxed cotton and in the cotton practically free of pectin are in complete agreement with those found by Whistler, Martin, and Harris (5).

The material recovered from the sodium carbonate solution by the method outlined in the section on methods had a pectin content of 69.8%, which corresponds closely to that of a commercial pectin.

Fluidity determinations of cuprammonium hydroxide solutions of cotton extracted with sodium carbonate and with ammonium oxalate solutions at various stages of pectin removal, have been carried out, and the results are given in Table I. These show that the fluidity does not depend on pectin content.

In Table I are also included the results of the determination of α-cellulose in the cotton at various stages of pectin removal. These results indicate a close agreement between the α-cellulose content and total non-pectin material in the fibre. This holds only when there is no degradation as shown by the fluidity values. Some of the original cotton was treated for 0.5 hr. according to Farr's method for the removal of pectin (3, 4), and the resulting cotton tested for α-cellulose and fluidity. The results are given in Table III.

TABLE III

EFFECT OF TREATMENT WITH HYDROCHLORIC ACID ON α-CELLULOSE CONTENT AND FLUIDITY OF COTTON

Sample	Original	Treated
α-cellulose, %	99.0	91.4
Fluidity, rhes.	1.93	25.8

Original—dewaxed cotton.
Treated—Original, treated 30 min. at 25° C. with hydrochloric acid (sp. gr. = 1.18).

The change in α-cellulose content from 99.0 to 91.4% definitely indicates that degradation has taken place, and it is reasonable to conclude, therefore, that the change in fluidity is due to this degradation and not to the removal of pectin. This substantiates recent work by Harris (5), in which it is shown that treatment of cotton with concentrated hydrochloric acid removes only a small part of the pectin present. From the foregoing, an α-cellulose content of less than 98.5% would indicate possible degradation of the cotton, with correspondingly higher fluidity values.

References

1. DICKSON, A. D., OTTERSON, H., and LINK, K. P. J. Am. Chem. Soc. 52 : 775-779. 1930.
2. DOREE, C. The methods of cellulose chemistry. Chapman and Hall, Ltd., London. 1933.
3. FARR, W. K. Contrib. Boyce Thompson Inst. 10 (1) : 71-112. 1938.
4. FARR, W. K. and ECKERSON, S. Contrib. Boyce Thompson Inst. 6 (3) : 309-313. 1934.
5. HOCK, L. W. and HARRIS, M. Textile Research, 10 : 323-333. 1940.
6. WHISTLER, R. L., MARTIN, A. R., and HARRIS, M. Am. Dyestuff Reptr. 29 (10) : 244-258. 1940.
7. WHISTLER, R. L., MARTIN, A. R., and HARRIS, M. J. Research Natl. Bur. Standards. 24 : 13-25. 1940.

Canadian Journal of Research

Issued by The National Research Council of Canada

VOL. 19, SEC. B. MARCH, 1941 NUMBER 3

THERMAL STUDIES ON ASBESTOS

III. EFFECT OF HEAT ON THE BREAKING STRENGTH OF ASBESTOS CLOTH CONTAINING COTTON[1]

By D. Wolochow[2]

Abstract

Commercial, Underwriters', and A grades of asbestos cloth begin to lose strength as soon as heat is applied. On heating for five minutes at 300° C. these three grades of asbestos cloth lose approximately 60, 35, and 25% of their original (conditioned) breaking strength, respectively. Charts are given showing the effect of heating, at temperatures up to 600° C., for periods up to one hour.

Supplementing the study of the effect of heat on the breaking strength of pure or Grade AAAA asbestos tape, which was the subject of the previous paper (1), there is now presented a summary of the results of similar tests on asbestos cloth that contains cotton.

Materials Tested

The samples of cloth tested fall into three grades: Commercial, Underwriters', and A grade. Several samples of each grade were studied, the average asbestos content of the samples in each grade being 79.5, 82.0, and 89.0%, respectively.

The samples had thicknesses ranging from 0.140 to 0.250 in., and weights of 1.5 to 2.5 lb. per yard.

Methods of Test

The samples were conditioned at 70° F., and 65% relative humidity, and the thickness, weight, and breaking strength determined. Strips, about 1½ in. wide and 6 in. long, were then prepared and at least 10 strips were taken for each heating test. After being heated in a well ventilated furnace, the samples were cooled in a desiccator and broken in a machine equipped with standard 1-in. jaws.

Results

The results of the tests are shown in Figs. 1 to 3, in which the percentage of the original breaking strength retained after heating at the temperatures indicated has been plotted against the time of heating. The values are averages for all samples within each grade.

[1] *Manuscript received September 16, 1940.*
Contribution from Division of Chemistry, National Research Laboratories, Ottawa. Issued as N.R.C. No. 972.

[2] *Chemist, Division of Chemistry.*

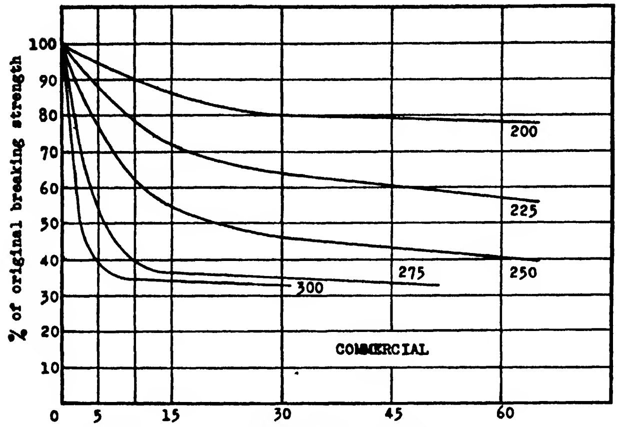

Fig. 1. Time heated - minutes

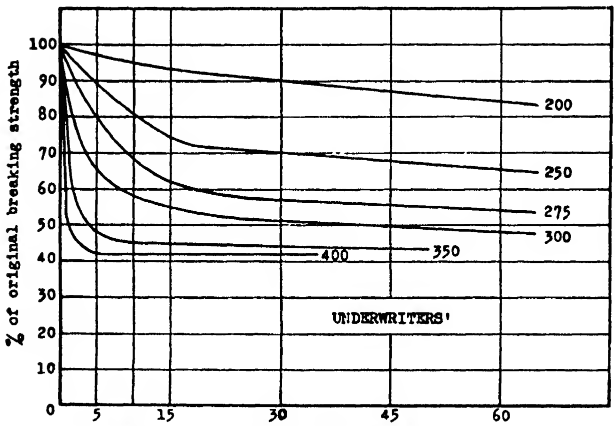

Fig. 2. Time heated - minutes

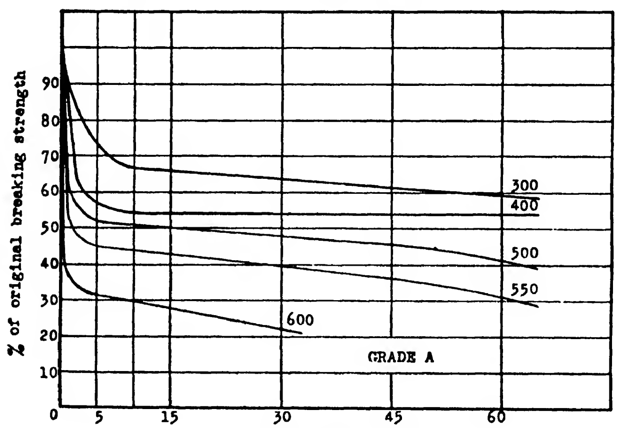

Fig. 3. Time heated - minutes

FIG. 1. *Breaking strength of commercial grade asbestos cloth after heating at 200-300° C.*
FIG. 2. *Breaking strength of underwriters' grade asbestos cloth after heating at 200–400° C.*
FIG. 3. *Breaking strength of Grade A asbestos cloth after heating at 300–600° C.*

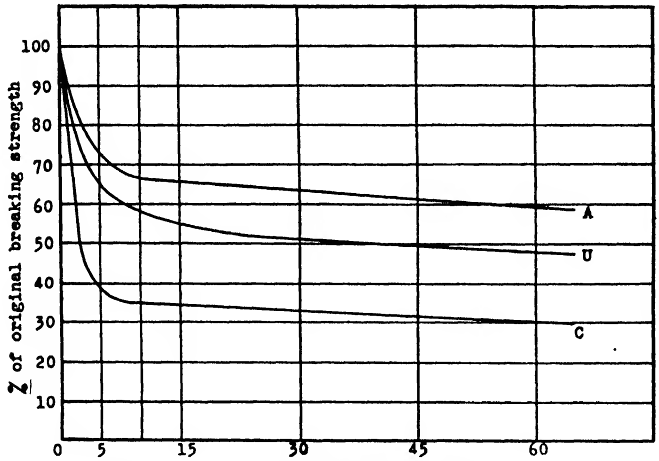

Fig.4. Time heated - minutes

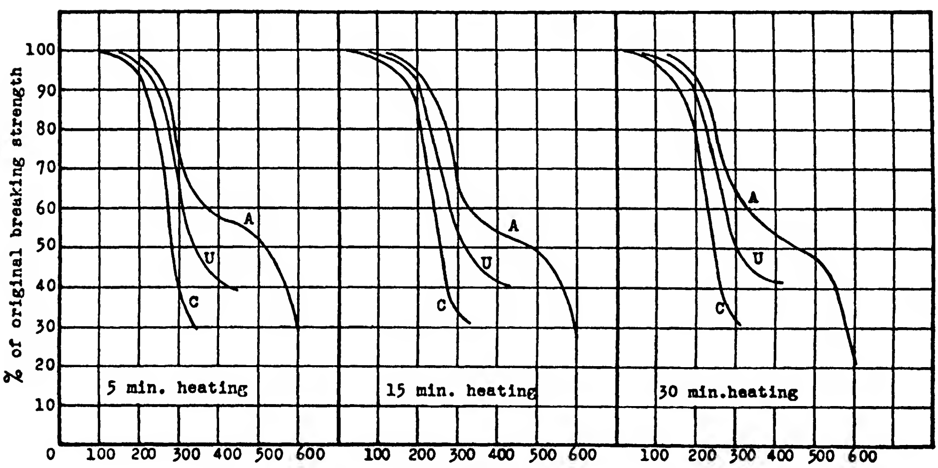

Fig.5. Temperature - °C.

FIG. 4. *Breaking strength of commercial, underwriters' and A grades of asbestos cloth after heating at 300° C.*

FIG. 5. *Breaking strength of commercial, underwriters' and A grades of asbestos cloth after heating for 5, 15, and 30 minutes.*

The effect of heating the three grades of cloth at 300° C. is shown in Fig. 4. In Fig. 5 the percentage of the original breaking strength retained by the three grades of cloth, after heating for 5, 15, and 30 min. has been plotted against the temperature of heating.

From these curves it is possible to predict with a fair degree of accuracy the percentage of the original (conditioned) breaking strength that is retained by Commercial, Underwriters', and A grades of asbestos cloth when heated up to temperatures of 300, 400, and 600°, respectively.

Reference

1. WOLOCHOW, D. Can. J. Research, B, 19 : 56-60. 1941.

THE ANALYTICAL PROBLEM OF MAPLE SAP PRODUCTS[1]

By Paul Riou[2] and Joachim Delorme[3]

Abstract

A systematic study of official methods of analysis of maple sap products has been made in order to investigate their validity as criteria of the purity of these products.

A new value, the manganese number, is being proposed as a safer criterion but, in some cases, even this may lead to error.

The conclusion of the writers is that, at the present time, it cannot be stated with certainty that a maple product is 100% pure; it is therefore necessary that research work be continued in order to find a criterion of purity that would be valid in every case.

Introduction

As a result of previous investigations involving a study of the manganese content of maple, beet, and cane sugars, the writers came to the conclusion that:

1. Manganese is present in all maple sugars, the amounts ranging from 0.75 to 17.50 mg. per 100 gm. (on dry basis), the average being 5.21 mg.

2. There is no manganese in refined beet and cane sugars.

3. In the majority of cases, manganese is absent in raw sugars, from beet and cane; if present, the content is very low.

In view of these results, certain conclusions concerning the purity of maple products were drawn, i.e., that:

1. A maple sugar containing no manganese is artificial.

2. A maple sugar with a manganese number* higher than 6 is likely to be pure.

3. If the manganese number* is lower than 6, a complete analysis of the product is required to ascertain a possible adulteration.

Since determination of the manganese number provides a test that is rapid and as reliable (or more so) than the usual methods,** the authors propose it as a criterion of the purity of maple sap products. In the present paper, a systematic study of all values used as criteria is made to determine its suitability.

[1] *Manuscript received in original form, October 15, 1940, and as revised, December 20, 1940.*
Contribution from the Department of Chemistry, Faculty of Commerce, University of Montreal, Montreal, P.Q.

[2] *Professor of Technology, Chairman of the Scientific Research Bureau of the Province of Quebec.*

[3] *Professor of Chemistry and Physics.*

* *The manganese number is the quantity of manganese in milligrams per 100 gm. of sugar on dry basis.*

** *For a review of these methods, see (1).*

Preliminary Work

In 1936, a determination of the Canadian Lead Number (1, 4) of 22 raw cane sugars was made; the results are given in Table I. It will be noticed that 12 of these (Samples 1–11, 17) have a Lead Value within the range of that for pure maple products. It is evident, therefore, that this value alone cannot be used as a criterion for determining the purity of a maple product (because it does not reveal adulteration with raw sugars).

TABLE I

Canadian lead number of raw cane sugars

No.	Sample	Value	No.	Sample	Value
1	West Ind. 113	7.40	12	West Ind. 121	12.45
2	Cuba 1a	5.82	13	Cuba 2740	12.48
3	West Ind. 134	5.58	14	Java 5209	10.17
4	Jamaica 1272	5.33	15	Java 5206	9.01
5	Jamaica 2471	4.30	16	West Ind. 8299	8.04
6	Natal (Afr.) 9760	4.03	17	Australia 9749	1.88
7	West Ind. 114	3.47	18	West Ind. 4612	1.63
8	West Ind. 4	3.46	19	West Ind. 121	1.50
9	Jamaica 5	3.23	20	Cuba 3	1.50
10	Trinidad 2472	2.20	21	West Ind. 6	1.48
11	Trinidad 116	2.15	22	Java 5205	1.38

Experimental

In view of the results of the preliminary work, 20 different samples of adulterated products were prepared and, in each, the following values were determined: *(a)* total ash; *(b)* soluble ash; *(c)* insoluble ash; *(d)* ratio of soluble to insoluble ash; *(e)* alkalinity of total ash; *(f)* alkalinity of soluble ash *(g)* alkalinity of insoluble ash; *(h)* ratio alkalinity soluble/alkalinity insoluble ash; *(i)* malic acid value (Cowles method); *(j)* Canadian Lead Number; *(k)* conductivity value; *(l)* manganese number.

Table II lists the different samples prepared and analyzed.

TABLE II

Composition of samples

Sample		Sample	
A	50% Raw cane sugar, "c"–134 50% Raw beet sugar Chatam-"b"	E	50% Raw cane sugar "c"–118 50% Maple sugar (Shefford)
B	50% Raw cane sugar "c"–120 50% Raw beet sugar Chatam-"c"	F	50% Raw cane sugar "c"–119 50% Maple sugar (Gaspé)
C	50% Raw cane sugar "c"–130 50% Raw beet sugar Chatam–"a"	G	50% Raw cane sugar "c"–120 50% Maple sugar (Rigaud)
D	50% Raw beet sugar Chatam–"b" 50% Maple sugar (St. Vincent)	H	50% Raw beet sugar "b"–3118 50% Maple sugar (Quebec)

TABLE II—*Concluded*

COMPOSITION OF SAMPLES—*Concluded*

Sample		Sample	
I	50% Raw beet sugar "b"–55035 50% Maple sugar (Sutton)	C–120	100% Raw cane sugar
J	50% Raw cane sugar "c"–132 50% Maple sugar (Nominingue)	C–130	100% Raw cane sugar
K	50% Raw cane sugar "c"–134 50% Maple sugar (Beauce)	C–132	100% Raw cane sugar
L	50% Raw cane sugar "c"–130 50% Maple sugar (Nominingue)	C–134	100% Raw cane sugar
C–118	100% Raw cane sugar	B–3118	100% Raw beet sugar
C–119	100% Raw cane sugar	B–55035	100% Raw beet sugar

Results

In Table III are given the analytical values found in the adulterated products and the minimum and maximum for corresponding values in pure maple products.

Discussion

A comparison of the analytical values found in adulterated maple products with those of pure products (Table III) show that, in numerous cases, e.g., samples E, C, A, several values were outside the range for pure products and were undoubtedly impure. In others, e.g., samples D, F, L, the only value lying outside the range was the manganese number (less than 6.00) and that alone led to a detection of the adulteration. In two samples (I, K) all values were within the pure product range but the manganese number (6.00), being at the lower limit of the range, suggested a possible adulteration. It is therefore evident that the manganese number is by far a safer criterion of the purity of a maple sap product than any of the other values.

In calculating the number of times the official methods have led to error with respect to the purity of the product, the following figures for each value were found.

Total ash:	80%	Alk. sol. ash:	70%
Soluble ash:	70	Ratio alk. sol./alk. ins. ash:	85
Insol. ash:	80	Malic acid value (Cowles):	45
Ratio sol./insol. ash:	75	Canadian lead number:	65
Alk. total ash:	65	Conductivity value:	65
Alk. insol. ash:	65	Manganese number:	10

TABLE III

COMPARISON OF ANALYTICAL VALUES OF PURE AND ADULTERATED MAPLE PRODUCTS

Values	Pure products*		Adulterated products									
			Samples									
	Min.	Max.	D	F	L	K	E	J	I	H	C	A
Total ash	0 56	1 70	1 18	0 96	0 99	0 76	0 61	0 70	0 92	1 10	1 65	0 71
Soluble ash	0 27	1 23	0 71	0 60	0 70	0 54	0 16	0 36	0 70	0 76	0 96	0 61
Insoluble ash	0 12	1 01	0 47	0 36	0 29	0 22	0 45	0 34	0 22	0 34	0 69	0 10
Ratio sol./insol. ash	0 43	4 07	1 51	1 67	2 41	2 45	0 36	1 06	3 18	2 24	1 25	6 10
Alkalinity-total ash	0 95	2 67	1 46	1 82	1 94	1 11	1 02	1 01	1 33	1 47	1 00	0 87
Alkalinity insol. ash	0 31	2 08	0 74	1 14	0 93	0 63	0 73	0 65	0 55	0 55	0 28	0 27
Alkalinity sol. ash	0 34	1 40	0 72	0 68	1 01	0 48	0 29	0 36	0 78	0 92	0 72	0 60
Ratio alk. sol./alk. insol. ash	0 21	2 29	0 97	0 60	1 09	0 76	0 40	0 55	1 42	1 67	2 57	2 22
Malic acid value (Cowles method)	0 21	1 82	0 40	0 61	0 66	0 38	0 31	0 32	0 27	0 23	0 14	0 17
Canadian lead number	1 74	7 55	2 99	4 82	5 10	3 21	2 77	2 79	3 32	2 85	1 19	2 00
Conductivity value	96 00	230 00	150 73	166 85	139 97	112 38	101 90	107 54	145 20	165 43	162 88	141 82
Manganese number	6 00	17 50	1 00	2 66	2 05	6 00	1 35	0 75	6 00	5 17	0	0
			B	G	C–120	B–3118	B–55035	C–134	C–142	C–130	C–119	C–118
Total ash	0 56	1 70	0 85	1 25	0 77	1 42	1 34	0 55	0 34	0 45	0 47	0 23
Soluble ash	0 27	1 23	0 75	0 68	0 24	0 96	0 84	0 31	0 26	0 13	0 25	0 20
Insoluble ash	0 12	1 01	0 10	0 57	0 53	0 46	0 50	0 24	0 08	0 32	0 21	0 03
Ratio sol./insol. ash	0 43	4 07	7 50	1 19	0 45	2 09	1 68	1 29	3 25	0 41	1 19	6 66
Alkalinity-total ash	0 95	2 67	0 97	1 72	0 60	1 14	1 13	0 68	0 47	0 68	0 50	0 24
Alkalinity insol. ash	0 31	2 08	0 30	1 30	0 46	0 17	0 15	0 22	0 33	0 44	0 34	0 16
Alkalinity sol. ash	0 34	1 40	0 67	0 42	0 14	0 97	0 98	0 46	0 14	0 24	0 16	0 08
Ratio alk. sol./alk. insol. ash	0 21	2 29	2 23	0 32	0 31	5 71	6 53	2 10	0 42	0 55	0 47	0 50
Malic acid value (Cowles method)	0 21	1 82	0 14	0 22	0 13	0 14	0 12	0 19	0 15	0 12	0 11	0 09
Canadian lead number	1 74	7 55	1 81	2 13	2 20	0 90	0 95	2 67	1 68	0 90	0 67	0 76
Conductivity value	96 00	230 00	167 38	91 11	93 79	157 71	152 01	82 06	78 04	65 73	83 30	44 61
Manganese number	6 00	17 50	0	0 50	0	0	0	0	0 50	0	0	0

* *Analytical values provided by Dr. J. F. Snell, Macdonald College, Faculty of Agriculture, McGill University.*

Conclusion

These investigations lead the writers to the conclusion that the present methods of analysis in evaluating the purity of maple products are far from being safe. This can be explained by the fact that the methods, as those for testing wine, butter, honey, etc., are based upon a range for each value. In many cases, it can be stated that the product has been adulterated, but it can never be stated, on a scientific basis, that the product is 100% pure.

It may be said, in conclusion, that it would be advisable to continue research work on analytical methods of testing maple products until one is found that determines with certainty the purity of the analyzed product. Then only will the problem of analyzing maple products be solved.

References

1. DELORME, J. Contribution No. 7 du Laboratoire de l'Ecole des Hautes Etudes Commerciales (Montreal). 1937.
2. RIOU, P. and DELORME, J. Compt. rend. 200 : 1132-1133. 1935.
3. RIOU, P. and DELORME, J. J. Assoc. Official Agr. Chem. 18 : 505. 1935.
4. RIOU, P. and DELORME, J. Compt. rend. 202 : 1941-1942. 1936.

THE SYSTEM NAPHTHALENE-*p*-NITROPHENOL: AN EXPERIMENTAL INVESTIGATION OF ALL THE VARIABLES IN AN EQUATION OF THE FREEZING POINT CURVE[1]

BY A. N. CAMPBELL[2] AND A. J. R. CAMPBELL[3]

Abstract

With the object of determining the factors responsible for the inapplicability of the ideal equation of the freezing curve,

$$\log_e x = Q/R(1/T_0 - 1/T),$$

a number of experimental determinations have been carried out on the system naphthalene–*p*-nitrophenol. These were: (i) specific heat, (ii) heat of fusion, (iii) heat of mixing, (iv) vapour pressure, (v) vapour composition, (vi) density, (vii) surface tension, (viii) viscosity.

The conclusion is arrived at that the discrepancy is due principally to the invalidity of Raoult's law in this case. Since the deviation is positive with respect to both components, it cannot be ascribed to compound formation in solution. Apart from the deviation from Raoult's law, the solution does not exhibit marked abnormality.

The data obtained also permit of the complete, or almost complete, construction of the *p–t–x* model for this system.

Introduction

An ideal equation, connecting the mole fraction with the depression of the freezing point over the whole range of the freezing point curve, has been given at various times (9):

$$\log_e x = Q/R\,.\,(1/T_0 - 1/T),$$

in which Q is the molar heat of fusion (as a first approximation) of the solid phase separating, and T_0 the freezing point of pure solid phase, in absolute degrees. The validity of the equation is unrestricted, if the solution be ideal. It results from this equation that if $\log_{10} x$ be plotted against $1/T$ a straight line should be obtained. According to Andrews and Johnston (1) this behaviour is quite frequently found with metallic systems, but in other cases, e.g., organic systems, this straight-line relation is rather rare. This being the case, it becomes of interest to enquire in what manner a given system deviates from the ideal. A lengthy theoretical discussion of this is given by Roozeboom (9). The absence of straight-line behaviour may be summarized as due to:— (i) inconstancy of Q; (ii) non-obedience to Raoult's law, i.e., the partial pressure does not vary with the mole fraction.

Only if the heat of mixing of the liquid components is zero, and if the heat of fusion is independent of temperature, is it possible to identify Q with the heat of fusion of the pure component separating from the melt. The heat of mixing is not usually zero and, moreover, it varies with concentration. The heat effect in question here is obviously that involved in the introduction of

[1] *Manuscript received in original form October 23, 1940, and as revised, January 3, 1941. Contribution from the Chemistry Department, University of Manitoba, Winnipeg, Man.*

[2] *Associate Professor of Chemistry.*

[3] *Wife of the senior author.*

a mole of solid component into an infinite quantity of the equilibrium liquid melt. Roozeboom (9) shows how this quantity can be obtained from a knowledge of the heat of fusion and the "differential heat of mixing". The effect of temperature on the heat of fusion over the relatively restricted temperature range of the present equilibrium diagram (39.5° C.) is not likely to be appreciable. Unfortunately, the integration of the above equation assumes a constant value of Q: it is not possible to introduce a variable Q into the equation in the above form. If, however, the heat of mixing is not zero, the ideal equation cannot be expected to apply.

Apart from the above source of deviation, the straight-line relation will also not be followed if Raoult's law is not obeyed. Of the two sources of discrepancy, the latter effect is likely to be much the more important.

The writers chose for investigation the system naphthalene–*p*-nitrophenol, since this is a simple system, showing only a eutectic unaccompanied by compound separation. The equilibrium diagram has been well established by different workers (6, p. 1291; 8). The quantities that are required to be known for the application of the ideal equation are the heats of fusion and the freezing temperatures (taking log x as the unknown). The writers determined, in addition to these quantities, the heats of mixing and, as a direct investigation of Raoult's law, the vapour pressures of several different mixtures. Since the latter study showed a marked deviation from Raoult's law, the writers were led to investigate the molar volumes, surface tensions, and viscosities of mixtures as a possible measure of their abnormality. There is no necessary connection between non-conformity with thermodynamically ideal behaviour and other physical properties, but the possibility at least exists that this non-conformity might be reflected as a non-adherence to additivity in the case of some other physical properties.

In addition, a few determinations of the composition of the vapour phase were made. The data obtained permit of the construction of the p t x model (excepting high pressure curves; cf. Roozeboom (9), the whole volume and diagrams at end) or, what amounts to the same thing, the p–x and p–t sections in addition to the conventional t-x diagram.

Experimental and Results

Materials Used

The naphthalene was obtained as pure from the Eastman Kodak Company. The *p*-nitrophenol was a "certified chemical" from British Drug Houses, and had a melting point of 114° C.*

Specific Heat of Solid p-Nitrophenol

As the heat of fusion was determined by the method of mixtures, it was necessary to know the specific heat of solid *p*-nitrophenol. This was determined by a method previously described (3). The value found was 0.248 ± 0.009 cal. per gm., this being a mean figure for the range 0 – 20° C

**All melting points are uncorrected.*

Heat of Fusion

This was determined by the method of mixtures. The heats of fusion of pure *p*-nitrophenol and of the eutectic mixture were obtained. About 100 gm. of substance, contained in a glass bulb, was kept in a fused condition in an electrically controlled thermostat at the temperatures of the respective melting points (114° and 73° C. respectively). The bulb, after attaining the temperature of the thermostat, was dropped into a jacketed calorimeter and the corrected temperature rise obtained in the usual way. The heat of fusion of pure *p*-nitrophenol was found to be 41.7 ± 1.0 cal. per gm., and that of the eutectic mixture, 37.0 ± 1.0 cal. per gm.

Heat of Mixing of the Liquid Components

The heat of fusion of the eutectic mixture (25.3% *p*-nitrophenol) calculated by the mixture rule from the heats of fusion of the components is 37.0 cal. per gm., i.e., identical with the experimental value within the limits of experimental error. Since, however, the experimental error is ± 1.0 cal. per gm., this merely means that the heat of mixing has a maximum value of ± 130 cal. per mole for the eutectic mixture. Subsequent direct experiment showed it to be somewhat larger than this and negative in sign.

Since the heat of mixing was small, it became necessary to determine it directly. This was done by introducing a weighed quantity of naphthalene or *p*-nitrophenol (about 100 gm.) into a Dewar flask which served as a calorimeter. This flask carried a Beckmann thermometer, a direct reading thermometer graduated in tenths of a degree, and a heating coil. The Dewar flask was immersed in a thermostat (containing "Paraffinol", a high-boiling, colourless petroleum product) at a temperature of 120° C. The contents of the Dewar flask was stirred with a fine stream of dry air passing through a copper heating coil in the thermostat and through thermometer tubing in the Dewar. A weighed quantity (about 20 gm.) of *p*-nitrophenol or of naphthalene was placed in a large test-tube, carrying a thermometer graduated in tenths of a degree, and kept in the thermostat. When temperature equilibrium was established, the contents of the test-tube was poured into the Dewar flask, and the temperature restored to its original value electrically.

TABLE I

HEAT OF MIXING

Final composition of mixture produced, mole fraction *p*-nitrophenol	Heat of mixing per mole of mixture, cal.	Final composition of mixture produced, mole fraction *p*-nitrophenol	Heat of mixing per mole of mixture, cal.
0.159	−200	0.812	−438
0.284	−350	0.657	−690
0.377	−470	0.563	−680
0.450	−560	0.493	−600
0.640	−700		

The results are contained in Table I. The negative sign indicates that heat is absorbed from the surroundings on mixing.

Vapour Pressures

Some of these were determined in a differential apparatus, some in an absolute apparatus. For solutions having vapour pressures greater than half that of pure naphthalene, a differential method is more accurate, for solutions with vapour pressure less than half that of pure naphthalene, and for pure *p*-nitrophenol, an absolute method is preferable. In the differential method, the mixture was placed in one of two flasks and pure naphthalene in the other; both flasks had the same volume and were connected by a U-shaped glass tube. The U-tube was connected by a short horizontal tube to a long vertical glass tube which in turn was connected at its upper end to a Hyvac pump: a manometer in the circuit showed that the pressure on this side was never greater than 10^{-1} mm. The lower limb, which had a length greater than 760 mm., was connected by pressure tubing to a mercury reservoir. All the limbs of the apparatus had a diameter of about 1 cm., to avoid capillary errors. An inverted bell-jar, filled with Paraffinol, which formed the heating bath, was heated electrically, stirred well, and illuminated from behind. It was not thermostatically controlled, measurements being taken with both rising and falling temperature. The great advantage of this simple apparatus is that it permits of the complete removal of dissolved and occluded gas. No traps were necessary in the pumping train since the vapour pressure, even of pure naphthalene, is almost zero at room temperature. The method of working was to exhaust the apparatus at room temperature, with the mercury level below the U-junction, then by raising the mercury to sever connection between the limbs. Heating was then begun and the difference of level in the limbs joining the two flasks measured with a cathetometer. After measurements had been carried to the highest temperature, the mercury was momentarily lowered to permit of the escape of any dissolved air that might have been evolved. Measurements were repeated with falling temperature. The whole process was then repeated until check determinations were obtained.

The method of operating the absolute apparatus, which was used only for pure *p*-nitrophenol and for mixtures containing 89.8% and 95.0% *p*-nitrophenol, was similar, except that pressures were read directly on the limb connecting with the pump, instead of by reference to the known vapour pressure of naphthalene in a second flask. It was found that mixtures rich in *p*-nitrophenol tended to give a small residual pressure at room temperature, after having been heated to a somewhat higher temperature than usual. This is no doubt due to a slow decomposition of the *p*-nitrophenol, which the writers observed to be appreciably rapid above 186° C. Measurements were therefore never taken above 120° except in the case of *p*-nitrophenol itself, where the smallness of the vapour pressure rendered this unavoidable. The results for pure *p*-nitrophenol are expressed in Table II. All figures are corrected for density and vapour pressure of mercury.

TABLE II

VAPOUR PRESSURES OF *p*-NITROPHENOL

Temp., °C.	Press., mm. Hg	Temp., °C.	Press., mm. Hg	Temp., °C.	Press., mm. Hg
120	0.60	130	0.93	142	1.91
146	2.24	149	2.82	150.5	3.17
153	3.47	156	3.81	157	4.27
162	5.63	165	6.92	168	7.59
169	8.71	177	12.62	182	15.2
184	17.4	186	18.7		

As an economy of space, the somewhat extensive tables giving the vapour pressures of mixtures are not presented here, but certain figures are utilised in the discussion.

Vapour Composition

A series of experiments were carried out at 120° C., a temperature at which all mixtures are completely liquid, to determine the composition of the vapour in equilibrium with different liquids. The liquid mixture was contained in a gas-washing bottle in the thermostat and air passed slowly, after purification and drying, through a copper worm in the thermostat, then through the mixture, then through absorption tubes packed with glass wool. Some of the tubes were on the surface of the thermostat and others immersed in ice-water, immediately outside the thermostat. After weighing the absorption tubes, they were extracted with ether, and nitrogen determined by the Kjeldahl method, the usual precautions being taken for presence of a nitro group. The results shown in Table III were obtained.

TABLE III

VAPOUR COMPOSITION

Composition of liquid mixture, % *p*-nitrophenol	Composition of vapour, % *p*-nitrophenol
73.0	2.00
89.8	4.32
95.0	12.4

Densities

The densities of liquid *p*-nitrophenol, of liquid naphthalene, and of mixtures of *p*-nitrophenol and naphthalene were determined at 117.3° C. The mixtures were prepared by weighing into stoppered flasks and melting in the thermostat. An Ostwald pyknometer was not used because of the difficulty of adjusting the liquid in the arms when the liquid solidifies immediately above the surface of the thermostat. An ordinary specific gravity bottle was employed. The

TABLE IV

DENSITIES

p-Nitrophenol, %	Mole fraction *p*-nitrophenol	$d_{4°}^{117.8°}$	Molar volume, cc.	*dV*	
				Cc.	%
0.00	0.00	0.9554	134.8	—	—
10.09	0.0937	0.9779	132.4	+0.04	+0.03
14.77	0.1376	0.9879	131.1	−0.02	−0.02
21.52	0.2015	1.007	129.3	+0.10	+0.07
27.54	0.2592	1.023	127.9	−0.05	−0.04
44.28	0.4226	1.070	124.0	+0.35	+0.28
48.38	0.4633	1.084	122.7	+0.11	+0.09
59.62	0.5762	1.121	119.8	+0.21	+0.18
66.49	0.6463	1.148	117.9	+0.16	+0.14
79.89	0.7854	1.195	114.4	+0.32	+0.28
89.71	0.8892	1.236	111.5	+0.17	+0.15
100.00	1.0000	1.282	108.4	—	—

results are given in Table IV. The density of *p*-nitrophenol is given by Hewitt and Winmill (4) as 1.2613 at 129.7° and 1.2329 at 162.5° C.

The experimental molecular volumes of liquid mixtures correspond very closely with those calculated from the mixture rule. There is, however, definitely a small expansion of not more than +0.4%, lying presumably, though not necessarily, at 50 mole per cent. Positive deviations from Raoult's law are usually, though not always, accompanied by an expansion in volume (5).

Surface Tension

The surface tension of *p*-nitrophenol and of mixtures was determined at 121° C. by the method of capillary rise, using naphthalene, for which the surface tension is known (International Critical Tables), as calibrating fluid. The capillary bore (0.353 mm.) was also checked by the mercury thread method. The results are given in Table V.

TABLE V

SURFACE TENSION

Composition of mixture, % *p*-nitrophenol	Mole fraction	Surface tension, dynes/cm.	Mol. surface energy, $\gamma(Mv)^{2/3}$
0.00	0.00	29.3	771
11.8	0.11	29.9	775
25.3	0.24	31.0	788
33.3	0.315	31.8	801
49.8	0.48	33.7	831
62.3	0.60	34.8	842
73.0	0.71	37.7	896
89.8	0.88	41.8	968
95.0	0.93	43.4	995
100.0	1.00	46.3	1053

When surface tension is plotted against composition in mole fraction, a smooth curve is obtained, convex to the axis of composition. A similar type of curve is obtained when molecular surface energy is plotted against mole fraction.

Viscosity

The viscosity at 121° C. was determined in an Ostwald viscometer, using naphthalene as calibrating fluid. The results are expressed in Table VI, which also gives the observed fluidities and those calculated from Bingham's rule (2): $\phi = m\phi_1 + n\phi_2$, where m and n are the volumes of the two liquids in unit volume of the mixture.

TABLE VI

VISCOSITY

Composition of mixture, % *p*-nitrophenol	Viscosity, centipoises	$\phi_{obs.}$	$\phi_{calc.}$
0.0	0.440*	2.270	—
11.8	0.478	2.090	2.095
25.3	0.600	1.670	1.894
33.3	0.750	1.335	1.761
49.8	1.055	0.946	1.471
62.3	1.350	0.742	0.235
73.0	1.615	0.619	1.011
89.8	2.045	0.489	0.639
100.0	2.560	0.391	—

* *International Critical Tables.*

When viscosity is plotted against mole fraction, the curve does not deviate greatly from a straight line, but it is still slightly convex to the axis of composition. The fluidities show a very marked deviation from Bingham's rule, the calculated values being much greater than the observed. On the other hand, the deviations from Egner's rule (7, p. 102), $\log \mu = x_1 \log \eta_1 + x_2 \log \eta_2$, are less and occur principally at the naphthalene end of the series.

TABLE VII

DEVIATION FROM EGNER'S RULE

p-nitrophenol, %	$\eta_{obs.}$	$\eta_{calc.}$	Deviation, %
11.8	0.478	0.535	+11.9
25.3	0.600	0.659	+ 9.85
33.3	0.750	0.767	+ 2.3
49.8	1.055	1.026	− 2.8
62.3	1.350	1.266	− 6.2
73.0	1.615	1.536	− 4.9
89.8	2.045	2.07	+ 1.2

Discussion of Results

For purposes of comparison, the equilibrium data of Rheinboldt (8) are reproduced in Table VIII, together with the values of $1000/T$ and of $\log_{10} . 100 N$, as calculated from the ideal equation on the simple assumption that Q is the heat of fusion of pure component. We take as the heat of fusion of naphthalene 35.6 cal. per gm. (International Critical Tables) and as the heat of fusion of *p*-nitrophenol 41.7 cal. per gm. (see Experimental Part). The heat of fusion was also calculated from the experimental values of temperature and mole fraction.

TABLE VIII

EQUILIBRIUM DATA—OBSERVED AND CALCULATED

Mixture No.	Per cent *p*-nitrophenol	T, ° Abs.	$\frac{1000}{T}$	$N_{exp.}$	$\log_{10} . 100N_{exp.}$	$\log_{10} . 100N_{calc.}$	Calc. heat of fusion, cal./gm.
Naphthalene separating							
1	0.00	353.5	2.83	1.00	2.00	2.00	—
2	11.8	250.0	2.86	0.89	1.949	1.972	64.0
3	25.3	346.5	2.89	0.762	1.882	1.943	73.4
Nitrophenol separating							
4	33.3	350	2.855	0.315	1.498	1.663	62.0
5	49.8	358	2.793	0.477	1.679	1.743	52.0
6	62.3	365	2.740	0.604	1.781	1.811	48.4
7	73.0	371	2.695	0.714	1.854	1.868	46.0
8	75.7	372	2.687	0.742	1.870	1.879	43.4
9	89.1	380.5	2.633	0.883	1.946	1.953	47.4
10	100.0	386	2.59	1.000	2.000	2.000	—

When $\log_{10} . 100 N_{exp.}$ is plotted against $1000/T$ the straight line relation is far from being obeyed, particularly on the *p*-nitrophenol side of the diagram.

Roozeboom (9) has given a graphical method whereby the differential heat of mixing can be obtained from the graph of the heat of mixing plotted against mole fraction of the mixture produced. This has been done in Fig. 1. By drawing tangents at the corresponding concentrations the differential heats of mixing are obtained. It is obvious at once that the differential heat of mixing for naphthalene separating is zero, and that, for *p*-nitrophenol separating, it has a constant value from 0 to about 50 mole per cent *p*-nitrophenol. The true heat effect involved is then obtained as the algebraic sum of the heat of fusion and the differential heat of mixing. These corrected values of Q cannot be introduced into the equation, because the integration of that equation assumed a constant Q, but it is of interest to compare this true, or corrected, heat effect with the simple molar heat of fusion. This has been done in Table IX for the mole fractions used by Rheinboldt.

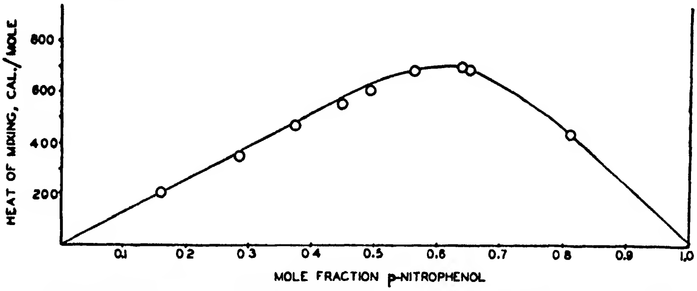

FIG. 1. *Relation between molar heat of mixing and mole fraction of p-nitrophenol.*

TABLE IX

DIFFERENTIAL HEAT OF MIXING

Per cent *p*-nitrophenol	Corrected heat effect, Cal./mole	Per cent *p*-nitrophenol	Corrected heat effect, Cal./mole
11.8	−4.56	62.3	−6.52
25.3 } Eutectic	−4.56	73.0	−5.93
25.3 } Eutectic	−7.10	75.7	−5.87
33.3	−7.10	89.1	−5.80
49.8	−7.10		

It is apparent from the above that, as far as the heat effect is concerned, the behaviour should be ideal along the naphthalene branch and along the *p*-nitrophenol branch from 100% *p*-nitrophenol to about 73% *p*-nitrophenol, the greatest deviation lying in the range 49.8 to 25.3% *p*-nitrophenol.

In regard to the vapour pressure measurements, when $\log_{10}p$ for pure *p*-nitrophenol is plotted against T in the form of the Clausius-Clapeyron equation, the following equation is obtained for the vapour pressure of liquid *p*-nitrophenol:—

$$\log_{10} p = \frac{-0.05223 \times 76500}{T} + 9.95$$

This equation can be used to calculate the vapour pressure at the melting point, and the temperature of the boiling point ($p = 760$). There is obtained:

$$p_{114°} = 0.396 \text{ mm.}$$

and

$$t_{p=760} = 294° \text{ C.}$$

The literature gives as the boiling point 279°, "with decomposition". Since the writers have found incipient decomposition to begin at 186°, this agreement is as good as could be expected. The vapour pressure up to 100° is low and this is in agreement with the fact that *o*- and *m*-nitrophenols can be separated from *p*-nitrophenol by steam distillation, the *p*-nitrophenol remaining behind.

Knowing the heat of fusion, an equation corresponding to the above can be derived for the sublimation curve. This equation is:—

$$\log_{10} p = \frac{-0.05223 \times 100800}{T} + 13.25$$

By means of these equations, the true partial pressure of the solid component can be determined along the freezing point curve and hence the mole fraction according to Raoult's law ($p' = np$) can be compared with that calculated from the weight composition. This has been done in Table X, in which p' means partial pressure (vapour pressure of solid component) and p the vapour pressure of the pure (supercooled) liquid at the equilibrium temperature. The corresponding equations for naphthalene are taken from the International Critical Tables. They are, for solid naphthalene:—

$$\log_{10} p = \frac{-0.05223 \times 71401}{T} + 11.45,$$

whereas for liquid naphthalene, the data of the International Critical Tables give rise to the following equation:—

$$\log_{10} p = \frac{-0.05223 \times 47700}{T} + 7.946.$$

The mole fraction calculated from Raoult's law ($n = p'/p$) is symbolized n' and that from the weight composition n. The temperatures are taken from Rheinboldt (8)

TABLE X

OBSERVED AND CALCULATED MOLE FRACTIONS

Temp., °C.		p	p'	n'	n
$C_{10}H_8$ separating	80.5	7.954	7.954	—	—
	77.0	6.746	6.31	0.937	0.882
Eutectic	73.5	5.84	5.02	0.86	0.747
	73.5	0.0252	0.00892	0.354	0.253
p-nitrophenol separating	77.0	0.0355	0.0178	0.503	0.315
	85.0	0.0563	0.0355	0.63	0.477
	92.0	0.100	0.0708	0.708	0.604
	98.0	0.148	0.118	0.797	0.714
	107.5	0.276	0.269	0.99	0.883
	113.0	0.399	0.399	1.000	1.000

The values of n' indicate a wide divergence from n. Raoult's law is not obeyed, the divergence being in the sense that both components are more volatile than is calculated from their mole fractions. Such behaviour cannot be accounted for on the basis of compound formation.

The vapour pressure data, in combination with the equilibrium-composition data of Rheinboldt and Kremann, have been utilized to construct Fig. 2, in which, against a common composition axis, are expressed (i) equilibrium temperatures (R and K), (ii) equilibrium pressures, and (iii) composition of the vapour phase. The data of (ii) are obtained from the vapour pressure measurements by a simple interpolation. The data of (iii) are obtained from (ii) knowing the vapour pressure of the solid phase separating. The complete data are assembled in Table XI.

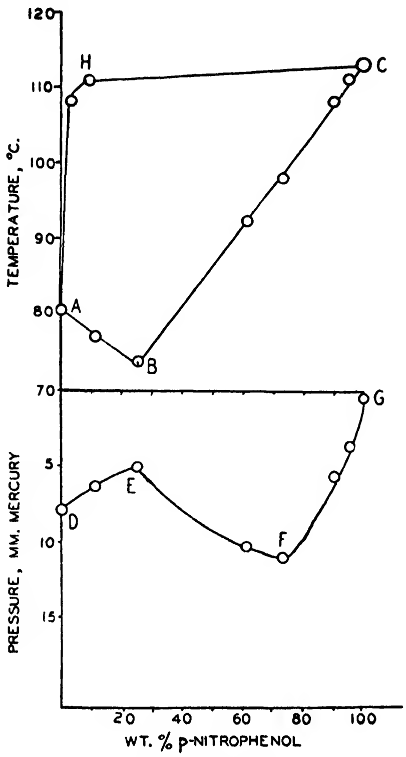

FIG. 2. *ABC—liquidus. DEFG—vapour pressure curve. AHC—vapour composition curve.*

TABLE XI

EQUILIBRIUM VAPOUR PRESSURE AND COMPOSITION

Per cent *p*-nitrophenol in liquid	T°, C.	Total pressure, mm.	Weight % *p*-nitrophenol in vapour
0.0	80.5	7.95	0.00
11.8	77	6.5	—
25.3	73.5	5.1	0.215
62.3	92	10.5	0.687
73.0	98	11.0	1.155
89.8	108	5.75	5.17
95.0	111	3.8	9.85
100.0	113	0.39	100.0

The form of the vapour pressure-composition graph is very uncertain, owing to the fact that an insufficient number of points were determined: the form indicated is a mere suggestion. It is, however, certain that both a maximum and a minimum must occur on the curve.

The vapour pressure figures were now combined with those for vapour composition to obtain Fig. 3. This is an isothermal for 120° C., giving vapour

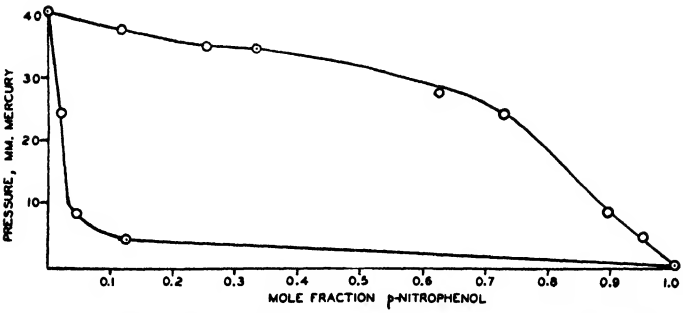

FIG. 3. *Relation between pressure and mole fraction of p-nitrophenol.*

pressures, total and partial, against liquid composition, as well as vapour composition. The data on which the figure is constructed, together with certain derived quantities, are given in Table XII.

TABLE XII

Composition of liquid, % *p*-nitrophenol	Total vapour pressure, mm.	Partial pressures		Mole fraction from liquid composition		Mole fraction from partial pressures	
		Naphthalene	*p*-Nitrophenol	Naphthalene	*p*-Nitro phenol	Naphthalene	*p*-Nitrophenol
0.00	40.8	40.8	—	1.00	0.00	1.00	0.00
11.8	37.6	37.4	0.20	0.89	0.11	0.915	0.33
25.3	35.1	34.8	0.30	0.76	0.26	0.85	0.50
33.3	34.7	34.3	0.30	0.68	0.32	0.84	0.50
62.3	27.4	26.9	0.5	0.40	0.60	0.66	0.83
73.0	24.2	23.7	0.5	0.29	0.71	0.58	0.83
89.8	8.5	8.0	0.5	0.12	0.88	0.20	0.83
95.0	4.7	4.1	0.6	0.06	0.94	0.10	1.00
100.0	0.6	0.0	0.6	0.00	1.00	0.00	1.00

The partial pressures are obtained from the vapour composition curve, after conversion to mole fractions. Scrutiny of the two preceding tables reveals that the molar fraction, both for naphthalene and for *p*-nitrophenol, calculated from the Raoult relation is always greater than that calculated from the liquid composition.

As a general summary, it may be said that the principal cause of non-adherence to the ideal equation of the freezing point curve is the deviation from Raoult's law. This deviation from Raoult's law is not, however, accompanied by any very marked abnormality in other physical properties, such as molecular volume, surface tension, and viscosity. It is perhaps connected with the difference in electric moment of the molecules of naphthalene and *p*-nitrophenol, and it is proposed subsequently to investigate this point.

References

1. ANDREWS, D. H. and JOHNSTON, J. J. Inst. Metals, 32 : 385-404. 1924.
2. BINGHAM, E. C. Fluidity and plasticity. McGraw-Hill Book Company, New York and London. 1922.
3. CAMPBELL, A. N. and CAMPBELL, A. J. R. J. Am. Chem. Soc. 62 : 291-297. 1940.
4. HEWITT, J. T. and WINMILL, T. F. J. Chem. Soc. 91 : 441-448. 1907.
5. HILDEBRAND, J. H. Solubility. 2nd Edition. Reinhold Publishing Company, New York. 1936.
6. KREMANN, R. Monatsh. 25 : 1215-1310. 1904.
7. MILLARD, E. B. Physical chemistry for colleges. 4th Edition. McGraw-Hill Book Company, New York and London. 1936.
8. RHEINBOLDT, H. J. prakt. Chem. 111 : 242-272. 1925.
9. ROOZEBOOM, B. Die heterogenen Gleichgewichte, 2 (1), pp. 267-328. F. Vieweg and Son. Braunschweig. 1904.

DETERMINATION OF T.N.T. (2,4,6-TRINITROTOLUENE) IN AIR[1]

By Kingsley Kay[2]

Abstract

A practical method for determining the concentration of T.N.T. in workroom atmospheres has been developed and has been given successful field tests. The accuracy of the method described is approximately ± 10%. The method is a comparative one, depending upon the red coloration produced when 2,4,6-trinitrotoluene in acetone is treated with a solution of sodium hydroxide in water. The stability of the coloration has been studied and the optimum conditions of temperature and concentrations of reactants have been determined. In addition the range of colour that allows the most accurate comparison has been evaluated. Minor refinements are at present in progress with a view to increasing the accuracy of the test.

Shortly after the beginning of the war, the Division of Industrial Hygiene of the Department of Pensions and National Health, Ottawa, was faced with the problem of supervising health conditions in plants manufacturing and handling T.N.T. (2,4,6-trinitrotoluene). In order that the control of environmental conditions as affecting health might be accomplished, it was necessary to have a means for determining the quantity of T.N.T. in workroom atmospheres. No safe limits for T.N.T. in air were established during the last war, mainly on account of the fact that no satisfactory method for determining this substance in air was developed at that time. This Division, therefore, set about developing a satisfactory method for determining T.N.T. in air that might be available for correlating clinical findings among workers with the concentrations of T.N.T. in the atmospheres in which exposure took place.

A search of the literature disclosed only two investigations in which methods of air analysis for T.N.T. were employed. In 1917, Moore (1) in England, reported analyses of factory air for T.N.T. dust and fumes by a method involving the bubbling of the contaminated air through water. The method required that the air be drawn through water for the full working day and the actual amount of T.N.T. weighed after evaporation of the absorbing liquid. His method gave no indication of the peaks of concentration during the course of a working day and, hence, it was necessary to develop a method of determination that would allow testing of the air over shorter periods, such as one-half to two hours. In connection with this method, it might be pointed out that the efficiency of extraction of T.N.T. from the air was proved by testing the glass tubing on the exit side of the liquid with alcoholic potash. The reaction of T.N.T. with alcoholic potash, which produces a red coloration, was not described. The source of the original observations in this connection has not been found. However, it would appear that this phenomenon was observed at least early in the large-scale production of commercial T.N.T.

[1] *Manuscript received January 4, 1941.*

Contribution from the Division of Industrial Hygiene, Department of Pensions and National Health, Ottawa, Canada.

[2] *Industrial Hygiene Engineer.*

Textbook descriptions of the washing of crude trinitrotoluene point out that attempts were made to wash the acids from T.N.T. with sodium hydroxide, as in the manufacture of nitroglycerine. This proved impracticable, owing to the action of alkali upon T.N.T. which produced dangerously sensitive products of decomposition.

Estimations of T.N.T. in air were also carried out by Phelps and Casselman in the United States and are referred to in a paper by Voegtlin, Hooper, and Johnson (2), published in 1922. No description of the method was given and it was not published elsewhere by these investigators.

However, recent communication with the United States Public Health Service has disclosed that Phelps and Casselman investigated two methods, and in addition that similar methods had been described by Elvove under a title "The detection and estimation of certain organic nitro compounds with special reference to the examination of the urine of T.N.T. workers" (J. Ind. Eng. Chem. 11, 861, 1919). The first method, dependent on the action of alkali on T.N.T., is similar to the method described in this paper. However, the present method, while employing a similar reaction, allows accurate detection of quantities of T.N.T. about five times as small. This is an important consideration in lowering air sampling times to suit modern levels of T.N.T. in workroom air.

Method

In the Industrial Hygiene Laboratory of the Department of Pensions and National Health, Ottawa, the reaction of T.N.T. with alkali was studied, with a view to developing it as a method of determination of T.N.T. in air. Crude T.N.T. provided by Canadian Industries, Limited, was purified by precipitation from hot alcohol and acetone, and purity of the 2,4,6-trinitrotoluene recovered was confirmed by melting point determinations. A standard solution of 2,4,6-trinitrotoluene in acetone (0.5000 gm. per 250 cc.) was made up, and the effects of various concentrations and amounts of sodium hydroxide in water and in alcohol on this test solution and dilutions made from it were studied.

Briefly, it was found that addition of 0.1 cc. of a 20% (by weight) solution of sodium hydroxide in water to 1 cc. of a solution of 2,4,6-trinitrotoluene in acetone produced the maximum red coloration in a series of dilutions made from the standard solution. The dilutions were made by adding acetone to the standard in various proportions, and ranged from 1 cc. of the standard in 500 cc. of acetone to 1 cc. of standard in 50 cc. of acetone. The test was conducted by first adding the sodium hydroxide solution to small 1.5 cc. test tubes. Thereafter, the T.N.T. solution was added, the tubes were inverted several times, and allowed to stand. Two phases, of course, were formed, the colour developing at the partition of the phases and migrating into the acetone phase.

The stability of the red coloration was studied and it was found that the colour developed within 10 min. at room temperature and was stable up to

30 min., after which time it gradually faded, leaving the sodium hydroxide phase orange in colour and the acetone phase almost colourless. Stability of the colour product decreased with increase of temperature, and, in the case of heating over a steam bath, the orange decomposition product was formed almost immediately. No investigations were conducted on the chemical constitution of this unstable colour compound. The shade of colour obtained was similar to that of phenolphthalein in solution. It was found that a measurable colour could be developed in acetone solutions of T.N.T. containing as little as 0.000004 gm. per cc.

Experiments were conducted for the purpose of determining the best range of colour over which comparisons might be made with accuracy. It was proved that several different subjects, with the naked eye, could differentiate colour produced in test solutions varying in concentration by ± 10% over the range 0.000004 gm. per cc. to 0.00004 gm. per cc. In order to determine the accuracy of the naked eye in comparison of these acetone dilutions of the standard, they were made up in tubes numbered on the bottom. The order of the tubes was destroyed and an attempt made to rearrange them in the correct order. No special efforts were made to standardize the lighting conditions under which the tests were carried out. The tubes were placed in line in a white test tube holder and were viewed in the daylight. In this manner the above-mentioned standard concentrations for colour comparison of unknown concentrations were established.

The accuracy of the method as described above can be regarded as sufficient for the purpose for which the test is required at the present time. Considerable study correlating clinical data with concentrations of T.N.T. in air will be necessary before it can be proved that variations of 10% in concentration can be regarded as significant from a health point of view.

In order to establish that the red colour was due to 2,4,6-trinitrotoluene rather than to impurities such as isomers of trinitrotoluene, dinitrotoluene, etc., in the standard material, a standard solution containing 0.500 gm. of crude T.N.T. in 250 cc. of acetone was made up, and various dilutions of this standard solution were treated with the hydroxide solution. Similar dilutions of pure 2,4,6-trinitrotoluene in acetone were prepared. No difference in colour was perceptible between comparable solutions prepared from the crude and pure materials. Hence, it would appear unlikely that the colour could be due to substances other than 2,4,6-trinitrotoluene. As further confirmation, it was found that in workroom tests in which air containing 2,4,6-trinitrotoluene was passed through acetone the same colour reaction and shade were obtained on treating the absorbing solution with base. In these experiments the likelihood that T.N.T. dust or vaporized impurities were present was remote, since the material was in the molten state and the impurities in the crude T.N.T. would not evaporate at the temperature of 82° C. which was maintained in the T.N.T. pots from which the vapour emanated.

Field Tests

In extending this method of testing to actual air analysis the procedure used was as follows:—

The air was drawn through a sintered glass bubbling tube containing approximately 150 cc. of acetone, at a rate of 0.5 litre per min. (measured by means of a standardized flowmeter), for a period of about one hour. Concomitantly, absorption was carried out using two bubbling tubes set up in series, drawing air from the same point in the room. This procedure eventually showed that one bubbling tube collected all the T.N.T. in a given volume of air.

The acetone solution containing the T.N.T. absorbed from the air was evaporated at a temperature well below 82° C. (to avoid the possibility of the loss of T.N.T., which melts and evaporates above 82° C.). As concentration continued, 1 cc. of the solution being concentrated was withdrawn and tested for the presence of T.N.T. in the manner previously described. This procedure was carried out in order that the concentration of the solution should not be increased by evaporation to such an extent that the reaction obtained with the base would result in a colour outside the range of colour of the standard solutions prepared for comparison.

The method has been employed in numerous plant tests and can be conducted with facility. However, experiments continue to be carried out with a view to cutting the absorption time from one hour to a shorter period. This absorption time, it may be mentioned, is, of course, a function of the concentration of T.N.T. in the air being tested, as enough T.N.T. must be absorbed to provide a concentration greater than 0.000004 gm. of T.N.T. in 1 cc. of concentrated solution. With a few preliminary tests a suitable absorption time can be set.

References

1. MOORE, B. Medical Research Committee, Great Britain. Special Report Series, No. 11. 1917.
2. VOEGTLIN, C., HOOPER, C. W., JOHNSON, J. M. J. Ind. Hyg. 3: 280-292. 1922.

Canadian Journal of Research

Issued by The National Research Council of Canada

VOL. 19, SEC. B. APRIL, 1941 NUMBER 4

A TRYPSIN-INHIBITING FRACTION OF ASCARIS[1]

By H. Bruce Collier[2]

Abstract

A crude extract of *Ascaris lumbricoides* strongly inhibits pepsin and trypsin but not papain; the extract shows no proteolytic activity. An active trypsin inhibitor was isolated by fractional precipitation. It is not precipitated by trichloracetic acid and has the properties of a polypeptide.

The inhibitor acts instantaneously on trypsin, exerting its maximum effect at neutral and acid reactions, with a minimum at pH 5. The effect of concentration suggests a reversible combination between enzyme and inhibitor. The inhibitor has no effect on papain, but stimulates peptic digestion.

Introduction

Weinland (18) in 1903 suggested that intestinal helminths produce anti-enzymes that protect them from attack by the digestive enzymes of the host. (Although the term 'anti-enzyme' has been current, it seems preferable to follow Northrop's usage and employ 'enzyme inhibitor' in order to avoid confusion with immunological phenomena.) Mendel and Blood (10) a few years later showed that extracts of Ascaris inhibited pepsin and trypsin but not papain.

The present investigation records an attempt to isolate the enzyme inhibitor of Ascaris. A trypsin-inhibiting fraction was obtained and partially purified; the very small yield made further purification impracticable. However, in view of the fact that the investigation is not being pursued further at the present time, it seemed worth while to record the methods employed and the general results obtained.

Sang (14) has recently prepared from Ascaris an extract that showed both inhibitory and proteolytic activity. Since he measured digestion by means of the formol titration, which is not specific for proteolysis, it is probable that the results were complicated by the presence of peptidases. Von Bonsdorff (4) prepared an extract that showed proteolytic activity but no inhibitory effect on pepsin, trypsin, or papain.

Trypsin inhibitors have been isolated from other sources: from egg-white by Balls and Swenson (2); from pancreas by Kunitz and Northrop (8); and from blood plasma by Schmitz (15). The preparation of a crystalline, specific inhibitor from pancreas removes any doubt that such 'anti-enzymes'

[1] *Manuscript received in original form, November 13, 1940, and as revised, January 3, 1941. Contribution from the Institute of Parasitology, McGill University, Macdonald College, Que., with financial assistance from the National Research Council of Canada.*

[2] *Lecturer.*

actually exist. It is interesting that these inhibitors from various sources all have somewhat similar properties.

Experimental

Methods

Crystalline pepsin was prepared from Merck's U.S.P. Pepsin by the method of Philpot (12). Commercial papain was partially purified by thrice repeated precipitation from aqueous solution by ethanol at a concentration of 55% by volume. Trypsin was prepared from active pancreatic extracts by the method of Northrop (11, p. 141). It failed to crystallize but had a specific activity, $[T.U.]_{mg.N.} = 0.07$, approaching that of crystalline trypsin.

Proteinase activity was measured by the elegant method of Anson (1), using a dialyzed solution of "Difco" Bacto-Haemoglobin as substrate, the concentration of the stock solutions being determined by iron estimations. This preparation was found to give a very low blank—only 0.0001 m.e. of tyrosine per 5 ml. of filtrate. The digestions were carried out for 10 min. at 37° C. but temperature corrections have been applied and the results converted to Anson units. The samples may be either centrifuged or filtered, after precipitation with trichloracetic acid. Filtration was found to give slightly higher values, using Whatman No. 2 paper, which contains a trace of chromogenic material extractable by the acid. ($N/5$ trichloracetic acid passed through the paper gave a colour value equal to 0.000016 m.e. of tyrosine per 5 ml.)

The colorimetric measurements were made in a Klett-Summerson photoelectric colorimeter, a Corning red filter No. 241 being used. The volumes employed were smaller than those recommended by Anson. Into a colorimeter tube were pipetted 1.5 ml. of trichloracetic acid filtrate, 3.0 ml. of 0.5 N sodium hydroxide, and 1.0 ml. of the Folin-Ciocalteu reagent, diluted three times. The method was standardized against pure tyrosine, estimated under identical conditions. Up to a tyrosine concentration of 0.0016 m.e. per 5 ml. there was a virtually linear relation between concentration and colorimeter reading, against a reagent blank.

Enzyme or buffer solutions must not be preserved with thymol, which reduces the reagent. Purified enzyme and inhibitor solutions give a virtually negligible blank, but with crude extracts the method of performing control determinations is of great importance. The blank values for substrate, enzyme, and inhibitor, determined separately, are greater than when enzyme and inhibitor are mixed, and substrate added, followed immediately by trichloracetic acid. The latter procedure was always adopted. Boiled enzyme controls also deviated considerably from the above. In each case the values for the appropriate blanks have been deducted from the published results, or more frequently, the blank tube was used in adjusting the colorimeter to zero reading.

Activity of Crude Ascaris Extracts

Live specimens of *Ascaris lumbricoides* were obtained from hogs (through the kind co-operation of Dr. E. Dufresne, Inspector-in-Charge, Wilsil, Ltd., Montreal), and were kept in normal saline at 37° C. until used. Preliminary tests were made for proteinase activity. The worms were dissected and body wall, ovaries, intestine, and oesophagus separately ground with sand and extracted with saline, the filtered extracts being tested for pepsin, trypsin, cathepsin, and papain. The ovary and gut showed traces of cathepsin activity, and the gut, traces of trypsin; the other tests were negative. In any case, the observed activities were not sufficient to interfere with the inhibition tests. In view of the proteolytic activity frequently reported by other workers, it was thought that the worms might contain a proteinase capable of digesting albumin or casein, but not haemoglobin. However, extracts of whole Ascaris had no effect on egg albumin at pH 5 or on casein at pH 6, using the colorimetric method. Nor did a concentrated inhibitor preparation digest casein at pH 4, as measured by 'tyrosine' and nitrogen determinations on the trichloracetic acid filtrate.

For tests of inhibitor activity, body walls of fresh worms were dissected out, washed in cold running water, ground with sand and extracted with 1% sodium chloride (100 ml. per 25 gm.) overnight in the presence of toluene. The extract was filtered, shaken with ether, separated and dialyzed. This yielded a pink, opalescent liquid containing much glycogen. Preliminary tests indicated that this extract strongly inhibited pepsin and trypsin, but had no effect on papain.

In the case of crystalline pepsin, 0.05 ml. of 0.005% solution was treated with Ascaris extract, in a total volume of 1.0 ml. at pH 2, for 15 min. at room temperature, then was allowed to act on haemoglobin. The results were as follows:—

Pepsin alone	1.15×10^{-4} P.U.	
plus 0·2 ml. extract	1·07	= 7% inhibition
0.6	0.36	= 69
1.0	0	= 100

One millilitre of extract, at pH 7, was added to 0.10 ml. of 0.01% trypsin, which after 15 min. at room temperature was allowed to act upon substrate:

Trypsin alone	2.35×10^{-4} T.U.	
plus extract	1.20	= 49% inhibition

Using 0.10 ml. of 0.125% papain, activated with potassium cyanide, and 1 ml. of extract, the following results were obtained:—

Papain alone	5.1×10^{-4} m.c. per ml.
plus extract	5.0

Purification of Inhibitor

Preliminary tests showed that the inhibitor in the crude extract was not affected by boiling nor by 2.5% trichloracetic acid. It was precipitated by 85% ethanol and by 0.7 saturated ammonium sulphate. As the inhibitor

seemed similar to that of Northrop (11, p. 135), his procedure was applied, with certain modifications.

Whole specimens of Ascaris were minced and extracted with 0.25 N sulphuric acid. Addition of ammonium sulphate to 0.3 saturation resulted in the precipitation of much inert protein, together with the pepsin inhibitor and some trypsin inhibitor. Addition of ammonium sulphate to 0.7 saturation gave a precipitate containing trypsin inhibitor and a large quantity of glycogen. Attempts to recover the pepsin inhibitor by reprecipitation resulted in complete loss of activity, and this phase of the investigation has not been pursued further.

For direct isolation of trypsin inhibitor the method has been simplified as follows. Several methods of mincing the worms were tried, the use of the Waring Blendor* having been found most convenient. The worms, being placed in 1% saline in the Blendor, are reduced in a few minutes to a fine suspension. This was autolyzed under toluene for several days, in the presence of a little diastase to insure removal of glycogen. Trichloracetic acid was then added to 2.5% concentration and the fluid was heated to 80 °C. for five minutes, then cooled and filtered. Treatment with charcoal removed the colour and the very disagreeable odour but did not affect the inhibitor. This extract was adjusted to pH 3.0 by addition of 5 N sodium hydroxide and was saturated with magnesium sulphate, which precipitated the inhibitor. The precipitate was filtered off by suction through hardened paper and was found to be a very active inhibitor. Since treatment of several kilograms of worms yielded only 300 mg. of moist precipitate at this stage, the purification was not carried further. The precipitate was dissolved in 3 ml. of water, giving a stock solution that contained 7.0 mg. of total nitrogen per ml. This was diluted tenfold for the following experiments.

Properties of Inhibitor

The inhibitor was not affected by boiling nor precipitated by 2.5% trichloracetic acid. It was precipitated by saturated magnesium sulphate and by 0.7 saturated ammonium sulphate. It gave a pink biuret test, positive Sakaguchi test for arginine, positive Millon's test, negative Molisch test, negative nitroprusside test for free or oxidized sulphydryl groups, negative Sullivan test (17) for guanidine, negative Lison's toluidine blue test (9) for sulphuric acid esters, negative lead acetate test for unoxidized sulphur.

Ferrocyanic, picric, and trichloracetic acids failed to precipitate the inhibitor. However, phosphotungstic acid gave a slight precipitate, and tannic acid a heavy one. Copper sulphate and mercuric chloride gave precipitates in slightly alkaline solution. The inhibitor has the properties of a proteose or polypeptide; it dialyzed only very slowly through cellophane.

* *Waring Corporation, 1697 Broadway, New York City. The Blendor is very useful for mincing and extracting animal tissues, suspended in a fluid medium.*

Effect on Papain

One millilitre of 0.025% papain, activated with potassium cyanide, was treated with 0.20 ml. of 1/10 inhibitor for 15 min. at room temperature, and the activity determined in the usual manner. No inhibition was apparent.

Papain alone	1.71×10^{-4} m.e. per 5 ml.
plus inhibitor	1.74

Effect on Pepsin

One millilitre of 0.001% pepsin was treated with 0.20 ml. of 1/10 inhibitor for 15 min. at room temperature, and the activity was determined. In one pair of tubes the pepsin was dissolved in 0.1 *N* hydrochloric acid; in another, in 0.1 *M* acetate buffer, pH 5.5. The results showed a strong stimulation of pepsin digestion by the inhibitor. This was not due to protection from destruction at the higher pH, as the results indicate. Nor was it due to action of pepsin on the inhibitor itself, as controls showed no increase in the blank values.

pH 1.1	Pepsin alone	0.75×10^{-4} P.U.
	plus inhibitor	1.30
pH 5.5	Pepsin alone	0.68
	plus inhibitor	0.90

Effect on Trypsin

The effect of time on trypsin inhibition was investigated as follows. To 1.00 ml. of 0.003% trypsin was added 0 05 ml. of 1/10 inhibitor, both being at pH 7. After a predetermined time at room temperature, substrate was added, and the activity determined. The results (Table I) indicate that maximum inhibition occurred at zero time, and that a prolonged interval slightly decreased the effect. The blank did not change with time.

TABLE I

EFFECT OF TIME INTERVAL ON TRYPSIN INHIBITION

	Activity, T.U. $\times 10^{1}$	Inhibition, %
Trypsin alone	3.32	0
Trypsin plus inhibitor, 0 min	1.05	68
Trypsin plus inhibitor, 10 min.	1.55	53
Trypsin plus inhibitor, 20 min.	1.57	53
Trypsin plus inhibitor, 30 min.	1.57	53

The effect of inhibitor concentration is illustrated in Table II. In each case, inhibitor was added to 0.10 ml. of 0.03% trypsin and the volume made up to 1.00 ml. After 10 min. at room temperature, the resultant activity was determined. The degree of inhibition does not vary directly as inhibitor concentration; this suggests an equilibrium between free trypsin, inhibitor, and the inhibitor-enzyme complex.

In investigating the effect of pH on inhibition, 0.10 ml. of 0.03% trypsin and 0.05 ml. of 1/10 inhibitor were added to 1 ml. of 0.1 *M* phosphate buffer

TABLE II

EFFECT OF CONCENTRATION ON TRYPSIN INHIBITION

	Activity, T.U. × 10^4	Inhibition, %
Trypsin	3.50	0
Trypsin plus 0.02 ml. inhibitor	2.60	26
Trypsin plus 0.05 ml. inhibitor	1.50	57
Trypsin plus 0.10 ml. inhibitor	0.70	80
Trypsin plus 0.20 ml. inhibitor	0.10	98

of the desired pH. After 10 min. at room temperature, the activity was determined. In each case, parallel controls without inhibitor were run to determine the effect of the reaction on the enzyme alone. In the tests at pH 1 and pH 3, immediately after addition of substrate sufficient alkali was added to neutralize the buffer. If the buffer were neutralized *before* the addition of substrate, the observed inhibition was somewhat less. The results (Table III) indicate that minimum inhibition occurred at pH 5. There was no evidence of a reversal of inhibition in strongly acid reaction, such as was observed by Northrop in the case of pancreas inhibitor.

TABLE III

EFFECT OF pH ON TRYPSIN INHIBITION

pH		Activity, T.U. × 10^4	Inhibition, %
1	Trypsin	3.17	
	Trypsin plus inhibitor	1.03	67
3	Trypsin	3.20	
	Trypsin plus inhibitor	1.50	53
5	Trypsin	3.23	
	Trypsin plus inhibitor	1.76	45
7	Trypsin	3.20	
	Trypsin plus inhibitor	0.84	74

Enzyme-inhibitor Interaction

The reactive 'tyrosine' and acid- and alkali-titratable groups of enzyme and inhibitor before and after mixing were determined, in the hope that any observed changes might throw light on the nature of the active groups involved. The observed changes were small, and since the inhibitor was not pure, probably are of little significance. There was found to be a small decrease in the acid- and alkali-titratable groups, and a very small increase in reactive 'tyrosine'. Exactly neutral solutions of enzyme and inhibitor showed no pH change on mixing.

In the course of these experiments it was observed that trypsin, treated with inhibitor, was no longer precipitable by trichloracetic acid, even on boiling. The precipitate given by phosphotungstic acid was appreciably less than that given by the separate components, whereas that given by tannic acid was not noticeably altered, nor was the precipitation by heavy metals affected. The complex resembles pepsin in not being precipitable by trichloracetic acid (2.5%), but showed no peptic activity. A solution of crystalline pepsin was no longer coagulated by boiling, after the addition of trypsin inhibitor.

Discussion

It has been demonstrated that crude extracts of Ascaris strongly inhibit pepsin and trypsin but have no effect on papain, thus confirming the results of previous workers. The extracts were devoid of proteinase activity. Ascaris probably cannot assimilate undigested protein, but it is surprising that cathepsin was not found in more than traces, for protein synthesis certainly takes place. Demonstration of strong proteinase activity by other workers may have been due to bacterial contamination or to the use of non-specific methods of estimation.

The trypsin inhibitor isolated from Ascaris has the properties of a proteose or polypeptide and is similar to the inhibitors that have been obtained from egg-white, pancreas, and blood plasma. Its function presumably is to protect the parasite from attack by the proteinases of the digestive tract of the host: there is no inhibitor for the papain-like enzymes, which are able to destroy live worms. This has been demonstrated by Robbins (13) with ficin, and with papain and bromelin by Berger and Asenjo (3). On the other hand, Burge and Burge (5) have found that *dead* parasites are digested by trypsin, so that the presence of inhibitor cannot be the only protective factor. Northrop (11, p. 14) has discussed the resistance of living tissue to digestion, and has concluded that permeability is an important factor.

The occurrence of inhibitors in various sources associated with the presence of trypsin suggests that this may be a general biological phenomenon; that is, the inhibitor may appear whenever living tissue is in contact with active enzyme. If the inhibitor is actually functional, and not accidental, and if the intestinal helminths have evolved from free-living forms, it is highly improbable that this mechanism has arisen *de novo*, but more likely that it is an adaptation of an already existent physiological mechanism.

It has been assumed that the inhibitor can diffuse from the worm into the gut of the host. Stewart (16) concluded that protein digestion by the host is thus inhibited, but gave no evidence that the inhibitor is actually excreted by the parasite. Sang (14) found that a living worm inhibited a tryptic digest of casein, but he did not eliminate the possibility of pH change due to production of organic acids. The author observed that living Ascaris imparted an antitryptic effect to saline, tested after neutralization, but it is not known whether the specific inhibitor was responsible.

The mode of action of the trypsin inhibitor is a problem of great theoretical interest, but the examination of a relatively impure preparation cannot shed much light on the actual mechanism of inhibition. However, it seems worth recording that when enzyme and inhibitor combine there is a decrease in acid- and alkali-titratable groups, and a small increase in reactive 'tyrosine'. This may possibly be related to the increase in 'tyrosine' during protein digestion.

The properties of the inhibitor are somewhat different from those observed by Northrop with his pancreatic preparation, in that minimum inhibition takes place at pH 5, being greater at pH 1 and pH 7; further, the reaction appears to be instantaneous. Horwitt (7) has pointed out that trypsin is inhibited by acid substances, as heparin, and by certain basic dyes; it is possible that the Ascaris inhibitor may be either an acid or a basic peptide. (Herriott's (6) pepsin inhibitor appears to be a strongly basic peptide.) Since the trypsin-inhibitor complex resembles pepsin in its precipitation properties, the complex may be a more acid protein than trypsin itself, and the inhibitor an acid peptide.

References

1. Anson, M. L. J. Gen. Physiol. 22 : 79-89. 1938.
2. Balls, A. K. and Swenson, T. L. J. Biol. Chem. 106 : 409-419. 1934.
3. Berger, J. and Asenjo, C. F. Science, 90 : 299-300. 1939. Science, 91 : 387-388. 1940.
4. Bonsdorff, B. von. Acta Med. Scand. 100 : 459-482. 1939.
5. Burge, W. E. and Burge, E. L. J. Parasitol. 1 : 179-183. 1915.
6. Herriott, R. M. Cold Springs Harbor Symposia on Quantitative Biology, 6 : 318-324. 1938.
7. Horwitt, M. K. Science, 92 : 89-90. 1940.
8. Kunitz, M. and Northrop, J. H. J. Gen. Physiol. 19 : 991-1007. 1936.
9. Lison, L. Compt. rend. soc. biol. 118 : 821-824. 1935.
10. Mendel, L. B. and Blood, A. F. J. Biol. Chem. 8 : 177-213. 1910.
11. Northrop, J. H. Crystalline enzymes. Columbia University Press, New York. 1939.
12. Philpot, J. St. L. Biochem. J. 29 : 2458-2464. 1935.
13. Robbins, B. H. J. Biol. Chem. 87 : 251-257. 1930.
14. Sang, J. H. Parasitology, 30 : 141-155. 1938.
15. Schmitz, A. Z. physiol. Chem. 255 : 234-240. 1938.
16. Stewart, J. Rept. Inst. Anim. Path. Univ. Camb. 3 : 77-86. 1932–3.
17. Sullivan, M. X. Proc. Soc. Exptl. Biol. Med. 33 : 106-108. 1935.
18. Weinland, E. Z. Biol. 44 : 1-15. 1903.

FACTORS AFFECTING THE PETT VISUAL TEST FOR VITAMIN A DEFICIENCY[1]

By L. B. Pett[2] and Marian K. Lipkind[3]

Abstract

Under the conditions prescribed for the Pett test, which is described, it has been found that: (i) antecedent light does not affect the median of the three tests usually performed; (ii) no error results from the wearing or not wearing of glasses; (ii) the use of pilocarpine to contract the pupils is not advisable; (iv) some light may be admitted into the test room; (v) the time of exposure to the bright light (30 sec.) is suitable; (vi) repeated tests cause a 'learning' effect so rarely as to be of little concern; (vii) the standard error of the mean is ± 1.4 and of the median is ± 2.4 sec. Some results are presented suggesting that a diurnal rhythm in the vitamin A content of the blood exists.

Introduction

The last ten years of vitamin research have suggested the importance of accurate tests for vitamin deficiencies in human beings, in order to facilitate the application of results obtained in animal experimentation. Such tests are also important because recent research tends to show that slight deficiencies of vitamins, often called 'subclinical', may be the causes of various vague ills of mankind. This paper reviews some details of a rapid visual test for vitamin A deficiency, and presents new information on factors that may affect it. The paper might be considered No. 4 of a series.

Many factors affect visual tests for vitamin A deficiency. The importance of studying these factors has been emphasized in recent papers by Harris and Abbasy (2, 3), and by Thomson *et al.* (8, 9). The latter give detailed accounts of investigations with a somewhat limited number of subjects, using certain methods, followed by sweeping generalizations. Of all the methods for detecting vitamin A deficiency, the Pett test is the simplest and most rapid, and is the only test correlated with blood analyses. Since it was not included in the study made by Thomson *et al.* (8, 9), a similar but more extensive study of influencing factors is here reported.

Numerous tests for night blindness, dark adaptation, etc., have been described and are reviewed by Pett (6). Several of these tests have been studied in regard to influencing factors, and several seem to fail in the most important factor, one that should influence all tests purporting to measure vitamin A deficiency, namely, the actual relationship of vitamin A therapy to the test.

[1] *Manuscript received in original form September 30, 1940, and as revised, January 13, 1941.*
Contribution from the Department of Biochemistry of the University of Alberta, Edmonton, Alta., assisted from a grant to Prof. G. Hunter from the Associate Committee on Medical Research of the National Research Council. Part of this work was included in a thesis for the degree of Master of Science in the University of Alberta.

[2] *Lecturer in Biochemistry.*

[3] *Research Assistant, 1939–40.*

It has been shown (5, 6, 7) that the testing of hundreds of people for vitamin A deficiency permits construction of a frequency distribution graph. The importance of such a graph was first emphasized by Pett (6). Part of this graph represents people deficient in vitamin A, and the dividing line can be decided only by selecting some as "deficient", administering vitamin A, and finding whether the test shows a difference or change toward the "normal" end of the curve. Pett (6) reported 200 serial cases classified as "deficient", who responded to vitamin A therapy. Since that publication many hundreds more have shown the same result, thus proving that the Pett instrument (now called the Vitometer) responds to vitamin A therapy of "deficient" individuals. Correlation with actual blood analyses for vitamin A has also been reported (7). These two important factors are frequently lost sight of in the discussions of other instruments and the accuracy with which they measure 'subnormal dark adaptation', etc.

The following factors are discussed in the present paper: the effects (i) of antecedent light, (ii) of wearing or not wearing glasses, (iii) of contracting the pupil with pilocarpine, (iv) of the lightness of the test room, (v) of the duration of exposure to bright light, (vi) of repeated tests in causing "learning", and (vii) the variability to be expected in different tests on one person. In addition some results are presented suggesting the possibility of a diurnal rhythm in the vitamin A content of the blood.

Experimental Procedure

It is supposed that the recovery of vision after blinding by a bright light depends on a re-formation of the retinal visual purple from vitamin A. Since 1865 many means have been used for studying this general process, and many of them are very complicated. Since the relationship to vitamin A became clearer, numerous tests have been suggested. The conditions embodied in the Vitometer were arranged after many variations had been tried by actual experimentation on many subjects. The resulting test has a simplicity and rapidity of definite advantage, and an accuracy sufficient for most purposes. The following extracts from Pett (6) will serve to describe the apparatus:

"*Description of Apparatus*—The instrument here outlined consists of a black metal (or wooden) box, about 1 cubic foot in volume. Protruding from the front is a headpiece, and on the back are various instruments. Inside the box are: (1) a source of bright white light for bleaching visual purple in the eyes, coming from either one or several bulbs. (2) A surface for reflecting this bright light into the eyes, while looking into the headpiece, such that 50 foot-candles is the intensity at the eyes; the bright light is connected to a voltmeter and rheostat, and each instrument is calibrated by a photometer to operate at a certain voltage; the reflecting surface is paper (English Cartridge Paper, 100 pounds), is 12 inches square, and covers a metal shield from which two rectangles are cut out. (3) Behind the metal shield is a dim light, so placed as to shine evenly through the two rectangles. In passing through the paper this light loses 90 per cent of its intensity and at

the eye has an intensity of about 4 millifoot-candles, and is slightly reddish. A mechanical device controlled from the back of the box is used to cover one of the rectangles of dim light, while the other remains visible, the subject then having to distinguish between vertical and horizontal directions.

"*Description of a Test*—The subject adjusts his head comfortably against the rubber forehead rest, wearing glasses if they are usually worn, and is shown the rectangles of dim light, one "Up", one "Across". The bright light is put on, and he is asked to look at a black spot marking the position where the bar of dim light will later appear when the bright light goes out. During this period of thirty seconds, the name, date, etc., can be recorded on a card and the voltage checked. As the watch hand crosses thirty seconds the bright light is turned off and the subject reminded to say "Up" or "Across," indicating the direction of the rectangle seen, as soon as the direction can be made out. The time is noted when this is said, and represents the recovery time from thirty seconds of standard bright light.

"Tests are repeated at minute intervals, three usually sufficing. In some cases the three values may be rather divergent, especially when the first value is long. It is then considered more accurate to use the median or midvalue, rather than the mean; e.g., of three values 23, 15, 16, use 16 rather than 18. The range of recovery times is from three to sixty seconds, with a mode at eight. Thirty to forty persons an hour have been tested by one operator with one instrument.

"*Discussion of Apparatus*—Previous investigations in this field have been hampered by instruments too slow and complicated to permit the testing and retesting of large numbers of people, thereby lacking statistical weight for their findings. Hence the insistence on a test that would be rapid and simple. Every step in the development of this design was tested on numerous subjects not for the accuracy with which it would show new laws of optic physiology, but rather for the avoidance of complications in practice when testing for vitamin A deficiency. Repeated tests were made on each person at each stage, permitting calculations of means, and their standard errors, thus giving mathematical assurance of the validity of every modification. The result is a nice balance, obtained by experimentation of numerous factors, including the colour, duration and intensity of the bright light, the size, colour, duration, and intensity of the dim light, and the area and location of the retina affected and other points.

"Reflection of the bright light from paper makes it more diffuse than reflection from or transmission through glass. Diffusion of the light helps to avoid the afterglow in the eyes from bright spots of light that causes some confusion otherwise. Confusion may also be lessened by having the outer edges of the reflecting surface actually, but not apparently, brighter than the center where the dim light is to be seen. This is done by having a circle of lights for bright illumination.

"Having the dim light in the form of a small rectangle which may be vertical or horizontal gives a more constant recovery time and eliminates guessing

which is common in children. A suitable size was found that would be independent of astigmatism in the subject. Glasses are worn, if they are usually worn, only for the sake of speed, since no effect of removing them has been found, even in extreme myopia and hyperopia. There must, of course, be light transmission and perception. The terms "Up" and "Across" are used because they are much more familiar to the average subject and much faster than any others tried.

"Since the standard error of the mean has been found to be about one second for many people, checks are required only within about one second, and the "reaction times" of subject and operator are unimportant. A practice effect—tests gradually getting shorter— has sometimes been observed if more than three tests were made at one-minute intervals, but if the interval was lengthened to five or ten minutes this effect disappeared."

Results

1. *Effects of Antecedent Light*

Thomson *et al.* (8, 9) have criticized all visual tests of vitamin A deficiency in regard to inadequate consideration of the effects of previous exposure to light. They consider that the eyes must be fully dark adapted; this requires at least 15 min. in the dark. They report a pronounced effect on their tests if this procedure is not carried out. Since their tests required another 15 or 20 min. to perform, it was not usual to do several tests on one individual. The design of the Pett apparatus permits several tests in a short space of time (three tests in five minutes), giving some mathematical reliability to the results. This procedure is not only easier on patient and operator, but obviates the necessity of trying to achieve the somewhat illusory 'perfect' dark adaptation.

Tables I and II show that this approach overcomes any difficulty from antecedent light. Although the first of the prescribed three tests may be longer than normal (in about one-third of the cases) the subsequent tests are usually uniform. It is not suggested that the eyes after the first test are in

TABLE I

THE EFFECTS OF PREVIOUS EXPOSURE TO LIGHT ON THE TEST FOR VITAMIN A DEFICIENCY

Figures give recovery times in seconds. Three tests were done at one minute intervals, and the median is the value used

Subject	Ordinary tests		Tests after looking at a 1000 watt lamp for:							
			2 min.		5 min.		15 min.		30 min.	
		Med.		Med.		Med.		Med.		Med.
G.A.L.	8, 6, 6	6	8, 6, 5	6	–	–	9, 6, 5	6	–	–
L.B.P.	6, 6	6	7, 6, 7	7	–	–	7, 7, 6	7	–	–
F.H.I.	11, 7, 6	7	–	–	5, 6, 7	6	–	–	9, 7, 6	7
J.A.N.	7, 9, 10	9	–	–	13, 6, 7	7	–	–	–	–
R.C.	4, 6, 6	6	–	–	–	–	–	–	8, 6, 6	6
P.B.	11, 9, 9	9	12, 10, 9	10	–	–	13, 9, 9	9	–	–

TABLE II

THE EFFECTS ON THE TEST OF VARIOUS AMOUNTS OF SUNLIGHT

The median of three tests, expressed in seconds, is used

Subject	Ordinary tests		Tests after exposure to:					
			Bright sunlight		Bright sun on snow		Late afternoon sun, about 1000 ft.-c.	
		Med.		Med.		Med.		Med.
L.B.P.	9, 8, 8	8	9, 8, 10	9	21, 8, 8	8	8, 7, 7	7
D.S	12, 14, 13	13	13, 14, 15	14	18, 15, 15	15	–	–
M.L.	13, 11, 10	11	19, 11, 8	11	–	–	–	–

a physiologically constant condition (if such can ever be), but they are in a sufficiently standard condition to give reproducible results, correlated with vitamin A (7). It will be seen in the tables that the median for a given subject remains constant, within the accuracy expected of the method, regardless of the previous exposure to light.

2. *Effects of Wearing Glasses*

Subjects who enter the test room wearing glasses are told to leave them on, unless they are tinted, since this saves time and avoids the danger of breaking them by leaving them exposed. Most people who wear glasses all the time require a moment's adjustment after removing them. Following this period the Pett test has been found to be the same as before removing the glasses.

TABLE III

THE RECOVERY TIMES OF PERSONS BEFORE AND AFTER REMOVING GLASSES

Median of three tests is given in seconds

	T.R.	R.H.	B.P.	H.W.	A.N.	S.L.	E.L.	J.Mc.	L.F.	A.L.	J.C.	E.P.	J.G.
On	5	8	9	10	10	10	11	11	12	13	17	21	27
Off	6	7	8	10	11	9	10	12	10	11	19	18	27

The results in Table III show clearly that leaving the glasses on does not affect the test seriously. More than 50 persons have been tested in this way, and the conclusion may be drawn that this test is not appreciably affected by myopia, hyperopia, or astigmatism.

3. *Effects of Contracting the Pupils*

Feldman (1) has advocated the use of pilocarpine before a test. Table IV shows our results using this procedure.

In this experiment the subjects had some distress in becoming accustomed to their condition. Although this feeling wore off before the effects of the

drug wore off, it is clear from the table that a great prolongation of the recovery time was caused. In addition great variation in the results was observed. The procedure is therefore considered unsatisfactory.

TABLE IV

RECOVERY TIMES OF SIX PERSONS BEFORE, AND ONE OR TWO HOURS AFTER, THE ADMINISTRATION OF TWO DROPS OF 1% PILOCARPINE NITRATE

Subject	Normal test	Test 1 hour after	Test 2 hours after
A.L.	12	45	16
W.D.	12	57	24
M.P.	6	18	11
B.P.	9	77	32
P.B.	16	80	33
M.L.	9	24	18

4. *Lightness of the Test Room*

The possibility that extraneous light would bother the subject and affect the results of the test has been suggested by all investigators, but no systematic study has been reported. The custom is to use a completely dark room, but in practice this is not always convenient. The Pett apparatus (6) introduced one advantageous procedure by incorporating the bright light within itself, so that the subject's head is in the head-piece all the time.

Stress was also laid on the use of an area of bright light large enough to affect a suitable area of retina, and on the need for uniformity of light over this area. These points have since been emphasized by Thomson (8, 9).

TABLE V

THE RECOVERY TIMES (MEDIAN OF THREE TESTS) OF PERSONS TESTED WITH SIX DIFFERENT LIGHT INTENSITIES IN THE TEST ROOM

Subject	Amount of light, outside the head-piece, in foot-candles					
	Dark	1½	2	4	5	6
T.R.	5	7	7	7	6	5
M.P.	6	8	8	8	7	8
A.L.	7	6	11	11	10	11
R.C.	8	11	12	10	9	7
E.L.	8	10	17	8	11	10
J.C.	10	12	10	11	13	14
A.W.	10	7	10	10	8	9
M.H.	10	9	9	12	9	11
M.P.	12	12	12	12	13	12
V.D.	12	10	12	9	9	9
J.J.	15	17	13	12	14	18
M.L.	14	16	13	20	15	15
D.B.	14	15	13	17	10	19
B.F.	20	26	23	24	27	25
M.M.	24	17	22	21	22	21

Table V shows the effects of varying the amount of light in the test room on the recovery times of various persons. The light in the room is expressed in terms of foot-candles at the head-piece of the apparatus, which is placed so that no bright light, direct or reflected, comes from behind the subject.

The table shows that great variation was found from one person to another in the effect of light in the test room, some cases showing a marked lengthening of the test. Nevertheless, some light may safely be admitted into the room. This amount of light is taken as 1½ ft.-c. at the head-piece, and corresponds to the light from a 200 w. frosted lamp at a distance of about 15 feet. Table lamps can be used in suitable positions in the room, without materially altering this value. Since some people are bothered, even by this much light, routine testing should be carried out in a corner as obscure as convenient.

5. *Effects of Time of Exposure to the Bright Light*

Different workers use different intensities of bright light (not always clearly stated) and also different times of exposure to the light. A great deal of work was done in this connection in evolving the Pett apparatus, but only one interesting point will be mentioned here.

Twenty persons were used in an experiment in which three tests were given at each of 10 different exposure times, varying from 5 to 60 sec. Typical curves for three persons are given in Fig. 1.

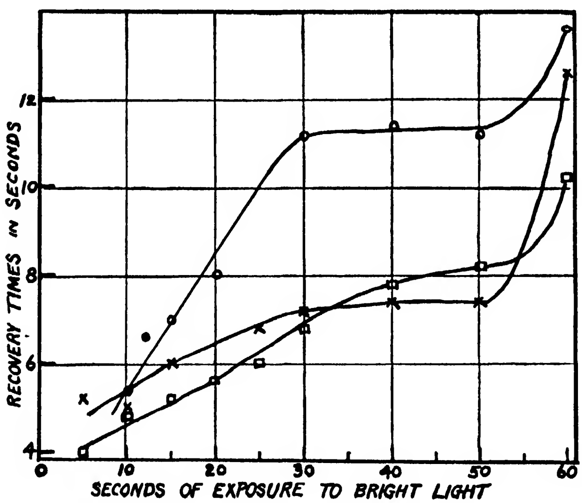

FIG. 1.

It will be seen in Fig. 1 that each curve has a flattened part (or constant Recovery Time) for a range of about 30 to 50 sec. exposure. The flat part of the curve varies slightly with each individual, and at different times with the same individual. A similar result was found when the time was held constant and the brightness of the light varied. Within the range of this flat part easily reproducible measurements can be made, and the recovery

times of all 20 people studied could be safely measured with the 30 sec. exposure prescribed for the test. Some evidence was found that the curve again flattens out with much brighter lights or longer exposure times. Restlessness and fatigue of the subjects are more marked when looking at the bright light more than one minute, or at very bright lights, so these are not considered suitable conditions for this test.

6. Practice Effects

The important possibility of people becoming so acquainted with the test that the results show improvement without dietary cause has received only slight attention. In actual practice, where it is desired to follow the course of treatment by repeated tests, such a 'learning' effect might lead to erroneous conclusions. With rapid tests, repeated testing is encouraged, and consequently extensive investigation of the possibility of "learning" has been carried out with the Pett test.

Careful examination by one of the writers (L. B. P.) of the last three years' results, during which nearly 4,000 persons have been tested, did not show much suggestion of practice effects. More than 500 persons have had many repeated tests without showing a "learning" effect. In addition some experiments have been designed especially to elucidate this point.

A group of 17 persons received 15 tests each, with only one minute interval between tests. One person showed a significant practice effect, i.e., the first few recovery times gradually became shorter until a significantly lower level was reached. Lengthening the interval between tests to two minutes removed this effect.

A different group of 25 persons, never before tested, received a single test daily (not the prescribed three tests) for 21 days. Of the 25, 11 persons showed learning curves. Thus with one observation only learning may be a disturbing factor in certain cases, but the procedure prescribed for this test, requiring three tests, successfully guards against this error.

7. Dispersion or Variability of Tests on One Person

The arithmetical mean (or median) of two or more figures represents those figures with a degree of accuracy depending on how much the figures differ from each other, and from the mean or median. The usual measure of such dispersion is the standard deviation:

$$\sigma = \sqrt{\frac{\Sigma\ (d^2)}{n-1}}\ .$$

This deviation marks off a distance above and below the mean or median, making its accuracy comparable with other similarly calculated means. The standard error of the mean (or median) expresses the limits within which will fall any future mean (or median) of the same experiment, no matter how many times the experiment is repeated. It is the result of dividing the standard deviation of the observations by the square root of the number of observations.

The latter calculation was carried out on every twentieth card in the writers' files, until 100 had been done. Table VI summarizes some statistical information resulting. It will be seen that the most likely deviation is 0.9 if the mean is used, and 1.7 if the median is used. The use of the median was recommended by Pett (6) owing to convenience. Actually in more than half the cases it gives just as great accuracy as using the mean, even though the above figures show a greater error. This means that observations within two seconds of each other are satisfactory. It may be noted that with recovery times of more than 20 sec. the variation is greater, but the percentage error remains about the same.

TABLE VI

STANDARD ERRORS OF THE MEAN (OR MEDIAN) OF THE PRESCRIBED THREE TESTS ON EACH OF 100 PERSONS, TAKEN AT RANDOM FROM 2,000 CASES

The figures are in seconds

Of three tests	Range of deviations		Mean of deviations	Mode of deviations
	Low	High		
Means	±0	±4.4	±1 4	±0 9
Medians	±0	±8.9	±2.4	±1.7

8. *Possibility of a Diurnal Rhythm*

Since vitamin A storage is most marked in the liver, some functional role of this organ in vitamin A metabolism might be suspected. The liver is believed by some (4) to change in activity at different times of day, in releasing bile and sugar, so it seemed possible that vitamin A might be similarly affected. If changes during the day in the vitamin A content of the blood, reflected in a visual test, were large, they might be an important factor in deciding when such visual tests should be done. Since this test has been correlated with blood analysis (7) it may be taken as an indication of the blood level. Tests were therefore done at intervals during the day. These are summarized in Table VII. Table VII shows that in non-fasting persons the tests varied from one time of day to another. Great individual variation was found, but a tendency may be noted to show low values in the early morning, increasing to a peak late in the morning, and decreasing again. These data are suggestive but not conclusive. The idea of a change during the day receives support from the results on a fasting person (L. B. P.) also shown in Table VII. In this case the values were low in the early morning (indicating high blood vitamin A), high at 11 a.m., decreased to 7 p.m., increased and later decreased again. These figures are averages of five tests at each time. The standard error of the differences between any two figures in this fasting experiment is ±0.25, so most of the differences are significant. (i.e., more than twice the standard error). These results are not subject to the influences of current food intake or exercise, but they cannot be taken

as conclusive until more tests are made. There is, however, a definite suggestion of a diurnal rhythm of vitamin A in the blood.

TABLE VII

RECOVERY TIMES (IN SECONDS) AT INTERVALS DURING THE DAY OF *(a)* A FASTING PERSON, AND *(b)* SEVERAL PERSONS NOT FASTING

Longer times mean lower vitamin A

Time of day	Fasting	Not fasting						
		1	2	3	4	5	6	7
8 a.m.	5.8	–	–	–	–	–	–	–
9 a.m.	5.6	20	8	7	12	4	14	10
10 a.m.	7.4	24	12	7	16	5	11	13
11 a.m.	7.5	34	12	10	10	6	14	14
12 noon	7.2	24	11	14	11	6	13	15
1 p.m.	6.8	–	–	–	–	–	–	–
2 p.m.	7.6	29	9	8	11	6	13	13
3 p.m.	7.2	29	9	12	13	5	13	11
4 p.m.	6.7	25	7	15	12	6	16	13
5 p.m.	6.8	25	6	11	8	4	12	12
6 p.m.	6.5							
7 p.m.	6.3							
8 p.m.	7.1							
9 p.m.	7.2							
11 p.m.	6.5							
8 a.m.	6.0							

References

1. FELDMAN, J. B. *in* Nutrition: The newer diagnostic methods. The Milbank Memorial Fund. New York. 1938.
2. HARRIS, L. J. and ABBASY, M. A. Lancet, 237 : 1299-1305. 1939.
3. HARRIS, L. J. and ABBASY, M. A. Lancet, 237 : 1355-1359. 1939.
4. MÖLLERSTRÖM, J. Arch. Internal Med. 52 : 649-663. 1933.
5. PETT, L. B. Nature, 143 : 23. 1939.
6. PETT, L. B. J. Lab. Clin. Med. 25 : 149-159. 1939.
7. PETT, L. B. and LEPAGE, G. A. J. Biol. Chem. 132 : 585-593. 1940.
8. THOMSON, A. M., GRIFFITH, H. D., MUTCH, J. R., and LUBBOCK, D. N. Brit. J. Ophth. 23 : 461-478. 1939.
9. THOMSON, A. M., GRIFFITH, H. D., MUTCH, J. R., and LUBBOCK, D. N. Brit. J. Ophth. 23 : 697-723. 1939.

THE COMPOSITION OF THE "5 : 3" CALCIUM ALUMINATE[1]

BY T. THORVALDSON[2] AND W. G. SCHNEIDER[3]

Abstract

When the isotropic hexahydrate of tricalcium aluminate is dehydrated, calcium oxide is liberated with the formation of a calcium aluminate lower in lime. A quantitative study of this reaction was made in order to determine the composition of the aluminate formed. Errors due to impurities in the tricalcium aluminate used, incompleteness of hydration to the hexahydrate, carbonation during treatment, retention of water by the final product, and recombination of the free lime with the aluminate formed were eliminated. The results indicated the formation of an aluminate of the composition $12CaO \cdot 7Al_2O_3$. The aluminate formed during the dehydration was found to give the same X-ray diffraction pattern as apparently homogeneous samples of the compositions $5CaO \cdot 3Al_2O_3$ and $12CaO \cdot 7Al_2O_3$ prepared directly from lime and alumina by thermal methods. The results support the assumption that the so-called "5 : 3" calcium aluminate should be assigned the formula $12CaO \cdot 7Al_2O_3$.

In their pioneer investigation on the system $CaO–Al_2O_3$ Shepherd, Rankin, and Wright (6) prepared four aluminates of calcium to which they assigned the compositions $3CaO \cdot Al_2O_3$, $5CaO \cdot 3Al_2O_3$, $CaO \cdot Al_2O_3$ and $3CaO \cdot 5Al_2O_3$. In 1931 Koyanagi (4), after studying melts of lime and alumina in various ratios, suggested the existence of an aluminate of the composition $3CaO \cdot 2Al_2O_3$. Later, on the basis of structural analysis, Büssem and Eitel (2) proposed the formula $12CaO \cdot 7Al_2O_3$ instead of the 5 : 3 ratio. A study of X-ray patterns of crystallized melts led Lagerquist, Wallmark, and Westgren (5) to a similar conclusion, although they considered the composition $9CaO \cdot 5Al_2O_3$ as an alternative possibility.

It is difficult to obtain conclusive results in the case of compositions as close together as the 5 : 3 and 12 : 7 lime–alumina mixtures (47.8 and 48.5% CaO) by either the microscopic study of quenched melts or by X-ray diffraction studies. It would, therefore, be desirable to find other experimental methods which would give evidence as to the true composition of the aluminate.

Shepherd, Rankin, and Wright (6) found that tricalcium aluminate melts incongruently producing free lime and the next aluminate lower in lime. If this decomposition could be made quantitative and the free lime in the product determined, the composition of the aluminate formed could be calculated. It is, however, unlikely that this could be done with the necessary accuracy. Thorvaldson and Grace (7) found that the hexahydrate of tricalcium aluminate decomposes in a similar manner when dehydrated at temperatures above 275° C. The maximum liberation of lime observed was 26.6% (anhydrous basis) while the formation of the 5 : 3 aluminate calls for liberation of 27.7% free lime. Büssem (1, p. 150) cites this result as evidence for the correctness

[1] *Manuscript received February 8, 1941.*
Contribution from the Department of Chemistry, University of Saskatchewan, Saskatoon, Sask.

[2] *Professor of Chemistry.*
[3] *Holder of a Bursary under the National Research Council of Canada.*

of the formula $12CaO . 7Al_2O_3$, which would require 26.69% free lime. There are, however, several factors that may interfere with the accuracy of the determination of the maximum free lime liberated on decomposition of the hexahydrate of tricalcium aluminate, and the experimental work of Thorvaldson and Grace (7) was not done with the object of determining the exact composition of the anhydrous aluminate formed. It was therefore decided to make a careful quantitative study of the thermal decomposition of $3CaO . Al_2O_3 . 6H_2O$.

It is evident that the tricalcium aluminate used must be very pure, with no appreciable excess of either lime or alumina, and that it must be converted completely to the hexahydrate. Incomplete hydration would result in incomplete thermal decomposition of the aluminate at the temperatures used, and would therefore give low values for the free lime liberated. In the lower part of the range of temperatures causing decomposition of the hexahydrate with liberation of lime, the dehydration is never complete. If this retention of water is due to the presence of some undecomposed hexahydrate, the results for free lime in the product would be low. However, if temperatures that are high enough to cause complete dehydration are used there is always some recombination of the lime and the lower aluminate to give anhydrous tricalcium aluminate, again resulting in a low maximum value for the free lime. Any contamination with carbon dioxide of the air during the dehydration would also give low results. It will thus be seen that all the most likely errors would give low results for the free lime in the decomposition mixture and thus lead one to favour the formula $12CaO . 7Al_2O_3$ as against the formula $5CaO . 3Al_2O_3$ for the lower aluminate. The object of the present investigation was to eliminate every possibility of error in the determination of the maximum free lime liberated on the decomposition of the hexahydrate of tricalcium aluminate and thus to obtain reliable evidence as to the composition of the aluminate formed. Table I shows the maximum amount of free lime to be expected according to each of the formulae mentioned above.

TABLE I

CALCULATED LIME MAXIMA FOR THERMAL DECOMPOSITION OF $3CaO . Al_2O_3 . 6H_2O$

Composition of final product	Maximum percentage free lime expected
$3CaO . 2Al_2O_3$	31.13
$5CaO . 3Al_2O_3$	27.67
$12CaO . 7Al_2O_3$	26.69
$9CaO . 5Al_2O_3$	24.91

Experimental

Preparation of $3CaO . Al_2O_3 . 6H_2O$

Calcium carbonate (low alkali analytical reagent) was dissolved in freshly redistilled hydrochloric acid and the solution made alkaline by addition of calcium oxide, prepared from the same material, to precipitate traces of iron,

alumina, etc. After filtering, the solution was diluted and the calcium precipitated by means of pure ammonium carbonate. The ammonium carbonate contained no insoluble matter and negligible non-volatile residue. The calcium carbonate was then washed free of chloride, dried, and analyzed. The analysis gave 56.10% CaO.

The alumina was prepared from "iron-free" ammonia alum by double precipitation using freshly redistilled ammonia and hydrochloric acid and washing free of sulphates and chlorides. The alumina after drying at 105° C. was found to contain 69.15% Al_2O_3 and less than 0.01% Fe_2O_3.

The calcium carbonate and alumina were then weighed out in the required proportions, mixed in a stoppered bottle, transferred to platinum crucibles, and the carbon dioxide and most of the water slowly driven off in a muffle furnace (maximum temperature 850° C.). The platinum crucibles were then heated in an induction furnace at 1450 to 1500° C. for 20- to 50-min. periods with intermediate grinding in an agate mortar to pass a 200 mesh sieve. Samples *A* and *B* contained 2 and 8% free lime respectively after the first heating in the induction furnace, while the last trace of free lime disappeared after the seventh and the fifth heatings, respectively. Examination of the product by means of the petrographic microscope showed it to be homogeneous and isotropic with a refractive index of 1.710. The analysis is given in Table II.

TABLE II

ANALYSIS OF IGNITED SAMPLES OF TRICALCIUM ALUMINATE

	Experimental		Calculated
	A	*B*	
Per cent CaO	62.24	62.27	62.27
Per cent Al_2O_3	37.80	37.86	37.73

Small samples of the aluminate were hydrated in platinum crucibles in an autoclave, which was heated slowly to 150° C. and kept at that temperature completely protected from contamination with carbon dioxide. In some cases the platinum crucibles containing the samples were placed over water in small silver lined steel autoclaves, which were heated in an electric oven at 120° C. After hydration, the samples were dried *in vacuo* over freshly ignited lime. All the samples were examined by means of the polarizing microscope and only those that were homogeneous and completely isotropic were used for the dehydration experiments. Eleven separately prepared samples were used for the final series of dehydrations. The hydration period varied from 5 to 14 days, the water content from 39.93 to 40.09% (which corresponds to a molar ratio of 5.98 to 6.01). The refractive index of the hydrate was 1.604.

The Thermal Decomposition of $3CaO \cdot Al_2O_3 \cdot 6H_2O$ *and the Determination of Free Lime*

The furnace was a vertical fused silica tube, 24 by 1 in., the middle portion being wound with a heating element and insulated with alundum and asbestos packing. The temperature was measured by means of a calibrated platinum–platinrhodium thermocouple, the junction being placed just above the 4 cc. platinum crucible containing the hydrate. To avoid violent evolution of moisture the sample was placed in the cold furnace and the temperature gradually raised to that desired. A slow current of air, thoroughly purified and then dried by passing over soda-lime and finally over anhydrous magnesium perchlorate, was passed upwards through the furnace during the heating. On removal, the sample was cooled over freshly ignited lime in a desiccator and the crucible after weighing transferred directly into a boiling-flask containing 60 cc. of 1 : 5 anhydrous-glycerol–alcohol mixture. The free lime was then determined according to the method of Lerch and Bogue. The end-point was very definite, except with the samples dehydrated at low temperatures (275 to 500° C.), and most of the lime was titrated within the first ten minutes while the end-point was usually reached within one hour. Using 0.5 gm. samples containing about 26% free lime, replicate determinations usually agreed within ±0.05%. Contamination with carbon dioxide, which is probably the most serious cause of error, was carefully avoided.

The first indication of the decomposition of the aluminate appears on prolonged heating of the hexahydrate at about 275° C., when the dehydration product turns pink when boiled in the glycerine-alcohol-phenolphthalein mixture. Higher temperatures must, however, be used before any free lime is readily extracted, and the free lime determination is somewhat uncertain when the dehydration temperature used is below 500° C.

In all cases the product of dehydration contained considerable amounts of water, as shown by ignition at 1100° C. to constant weight. A series of dehydrations at various temperatures was therefore made to ascertain whether the amount of water retained affects the amount of lime liberated. A short period of heating (three hours) was chosen to reduce the amount of possible recombination of lime with the aluminate. The results are given in Table III.

TABLE III

COMPARISON OF WATER RETAINED AND LIME LIBERATED

Temperature, °C.	Time of heating, hr.	Per cent water retained	Per cent CaO liberated
550	3	1.92	26.63
650	3	1.49	26.66
750	3	1.38	26.64
850	3	0.77	26.58
950	3	0.74	26.61

It is evident from the data of Table III that the amount of lime liberated remains constant over a considerable range of temperature while the amount of water held varies, and, that, when the water content of the product drops below approximately 2%, further dehydration does not affect appreciably the amount of lime liberated. This indicates that in a three-hour heating in a very dry atmosphere at 550° C. or above, none of the hexahydrate of tricalcium aluminate remains undecomposed. Possible error from this source is thus eliminated.

Three series of determinations of the lime liberated on heating the isotropic hexahydrate for various periods of time at 650, 750, and 850° C. were also made for the purpose of determining definitely the rate of recombination of the lime and the aluminate formed. The platinum crucibles containing the hexahydrate were placed in the cold furnace to prevent the sudden liberation of water with possible hydrolysis, and a fresh sample was used for each run. The results are given in Table IV and in Fig. 1.

TABLE IV

THERMAL DECOMPOSITION OF TRICALCIUM ALUMINATE HEXAHYDRATE

Temperature, °C.	Time of heating, hr.	Per cent water retained (anhydrous basis)	Per cent free CaO (anhydrous basis)
650	1	6.09	23.58
	2	1.84	26.33
	3	1.60	26.60
	6	1.36	26.63
	12	1.49	26.62
	24	1.35	26.50
750	1	0.86	26.64
	3	1.05	26.66
	6	1.03	26.63
	12	0.80	26.54
	24	0.72	26.24
850	1	0.81	26.65
	3	0.61	26.60
	6	0.60	26.44
	12	0.85	26.29
	24	0.63	26.03

From Table IV it is apparent that at 650° C. the decomposition is not complete until the heating has continued from three to six hours and that the rate of recombination is approximately 0.1% of lime in 12 hr. At 750° C. the decomposition appears complete in from one to three hours, with recombination apparent between 6 and 12 hr. at a rate of approximately 0.3% of lime in 12 hr., while at 850° the decomposition is probably complete in one hour and the average rate of recombination is somewhat greater than at 750°. The value for the free lime obtained by extrapolation to zero time

(Fig. 1) in order to eliminate the effect of recombination does not differ appreciably from the maximum for each curve.

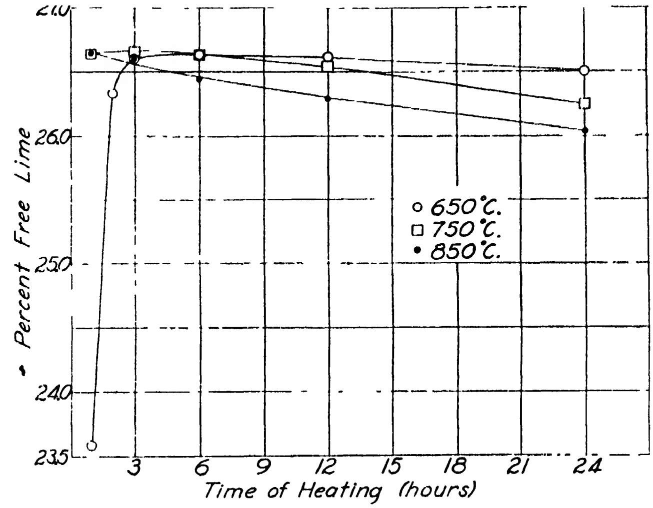

FIG. 1. *The thermal decomposition of* $3CaO \cdot Al_2O_3 \cdot 6H_2O$.

Considering the results as a whole, there does not seem to be any reason to suspect that the value obtained for free lime might be too high. It would therefore appear that the possibility of the composition $9CaO \cdot Al_2O_3$ (corresponding to 24.91% free CaO) may be eliminated. The formula $3CaO \cdot 2Al_2O_3$ (31.13% free CaO) may also doubtlessly be ruled out. The experimental evidence supports strongly the composition represented by $12CaO \cdot 7Al_2O_3$ rather than $5CaO \cdot 3Al_2O_3$ as the aluminate formed on dehydration.

There remains the question whether the anhydrous aluminate obtained after dissolving the free lime from the mixture obtained on dehydration of the hexahydrate of tricalcium aluminate is identical with the aluminate obtained by thermal treatment of the corresponding mixture of lime and alumina. X-ray powder patterns were made using the solid residue remaining after the determination of free lime and the apparently homogeneous products obtained on thermal treatment of lime and alumina in the ratios $12CaO \cdot 7Al_2O_3$ and $5CaO \cdot 3Al_2O_3$. All the X-ray patterns appeared identical and the readings were those given by Harrington (3) for the product $5CaO \cdot 3Al_2O_3$.

It therefore appears that on dehydration of the hexahydrate of tricalcium aluminate a crystalline aluminate of the composition $12CaO \cdot 7Al_2O_3$ (48.53% CaO and 51.47% Al_2O_3) is formed with the liberation of 26.7% of calcium oxide, and that X-ray diffraction photographs show that the same product is obtained by direct thermal combination of lime and alumina in the above proportions. If the formula $5CaO \cdot 3Al_2O_3$ were to be accepted as representing the composition of the compound, it would be necessary to assume that in all

the experiments described above, 98.66 parts of this compound retain 1.34 parts of calcium oxide in solid solution, and that this dissolved lime cannot be extracted under the conditions existing during the determination of free lime. Without further evidence such an assumption appears unwarranted.

References

1. BÜSSEM, W. Proc. Symposium on the Chemistry of Cements, Ingeniörsvetenskapsakademien, Stockholm. 1938.
2. BÜSSEM, W. and EITEL, A. Z. Krist. A95 : 175. 1936.
3. HARRINGTON, A. E. Am. J. Sci., (5) 13 : 467-479. 1927.
4. KOYANAGI, K. Zement, 20 : 72-75. 1931.
5. LAGERQUIST, K., WALLMARK, A., and WESTGREN, A. Z. anorg. allgem. Chem. 234 : 1-16. 1937.
6. SHEPHERD, E. S., RANKIN, G. A., and WRIGHT, F. E. Am. J. Sci. (4) 28 : 293-333. 1909.
7. THORVALDSON, T. and GRACE, N. S. Can. J. Research, 1 : 36-47. 1929.

PASTURE STUDIES. XIX.

A SIMPLIFIED APPARATUS FOR THE CONTINUOUS EXTRACTION OF MOISTURE AND FAT FROM BIOLOGICAL MATERIALS[1]

By E. W. Crampton[2] and T. L. Purdy[3]

Abstract

A modification of the Kaye apparatus for the determination of moisture by distillation and of lipids by isopropyl ether extraction is described. The modified apparatus has been used in the analysis of plant material and faeces, and typical results are presented. It appears that isopropyl ether and ethyl ether yield similar amounts of extract, but that oven-drying may result in values that are too low.

The present chemical methods of analysis of food stuffs and of faeces are being re-examined from a biological standpoint and one fraction under consideration is the ether extract. Two criticisms of the standard A.O.A.C. method have been raised. One is that the process of oven-drying, to which samples are subjected, is liable to volatilize certain fractions of the ether extract and also theoretically, at least, may permit oxidation of the extractives. In the second place, the 'ether extract' includes a variety of substances of differing nutritional significance depending on the parent material.

A method of analysis that would eliminate the necessity of drying the sample by heat should give a truer picture of the composition of the lipid fraction. Kaye (1) has proposed such a procedure and has designed an apparatus that in principle consists of a water collection trap combined with a Soxhlet type extractor. The method requires a fat solvent, insoluble in water, and with a boiling point close to that of water. Isopropyl ether possesses the desired properties. With it, Kaye extracted from human faeces 30% more neutral fats than was obtained by standard methods with ethyl ether.

This procedure seemed to be applicable to the solution of one of the problems involved in the study of the nutritive value of pasture herbage. The design of the apparatus, however, appeared more complicated and expensive than necessary, and an attempt was made in this laboratory to simplify it, particularly with respect to: (i) quantities of solvent required per unit of sample, (ii) ease of assembly, (iii) operation as to temperature control, and (iv) reduction in the number of separate parts and standard joints necessary.

The new design (Fig. 1) is based on the standard Soxhlet apparatus and includes the following modifications of the Kaye apparatus:

[1] *Manuscript received January 20, 1941.*
Contribution from the Faculty of Agriculture, McGill University, Macdonald College, Que. Journal Series No. 155.
[2] *Associate Professor of Animal Nutrition.*
[3] *Research Associate, Nutrition Section, Department of Animal Husbandry.*

1. The ground glass joint between the boiling-flask and the extraction chamber was eliminated. This was thought advisable in that the entire unit is immersed in a water or steam bath.

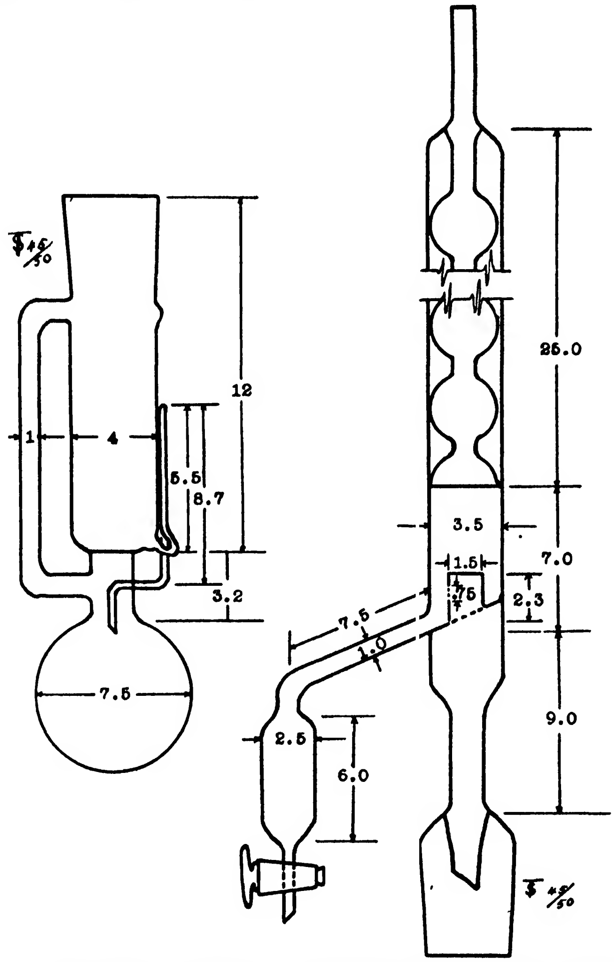

FIG. 1. *Diagram of apparatus. All measurements are in centimetres.*

2. Attached to the condenser and above the standard ground glass joint between the condenser and the extraction chamber is a water-solvent separator, connected by an offset tube to a water trap. The essential parts of this are: *(a)* a sloping floor leading to an offset collection bulb, fitted with a stopcock so that the water collected may be drained off completely and measured or weighed; *(b)* a central tube in this floor through which the ascending vapours may pass without interference from the returning condensate. The condensate runs down the walls of the collection chamber, and the ether returns through an aperture in the side of the vapour conduction tube. In this way the droplets of water are not so readily carried back to the thimble by surface

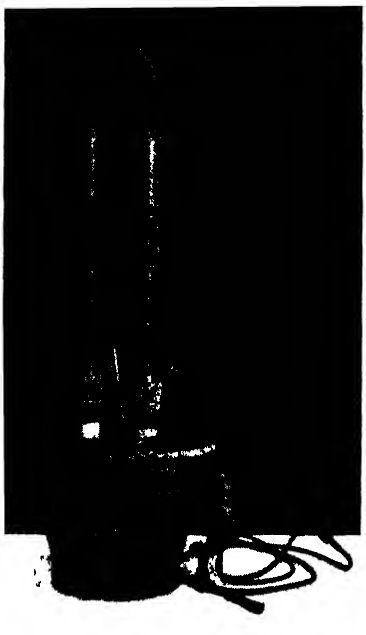

FIG. 2. *Apparatus assembled in deep steam bath.*

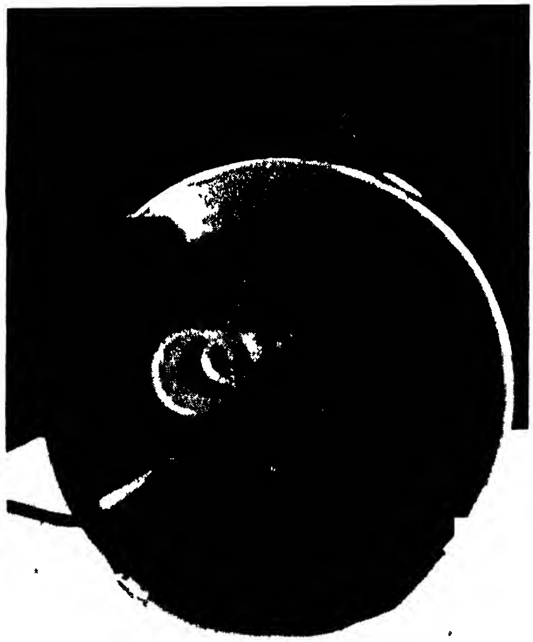

FIG. 3. *Inside view of steam bath showing arrangement of steam coil and rubber seats for extractors.*

tension of the solvent, since most of them must pass around the circumference of the collection chamber.

Heating is accomplished by means of a deep steam bath. This was made from a pail that was of a depth sufficient to enclose the extracting unit to the level of the top of the thimble. Three turns of flexible-metal tubing about the lower inside circumference of the bath, attached to a steam line, supplies the heating element. The water is kept at constant level by means of a constant level chamber on one side of the bath. The water is maintained at a level sufficient to cover the flasks of the unit as it stands on a notched rubber ring on the bottom of the bath. The weight of the apparatus overcomes the buoyancy of water of this depth and with the rubber ring seat, clamps other than for the condenser are unnecessary. One such steam bath accommodates two extractor units. A divided cover, cut out to accommodate the units, completely encloses the extraction units. A rubber mat cut to fit exactly around the extraction chambers prevents escape of steam. Thus the whole extraction unit may be heated uniformly at a constant temperature, regulated by the steam allowed into the coils.

Operation

Two steps are involved in the procedure.

(I) A standard thimble 33 by 80 mm. is used to hold the sample of approximately 10 gm. As soon as this is placed in the extraction chamber the con-

denser unit is fitted. (A very light coating of glycerol and glucose (1 : 1) was found advantageous on the ground glass joint, making it possible to dismantle the apparatus without waiting for it to cool.) The isopropyl ether is then added through the top of the condenser filling the water collection bulb and the separation chamber to the aperture in the vapour conduction tube.

Additional ether is added to cover the sample in the thimble but not more than sufficient to rise half-way up the syphon. From 65 to 75 ml. are needed for the water distillation, the amount depending on the bulk of the sample. If more than this is added there is, on heating, a tendency for the ether to bubble over the syphon, with the possibility of carrying water soluble material into the flask at the beginning of the distillation. It seems difficult to prevent this in the Kaye apparatus. The use of the deep steam bath with the modified apparatus, completely enclosing the extraction unit, overcomes this difficulty.

Distillation is carried out with the steam bath brought slowly to 85° C. At this temperature no droplets of moisture collect high enough in the condenser to make their removal difficult. Distillation takes from two to four hours, the time depending on the nature of the sample. With material that might become compact, operations can be facilitated by mixing pre-dried asbestos with the sample.

(II) When the distillation is completed, one-half of the cover of the steam bath is raised. This reduces the temperature of the extraction chamber below the boiling point of the ether. Extraction is then continued with the addition of sufficient ether (about 20 to 30 cc.) to allow the syphon to operate as a standard Soxhlet.

The collected water may be removed and measured or weighed. In this laboratory, graduated 15 ml. centrifuge tubes were found useful for this purpose. A small amount of ether drawn off with the water provides an easily read meniscus.

Following removal of the water, the water trap becomes a unit through which the solvent may be recovered merely by closing the cover of the bath and heating the whole unit as for distillation of the water. (Recovery of solvent has been 80 to 85%.) The ether thus recovered requires no further distillation for immediate subsequent use.

On completion of the extraction and recovery of the solvent, the ether extract may be transferred with warm ether to a tared beaker, dried *in vacuo*, and weighed.

Discussion

It is important that freshly prepared, dry ether be used. The writers' results indicate that ether that has been unused for as long as two days should be redistilled before further use. A comparison of the results of extraction with peroxide-free and peroxide-containing ether emphasizes this point (Table I). Not only was there a difference in weight of extract obtained from fresh cereal grass, but also the green colour of the extract obtained with peroxide-free ether was completely destroyed by the peroxide-containing

solvent. Determinations also indicated a complete loss of carotene in extracts obtained with peroxide-containing ether.

TABLE I

RESULTS OF EXTRACTION OF CEREAL GRASS IN MODIFIED APPARATUS, SHOWING THE EFFECTS OF PEROXIDE IN THE SOLVENT

	Extracted with isopropyl ether, peroxide-containing	Extracted with isopropyl ether, peroxide-free
Original sample	100	100
Water	74.0	73.2
Ether extractives	1.4	1.2
Residue	24.7	24.5
Total accounted for	100.1	98.9
Error	+0.1	−1.1
Per cent loss of extractives on subsequent oven drying	14.6	9.0
Colour of extract	Brown	Green
Carotene in extract	Absent	Normal

It would appear that isopropyl ether extracts do not differ quantitatively from ethyl ether extracts (Table II). Removal of water by distillation, followed by extraction with ether, yields a definitely larger proportion of ether extract from plant materials than does the A.O.A.C. method.

TABLE II

COMPARISONS OF METHODS OF MOISTURE AND LIPID DETERMINATION ON FRESH FAECES, FRESH GRASS, AND DRIED GRASS

Material	Fractions	Oven drying at 105° C. followed by Soxhlet extraction		Vacuum drying at 90° C. followed by Soxhlet extraction	Moisture by distillation, followed by extraction with isopropyl ether	
		Ethyl ether	Isopropyl ether	Ethyl ether	Crampton apparatus	Kaye apparatus
Fresh steer faeces	Sample	100.00		100.00	100.00	
	Moisture	82.38		81.66	82.39	
	Ether extract	1.27		1.36	1.22	
	Residue	16.40		15.60	17.40	
	Total accounted for	100.05		98.62	101.01	
Fresh grass	Sample	100.00	100.0		100.00	
	Moisture	79.81	79.49		79.50	
	Ether extract	0.54	0.56		0.62	
	Residue	19.73	19.86		20.85	
	Total accounted for	100.08	99.91		100.97	
Dried cereal grass (commercial)	Sample	100.00			100.00	100.00
	Moisture	7.43			5.67	5.63
	Ether extract	4.30			5.93	5.86
	Residue	88.27 (dif.)			88.76	88.00
	Total accounted for	100.00			100.36	99.49

The authors are indebted to V. K. Collins and R. A. Chapman, Department of Chemistry, Macdonald College, for assistance with the chemical analyses.

Sufficient work has not been done on faeces to make certain that the example cited is typical: but indications are that the ether extractives lost from fresh herbage material by standard procedures are not present in measurable quantities in the faeces of steers fed on such herbage.

That a part of the ether extractable material may be lost through oven-drying certain substances is indicated in Table III.

TABLE III

LOSS OF ETHER EXTRACT BY HEATING IN OPEN OVEN AT 105° C.

Sample	Per cent moisture by distillation	Per cent ether extract by extraction in Crampton apparatus	Per cent ether extract lost by subsequent heating in oven at 105° C. for 12 hr.
Dried grass (commercial)	5.7	5.9	9.4
Fresh pasture grass	79.9	0.6	10.3
Fresh cereal grass (rye)	73.2	1.2	9.0

Presumably the extract was moisture-free and consequently the loss (Table III, Col. 3) was not water but some fraction of the dry ether extract. It is perhaps significant that a comparable loss was obtained with three forms of similar plant material.

Reference

1. KAYE, I. A., LEIBNER, I. W., and CONNOR, E. B. J. Biol. Chem. 132(1) : 195-207. 1940.

Canadian Journal of Research
Issued by The National Research Council of Canada
VOL. 19, SEC. B. MAY, 1941

THE DEHYDRATION OF TRICALCIUM ALUMINATE HEXAHYDRATE[1]

By W. G. Schneider[2] and T. Thorvaldson[3]

Abstract

Samples of the isotropic hexahydrate of tricalcium aluminate were dehydrated in a current of dry air at various temperatures up to 1050°*. The water retained and the lime liberated were determined. The results of earlier preliminary studies in this laboratory were confirmed. At low temperatures an isotropic hydrate of the composition $3CaO \cdot Al_2O_3 \cdot 1\frac{1}{2}H_2O$, having a refractive index of 1.543 ± 0.003, is formed. This hydrate is stable in dry air up to a temperature of approximately 275° and when once formed at lower temperatures has a very slow rate of decomposition below 350°. On continued dehydration above 275° decomposition occurs with the liberation of calcium oxide. Between 550° and 950° quantitative decomposition occurs into calcium oxide and an aluminate of the composition $12CaO \cdot 7Al_2O_3$. In the upper part of this temperature range prolonged heating causes slow recombination of the solid decomposition products, and above 950° this effect becomes marked. Dehydration of the hexahydrate in a current of dry nitrogen gives similar results. The experiments indicate that the system $3CaO.Al_2O_3 \cdot 1\frac{1}{2}H_2O–3CaO \cdot Al_2O_3 \cdot 6H_2O$ would serve as an efficient drying agent at temperatures below 100°.

In previous work in this laboratory (6) it was found that when the isotropic hexahydrate of tricalcium aluminate is heated in a current of dry air at temperatures below 275° to 300°, simple dehydration of the aluminate takes place with the formation of a hydrate of the composition $3CaO \cdot Al_2O_3 \cdot 1\frac{1}{2}H_2O$, while, on the other hand, heating at higher temperatures causes simultaneous dehydration and decomposition of the aluminate with the liberation of a part of the lime present. At still higher temperatures recombination of the two solid decomposition products occurs, so that the heating of the hydrate at 1000 to 1100° may show no ultimate liberation of calcium oxide, anhydrous tricalcium aluminate being produced. A recent study (7) has shown that this recombination is very slow if the temperature is kept below 850°.

Köberich (2) made a eudiotensimetric study of the dehydration of the hydrate over a wide range of temperature. He reported that between 180° and 260° the dehydration from $3CaO \cdot Al_2O_3 \cdot 6H_2O$ to $3CaO \cdot Al_2O_3 \cdot 1\frac{1}{2}H_2O$ is reversible and takes place without change in the crystal structure except that there is a shrinkage in the unit cell corresponding to a decrease in the

[1] *Manuscript received February 8, 1941.*
Contribution from the Department of Chemistry, University of Saskatchewan, Saskatoon, Sask.
[2] *At the time, holder of a Bursary under the National Research Council of Canada.*
[3] *Professor of Chemistry.*
* *All temperatures in this report are given in degrees Centigrade.*

lattice constant from 12.542 to 11.94 Å. On the other hand, he found that dehydration below the $1\frac{1}{2}$-H_2O hydrate at temperatures between 400° and 500° is irreversible with destruction of the crystal lattice and liberation of lime. From this he concludes that 12 of the 48 molecules of water in the unit cell of the hexahydrate are present in the lattice in the form of OH groups.

Büssem (1, pp. 156–157) suggests that the behaviour on dehydration as outlined by Köberich may be explained by assuming that a transformation of $Al(OH)_6$ groups into $Al(OH)_4$ and AlO_4 groups takes place. This leads him to the assumption that a hydrate having 2 instead of $1\frac{1}{2}$ moles of water is formed. Büssem considers that Köberich's curves for the dehydration tend to give values approaching $1.8H_2O$ and support the assumption that the lower hydrate contains 2 moles of water.

Nacken (5) also made a eudiotensimetric study of the dehydration and came to the conclusion that hydrates having 4 and 2 moles of water are formed. During the dehydration of the dihydrate he found that lime was liberated, the maximum value obtained being 25.73% CaO after heating for three hours at 611°, while no free lime was found when the product was heated for three hours at 1260°.

Köberich (2) gives a critical discussion of the eudiotensimetric method of studying dehydration and shows how easy it is to come to misleading conclusions as to the composition of stable hydrates. The information as to experimental conditions given by Nacken (5) is hardly sufficient to determine whether he took the precautions that Köberich considers essential in order to obtain reliable results.

Lefol (3, 4) also studied the dehydration of the hexahydrate and found that below 260° the loss of water is very slow, while between 260° to 300° there is a very rapid increase in the rate. Between 315° and 350° a product of constant composition, $3CaO \cdot Al_2O_3 \cdot 1\frac{1}{2}H_2O$, was obtained under the conditions used.

Travers (8, pp. 225–226) and Travers and Zahabi (9) report that when the hexahydrate is heated in a current of nitrogen no loss in weight is shown below 175°; that, between 275° and 450°, 67% of the water is given off, the dihydrate being formed; that only towards 1000° is the dehydration complete and that no free lime is in any case obtained during the dehydration. These authors attribute the absence of free lime to the use of an inert medium (nitrogen).

The lack of agreement of the results obtained by different experimenters led the authors to conduct the present series of experiments.

Experimental

For the details of the preparation of the anhydrous tricalcium aluminate, the conversion of the same to the hexahydrate, the type of furnace used for the dehydration, and the precautions taken against contamination of the samples, the reader is referred to a preceding paper (7). The temperatures were measured by means of calibrated thermocouples; copper-constantan

being used for the low, iron-constantan for the medium, and platinum-platinrhodium for the higher temperatures. The temperature of the furnace remained constant to within $\pm 5°$ during a run. Attention should be drawn to the purification and thorough drying of the air circulating through the furnace. The air, in the form of small bubbles, was passed through a series of towers, packed with glass beads, countercurrent to a solution of caustic potash and sulphuric acid, then through a tower of soda-lime, while the last traces of moisture were removed by a long column packed with anhydrous magnesium perchlorate (10).

Dehydration at Low Temperatures

Several series of dehydrations of the hexahydrate at temperatures between 150° and 400° were made. In dehydrations below 200° the loss in weight was very slow (12 hr. at 200° caused a change from $6H_2O$ to $5H_2O$) and a temperature of 275° or higher had to be used in order to obtain a product of constant weight in a reasonable time. When the samples of the hydrate were heated rapidly by introducing them into the hot furnace at temperatures above 275°, somewhat erratic results were obtained. This was probably due to the violent evolution of steam, favouring hydrolysis and causing the sudden collapse of the crystal lattice. On the initial heating of a sample of the hexahydrate it was therefore placed in the cold furnace and the temperature raised gradually to the one desired. If the sample was to be reheated it was then introduced into the furnace at the temperature of the dehydration. In some of the series the samples were heated for various time intervals, each sample being used only once, while in other series the one sample was heated at a given temperature for successive intervals of time with intermediate weighings. In the first type of experiment the loss of moisture was more rapid for a given total time of heating and free lime was obtained at a lower temperature. Thus free lime was present after prolonged heating at 300° or even at 275° (after heating for 40 hr.) as shown by a pink coloration imparted to the solid by phenolphthalein. When the second method was used, the loss of water was somewhat retarded after one or two periods of heating and a product of almost constant weight was obtained at temperatures up to 350° before any free lime could be detected.

Table I and Fig. 1 give the results of a typical series of experiments using 0.5 gm. samples of the hexahydrate, the one sample being used for all the determinations at each temperature. On completion of a series at a given temperature the sample was tested for free lime.

The experimental data of Table I and Fig. 1 confirm the previous results obtained in this laboratory. In all the dehydrations between 275° and 325° the loss of water to below $1.6H_2O$ is comparatively rapid; below this point it is very slow, the product approaching a constant composition at approximately $3CaO . Al_2O_3 . 1\frac{1}{2}H_2O$. The lag in dehydration at this composition is noticeable even when the temperature is high enough to cause liberation of lime on prolonged heating (cf. 350° series). In no case was free lime detected in the product until the hydration had dropped below $1.50H_2O$. It would

TABLE I

DEHYDRATION OF TRICALCIUM ALUMINATE HEXAHYDRATE

Total time of heating, hr.	Moles of water retained at given temperature					
	275°	300°	325°	350°	375°	400°
¼						1.65
½				1.98		–
1	2.99	1.79	1.62	1.62	1.61	1.37
2	1.89	1.62	1.58	1.57	1.57	1.31
3	1.73	1.58	1.53	1.54	1.42	–
4	1.71	1.54	1.52	1.53	1.40	1.04
6	1.67	–	1.52	1.53	1.38	–
8	1.65	1.51	1.51	1.51	1.37	0.72
15	1.59	1.50	1.51	1.46	1.36	–
26	1.57					
50	1.53					
75	1.53					
Test for free lime	Negative	Negative	Negative	Trace[1]	Present[2]	Present[2]

[1] *The tests for free lime were made by transferring the platinum crucible with the sample into 60 cc. of an anhydrous alcohol-glycerine mixture (5 : 1) with phenolphthalein as an indicator and refluxing the mixture. In this case the solid turned pink while the solution remained colourless, the colour of the adsorbed phenolphthalein being changed to the alkaline tint.*

[2] *Although considerable amounts of free lime were present, the titration with a standard solution of ammonium acetate in absolute alcohol was not satisfactory. The lime was extracted from the solid very slowly and the end-point was very indefinite. This was always found to be the case with the partly dehydrated aluminate.*

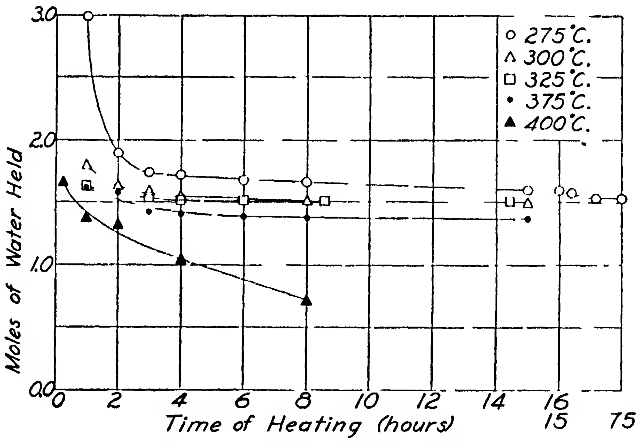

FIG. 1. *The dehydration of* $3CaO \cdot Al_2O_3 \cdot 6H_2O$.

therefore appear that this composition represents a definite hydrate of tricalcium aluminate and, also, as concluded by Köberich (2), the limit of the zeolitic dehydration. The refractive index of this isotropic lower hydrate was found to be 1.543 ± 0.003 (sodium light).

Dehydration at High Temperatures

Samples of the hexahydrate dehydrated at temperatures between 350° and 550° (and down to 300° when the heating was for one continuous long

period) always showed the presence of free lime when refluxed with the anhydrous alcohol-glycerine mixture. The quantitative determination of free lime in these products was, however, not satisfactory owing to the very long refluxing necessary and the uncertainty of the end-point of the titration. The qualitative test appears to be reliable, as a negative result under the same conditions was always obtained when the dehydration had not proceeded below the $1\frac{1}{2}$-H_2O hydrate. In addition X-ray powder patterns of dehydration products with less than $1\frac{1}{2}H_2O$ showed lines of CaO. This is in agreement with the results obtained with the product of dehydration over phosphorus pentoxide at 400° by Köberich (2, p. 17), who observed the lines of both decomposition products and in addition found 17.5% CaO by analysis.

Samples dehydrated at temperatures above 500° give consistent values for free lime, namely, a maximum of 26.7% CaO with the formation of an aluminate of the composition $12CaO . 7Al_2O_3$. Some recombination on prolonged heating is apparent but this is very slow at temperatures below 950°. The results of dehydration in this temperature range are given in a preceding paper (7). Above 950° the recombination to form anhydrous tricalcium aluminate is rapidly accelerated with increasing temperature. Samples of the hexahydrate heated in the furnace at 1050° for seven hours showed free lime absent.

Dehydration in an Atmosphere of Nitrogen

Dehydration of the isotropic hexahydrate in a current of nitrogen instead of air was also studied. The nitrogen was purified as described above for air. No difference in the behaviour during dehydration was discovered. Thus a sample of the hexahydrate after heating for one hour at 375° still held 1.4 moles of water. After further heating at 750° to 775° for three hours, 1.13% of water was held, and the sample was found to contain 26.4% of free lime. The authors are at a loss to explain the conflicting results of Travers and Zahabi (8, 9), unless the cause lies in the difference in the method of testing for the presence of free lime.

The System $3CaO . Al_2O_3 . 1\frac{1}{2}H_2O$-$3CaO . Al_2O_3 . 6H_2O$ *as a Drying Agent*

The experiments described in this paper show that air dried at room temperature by the very efficient drying agent, magnesium perchlorate, does not remove any water from the hydrate $3CaO . Al_2O_3 . 1\frac{1}{2}H_2O$ even when passed over the hydrate at temperatures up to 275° C. Further, the system $3CaO . Al_2O_3 . 6H_2O$–$3CaO . Al_2O_3 . 1\frac{1}{2}H_2O$ has a lower vapour pressure than the system CaO–$Ca(OH)_2$. The $1\frac{1}{2}$-hydrate of tricalcium aluminate when exposed to water vapour takes up moisture to the extent of 27% of its own weight to form the hexahydrate (2, p.17) and the $1\frac{1}{2}$-hydrate may be readily regenerated at 275° to 300° C. These facts indicate that the $1\frac{1}{2}$-hydrate of tricalcium aluminate is well suited for use as a drying agent. The great stability of the hexahydrate at 100° C. also indicates that the system $3CaO . Al_2O_3 . 1\frac{1}{2}H_2O$–$3CaO . Al_2O_3 . 6H_2O$ would be an effective drying agent at temperatures considerably above room temperatures.

References

1. BÜSSEM, W. Proc. Symposium on the Chemistry of Cements. Ingeniörsvetenskaps-akademien. Stockholm. 1938.
2. KÖBERICH, F. Inaugural-dissertation. Berlin. 1934.
3. LEFOL, J. Compt. rend. 197 : 919-921. 1933.
4. LEFOL, J. Sur l'hydration des aluminates, des sels doubles du silicate et du sulfate de calcium. Thèse (Université). Paris. 1937.
5. NACKEN, R. Zement, 26 : 715-719. 1937.
6. THORVALDSON, T. and GRACE, N. S. Can. J. Research, 1 : 36-47. 1929.
7. THORVALDSON, T. and SCHNEIDER, W. G. Can. J. Research, B, 19 : 109-115. 1941.
8. TRAVERS, A. Proc. Symposium on the Chemistry of Cements. Ingeniörsvetenskaps-akademien. Stockholm. 1938.
9. TRAVERS, A. and ZAHABI, H. Compt. rend. 206 : 55-57. 1938.
10. WILLARD, H. H. and SMITH, G. F. J. Am. Chem. Soc. 44 : 2255-2259. 1922.

A NEW LOW PRESSURE GAUGE[1]

By C. C. Coffin[2] and J. R. Dingle[3]

Abstract

A heat-conductivity, low-pressure gauge based on the rate of sublimation of solid carbon dioxide is described. The gauge, which also serves as a trap in the vacuum line, is sensitive enough for most purposes. It is extremely simple and inexpensive to construct and operate.

Introduction

The fact that apparatus dimensions set an upper limit to the mean free path of gas molecules enables variations in the transfer properties of gases to be used for the measurement of low pressures. The Pirani-Hale heat conductivity gauge (3) and the Langmuir viscosity gauge (4, p. 107) are well known and thoroughly tested examples of such manometers. The present note describes a heat-conductivity, low-pressure manometer the operation of which is based on the rate of escape of gaseous carbon dioxide from a slush of solid carbon dioxide and ether. This gauge, which has been in use in this laboratory for several years, is very simple to construct and use. The fact that it cannot compete in precision with the more elaborate and expensive Pirani and ionization gauges is of no consequence in the many cases where a rough estimation rather than a measurement of the pressure is all that is desired. The fact that solid carbon dioxide makes a necessary and sufficient (if used with a phosphorus pentoxide tube (2, p. 74)) trap for both mercury and oil condensation pumps is a point in favour of this manometer, which of course also acts as an efficient trap. A distinct advantage is that since its range covers that of the McLeod gauge and even lower pressures it can be used in place of the latter in systems where the presence of mercury vapour is not desired. The functional disadvantages peculiar to the Pirani gauge are of course accentuated in this cruder variation of the instrument which has, however, the distinct advantage that no expensive corrodible auxiliary equipment is required.

Experimental

The gauge is shown in Fig. 1. The inner carbon dioxide chamber, A, and the outer air-stirred ice bath, B, are separated by the vacuum to be measured. The time taken for a given volume (20 to 50 cc.) of carbon dioxide to collect in a brine-filled gas burette (i.e., the time taken for a given change of liquid level in the burettes) is measured on a stop-watch and translated into pressure from a calibration curve made with a McLeod gauge and a pipette system (e.g., see (5)). A typical calibration curve is shown in Fig. 2. The bath

[1] *Manuscript received February 24, 1941.*
Contribution from the Department of Chemistry, Dalhousie University, Halifax, N.S.

[2] *Professor of Chemistry.*
[3] *Honours Student in Chemistry.*

must be stirred or a sheath of ice at an indeterminate temperature will form on the gauge at the higher pressures.

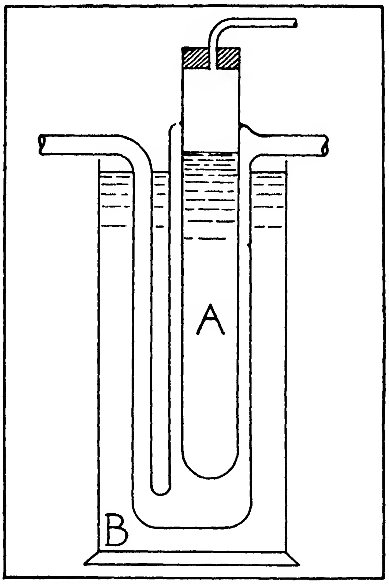

FIG. 1 *Carbon dioxide trap and pressure gauge.*

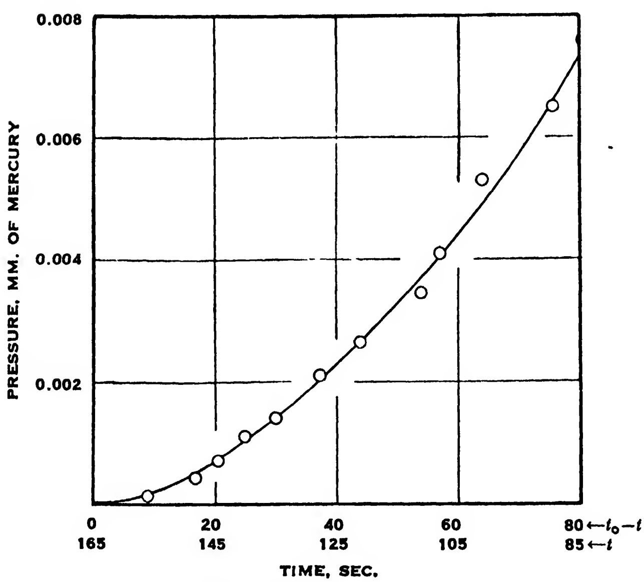

FIG. 2. *Calibration curve of pressure gauge No. 3*

The slush, which can be made with either "dry-ice" or carbon dioxide snow from a cylinder, requires rather careful preparation. It should contain as much carbon dioxide as possible and yet not be heavy enough to channel

clot or pack into wads with the gas evolution. A variation of several centimetres in the depth of the slush has no appreciable effect on the rate of escape of carbon dioxide for any given pressure in the gauge. At the higher pressures where carbon dioxide is being rapidly evolved frequent additions of solid carbon dioxide may be necessary. Measurements seem to be more reproducible if several minutes are allowed to elapse between readings. A multi-range flowmeter has been used successfully in place of the gas burettes and, while not so sensitive as the latter, has the advantage that any sudden changes in pressure are instantly visible.

A typical calibration curve (Gauge No. 3: *A;* 3 by 26 cm.; *B*, 4.5 by 30 cm.) is shown in Fig. 2 in which pressures as measured with a McLeod gauge are plotted against time in seconds. The abscissa gives both t and $t_0 - t$, where t_0 is the longest time taken for a given amount of carbon dioxide to escape (i.e., the lower limit of the gauge) and t is the time taken for the same amount of gas at any pressure. The volume of carbon dioxide used in obtaining the curve shown was 50 cc. at a pressure of 76 cm. of mercury plus 40 cm. of brine. The fact that any gauge has the same value of t_0 with any reasonably good pumping system indicates that the gauge will not measure extremely low pressures and that its lower limit is in that pressure region where the energy conducted becomes negligible in comparison with that radiated.

Radiation to the carbon dioxide chamber may be decreased and the usefulness of the gauge extended to lower pressures by silvering the outer wall of *A* and the inner wall of *B*. A silvered gauge was found to take about twice as long to deliver a given volume of carbon dioxide at the lowest possible pressure as the same gauge before silvering. The outside of tube *A* of the gauge used in obtaining Fig. 2 was platinized (1) for use in the presence of mercury vapour. A narrow observation strip was left for observing the slush level. Subsequent removal of the platinum and total silvering increased t_0 by about 50%. An observation strip is not essential as the rubber stopper of *A* may be removed at any time and the slush level determined with a probe.

References

1. COFFIN, C. C. Can. J. Research, B, 18 : 318-321. 1940.
2. DUSHMAN, S. Production and measurement of high vacuum. Gen. Elec. Co., Schenectady, N.Y. 1922.
3. HALE, C. F. Trans. Am. Electrochem. Soc. 20 : 243-258. 1911.
4. LANGMUIR, I. J. Am. Chem. Soc. 35 : 105-127. 1913.
5. SODDY, F. and BERRY, A. J. Proc. Roy. Soc. (London), 83 : 254-264. 1910.

THE OXIDATION OF *p*-NITRO-*p'*-HYDROXYAZOBENZENE AND SOME RELATED COMPOUNDS WITH HYDROGEN PEROXIDE[1]

By E. P. Linton[2], C. H. Holder[2], and H. E. Bigelow[3]

Abstract

p-Nitro-*p'*-hydroxyazobenzene, *p*-hydroxyazobenzene, and *p*-aminoazobenzene have been oxidized with 30% hydrogen peroxide. It has been found that in the case of the first two compounds prolonged treatment (25 hr.) disrupts both benzene rings and results in their complete oxidation to carbon dioxide, water, and nitrogen, or oxides of nitrogen. Oxidation of the third compound is not complete after six days.

Introduction

A number of instances of the direct oxidation of azo compounds to the corresponding azoxy compound are recorded in the literature (1–5, 7, 10). It has generally been found that oxidation is complete at this stage. Bamberger (8, p. 1953), however, observed that during the oxidation of both the α and β forms of *o*-hydroxyazoxybenzene with permanganate in a potassium hydroxide solution one benzene ring was removed and the final product was potassium isodiazotate. Angeli (6) obtained a similar result with the para isomer of this compound.

In an attempt by the authors to prepare the two isomeric azoxy compounds from *p*-nitro-*p'*-hydroxyazobenzene by treatment with hydrogen peroxide, it was found that on prolonged boiling the original compound entirely disappeared, being apparently oxidized to carbon dioxide, water, and nitrogen or an oxide of nitrogen. Since no case could be found in the literature in which a compound containing two benzene rings was completely oxidized in this way, it was decided to study the reaction quantitatively in order to determine the extent of the oxidation.

Experimental

A. Preparation of the Materials

Azoxybenzene was prepared by the action of sodium arsenite on nitrobenzene (9). This was treated with concentrated nitric acid at about 40° C. and the *o*- and *p*-mononitro derivatives obtained were readily separated by crystallization from alcohol, which yields the para compound in crystalline form. The ortho compound was obtained as an oil, which later solidified.

p-Nitroazoxybenzene was treated at about 100° C. for two to three hours with concentrated sulphuric acid. Under these conditions Wallach's rearrangement occurred, and *p*-nitro-*p'*-hydroxyazobenzene was formed. The resulting red solution was poured into ice and water. The insoluble product was

[1] *Manuscript received March 12, 1941.*
Contribution from the Department of Chemistry, Mount Allison University, Sackville, N.B.
[2] *Instructors, at time of the research.*
[3] *Professor of Chemistry.*

filtered and then treated with ether, which eliminated a black powder consisting of polymerization products. The ethereal solution was extracted with 5% sodium hydroxide solution. *p*-Nitro-*p'*-hydroxyazobenzene was precipitated by acidifying the alkaline solution and was then recrystallized from alcohol. The product obtained was in the form of brilliant red or yellow flakes, which were purified by sublimation under reduced pressure.

The preparation of the *p*-hydroxyazobenzene was carried out by Wallach's rearrangement of azoxybenzene by a method similar to that described above. The *p*-aminoazobenzene was an Eastman Kodak Company product and was recrystallized from alcohol. The hydrogen peroxide was of 30% strength as supplied by Merck and Company.

B. The Apparatus

Fig. 1 is a diagram of the apparatus. *A* is the reaction flask, which is fitted with a ground glass joint, lubricated with phosphoric acid. The purpose of the silver wire in tube *G* was to decompose hydrogen peroxide vapour. *H* is a tube containing ignited wire-form copper oxide, at a dull red heat, used to convert carbon monoxide to carbon dioxide. *I* is a tube containing lead peroxide, which is heated in an oil bath at 185° ± 5° C. The

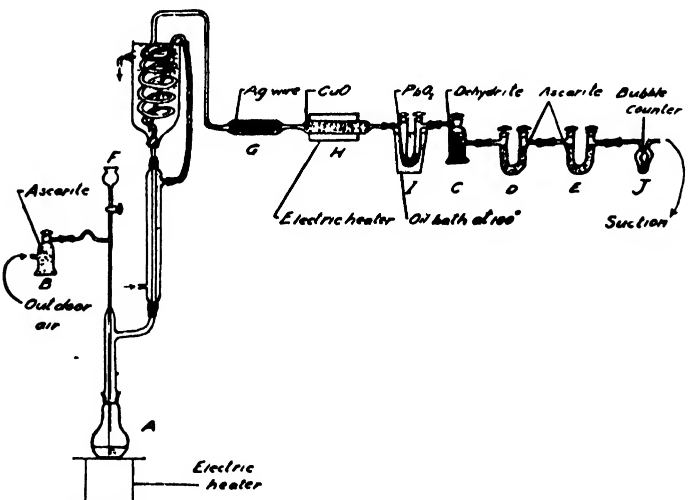

FIG. 1

lead peroxide was prepared according to Pregl's method, and was used to remove the oxides of nitrogen. Moisture was removed from the gases by tube *C*, which contains dehydrite. *D* is a weighing tube containing ascarite, and the progress of the oxidation was followed by observing the gain in weight of *D*; *E* is an ascarite tube that served as a check to determine if complete absorption of carbon dioxide was taking place in *D*. *J* is a bubble counter that gave an indication of the speed of gas flow.

In making a run, air was swept through the apparatus containing a weighed sample in *A* until the ascarite tube *D* gave a constant weight for four or five hours. The hydrogen peroxide was then added through the funnel *F*. The stopcocks at *F* and *B* were closed and the heater under *A* turned on. The evolved gases passed through the reflux condensers to the purifying train and the carbon dioxide constituent was absorbed in the ascarite tube *D*. The boiling hydrogen peroxide was coloured slightly by the red azo compound, which slowly dissolved and finally disappeared in six or seven hours. Suction was then applied at *J* and the evolved gases were slowly swept through the absorption train by allowing air to enter the system through the ascarite tube *B*. *D* was weighed at intervals and when it finally reached a constant maximum value it was concluded that oxidation was complete.

Results

Table I gives the results obtained in the oxidation of three closely related compounds. From the results listed it is clear that the first two compounds are completely oxidized by prolonged treatment with 30% hydrogen peroxide. It may be said that not all the results gave as good agreement as those listed. The unlisted results, however, showed no regularities among themselves so that it was concluded that those of Table I represent the normal results. Moreover, in most cases the anomalous results could be traced to the erratic behaviour of the lead peroxide. With a period of conditioning and proper

TABLE I

RESULTS

Run No.	Time required for weight to become constant	Weight of sample oxidized, gm.	Per cent oxidized
p-Nitro-p'-hydroxyazobenzene			
1	35 hr.	0 0567	100.5
2	30 hr.	0.0439	100 4
3	25 hr.	0.2365	98.1
4	40 hr.	0.1145	99.5
p-Hydroxyazobenzene			
5	35 hr.	0.1172	100.8
6	45 hr.	0.0849	100.7
p-Aminoazobenzene			
7	6 days	0.1279	Incomplete

temperature control of the bath surrounding the lead peroxide this difficulty was overcome. The lack in uniformity in the number of hours required for the weight to become constant is due to variation in heater temperatures and gas flow.

In order to show the progressive increase in weight of the ascarite tube, which finally reached a maximum as oxidation became complete, Table II has been included. This table gives the complete data for a typical run. The calculated gain for the ascarite tube is made on the assumption that complete oxidation to carbon dioxide occurs.

After refluxing the para aminoazobenzene for six days a small amount of a yellow solid of high melting point remained in the flask. On the other hand, the hydrogen peroxide solution left after oxidizing the other two compounds was water white and left no visible deposit on complete evaporation.

TABLE II

DATA FROM A TYPICAL RUN

No. of hours between weighings	Weight of ascarite tube, gm.	Total number of hours since adding H_2O_2
0	18 3953	
2	18.3960	
5	18.3962	
2	18 3963	
H_2O_2 *added*		
13	18.5053	13
6	18 5105	19
4	18.5147	23
5	18.5198	28
1	18.5198	29
2	18.5199	31
4	18.5200	35

Total gain in weight of ascarite tube 18.5200 − 18.3963 = 0.1237 gm.
Weight of sample oxidized, 0.0567 gm.

Calculated gain if completely oxidized $\frac{528 \times 0.0567}{243} = 0.1231$ *gm.*

Per cent oxidized $\frac{0\ 1237}{0\ 1231} = 100.5\%$.

References

1. ANGELI, A. Atti accad. Lincei, 19, Part 1 : 793-795. 1910.
2. ANGELI, A. Atti accad. Lincei, 23, Part 2 : 30-39. 1914.
3. ANGELI, A. Atti accad. Lincei, 23, Part 1 : 557-570. 1914.
4. ANGELI, A. Atti accad. Lincei, 26, Part 1 : 95-101. 1917.
5. ANGELI, A. Atti accad. Lincei, 26, Part 1 : 207-213. 1917.
6. ANGELI, A. Gazz. chim. ital. 51, Part 1 : 35-42. 1921.
7. ANGELI, A. and VALORI, B. Atti accad. Lincei, 21, Part 1 : 155-165. 1912.
8. BAMBERGER, E. Ber. 33 : 1939-1957. 1900.
9. BIGELOW, H. E. and PALMER, A. Org. Syntheses, 11 : 16-18. 1931.
10. BIGIAVI, D. Gazz. chim. ital. 57 : 555-556. 1927.

PASTURE STUDIES. XXI.

AN IMPROVED THIOCHROME METHOD FOR THE ESTIMATION OF VITAMIN B_1[1]

By W. D. McFarlane[2] and R. A. Chapman[3]

Abstract

The thiochrome method as applied to foodstuffs by Pyke (10) has been modified to permit the use of the fluorimeter described by Froman and McFarlane (3). Interfering pigments are destroyed by adding hydrogen peroxide to the "blank" and test solutions before extracting with isobutanol. Hydrogen peroxide does not oxidize thiamine to thiochrome nor does it destroy the latter. The procedure described is based on a reinvestigation of the various methods proposed for extracting thiamine from tissues and also of the optimum amount of each reagent used in the thiochrome test.

The literature contains numerous recommendations for the modification of Jansen's method (5) for the estimation of thiamine (vitamin B_1), which is based on the measurement of the intense blue-violet fluorescence of its oxidation product, thiochrome. To separate thiamine from substances that interfere in the thiochrome test, Hennessy and Cerecedo (4) employed a base-exchanging zeolite (Decalso). Although recoveries of thiamine chloride of 91 to 97% are reported (4), it has become evident that the behaviour of "Decalso" adsorption columns is erratic, so that to obtain values approaching quantitative recovery the most exacting attention must be given to technical details, and "recovery checks" must be conducted with each assay and under identical conditions. According to Jowett (7) the recovery from pure solutions of vitamin is about 68% over a wide range of concentrations, and he has concluded that the loss is due to incomplete elution of the vitamin or to its destruction during elution.

Pyke (10) has applied the thiochrome test to foodstuffs by a method that omits the adsorption step, and this procedure seemed to be most suitable for the writers' purposes, namely, to investigate the thiamine content of pasture grasses. The analysis of grass by Pyke's method was attempted but in place of the prescribed visual-titration technique the writers employed the fluorimeter described by Froman and McFarlane (3). This instrument is of the compensating two-photocell type and had previously been found to perform satisfactorily when measuring the fluorescence of thiochrome solutions prepared from thiamine chloride. However, on applying the thiochrome test to grass extracts the final butyl alcohol solution was found to have a distinct greenish-yellow colour. The absorption of light by these pigments resulted in the "total blank" (ferricyanide omitted) giving a large negative reading

[1] *Manuscript received March 3, 1941.*

Contribution from the Macdonald College Pasture Committee, Faculty of Agriculture (McGill University), Macdonald College, Que., with financial assistance from the National Research Council of Canada. Macdonald College Journal Series No. 158.

[2] *Professor of Chemistry.*

[3] *Research Assistant, Macdonald College Pasture Committee.*

when compared with the "reagent blank" (grass extract omitted). Repeated extraction with isobutanol, ethyl ether, or petrol ether, before applying the thiochrome test did not remove all the interfering pigments. Apparently some of the chromogens are extracted by isobutanol from strongly alkaline solution only, or they are formed by the action of strong alkali. Certainly their colour is intensified by alkali, and of course it is impossible to carry out a preliminary extraction with isobutanol from alkaline solution because of the known instability of thiamine. Even at pH 6 to 7, prior extraction with isobutanol resulted in some loss of thiamine; apparently, thiamine in neutral solution is slightly soluble in isobutanol. The colour of the test solution (ferricyanide added) was perceptibly less than that of the "total blank" owing to oxidation of the pigments. Furthermore, the addition of a known amount of thiochrome to the "total blank" gave a larger instrument reading than was to be expected. It was evident that the results would be too high if the estimations were made by adjusting the galvanometer to "zero" with the "total blank" and then reading the test solution; therefore, the "total blank" had to be reduced to a minimum and must not greatly exceed the reading of the "reagent blank".

Consequently, it was decided to investigate the method as applied to materials such as wheat germ, yeast, and flour, etc., the analyses of which have been reported by numerous investigators. The same difficulty was again encountered although to a lesser degree. It was found that the isobutanol extracts were colourless if hydrogen peroxide was added to the "blank" and "test" solutions before extracting with isobutanol, and the reading of the "total blank" was now virtually identical with that of the "reagent blank". This is true of all the analyses recorded in this paper, provided that methanol or ethanol is not present. Hydrogen peroxide does not oxidize thiamine to thiochrome, a fact that had previously been observed by Kinnersley, O'Brien, and Peters (8), nor does it destroy thiochrome, but in alkaline solution it rapidly oxidizes anthoxanthins and non-thiochrome fluorescing substances contained in the blank and test solutions.

The procedure that the writers are now using, as described below, is based on a reinvestigation of the various methods proposed for extracting the vitamin from tissues and also of the optimum amount of each reagent used in the thiochrome test.

Procedure

Grind solids as fine as possible to facilitate quantitative extraction of the vitamin. Transfer a 5 to 20 gm. sample, the weight depending on its thiamine content, e.g., 5 gm. of yeast or of wheat germ and 10 to 20 gm. of bread or flour, to a 250 ml. centrifuge bottle and add a 0.2% solution of pepsin in 0.33% hydrochloric acid (50 ml. to the 5 to 10 gm. sample and 75 ml. to the 20 gm. sample). Let stand for one hour, then adjust to pH 2.0 with *N* hydrochloric acid or *N* sodium hydroxide, using thymol blue as an external indicator, and incubate overnight at 37° C. Adjust to pH 4.5 with bromcresol green as an external indicator, add 0.1 gm. of takadiastase and incubate

at 37° C. for a further three to four hours. Centrifuge at maximum speed, transfer the supernatant to a 100 ml. volumetric flask and wash the residue twice with distilled water. Combine the extract and washings and dilute to volume with distilled water. At this point it may be advantageous, with some extracts, to further clarify a portion of the solution by filtering through a dry filter paper before applying the thiochrome test, which is carried out as follows:—

Pipette a 1 ml. aliquot of the extract into each of three 10 ml. graduated, glass-stoppered cylinders. The optimum amount of potassium ferricyanide in the test solutions varies according to the amount of organic matter present and, under the conditions prescribed here for 1 cc. of the extract, falls within a range of 0.1 to 0 4 ml. of a 1% solution. If 2 or 3 ml. of the extract is taken for the test, the optimum range of ferricyanide concentrations must be redetermined. To cylinders No. 1 and No. 2 add 0 2 and 0 3 ml., respectively, of a 1% aqueous solution of potassium ferricyanide. Dilute the contents of the three cylinders to 3 ml. with distilled water. Cylinder No. 3 contains no ferricyanide and acts as a blank. Add 1 ml. of 40% sodium hydroxide to each cylinder, mix thoroughly and let stand for two minutes. Add 1 ml. of 30% hydrogen peroxide, again mix thoroughly, and allow to stand for about five minutes. Add 5 ml. of isobutanol, stopper, and shake vigorously for one minute. Remove the stoppers and centrifuge at minimum speed (zero step on Q.V. circular rheostat), using the 250 ml. trunnion cups, containing the customary rubber pads. In addition, hold the cylinder in position with a No. 11 stopper bored so as to fit over the neck of the cylinder. Record the volume of the isobutanol layer.

Carry out the fluorescence measurements as follows:— Transfer a 4 ml. aliquot of each supernatant to three fluorimeter tubes (3) and add 1 ml. of 95% methanol to remove a slight turbidity due to moisture. Special care should be taken to ensure complete mixing, and the outside of the test tube should be perfectly clean. The writers have modified the procedure previously described (3) for making the readings. At least 15 min. before making a reading, switch on the ultra-violet lamp, with the galvanometer connected in the circuit. During that time a test-tube, painted inside with black enamel, is in the test-tube block and the polaroids are set at zero reading.

About five minutes before making a reading remove the blackened test tube and open the polaroids. Place tube No. 3 (which has not been treated with potassium ferricyanide) in the instrument, with the polaroids at zero and the resistance adjusted to give no deflection of the galvanometer. Replace the blank with one of the test solutions and rotate the polaroids until the galvanometer again reads zero. Record the polaroid reading and ensure that the voltage has not changed appreciably in the interim; this is done by replacing the test solution with the blank solution and observing that there is no deflection of the galvanometer at zero reading on the polaroids. If the results of the two tests do not agree closely, repeat the test making a small change in the volumes of 1% potassium ferricyanide solution. Calculate the

thiamine content of the solution by reference to a calibration curve (Fig. 1) or from the equation (3)

$$C = K' \sin^2 \theta,$$

where K' is a constant for the instrument and fluorescent substance which, by calculation from the data plotted in Fig. 1, is found to be 0.523 ± 0.021. With the higher concentrations of thiochrome, the fluorescence decreases rapidly in ultra-violet radiations and the polaroid reading should therefore not exceed 60. The observations on the thiochrome method which form the basis of this procedure are discussed below.

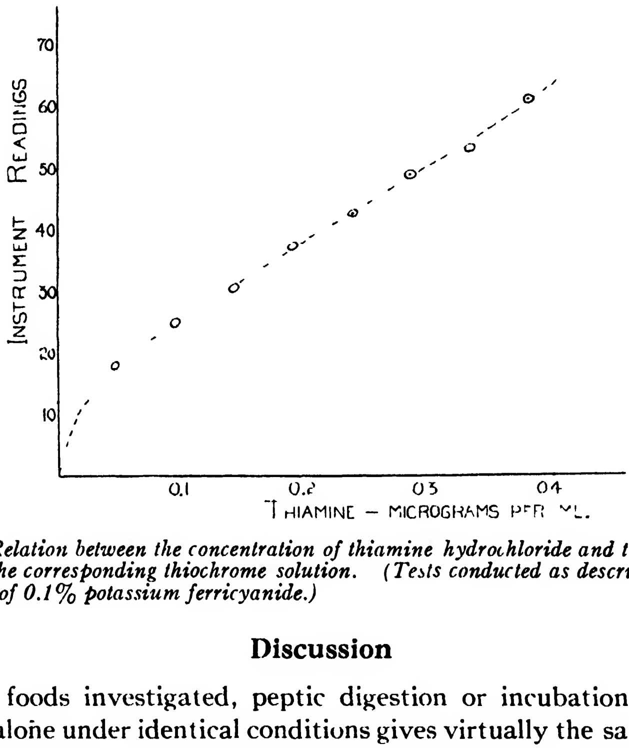

FIG. 1. *Relation between the concentration of thiamine hydrochloride and the fluorescence intensity of the corresponding thiochrome solution. (Tests conducted as described in text but with 0.2 ml. of 0.1% potassium ferricyanide.)*

Discussion

With the foods investigated, peptic digestion or incubation with hydrochloric acid alone under identical conditions gives virtually the same extraction of thiamine (Table I). Papain digestion as recommended by Emmett *et al.* (2) gives low results. These observations indicate that, in the extraction of thiamine, the pH is the important factor. However, peptic digestion may be advantageous, with some foods, as pointed out by Pyke (10), so that the simple addition of pepsin is adopted by the writers as a standard procedure. Less consistent results are obtained by refluxing and, with these products, autoclaving is definitely unsatisfactory. The data in Table I also indicate the reproducibility of the results obtained by the writers' procedure.

According to Booth (1), wheat contains little or no cocarboxylase so that, with wheat products, takadiastase digestion might be considered unnecessary. However, a clearer extract is obtained by this treatment, and it is probable that with some starchy foods it may be advantageous to use a longer digestion period than that recommended by the writers.

TABLE I

COMPARISON OF VARIOUS METHODS OF EXTRACTING THIAMINE FROM DIFFERENT MATERIALS
(Results expressed in International Units (micrograms × 3) per 100 gm.)

Method of extraction*	Dry yeast**			Wheat germ***	Special breads—Dried***	
	Number of determinations	Range	Average		*A*	*B*
I. Incubating at 37° C. for 12 hr.						
(a) Pepsin—HCl at pH 2.0	6	730–737	733	980	92	112
(b) HCl at pH 2 0	2	725–730	727	991	—	—
(c) Papain at pH 4.5	4	675–680	677	698	—	—
II. Refluxing for 1 hr.						
(a) HCl at pH 2.5	2	722	722	976	88	95
(b) CH_3COOH at pH 2.5	4	570–604	590	1023	66	90
III. Autoclaving at 120° C. for 40 min.						
H_2SO_4 at pH 3.0	2	360–397	379	446	—	—

* *Followed, in all cases, by takadiastase treatment at pH 4.5.*

** *Standard Brands Incorporated; Type 700-H; Guaranteed 600-900 I.U. per 100 gm.*

*** *Average of two determinations agreeing closely in each case. Bread A contained 5% wheat germ and Bread B was made from flour produced by a special milling process.*

In the earlier work the writers employed alcohol precipitation to reduce the organic matter content of the extracts, as suggested by Melnick and Field (9). Very satisfactory extracts are obtained when the takadiastase treatment is followed by the addition of 95% methanol to give a final concentration of 50 or 80% and provided that hydrogen peroxide is used in the thiochrome test. With yeast, wheat germ, and flour, the results are not significantly different from those obtained when the alcohol treatment is omitted. However, Johannson and Rich (6) find that in the analysis of flour this procedure greatly facilitates reading by the visual-titration technique.

Alcohol extracts of bran and grass give a large blank reading that is not satisfactorily reduced by the inclusion of hydrogen peroxide. For example, the apparent thiamine content of bran is 418 I.U. per 100 gm. when alcohol is employed and 214 when it is omitted. In the latter case, the blank reading is negligible and the value obtained is in good agreement with the average value obtained by bio-assay as recorded in the literature. This led the writers to investigate the common practice of adding alcohol in the thiochrome test, where it is said to stabilize the ferricyanide oxidation. The writers have found that the optimum amount of ferricyanide is not more critical when methyl alcohol is omitted, nor is the extraction of thiochrome by isobutanol diminished. Methyl alcohol facilitates the transfer of interfering pigments to the isobutanol layer and this is particularly evident with bran or grass extracts.

The amount of sodium hydroxide used in the test has been thoroughly investigated with extracts or pure solutions of thiamine and with varying concentrations of ferricyanide. Under the conditions of the test, maximum fluorescence is obtained with 1 ml. of 40 or 50% sodium hydroxide. Solid sodium peroxide can replace hydrogen peroxide in the test but it is less convenient. A larger amount of hydrogen peroxide than that recommended may be advantageous in some cases, but the writers have never found it advisable to reduce the amount. The test solution is extracted with an equal volume of isobutanol and the same ratio is employed in preparing the standard calibration data. Other investigators have used a larger proportion of isobutanol, usually 13 ml. to about 7 ml. of test solution. The writers have reduced the proportion of isobutanol so as to increase the sensitivity, having found that moderate variations in the ratio do not influence the amount of thiochrome extracted. The results in Fig. 1 are further evidence that, under the conditions of the test, sufficient isobutanol is being employed. The volume of extract may be varied but the amount of the reagents, including isobutanol, should be changed proportionately.

Two samples of bread analyzed by the writers' method or by a modification employing visual titration gave results that are of the same order as those obtained by bio-assay, whereas the introduction of Decalso adsorption gave results that are much lower (see Table II). This collaborative study is being

TABLE II

A COMPARISON OF THE THIAMINE CONTENT OF TWO SPECIAL BREADS* AS DETERMINED IN DIFFERENT LABORATORIES BY DIFFERENT METHODS

(Results expressed in International Units per 100 gm.)

Methods of analysis	Bread *A*	Bread *B*
Biological assay	99	113 and 130
Thiochrome method:		
(1) Decalso adsorption		
Laboratory *A*—photoelectric fluorimetry	58	78
Laboratory *B*—photoelectric fluorimetry	53	91
(2) Modified Pyke's Method		
Laboratory *C*—visual titration	86	132
Authors—photoelectric fluorimetry	92	112

* *See footnote—Table I.*

continued and extended to include other products. The writers' procedure gives equally satisfactory results (so far as the blank readings, etc., are concerned) when applied to beef liver, cabbage centre-leaves, carrots, and milk. Values of 105, 37, 36, and 15 international units of thiamine per 100 gm., respectively, were obtained; these appear reasonable when compared with the average values obtained by bio-assay as recorded in the literature.

Acknowledgments

The authors wish to thank Mr. C. E. Rich and Mr. H. Johannson, Ogilvie Flour Mills Co. Ltd., Montreal, for supplying samples and rendering other valued assistance. They are also grateful to Dr. C. A. Morrell and Mr. W. A. Crandall of the Department of Pensions and National Health, Ottawa, who conducted the bio-assays.

One of the writers (R.A.C.) is the recipient of a grant from the Macdonald College Pasture Committee through Prof. L. C. Raymond.

References

1. BOOTH, R. G. J. Soc. Chem. Ind. 59 : 181T-184T. 1940.
2. EMMETT, A. D., PEACOCK, G., and BROWN, R. A. J. Biol. Chem. 135 : 131-138. 1940.
3. FROMAN, D. K. and MCFARLANE, W. D. Can. J. Research, B, 18 : 240-245. 1940.
4. HENNESSY, D. J. and CERECEDO, L. R. J. Am. Chem. Soc. 61 : 179-183. 1939.
5. JANSEN, B. C. P. Rec. trav. chim. 55 : 1046-1052. 1936.
6. JOHANNSON, H. and RICH, C. E. Cereal Chem. (in press).
7. JOWETT, M. Biochem. J. 34 : 1348-1355. 1940.
8. KINNERSLEY, H. W., O'BRIEN, J. R., and PETERS, R. A. Biochem. J. 29 : 2369-2384. 1935.
9. MELNICK, D. and FIELD, H. J. Biol. Chem. 127 : 515-530. 1939.
10. PYKE, M. J. Soc. Chem. Ind. 58 : 338T-340T. 1939.

Canadian Journal of Research

Issued by The National Research Council of Canada

VOL. 19, SEC. B. JUNE, 1941 NUMBER 6

THE SYSTEM NAPHTHALENE-BENZENE CONSIDERED AS AN IDEAL SOLUTION[1]

By A. N. Campbell[2]

Abstract

An experimental study of the vapour pressure, and other physical properties, of an ideal system is described. Raoult's law is followed closely by benzene up to high concentrations of naphthalene. Such behaviour may be connected with the smallness of the dipole moments, although that of naphthalene is far from zero. Other physical properties investigated, viz., density, viscosity, and surface tension, show fairly close, but not exact, additive behaviour. In this respect, the behaviour is very similar to that of a system previously investigated, naphthalene–*p*-nitrophenol, where, however, the partial pressures show marked deviation from Raoult's law: this is in harmony with the (presumed) high electric moment of *p*-nitrophenol. It appears, in so far as the two systems studied are concerned, that marked deviation from Raoult's law may be associated with high dipole moment, but that this deviation does not necessarily cause any marked deviation from additivity in other physical properties not dependent on vapour pressure.

Introduction

This work was undertaken as a corollary to previous work on the system naphthalene–*p*-nitrophenol, whose behaviour was shown to be far from ideal (1). The present system was shown by Washburn and Read (6) to exhibit almost ideal behaviour. From the equation

$$d \log N/dT = \Delta H/RT^2$$

they calculated the eutectic temperature as $-3.56°$ C., against an experimental value of $-3.48°$. Using their data, the eutectic composition is calculated as 20.2% naphthalene (benzene separating) and as 21.0% (naphthalene separating), against an experimental value of about 20.2%. There is, therefore, no doubt of the ideal behaviour of this solution. The aim of this work was to exhibit this ideal behaviour in other relations. The physical properties investigated were those listed in the previous paper, with the exception of the properties previously determined by other workers.

Experimental

The heats of fusion of benzene and of naphthalene are known with considerable accuracy (Cf. International Critical Tables). The freezing point diagram has been determined by Pickering (3, pp. 1022 and 1027) and by Lee Ward

[1] *Manuscript received February 5, 1941.*
Contribution from the Department of Chemistry, University of Manitoba, Winnipeg, Man.
[2] *Associate Professor of Chemistry.*

(5, p. 1322), with results in good agreement. The heat of solution of naphthalene in benzene is almost identical with the heat of fusion of naphthalene (4), implying an almost negligible heat of mixing of the liquid components. Gehlhoff (2, p. 254) gives the heat of solution of naphthalene in benzene as -34.5 cal. per gm. (for very weak solutions) as against a heat of fusion of -35.7 cal. per gm. It was therefore not necessary to determine any of the above quantities.

Vapour Pressure

The vapour pressures of solutions of naphthalene in different concentrations in benzene over a range of temperatures were determined by a differential method described in a previous paper (1). This method could be used only up to a content of 60% naphthalene. Beyond this, the method became seriously inaccurate because the preliminary evacuation altered appreciably the concentration of a solution already rich in naphthalene. For solutions richer in naphthalene the expedient of finding the boiling point in an electrically heated Beckmann boiling point apparatus was resorted to, the barometric pressure being followed throughout the experiment.

Vapour Composition

This was not determined directly, but was calculated from the observed total vapour pressure, assuming that naphthalene obeys Raoult's law. The evidence is that in this solution naphthalene does obey Raoult's law, but, even if it deviated considerably, the error involved in the calculation is much smaller than that of any experimental determination.

Density, Viscosity, and Surface Tension

These were determined by the standard methods, mentioned in the previous paper (1), at 79.5° C.

Results

The vapour pressure of pure benzene, in terms of the Clausius-Clapeyron equation, is expressed by the equation

$$\log_{10} p_{mm.} = \frac{-0.05223\,A}{T} + B,$$

where A and B have the values, respectively, 32,295 and 7.6546, for the range 42° to 100° C. (Int. Crit. Tables). To save space, the extensive experimental results for solutions of naphthalene in benzene are expressed in the same form in Table I, by simply reproducing the constants A and B. This table also gives the value of the ratio $\frac{p_{solution}}{p_{benzene}}$ for 80°, which, in terms of Raoult's law, is equal to the mole fraction of benzene, if the partial pressure of naphthalene be neglected, as can be done with the more dilute solutions; the term Δn represents the deviation of this ratio from the mole fraction as calculated from the weight composition. The values of A and B apply to the range of measurement, viz., from the temperature of homogeneity to about 80°.

TABLE I

RESULTS OBTAINED WITH SOLUTIONS OF NAPHTHALENE IN BENZENE

Wt. % naphthalene	Mole fraction of benzene	A	B	p'/p	Δn, %
11.2	0.929	32300	7.6168	0.918	−1.2
24.2	0.8375	31300	7.4006	0.787	−6.1
32.7	0.769	30900	7.3071	0.730	−5.1
43.3	0.683	30500	7.2136	0 692	+1.3
53.8	0.585	33400	7.5921	0.600	+2.6

The value of A is not constant, as perhaps it should be, since it represents essentially the latent heat of evaporation of benzene from solution. If A be constant the observed variations in A then represent the experimental error, viz., about 5%. It is doubtful, however, whether A is really constant, since the temperature coefficient of heat of evaporation may not be the same for solutions of different naphthalene content. Assuming that A is constant at the value of pure benzene (32,295), the figures in Table II are obtained.

TABLE II

VALUES OBTAINED ON THE ASSUMPTION THAT A IS CONSTANT AND EQUAL TO 32,295

Wt. % naphthalene	Mole fraction of benzene	B	p'/p	Δn, %
11.2	0.929	7.6168	0.918	−1.2
24.2	0.8375	7.6006	0.842	+0.9
32.7	0.769	7.5511	0.740	−3.8
43.3	0.683	7.4836	0.643	−6.7
53.8	0.585	7.4321	0.573	−2.0

By the boiling point method, the figures in Table III were obtained.

TABLE III

RESULTS OBTAINED WITH BOILING POINT METHOD

Wt. % naphthalene	Mole fraction of benzene	Boiling point, °C.	P	p'	p	n	Δn, %
50.0	0.620	95.4	738.1	4.9	733.2	0.615	−0.8
60.0	0.523	102.6	745.9	9.2	736.7	0.507	−3.1
70.0	0.413	112.0	742.9	17.9	725.0	0.394	−4.6
80.0	0.293	124.6	741.7	32.7	709.0	0.274	−6.2
90.0	0.155	148.8	738.7	91.4	647.3	0.144	−7.4

NOTE: *P = barometric pressure, p' = partial pressure of naphthalene (calculated from Raoult's law), p = partial pressure of benzene = $P - p'$, $n = \frac{p_{\text{benzene in solution}}}{p_{\text{pure benzene}}}$ and Δn = the deviation of this calculated value of mole fraction from that calculated from weight composition.*

On the assumption that the latent heat of evaporation of benzene is constant and equal to 32,295, it is possible to calculate B values from the boiling point experiments, with the results shown in Table IV.

TABLE IV

RESULTS OBTAINED ON ASSUMPTION THAT LATENT HEAT OF BENZENE IS CONSTANT AND EQUAL TO 32,295

Naphthalene, %	50.0	60.0	70.0	80.0	90.0
B	7.4651	7.3673	7.2403	7.0906	6.8311

For the purpose of constructing the complete equilibrium diagram (Fig. 1), the equilibrium temperatures corresponding to the compositions used in the vapour pressure determinations have been read from the plotted data of Pickering (3, pp. 1022 and 1027) and of Ward (5, p. 1322): for these temperatures the vapour pressures, total and partial, have been calculated, as well as the vapour composition.

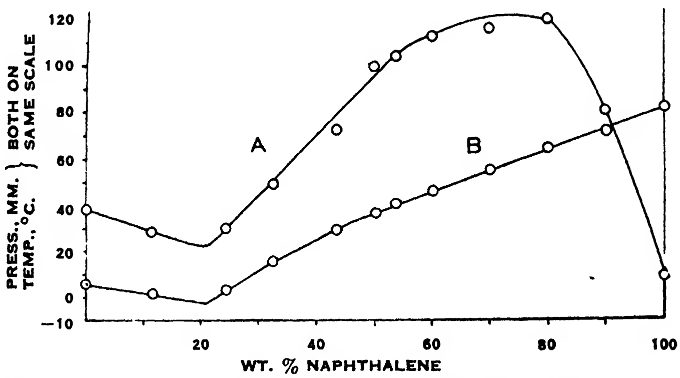

FIG. 1. *Freezing point diagram of system naphthalene-benzene: equilibrium concentrations and pressures. Curve A—vapour pressure; Curve B—equilibrium temperature.*

TABLE V

VAPOUR PRESSURES AND VAPOUR COMPOSITION AT VARIOUS EQUILIBRIUM TEMPERATURES

Wt. % naphthalene	t, °C.	P	p'	p	Per cent naphthalene in vapour
11.2	1.0	27.98	0.00495	27.98	0.0291
24.2	3.0	29.55	0.0112	29.54	0.0618
32.7	15.0	47.99	0.0501	47.94	0.171
43.3	28.0	71.39	0.112	71.28	0.257
50.0	36.0	98.88	0.251	98.63	0.416
53.8	40.0	102.8	0.355	102.4	0.563
60.0	45.0	111.5	0.537	111.0	0.875
70.0	54.0	114.9	1.12	113.8	1.59
80.0	64.0	117.7	2.24	115.5	3.09
90.0	71.0	79.63	3.98	75.6	7.98
100.0	80.0	7.94	7.94	0.0	100.0

The figures obtained for density and molecular volume are contained in Table VI: ΔV represents the deviation from additivity.

TABLE VI

DENSITY AND MOLECULAR VOLUME

Naphthalene, %	$d_{4°}^{79.5°}$	Mol. volume, cc.	ΔV, %
*0.00	0.8154	95.7	—
10.0	0.8267	98.3	+0.39
20.0	0.8390	100.9	+0.57
30.0	0.8551	103.4	+0.39
40.0	0.8738	105.9	+0.05
50.0	0.8896	109.0	−0.02
60.0	0.9076	112.3	−0.16
70.0	0.9236	116.3	−0.03
80.0	0.9424	120.5	−0.12
90.0	0.9598	125.4	−0.06
100.0	0.9779	131.0	—

* *Not determined: taken from International Critical Tables.*

The values of viscosity and surface tension are incorporated in Table VII. The temperature of determination was 79.5° C.

TABLE VII

VISCOSITY AND SURFACE TENSION

Naphthalene, %	Viscosity, poises	S.T., dynes/cm.	Naphthalene, %	Viscosity, poises	S.T., dynes/cm.
0.00	0.00321	—	50.0	0.00520	27.80
10.0	0.00347	22.68	60.0	0.00590	29.20
20.0	0.00385	23.42	70.0	0.00662	30.44
30.0	0.00412	25.00	80.0	0.00765	31.70
40.0	0.00462	26.70	90.0	0.00837	33.00

It was attempted to determine the dielectric constants of solutions of *p*-nitrophenol in benzene with a view to determining the electric moment of *p*-nitrophenol. As a preliminary to this work, the solubility of *p*-nitrophenol in benzene was determined at 30.3° C. It was found to be 2.68 gm. per 100 gm. of benzene. With the available apparatus, however, it was not possible to make the determination of the dielectric constant with accuracy, even in very dilute solution, owing to the high dielectric loss. The mere existence of this dielectric loss, however, is an indication that the dielectric constant and dipole moment of *p*-nitrophenol are high. The dipole moments of benzene and naphthalene are known (8).

Discussion of Results

When the observed values of $\log_{10} 100\,N$ (from the equilibrium figures of Pickering (3, pp. 1022 and 1027) and of Ward (5, p. 1322)) and the values of $\log_{10} 100\,N$ calculated from the ideal equation:—

$$\log_{10}N = \frac{\Delta H}{4.579}\left\{\frac{T_0 - T}{T_0T}\right\}$$

are plotted against $1000/T$, straight lines of almost identical slope are obtained. The agreement in so far as benzene is concerned is extremely good, indicating that the heat of mixing is zero, or, in other words, that the heat of solution of solid benzene in a solution of benzene in naphthalene equals the heat of fusion of benzene. As regards naphthalene the agreement, though good, shows a small deviation in the sense that the calculated value is almost always slightly lower (maximum deviation at the eutectic = 5.5%) than the observed value. If the calculation is repeated for naphthalene, using instead of the heat of fusion, Gehlhoff's (2) value for the heat of solution, the agreement is better, giving a maximum deviation of 3.5% at the highest concentration of benzene.

Considering the figures for the partial pressures of benzene in solutions of naphthalene in benzene in the light of Raoult's law, it may be said that the deviation from Raoult's law does not exceed 5% up to a concentration of 70% naphthalene, and does not exceed 7.4% at 90.0% naphthalene. The experimental error is assessed as a ±5% (a maximum value), so that the above are limiting values. Probably the actual deviation is less than the limits set. The sign of the deviation is negative, i.e., the observed partial pressure is less than the calculated. For a concentration of 20% naphthalene (benzene solid phase) and an equilibrium temperature of −3.5° C., the vapour pressure of solid benzene is calculated (from the data of the International Critical Tables) to be 18.92 mm., and that of liquid benzene as 21.94 mm., i.e. an apparent mole fraction of 0.860 as compared with 0.8685 from weight composition. This gives a deviation of −0.93%. A similar calculation can be made for the naphthalene side of the diagram, using the data of the International Critical Tables: the constants of the equation for liquid naphthalene were evaluated in the previous paper (1). The constants of this equation have been recalculated as:— A = 47,360, B = 7.9012. When this is done, the deviation from Raoult's law is negligible up to 20% benzene (equilibrium temperature = 64°), but after that increases to an apparent value of about −50% at the eutectic. This figure obviously does not represent the truth, in view of the results of Washburn and Read (6). The discrepancy is almost certainly due to the attempt to apply the Clausius-Clapeyron equation over too great a range (in the case of liquid naphthalene); in other words, the heat of evaporation of liquid naphthalene at a temperature about 80° below the freezing point is not the same as it is above the freezing point. The calculation of Washburn and Read (6) shows that the partial pressure of naphthalene must obey Raoult's law almost equally well with that of benzene.

Little comment is necessary on the density determinations, except to say that there is definitely a slight expansion (mean value = 0.35%) in solutions containing from 0 to 40% naphthalene, which then changes to a slight contraction for higher concentrations of naphthalene (mean value = 0.08%).

International Critical Tables give figures for the viscosity of solutions of naphthalene in benzene at 25° C., of concentrations from 0 to 37.69% naphthalene. When plotted against mole fraction these figures give an almost straight line relation: the fluidity plot has a slight convexity to the axis of concentration. Similar plotting of the experimental results of this paper, for 79.5° C. and the whole range of composition, gives a slight but distinct S-curve: solutions of mole fraction of naphthalene less than 0.55 are less viscous, solutions of mole fraction greater than 0.55 more viscous, than the mixture rule requires. The fluidity curve is smooth with slight convexity towards the axis of concentration.

The curve of surface tension against mole fraction of naphthalene is slightly concave towards the axis of concentration.

According to Williams and Ogg (8), the electric moments of benzene and naphthalene are respectively 0.085 and 0.705. Both values are low, and this is no doubt connected with the ideal behaviour of the solutions. It was found impossible, with the apparatus available, to determine the dipole moment of *p*-nitrophenol experimentally, but it can be calculated with some accuracy. According to Williams (7), the dipole moment of a benzene molecule substituted in the para-position can be calculated additively, provided that the substituents are not too complicated in nature. He gives a table of group moments from which the values are taken:— $OH = -1.7 \times 10^{-18}$ and $NO_2 = -3.9 \times 10^{-18}$. From this, the dipole moment of *p*-nitrophenol results as:— $-1.7 - (-3.9) = 2.2 \times 10^{-18}$. This is an average high value and no doubt accounts for the much greater deviation of the system *p*-nitrophenol–naphthalene from Raoult's law (1).

A general conclusion from the study of only two systems would be unjustifiable, but the following observations may be made:

1. Pronounced deviations from Raoult's law are observed in the system, one of whose components has a high dipole moment.

2. Ideal behaviour is observed in the system, both of whose components have a small dipole moment, one being almost zero.

3. Pronounced deviations from Raoult's law and derived equations are not necessarily associated with marked departure from additivity in regard to other physical properties.

References

1. Campbell, A. N. and Campbell, A. J. R. Can. J. Research, B, 19 : 73-85. 1941.
2. Gehlhoff, G. Z. physik. Chem. 98 : 252-259. 1921.
3. Pickering, S. U. J. Chem. Soc. 63 : 998-1027. 1893.
4. Timofejew, W. Chem. Centr. 76 (2) : 429-438. 1905.
5. Ward, H. L. J. Phys. Chem. 30 : 1316-1333. 1926.
6. Washburn, E. W. and Read, J. W. Proc. Nat. Acad. Sci. U.S. 1 : 191-195. 1915.
7. Williams, J. W. J. Am. Chem. Soc. 50 : 2350-2357. 1928.
8. Williams, J. W. and Ogg, E. F. J. Am. Chem. Soc. 50 : 94-101. 1928.

SYNTHESIS OF 4-HYDROXY-3-METHOXYMANDELAMIDE[1]

BY HARRY SCHWARTZ[2] AND JOSEPH L. MCCARTHY[3]

Abstract

4-Hydroxy-3-methoxymandelamide was synthesized from vanillin through the cyanohydrin, the imino ether hydrochloride, and the ethyl ester. Its dibenzoate was prepared from vanillin cyanohydrin dibenzoate by the method of Albert.

The substance 4-hydroxy-3-methoxymandelamide, required as an intermediate in the preparation of hydroxyketones by the Grignard reaction, could not be synthesized directly but was finally prepared, after considerable experimentation as to proper conditions, from vanillin by its conversion successively through vanillin cyanohydrin, the imino ether hydrochloride, and the ethyl ester.

Vanillin cyanohydrin, prepared by the method of Buck (4), was not isolated in crystalline form for the preparation of the imino ether hydrochloride, but was kept in ether solution and the latter treated with ethanol-hydrochloric acid. It was found that when the cyanohydrin is isolated in crystalline form and then treated with ethanol-hydrochloric acid, the yield of the ethyl ester is extremely low (3·5%), presumably owing to decomposition of the cyanohydrin into vanillin and hydrogen cyanide on exposure to the atmosphere

When the *p*-hydroxyl group of vanillin cyanohydrin is blocked, a substituted derivative of the required amide can be obtained directly. Thus vanillin was treated with potassium cyanide and benzoyl chloride to yield stable vanillin cyanohydrin dibenzoate, a product previously described by Aloy and Rabaut (2). Using the method of Albert (1), the conversion in good yield to the amide dibenzoate was accomplished by refluxing the cyanohydrin derivative with zinc oxide and acetic acid for two hours, instead for one-half hour as recommended by Albert (1). However, the method of Hahn, Stiehl, and Schulz (5) for converting acetyl aryl cyanohydrins of methyl vanillin, isovanillin, and piperonyl into α-chloroacetamides by treatment with anhydrous hydrogen chloride in ether-benzene solution is apparently not applicable to diacetylated vanillin cyanohydrin; this is a good example of the peculiarities encountered in the study of vanillin derivatives as compared with those of other *p*-substituted benzaldehydes (3).

Somewhat surprisingly, neither of the substances, under the conditions employed, could be converted by the Grignard reaction to its corresponding guaiacyl acetyl carbinol derivative.

[1] *Manuscript received in original form November 7, 1940, and as revised, May 8, 1941.*
Contribution from the Division of Industrial and Cellulose Chemistry, McGill University, Montreal, Que.

[2] *Postdoctorate Research Assistant, Division of Industrial and Cellulose Chemistry, McGill University.*

[3] *Sessional Lecturer, McGill University, and holder of a Canada Paper Company Fellowship.*

Experimental

Preparation of Ethyl 4-Hydroxy-3-methoxymandelate

An ether solution (250 cc.) of vanillin cyanohydrin, prepared from 100 gm. of vanillin by the method of Buck (4), was treated with dry ethanol (20 cc.) and anhydrous hydrogen chloride (10 gm.) dissolved in anhydrous ether (50 cc.). On standing overnight at 10° C., the yellowish white salt of the imino ether hydrochloride settled out. The supernatant liquid was decanted off and the salt washed once with anhydrous ether, then hydrolysed as follows: It was dissolved in water (1500 cc.) containing an excess of calcium carbonate, filtered from any insoluble material, made just acid to litmus paper, and then allowed to stand at room temperature for three hours. The solution was then continuously extracted with ether, the ether solution extracted once with saturated sodium bisulphite and twice with saturated sodium bicarbonate solution, dried over calcium chloride, and then the ether was removed under reduced pressure. The residual dark yellow oil was distilled under vacuum. The ester fraction (150 to 170° C. (1 mm.)) was collected, crystallized by scratching, and recrystallized from benzene-petroleum ether. Yield, 25% based on the weight of vanillin taken; m.p., 75 to 77° C.*; mixed m.p. with vanillin cyanohydrin, 55 to 67° C. Found: Alkoxyl (as methoxyl) (6), 26·8%. Calc. for $C_{11}H_{14}O_5$: Alkoxyl (as methoxyl), 27·40%.

Preparation of 4-Hydroxy-3-methoxymandelamide

Ethyl 4-hydroxy-3-methoxymandelate (21 gm.) was dissolved in a minimum amount of ethanol, cooled to 0° C., saturated with anhydrous ammonia gas, and allowed to stand at 0° C. for four days, when the amide (8·6 gm.) settled out. After a further seven days at 0° C., more material (3·2 gm.) separated. Total yield of the amide, 65%. The product was ground in a mortar with ether and recrystallized twice from dioxane-petroleum ether (b.p. 60 to 70° C.) and twice from ethanol; m.p., 136·5 to 137·5° C. Found: C, 54·94; H, 5·83; N (Kjeldahl), 6·9; OCH_3 , 16·0%. Calc. for $C_9H_{11}O_4N$: C, 54·82; H, 5·58; N, 7·1; OCH_3 , 15·76%.

Preparation of 4-Hydroxy-3-methoxymandelamide Dibenzoate

To vanillin cyanohydrin dibenzoate (2 gm., m.p. 145 to 146·5° C.), prepared in 23% yield by the method of Aloy and Rabaut (2), was added zinc oxide (1 gm.), glacial acetic acid (10 cc.), and water (2 cc.), and the mixture refluxed for two hours. The solution was poured into water (250 cc.), and the resulting precipitate was filtered off and recrystallized from ethanol. Yield, 80%; m.p., 176·5 to 177·5° C. Found: OCH_3, 7·8; N (Kjeldahl), 3·40%. Calc. for $C_{23}H_{19}O_6N$: OCH_3 , 7·71; N, 3·45%.

Action of Methyl Magnesium Iodide on 4-Hydroxy-3-methoxymandelamide and its Dibenzoate

4-Hydroxy-3-methoxymandelamide dibenzoate (1 mole) in benzene suspension was added to an ether solution of methyl magnesium iodide (4 moles),

* *Melting points are uncorrected.*

and the suspension refluxed for five hours. Ten per cent sulphuric acid was added, the aqueous layer extracted with ether, and the latter then combined with the benzene layer. This ether-benzene solution yielded a sodium bicarbonate fraction from which benzoic acid was isolated and identified. On evaporation of the residual solution to dryness, there was obtained a dark coloured oil, which did not yield the desired ketone fraction on distillation. When free 4-hydroxy-3-methoxymandelamide was treated with methyl magnesium iodide (using a 5 to 1 ratio of Grignard reagent to amide) and the reaction mixture examined in the same way as described for the dibenzoylated amide, again the expected ketone was not obtained.

Acknowledgment

The authors appreciate the advice and encouragement given by Prof. Harold Hibbert of McGill University.

References

1. ALBERT, A. Ber. 49 : 1382-1385. 1916.
2. ALOY, J. and RABAUT, C. Bull. soc. chim. 11 : 389-393. 1912.
3. BRICKMAN, L., HAWKINS, W. L., and HIBBERT, H. Can. J. Research, B, 19 : 24-33. 1941.
4. BUCK, J. S. J. Am. Chem. Soc. 55 : 3388-3390. 1933.
5. HAHN, G., STIEHL, K., and SCHULZ, H. J. Ber. 72 : 1291-1301. 1939.
6. VIEBÖCK, F. and SCHWAPPACH, A. Ber. 63 : 2818-2823. 1930.

Canadian Journal of Research

Issued by THE NATIONAL RESEARCH COUNCIL OF CANADA

VOL. 19, SEC. B. JULY, 1941 NUMBER 7

THE EFFECT OF DISHWASHING COMPOUNDS ON ALUMINUM[1]

BY J. F. J. THOMAS[2]

Abstract

Several proprietary dishwashing compounds, in ½% solution, were found to appreciably attack commercial aluminum and aluminum utensils. Curves are shown illustrating also the corrosive effect on commercial aluminum (2S½H) of ½% aqueous mixtures, in various proportions, of the salts usually present in such compounds. Sodium metasilicate was found to be a more efficient inhibitor than either trisodium phosphate or sodium pyrophosphate. Replacement of the soda ash by either trisodium phosphate or sodium pyrophosphate so as to give a final soda ash content of 40 to 45% was required before less sodium metasilicate than about 20% produced inhibition of the attack. The author concludes that the addition of about 25% sodium metasilicate to such proprietary compounds is advisable.

Proprietary compounds have been used for the washing of aluminum utensils. These compounds appear to be mixtures in various proportions of sodium carbonate, sodium metasilicate, trisodium phosphate, and sodium pyrophosphate. This investigation was made in order to ascertain the corrosive effect on aluminum of the several components usually present in such proprietary compounds.

Panels of ordinary commercial aluminum (2S½H) and of three brands of aluminum kitchen utensils were tested by total immersion in aqueous solutions of the compounds and of mixtures of the mentioned salts at 60 ± 2° C. for one hour. The strength of the aqueous solutions was ½% by weight of the compound, which is the strength commonly used in practice. Unless otherwise stated, the ratio of the area of exposed metal to the volume of the test solution was 2 sq. dm. per litre. All the panels, except those cut from the kitchen utensils, which were tested as received, were etched for two minutes in an aqueous 10% sodium hydroxide solution prior to testing. These conditions of test procedure were determined in preliminary work.

Results are shown in Figs. 1 to 9. In Fig. 1 are given some results obtained with the kitchen utensils, using proprietary compounds. The loss in weight of the panels is plotted against the time of exposure. Figs. 2 to 9 inclusive illustrate the corrosive attack of different mixtures of the salts on commercial aluminum. The abscissa shows the proportion by weight of each salt in the

[1] *Manuscript received April 29, 1941.*
Contribution from the Division of Chemistry, National Research Laboratories, Ottawa, Canada. Issued as N.R.C. No. 1003.

[2] *Chemist.*

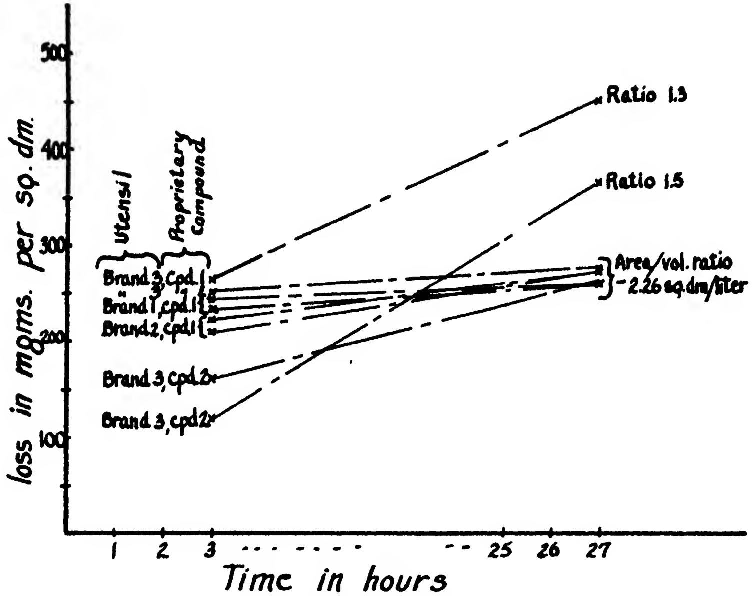

FIG. 1. *The effect of dishwashing compounds on aluminum utensils.*

½% solution. Many of the points plotted represent check results of four or five tests.

In Fig. 1 little difference in attack is found with the three different brands of utensils using the same proprietary compound. However, a change in the slope of the curve of weight-loss against time is found when using the same utensil but different proprietary compounds, although the total attack after considerable time has elapsed is approximately the same. The effect of a change in the ratio of the area of exposed metal to the volume of the solution is also shown; the slope of the curve changes. The total attack increases markedly with a decreasing ratio with both proprietary compounds.

The attack, with various mixtures of soda ash and trisodium phosphate (Fig. 2), shows that, in general, increasing percentages of trisodium phosphate typically decrease the attack by the soda ash.

Fig. 3 indicates the effect of increasing percentages of sodium metasilicate on the attack by soda ash. It will be noted that the attack diminishes very rapidly until at about 20% and greater proportions of sodium metasilicate the attack is practically zero. The results obtained with Brand 2 kitchen utensil also followed this general curve and also the curves in Figs. 5 and 6.

The attack with mixtures of trisodium phosphate and sodium metasilicate is found to be at no time appreciable (Fig. 4), but it is evident from Figs. 2, 3, and 4 that sodium metasilicate is a more efficient inhibitor than trisodium phosphate.

The effect of mixtures of soda ash, with various equal proportions of sodium metasilicate and trisodium phosphate added, is shown in Fig. 5. Again, 20%

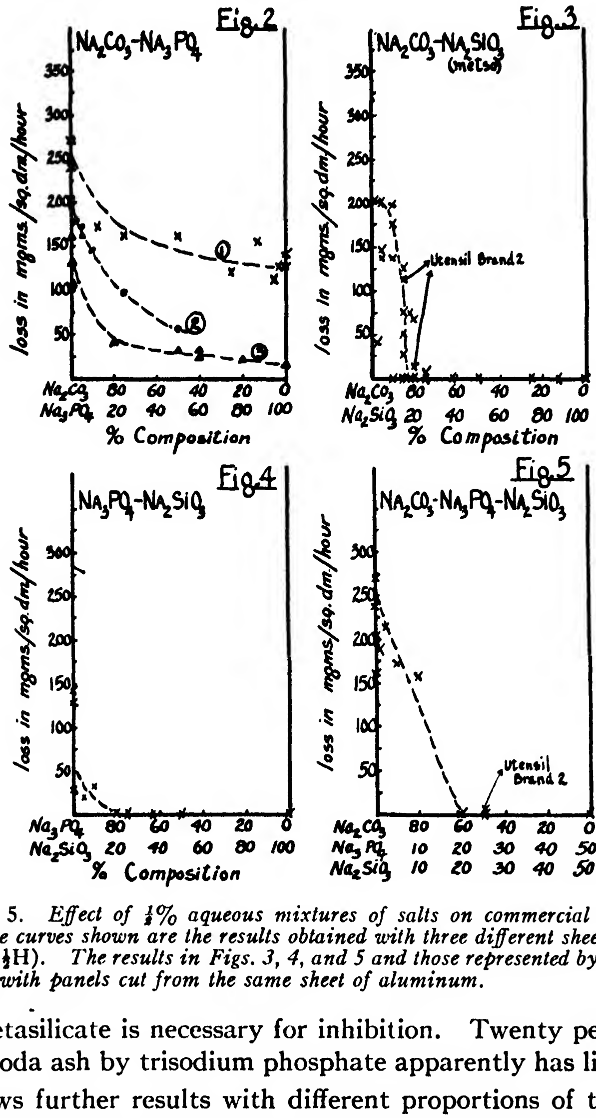

FIGS. 2 TO 5. *Effect of ½% aqueous mixtures of salts on commercial aluminum. In Fig. 2 the three curves shown are the results obtained with three different sheets of commercial aluminum* (2S½H). *The results in Figs. 3, 4, and 5 and those represented by Curve 1, Fig. 2, were obtained with panels cut from the same sheet of aluminum.*

of sodium metasilicate is necessary for inhibition. Twenty per cent replacement of the soda ash by trisodium phosphate apparently has little effect.

Fig. 6 shows further results with different proportions of these salts. In these mixtures larger amounts of the soda ash are replaced by trisodium phosphate, but again it is found that 20% or more of the metasilicate is necessary to inhibit attack, despite the fact that the concentration of the aggressive soda ash is lowered to 40% of the mixture.

The inhibitive efficiency of sodium pyrophosphate is shown in Fig. 7. The curve is similar to that obtained with trisodium phosphate. Mixtures of sodium pyrophosphate and sodium metasilicate, containing very small percentages of metasilicate (Fig. 8), show no appreciable action on aluminum; in fact, a slight gain in weight was usually found.

The effect of various mixtures of soda ash, sodium pyrophosphate, and sodium metasilicate is shown in Fig. 9, which confirms the conclusion that not

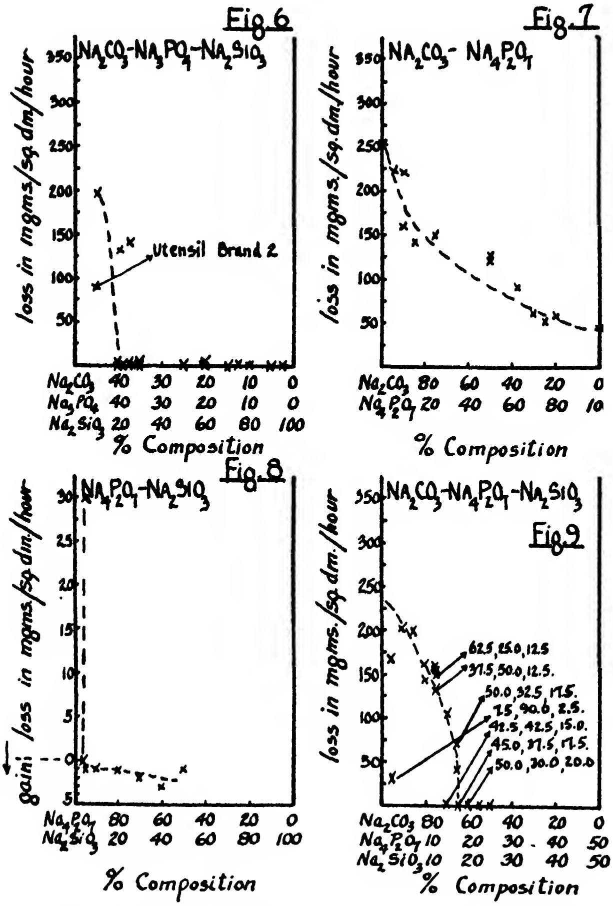

FIGS. 6 TO 9. *Effect of ½% aqueous mixtures of salts on commercial aluminum. These results and those represented by Curve 1, Fig. 2, were obtained with panels cut from the same sheet of aluminum. In Fig. 9, the inserted numbers, e.g., 62.5, 25.0, and 12.5, refer to the percentage composition of the test solution with which the indicated point was obtained, i.e., 62.5% sodium carbonate, 25.0% sodium pyrophosphate, and 12.5% sodium metasilicate.*

less than 20% of the metasilicate is necessary to inhibit all attack. Results obtained with various odd mixtures of these salts are plotted, and it is seen that in general 20% of the metasilicate is necessary to inhibit attack except when the soda ash is replaced by pyrophosphate until only about 40 to 45% of the soda ash remains.

Summary

It is indicated that several of the proprietary compounds tested showed appreciable attack on kitchen utensils in short periods of time under the mentioned test conditions. These test conditions were found to give fairly reproducible results.

Trisodium phosphate, sodium pyrophosphate, and sodium metasilicate were all inhibitors of attack on aluminum by sodium carbonate solution, the metasilicate being more efficient than the phosphates.

It was found that discoloration of the panels gave no indication of the degree of attack.

Different sheets of the 2S½H aluminum gave slightly different weight-losses under otherwise constant conditions.

Since in the curves of Figs. 3, 5, and 9 the rate of change in loss in weight is greatest in the range of substantially 15 to 20% of sodium metasilicate and since amounts of 25% gave practically no weight-loss, it appears logical to conclude that in all proprietary washing compounds of the type mentioned for aluminum a sodium metasilicate content greater than 20% is advisable.

CONTRIBUTION À L'ÉTUDE DES SEMICARBAZIDES δ-SUBSTITUÉES[1]

I. SYNTHÈSE DE QUELQUES DÉRIVÉS

PAR ROGER BARRÉ[2] ET LUCIEN PICHÉ[3]

Sommaire

Afin d'étudier l'influence des substitutions aromatiques sur la réactivité de la semicarbazide avec les aldéhydes et les cétones et sur les propriétés des semicarbazones correspondantes, nous avons préparé quelques semicarbazides δ-substituées. Connaissant l'insolubilisation qui résulte généralement de la nitration des hydrazones, des osazones et des semicarbazones elles-mêmes, nous avons surtout préparé des dérivés nitrés de la phényl-4-semicarbazide: *p*-nitrophényl, 2,4-dinitrophényl, *p*-nitrobenzyl et *p*-nitroxényl-4-semicarbazides.

Nous donnons présentement une description de la synthèse de ces dérivés et nous y joignons une discussion du mécanisme probable de formation des semicarbazides δ-substituées. En nous basant sur les données de la théorie des capacités affinitaires, telles qu'énoncées par Meerwein et précisées par Tiffeneau, nous avons interprété les rendements que nous avons obtenus dans nos synthèses ainsi que ceux qui ont été rapportés par d'autres auteurs. Ces rendements sont en accord constant avec la classification usuelle des radicaux organiques par ordre de capacités affinitaires croissantes, et ils nous amènent à proposer l'équation suivante comme réaction type des amines sur l'urée:—

$$R\text{—}NH_2 + \begin{matrix}H\\ \\ H\end{matrix}\!\!>N\text{—}CO\text{—}NH_2 \rightarrow R\text{—}NH\text{—}CO\text{—}NH_2 + NH_3$$

Cette équation s'applique aussi à la réaction des amines sur l'acétone-semicarbazone ainsi qu'à la réaction de l'hydrazine sur les urées substituées. L'ammoniac libéré au cours de la condensation proviendrait par conséquent de l'amine; il n'est donc pas fourni par voie d'isomérisation préalable de l'urée, comme le veulent les interprétations actuelles de ces réactions.

La théorie dite du "réarrangement" de l'urée et des urées substituées ne rend pas compte des rendements anormaux que nous avons parfois obtenus et qui ont été observés par ceux même qui proposent cette interprétation. Au contraire, l'équation que nous proposons en nous basant sur la théorie des capacités affinitaires, fournit une interprétation générale, conforme aux faits observés et ne donnant lieu à aucune exception.

Introduction

En prévision de l'application d'un dérivé de la semicarbazide à des essais de précipitation quantitative du glucose, nous avons voulu étudier l'influence des substitutions aromatiques sur la réactivité de la semicarbazide et sur les propriétés des semicarbazones correspondantes.

Nous avons préféré préparer les dérivés de la position δ (ou 4) de la semicarbazide: $\underset{\alpha}{\overset{1}{N}}H_2\text{—}\underset{\beta}{\overset{2}{N}}H\text{—}\underset{\gamma}{\overset{3}{C}}O\text{—}\underset{\delta}{\overset{4}{N}}H\text{—}Ar$ de préférence aux dérivés des autres positions parce qu'ils conviennent particulièrement bien à l'étude que nous

[1] *Manuscrit original reçu le 10 avril 1941, et sous forme revisée le 17 mai 1941.*

Contribution de l'Institut de Chimie de la Faculté des Sciences, Université de Montréal, Montréal, Qué.

[2] *Professeur titulaire de Chimie organique.*

[3] *Chargé de cours en Chimie générale.* *Boursier du Conseil National de Recherches (Bursary 1936–37; Studentship 1937–38).*

nous proposons: en effet, c'est par l'intermédiaire des hydrogènes du groupement aminé α que la semicarbazide fournit, avec les aldéhydes et les cétones, les semicarbazones si précieuses en analyse organique parce qu'elles se forment facilement, sont peu solubles, bien cristallisées et parce qu'elles sont facilement hydrolysables. Or non seulement la substitution sur la position δ conserve-t-elle cette aptitude réactionnelle du groupe α, mais il nous a semblé qu'elle pouvait permettre de l'amplifier très avantageusement.

Guidés par les notions de capacités affinitaires variables des radicaux organiques et de distribution alternée des forces d'attache entre les éléments d'une chaîne carbonée, nous avons cherché à amplifier ces caractères de la position α par des substitutions aromatiques, tout en apportant par des groupes secondaires de substitution (particulièrement des groupes NO_2), des particularités intéressantes au point de vue analytique: insolubilité des semicarbazones, élévation de leurs points de fusion, etc.

Le mécanisme de l'alternance des forces d'attache, auquel nous venons de faire allusion, est celui que suppose la théorie des relations interatomiques basées sur les capacitées affinitaires variables des radicaux organiques; ce mode de représentation des formules organiques permet, surtout sous la forme généralisée que lui ont donnée Meerwein, Swarts (14), Tiffeneau et Orékhoff (16, 17), de prévoir le sens d'un grand nombre de réactions, de modifier le rendement de certaines autres et même, dans plusieurs cas, d'expliquer des réactions qui pourraient sans elle paraître anormales. Nous aurons recours à ce procédé non seulement pour tenter d'expliquer le mécanisme des réactions de synthèse des semicarbazides, mais pour interpréter aussi l'influence des substitutions organiques sur leur réactivité.

Or les dérivés nitrés de la phényl-4-semicarbazide sont encore peu connus; nous avons ainsi synthétisé quelques semicarbazides δ-substituées qui n'étaient pas jusqu'ici connues; ces synthèses feront le sujet de la première partie de notre communication; nous y joindrons une discussion du mécanisme probable de formation des semicarbazides δ-substituées, discussion basée sur le rendement des synthèses que nous avons réalisées ou sur les résultats obtenus par d'autres auteurs.

Partie expérimentale

1. Préparation de la *p*-nitrophényl-4-semicarbazide

Trois procédés nous ont fourni ce dérivé de la semicarbazide que Wheeler et Walker (22) ont déjà tenté en vain de préparer:

A. Par condensation de p-nitrophénylurée avec l'hydrazine

Ce procédé suppose, comme phase préliminaire, la préparation de *p*-nitrophénylurée, déjà décrite par Pierron (10), mais que Wheeler et Walker n'ont pas pu obtenir; nous avons nous-mêmes connu des échecs répétés en tâchant de l'obtenir par application des principes de substitution de l'urée par les amines, principes qui ont été énoncés par Davis, Blanchard et Underwood (3, 4).

C'est la méthode mise au point et décrite par Shriner, Horne et Cox (7, 13), modification de la méthode originale de Vittenet (19), qui nous a permis d'obtenir la *p*-nitrophénylurée. On traite la *p*-nitraniline, en solution dans l'acétate d'éthyle, par un excès de phosgène; on obtient ainsi l'isocyanate de *p*-nitrophényle. La solution d'isocyanate de *p*-nitrophényle dans le tétrachlorure de carbone est ensuite saturée par un courant lent de gaz ammoniac sec; ce procédé avait fourni à Swartz (15) les phényl et *o*-nitrophénylurées. L'isocyanate absorbe rapidement l'ammoniac et fournit un abondant précipité de *p*-nitrophénylurée à peine colorée en jaune et fondant à 242°C.*. Le rendement de cette opération est absolument quantitatif et le produit très pur n'exige pas de recristallisation.

On est conduit sans autre intermédiaire à la *p*-nitrophényl-4-semicarbazide par condensation de la *p*-nitrophénylurée avec l'hydrate d'hydrazine en solution alcoolique:

$$p\text{-}NO_2C_6H_4\text{—}NH\text{—}CO\text{—}NH_2 + NH_2NH_2 \cdot H_2O \rightarrow p\text{-}NO_2C_6H_4\text{—}\underset{\delta}{NH}\text{—}\underset{\gamma}{CO}\text{—}\underset{\beta}{NH}\text{—}\underset{\alpha}{NH_2} + NH_3$$

A cette fin, 30 g. de *p*-nitrophénylurée dissous dans 200 cm.³ d'alcool absolu bouillant, sont additionnés de 60 cm.³ d'une solution aqueuse d'hydrate d'hydrazine à 50% (soit un excès égal à quatre équivalents moléculaires). Le mélange a été mis à bouillir sous un réfrigérant à reflux pendant environ 50 h., puis versé dans l'eau froide, de façon à provoquer la précipitation de la *p*-nitrophényl-4-semicarbazide produite; la *p*-nitrophénylurée non transformée s'y joint. Ce mélange urée-semicarbazide est dissous dans le volume minimum d'alcool bouillant (20 cm.³ par gramme), puis additionné d'acide chlorhydrique concentré; par refroidissement, le chlorhydrate de *p*-nitrophényl-4-semicarbazide précipite en masse feutrée jaune pâle; une recristallisation dans l'alcool le fournit sous forme d'aiguilles presque incolores, fondant avec décomposition à 265° C. Cette condensation fournit 26.1 g. de chlorhydrate, soit 67% du rendement théorique. La *p*-nitrophénylurée est facile à récupérer et à mettre en œuvre à nouveau.

B. Par condensation directe d'isocyanate avec l'hydrazine

Nous avons étudié l'action de l'hydrazine sur l'isocyanate de *p*-nitrophényle, en vue de l'obtention directe de la *p*-nitrophényl-4-semicarbazide:

$$p\text{-}NO_2C_6H_4\text{—}N\text{=}C\text{=}O + NH_2NH_2 \rightarrow p\text{-}NO_2C_6H_4\text{—}\underset{\delta}{NH}\text{—}\underset{\gamma}{CO}\text{—}\underset{\beta}{NH}\text{—}\underset{\alpha}{NH_2}$$

Le procédé ne doit évidemment mettre en œuvre que des produits anhydres, car l'eau transforme près de vingt fois son poids d'isocyanate en bis-*p*-nitrophénylurée symétrique. Mais la préparation d'hydrazine anhydre donne lieu à de sérieuses difficultés techniques, ce qui nous a obligés à lui substituer un de ses sels. De tous les sels d'hydrazine que nous avons examinés, l'acétate basique, $CH_3CO_2H \cdot NH_2NH_2$, est celui qui nous a semblé le mieux convenir à cette fin, quoiqu'il soit très déliquescent.

* *Points de fusion déterminés par la méthode Maquenne, sans correction.*

La condensation de ce sel avec l'isocyanate de *p*-nitrophényle a été réalisée en dissolvant 1.2 g. d'isocyanate dans l'éther de pétrole et en y ajoutant peu à peu une solution de 0.67 g. d'acétate d'hydrazine dans l'acétone. Par suite de la présence d'acétone dans le milieu, il y a condensation simultanée qui conduit à l'acétone-semicarbazone correspondante. On obtient un produit très impur, contenant une proportion parfois considérable de bis-*p*-nitrophénylurée symétrique; une recristallisation dans l'acétone conduit cependant à un produit presque incolore, qui sublime sans fondre sur le bloc Maquenne au-dessus de 220° C. Le rendement d'acétone-*p*-nitrophényl-4-semicarbazone recristallisée a été de 0.70 g., soit 45% du rendement théorique.

Si ce procédé présente un certain intérêt théorique, il ne peut pas être considéré comme procédé de préparation des semicarbazides δ-substituées, à cause des difficultés que présentent la préparation et la manipulation des sels d'hydrazine; leur avidité pour l'eau est telle qu'il est pratiquement impossible de les isoler à l'état anhydre; certains essais n'ont ainsi fourni que de la bis-*p*-nitrophénylurée symétrique.

C. Par condensation de p-nitraniline avec l'acétone-semicarbazone

La condensation des amines avec l'acétone-semicarbazone, procédé qui a été mis au point par Borsche (2) et perfectionné par Wilson, Hopper et Crawford (6, 23, 24), fournit généralement un bon rendement d'acétone-semicarbazone correspondante, substituée en position δ:

$$Ar{-}NH_2 + NH_2{-}CO{-}NH{-}N{=}C\begin{matrix}\diagup CH_3\\ \diagdown CH_3\end{matrix} \rightarrow Ar{-}\underset{\delta}{NH}{-}\underset{\gamma}{CO}{-}\underset{\beta}{NH}{-}\underset{\alpha}{N}{=}C\begin{matrix}\diagup CH_3\\ \diagdown CH_3\end{matrix} + NH_3 \qquad (I)$$

Nous avons tenté d'appliquer cette réaction à la préparation de la *p*-nitrophényl-4-semicarbazide, en dépit de l'inertie dont la *p*-nitraniline a précédemment fait preuve vis-à-vis de l'urée.

Les meilleurs résultats ont été fournis par cette réaction conduite en solution dans le xylène; nous avons dissous 5 g. de *p*-nitraniline et 5 g. d'acétone-semicarbazone dans 250 cm.^{3} de xylène et mis le mélange à refluer pendant au moins six heures, période pendant laquelle il y a dégagement de gaz ammoniac. Par refroidissement, une masse jaunâtre cristalline précipite; elle est reprise par l'éther qui dissout la *p*-nitraniline non transformée et par l'eau chaude qui extrait l'excès d'acétone-semicarbazone. Le résidu dissous dans l'alcool bouillant et traité par l'acide chlorhydrique, fournit le chlorhydrate de *p*-nitrophényl-4-semicarbazide. Rendement: 1.55 g. de chlorhydrate, soit 18% du rendement théorique.

Description de la p-nitrophényl-4-semicarbazide et de ses dérivés

La *p-nitrophényl-4-semicarbazide* libre est une substance cristalline à peine colorée en jaune lorsqu'elle est pure; elle est soluble dans l'alcool et l'eau bouillante, mais elle est très peu soluble dans l'eau froide. Purifiée par précipitation à l'état d'acétone-semicarbazone et hydrolyse subséquente, elle fond avec décomposition à 191° C.

Son *chlorhydrate* s'obtient facilement par addition d'acide chlorhydrique concentré à la solution alcoolique chaude de la base; il cristallise lentement en belles aiguilles blanches jaunissant progressivement à l'air. Il fond sur le bloc Maquenne à 265° C.; il est soluble dans l'eau froide; l'eau bouillante l'hydrolyse rapidement.

L'acétone-p-nitrophényl-4-semicarbazone se présente sous forme d'aiguilles feutrées très blanches qui subliment entre 220° et 264° C.; à cette température, il y a fusion instantanée avec décomposition. Son hydrolyse est obtenue par ébullition de sa solution alcoolique en présence d'acide chlorhydrique. N, calculé, 23.73%. N, trouvé, 23.91%.

La *glucose-p-nitrophényl-4-semicarbazone* s'obtient facilement en faisant bouillir pendant quelques minutes la solution alcoolique de *p*-nitrophényl-4-semicarbazide additionnée de la quantité théorique de glucose en solution aqueuse concentrée. Par refroidissement, de belles aiguilles très blanches se forment lentement; cette semicarbazone fond vers 192° à 193° C. lorsqu'elle est bien sèche.

2. Préparation de la *p*-nitrobenzyl-4-semicarbazide

Nous avons obtenu ce dérivé de la semicarbazide en appliquant à la *p*-nitrobenzylamine le procédé de condensation avec l'acétone-semicarbazone; ce procédé de Borsche (2) fournit un rendement très satisfaisant de benzyl-4-semicarbazide. La *p*-nitrobenzylamine nécessaire à cette fin a été préparée par transformation du chlorure de *p*-nitrobenzyle en dérivé de la phtalimide puis hydrolyse, procédé décrit par Ing et Manske (8).

On décompose d'abord le chlorhydrate de *p*-nitrobenzylamine, en solution aqueuse (0.2 g.) par la soude normale et on extrait rapidement par l'éther l'amine ainsi libérée; cette solution est alors ajoutée à 50 $cm.^3$ de xylène contenant déjà en solution 0.9 g. d'acétone-semicarbazone simple; l'élimination de l'éther par distillation conduit rapidement à la température d'ébullition du xylène (132° C.) et il se produit à ce point un abondant dégagement d'ammoniac. Après avoir fait refluer le mélange pendant trois heures, le xylène fournit par refroidissement une masse cristalline blanche; c'est l'acétone-semicarbazone *p*-nitrobenzylée brute; les 1.8 g. de produit obtenu représentent 83% du rendement théorique.

Cette semicarbazone conduit, par hydrolyse en présence d'acide chlorhydrique, au chlorhydrate de *p*-nitrobenzyl-4-semicarbazide, fines aiguilles très blanches, fondant de 195° à 197° C.

Description de la p-nitrobenzyl-4-semicarbazide et de ses dérivés

La *p-nitrobenzyl-4-semicarbazide* obtenue par décomposition du chlorhydrate en solution aqueuse, par la soude diluée, fournit une poudre blanche fondant à 164° C.

Le *chlorhydrate*, tel qu'il vient d'être décrit, est très soluble dans l'eau et fond de 195° à 197° (déc.).

L'*acétone-semicarbazone*, recristallisée dans l'alcool, fond à 162°; c'est une poudre blanche amorphe, peu soluble dans l'eau. N, calculé, 22.40%. N, trouvé, 22.58%.

La *glucose-p-nitrobenzyl-4-semicarbazone* n'a pas pu être isolée à l'état pur; elle se présente sous forme de gelée difficile à purifier.

3. Préparation de la *p*-nitroxényl-4-semicarbazide

La *p*-nitroxényl-4-semicarbazide (*p*-nitro-*p'*-biphényl-4-semicarbazide) a été préparée par condensation de *p*-nitroxénylamine avec l'acétone-semicarbazone (équation I).

La *p*-nitroxénylamine a été préparée par nitration du diphényle à l'état de 4,4'-dinitrodiphényle par les méthodes combinées de Bell, Kenyon et Robinson (1) et de Guglialmelli et Franco (5) puis réduction sélective d'un seul groupe nitré par la méthode de Mascarelli et Gatti (9). Cette *p*-nitroxénylamine, recristallisée dans l'alcool, fond à 185° C.

Nous avons obtenu la *p*-nitroxényl-4-semicarbazide en dissolvant 14.5 g. de *p*-nitroxénylamine et 7.8 g. d'acétone-semicarbazone simple dans 100 cm.^{3} d'acétone; on ajoute à chaud, 350 cm.^{3} de xylène et on fait bouillir afin d'éliminer l'acétone; on continue ensuite l'ébullition sous réfrigérant à reflux pendant au moins cinq heures. Puis on distille jusqu'à volume final de 75 à 100 cm.^{3} et l'on porte à la glacière pendant 24 h.; la substance qui précipite est recueillie par filtration, broyée puis lavée à l'éther pour dissoudre l'amine non transformée et à l'eau chaude pour extraire l'acétone-semicarbazone qui n'a pas réagi. La masse est ensuite reprise par 150 cm.^{3} d'alcool chaud auquel on ajoute 25 cm.^{3} d'acide chlorhydrique concentré. Après dissolution, on laisse cristalliser; le chlorhydrate de *p*-nitroxényl-4-semicarbazide précipite lentement sous forme d'une poudre jaune pâle.

Description de la p-nitroxényl-4-semicarbazide et de ses dérivés

La *p-nitroxényl-4-semicarbazide* se présente sous forme d'une poudre amorphe jaune pâle, qui fond en se décomposant sur le bloc à 178° C. Elle est insoluble dans l'eau, mais très soluble dans l'alcool.

Son *chlorhydrate*, en paillettes jaunes, fond à 219°.

L'*acétone-semicarbazone* fond à 261°; elle est légèrement colorée en jaune. N, calculé, 17.95%. N, trouvé, 18.03%.

La *glucose-semicarbazone* s'obtient en faisant bouillir la solution aqueuse de la *p*-nitroxényl-4-semicarbazide, acidifiée par quelques gouttes d'acide acétique, avec la quantité équimoléculaire de glucose. Elle cristallise difficilement et fond à 172° C.

4. Préparation de la 2,4-dinitrophényl-4'-semicarbazide

Sah et Tao (12) ont déjà obtenu et décrit la 3,5-dinitrophényl-4-semicarbazide par un procédé qui diffère totalement des procédés ordinaires de préparation des semicarbazides δ-substituées; c'est d'ailleurs le seul dérivé

dinitré de la phényl-4-semicarbazide qui ait jusqu'ici été préparé. Nous avons préparé la 2,4-dinitrophényl-4'semicarbazide; il ne nous a pas été possible d'obtenir ce dérivé par l'une ou l'autre des deux méthodes ordinaires de synthèse des dérivés δ-substitués de la semicarbazide; en effet, non seulement retrouve-t-on dans la 2,4-dinitro-aniline l'inertie dont la *p*-nitraniline a fait preuve dans certaines de ses réactions, mais il semble qu'elle se soit amplifiée de façon très sensible.

Nous avons obtenu la 2,4-dinitrophényl-4'-semicarbazide par condensation d'une solution d'hydrate d'hydrazine avec l'urée correspondante, une fois que celle-ci eût été préparée par nitration de la phénylurée. La nitration des phényluréthanes méthylique et éthylique ayant fourni à Van Romburgh (18) des dérivés polynitrés dont une proportion importante de 2,4-dinitrophényluréthanes, Reudler (11) a repris cette réaction pour l'appliquer à la phénylurée. Ce procédé de Reudler nous a fourni la 2,4-dinitrophénylnitrourée (p.f. 164° C.) que nous avons transformée en 2,4-dinitrophénylurée (p.f. 176°) par l'action prolongée d'un courant de gaz ammoniac sec.

L'urée substituée précédemment obtenue (5.0 g.), dissoute dans dix fois son poids d'alcool absolu et traitée par quatre équivalents moléculaires d'hydrate d'hydrazine (8 cm.³ sol. à 50%) fournit, après 48 h. de condensation sous réfrigérant à reflux, un rendement de 75% en 2,4-dinitrophényl-4'-semicarbazide.

Description de la 2,4-dinitrophényl-4'-semicarbazide et de ses dérivés

La *2,4-dinitrophényl-4'-semicarbazide*, recristallisée dans l'alcool, est un corps jaune fondant à 178° C.

L'*acétone-semicarbazone* correspondante, de couleur jaune pâle, fond à 248°.

La condensation de ce dérivé avec le glucose n'a fourni que des produits mal définis.

Discussion

Le mécanisme des réactions de condensation de l'urée avec les amines a été l'objet de plusieurs tentatives d'interprétation. La théorie dite du "réarrangement" de l'urée, exposée par Walker et Hambly (20), puis confirmée par Werner et Fearon (21), est celle que l'on admet le plus généralement aujourd'hui: l'urée chauffée à sec à 160° C. ou en solution aqueuse à 100° se transforme partiellement en isocyanate d'ammonium. Inversement, dans les mêmes conditions, le cyanate d'ammonium serait lui-même transformé en urée; d'autre part, par hydrolyse, il serait susceptible de fournir de l'acide isocyanique et de l'ammoniac, ce qui conduit à représenter la transformation de l'urée en solution aqueuse bouillante par le double équilibre suivant:

$$NH_2—CO—NH_2 \rightleftarrows O{=}C{=}N—NH_4 \rightleftarrows O{=}C{=}N—H + NH_3 \qquad (II)$$

L'existence de ces transformations ne laisse aujourd'hui aucun doute, car elles ont reçu l'appui de vérifications expérimentales très démonstratives.

Davis, Blanchard et Underwood (3, 4) ont adopté cette théorie du réarrangement de l'urée pour rendre compte du mécanisme de formation des urées

substituées par réaction des amines sur l'urée; l'acide isocyanique naissant (équation II) fixerait immédiatement une molécule d'amine, par ouverture d'une valence de la double liaison de son azote, et il conduirait ainsi directement à l'urée substituée:

$$O{=}C{=}N{-}H + \begin{array}{l} H \\ \quad \rangle N{-}R \\ H' \end{array} \rightarrow \begin{array}{ccccc} O{=} & C & {-} & N & {-}H \\ & | & & | & \\ H{-} & N & & H & \\ & | & & & \\ & R & & & \end{array} \qquad \text{(III)}$$

Si l'urée se trouve en présence d'un excès d'amine, la réaction conduit généralement à l'urée disubstituée symétrique. Davis et Blanchard donnent ici une extension importante à leur hypothèse originale en admettant que les dérivés de substitution de l'urée sont eux-mêmes isomérisés par ébullition de leurs solutions; ainsi la phénylurée serait transformée en isocyanate de phényle par la réaction réversible suivante:

$$C_6H_5{-}NH{-}CO{-}NH_2 \rightleftarrows C_6H_5{-}N{=}C{=}O + NH_3$$

La formation de diphénylurée symétrique en présence d'un excès d'amine s'expliquerait alors par un mécanisme analogue au précédent, c'est-à-dire, par ouverture d'une valence de la double liaison de l'isocyanate et fixation d'une seconde molécule d'amine.

Ce mode de représentation a le mérite de permettre des corrélations très avantageuses entre les réactions fournies par l'urée, la nitrourée, la thiourée et la guanidine; il se montre toutefois insuffisant devant un certain nombre de réactions, vraisemblablement identiques aux précédentes, mais qui conduisent à des résultats inattendus. Ainsi, Davis et Underwood (4) notent avec perplexité que les amines secondaires ne se condensent pas avec l'urée:

> "We have heated urea with diphenylamine and with ethylaniline, but have found no evidence that any reaction took place—a fact which may perhaps be due to the inactivity of the hydrogen atoms in these substances . . ."

Nous avons nous-mêmes déjà indiqué (page 159) jusqu'à quel point la *p*-nitraniline est inerte lorsqu'on tente de la condenser avec l'urée pour l'obtention de la *p*-nitrophénylurée; pourtant, dans les mêmes conditions l'aniline, de structure très voisine, donne un excellent rendement de phénylurée. Bien plus, le nombre des amines aromatiques ou aliphatiques qui donnent cette réaction est si grand que le procédé est considéré comme méthode générale de préparation des urées monosubstituées.

Nous allons tenter de démontrer que la théorie des capacités affinitaires rend non seulement compte de ces observations, mais qu'elle permet d'établir une relation très étroite entre les rendements obtenus au cours des synthèses d'urées substituées et les capacités affinitaires des radicaux organiques combinés à l'urée. Elle conduit ainsi à une interprétation plus générale, plus conforme aux faits observés, des réactions de synthèse des semicarbazides δ-substituées.

La théorie des capacités affinitaires variables des radicaux organiques offre un mode relativement nouveau de représentation des formules chimiques qui n'a évidemment pas encore pris une forme définitive à cause de la nature

essentiellement qualitative de beaucoup de ses résultats. Elle facilite néammoins l'interprétation de bien des réactions chimiques qui sans elle semblent tout à fait anormales et elle permet même, dans bien des cas, d'en prévoir l'orientation et d'en déterminer, à priori, le rendement approximatif. Elle constitue ainsi un guide précieux dans les synthèses organiques.

Or la représentation des formules chimiques en fonction des capacités affinitaires est une pratique peu usitée et nous renvoyons aux communications des auteurs de la méthode pour une discussion de leurs procédés (14, 16, 17). Nous désirons toutefois préciser que des comparaisons expérimentales entre divers radicaux organiques démontrent qu'ils se distinguent par des valeurs affinitaires très inégales; certains radicaux échangent, dans les combinaisons chimiques, une plus grande affinité que les autres, ce que l'on représente par des liaisons d'intensité relative variable: p-$NO_2C_6H_4$▬ a une capacité affinitaire plus grande que C_6H_5— et que CH_3—; on admet généralement que leur force ou solidité d'attache est proportionnelle à leur capacité affinitaire et que par conséquent un radical à faible capacité affinitaire se détache plus facilement, dans les réactions chimiques, du groupement auquel il est attaché, qu'un radical à forte capacité affinitaire. L'intensité du lien est donc jusqu'à un certain point une mesure de la solidité d'attache des radicaux organiques.

Admettant en outre que tout radical tend à échanger avec le voisin le maximum d'affinité correspondant à sa capacité affinitaire, l'on conçoit aisément qu'il s'établisse au sein de la molécule une sorte de concurrence pour le partage de l'affinité; ceci conduit à la notion de distribution alternée des forces d'attache entre les atomes d'une chaîne organique; un radical "R" à capacité affinitaire élévée étant introduit à l'extrémité d'une chaîne organique, il y détermine une alternance de valences fortes et de valences faibles par suite de la concurrence qui s'établit entre les atomes de la chaîne:—

R▬ CH_2----CH_2▬ CH_2----CH_2▬

La présence de ce radical à une extrémité de la chaîne induit donc à l'autre extrémité une capacité affinitaire plus petite si la chaîne comprend un nombre pair d'atomes de carbone, plus grande si ce nombre est impair.

(a) Condensation des amines avec l'urée

Si, pour l'étude des réactions de condensation des amines avec l'urée, l'on adopte le point de vue offert par l'hypothèse de Davis et qu'on les examine à l'aide des notions de capacités affinitaires, il est facile de concevoir que les réactions de ce genre soient d'autant plus faciles et complètes que les hydrogènes aminés sont moins fortement liés:

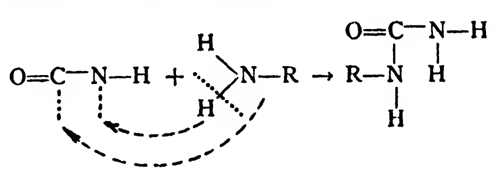

(IV)

Pourtant, le relevé des rendements obtenus par ces auteurs et par nous-mêmes démontre au contraire que la réaction est d'autant plus favorisée que

ces hydrogènes sont plus fortement liés; le tableau I de classification des amines par ordre de réactivité vis-à-vis de l'urée le montre suffisamment: les liaisons entre groupes d'atomes ont été représentées suivant les règles de la périodicité des valences, de façon à illustrer la force d'attache des hydrogènes aminés dans chacune des amines.

TABLEAU I

Amine		Rendement d'urée substituée	Préparation
$p\text{-}NO_2C_6H_4\text{—}N{<}^{H}_{H}$	→	0% de p-nitrophénylurée	Synth. 1, A.
$(C_6H_5)_2{>}N\text{----}H$	→	0% de diphénylurée asym.	D. et B. (3)
$C_6H_5(CH_3){>}N\text{----}H$	→	0% de méthyl-phénylurée	(*)
$C_6H_5\text{—}N{<}^{H}_{H}$	→	26% de monophénylurée. 90% de diphénylurée sym.	D. et B. (3)
$C_6H_5CH_2\text{-----}N{<}^{H}_{H}$	→	97% de benzylurée.	D. et B. (3)

(*) *En changeant entièrement les conditions ordinaires de condensation, par additio l'acide chlorhydrique au mélange, les auteurs cités (4) ont obtenu de très faibles rendements d méthyl-phénylurée asymétrique.*

Les deux cas extrêmes, représentés par les rendements obtenus en condensant la p-nitraniline et la benzylamine avec l'urée constituent une démonstration excellente de l'indépendance de cette réaction vis-à-vis des hydrogènes de l'amine; la p-nitraniline, dans laquelle ils sont très peu liés, a obstinément refusé de fournir la moindre trace de p-nitrophénylurée. Au contraire, la benzylamine dont les hydrogènes sont fortement liés, fournit un rendement théorique de benzylurée.

On observe, par conséquent, que les rendements augmentent à mesure que la capacité affinitaire du groupe aminé diminue. La formation des urées substituées est donc facilitée par la mobilité du groupe aminé, qui fournit l'ammoniac dégagé au cours de la condensation; ceci nous amène à proposer l'équation suivante comme interprétation de la réaction des amines sur l'urée

$$R\text{—}NH_2 + {}^{H}_{H}{>}N\text{—}CO\text{—}N{<}^{H}_{H} \rightarrow R\text{—}NH\text{—}CO\text{—}NH_2 + NH_3 \qquad (V)$$

La condensation de l'urée avec une amine s'effectuerait par l'union du groupe —NH_2 de l'amine à l'un des hydrogènes de l'urée, le radical aromatique de l'amine se substituant à cet hydrogène; ce mode de représentation permet d'établir une relation très régulière entre les rendements obtenus et la force d'attache de chacun des groupements aminés; il explique aussi le fait que les amines secondaires soient incapables de donner cette réaction, comme le rapportent Davis et Blanchard, ou qu'ils la donnent avec difficulté.

(b) Condensation de l'hydrazine avec les urées substituées

Les réactions de condensation des amines avec l'urée sont donc fidèlement interprétées sans qu'il soit nécessaire d'avoir recours au phénomène accessoire d'isomérisation de l'urée. Cette conclusion est corroborée par la réaction de condensation de l'hydrazine avec les urées substituées, pour la préparation des semicarbazides correspondantes. Ici encore, comme le tableau II permet d'en rendre compte, l'influence des radicaux aromatiques se fait sentir dans le sens de leurs capacités affinitaires respectives, car les rendements obtenus sont d'autant plus faibles que les hydrogènes terminaux des urées substituées sont plus fortement retenus:

TABLEAU II

Urée substituée		Rendement de semicarbazide	Préparation
$C_6H_5CH_2-NH-CO-N\langle^{H}_{H}$	→	0% benzyl-4-semicarbazide	(*)
$C_6H_5-NH-CO-N\langle^{H}_{H}$	→	55% phényl-4-semicarbazide	(**)
p-$BrC_6H_4-NH-CO-N\langle^{H}_{H}$	→	59% p-bromophényl-4-s.c.	(***)
p-$NO_2C_6H_4-NH-CO-N\langle^{H}_{H}$	→	67% p-nitrophényl-4-s.c.	Synth. 1, A
$\begin{matrix}(2)NO_2\\(4)NO_2\end{matrix}\rangle C_6H_3-NH-CO-N\langle^{H}_{H}$	→	75% dinitrophényl-4-s.c.	Synth. 4

(*) *À la solution de 5 g. de benzylurée dans 50 cm.³ d'alcool absolu, on a ajouté 12 cm.³ de solution aqueuse à 50% d'hydrate d'hydrazine, soit au-delà de trois équivalents moléculaires; après une ébullition de 70 h., tout indiquait encore l'absence complète de benzyl-4-semicarbazide dans cette solution.*

(**) *Rendement obtenu en faisant refluer pendant 12 h. un mélange de 34 g. de phénylurée et de 40 cm.³ d'hydrate d'hydrazine à 50%; 31 g. de chlorhydrate de phényl-4-semicarbazide (p.f. 215° C.) ont été recueillis.*

(***) *8.1 g. de bromophénylurée dissous dans 45 cm.³ d'alcool absolu ont été additionnés de 11 cm.³ de solution à 50% d'hydrate d'hydrazine et mis à refluer pendant 48 h.; on a ainsi obtenu 5.9 g. de chlorhydrate de p-bromophényl-4-semicarbazide, soit 59% du rendement théorique.*

Il faut admettre, comme précédemment, que l'ammoniac qui est éliminé au cours de la réaction ne provient pas uniquement de l'isomérisation de l'urée, comme le voudrait l'hypothèse de Davis, Underwood et Blanchard, mais en grande partie de l'hydrazine:

$$R-NH-CO-N{<}^{H}_{H} + NH_2NH_2 \rightarrow R-\underset{\delta}{NH}-\underset{\gamma}{CO}-\underset{\beta}{NH}-\underset{\alpha}{NH_2} + NH_3 \qquad \text{(VI)}$$

(c) Condensations d'amines avec l'acétone-semicarbazone

On observe également cette correspondance régulière entre les rendements fournis par condensation d'amines avec l'acétone-semicarbazone et la classification des radicaux par ordre de capacités affinitaires:

TABLEAU III

Amines		Pour cent d'acétone-semicarbazones	Préparation
$NO_2C_6H_4CH_2\cdots N{<}^{H}_{H}$	→	83% *p*-nitrobenzyl-4-s.c.	Synth. 2
$C_6H_5CH_2\cdots N{<}^{H}_{H}$	→	74% benzyl-4-semicarbazone	(*)
p-$C_6H_5C_6H_4-N{<}^{H}_{H}$	→	66% *p*-xényl-4-semicarbazone	(**)
p-$BrC_6H_4-N{<}^{H}_{H}$	→	26% *p*-bromophényl-4-s.c.	(***)
p-$NO_2C_6H_4-N{<}^{H}_{H}$	→	18% *p*-nitrophényl-4-s.c.	Synth. 1, C.
$^{(2)NO_2}_{(4)NO_2}{>}C_6H_3-N{<}^{H}_{H}$	→	0% 2, 4-dinitrophényl-4-s.c.	Synth. 4.

(*) *10 g. de benzylamine et 10 g. d'acétone-semicarbazone sont fondus à 130° C. et maintenus à cette température pendant 30 min. Par précipitation du produit dans l'eau froide, on recueille 14.4 g. d'acétone-benzyl-4-semicarbazone, soit 74% du rendement théorique.*

(**) *2 g. d'acétone-semicarbazone en solution dans 40 cm.³ de xylène sont additionnés de 3.25 g. de p-xénylamine; après condensation pendant quatre heures puis hydrolyse chlorhydrique, on obtient 3.38 g. de chlorhydrate, soit 66% du rendement théorique.*

(***) *3.54 g. de p-bromoaniline et 2.3 g. d'acétone-semicarbazone ont été mis à condenser pendant 12 h. dans 100 cm.³ de xylène; on obtient, après hydrolyse 1.38 g. de semicarbazide, soit 26% du rendement théorique.*

Ici encore, les groupements aminés par leur rigidité d'attache sont responsables des rendements observés; en somme, le mécanisme de la condensation est le même que celui auquel nous avons conclu dans les réactions précédentes, c'est-à-dire, que c'est toujours le groupement fonctionnel de l'amine qui est éliminé à l'état d'ammoniac:

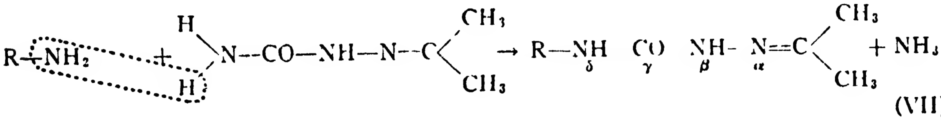

(VII)

Conclusions

Si l'on admet le principe initial de la valeur relative des radicaux organiques au point de vue des capacités affinitaires, on est conduit aux conclusions suivantes, dans l'étude des réactions de synthèse des semicarbazides δ-substituées:

1. Les rendements obtenus au cours de la réaction de condensation de l'urée et de l'acétone-semicarbazone avec les amines ou celle des urées substituées avec l'hydrazine sont conformes aux tableaux de classification des radicaux organiques par ordre de capacités affinitaires.

2. L'alternance des forces d'attache entre les éléments d'une chaîne organique conduit à admettre que le mécanisme de toutes ces réactions est le même, à savoir: élimination du groupement fonctionnel de l'amine à l'état d'ammoniac et union du reste aryle ou alcoyle avec l'amide (équations V, VI et VII).

3. La théorie du "réarrangement" de l'urée en isocyanate d'ammonium et l'hypothèse de l'isomérisation des urées substituées en isocyanates correspondants se montrent insuffisantes pour interpréter un bon nombre de ces réactions, et elles entrent même en conflit avec les rendements observés. Nous en déduisons que l'isomérisation de l'urée et des urées substituées est un phénomène accessoire, dont l'existence est bien démontrée, mais qui ne s'applique pas aux réactions de synthèse des semicarbazides.

Bibliographie

1. Bell, F., Kenyon, J., et Robinson, P. H. J. Chem. Soc. 129 : 1239-1247. 1926.
2. Borsche, W. Ber. 38 : 831-837. 1905.
3. Davis, T. L. et Blanchard, K. C. J. Am. Chem. Soc. 45 : 1816-1820. 1923.
4. Davis, T. L. et Underwood, H. W. Jr. J. Am. Chem. Soc. 44 : 2595-2604. 1922.
5. Guglialmelli, L. C. et Franco, M. R. Anales asoc. quím. argentina, 17 : 340-351. 1929.
6. Hopper, I. V. J. Roy. Tech. Coll. Glasgow, No. 4 : 48-57. 1927.
7. Horne, W. H. et Cox, R. F. B. J. Am. Chem. Soc. 53 : 3186. 1931.
8. Ing, H. R. et Manske, R. H. F. J. Chem. Soc. 129 : 2348-2351. 1926.
9. Mascarelli, L. et Gatti, D. Atti accad. Lincei (Ser. 6), 10 : 441-446. 1929.
10. Pierron, P. Bull soc. chim. Mém. (Sér. 3) 33 : 69-74. 1905.
11. Reudler, J. F. L. Rec. trav. chim. 33 : 35-84. 1914.
12. Sah, P. P. T. et Tao, P.-C. J. Chinese Chem. Soc. 4 : 506-512. 1936.
13. Shriner, R. L. et Cox, R. F. B. J. Am. Chem. Soc. 53 : 1601-1605. 1931.
14. Swarts, F. Inst. intern. chim. Solvay, Conseil chim., 2ième Conseil, 199-236. 1926.

15. SWARTZ, S. E. Am. Chem. J. 19(4) : 295-319. 1897.
16. TIFFENEAU, M. Bull. soc. chim. Mém. (Sér. 4) 49 : 1595-1605. 1931.
17. TIFFENEAU, M. et ORÉKHOFF, A. Inst. intern. chim. Solvay, Conseil chim., 2ième Conseil, 247-321. 1926.
18. VAN ROMBURGH, P. Rec. trav. chim. 10 : 135-143. 1891.
19. VITTENET, H. Bull. soc. chim. Mém. (Sér. 3) 21 : 586-593. 1899.
20. WALKER, J. et HAMBLY, F. J. J. Chem. Soc. 67 : 746-767. 1895.
21. WERNER, E. A. et FEARON, W. R. J. Chem. Soc. 117 : 1356-1362. 1920.
22. WHEELER, A. S. et WALKER, T. T. J. Am. Chem. Soc. 47 : 2792-2796. 1925.
23. WILSON, F. J. et CRAWFORD, A. B. J. Chem. Soc. 127 : 103-109. 1925.
24. WILSON, F. J., HOPPER, I. V., et CRAWFORD, A. B. J. Chem. Soc. 121 : 866-870. 1922.

… Canadian Journal of Research

Issued by THE NATIONAL RESEARCH COUNCIL OF CANADA

VOL. 19, SEC. B. AUGUST, 1941 NUMBER 8

SELENIUM IN SOILS, GRAINS, AND PLANTS IN ALBERTA[1]

BY OSMAN J. WALKER[2], WALTER E. HARRIS[3], AND MICHAEL ROSSI[4]

Abstract

Two hundred and twenty-seven samples of wheat, forty soils, and four plants of the *Astragalus* family, all from the province of Alberta, have been analysed for their selenium content. The selenium content of the soils varied from less than 0.1 to 1 p.p.m., that of wheat, from less than 0.1 to 1 p.p.m., and that of *Astragalus* plants, from 0.3 p.p.m. in the root of one plant to 600 p.p.m. in the stalks of another. The majority of the wheat samples contained only traces of selenium, and in no case can any one be considered as dangerous. Some of the soils contained over 0.5 p.p.m. of selenium and these may be looked upon as seleniferous. Not enough data are available to indicate the extensiveness of seleniferous soils. Although the underlying strata of much of Alberta is of Upper Cretaceous Age, the soil is derived mostly from glacial drift formed from other types of rock, so that the seleniferous area may be much smaller than that earlier suspected. Analyses of wheat and soils indicate that dangerous areas are more likely to be found in southern Alberta than in central Alberta. Analyses of vetches show that the amount of selenium absorbed is independent of the species and the selenium content of the soil and varies with the part of the plant examined.

In recent years a great deal of attention has been paid to elements occurring in small amounts in water, soils, rocks, and plants, especially from the standpoint of their effect on humans and animals. Selenium is one that has been found to be harmful, as Beath and his coworkers in Wyoming (17, p. 14) and Franke and his coworkers (7, 8) in South Dakota have shown that "alkali disease" and "blind staggers" are caused by selenium in the diet. The toxicity of this element depends on the form in which it is ingested, in the following order: wheat >corn >barley >selenate >selenite (6). In plants, the selenium is present in the protein fraction and it has been shown that the toxic fraction is concentrated when a separation of proteins from other material is carried out. In foodstuffs, a selenium content of about 4 p.p.m. prevents normal growth.

Selenium in plants is derived from the soils in which they grow, but there seems to be no relation between the selenium content of the soils and that of the plants. Plants may be divided into three classes depending on their tolerance for selenium (9); (*a*) those that absorb large amounts of selenium

[1] *Manuscript received June 2, 1941.*
Contribution from the Department of Chemistry, University of Alberta, Edmonton, Alta.
[2] *Professor of Chemistry.*
[3] *Former holder of Board of Governors Research Fellowship. At present, graduate student, University of Minnesota, Minneapolis, Minn., U.S.A.*
[4] *Former graduate student.*

even from inorganic material, (*b*) those that absorb moderate amounts, (*c*) those that have a limited tolerance for the element and are either absent from, or grow very poorly in, soils containing much selenium.

Examples of plants of the first type are certain of the vetches of the *Astragalus* family. Cereals fall into the second class and some of the grasses as well as many other native plants fall into the third group. The vetches grow vigorously on seleniferous soils and may contain many times more selenium than the soils on which they grow. These may be and are used as "indicator" plants (15) for locating the presence of selenium in the soil. It is believed that these are the only plants that can utilize the selenium from such inorganic substances as selenides, selenites, and selenates. The selenium is stored in these plants in proteins which contain the selenium tied up in the same manner as sulphur in the commoner proteins. When these plants decay, the selenium is returned to the soil in the form of organic selenium (1). Cereals and other plants of the second class do not utilize inorganic selenium but grow fairly well on seleniferous soils and absorb moderate amounts of selenium if the element is present in organic compounds generally formed from the decay of "indicator" plants. Plants of the third group seem to have their growth retarded by selenium in the soil.

The consensus of opinion at the present time is that soils containing 0 5 p.p.m. of selenium or more should be suspected of being producers of toxic crops (10). It has also been found that the tendency of plants to absorb selenium is decreased if the rainfall is more than 21 in.

All soils contain some selenium but those derived from rocks of the Upper Cretaceous Period generally contain larger amounts than those derived from rocks of other Periods, so that the crops grown on such soils are more likely to be toxic than those grown on soils from other sources. Rocks of this Period extend from the Prairie Provinces down to the Gulf of Mexico, east of the Rocky Mountains, and there is a possibility that vegetation grown in soils derived from them will contain quantities of selenium. In such states as Wyoming, South Dakota, North Dakota, and Montana the more outstanding seleniferous soils are on the Pierre and Niobrara formations of the Upper Cretaceous system, the former of which correspond in age to the Belly River series and the Bearpaw series of Alberta and Saskatchewan. Since in the neighbouring states of Montana and North Dakota selenium poisoning is endemic, it would naturally be expected that similar conditions would prevail in the Prairie Provinces, because of the selenium in the soils and in the plants grown on these soils. The first positive proof of this was found by Robinson (12) who noted the presence of 1.9 p.p.m. of selenium in a sample of Saskatchewan wheat.

Since wheat is one of the main crops of the Prairie Provinces it would seem to be logical to examine this cereal as well as soils in order to determine whether any district produces wheat of high enough selenium content to render it toxic and thus dangerous for human consumption. Three studies of this nature were begun in 1938, by Byers of the U. S. Department of

Agriculture (4, 16), by Thorvaldson of the University of Saskatchewan (14), and by the writers at the University of Alberta. The present project had been under way for nearly a year before it was known that other investigators were interested in the selenium problem in Canada.

Byers' reports indicate the presence of large areas of seleniferous soils in Alberta, Saskatchewan, and Manitoba, with selenium content from 0.1 to 6 p.p.m., and vegetation, chiefly from the *Astragalus* family, with selenium content from 3 to 4190 p.p.m. His soils were mostly those in which "indicator" plants were growing. Thorvaldson examined 230 composite wheat samples and found an average selenium content of only 0.44 p.p.m., with a maximum of 1.5 p.p.m.

The present investigation was carried out primarily on samples of wheat. The examination was restricted to the ripened seeds even though it is known that the stem and the leaf may contain more selenium. A number of soils also were examined as well as some plants of different species of *Astragalus*, namely, *A. bisulcatus* and *A. pectinatus*. Samples of wheat of the 1938 crop were supplied by the Department of Field Crops of the University and by several mills at Medicine Hat. Many of the soils were collected from garden plots in 1935 by graduates of the University; the remainder, along with selenium bearing plants growing thereon, were gathered in 1939 by the Alberta Soil Survey unit of the Dominion Department of Agriculture.

The samples were so selected that a fair distribution from different parts of the province was obtained, with considerable emphasis placed on the southern half of the province, where outcrops of shales of Belly River and Bearpaw formations are more frequent.

Many methods for determining selenium in small quantities were examined critically, and for wheat and soils the one chosen was that of Robinson, Dudley, Williams, and Byers (13) with the modifications suggested by Curl and Osborn (5). In this procedure large amounts of hydrobromic acid are used, so it was found necessary to recover this by distillation as the constant boiling acid. Some of the waxy material from the wheat distilled over with the hydrobromic acid, giving a cloudy liquid with which it was difficult to obtain a satisfactory value for selenium. Satisfactory results were obtained by adding one-tenth of one per cent by weight of fresh bentonite to the hydrobromic acid filtrates, allowing to stand overnight, and then filtering. Fractional distillation was then carried out. The first third of the constant boiling acid was decolorized with sulphur dioxide, allowed to stand overnight, and filtered. It was then ready for use once more.

The weight of sample of wheat or soil used was 10 gm. although some determinations were carried out with 30-gm. samples. Weights were based on air dried material. Grains were ground up in a mill, and soils were ground in a mortar.

Two hundred and twenty-seven (227) samples of wheat were analysed. The results are summarized in Table I. Two hundred and six (206) of these

TABLE I

SELENIUM CONTENT OF WHEAT SAMPLE

Se, p.p.m.	Number of samples	Se, p.p.m.	Number of samples
<0.1	110	0.5	7
0.1	50	0.6	5
0.2	21	0.7	2
0.3	17	0.9	2
0.4	10	1.0	3

samples were grown in soil over Upper Cretaceous rocks, ninety-seven (97) over Belly River, and thirty-six (36) over the Bearpaw series. The classification of rocks used in this paper is taken from the geological map of Alberta published by Dr. J. A. Allan in 1937 under the auspices of the Research Council of Alberta. The underlying rocks may be of little significance in this province as they are covered in most places by layers of glacial drift differing greatly in thickness, so that only in a few places are beds covered by soils formed directly from rock strata below. It would be supposed that erosion would lower the selenium content of glacial drift by removal of soluble selenium compounds by washing them away. Then again the glacial drift may have been formed to a great extent from rocks that are not seleniferous. This may account for the lack of absorption of selenium as shown by the bulk of the wheat samples examined. As 4 p.p.m. of selenium is looked upon as the minimum amount of the element that is toxic in foods, it can be seen that the selenium content of the wheat examined is well below the toxic level.

Similar results were obtained in the examination of the soils. Twenty-seven of these soils, which had not been collected from the same plots as the samples of wheat, were stored in glass stoppered bottles from 1935 to 1938. These were so chosen as to represent a cross-section of the province. Thirteen were collected in 1939 and were taken from spots from which the *Astragalus* plants were obtained. Table II contains the results of analysis of the first series of soils. The results for the remaining 13 soils are shown with those for the selenium collecting plants in Table III.

If we look upon a soil containing 0.5 p.p.m. of selenium as dangerous, it can be seen that six of these fall in this category. These high selenium soils were taken at Coutts, Nemiscam, and Medicine Hat in the southern part of the province and at Blackfalds, Delburne, and Raven in the central part. Soils with low values for selenium were widely distributed over the southern and central parts of the province. These results compare favourably with those of Byers (16) whose values for soils from Alberta vary from 0.1 to 1.5 p.p.m. of selenium. It must be remembered, however, that all his samples came from southern Alberta and were chosen mostly because of the proximity of "indicator" plants.

TABLE II

SELENIUM CONTENT OF ALBERTA SOILS

Se, p.p.m.	Number of samples	Se, p.p.m.	Number of samples	Se, p.p.m.	Number of samples
<0.1	16	0.3	1	0.8	1
0.1	1	0.4	1	0.9	2
0.2	2	0.7	2	1.0	1

TABLE III

ANALYSIS OF SOILS AND PLANTS

Sample		Location	Geological formation	Se, p.p.m.
Soil	0-12 in.	12-5-6-W4	Belly River	0.5
"	12-24	"	"	0.4
"	24-36	"	"	0.4
"	36-48	"	"	0.4
A. bisulcatus	Roots	"		0.3
"	Stalks	"		3.0
"	Leaves	"		5.0
Soil	0-12 in.	34-6-5-W4	Bear Paw	0.3
"	12-24	"	"	0.4
"	24-36	"	"	0.3
"	36-48	"	"	0.5
A. bisulcatus	Roots	"		360
"	Stalks	"		465
"	Leaves *	"		170
Soil	0-12 in.	10-2-4-W4	Bear Paw	0.7
"	12-24	"	"	0.3
"	24-36	"	"	0.3
"	36-48	"	"	0.4
A. pectinatus	Stalks	"		30
"	Leaves	"		120
A. bisulcatus	Roots	"		220
"	Stalks	"		200
"	Leaves	"		600
Soil	0-12 in.	20 ft. from previous	Bear Paw	0.4

* *This sample contained some soil that could not be separated. This may explain the low selenium content for these leaves.*

Astragalus plants, along with the soils in which they grew, were collected in late July, 1939, from the southeastern corner of the province on and near the Dominion Range Experimental Station at Manyberries. The plants were about a week beyond the blossoming stage. The soils come from both the Belly River and the Bearpaw formations and samples were taken at various depths. The plants were air dried and separated roughly into roots, stalks, and leaves. Table III contains the results of the analysis of these portions of the plants and the corresponding soils. Plants of this family collected by Byers (16) in Alberta varied in selenium content from 12 to 3690 p.p.m.

Even though the maximum amount of 0.7 p.p.m. of selenium was found in these samples of soil, the vegetation grown on them was quite seleniferous. There is no relation between the selenium content of the plant and that of the soil. It will be noticed that plants of the same species grown on soils of similar selenium content differ greatly in the amount of selenium absorbed. It will also be noted that the selenium content of the plants generally increases from the root, to the stalk, and to the leaves. The results shown here correspond to those found by Byers (2, 3, 4, 15, 16), by Painter (11), and other workers.

The results presented in this paper must be regarded as preliminary in character. Sufficient evidence has been collected to indicate that there are areas in the province of Alberta where the soil contains sufficient selenium to render certain plants dangerous to the health of man and animals. From the examination of wheat it would seem that the selenium content is sufficiently low that the possibility of harmful effects from this source is very remote. No work has yet been done on vegetables, hay, grass, or other forage crops. The whole matter of possible selenium poisoning in Alberta can be cleared up only by an intensive survey of the area from the standpoint of selenium content of soils and all types of vegetation.

Acknowledgment

The writers wish to express their appreciation to those who assisted in collecting the soil, the vetches, and the grain for this research.

References

1. Beath, O. A. Wyoming Agr. Expt. Sta. Bull. 221, pp. 29-62. 1937.
2. Byers, H. G. U.S. Dept. Agr. Tech. Bull. 482. 1935.
3. Byers, H. G. U.S. Dept. Agr. Tech. Bull. 530. 1936.
4. Byers, H. G. and Lakin, H. W. Can. J. Research, B, 17 : 364-369. 1939.
5. Curl, A. L. and Osborn, R. A. J. Assoc. Official Agr. Chem. 21(2) : 228-235. 1938.
6. Franke, K. W. and Painter, E. P. Cereal Chem. 15 : 1-24. 1938.
7. Franke, K. W. and Potter, V. R. J. Nutrition, 10(2) : 213-221. 1935.
8. Franke, K. W., Rice, T. D., Johnson, A. G., and Schoening, H. W. U.S. Dept. Agr. Circ. 320. 1934.
9. Miller, J. T. and Byers, H. G. J. Agr. Research, 55(1) : 59-68. 1937.
10. Moxon, A. L. South Dakota Agr. Expt. Sta. Bull. 311. 1937.
11. Painter, E. P. Chem. Reviews, 28 : 179-213. 1941.
12. Robinson, W. O. Ind. Eng. Chem. 28 : 736-738. 1936.
13. Robinson, W. O., Dudley, H. C., Williams, K. T., and Byers, H. G. Ind. Eng. Chem. Anal. Ed. 6(4) : 274-276. 1934.
14. Thorvaldson, T. and Johnson, L. R. Can. J. Research, B, 18 : 138-150. 1940.
15. Williams, K. T., Lakin, H. W., and Byers, H. G. U.S. Dept. Agr. Tech. Bull. 702. 1940.
16. Williams, K. T., Lakin, H. W., and Byers, H. G. U.S. Dept. Agr. Tech. Bull. 758. 1941.
17. Wyoming Agr. Expt. Sta., Ann. Rept. 1932-33.

CONTRIBUTION TO THE STUDY OF THE PRECIPITATION OF CARBONATES, BORATES, SILICATES AND ARSENATES[1]

BY PAUL E. GAGNON[2], LOUIS CLOUTIER[2] AND R. MARTINEAU[3]

Abstract

A study was made of the precipitation, at room temperature, of the carbonates of cadmium, cobalt, and nickel, of the chromate of beryllium, of the borates of zinc, of the silicates of copper and of the arsenates of lead. A rapid-mixing apparatus that insured that the precipitations took place in homogeneous liquid medium was used. In each series of experiments, the concentration of one reacting solution was kept constant and that of the other systematically varied. The values of the molar ratio of oxides, CdO/CO_2 for example, in the precipitates were found by analysis. If they remained constant with different concentrations of reactants, a definite compound was indicated. The normal cadmium carbonate was obtained. Three definite basic compounds, not described in the literature, were prepared: a definite basic carbonate of cobalt, $5CoCO_3.Co(OH)_2$, and two definite basic arsenates of lead, $4Pb_3(AsO_4)_2.Pb(OH)_2$ and $9Pb_3(AsO_4)_2.Pb(OH)_2$. Dilead arsenate, $PbHAsO_4$, was easily precipitated, but trilead arsenate, $Pb_3(AsO_4)_2$, only under very specific conditions. The other precipitates were all mixtures. The influence of the hydrogen ion concentration of the solutions on the composition of the precipitates formed was determined.

Introduction

The composition of precipitates obtained by mixing solutions often varies not only according to the concentration of the reagents and to the temperature but also according to the method of precipitation. The last factor is much more important than it was at first believed to be. This explains why so many authors have obtained different results although using the same solutions. In the case of solutions apt to form basic salts, a whole series of mixtures may be obtained, their composition ranging from that of the hydroxide to that of the normal salt. These mixtures have often been assumed to be definite compounds. Consequently, when the study of a precipitation is planned, the method of mixing the solutions must be taken into account so that the precipitates be formed in homogeneous medium.

To realize a rapid mixing of two solutions and obtain homogeneous precipitates, Pierre Jolibois has designed an apparatus and proposed a procedure that has been followed for the study of numerous precipitations (2, 3, 7, 8, 9, 10, 12).

The main object of this work was to apply Jolibois' method to the study of the precipitation, at room temperature, of the carbonates of cadmium, cobalt and nickel, of the chromate of beryllium, of the borates of zinc, of the silicates of copper and of the arsenates of lead.

[1] *Manuscript received January 29, 1941.*
Contribution from the Department of Chemistry, Laval University, Quebec, Que.
[2] *Professor of Chemistry.*
[3] *Graduate student, and holder of a bursary (1938-1939) and of a studentship (1939-1940) under the National Research Council of Canada.*

Procedure

Since a detailed description of the apparatus used can easily be found in the literature (3, 7, 12), it is not necessary to repeat it here.

The present authors generally used only two reactants, e.g., four litres of a solution of cadmium nitrate, $M/20$, was mixed very rapidly with four litres of a solution of potassium acid carbonate, $M/20$. The precipitate formed was filtered off and analysed. The experiment was repeated with four litres of solutions of cadmium nitrate of the same concentration, $M/20$, and four litres of solutions of potassium acid carbonate of different concentrations ranging from $M/20$ to $M/2$. The values of the molar ratio of oxides CdO/CO_2 found for the precipitates were tabulated and plotted against the corresponding values of the molar ratio of oxides CO_2/CdO in the solutions.

Whenever the value of the molar ratio of oxides in the precipitates remained constant for successive increasing values of the molar ratio of oxides in the solutions, a definite compound was indicated, whereas, if the composition of the precipitates varied, a mixture had been obtained.

General Results

The reactions of solutions of cadmium nitrate with solutions of potassium acid carbonate always yielded the normal carbonate of cadmium, whereas with solutions of ammonium carbonate more basic precipitates were obtained.

The precipitation of solutions of cobalt nitrate by those of potassium acid carbonate gave a definite basic compound, $5CoCO_3 . Co(OH)_2$, which has not been described in the literature, whereas solutions of ammonium carbonate gave unstable products that decomposed with loss of carbon dioxide.

When solutions of nickel nitrate and of ammonium carbonate were used, basic mixtures were first formed, but, when the value of the molar ratio CO_2/NiO in the solutions was higher than 7.0, the nickel remained in solution as nikelo-ammonic cations. Potassium acid carbonate did not give precipitates in sufficient quantity to be studied.

The hydrogen ion concentration has a marked influence on the composition of the carbonates obtained by precipitation. The influence of the carbonate ions is lessened by the concentration of the hydrogen ions.

The beryllium carbonates decomposed immediately after their formation by giving off carbon dioxide, and the beryllium chromate was hydrolysed by washing. Hence, it was impossible to study these compounds.

The precipitates prepared from solutions of zinc nitrate and solutions of borax, or of borax and sodium hydroxide, were all basic mixtures.

Solutions of copper sulphate treated with those of sodium metasilicate gave basic or acid mixtures, and, when treated with solutions of sodium metasilicate and sodium hydroxide, yielded only basic mixtures.

When solutions of lead nitrate reacted with those of arsenic acid or of monopotassium arsenate, dilead arsenate was always precipitated. However,

when there was an excess of arsenate ions, the precipitates adsorbed some and were not pure.

The reaction between solutions of lead acetate and of arsenic acid gave the same results, although, in this case, a slight excess of arsenic ion had no influence on the purity of the precipitates.

Solutions of lead chloride gave by reaction with arsenic acid indefinite lead chloroarsenates.

Solutions of lead nitrate and of dipotassium arsenate produced, depending on the concentration, dilead arsenate, $PbHAsO_4$, trilead arsenate, $Pb_3(AsO_4)_2$, and the definite basic arsenate $9Pb_3(AsO_4)_2 . Pb(OH)_2$. The first two are well known, whereas the last has not yet been mentioned in the literature.

Solutions of lead nitrate treated with those of arsenic acid and potassium hydroxide gave basic mixtures. However, with very dilute solutions of potassium hydroxide, dilead arsenate was obtained.

Finally, solutions of lead nitrate and of arsenic acid containing ammonium hydroxide yielded dilead arsenate and a definite basic arsenate $4Pb_3(AsO_4)_2 . Pb(OH)_2$, which has not yet been described.

None of the basic arsenates of lead mentioned in the literature could be obtained by the present authors under the conditions maintained.

The composition of the arsenates that were prepared did not change when stirred for 24 hr. with their mother liquors.

The pH values of all the mother liquors of the arsenates were determined and the influence of the hydrogen ion concentration on the composition of the precipitates was ascertained.

Experimental and Results

Cadmium Carbonates

Schulten (18) obtained crystals of the normal carbonate by washing with aqueous ammonia the precipitate obtained by adding an excess of ammonium carbonate to a concentrated solution of cadmium chloride and heating the diluted mixture on a water-bath.

The present authors, using solutions of cadmium nitrate, $M/20$, and of potassium acid carbonate of different concentrations, $M/20$ to $M/2$, always obtained the normal carbonate of cadmium. With solutions of cadmium nitrate, $M/20$, and of ammonium carbonate of different concentrations, $M/20$ to $M/2$, precipitates slightly more basic than the normal cadmium carbonate were obtained.

Since other authors (3) obtained two definite basic carbonates but no normal carbonate of cadmium by interaction of solutions of cadmium nitrate $M/20$, and of normal potassium carbonate, $M/40$ to $3/4$ M, instead of solutions of potassium acid carbonate or ammonium carbonate, it may be concluded that the composition of the cadmium carbonate formed by precipitation is greatly influenced by the hydrogen ion concentration.

Before being analysed, the precipitates were filtered off, washed thoroughly with cold distilled water, and dried at 80° C. Qualitative tests indicated that the precipitates were free from potassium or ammonium ions. Since the carbonates still contained water, the carbon dioxide and the metal were determined on the same portion of the sample. Carbon dioxide liberated by hydrochloric acid (1 : 1) was absorbed in weighed soda-lime tubes and the resulting cadmium chloride solution was treated with concentrated sulphuric acid and evaporated to dryness on the steam-bath. The residue was dissolved in water and the solution brought up to 250 cc. in a graduated flask. Cadmium was then determined electrolytically on 50 cc. portions of the solution.

The results are given in Tables I and II.

TABLE I

CADMIUM NITRATE ($M/20$) AND POTASSIUM ACID CARBONATE ($M/20$ TO $M/2$)

Conc. of solutions, moles per litre		Molar ratio CO_2/CdO in solutions	Analysis of precipitates, gm.		Molar ratio CdO/CO_2 in precipitates	Average
$Cd(NO_3)_2$	$KHCO_3$		CdO	CO_2		
0.05	0.05	1.0	1.2485	0.4744	1.03	
			1.2685	0.4819	1.03	1.03
0.05	0.25	5.0	1.3115	0.4930	1.037	
			1.2470	0.4806	1.015	1.02
0.05	0.50	10.0	1.2760	0.4888	1.022	
			1.2485	0.4772	1.024	1.02

TABLE II

CADMIUM NITRATE ($M/20$) AND AMMONIUM CARBONATE ($M/20$ TO $M/2$)

Conc. of solutions, moles per litre		Molar ratio CO_2/CdO in solutions	Analysis of precipitates, gm.		Molar ratio CdO/CO_2 in precipitates	Average
$Cd(NO_3)_2$	$(NH_4)_2CO_3$		CdO	CO_2		
0.05	0.05	1.0	1.2100	0.4528	1.046	
			1.2740	0.4684	1.065	1.06
			1.2925	0.4775	1.059	
0.05	0.25	5.0	1.2685	0.4800	1.034	
			1.3300	0.5013	1.036	1 03
0.05	0.50	10.0	1.3070	0.4869	1.050	
			1.3340	0.4960	1.052	1.05

COBALT CARBONATES

Since the normal cobalt carbonate is easily hydrolysed and transformed into basic carbonate, it is difficult to prepare by precipitation even when using potassium acid carbonate. Under the conditions of the present experiments, only one basic carbonate, which has not yet been described, could be obtained.

The solutions used were: cobalt nitrate, $M/20$, potassium acid carbonate $M/10$ to $M/2$. The precipitate obtained with a $M/10$ potassium acid carbonate solution was a basic mixture More concentrated solutions of the acid carbonate yielded precipitates having the composition $5CoCO_3\ Co(OH)_2$.

TABLE III

COBALT NITRATE ($M/20$) AND POTASSIUM ACID CARBONATE ($M/10$ TO $M/2$)

Conc of solutions, moles per litre		Molar ratio CO_2/CoO in solutions	Analysis of precipitates, gm		Molar ratio CoO/CO_2 in precipitates	Average
$Co(NO_3)_2$	$KHCO_3$		CoO	CO_2		
0 05	0 10	2 0	1 6880	0 9935	1 268	1 27
0 05	0 30	6 0	1 4440	0 8862	1 213	
			1 0480	0 6414	1 220	1 22
0 05	0 50	10 0	0 9660	0 6024	1 197	
			0 9545	0 5909	1 206	1 20

TABLE IV

COBALT NITRATE ($M/20$) AND AMMONIUM CARBONATE ($M/40$ TO $M/2$)

Conc of solutions moles per litre		Molar ratio CO_2/CoO in solutions	Analysis of precipitates, gm		Molar ratio CoO/CO_2 in precipitates	Average	Days between precipitation and analysis
$Co(NO_3)_2$	$(NH_4)_2CO_3$		CoO	CO_2			
0 05	0 025	0 5	0 7640	0 2740	2 082	2 10	2
			0 7390	0 2589	2 131		
0 05	0 05	1 0	0 5850	0 1965	2 222		
			0 6810	0 2271	2 239	2 23	5
0 05	0 05	1 0	1 3050	0 4998	1 949		
(Second precipitation)			1 1765	0 4483	1 959	1 95	1
0 05	0 10	2 0	1 5020	0 6727	1 667		
			1 4135	0 6234	1 693	1 68	1
0 05	0 15	3 0	0 9815	0 4016	1 824		
			0 9910	0 4074	1 816	1 82	1
(Second analysis of			1 2570	0 4094	2 292		
same precipitate)			1 3610	0 4434	2 291	2 29	15
0 05	0 25	5 0	1 3740	0 4933	2 079		
			1 2800	0 4621	2 069	2 07	2
0 05	0 375	7 5	1 4480	0 6158	1 755		
			1 5420	0 6596	1 745	1 75	1
(Second analysis of			1 3035	0 4328	2 248		
same precipitate)			1 4310	0 4728	2 259	2 25	10
0 05	0 50	10 0	1 5355	0 5308	2 159		
			2 1560	0 7616	2 113		
			2 1740	0 7616	2 131	2 13	3

The precipitates obtained with solutions of cobalt nitrate, $M/20$, and of ammonium carbonate, $M/40$ to $M/2$, decomposed rapidly. The curve (Fig. 3) prepared by plotting the time elapsed between filtration and analysis against the value of the CoO/CO_2 molar ratio of each precipitate shows a rapid loss of carbon dioxide during the first five days, and indicates that at equilibrium the value of the molar ratio CoO/CO_2 is more than 2.3.

Other investigators (3) carried out a series of precipitations with solutions of cobalt nitrate, $M/20$, and of normal potassium carbonate, $M/40$ to $M/2$. They obtained indefinite basic carbonates in which the values of the CoO/CO_2 molar ratio were always more than 2. Hence, it can be concluded that the

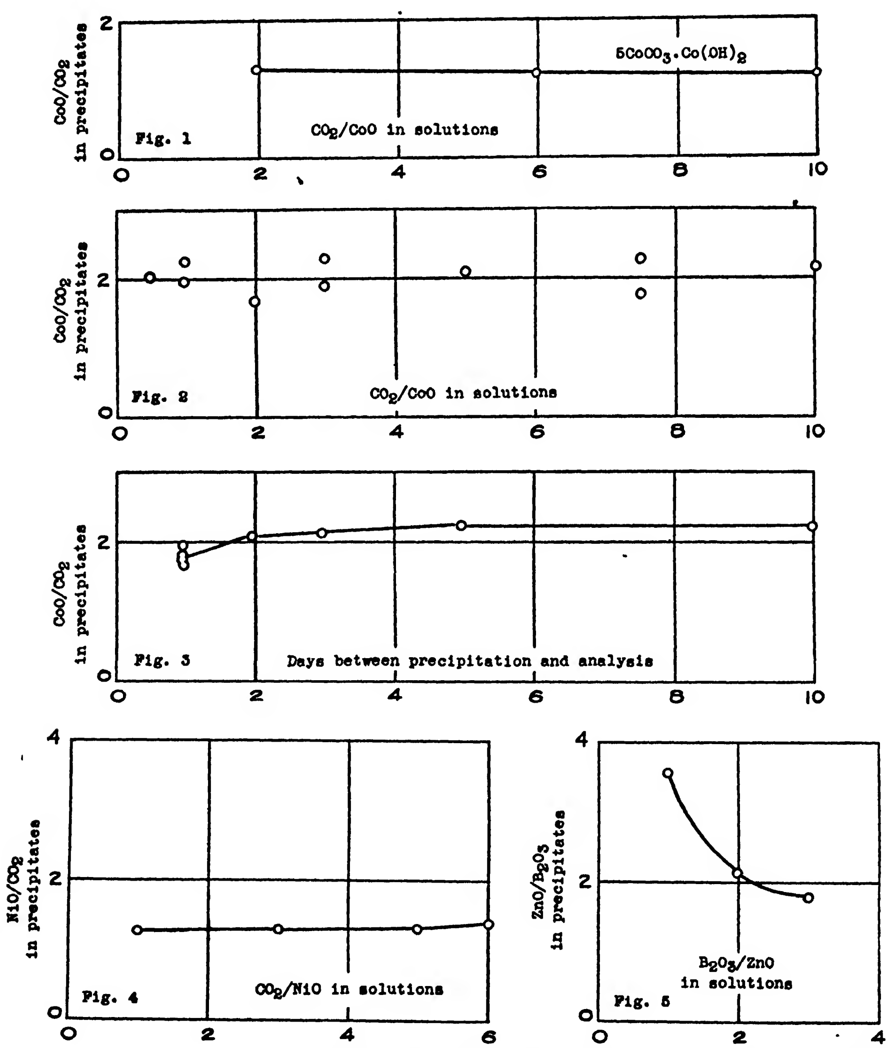

FIGS. 1 - 5. FIG. 1. *Cobalt nitrate and potassium acid carbonate.* FIG. 2. *Cobalt nitrate and ammonium carbonate.* FIG. 3. *Cobalt nitrate and ammonium carbonate.* FIG. 4. *Nickel nitrate and ammonium carbonate.* FIG. 5. *Zinc nitrate and borax.*

composition of the cobalt carbonates, like that of the cadmium carbonates, is greatly influenced by the hydrogen ion concentration.

After filtration, the precipitates were washed thoroughly with cold distilled water and allowed to dry in the air at room temperature. Tests for the presence of potassium or ammonium were negative. The carbon dioxide and the metal were determined on the same portion of the sample: carbon dioxide was displaced with hydrochloric acid and absorbed in weighed soda-lime tubes; cobalt was determined electrolytically.

The results are given in Tables III and IV and Figs. 1, 2, and 3.

Nickel Carbonates

Attempts were made to obtain nickel carbonates by treating nickel nitrate solutions with potassium acid carbonate solutions, but the amounts of the precipitates were not sufficient for study.

The solutions used were: nickel nitrate, $M/20$; ammonium carbonate, $M/20$ to $M/2$. When the value of the CO_2/NiO molar ratio in the solutions was less than 7, indefinite basic carbonates were obtained and when the value was more than 7, no precipitate was formed. When using nickel nitrate solutions, $M/20$, and solutions of potassium carbonate, $M/20$ to $3/4\ M$, other investigators (3) prepared nickel carbonates that were more basic. Hence, the composition of the nickel carbonates, like that of the carbonates of cadmium and cobalt, depends greatly on the hydrogen ion concentration.

The precipitates were treated and analysed as indicated for the carbonates of cobalt. They contained no ammonium. The results are given in Table V and Fig. 4.

TABLE V

Nickel nitrate ($M/20$) and ammonium carbonate ($M/20$ to $3/10\ M$)

Conc. of solutions, moles per litre		Molar ratio CO_2/NiO in solutions	Analysis of precipitates, gm.		Molar ratio NiO/CO_2 in precipitates	Average
$Ni(NO_3)_2$	$(NH_4)_2CO_3$		NiO	CO_2		
0.05	0.05	1.0	0.5800	0.3391	1.282	
			0.5670	0.3304	1.287	1.28
0.05	0.15	3.0	0.9230	0.5324	1.300	
			0.9560	0.5500	1.303	1.30
0.05	0.25	5.0	0.8600	0.4839	1.332	
			0.8980	0.5052	1.332	1.33
0.05	0.30	6.0	0.7810	0.4176	1.402	
			0.8070	0.4316	1.402	1.40

Effect of hydrogen ion concentration on the composition of the carbonates

It has already been mentioned that the hydrogen ion concentration exerts a strong influence on the composition of the carbonates of cadmium, cobalt, and nickel obtained by precipitation. The degree of this influence is indicated qualitatively in Table VI, in which the results obtained by the authors, with potassium acid carbonate and ammonium carbonate solutions, are compared with the results that Cloutier, Pelletier, and Gagnon obtained with normal potassium carbonate solutions (3). The values of the molar ratio of oxides in the precipitates increased when the pH values of the mother liquors were increased.

TABLE VI

Composition of the carbonates for different pH values

Reactant	Values of the molar ratio of oxides in the precipitates		
	CdO/CO_2	CoO/CO_2	NiO/CO_2
Solutions of low pH values $KHCO_3$	1.0	From 1.22 to 1.27	
Solutions of higher pH values $(NH_4)_2CO_3$	1.0	From 1.75 to 2.29	From 1.28 to 1.40
Solutions of still higher pH values K_2CO_3	From 1.1 to 1.2	From 2.15 to 2.58	From 1.45 to 3.53

Beryllium Chromate and Carbonates

A few unsuccessful attempts to precipitate beryllium chromate and beryllium carbonate were made.

When a solution of beryllium nitrate, $M/20$, was used with a potassium chromate solution, $M/20$, no precipitate was formed. With a $M/4$ solution of potassium chromate, the precipitate obtained was hydrolysed by washing. To measure the extent of its decomposition, it was boiled four times with large quantities of water, filtered off, and analysed by the following method. It was dissolved in hydrochloric acid, and the solution was treated with an excess of a sodium hydroxide solution, 6 N, until the precipitate formed at first redissolved. The solution was then diluted to 500 cc. and boiled for 50 min. The beryllium hydroxide precipitated was filtered off on a hot filter, washed thoroughly with hot water, dried, ignited, and weighed as BeO. The chromic acid in the filtrate was determined by iodometric titration. The results found indicate nearly complete hydrolysis: BeO, 0.3482 gm., CrO_3, 0.0077 gm.; molar ratio, BeO/CrO_3, 181.

Beryllium nitrate solutions treated with either potassium acid carbonate or ammonium carbonate solutions gave unstable compounds; carbon dioxide was immediately evolved. These results confirm those of Parsons (11).

Zinc Borates

No definite zinc borate could be obtained under the present experimental conditions.

(*a*). *Zinc Nitrate and Borax*

Solutions of zinc nitrate $M/20$, and of borax, B_2O_3 $M/20$ to $3/20$ M, were used. Indefinite basic borates were obtained. When the concentrations of the solutions of borax were increased, the precipitates became less basic. The pH values of the mother liquors were determined within 0.2. It was thus established that the more basic precipitate of this series was formed in a slightly acid medium, whereas the others were formed in a slightly alkaline medium. This was probably due to the solubility of zinc hydroxide in the sodium hydroxide formed by the hydrolysis of borax.

For analysis, the precipitates were filtered off, washed thoroughly with cold distilled water, and dried at red heat. A weighed portion was fused with a mixture of potassium and sodium carbonates. The melt was digested with distilled water on the water-bath until disintegration was complete. The zinc carbonate was filtered off, washed with 1% solution of sodium carbonate and then with cold distilled water, dried, ignited, and weighed as ZnO. The filtrate was acidified, refluxed to remove all the carbon dioxide, and diluted to 250 cc. with freshly boiled distilled water. A 50 cc. portion was neutralized with a sodium hydroxide solution, $N/10$, using methyl orange as indicator. Another 50 cc. portion of the borate solution was neutralized, without methyl orange, by the addition of the same volume of standard sodium hydroxide solution, $N/10$. The boric acid was titrated by further addition of standard sodium hydroxide solution in the presence of neutral glycerol and phenolphtalein as indicator. Later it was found sufficient to determine ZnO by the pyrophosphate method and B_2O_3 by difference. The precipitates contained no sodium.

The results are given in Table VII and Fig. 5.

TABLE VII

Zinc nitrate ($M/20$) and Borax (B_2O_3 $M/20$ to $3/20$ M)

Conc. of solutions, moles per litre		Molar ratio B_2O_3/ZnO in solutions	Analysis of precipitates, gm.		Molar ratio ZnO/B_2O_3 in precipitates	Average	pH values of the mother liquors
$Zn(NO_3)_2$	B_2O_3(borax)		ZnO	B_2O_3			
0.05	0.05	1.0	1.2024	0.2911	3.53	3.53	6.6
0 05	0.10	2.0	0.4005	0.1611*	2.127		
			0.3217	0.1305*	2.110	2.12	7.8
0.05	0.15	3.0	1.2746	0.6100	1.788	1.79	7.8

* *By difference.*

(*b*). *Zinc Nitrate, Borax, and Sodium Hydroxide*

The authors used four litres of zinc nitrate solutions, $M/20$, and solutions made up of two litres of borax solutions, B_2O_3 $M/20$, and two litres of sodium hydroxide solutions of different concentrations, Na_2O $M/20$ to $M/5$. Another precipitation was made in which boric acid, $M/10$, was used instead of sodium hydroxide. All the precipitates were basic and the basicity was found to increase very quickly with the alkalinity of the medium. When the value of the molar ratio of oxides, Na_2O/ZnO, in the solutions reached 4.0, the precipitate consisted almost entirely of zinc hydroxide. This can be explained by the law of mass action. The addition of sodium hydroxide prevents the hydrolysis of the borax.

The pH values of the mother liquors were determined within 0 2. The precipitates were treated and analysed as indicated above. They contained no sodium.

The results are given in Table VIII and Fig. 6, together with the results of an experiment with a zinc nitrate solution, $M/20$, and a borax solution, $M20$.

TABLE VIII

ZINC NITRATE ($M/20$), BORAX (B_2O_3 $M/20$), SODIUM HYDROXIDE (Na_2O $M/20$ TO $M/5$), AND BORIC ACID (B_2O_3 $M/10$)

Conc of solutions, moles per litre			Molar ratio Na_2O/ZnO in solutions	Analysis of precipitates, gm.		Molar ratio ZnO/B_2O_3 in precipitates	Average	pH values of the mother liquors
$Zn(NO_3)_2$ 4 litres	B_2O_3 (borax) 2 litres	Na_2O 2 litres		ZnO	B_2O_3			
0 05	0 05	0 05	0 5	1 6176	0 2598*	5 328	5 33	6 6
0 05	0 05	0 10	1 0	1 5272	0 0522	25 03	25 0	9 2
0 05	0 05	0 20	2 0	1 4086	0 0045	269 06	269	9 6
		B_2O_3 (boric ac) 2 litres	Molar ratio B_2O_3(bor ac)/ZnO in solutions					
0 05	0 05	0 10	1 0	0 3986 0 3572	0 1278* 0 1148	2 669 2 663	2 67	6 8
0.05	0 05	—	0 0	1 2024	0 2911	3 53	3 53	6 6

* *By difference.*

COPPER SILICATES

(*a*). *Copper Sulphate and Sodium Metasilicate*

Solutions of copper sulphate, $M/20$, and of sodium metasilicate, Na_2SiO_3, $M/40$ to $M/2$, were used. Indefinite basic and acid copper silicates were obtained.

The precipitates formed were filtered off immediately. They were gelatinous and could not be filtered rapidly. They were washed with distilled water until the filtrate gave no brown precipitate or colour with silver nitrate solution. All were pale blue but some darkened and became greenish during washing and drying. After drying at 80°, they were powdered and analysed.

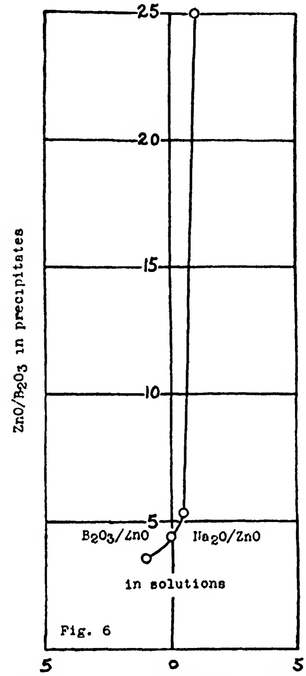

FIG. 6. *Zinc nitrate, borax, sodium hydroxide and boric acid*

The material (1.5 gm.) was weighed into a small porcelain dish and covered with water. Concentrated hydrochloric acid (5 cc.) was added and the solution evaporated to dryness on the water-bath. The addition of concentrated hydrochloric acid and evaporation to dryness were repeated twice. The mass was then moistened with concentrated hydrochloric acid and allowed to stand for 15 min. After addition of hot water, the silica was filtered off and washed with hot water until free from hydrochloric acid. The filtrate was evaporated to dryness and the residue treated as the original material. The two filter papers were dried and ignited together in a weighed platinum crucible in the electric furnace at red heat. The silica was then weighed. It was almost pure silica, leaving virtually no residue when treated with hydrofluoric acid.

The filtrate containing the copper was treated with concentrated sulphuric acid (3 cc.), evaporated on the water-bath, and diluted to exactly 100 cc. Copper was then determined by electrolysis on an aliquot portion. The precipitates contained no sodium.

The results are given in Table IX and Fig. 7.

TABLE IX

COPPER SULPHATE ($M/20$) AND SODIUM METASILICATE ($M/40$ TO $M/2$)

Conc. of solutions, moles per litre		Molar ratio SiO_2/CuO in solutions	Analysis of precipitates, gm.		Molar ratio CuO/SiO_2 in precipitates	Average
$CuSO_4$	Na_2SiO_3		CuO	SiO_2		
0.05	0.025	0.5	0.9423	0.2216	3.210	
			0.9788	0.2322	3.182	3.20
0.05	0.05	1.0	0.8004	0.5076	1.187	
			0.9132	0.5812	1.186	1.19
0.05	0.10	2.0	0.8206	0.5726	1.082	
			0.8151	0.5706	1.078	1.08
0.05	0.15	3.0	0.6424	0.5294	0.916	
			0.6053	0.4926	0.928	
			0.6654	0.5554	0.904	0.92
0.05	0.25	5.0	0.7350	0.5854	0.948	0.95
			0.7515	0.5982	0.948	
0.05	0.50	10.0	0.6294	0.6256	0.759	
			0.6349	0.6442	0.744	0.75

(*b*) *Copper Sulphate, Sodium Metasilicate, and Sodium Hydroxide*

Copper sulphate solution, $M/20$, and solutions made up of two litres of sodium silicate solutions, $M/20$, and two litres of sodium hydroxide solutions of different concentrations, Na_2O $M/40$ to $M/4$, were used. Indefinite basic silicates were obtained. The precipitates had apparently the same physical properties as those of the preceding series, and were treated and analysed in the same way. They contained no sodium. The results are given in Table X.

TABLE X

COPPER SULPHATE ($M/20$), SODIUM METASILICATE ($M/20$), AND SODIUM HYDROXIDE (Na_2O $M/40$ TO $M/4$)

Conc. of solutions, moles per litre			Molar ratio Na_2O/CuO in solutions	Analysis of precipitates, gm.		Molar ratio CuO/SiO_2 in precipitates	Average
$CuSO_4$ 4 litres	Na_2SiO_3 2 litres	Na_2O 2 litres		CuO	SiO_2		
0.05	0.05	0.025	0.25	1.0249	0.2478	3.122	
				0.9708	0.2368	3.095	3.11
0.05	0.05	0.125	1.25	1.1015	0.2332	3.565	
				1.0990	0.2320	3.575	3.57
0.05	0.05	0.25	2.5	1.1175	0.1992	4.235	
				1.1290	0.2010	4.240	4.24

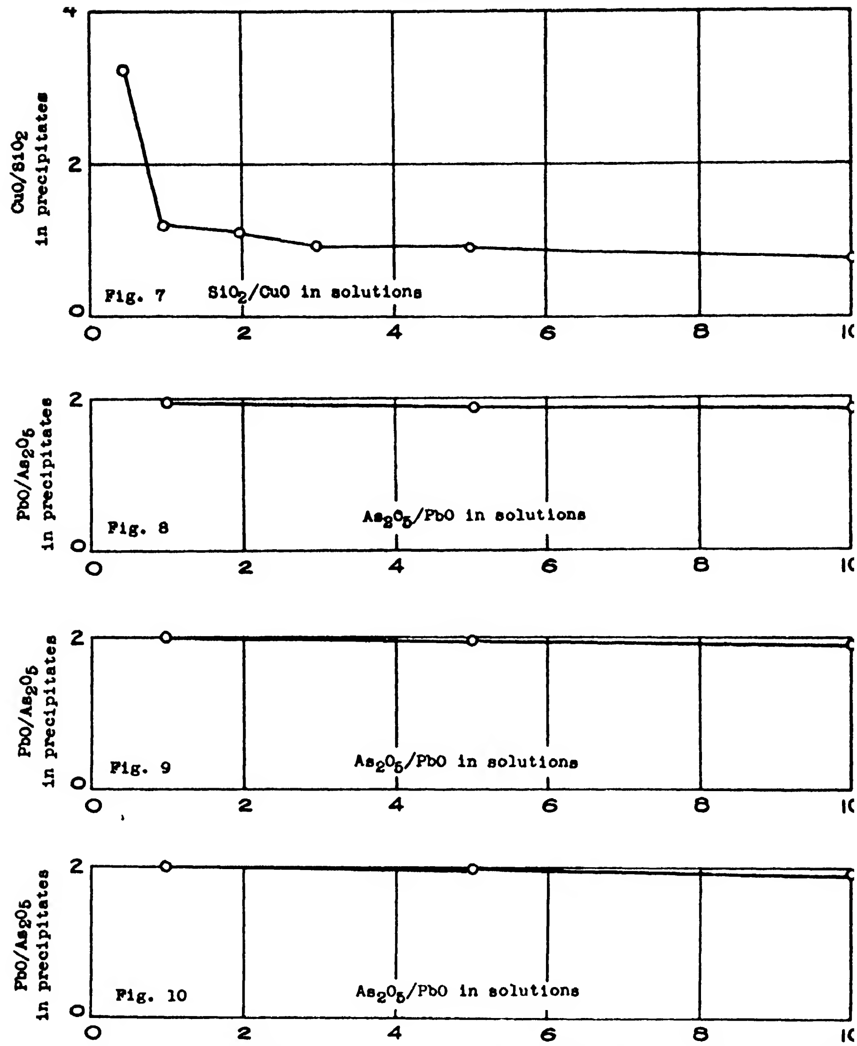

FIGS. 7 - 10. FIG. 7. *Copper sulphate and sodium metasilicate.* FIG. 8. *Lead nitrate and arsenic oxide.* FIG. 9. *Lead nitrate and monopotassium arsenate.* FIG. 10. *Lead acetate and arsenic oxide.*

LEAD ARSENATES

(*a*) *Lead Nitrate and Arsenic Acid*

Solutions of arsenic oxide, $M/20$, and of lead nitrate, $M/10$ to $M/2$, were used. Pure dilead arsenate was always obtained.

With solutions of lead nitrate, $M/20$, and of arsenic oxide, $M/20$ to $M/2$, precipitates that were more acidic were formed. They probably consisted of dilead arsenate, $PbHAsO_4$, with adsorbed arsenate ions, since the acidity of the precipitates increased with the excess of arsenic oxide used.

These results show clearly that if pure dilead arsentate is to be precipitated from solutions of lead nitrate and arsenic oxide, the arsenic oxide must not be

in excess. If the precipitation is to be made in the ordinary manner, the solution of arsenic oxide must be poured into the lead nitrate solution, so that at no time there can be an excess of arsenic oxide. This was known by Rose (17) who precipitated pure dilead arsenate from solutions of lead nitrate with solutions of arsenic acid.

All precipitations took place in a strongly acid medium (pH less than 1.7). Two of the precipitates were divided into two portions, one being filtered immediately after formation and the other being left in the mother liquor, which was stirred for 24 hr. The stirring did not change the composition of the arsenates; this indicated that equilibrium was attained quickly in every case. Precipitates were always filtered off on a Büchner funnel and washed with distilled water until the filtrate gave no reaction for lead with hydrogen sulphide water, nor for arsenic acid with silver nitrate solution. They were then dried at 80 to 90° C., pulverized, and analysed.

Lead oxide was determined according to the Official Method No. 1 of the A.O.A.C. (1) for total lead oxide in lead arsenate, and arsenic oxide according to the Tentative Method of the A.O.A.C. (1) for total arsenic oxide in lead arsenate. However, the purity of the lead arsenates precipitated made unnecessary the following operations: (*a*) in the lead oxide determination, the heating and filtration following the dissolving of the sample in 1 : 4 nitric acid; (*b*) in the arsenic oxide determination, the initial addition of 25 ml. of concentrated hydrochloric acid and the subsequent evaporation.

The results are given in Tables XI*a*, XI*b*, XII*a*, XII*b*, and Fig. 8.

TABLE XI*a*

LEAD NITRATE ($M/10$ TO $M/2$) AND ARSENIC OXIDE ($M/20$)

Precipitate No.	Analysis of precipitates, gm.				Molar ratio PbO/As_2O_5 in precipitates	Average
	PbO determination samples	PbO	As_2O_5 determination samples	As_2O_5		
55-1	0.5020	0.3226	0.5012	0.1656	2.00	
	0.5049	0.3242	0.5024	0.1660	2.00	2.00
56-1	0.5004	0.3220	0.5082	0.1657	2.03	
	0.5035	0.3236	0.5056	0.1643	2.03	2.03
56-11	0.5249	0.3360	0.5253	0.1729	2.00	
	0.5499	0.3529	0.5253	0.1735	2.00	2.00
57-1	0.5131	0.3294	0.4913	0.1615	2.01	
	0.4897	0.3131	0.5108	0.1681	2.00	2.01
57-11	0.4938	0.3160	0.5062	0.1664	2.00	
	0.5558	0.3539	0.4982	0.1640	1.99	2.00

TABLE XI*b*

Lead nitrate (*M*/10 to *M*/2) and arsenic oxide (*M*/20)

Precipitate No.	Conc. of solutions, moles per litre		Molar ratio PbO/As_2O_5 in solutions	Molar ratio PbO/As_2O_5 in precipitates	pH values of the mother liquors
	$Pb(NO_3)_2$	As_2O_5			
55-1	0.10	0.05	2.0	2.00	1.2
56-1	0.25	0.05	5.0	2.03	1.1
56-11	0.25	0.05	5.0	2.00	
57-1	0.50	0.05	10.0	2.01	1.0
57-11	0.50	0.05	10.0	2.00	

1 : *filtered immediately after precipitation.*
11 : *filtered after stirring 24 hr. in the mother liquor.*

TABLE XII*a*

Lead nitrate (*M*/20) and arsenic oxide (*M*/20 to *M*/2)

Precipitate No.	Analysis of precipitates, gm.				Molar ratio PbO/As_2O_5 in precipitates	Average
	PbO determination samples	PbO	As_2O_5 determination samples	As_2O_5		
51-1	0.5004	0.3161	0.5002	0.1673	1.94	
	0.5006	0.3176	0.5006	0.1679	1.95	1.95
51-11	0.5004	0.3194	0.5020	0.1671	1.97	
	0.5000	0.3188	0.5028	0.1676	1.97	1.97
52-1	0.5000	0.3122	0.5016	0.1703	1.89	
	0.5002	0.3104	0.5000	0.1700	1.88	1.89
52-11	0.5007	0.3102	0.5015	0.1709	1.87	
	0.5002	0.3111	0.5001	0.1702	1.88	1.88
53-1	0.5007	0.3040	0.5015	0.1724	1.82	
	0.5008	0.3049	0.5011	0.1721	1.82	1.82
53-11	0.5024	0.3083	0.4054	0.1398	1.83	
	0.5011	0.3067	0.4002	0.1378	1.83	1.83

TABLE XII*b*

Lead nitrate (*M*/20) and arsenic oxide (*M*/20 to *M*/2)

Precipitate No.	Conc. of solutions, moles per litre		Molar ratio As_2O_5/PbO in solutions	Molar ratio PbO/As_2O_5 in precipitates	pH values of the mother liquors
	$Pb(NO_3)_2$	As_2O_5			
51-1	0.05	0.05	1.0	1.95	1.7
51-11	0.05	0.05	1.0	1.97	
52-1	0.05	0.25	5.0	1.89	1.7
52-11	0.05	0.25	5.0	1.88	
53-1	0.05	0.50	10.0	1.82	1.2
53-11	0.05	0.50	10.0	1.83	

1 : *filtered immediately after precipitation.*
11 : *filtered after stirring 24 hr. in the mother liquor.*

(*b*) *Lead Nitrate and Monopotassium arsenate*

Solutions of lead nitrate, $M/20$, and of monopotassium arsenate, KH_2AsO_4, $M/10$ to M, were used. The monopotassium arsenate solution was prepared by mixing solutions of arsenic acid and of potassium hydroxide in equivalent quantities.

The first precipitation with monopotassium arsenate, $M/10$, gave pure dilead arsenate. The other two experiments, in which greater excesses of monopotassium arsenate were used, yielded precipitates that are more acidic and that are believed to consist of dilead arsenate with adsorbed arsenate ions. A slight excess of monopotassium arsenate may be used to prepare pure dilead arsenate from lead nitrate solutions whereas, as indicated above, if a slight excess of arsenic acid is present, the precipitate is not pure. In any case, it is safer to have an excess of lead nitrate present. McDonnell and Smith precipitated pure dilead arsenate from solutions of lead nitrate and solutions of monopotassium arsenate (13).

The precipitates were filtered off immediately after formation. They were treated and analysed as described before. None contained potassium. The mother liquors were all strongly acid (pH less than 3.2). The results are given in Tables XIII*a* and XIII*b* and in Fig. 9.

TABLE XIII*a*

LEAD NITRATE ($M/20$) AND MONOPOTASSIUM ARSENATE ($M/10$ TO M)

Precipitate No.	Analysis of precipitates, gm.				Molar ratio PbO/As_2O_5 in precipitates	Average
	PbO determination samples	PbO	As_2O_5 determination samples	As_2O_5		
84	0.5194	0.3358	0.4957	0.1642	2.01	
	0.5351	0.3459	0.5618	0.1851	2.02	2.01
85	0.5093	0.3242	0.5133	0 1730	1.94	
	0.4954	0.3160	0.5230	0.1761	1.95	1.95
86	0.5012	0.3166	0.4874	0.1655	1.91	
	0.4798	0.3028	0.4869	0.1653	1.91	1.91

TABLE XIII*b*

LEAD NITRATE ($M/20$) AND MONOPOTASSIUM ARSENATE ($M/10$ TO M)

Precipitate No.	Conc. of solutions, moles per litre			Molar ratio As_2O_5/PbO in solutions	Molar ratio PbO/As_2O_5 in precipitates	pH values of the mother liquors
	$Pb(NO_3)_2$ 4 litres	As_2O_5 2 litres	K_2O 2 litres			
84	0.05	0.10	0.10	1.0	2.01	2.0
	0.05	0.50	0.50	5.0	1.95	2.8
86	0.05	1.00	1.00	10.0	1.91	3.2

(c) Lead Acetate and Arsenic Acid

The solutions used were: lead acetate, $M/20$; arsenic oxide, $M/20$ to $M/2$. With the $M/20$ solution of arsenic oxide pure dilead arsenate was obtained. With the others, the precipitates were more acid and consisted probably of dilead arsenate with adsorbed arsenate ions. Arsenic oxide when not in greater excess than twice the equivalent quantity will precipitate pure dilead arsenate from lead acetate solutions, whereas with lead nitrate solutions such an excess yielded an impure product.

All precipitates were formed in a strongly acid medium (pH under 2.1). They were filtered off immediately, treated, and analysed as mentioned before.

The results are given in Tables XIV*a* and XIV*b* and Fig. 10.

TABLE XIV*a*

LEAD ACETATE ($M/20$) AND ARSENIC OXIDE ($M/20$ TO $M/2$)

Precipitate No.	Analysis of precipitates, gm.				Molar ratio PbO/As_2O_5 in precipitates	Average
	PbO determination samples	PbO	As_2O_5 determination samples	As_2O_5		
66	0.5386	0.3479	0.5167	0.1720	1.99	
	0.5106	0.3298	0.5169	0.1722	1.99	1.99
67	0.4776	0.3046	0.4789	0.1607	1.96	
	0.4894	0.3135	0.4965	0.1666	1.97	1.96
68	0.5198	0.3320	0.5013	0.1697	1.94	
	0.4981	0.3177	0.5325	0.1801	1.94	1.94

TABLE XIV*b*

LEAD ACETATE ($M/20$) AND ARSENIC OXIDE ($M/20$ TO $M/2$)

Precipitate No.	Conc. of solutions, moles per litre		Molar ratio As_2O_5/PbO in solutions	Molar ratio PbO/As_2O_5 in precipitates	pH value of mother liquors
	$Pb(C_2H_3O_2)_2$	As_2O_5			
66	0.05	0.05	1	1.99	2.1
67	0.05	0.25	5	1.96	1.5
68	0.05	0.50	10	1.94	1.5

(d) Lead Chloride and Arsenic Acid

Solutions of lead chloride, $M/30$, and of arsenic oxide, $M/30$ to $M/2$, were used. Indefinite lead chloroarsenates were formed. McDonnell and Smith (15) prepared a lead chloroarsenate having nearly the same composition as mimetite, $Pb_4(PbCl)(AsO_4)_3$, the only difference being in its chlorine content,

which was slightly higher than in mimetite. The first precipitation of this series with arsenic oxide, $M/30$, gave also a chloroarsenate with a composition close to that of mimetite, although the chlorine content is still higher than that of the chloroarsenate prepared by McDonnell and Smith. Gmelin (5, p. 173) states that dilead arsenate is the product of the reaction of lead chloride and arsenic acid or a soluble arsenate. McDonnell and Smith (13) say that a chloroarsenate is usually formed but that dilead arsenate can also be formed. No definite lead chloroarsenate nor dilead arsenate were obtained in the present experiments. All the mother liquors were strongly acid (pH less than 1.6).

As soon as formed, the precipitates were filtered off, thoroughly washed, and dried at 80° C. Arsenic oxide and lead oxide were determined by the methods already mentioned, and chlorine, by means of silver nitrate, on 0.5 gm. of precipitate dissolved in dilute nitric acid.

The results are given in Table XV and Fig. 11.

TABLE XV

LEAD CHLORIDE ($M/30$) AND ARSENIC OXIDE ($M/30$ TO $M/3$)

Conc. of solutions, moles per litre		Molar ratio As_2O_5/PbO in solutions	Analysis of precipitates, %				Total
$PbCl_2$	As_2O_5		PbO	As_2O_5	Cl	Minus oxygen equiv. to Cl	
0.033	0.033	1.0	74.65 74.66	22.86 22.84	2.91 2.92	0.66 0.66	99.76 99.76
0.033	0.166	5.0	72.72 72.55	24.40 24.38	2.70 2.70	0.61 0.61	99.21 99.02
0.033	0.333	10.0	69.75 69.84	27.60 27.59	1.82 1.82	0.41 0.41	98.76 98.84
Composition of mimetite $Pb_4(PbCl)(AsO_4)_3$:			74.99	23.17	2.38	0.54	100.00
Composition of McDonnell and Smith's lead chloroarsenate:			74.64	22.81	2.72	0.61	99.56

(*e*) *Lead Nitrate and Dipotassium Arsenate*

Solutions of lead nitrate, $M/20$, and of dipotassium arsenate, K_2HAsO_4, $M/20$ to M, were used. The dipotassium arsenate solutions were prepared by mixing solutions of arsenic acid with those of potassium hydroxide in equivalent quantities. The precipitation with the $M/20$ dipotassium arsenate took place in a strongly acid medium and yielded dilead arsenate. With more concentrated solutions of dipotassium arsenate, the pH values were higher and the precipitates became more basic. Trilead arsenate, $Pb_3(AsO_4)_2$, was obtained when the values of the molar ratio As_2O_5/PbO in the solutions were between 2.5 and 4.0 at a pH of 7.45–7.6.

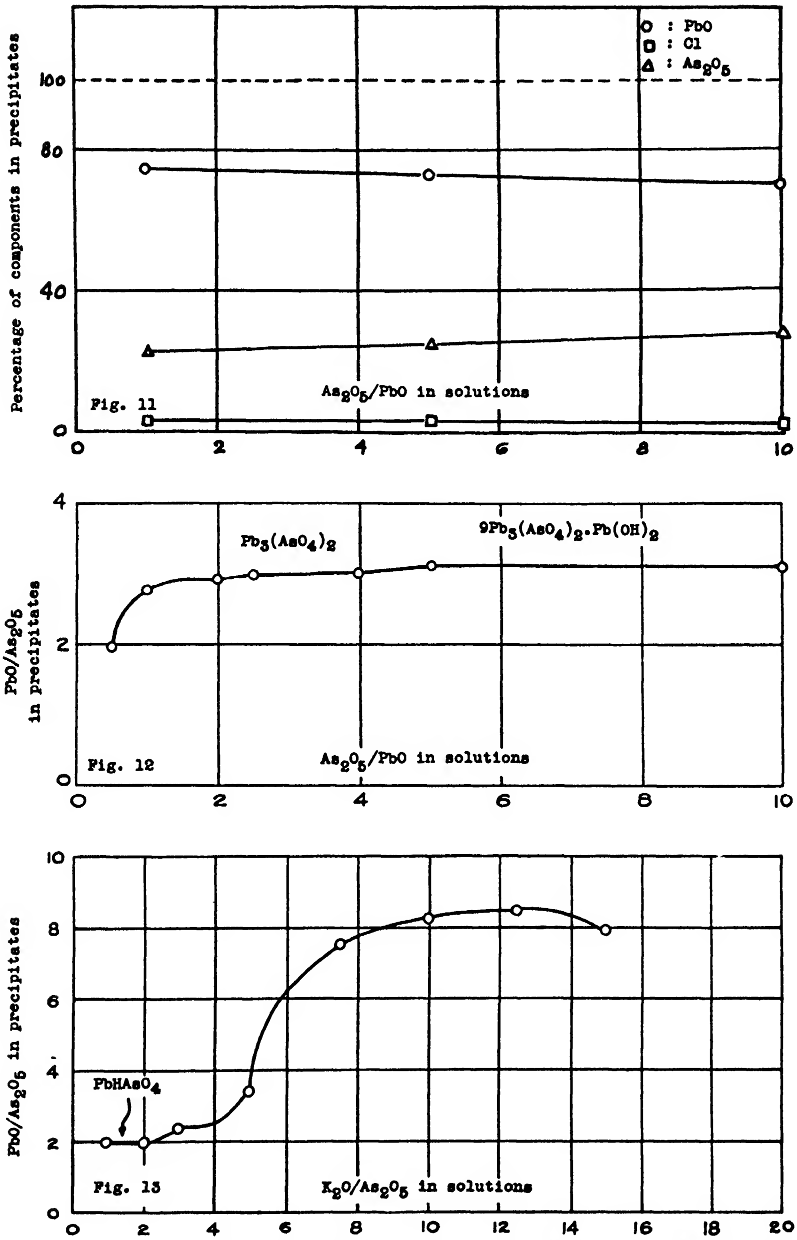

FIGS. 11 - 13. FIG. 11. *Lead chloride and arsenic oxide.* FIG. 12. *Lead nitrate and dipotassium arsenate.* FIG. 13. *Lead nitrate, arsenic oxide, and potassium hydroxide.*

These results confirm those of McDonnell and Smith (14) who found that trilead arsenate exists in solution only under specific conditions as an intermediate product between dilead arsenate and a basic arsenate.

The experiments made with great excess of arsenate yielded a definite compound, which has not yet been described. The value of its PbO/As_2O_5

molar ratio was 3.11 to 3.12, corresponding to the formula $9Pb_3(AsO_4)_2 \cdot Pb(OH)_2$.

In the literature no mention was found of precipitations of a lead salt solution by dipotassium arsenate, but numerous authors have used lead nitrate solution with solutions of the sodium salt, Na_2HAsO_4, which is more common than the potassium salt. Most of these investigators (13, 22, 19) obtained a slightly basic dilead arsenate but a few (4, 6) prepared pure dilead arsenate with dilute solutions. The present results show that there must be no excess of arsenate if pure dilead arsenate is to be obtained, because otherwise the solution would be too alkaline and would prevent its formation. Moreover, as seen previously, there must be no excess of arsenic oxide in solution since the precipitate will adsorb arsenate ions. Briefly, if pure dilead arsenate is to be precipitated from lead nitrate solutions, there must be no excess of arsenate ion and the medium must be strongly acid.

The precipitates were filtered off as soon as formed, treated, and analysed as before. They contained no potassium. The results are given in Tables XVI*a* and XVI*b* and Fig. 12.

TABLE XVI*a*

LEAD NITRATE ($M/20$) AND DIPOTASSIUM ARSENATE ($M/20$ TO M)

Precipitate No.	Analysis of precipitates, gm.				Molar ratio PbO/As_2O_5 in precipitates	Average
	PbO determination samples	PbO	As_2O_5 determination samples	As_2O_5		
63-1	0.4837	0.3084	0.4812	0.1597	1.98	
	0.4820	0.3079	0.4798	0.1596	1.98	1.98
88	0.4891	0.3531	0.4811	0.1294	2.76	
	0.4851	0.3503	0.5019	0.1355	2.75	2.76
90	0.5139	0.3762	0.5133	0.1332	2.90	
	0.5061	0.3704	0 5307	0.1373	2.91	2.91
77	0.5618	0.4118	0.5057	0.1278	2.98	
	0.5066	0.3713	0.5187	0.1313	2.98	2.98
91	0.5102	0.3761	0 4976	0.1252	3.02	
	0.4884	0.3601	0.5016	0.1264	3.01	3.02
78	0.5322	0.3955	0.5014	0.1230	3.12	
	0.5120	0.3802	0.5092	0.1253	3.11	3.11
87	0.5361	0.3965	0.5003	0.1223	3.11	
	0.5206	0.3853	0.5111	0.1250	3.12	3.12

(*f*) *Lead Nitrate, Arsenic Acid and Potassium Hydroxide*

Solutions of lead nitrate, $M/20$, and solutions made up of two litres of arsenic oxide solutions, $M/20$, and two litres of potassium hydroxide solutions of different concentrations, K_2O $M/20$ to $3/4\ M$, were used. The first

TABLE XVI*b*

LEAD NITRATE ($M/20$) AND DIPOTASSIUM ARSENATE ($M/20$ TO M)

Precipitate No.	Conc. of solutions, moles per litre			Molar ratio As_2O_5/PbO in solutions	Molar ratio PbO/As_2O_5 in precipitates	pH values of the mother liquors
	$Pb(NO_3)_2$ 4 litres	As_2O_5 2 litres	K_2O 2 litres			
63-1	0.05	0.05	0.10	0.5	1.98	2.0
88	0.05	0.10	0.20	1.0	2.76	6.8
90	0.05	0.20	0.40	2.0	2.91	7.4
77	0.05	0.25	0.50	2.5	2.98	7.45
91	0.05	0.40	0.80	4.0	3.02	7.6
78	0.05	0.50	1.00	5.0	3.11	7.8
87	0.05	1.00	2.00	10.0	3.12	9.0

experiments with dilute potassium hydroxide gave dilead arsenate in a strongly acid medium. With more concentrated solutions of potassium hydroxide, the mother liquors became alkaline and the precipitates more basic. The definite compound, $Pb_5(PbOH)_2(AsO_4)_4$ or $2Pb_3(AsO_4)_2.Pb(OH)_2$, prepared by McDonnell and Smith (16) by the action of sodium or potassium hydroxide solutions on dilead arsenate, was not precipitated.

Moreover, investigations suggested by results obtained by Strömholm (21) led McDonnell and Smith (16) to the preparation of a basic arsenate of lead $8PbO.As_2O_5.1/2H_2O$, which they called octo-arsenate. One of their methods of preparation consisted in the addition of a lead nitrate solution in successive equal portions to a solution of sodium hydroxide and trisodium arsenate in which the value of the Na_2O/As_2O_5 molar ratio was 15. The precipitate was filtered off after each addition and the filtrate used for the next precipitation. The PbO/As_2O_5 molar ratio of the successive precipitates decreased from high values to values close to 8.4 and remained there. The authors concluded that free lead hydroxide was precipitated together with the octo-arsenate at first, and then, when the excess of sodium hydroxide had been thus somewhat removed from the solution, only the octo-arsenate precipitated. The values of the molar ratio, Na_2O/As_2O_5, in solution corresponding to the precipitations of the octo-arsenate are not given. In other experiments the values of the PbO/As_2O_5 molar ratio in the octo-arsenate ranged from 7.94 to 8.20, the average being 8.07. It is evident that the octo-arsenate is not a very well defined compound.

For three precipitations in the present experiments, the values of the PbO/As_2O_5 molar ratio in the precipitates lie between 7.95 and 8.44, which corresponds with the values found by McDonnell and Smith for their octo-arsenate, but it cannot be said whether a definite compound was formed.

Before analysis, each precipitate was divided into two portions, one was dried immediately at 80° C., the other, after having been left in the mother liquor, which was stirred for 24 hr. No great difference in composition was noted between the two portions.

TABLE XVIIa

LEAD NITRATE ($M/20$), ARSENIC OXIDE ($M/20$), AND POTASSIUM HYDROXIDE (K_2O $M/20$ TO $3/4$ M)

Precipitate No.	Analysis of precipitates, gm.				Molar ratio PbO/As_2O_5 in precipitates	Average
	PbO determination samples	PbO	As_2O_5 determination samples	As_2O_5		
58-1	0.5041 0.5053	0.3220 0.3210	0.4884 0.5025	0.1610 0.1657	1.99 1.98	1.99
58-11	0.5047 0.4965	0.3219 0.3167	0.5225 0.4884	0.1721 0.1613	1.99 1.99	1.99
63-1	0.4837 0.4820	0.3084 0.3079	0.4812 0.4798	0.1597 0.1596	1.98 1.98	1.98
63-11	0.5030 0.4848	0.3222 0.3078	0.5350 0.5276	0.1767 0.1744	2.00 1.98	1.99
61-1	0.4956 0.4953	0.3366 0.3362	0.4985 0.4915	0.1487 0.1466	2.34 2.34	2.34
61-11	0.4936 0.4969	0.3260 0.3276	0.5002 0.5095	0.1553 0.1585	2.19 2.18	2.19
59-1	0.4896 0.4940	0.3671 0.3694	0.4823 0.4956	0.1099 0.1130	3.39 3.38	3.38
59-11	0.5671 0.5229	0.4226 0.3925	0.5148 0.5378	0.1177 0.1233	3.36 3.37	3.36
62-1	0.4829 0.4831	0.4187 0.4186	0.5557 0.4787	0.0660 0.0570	7.52 7.49	7.51
62-11	0.5043 0.4855	0.4270 0.4154	0.4897 0.4825	0.0601 0.0593	7.11 7.17	7.14
60-1	0.5243 0.4816	0.4525 0.4217	0.4861 0.5495	0.0533 0.0597	8.24 8.30	8.27
60-11	0.4979 0.5057	0.4402 0.4471	0.5198 0.4814	0.0595 0.0529	8.31 8.29	8.30
65-1	0.4840 0.4823	0.4280 0.4303	0.4784 0.4814	0.0518 0.0522	8.41 8.47	8.44
65-11	0.4884 0.5004	0.4357 0.4469	0.4969 0.5220	0.0546 0.0573	8.37 8.38	8.37
64-1	0.4970 0.4778	0.4072 0.3916	0.5028 0.5126	0.0534 0.0544	7.95 7.96	7.95
64-11	0.4843 0.4825	0.4179 0.4168	0.4936 0.5172	0.0536 0.0563	8.19 8.17	8.18

Each portion was washed and analysed as already described. All the arsenates were free from potassium.

The results are given in Tables XVII*a* and XVII*b* and Fig. 13.

TABLE XVII*b*

LEAD NITRATE ($M/20$), ARSENIC OXIDE ($M/20$) AND POTASSIUM HYDROXIDE (K_2O $M/20$ TO $3/4$ M)

Precipitate No.	Conc. of solutions, moles per litre			Molar ratio K_2O/As_2O_5 in solutions	Molar ratio PbO/As_2O_5 in precipitates	pH values of the mother liquors
	$Pb(NO_3)_2$ 4 litres	As_2O_5 2 litres	K_2O 2 litres			
58-1	0.05	0.05	0.05	1.0	1.99	1.7
58-11	0.05	0 05	0.05	1.0	1.99	1.65
63-1	0.05	0.05	0.10	2.0	1.98	2.0
63-11	0.05	0.05	0.10	2.0	1.99	
61-1	0.05	0.05	0.15	3.0	2.34	7.35
61-11	0.05	0.05	0.15	3.0	2.19	7.25
59-1	0.05	0.05	0.25	5.0	3.38	
59-11	0.05	0.05	0.25	5.0	3.36	10.2
62-1	0.05	0.05	0.375	7.5	7.51	
62-11	0.05	0.05	0.375	7.5	7.14	12.0
60-1	0.05	0.05	0.50	10.0	8.27	12.55
60-11	0.05	0.05	0.50	10.0	8.30	12.45
65-1	0.05	0.05	0.625	12.5	8.44	12.8
65-11	0.05	0.05	0.625	12.5	8.37	
64-1	0.05	0.05	0.75	15.0	7.95	12.8
64-11	0.05	0.05	0.75	15.0	8.18	12.75

1 : *filtered immediately after precipitation.*
11 : *filtered after stirring 24 hr. in the mother liquor.*

(*g*) *Lead Nitrate, Arsenic Acid, and Ammonium Hydroxide*

Solutions of lead nitrate, $M/20$, and solutions made up of two litres of arsenic oxide solutions, $M/20$, and two litres of ammonium hydroxide solutions of different concentrations, $M/20$ to M, were used.

With the two most dilute solutions of ammonium hydroxide, dilead arsenate was precipitated in strongly acid liquors. Then, as the alkalinity increased, the molar ratio, PbO/As_2O_5, in the precipitates rose to 3.25 and remained there, indicating the formation of a definite compound: $4Pb_3(AsO_4)_2.Pb(OH)_2$.

The definite compound, $Pb_4(PbOH)(AsO_4)_3$ or $3Pb_3(AsO_4)_2\,Pb(OH)_2$, prepared by different authors by the action of ammonium hydroxide on dilead arsenate (13, 16, 19) was not formed, even when the mother liquors were stirred for 24 hr. before filtration. Streeter and Thatcher (20) could not prepare this compound when they repeated all the experiments given in the literature.

The precipitates were washed thoroughly, dried, and analysed as described before. They contained no ammonium.

The results are given in Tables XVIII*a* and XVIII*b* and Fig. 14.

TABLE XVIII*a*

LEAD NITRATE ($M/20$), ARSENIC OXIDE ($M/20$), AND AMMONIUM HYDROXIDE ($M/20$ TO M)

Precipitate No.	Analysis of precipitates				Molar ratio PbO/As_2O_5 in precipitates	Average
	PbO determination samples	PbO	As_2O_5 determination samples	As_2O_5		
74[1]		% 64.71 64.75 64.73		% 33.51 33.45 33.48		1 98
70	gm. 0.4961 0.5290	gm. 0.3221 0.3432	gm. 0.4795 0.5166	gm. 0.1588 0.1771	2.02 2.02	2.02
69	0.5626 0.5201	0.4193 0.3881	0.4807 0.5165	0.1214 0.1302	3.04 3.05	3.04
76	0.4995 0.5115	0.3764 0.3852	0.5063 0.5200	0.1207 0.1235	3.25 3.26	3.26
71[1]		% 75.51 75.42 75.46		% 23.86 23.86 23.86		3.24
72[1]		75.49 75.37 75.43		23.70 23.80 23.75		3.26

[1] *Determinations made by P. E. Pelletier.*

TABLE XVIII*b*

LEAD NITRATE ($M/20$), ARSENIC OXIDE ($M/20$), AND AMMONIUM HYDROXIDE ($M/20$ TO M)

Precipitate No.	Conc. of solutions, moles per litre			Molar ratio NH_3/As_2O_5 in solutions	Molar ratio PbO/As_2O_5 in precipitates	pH values of the mother liquors
	$Pb(NO_3)_2$ 4 litres	As_2O_5 2 litres	NH_4OH 2 litres			
74	0.05	0.05	0.05	1.0	1.98	1.5
70	0.05	0.05	0.15	3.0	2.02	2.0
69	0.05	0.05	0.25	5.0	3.04	6.7
76	0.05	0.05	0.35	7.0	3.26	9.0
71	0.05	0.05	0.50	10.0	3.24	9.4
72	0.05	0.05	1.00	20.0	3.26	9.9

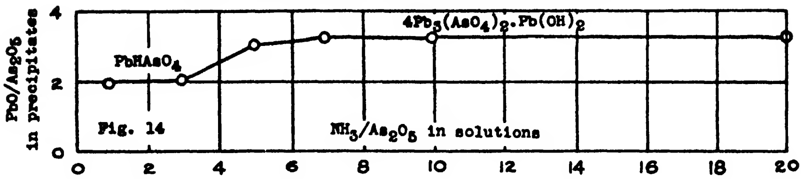

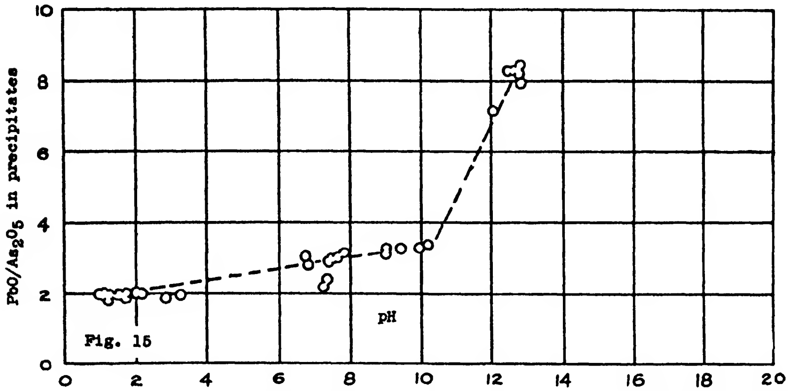

FIGS. 14 and 15. FIG. 14. *Lead nitrate, arsenic oxide, and ammonium hydroxide.* FIG. 15. *Influence of the pH on the composition of the precipitates.*

EFFECT OF HYDROGEN ION CONCENTRATION ON THE COMPOSITION OF THE LEAD ARSENATES

The pH values of the mother liquors were determined by means of the glass electrode. The results are shown in Table XIX and Fig. 15. The curve (Fig. 15), drawn from the data in this table, shows that, according to the hydrogen ion concentration, the precipitates obtained can be classified in three distinct groups: dilead arsenates in strongly acid solutions; slightly basic arsenates in neutral or slightly alkaline solutions; and strongly basic arsenates in strongly alkaline solutions.

TABLE XIX

INFLUENCE OF THE pH ON THE COMPOSITION OF THE LEAD ARSENATES

Molar ratio PbO/As_2O_5 in precipitates	pH values of the mother liquors	Molar ratio PbO/As_2O_5 in precipitates	pH values of the mother liquors	Molar ratio PbO/As_2O_5 in precipitates	pH values of the mother liquors
2.00	1.0	1.99	2.1	3.12	9.0
2.00	1.1	1.95	2.8	3.26	9.0
1.82	1.2	1.91	3.2	3.24	9.4
2.00	1.2	3.04	6.7	3.26	9.9
1.94	1.5	2.76	6.8	3.36	10.2
1.98	1.5	2.19	7.25	7.14	12.0
1.99	1.65	2.34	7.35	8.27	12.55
1.89	1.7	2.91	7.4	8.30	12.45
1.99	1.7	2.98	7.45	8.44	12.8
1.98	2.0	3.02	7.6	7.95	12 8
2.02	2.0	3.11	7 8	8.18	12.75

References

1. Association of Official Agricultural Chemists. Official and tentative methods of analysis. 4th ed. A.O.A.C., Washington, D.C. 1935.
2. Cloutier, L. Ann. chim. (Sér. 10) 19 : 5-77. 1933.
3. Cloutier, L., Pelletier, P. E., and Gagnon, P. E. Trans. Roy. Soc. Can., (Ser. 3), 30 (Sec. 3) : 149-164. 1936.
4. Curry, B. E. and Smith, T. O. J. Am. Chem. Soc. 37 : 1685-1688. 1915.
5. Gmelin, L. Hand-book of chemistry, tr. by H. Watts. Vol. 5. Cavendish Society, London. 1851.
6. Holland, E. B. and Reed, J. C. Massachusetts Agr. Expt. Sta. 24th Ann. Rept., Part I, 177-207. 1912.
7. Jolibois, P. Compt. rend. 169 : 1095-1098. 1919.
8. Jolibois, P. Compt. rend. 169 : 1161-1163. 1919.
9. Jolibois, P. and Bossuet, R. Compt. rend. 174 : 1625-1628. 1922.
10. Jolibois, P., Bossuet, R., and Chevry. Compt. rend. 172 : 373-375. 1921.
11. Parsons, C. L. J. Am. Chem. Soc. 26 : 721-740. 1904.
12. Pelletier, P. E., Cloutier, L., and Gagnon, P. E. Can. J. Research, B, 16 : 37-45. 1938.
13. McDonnell, C. C. and Smith, C. M. J. Am. Chem. Soc. 38 : 2027-2038. 1916.
14. McDonnell, C. C. and Smith, C. M. J. Am. Chem. Soc. 38 : 2366-2369. 1916.
15. McDonnell, C. C. and Smith, C. M. Am. J. Sci. (Ser. 4) 42 : 139-145. 1916.
16. McDonnell, C. C. and Smith, C. M. J. Am. Chem. Soc. 39 : 937-943. 1917.
17. Rose, J. Ausfüherliches handbuch der analytischen chemie. I : 381. 1851.
18. Schulten, A. de. Bull. soc. franç. minéral. 20 : 195-198. 1897.
19. Smith, G. E. J. Am. Chem. Soc. 38 : 2014-2027. 1916.
20. Streeter, L. R. and Thatcher, R. W. Ind. Eng. Chem. 16 : 941-942. 1924.
21. Strömholm, D. Z. anorg. Chem. 38 : 429-455. 1904.
22. Tartar, H. V. and Robinson, R. H. J. Am. Chem. Soc. 36 : 1843-1853. 1914.

Canadian Journal of Research

Issued by The National Research Council of Canada

VOL. 19, SEC. B | SEPTEMBER, 1941 | NUMBER 9

THE OXIDATION OF PYROLYTIC DISTYRENE[1]

By Léo Marion[2]

Abstract

The pyrolysis of polystyrene to distyrene is accompanied by the formation of 1,3,5-triphenylbenzene. When pyrolytic distyrene is oxidized with limited quantities of potassium permanganate, a mixture of β-phenylpropiophenone, benzoic acid, and α-hydroxy-α,γ-diphenylbutyric acid is obtained. This substituted butyric acid can further be oxidized to β-phenylpropiophenone, and when it is treated with hydrogen bromide and subsequently with sodium amalgam it gives rise to α,γ-diphenylbutyrolactone. The relation of these results to the structure of the ethylenic component of pyrolytic distyrene is discussed.

It is well known that when highly polymerized styrene is distilled *in vacuo* it is pyrolysed and yields a mixture of products from which one fraction can be separated which is generally termed distyrene. This fraction has been shown by Staudinger and Steinhofer (6) to consist of a mixture of α,γ-diphenylpropane and an unsaturated component that had been assumed by various authors to possess the structure of 1,3-diphenyl-3-butene (I).

$$CH_2.(C_6H_5).CH_2.C(C_6H_5)=CH_2 \qquad \text{(I)}$$

Staudinger and Steinhofer (6) were the first to attempt to support such a structure with chemical evidence. Having obtained β-phenylpropiophenone as a product of the oxidation of pyrolytic distyrene they considered structure I for the unsaturated component as established. It has been shown since (4), however, that α,γ-diphenylpropane, when oxidized, produces an excellent yield of β-phenylpropiophenone, so that the proof of the structure of the unsaturated component of pyrolytic distyrene no longer holds. In an attempt to elucidate the structure of this unsaturated substance a study of its oxidation products has been undertaken.

Polystyrene was pyrolysed and the product fractionated into styrene, distyrene, the so-called tristyrene, and a crystalline product identified as 1,3,5-triphenylbenzene. This confirms the observation of Staudinger and Steinhofer (6) who have already recorded the formation of 1,3,5-triphenylbenzene under the same conditions. It has now further been found that if the tristyrene fraction is redistilled under atmospheric pressure, it is cracked into styrene and distyrene, and the process is accompanied by the formation of an appreciable quantity of 1,3,5-triphenylbenzene.

[1] *Manuscript received July 17, 1941.*
Contribution from the Division of Chemistry, National Research Laboratories, Ottawa, Canada. Issued as N.R.C. No. 1008.

[2] *Chemist.*

Treatment of distyrene with nitrogen tetroxide yielded intractable gums which, after nitration and oxidation, produced *p*-nitrobenzoic acid. The nitration of distyrene with fuming nitric acid failed to yield the expected tetranitro-diphenylpropane but gave rise to a small quantity of *p*-nitrobenzoic acid. The failure to isolate the tetranitro derivative of diphenylpropane may be due to the presence of the other component of distyrene, which might prevent it from crystallizing. However, the readiness with which *p*-nitrobenzoic acid was obtained in these experiments harmonizes with the fact that all attempts to oxidize distyrene yielded benzoic acid as one of the products.

In the course of numerous experiments to oxidize pyrolytic distyrene in acetone solution with limited amounts of potassium permanganate, it was observed that the β-phenylpropiophenone produced was always accompanied by an appreciable quantity of an acid resembling benzoic acid. Repeated recrystallization, however, could not bring the melting point above 113 to 116° C. The acid was, therefore, esterified and the product fractionated into ethyl benzoate and an ester of higher boiling point. The latter, when saponified, gave rise to a crystalline acid yielding analytical figures in good agreement with $C_{16}H_{16}O_3$. The acid could not be distilled without decomposition, a characteristic of α-hydroxy acids. Furthermore, when the acid was oxidized with potassium permanganate, it gave an excellent yield of β-phenylpropiophenone (II). In view of the analytical results this characterizes

$$C_6H_5.CH_2.\,CH_2.\,CO.C_6H_5 \quad \text{(II)} \qquad C_6H_5.CH_2.CH_2.\overset{\displaystyle C_6H_5}{\overset{|}{\underset{\underset{\displaystyle OH}{|}}{C}}}\!-\!CO_2H \quad \text{(III)}$$

the acid as an α,γ-diphenylhydroxybutyric acid. Substituted α-hydroxy-acids can be oxidized to carbonyl compounds, as exemplified by α-hydroxyisobutyric and benzilic acids, which yield acetone and benzophenone respectively (2). Hence, the oxidation of the styrene degradation acid to β-phenylpropiophenone is a further and more definite indication that its hydroxyl group is attached to the α-position. The acid, therefore, must be α-hydroxy-α,γ-diphenylbutyric acid (III) and is an intermediate product in the oxidation of distyrene to β-phenylpropiophenone.

It was thought that were such an acid to be treated with hydrogen bromide and the resulting bromo acid reduced with sodium amalgam, the final product should be α,γ-diphenylbutyric acid. When these reactions were carried out, however, α,γ-diphenylbutyrolactone (IV) was produced. The rearrangement

$$\begin{array}{l} C_6H_5.CH{-}CH_2.CH.C_6H_5 \\ \quad\;\, | \qquad\qquad\;\; | \\ \quad\;\, O{-\!-\!-\!-\!-\!-}CO \end{array} \qquad \text{(IV)}$$

necessary to produce this lactone may have taken place in alkaline solution in the intermediate unsaturated acid formed after hydrogen bromide had been removed from the molecule. It is well known that α,β double bonds

of this type shift to the β,γ-position in the presence of alkali (3). In this case the β,γ double bond, being conjugated, would have no tendency to shift back to its original position. The elements of water would then be added at the double bond and the lactone formed, during the subsequent treatment of the acid. Whatever the mechanism of its formation, the production of α,γ-diphenylbutyrolactone is an additional proof that the oxidation acid is an α,γ-diphenylhydroxybutyric acid.

The mechanism of the formation of α-hydroxy-α,γ-diphenylbutyric acid from 1,3-diphenyl-3-butene (I) may be postulated as taking place through the intermediate formation of a glycol:

$$\overset{C_6H_5}{\overset{|}{C}H_2}.CH_2.\overset{C_6H_5}{\overset{|}{C}}{=}CH_2 \longrightarrow \overset{C_6H_5}{\overset{|}{C}H_2}.CH_2.\underset{\underset{OH}{|}}{\overset{C_6H_5}{\overset{|}{C}}}-\!\!-\underset{\underset{OH}{|}}{CH_2} \longrightarrow \overset{C_6H_5}{\overset{|}{C}H_2}.CH_2.\underset{\underset{OH}{|}}{\overset{C_6H_5}{\overset{|}{C}}}-CO_2H$$

It would not be possible, on the other hand, to obtain such a hydroxy-acid from the oxidation of any of the other isomeric forms of 1,3-diphenylbutene unless the oxidation were preceded by a rearrangement into 1,3-diphenyl-3-butene. It has been shown (4) that 1,3-diphenyl-3-butene is unstable and that it isomerizes on standing. If this hydrocarbon be assumed to be the ethylenic constituent of pyrolytic distyrene then the latter must consist of a mixture of α,γ-diphenylpropane, 1,3-diphenyl-3-butene, and one or more of its isomeric forms. Among its products of oxidation, one of these isomeric forms (i.e., 1,3-diphenyl-1-butene) should produce benzoic acid, while the other (i.e., 1,3-diphenyl-2-butene) should produce phenylacetic acid. Hence, the fact that α-hydroxy-α,γ-diphenylbutyric acid is always accompanied by an almost equal quantity of benzoic acid seems to support this assumption concerning the components of pyrolytic distyrene.

Experimental

Oxidation of Distyrene to p-Nitrobenzoic Acid

The gases produced by heating lead nitrate (40 gm.) were absorbed in hexane (100 cc.) cooled in an ice-salt mixture, and the solution was added to a chilled solution of distyrene (6.5 gm.) in hexane (100 cc.). The product gradually separated as an oil at the bottom of the flask. As nothing could be induced to crystallize from this oil it was treated in the cold with fuming nitric acid but, this failing again to give crystals, the product was oxidized in acetone solution with potassium permanganate. An acid was thus obtained which, after several recrystallizations from ethyl acetate, melted at 241° C.* In admixture with an authentic specimen of *p*-nitrobenzoic acid (m.p. 242°) it melted at 241°. Calc. for $C_7H_5O_4N$: C, 50.29; H, 2.99; N, 8.38%. Found: C, 50.88, 50.74; H, 3.35, 3.22; N, 8.25, 8.19%.

When distyrene was treated with fuming nitric acid, it also yielded a small quantity of *p*-nitrobenzoic acid accompanying the bulk of neutral, uncrystallizable product.

***All melting points are corrected.**

Pyrolysis of Polystyrene

Styrene was heated in a sealed tube at 170° C. for 72 hr. and the resulting polymer dissolved in benzene and fractionally precipitated with methanol. The fraction of average molecular weight 8000 was pyrolysed *in vacuo* according to the usual procedure (6). A total crude distillate weighing 979 gm. was obtained from 1150 gm. of polymer, representing a yield of 88.2%. The crude product was fractionated under diminished pressure. It yielded styrene, b.p. 28 to 34° (5 mm.), wt. 403 gm.; distyrene, b.p. 135 to 180° (3.5 mm.), wt. 161.5 gm.; and the so-called tristyrene, wt. 390.7 gm. Towards the end of the distillation, the temperature rose to 360 to 400° and a substance distilled over which crystallized in the receiver.

The tristyrene fraction was cracked, by distilling slowly under atmospheric pressure. It yielded styrene (188 gm.), distyrene (52.2 gm.), and finally a thick oil, which was dissolved in methanol and allowed to stand. This solution gradually deposited the same solid that was obtained in the pyrolysis *in vacuo* of the more highly polymerized styrene.

The combined crude distyrene fractions (213.7 gm.) were refractionated and the main cut, b.p. 140 to 145° C. (3 mm.) was collected. Wt. 186.4 gm. (17% of the polystyrene used).

Isolation of 1,3,5-Triphenylbenzene

The solid obtained in the pyrolysis of polystyrene and in the cracking of tristyrene was recrystallized from boiling methanol from which it separated as flat needles. It was sublimed *in vacuo*, 185° C. (0.5 mm.), and recrystallized repeatedly from alcohol. It was finally obtained as small colourless prisms, m.p. 176°. Wt. 7.5 gm. Calc. for $C_{24}H_{18}$: C, 94.12; H, 5.88%. Found: C, 94.43; H, 5.64%.

When this hydrocarbon was oxidized with chromic-acid–acetic-acid it yielded some unchanged hydrocarbon and an acid found to be benzoic acid; m.p. 124° C., either alone or in admixture with an authentic specimen.

1,3,5-Triphenylbenzene was synthesized from acetophenone, potassium pyrosulphate, and sulphuric acid by the method of Odell and Hines (5). The product, after several recrystallizations from benzene-methanol, melted at 176° C., either alone or in admixture with the pyrolytic solid hydrocarbon.

Oxidation of Pyrolytic Distyrene

Distyrene (50 gm.) was dissolved in acetone previously distilled over potassium permanganate, dried with calcium chloride, and redistilled (500 cc.). Finely ground potassium permanganate in portions each equivalent to one-quarter atom of oxygen (6.33 gm.) was added to the solution kept cool with running water. The total potassium permanganate added was equivalent to 3.5 atoms of oxygen. The manganese dioxide sludge was then filtered out and washed with acetone. The combined filtrate and washings were distilled on the steam-bath, the oily residue was dissolved in ether, washed repeatedly with dilute sodium hydroxide, and with water. After drying over

sodium chloride, the ether was distilled off and the oily residue allowed to cool. It crystallized immediately to a solid mass, wt. 38.3 gm. This was recrystallized from petroleum ether, from which it separated as flakes, m.p. 72° C. Admixture with β-phenylpropiophenone failed to depress the melting point. Some of the oxidation ketone was converted to the oxime which was recrystallized once from aqueous methanol and several times from petroleum ether; m.p. 83°, either alone or in admixture with an authentic specimen of β-phenylpropiophenoneoxime.

Isolation of Benzoic and α-Hydroxy-α,γ-diphenylbutyric Acids

The manganese dioxide sludge, which had been filtered, was suspended in water and a stream of sulphur dioxide passed through the suspension until all the manganese dioxide had dissolved. The acid that precipitated was collected in ether and the solution washed thoroughly with water, dried over sodium chloride, and distilled on the steam-bath. From 186 gm. of distyrene, 71.4 gm. of crude acid was obtained.

The crude acids were dissolved in dilute sodium hydroxide and the solution was extracted with ether, acidified with hydrochloric acid, and again extracted with ether. The second ether extract was washed with water, dried over sodium chloride, and distilled on the steam-bath. Wt. of crystalline acid, 46.7 gm. This was dissolved in absolute ethyl alcohol (235 cc.) containing concentrated sulphuric acid (23.5 gm.) and the solution refluxed for five hours on the steam-bath. About two-thirds of the alcohol was then distilled off and the residual oil poured into cold water (one litre). The precipitated oil was collected in ether, washed with water, with dilute sodium hydroxide, and again with water. It was dried over sodium chloride and distilled on the steam-bath. The residual ester (45.4 gm.) was distilled *in vacuo* through a fractionating column. Two fractions were collected: *(a)* b.p. 95° C. (6 mm.), wt. 17 gm., and *(b)* b.p. 195 to 200° (6 mm.), wt. 22.1 gm. The latter weight represents a yield of 9.6% calculated on the weight of distyrene used. The second fraction was redistilled and the cut, b.p. 184 to 187° C. (4 mm.), collected. Wt., 19.1 gm. From the dilute sodium hydroxide washings of the esters, 4 gm. of unchanged acids was recovered and this was esterified in ether solution with diazoethane. The product thus obtained was fractionated and the two fractions were combined with the corresponding fractions obtained from the main esterification.

The first fraction was saponified by refluxing with aqueous-alcoholic potassium hydroxide and the crystalline acid obtained was recrystallized twice from hot water. Alone or in admixture with an authentic specimen of benzoic acid, this acid melted at 124° C.

The ester collected in the second fraction could not be crystallized and it was saponified by refluxing with aqueous-alcoholic potassium hydroxide. It yielded a crystalline acid (20 gm.). This was recrystallized repeatedly from aqueous methanol and from methanol-benzene from which it separated in clusters of prismatic needles, m.p. 147° C. Calc. for $C_{16}H_{16}O_3$: C, 75.00;

H, 6.24%; mol. equiv. 256. Found: C, 75.04, 75.05; H, 6.31, 6.25%; mol. equiv. 252, 253. Some of the acid was dissolved in ether and esterified with diazomethane. The methyl ester was distilled twice and analysed. Calc. for $C_{17}H_{18}O_3$: OCH_3, 11.48%; mol. wt., 270. Found: OCH_3, 11.91, 11.93%; mol. wt. (Rast), 260. The Berg test (1) for α-hydroxy-acids was negative. This failure to give the test may possibly be due to the presence of the two phenyl groups in close proximity.

Oxidation of α-Hydroxy-α,γ-diphenylbutyric Acid

It was observed that α-hydroxy-α,γ-diphenylbutyric acid still reduced potassium permanganate. Therefore, the acid (1.0 gm.) was dissolved in purified acetone (50 cc.) and oxidized at room temperature by the addition of finely ground potassium permanganate in portions equivalent to one-quarter atom of oxygen. The first three portions were decolorized very rapidly but the fourth was not completely decolorized after four hours. A little methanol was added to destroy the remaining permanganate and the manganese dioxide filtered and washed with acetone. The combined acetone filtrate and washings were distilled on the steam-bath and the residue was dissolved in ether, washed with dilute sodium hydroxide, and with water. After drying over sodium chloride the ether was distilled off; the residue consisted of an oil that crystallized to a solid mass on cooling. Wt. 0.7 gm. This, after repeated recrystallization from petroleum ether, melted at 72 ° C. Admixture with β-phenylpropiophenone failed to depress the melting point. The oxime, m.p. 83°, was prepared and found to be identical with β-phenylpropiophenoneoxime.

Isolation of α,γ-Diphenylbutyrolactone

α-Hydroxy-α,γ-diphenylbutyric acid (1.5 gm.) was dissolved in glacial acetic acid (20 cc.) and the solution saturated with hydrogen bromide (action of bromine on tetralin). The solution was then refluxed for three hours, allowed to cool, and poured into cold water (300 cc.). The oil that separated was collected in ether, the solution washed repeatedly with water, and distilled on the steam-bath. The residue was dissolved in aqueous alcohol containing a little sodium hydroxide and the solution shaken in a mechanical shaker for 16 hr. with sodium amalgam. During the reduction the alkalinity was controlled by the occasional addition of acetic acid and the spent amalgam was replaced. After completion of the reduction, the liquor was decanted off and acidified with hydrochloric acid. The precipitated oil was dissolved in ether, washed with water, dried over sodium chloride, and distilled first on the steam-bath to remove the solvent and then *in vacuo*. The product was a yellowish oil, b.p. 195 to 200° C. (2.5 mm.), which crystallized on standing. After six recrystallizations from petroleum ether the melting point was constant at 107°. Calc. for $C_{16}H_{14}O_2$: C, 80.67; H, 5.88%. Found: C, 81.05, 81.41; H, 5.67, 5.75%. No depression in melting point was caused by admixture with α,γ-diphenylbutyrolactone prepared by the reduction of β-benzoyl-α-phenylpropionic acid with sodium amalgam.

Synthesis of β-Hydroxy-β,δ-diphenylvaleric Acid

It was believed originally that the styrene degradation acid might be β-hydroxy-β,δ-diphenylvaleric acid, and this was synthesized. The acid is new and although it is not identical with, but a homologue of, the degradation acid, it is thought desirable to put it on record. The ester of the acid was prepared by a Reformatzky reaction from β-phenylpropiophenone (11 gm.) and ethyl bromoacetate (8 gm.) in a mixture of dry benzene (20 cc.) and absolute ether (8 cc.) to which zinc spangles (4 gm.) was added. The product worked up as usual, yielded a crystalline ester which, after crystallization from petroleum ether, melted at 79.5° C. Calc. for $C_{19}H_{22}O_3$: C, 76.50; H, 7.38%. Found: C, 76.62, 76.97; H, 7.61, 7.75%. The ester, when saponified with aqueous-methanolic potassium hydroxide, yielded β-hydroxy-β,δ-diphenylvaleric acid which, after several recrystallizations from methanol-benzene and from hexane, melted at 155° C. Calc. for $C_{17}H_{18}O_3$: C, 75.54; H, 6.67%. Found: C, 75.46, 75.48; H, 6.51, 6.77%.

References

1. BERG, M. A. Bull. soc. chim. [3] 11 : 882-883. 1894.
2. CIUSA, W. Atti accad. Lincei, 25 : 632-637. 1937.
3. JOHNSON, J. D. A. and KON, G. A. R. J. Chem. Soc. 2748-2759. 1926.
4. MARION, L. Can. J. Research. B, 16 : 213-217. 1938.
5. ODELL, A. F. and HINES, C. W. J. Am. Chem. Soc. 35 : 81-84. 1913.
6 STAUDINGER, H. and STEINHOFER, A. Ann. 517 : 35-53. 1935.

THE TERNARY ALLOY SYSTEM: ALUMINIUM–LEAD–SILVER[1]

By A. N. Campbell,[2] L. Yaffe,[3] W. G. Wallace[4] and R. W. Ashley[3]

Abstract

1. The area of partial miscibility for the ternary system, aluminium–lead–silver, has been determined by thermal and chemical analysis. It is found to extend from the binary system aluminium–lead to alloys containing a maximum of 85.58% silver and 4.71% lead by weight.

2. The temperatures of separation of solid phase, bounding this area, have been found to fall at first with addition of silver to the system aluminium-lead, until a temperature of 548.5° C. is reached. This is the temperature of solidification of the alloy that contains silver and aluminium in their eutectic proportions, plus saturation with lead. The temperature then increases to a maximum of about 736° in the alloy containing about 80% silver and 14% lead. This temperature maximum does not coincide with the summit of the mutual solubility curve but lies well to the right of it.

3. No ternary compounds have been found.

4. The ternary eutectic practically coincides with the binary eutectic of the system silver–lead.

5. As far as can be determined by thermal analysis alone, it appears that there is no solid solution of lead in the α, β, or γ phases of the silver–aluminium system.

6. The first peritectic line formed by the addition of lead to the high temperature peritectic point of the silver–aluminium system intersects the partial miscibility curve at 7.90% Al, 7.60% Pb, and 84.50% Ag. The temperature drops from 779.0° to 727.0°.

7. The second peritectic line intersects the partial miscibility curve at 10.30% Al, 4.10% Pb, and 85.60% Ag. The temperature drops from 729.0° to 708.0°.

8. If the partial miscibility curve had not intervened, the two lines would have intersected at 11.00% Al, 15.50% Pb, and 73.50% Ag.

Introduction

Previous Investigations

The binary systems bounding the field of this ternary system are: lead–silver, aluminium–silver, and aluminium–lead. These binary systems are well known and have been worked out in detail so that extensive discussion of them is not necessary here. Bibliographies are given by Hansen (4) and Jänecke (6), but these are incomplete and we therefore subjoin our own, as follows:—

Bibliography

Lead–Silver

Chiswick, H. H. and Hultgren, R. Am. Inst. Mining Met. Engrs., Inst. Metals Div., Tech. Pub. No. 1169. 1940.

Heycock, C. T. and Neville, F. H. Trans. Roy. Soc. (London) A, 189 : 25-70. 1897.

Petrenko, G. J. Z. anorg. Chem. 53 : 200-211. 1907.

Yoldi, F. (with D. L. de A. Jimenez). Anales soc. españ. fis, quim. 28 : 1055-1065. 1930. *Abstract in* J. Inst. Metals, 47(3) : 76. 1931.

[1] *Manuscript received May 27, 1941.*
Contribution from the Chemistry Department, University of Manitoba, Winnipeg, Man.
[2] *Associate Professor of Chemistry.*
[3] *Holder of a Bursary under the National Research Council of Canada.*
[4] *Research Student.*

Aluminium–Silver

Ageew, N. and Shoyket, D. J. Inst. Metals, 52(2) : 119-126. 1933.
Ageew, N. and Shoyket, D. Metallurgia, 9(3) : 38-42. 1934.
Ageew, N. W. and Shoyket, D. N. Ann. inst. anal. phys. chim. (U.S.S.R.) 7 : 59-74. 1935.
Barrett, C. S. Metals and Alloys, 4 : 63-64, 74. 1933.
Beckmann, B. Intern. Z. Metallog. 6 : 246-255. 1914.
Broniewski, W. Compt. rend. 150 : 1754-1757. 1910.
Broniewski, W. Ann. chim. phys. (Sér. 8) 25 : 80-86. 1912.
Crepaz, E. Atti congr. naz. chim. pura applicata, 3rd Congr., Firenze Toscana, 1929. 371-379. 1930. *Abstract in* J. Inst. Metals, 47(3) : 378. 1931.
Gautier, H. Compt. rend. 123 : 109-112. 1896.
Gautier, H. Bull. soc. encour. ind. natl. (5) 1 : 1312. 1896.
Hansen, M. Z. Metallkunde, 20 : 217-222. 1928.
Hansen, M. Naturwissenschaften, 16 : 417-419. 1928.
Hansen, M. Mitt. deut. Materialprüfungsanstalt. 5 : 31. 1929.
Hansen, M. Mitt. deut. Materialprufungsanstalt. 10 : 29-33. 1930.
Hansen, M. and Sachs, G. Z. Metallkunde, 20 : 151-152. 1928.
Heycock, C. T. and Neville, F. H. Trans. Roy. Soc. (London) A, 189 : 25-70. 1897.
Hoar, T. P. and Rowntree, R. K. J. Inst. Metals, 45(1) : 119-124. 1931.
Hume-Rothery, W., Mabbott, G. W., and Evans, K. M. C. Trans. Roy. Soc. (London) A, 233 : 1-97. 1934.
Hume-Rothery, W., Raynor, G. V., Reynolds, P. W., and Packer, H. K. J. Inst. Metals, 66 : 209-239. 1940.
Jette, E. R. and Foote, F. Metals and Alloys, 4 : 78. 1933.
Kato, H. and Nakamura, S. J. Chem. Soc. Japan, 58 : 694-705. 1937.
Kokubo, S. Science Repts., Tôhoku Imp. Univ. (Ser. 1) 23(1) : 45-51. 1934.
Kroll, W. Metall u. Erz, 23 : 555-557. 1926.
Obinata, I. and Hagiya, M. Kinzoku-no-Kenkyu, 12 : 419-429. 1935.
Petrenko, G. I. Z. anorg. Chem. 46 : 49-59. 1905.
Petrenko, G. I. and Derkach, F. A. Ukraïn. Khem. Zhur. 13 : 69-79. 1938.
Phelps, R. T. and Davey, W. P. Trans. Am. Inst. Mining Met. Engrs., Inst. Metals. Div. 99 : 234-263. 1932.
Puschin, N. A. J. Russ. Phys. Chem. Soc. 39 : 528-566. 1907.
Tazaki, M. Kinzoku-no-Kenkyu, 4 : 34. 1927.
Tishtchenko, F. E. J. Gen. Chem. (U.S.S.R.) 3 : 549-557. 1933. *Abstract in* Met. Abstracts, Inst. Metals (Ser. 2), 1 : 7. 1934.
Tishtchenko, F. E. J. Gen. Chem. (U.S.S.R.) 9 : 729-731. 1939.
Tishtchenko, F. E. and Lukash, I. K. J. Phys. Chem. (U.S.S.R.) 9 : 440-448. 1937.
Ueno, S. Mem. Coll. Sci., Kyoto Imp. Univ. (Ser. A) 13(2) : 141-147. 1930.
Westgren, A. F. and Bradley, A. J. Phil. Mag. (Ser. 7) 6 : 280-288. 1928.
Wright, C. R. A. Proc. Roy. Soc. (London) 52 (315) : 11-27. 1892-93.
Zaziri, H. Tetsu-to-Hagane, 24 : 357-370. 1938.

Aluminium–Lead

Campbell, A. N. and Ashley, R. W. Can. J. Research, B, 18 : 281-287. 1940.
Claus, W. Aluminium, 18 : 544-545. 1936.
Gwyer, A. G. C. Z. anorg. Chem. 57 : 113-153. 1908.
Hansen, M. and Blumenthal, B. Metallwirtschaft, 10 : 925-927. 1931.
Kempf, L. W. and Van Horn, K. R. Am. Inst. Mining Met. Engrs., Inst. Metals Div., Tech. Pub. No. 990. 1938.
Pécheux, H. Compt. rend. 138 : 1042-1044. 1904.
Wright, C. R. A. and Thompson, C. J. Soc. Chem. Ind. 9 : 944-945. 1890.
Wright, C. R. A. and Thompson, C. J. Soc. Chem. Ind. 11 : 492-494. 1892.

To save discussion of such well known systems the binary diagrams, drawn from the best available data, are reproduced here for purposes of reference (Figs. 1, 2, and 3).

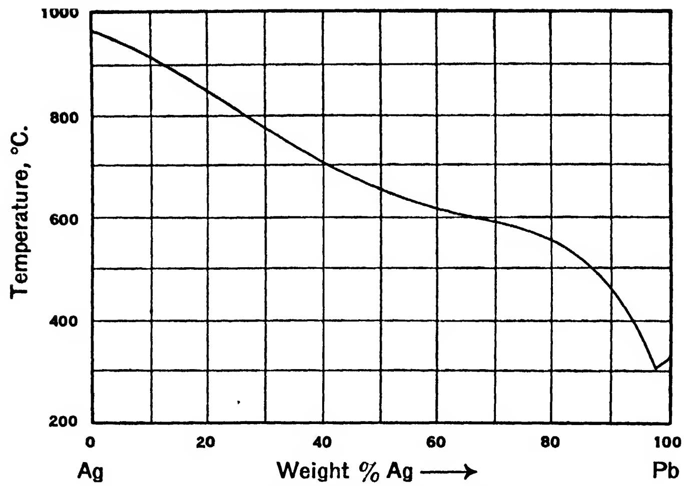

FIG. 1. *The system silver-lead (Petrenko).*

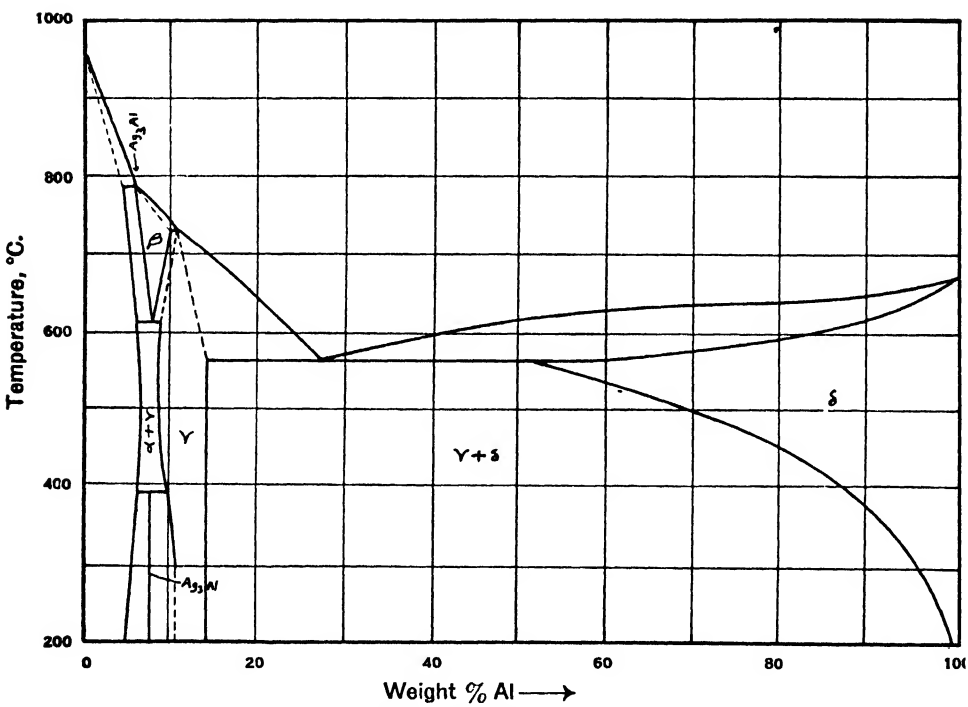

FIG. 2. *Composite diagram of the silver-aluminium system.*

Coming to the ternary system, we found that little had been done. Wright (16) obtained the critical curve for this system, but no record was made of temperature other than the statement that the alloys were first heated to about 870° C. It is apparent that the partial miscibility of the lead–aluminium system persists over a large area of the ternary diagram.

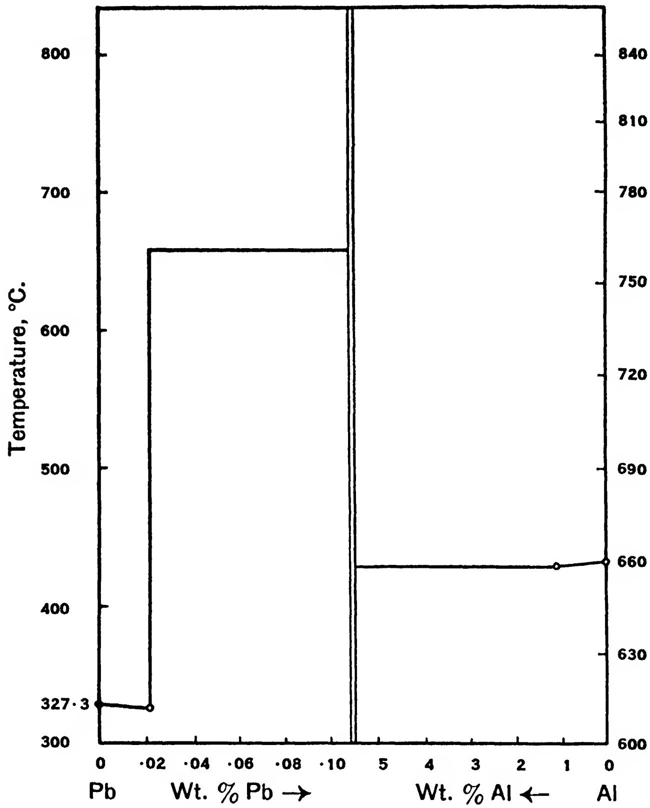

FIG. 3. *The system lead–aluminium (Campbell and Ashley).*

Lorenz and Erbe (7) studied the ternary system from the point of view of the application of the distribution law. The miscibility curve was plotted for 1000° and for 750° C. They found that at 750°, with a silver content of from 0 to 85% in the lighter phase, and from 0 to 8% in the heavier phase, lead was practically insoluble in aluminium. This conclusion was arrived at, however, on the assumption that all the lead present in the alloys could be explained as colloidal suspension, since it is known that part of it is present in that form. That this is not so has recently been shown by Kempf and van Horn (5) and by Campbell and Ashley (2). In other respects, the results of Lorenz and Erbe are in good agreement with the results of this paper.

Scheme of this Work

The work remaining to be done for completion of the liquidus diagram was:—

1. Redetermination of the miscibility curve for temperatures at which solid phases appear, or, in terms of the solid model, the curve of intersection of the solid of partial miscibility with the planes representing equilibrium of one solid phase with one liquid. In practice this means, the determination,

by thermal analysis, of the temperatures at which liquid alloys separate solid light alloy and solid heavy alloy, followed by chemical analysis of the separated layers.

2. Composition and temperature of the ternary eutectic.

3. The course of the eutectic curve running from the binary eutectic of the silver–aluminium system towards the ternary eutectic.

4. The peritectic lines, running from the two peritectic points of the silver–aluminium system.

In addition to the liquidus diagram, considerable information as to the nature of solid phases was obtained by carrying the thermal analysis down to about 300° C. It is apparent, of course, that for a complete knowledge of the solid phases, investigations by means of the microscope and by X-ray analysis are necessary, but, for these, apparatus was not available. As a matter of practical interest, some measurements of hardness were made.

Experimental

Thermal Analysis

The method employed was principally that of thermal analysis. The technique was standard and requires little explanation. Plato's method (10) of regulated cooling was used; a bank of rheostats was calibrated in equal amounts, so that the introduction of a certain amount of resistance per minute caused the furnace to cool at the rate of 2.5° C. per min. Two platinum–platinrhodium thermocouples were used, one inserted in the melt and the other in a neutral body of copper. The two thermocouples were opposed and connected through a delicate galvanometer, while the thermocouple in the melt was also connected to a potentiometer (method of Roberts-Austen (11)). Sudden displacement of the galvanometer indicated a thermal change at a temperature registered by the potentiometer. An accuracy of ±0.25° may be claimed as far as the determination of temperature alone is concerned.

Preparation of Alloys

The lead used had the following impurities: Ag = 0.0001%, Cu = 0.0025%. The writers are indebted to Dr. Frary and Mr. J. J. Bowman, of the Aluminum Company of America, for some very pure aluminium. This had the following composition:—

Si = 0.007%	Fe = 0.01%	Al = Remainder
Cu = 0.029%	Ti = 0.001%	

The silver used was highest purity fine silver.

Analysis of the Alloys

The alloys produced were occasionally analysed, especially those that had been heated to a high temperature for a length of time, in order to allow for change of composition due to oxidation of aluminium and lead; all the alloys used in the determination of the mutual solubility curve were analysed. Borings were taken from different parts of the alloy and mixed. In some cases

the solid phase is homogeneous, and in none was there evidence of segregation, except, of course, in the region of partial miscibility. In order to ensure homogeneity in the high temperature alloys (outside of the region of partial miscibility) these were quenched in a steel mould.

In the study of the region of partial miscibility, it was found that in alloys rich in aluminium and containing relatively small amounts of silver, the results obtained for the lead analysis were meaningless owing to the fact that aluminium may hold as much as 10% lead in the form of a dispersion. Heat treating these alloys, i.e., allowing them to remain for a long time at a high temperature, greatly reduced the amount of lead present but the results were still not satisfactory. It was finally found necessary to resort to thermal analysis in these cases. For this purpose, an alloy of aluminium and silver of known composition was made up, the temperature of primary crystallization found, and lead then added in quantities of ½% at a time. The temperature of primary crystallization was determined each time until a constant temperature was reached. Then, by plotting the temperature of primary crystallization against the percentage of lead added, the true amount of lead in the aluminium layer could be determined. As the percentage of silver in the alloy increased, and therefore the aluminium content decreased, this colloidal effect gradually diminished until, beyond about 80% silver, the phenomenon disappeared entirely and the chemical analysis could be taken as accurate.

The Ternary Eutectic

Since the temperatures in the neighbourhood of this eutectic were comparatively low, a mercurial thermometer was employed to determine the temperature. The thermometer was graduated in 0.5° C. and with the aid of a hand lens could be read to 0.05°. The eutectic alloy was contained in a hard glass test tube, heated electrically.

Enough aluminium was added to lead to saturate it, according to the figures of Campbell and Ashley (2) and thus reach that binary eutectic, and the temperature of solidification taken. Small quantities of silver were now added to the binary eutectic, the temperature of solidification being determined each time. At the attainment of the ternary eutectic an excess of silver was added to prove that the temperature of solidification would go no lower. Before analysis, the alloy was heat treated in the molten state for 24 hr. to allow excess aluminium and silver to separate out by gravity. The alloy was then analysed.

To show that the ternary eutectic is actually a condition of true equilibrium, it should be approached from both sides. Accordingly the binary eutectic, lead–silver, was prepared, and aluminium then added until a constant temperature of solidification was obtained. The alloy was then heat treated and analysed as before.

The Eutectic Curve

This is the curve running from the binary eutectic, silver–aluminium, towards the ternary eutectic point, but limited by its intersection of the area of partial miscibility. It was obtained in the same way as the ternary eutectic, by adding lead to the silver–aluminium binary eutectic until constant temperature was obtained. The higher temperature required the use of the thermocouple apparatus.

The Peritectic Lines

The diagram, outside the area of partial miscibility, was mapped in detail by the method of "sectioning". After each section line had been completed the alloy was analysed chemically and a small correction made for oxidation. Four such sections were studied. The results obtained in each case were plotted on rectangular co-ordinates, a vertical section through the solid model being thus obtained.

Hardness Measurements

These were carried out on most of the alloys prepared, on a standard Brinell hardness testing machine. As the alloys had all been cooled slowly, though not annealed, in the course of the thermal analysis, they are presumably in a more or less stable condition. The quenched alloys might have a different hardness, though the β-phase cannot be preserved by quenching.

Results

Thermal Analysis

Region of Partial Miscibility

In order to obtain the liquidus curve, 11 alloys of varying composition were prepared, such that the total composition of each alloy lay roughly on the mid-point of a tie-line. In each of these alloys two layers formed, of approximately equal weight. Cooling curves of each alloy were taken, the specimen was then cut vertically and samples were taken from each layer for analysis. The solidification temperatures and the analyses found are given in Table I. The curve obtained from these data is shown in Fig. 4. It should be emphasized that this curve is not strictly a mutual solubility curve, since it is not isothermal, though in fact it is almost so. The curve represents the intersection of an almost vertical sided solid (representing mutual solubility at different temperatures) with the planes of the solid model corresponding to the equilibrium of one liquid with one solid phase.

In Table I, A, the lead content of Alloys 2 to 5 inclusive was determined by means of thermal analysis, as described previously. The high value for lead in Alloy 6 is probably due to the colloidal phenomenon not yet having entirely disappeared. The values for the remaining alloys were obtained by chemical analysis. The figures for Alloy 1, containing no silver, are those of Campbell and Ashley (2).

The Ternary Eutectic

Starting from the aluminium–lead binary eutectic, the temperature of solidification fell, with additions of silver, from 327.0° to 304.1° C. Starting from the silver–lead eutectic and adding aluminium, the temperature remained

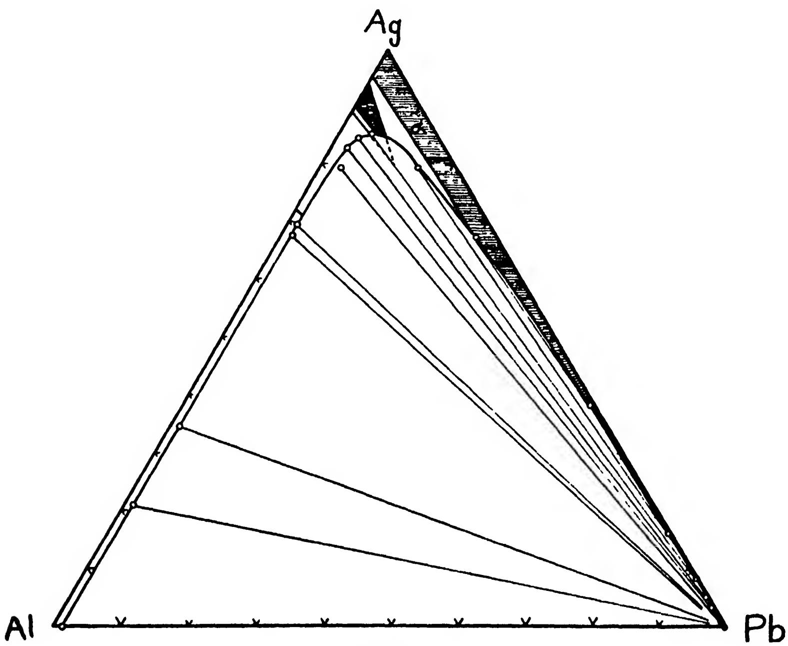

FIG. 4.

TABLE I

ANALYSIS AND TEMPERATURE ARRESTS

A. Lighter alloys					B. Lower alloys				
No. of alloy	Analysis, wt. % Ag	Al	Pb	Temp., ° C.	No. of alloy	Analysis, wt. % Ag	Al	Pb	Temp., ° C.
1	0.00	98.90	1.10	658 5	1	0 00	0.025	99 975	326.8
2	21.25	77.60	1.15	612 5	2	0 54	0.025	99.40	324.0
3	34.51	64.13	1.36	593.9	3	0.70	0.078	99.18	320.8
4	67.50	30.71	1.73	548.6	4	No data			
5	69.20	29.03	1 73	581.6 (Eutectic 548 7)	5	0.97	0 41	98.62	323.9
6	79.64	17.21	3.11	664 6 (Eutectic 548.1)	6	1.08	0.38	98 54	306.7
7	82.86	14.76	2.38	697.7	7	3.39	0 24	96.37	304.6
8	84.56	12.40	3.04	708.5	8	5.59	0.32	94.09	306 2
9	85.58	9.69	4.71	717.0	9	8.31	0.21	91.48	304.2
10	79.73	5.79	14.48	736 3	10	16.55	0.17	83.33	596.4, 398.9, 304.5
11	67.29	3.38	29.33	726.4	11	38.42	0.30	61 03	304.5

TABLE II

Composition and thermal effects in alloys of constant aluminium/lead ratio

Alloy No	Wt % Pb	Wt % Al	Wt % Ag	Temperature of thermal effect ° C	Nature of thermal effect	Comments
Section I Al/Pb = 6.8/1						
1	0.70	4.90	94.40	815.2	α Crystallization	Fig 5 (p 224) shows the plane vertical Section I drawn from these results The following deductions are made —
				769.2	First peritectic	
				601.8 (Very weak)	Eutectoid	
				396.8 (Very weak)	Compound separation	The limit of the α region = 4.90% Al and 0.70% Pb The first peritectic occurs at a composition of Al = 6.60% Pb = 1.00% Ag = 92.40% and at a temperature of 769.0° C
2	0.80	5.80	93.40	783.6	α Crystallization	
				764.8	First peritectic	
				597.7	Eutectoid	The second peritectic occurs at a composition of 10.60% Al 1.50% Pb and 87.90% Ag at a temperature of 716.0° C
				402.7	Compound separation	
3	1.00	6.60	92.40	773.8	β Crystallization (or peritectic)	Width of the first peritectic gap = 2.00% (1.70% Al and 0.30% Pb)
				602.5	Eutectoid	
				405.8	Compound separation	The maximum width of the β region = 2.80% (2.40% Al and 0.40% Pb)
4	1.10	7.90	91.00	762.8	β Crystallization	
				612.8 (Very weak)	Eutectoid	
				411.4 (Very weak)	Compound separation	Width of the second peritectic gap = 1.90% (1.60% Al and 0.30% Pb)
5	1.30	9.00	89.70	751.0	β Crystallization	
				718.0 (Very weak)	Second peritectic	The eutectoid temperature remains constant at 601° C
6	1.40	9.80	88.80	735.0	β Crystallization	The temperature of compound separation varies from 390 to 410° C
				705.7	Second peritectic	
7	1.50	10.60	87.90	712.3	Second peritectic	
8	1.60	11.30	87.10	714.5	γ Crystallization	
9	1.76	12.00	86.24	712.3	γ Crystallization	
Section II Al/Pb = 4.5/1						
1	1.00	3.90	95.10	844.0	α Crystallization	Fig 6 (p 225) shows the plane vertical Section II
2	1.10	4.60	94.30	817.6	α Crystallization	The limit of the α region = 4.06% Al and 1.10% Pb
				763.0	First peritectic	The first peritectic occurs at a composition of 7.20% Al 1.60% Pb 91.20% Ag and at a temperature of 764.0° C
				603.0	Eutectoid	
3	1.30	5.20	93.50	793.5	α Crystallization	
				766.7	First peritectic	The second peritectic occurs at a composition of 10.23% Al, 2.27% Pb and 87.50% Ag at a temperature of 720.0° C.
				598.0	Eutectoid	
				401.9	Compound separation	

TABLE II—*Continued*

COMPOSITION AND THERMAL EFFECTS IN ALLOYS OF CONSTANT ALUMINIUM/LEAD RATIO

Alloy No.	Wt. % Pb	Wt. % Al	Wt. % Ag	Temperature of thermal effect, ° C.	Nature of thermal effect	Comments
SECTION II—*Concluded*						
4	1.40	6.00	92.60	780.0 764.0 603.0 404.0	α-Crystallization First peritectic Eutectoid Compound separation	Width of the first peritectic gap = 3.10% (2.60% Al and 0.50% Pb). The maximum width of the β-region = 1.50% (1.20% Al and 0.30% Pb).
5	1.60	6.60	91.80	784.7 767.7 601.3 395.4	α-Crystallization First peritectic Eutectoid Compound separation	Width of the second peritectic gap = 2.20% (1.83% Al and 0.37% Pb) The eutectoid temperature remains constant at 601° C.
6	1.83	7.32	90.85	760.5 598.3 389.0	β-Crystallization Eutectoid Compound separation	The temperature of compound separation varies from 389° to 406° C.
7	1.90	8.40	89.70	760.5 725.0 709.1 599.2 406.2	β-Crystallization Second peritectic Intersects miscibility curve Eutectoid Compound separation	
8	2.00	9.25	88.75	747.7 720.8 705.2 598.0 389.0	β Crystallization Second peritectic Intersects miscibility curve Eutectoid Compound separation	
9	2.30	9.85	87.85	717.1 704.1	γ Crystallization Intersects miscibility curve	
SECTION III Al/Pb = 2.93/1						
1	1.60	4.40	94.00	834.5	α-Crystallization	Fig. 7 (p. 226) shows the plane vertical Section III.
2	1.80	5.20	93.00	815.2 774.5 606.7 380.7	α-Crystallization First peritectic Eutectoid Compound separation	The limit of the α-region = 5.20% Al and 1.80% Pb. The first peritectic occurs at a composition of 7.10% Al, 2.40% Pb and 90.50% Ag, at a temperature of 760.0° C.
3	2.00	6.00	92.00	768.5 604.5 377.0	First peritectic Eutectoid Compound separation	The second peritectic occurs at a composition of 10.40% Al, 3.60% Pb, and 86.00% Ag, at a temperature of 708.0° C.
4	2.30	6.70	91.00	774.0 761.0 599.0 397.0	α-Crystallization First peritectic Eutectoid Compound separation	The width of the first peritectic gap = 2.60% (1.86% Al and 0.64% Pb). The maximum width of the β-region = 0.50% (0.37% Al and 0.13% Pb).

TABLE II—*Concluded*

COMPOSITION AND THERMAL EFFECTS IN ALLOYS OF CONSTANT ALUMINIUM/LEAD RATIO

Alloy No.	Wt. % Pb	Wt. % Al	Wt. % Ag	Temperature of thermal effect, ° C.	Nature of thermal effect	Comments
SECTION III—*Concluded*						
5	2.60	7.40	90.00	760 0 717.0 (Very weak) 603.0 393.0	β-Crystallization Second peritectic Eutectoid Compound separation	The width of the second peritectic gap = 4.00% (3.00% Al and 1.00% Pb). The eutectoid temperature remains constant at 603° C.
6	2.80	8.20	89.00	751.5 709.5 600.5 (Very weak) 392.5 (Very weak)	β-Crystallization Second peritectic Eutectoid Compound separation	The temperature of compound separation varies from 377° to 397° C.
7	3.10	8.90	88.00	729.0 706.0	β-Crystallization Second peritectic	
8	3.30	9.70	87.00	725.0 707.0	β-Crystallization Second peritectic	
9	3.60	10.40	86.00	708.0	Second peritectic	
SECTION IV Al/Pb = 1.34/1						
1	4.70	6.30	89.00	799.5 750.5 710.3 (Very weak) 595.3 383.0	α-Crystallization First peritectic Intersects miscibility curve Eutectoid Compound separation	Fig. 8 (p. 227) shows the plane vertical Section IV. The first peritectic occurs at a composition of 7.55% Al, 5.59% Pb, and 86.86% Ag, at a temperature of 738.8° C.
2	5.00	6.70	88.30	777.7 749.7 713.7 (Very weak) 598.3 384.3	α-Crystallization First peritectic Intersects miscibility curve Eutectoid Compound separation	The second peritectic has disappeared because this section now intersects the area of partial miscibility. Finally an experiment was carried out with an alloy of the composition 81.00% Ag, 2 00% Al, 17.00% Pb. This showed only α-crystallization occurring at a temperature of 818.0° C., followed by ternary eutectic crystallization at 304.1° C.
3	5.35	7.23	87.42	757.8 740.8 708.1 (Weak) 591.5 380.0	α-Crystallization First peritectic Intersects miscibility curve Eutectoid Compound separation	
4	5.59	7.55	86.86	738.8 711.0 (Weak) 594.2 381.5	First peritectic Intersects miscibility curve Eutectoid Compound separation	

constant at 304.1°. The analyses of both alloys were identical and showed only traces of aluminium, less than 0.1%, with 2.30% silver. In order to improve the sensitivity of the chemical analysis, the aluminium was estimated, in this case, as its compound with 8-hydroxyquinoline. The composition and temperature of the binary eutectic, silver–lead, are given as 2.30% Ag and 300 to 305° by Yoldi and Jiminez (17).

The Eutectic Line

The binary eutectic, silver–aluminium, lies, according to Hansen (3) at 558° C., and contains, according to Petrenko (9), 69% silver. This temperature is lowered to 548.6° by the addition of lead, at a composition of 67.50% Ag, 30.71% Al, 1.73% Pb. Further addition of lead produces no change of temperature, the upper liquid layer being now saturated with lead.

Section Lines

These results are given in somewhat greater detail in Table II because of the importance and intricate nature of the phenomena.

Hardness Measurements

The comparative results of the Brinell hardness tests are given in Table III.

TABLE III

Alloy			Brinell number
Pure lead			4.2
Pure aluminium			15.9
Pure silver			12.7
Binary eutectic, Ag-Al			79.6
Binary eutectic, Ag-Al + 1.73% Pb			66.2
%Ag	%Al	% Pb	
34.51	64.13	1.36	58.3
21.25	77.60	1.15	55.3
79.64	17.21	3.11	63.7
87.50	12.50	–	109.0
94.40	4.90	0.70	124.0
90.85	7.32	1.83	50.3
87.85	9.85	2.30	119.0
91.00	6.70	2.30	116.5
86.00	10.40	3.60	74.0
86.86	7.55	5.59	59.0
81.00	2.00	17.00	17.5
20.00	80.00		50.3

Discussion of Results

Region of Partial Miscibility

In the lighter alloys, the silver content increases until it reaches a maximum of 85.58% (with 4.71% Pb) by weight, after which it falls again. With increasing silver content, the lead content also rises. This increase is very slight at first, rising from 1.10% in the alloy that contains no silver to 1.73%

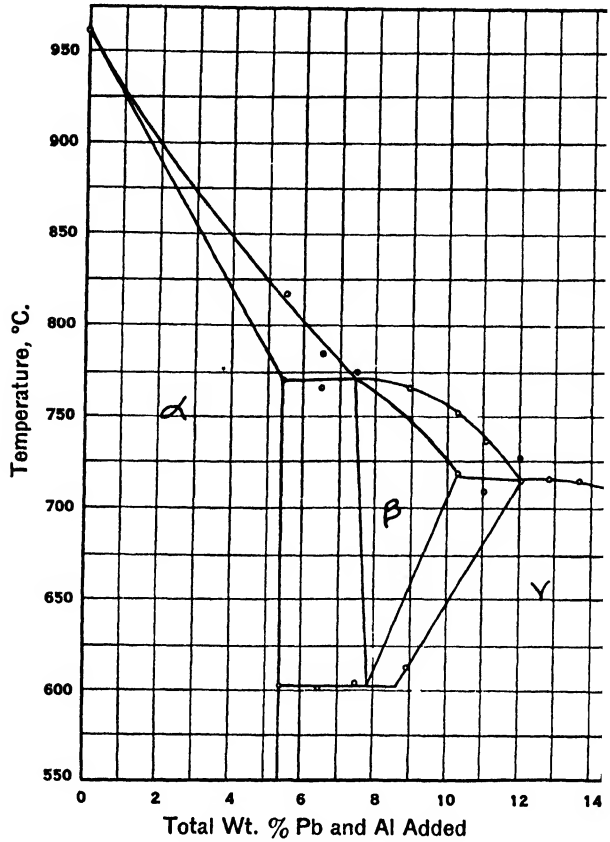

FIG. 5.

in the alloy containing silver and aluminium in the proportions of the binary eutectic of the silver–aluminium system. From this point, the lead content rises very rapidly.

As the amount of silver increases from 0 to 69% by weight, the temperature of solidification of the upper layer falls until it finally reaches a minimum value of 548.5° C. This is the temperature at which the γ-Al eutectic plus 1.73% lead strikes the miscibility curve. Beyond 69% silver, the temperature rises rapidly and continues to rise even in alloys whose composition lies past the summit of the miscibility curve. It finally attains a maximum value of about 736° C. in the alloy containing about 80% silver and 14% lead. Thus the temperature maximum does not coincide with the summit of the miscibility curve.

In the heavier alloys, the silver content rises very slowly until the conjugate lighter alloy has passed to the right of the summit of the curve, after which the content increases very rapidly. The aluminium content remains very small even in alloys with a silver content up to 40%.

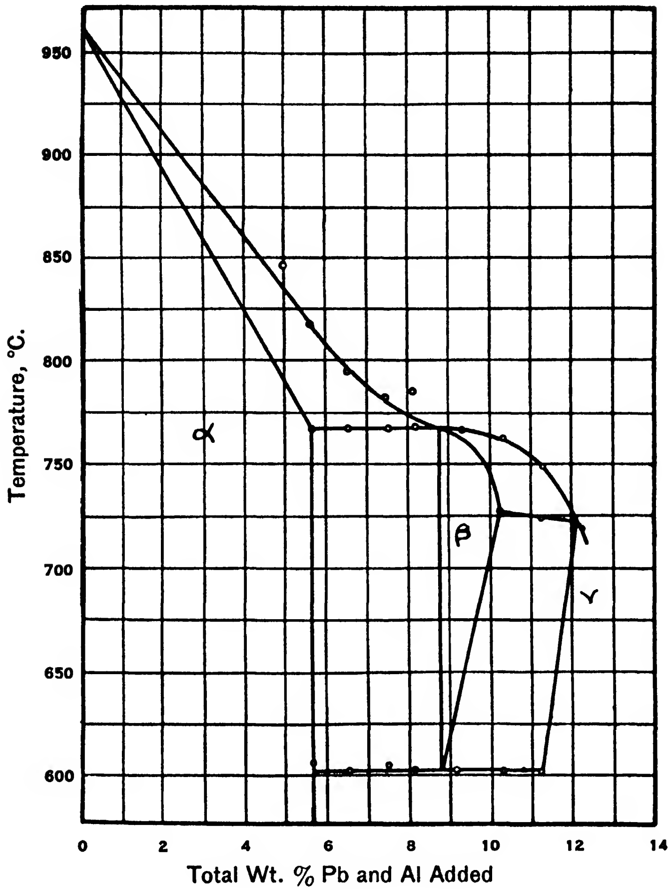

FIG. 6.

With reference to Table I, *B*, it is observed that, in Alloy 10, temperature arrests are observed at temperatures of 596.4° and 398.9° C. These are due to the fact that, in the aluminium-silver system, a β-phase forms owing to a peritectic reaction at 779° C. This phase is, however, stable only above 610° C; below that temperature it decomposes into a mixture of α and γ. This mixture also has a region of limited existence and at a temperature of about 400° C. the β′-phase ($AlAg_3$) is formed and this is stable at room temperature. Alloy 10 alone shows these transformations because it alone lies in the first peritectic gap. Alloy 9 might be expected to show the second peritectic transformation although it does not, but a very slight error, either in the position of the second peritectic line or in the analysis of Alloy 9, would account for this.

The analyses show that the light alloys always contain more silver than the corresponding heavy alloys and therefore the tie-lines slope uniformly to the right as shown in Fig. 4. To avoid complicating this diagram, the temperatures

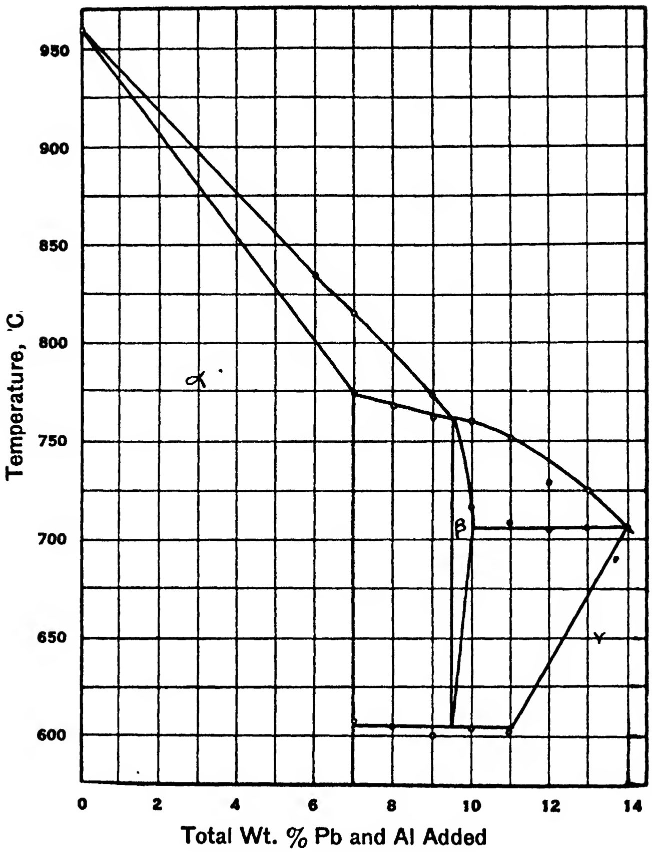

FIG. 7.

of the individual points have not been indicated: these may be found in the table. The diagram is a projection on the base of the solid model, not an isothermal section.

The Ternary Eutectic

The results show that the ternary eutectic point is almost identical with the binary eutectic, silver–lead. The solid phases here are silver, lead and (presumably) γ. The end member of the γ-series of solid solutions is either the compound $AgAl_2$, as found by most previous workers, or the compound $AlAg_2$, as found by Tishtchenko and Lukash (14).

Solubility of Lead in Solid Phases

Thermal analysis does not show any appreciable solid solubility of lead in the α, β, or γ-phases. The eutectoid reaction $\beta \rightleftarrows \alpha + \gamma$ would show a temperature change if solid solution of lead in any of these phases occurred, but, as Fig. 9 shows, the variation in eutectoid temperature is that only of experimental error, the temperature varying in different directions, regardless of the amount of lead added.

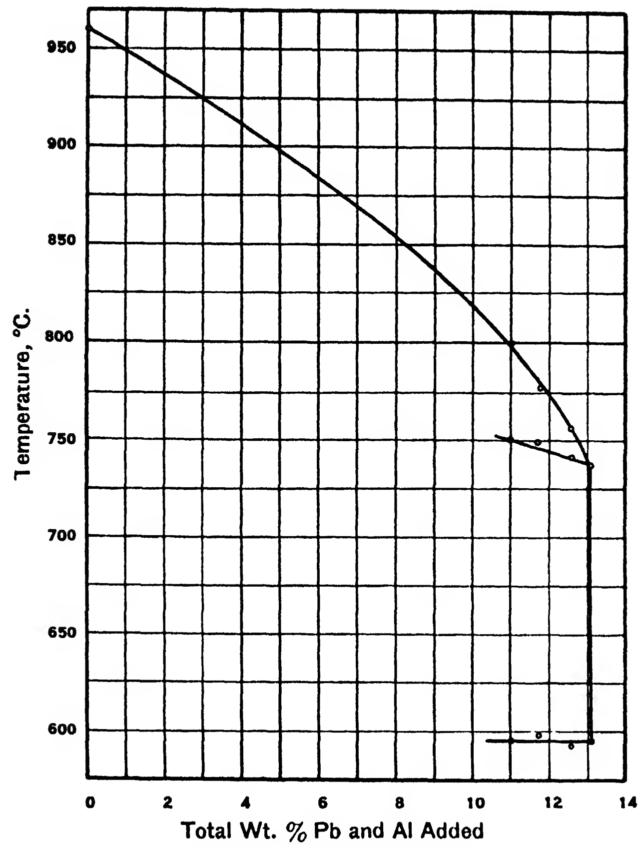

FIG. 8.

The eutectoid temperature has been variously given as 600° (1), 615° (8), 606° (12), and "around 610° C." (15). Our results show an average of 601°.

The temperature of compound separation ($\beta' = Ag_3Al$) likewise gives no indication of solid solubility. It was found to vary between 385° and 405° C., regardless of the amount of lead added. This variation is also found in the literature. Different investigators place this temperature at 400° (1), 400° (13), 420° (8), and 456° C. (12).

Investigation of δ-solid solubility proved fruitless since, even with very slow cooling (1° C. per min.), the effect could not be detected in the silver–aluminium system (without lead). This is borne out by Hansen (3), who determined the δ-region micrographically.

We have obtained some direct microscopic evidence of the insolubility of lead in γ-phase. Solubility of lead in α-phase is, a priori, improbable, since the α-phase will possess the silver space lattice, and the lead–silver binary system shows that lead and silver are mutually insoluble in the solid state. Micrographic determination is not possible for the β-region, since according to Obinata and Hagiya (8), Westgren and Bradley (15) and Ageew

and Shoyket (1), the reaction $\beta \rightleftarrows \alpha + \gamma$ cannot be repressed by quenching. X-ray analysis is necessary to settle the matter conclusively; thermal analysis indicates that lead is insoluble in β-phase.

Fig. 4 is a complete equilibrium diagram, showing all liquidus curves, and areas of solid separation.

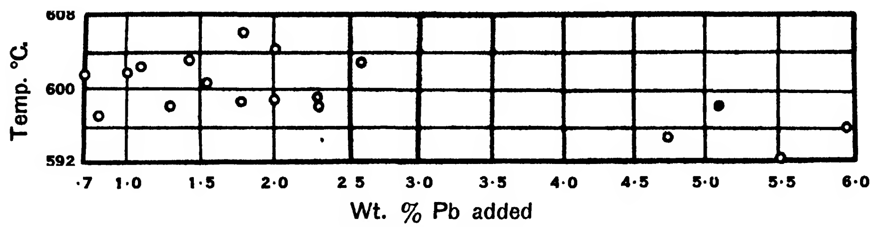

FIG. 9.

Fig. 10 is a magnified section of the silver apex, showing the peritectic lines and the (presumed) areas of solid solubility, together with some isothermal lines.

In the area *ABCK* primary crystallization of a solid solution of the α-series will take place, whose precise composition will depend on that of the melt. The lead will remain in the residual liquid, which will eventually solidify at the ternary eutectic point.

In the region bounded by the lines *BD*, *BC*, *DJ* and the miscibility curve, heterogeneous solid phases will be produced. A solid solution of the α-series will first separate. When temperature and composition cross the line *DJ*, interaction of separated α with liquid melt to form β-phase results, but excess α remains unchanged. The residual liquid, which (presumably) contains all the lead, solidifies at the ternary euctectic.

The region of occurrence of homogeneous β is bounded by the area *DJNE*. The β-phase is the primary crystallization. The lead will remain in the residual liquid which will finally solidify at the ternary eutectic.

The area *ENHG* is also an area of heterogeneity. The primary crystallization is that of β which will change (partially) to γ, when *GH* is crossed. The residual liquid containing the lead solidifies at the ternary eutectic. The $\beta/(\beta+\gamma)$ boundary *EN*, is drawn, like that of the $\alpha/(\alpha+\beta)$ boundary *BC*, by joining the point *E* (or *B*) to the opposed angular point, i.e., by assuming that the solid phases are free from lead. The thermal analysis, however, also presents some direct evidence for the position of *EN*, as reference to the data of the sections will show. Alloys showing eutectoid transformation but no second peritectic should all lie in the area *DJNE*, whereas alloys showing both eutectoid transformation and second peritectic should lie in the area *ENHG*. Owing to supercooling, delayed transition, slowness of solid diffusion, etc., this is not entirely borne out by the experimental data, but it is very

largely. It should be noted that the diagram only represents primary crystallization, in the sense that liquid melt is always present. The diagram does not represent the constitution of the cold alloy because of the impossibility of preserving β by quenching: β always transforms to the pure compound β' on cooling.

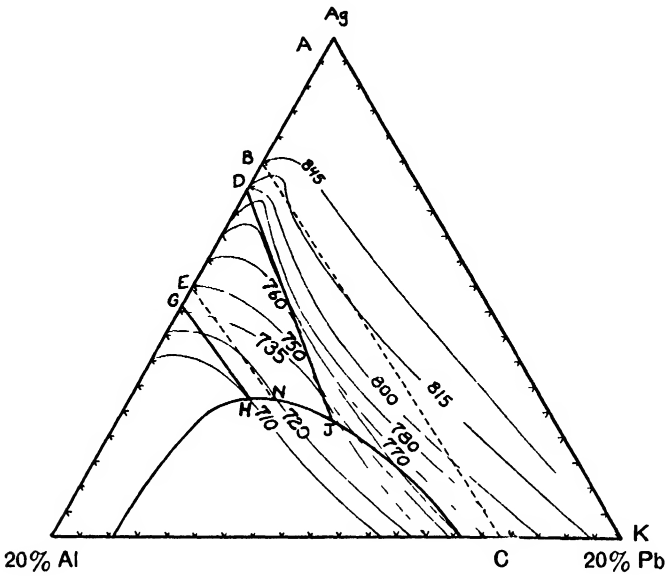

FIG. 10.

The first peritectic line in the silver–aluminium system with increasing addition of lead intersects the partial miscibility curve at 7.90% Al, 7.60% Pb, 84.50% Ag, the temperature dropping from 779° to 727° C. The second peritectic line intersects the partial miscibility curve at 10.30% Al, 4.10% Pb, and 85.60% Ag, the temperature dropping from 729° to 708°. If the partial miscibility curve had not intervened, the two lines would have intersected at 11.00% Al, 15.50% Pb, and 73.50% Ag.

Hardness Measurements

From the table of hardness it is evident that when silver is added to aluminium, the resultant alloy is very much harder than either of the two component metals. When lead is added to the aluminium–silver alloys, its presence reduces this hardness. Although the components are all soft, aluminium being the hardest, the hardness of alloys rich in α, β', and γ phases approaches that of mild steel. The heterogeneous solids are however much softer.

References

1. AGEEW, N. and SHOYKET, D. J. Inst. Metals, 52 : 119-126. 1933.
2. CAMPBELL, A. N. and ASHLEY, R. W. Can. J. Research, B, 18 : 281-287. 1940.
3. HANSEN, M. Z. Metallkunde, 20 : 217-222. 1928.
4. HANSEN, M. Der Aufbau der Zweistofflegierungen. J. Springer, Berlin. 1936.

5. KEMPF, L. W. and VAN HORN, K. R. Am. Inst. Mining Met. Engrs. Tech. Pub. 990. 1938.
6. JÄNECKE, E. Kurzgefasstes Handbuch aller Legierungen. O. Spamer, Leipzig. 1937.
7. LORENZ, VON R. and ERBE, F. Z. anorg. allgem. Chem. 183 : 311-339. 1929.
8. OBINATA, I. and HAGIYA, M. Kinzoku no-Kenkyu, 12 : 419-429. 1935.
9. PETRENKO, G. I. Z. anorg. allgem. Chem. 46 : 49-59. 1905.
10. PLATO, W. Z. physik. Chem. 55 : 721-737. 1906.
11. ROBERTS-AUSTEN, W. C. 5th Rept. Alloys Research Comm. Proc. Inst. Mech. Engrs. (London), 1899.
12. TISHTCHENKO, F. E. J. Gen. Chem. (U.S.S.R.) 9 : 729-731. 1939.
13. TISHTCHENKO, F. E. J. Gen. Chem. (U.S.S.R.) 3 : 549-557. 1933. *Abstract in* Met. Abstracts 1 : 7. 1934.
14. TISHTCHENKO, F. E. and LUKASH, I. K. J. Phys. Chem. U.S.S.R. 9 : 440-448. 1937.
15. WESTGREN, A. F. and BRADLEY, A. J. Phil. Mag. (Ser. 7) 6(35) : 280-288. 1928.
16. WRIGHT, C. R. A. Proc. Roy. Soc. (London) 52 : 11-27. 1892.
17. YOLDI, F. and JIMENEZ, D. L. DE A. Anales soc. españ. fís. quím. 28 : 1055-1065. 1930. *Abstract in* J. Inst. Metals, 47 : 76. 1931.

Canadian Journal of Research

Issued by THE NATIONAL RESEARCH COUNCIL OF CANADA

VOL. 19, SEC. B | OCTOBER, 1941 | NUMBER 10

PHASE EQUILIBRIA IN THE TWO COMPONENT SYSTEM, ETHYLENE-PROPYLENE, IN THE CRITICAL TEMPERATURE REGION[1]

BY W. G. SCHNEIDER[2] AND O. MAASS[3]

Abstract

Phase equilibria measurements have been made for a 1 : 1 ethylene-propylene system in the critical temperature region by means of an equilibrium apparatus described by Holder and Maass (3). The critical density of the system was found to be 0.230 gm. per cc. and the critical temperature 58.30° ± 0.05° C. For mass-volume ratios greater than 0.230, at constant volume, the temperature of liquid disappearance was lower than 58.30° C., while for mass-volume ratios less than 0.230, the temperature of liquid disappearance was higher than 58.30°C. With stirring, the phase compositions and phase densities of the liquid and vapour phases were shown to become equal at the critical temperature, whereas in the absence of stirring the attainment of equilibrium is slow and uncertain. The results are discussed on the basis of the liquid persistence theory (5), and the vapour-liquid dispersion theory (1, 9).

Introduction

A series of investigations in the critical temperature region has been carried out in this laboratory with one component systems, and in general the results indicated a discontinuity of property at the critical temperature (2, 3, 6, 7, 11, 15, 18, 20). This phenomenon was explained by the hypothesis of a liquid structure characterized by a regional orientation (5) which persists at the critical temperature and over a finite temperature range above the critical temperature. The present work is an attempt to study the behaviour of a two component system in the critical temperature region, and especially to determine whether a discontinuity in phase composition can be detected at the critical temperature.

Apparatus

To study the composition of the two phases of the system in the critical temperature region, it was necessary to obtain a representative sample of each phase in such a way that the equilibrium of the system would not be disturbed. This was possible with an apparatus similar in principle to that used in this laboratory by Holder and Maass (3). A new assembly was constructed which embodied several modifications of their apparatus. Fig. 1 shows a cross-section of the main features of the apparatus. It consisted of

[1] *Manuscript received July 25, 1941.*
Contribution from the Physical Chemistry Laboratory, McGill University, Montreal, Que., with financial assistance from the National Research Council of Canada.

[2] *Holder of a Fellowship under the National Research Council of Canada.*
[3] *Macdonald Professor of Physical Chemistry.*

a central main bomb to which two small sampling bombs, *B* and *C*, were attached. The main bomb was machined from a bar of stainless steel (18-8 composition, "Sta-brite"). This material was chosen because it was found that the phosphor-bronze bomb employed by Holder and Maass (3) was

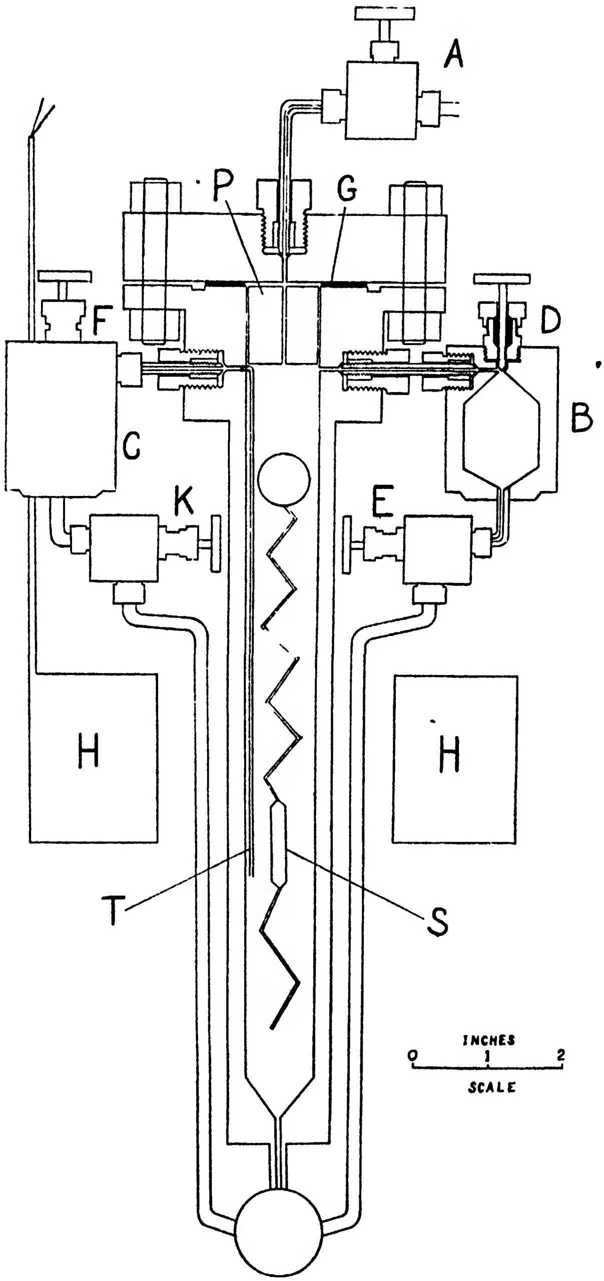

FIG. 1. *Schematic diagram of the equilibrium bomb assembly.*

slowly attacked by mercury. Moreover phosphor-bronze has not a sufficiently high tensile strength, and threads cut into it at the joints yielded. The stainless steel used is non-magnetic; this made possible the use of an electromagnetic stirrer. The depth of the main bomb was 11 in. and the inside diameter 13/16 in.; the wall thickness was $\frac{1}{4}$ in. These dimensions allowed mercury to run out of the sampling bombs readily. At the top of the bomb a shoulder was left to which the sampling bombs could be joined, and above this a flange $4\frac{1}{4}$ in. in diameter to which the cover could be bolted. The cover was 1 in. thick and was fastened to the bomb by means of four $\frac{3}{8}$ in. steel bolts. A lead gasket *G* was held in place by two V-grooves on the seat of the bomb, and two V-shaped tongues on the cover.

The sampling bombs, *B* and *C*, were made of cold rolled steel. These units were the same as used by Holder and Maass (3), and consisted of a reservoir and a needle valve combined in a single body. The sampling bombs were joined to the bottom of the main bomb by welding; this permitted the use of liquid air in charging the bomb. The bottom or liquid sample was drawn into the sampling bomb *C* through a fine stainless steel tube *T*, which extends approximately two-thirds of the distance down the main bomb. The plug *P* merely served to reduce the unavoidable dead space at this point. Graphite and string were used for the valve packings.

The stirrer *S* consisted of a glass-encased iron core with a sturdy glass spiral joined to each end; a bulb, about $\frac{5}{8}$ in. in diameter, at the top end steadied the stirrer in its up and down motion and set up a turbulence in the vapour phase to ensure efficient mixing. The stirrer was operated by a solenoid *H* enclosed in a brass case; the internal diameter of the solenoid ($3\frac{3}{4}$ in.) was sufficient to prevent any temperature gradient along the length of the tube due to heat from the solenoid.

The thermostat consisted of a cylindrical copper tank, fitted with two windows, and equipped with two high speed, four-blade stirrers. A high boiling hydrocarbon oil (Marcol HX) was used as the thermostat liquid. Heating as well as regulation of the thermostat was effected by means of a single intermittent 250 watt heater placed half-way down the side of the bath. Thermocouples placed at various points in the thermostat showed no temperature gradients either in the bath itself, or around the solenoid and along the length of the equilibrium bomb. Temperature control was good to within 0.01° C. The thermometer used throughout was calibrated against a platinum resistance thermometer.

Ethylene and propylene were obtained from the Ohio Chemical Co. The ethylene gas was certified 99.5% pure, and the propylene 99.8% pure. The gases were purified by fractional distillation. The critical properties of ethylene and propylene are summarized in Table I.

TABLE I

THE CRITICAL PROPERTIES OF ETHYLENE AND PROPYLENE

—	T_c,° C.	P_c, atm.	d_c, gm./cc.	Reference
Ethylene	9.2 (9.7)	50.9	0.22	(13, 16)
Propylene	91.4	45.4	0.233	(19)

Experimental Procedure

1. *Preparation for an Experiment*

In the equilibrium bomb 40.0 cc. of mercury was placed. The cover was then bolted on and the bomb connected to the gas reservoirs. The needle valves on the sampling bomb *B* were opened, while the valves of sampling bomb *C* were closed. The system was then evacuated. Valve *D* was closed; and ethylene or propylene admitted to the apparatus to a pressure of 1½ atm., forcing mercury up through valve *E* and filling the reservoir *B*. Valve *E* was then closed. Sampling bomb *C* was filled with mercury in the same manner. When both sampling bombs were filled, enough mercury remained in the main bomb to cover the bottom. The apparatus was then again thoroughly evacuated and flushed twice with propylene or ethylene.

2. *Filling the Equilibrium Bomb*

The volume of the equilibrium bomb, when it was ready to be charged (i.e., when the sampling bombs were filled and a little mercury remained in the bottom of the bomb) was calibrated by weighing with mercury. This volume was 87.4 cc. The amounts of ethylene and propylene required to give a 1 : 1 mixture and a mass volume ratio of 0.230 were calculated and condensed into the bomb with liquid air, propylene being condensed first. The amount of each gas condensed was measured accurately by the change in pressure in a calibrated volume, both gases being measured successively from the same volume. The error in the measurement of the masses of the gases condensed into the bomb is believed to be considerably less than 0.1%.

The charged bomb was placed in the thermostat at the desired temperature, and the stirrer started. Thermostating was continued for 14 hr. or longer with continuous stirring to allow the system to come to equilibrium. The rate of stirring varied from 75 to 120 strokes per min. (a stroke including one up and down motion of the stirrer). Between these limits the final equilibrium obtained was apparently independent of the rate of stirring.

3. *Sampling*

In withdrawing the phase samples, that of the "liquid" or lower phase was taken first. Valves *F* and *K* (Fig. 1) were opened for a sufficient time for the mercury to run down into the main bomb. In the same way the vapour or upper sample was drawn into the sample bomb *B* by opening valves *D* and *E*.

The apparatus was removed from the thermostat and the pressure in the main bomb was released. The samples were then expanded into calibrated volumes and the pressures and temperatures recorded.

4. *Analysis of the Samples*

The samples were analysed in a low temperature still of the Podbielniak type (17). By fractionating known samples of ethylene and propylene, analysis by this method was found to be accurate to 0.3%.

Results

1. *Critical Temperature and Critical Density of a 1 : 1 Ethylene-Propylene Mixture*

Before any measurements of the phase equilibria of the system in the critical region could be carried out, it was necessary to determine the critical temperature and the critical density of the system. This was accomplished by filling thick-walled glass bombs to various densities with the carefully purified gases and observing the temperature of meniscus disappearance as the bomb is gradually heated (0.1° C. per hour), the rate of stirring being the same as in the steel equilibrium bomb. The results of a number of measurements are summarized in Table II, and are plotted in Fig. 2. For a mass-volume ratio less than 0.230, the meniscus remained more or less stationary until the temperature was a few tenths of a degree below that of the liquid disappearance, when it gradually moved to the bottom and disappeared as the temperature was raised. On lowering the temperature again, the first traces of liquid appeared at the bottom of the bulb. The temperature of disappearance and reappearance of liquid was found to coincide to within 0.01° C.; this indicated therefore a true equilibrium, which cannot be attained without stirring. When the system was not agitated, the temperature of meniscus disappearance was somewhat indefinite, owing to the opalescence produced, and was generally about 0.2° C. higher than the equilibrium values given in Table II, whereas the temperature of liquid reappearance was about 0.3° C. lower.

TABLE II

RELATION OF THE CRITICAL TEMPERATURE TO THE MASS-VOLUME RATIO WITH STIRRING OF THE MEDIUM

Mass-volume ratio, gm./cc.	Temperature of disappearance of liquid, ° C.	Position of meniscus disappearance	Mass-volume ratio, gm./cc.	Temperature of disappearance of liquid, ° C.	Position of meniscus disappearance
0.190	59.89	Bottom	0.230	58.27	Middle
0.200	59.56	"	0.230	58.31	"
0.200	59.59	"	0.230	58.29	"
0.210	59.25	"	0.230	58.31	"
0.220	58.70	"	0.240	57.94	Top
0.220	58.74	"	0.250	57.59	"
0.225	58.48	Below middle			

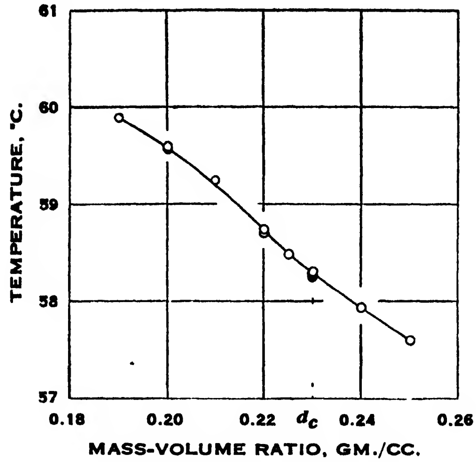

FIG. 2. *Curve showing the relation of the temperature of liquid disappearance to the mass-volume ratio in the critical temperature region for a 1 : 1 ethylene-propylene system.*

These results are in agreement with the experiments of Mason, Naldrett, and Maass (9, 13) using a shaking bomb in studying the critical behaviour of the one component systems ethylene and ethane.

For a mass-volume ratio greater than 0.230, the meniscus rose and disappeared at the top of the bulb as the temperature was raised. For a filling of 0.230 alone the meniscus remained almost stationary until it disappeared at the middle of the bulb, and this was therefore taken as the critical density. The temperature of liquid disappearance corresponding to this density, 58.30° ± 0.05° C., was taken as the critical temperature of the mixture. It will be observed that for a two component system the true critical temperature (corresponding to the critical density as defined above) is not the maximum of the classical parabolic vapour-liquid co-existence curve, as is true for a one component system. Fig. 2 represents one branch of this curve only, but it is obvious that the maximum of the complete vapour-liquid co-existence curve must lie at a density considerably less than the critical. This relation was early observed by Kuenen (4).

From the results of Table II it is further evident that true critical phenomena (characterized by a meniscus disappearance at the critical temperature near the middle of the bulb) for the system under investigation will occur only over a very limited density range near the critical density. Owing to this limited critical density range, and because it was necessary to have the meniscus disappear in the middle of the equilibrium bomb to ensure a true phase sampling near the critical temperature, the phase equilibrium measurements were confined to the critical density, 0.230 gm. per cc.

2. Results of Phase Equilibria Measurements in the Critical Temperature Region

Some preliminary experiments were carried out in which the medium was not stirred. It was found however that even after 12 hr. thermostating at the highest temperature studied, 63.23° C., the compositions of the liquid

and vapour phases differed by about 34 mole per cent of ethylene, and the phase densities were 0.13 and 0.36 for the vapour and liquid phases, respectively. It was also found that agreement in the results was poor. It therefore appeared that without stirring the attainment of equilibrium was slow and uncertain. In all subsequent experiments the measurements were carried out with stirring in the manner described above. The period of thermostating varied from 13 to 20 hr. With the rate of stirring used, equilibrium was no doubt reached in a considerably shorter time. It was found convenient however to thermostat the equilibrium bomb overnight.

TABLE III

PHASE EQUILIBRIUM DATA OF 1 : 1 ETHYLENE-PROPYLENE SYSTEM IN THE CRITICAL TEMPERATURE REGION

Expt. no.	Temp., ° C.	Vapour phase		Liquid phase	
		Density, gm./cc.	Composition, mole per cent ethylene	Density, gm./cc.	Composition, mole per cent ethylene
1	58.68	0.226	50.3	0.233	50.0
2	58.43	0.230	50.1	0.232	49.9
12	58.38	0.230	50.4	0.232	50.1
7	58.34	—	50.2	0.232	50.2
3	58.28	0.207	50.7	0.257	49.4
5	58.12	0.194	51.6	0.268	48.8
*11	58.14	0.196	51.3	0.266	48.9
8	57.67	0.182	51.8	0 284	48.2
14	57.67	0.182	52.2	0.?79	48.1
4	57.00	0.168	53 0	0.290	47.5
9	56.04	0.157	53.4	0.307	46.7
6	55.84	0.158	53.6	0.306	46.8
13	55.02	0.151	54.2	0.313	46.3
10	54.13	0.142	54.5	0.321	45.9

** Temperature raised to 58.70° C. and kept constant for 12 hr., then lowered to 58.14° C. and thermostating continued for 13 hr.*

The results of the phase equilibrium measurements are summarized in Table III. The first column gives an indication of the order in which the runs were carried out. The phase densities were calculated from the volume, pressure, temperature, and composition of the expanded samples, and the volume of the sample bombs. The volumes of the sample bombs were calibrated by weighing with mercury, and were 15.43 and 15.40 cc. for the vapour and liquid sample bombs, respectively. It is difficult to estimate the error of the phase densities obtained in this way. The detailed manipulation of the phase samples concerned limits the accuracy with which these values can be determined. Another difficulty was the occasional failure of the mercury to drain out of the sampling bombs completely when the phase samples were being withdrawn. However the regularity of the results in Table III seems to indicate that the error due to this cause is not as great as might be expected. Taken as a whole, the calculated densities are considered

to represent fairly good approximations of the relative phase densities, rather than absolute values of the phase densities.

The calculated phase densities are plotted in Fig. 3 and the phase compositions in Fig. 4. The density-temperature curve exhibits a very flat crest at the critical temperature, which, considering the limits of experimental error, could be drawn as a horizontal line. In this respect the curve is very similar to the density-temperature curve obtained by Mason, Naldrett, and Maass (9, 13) in studying the critical behaviour in a one component system using a shaking bomb.

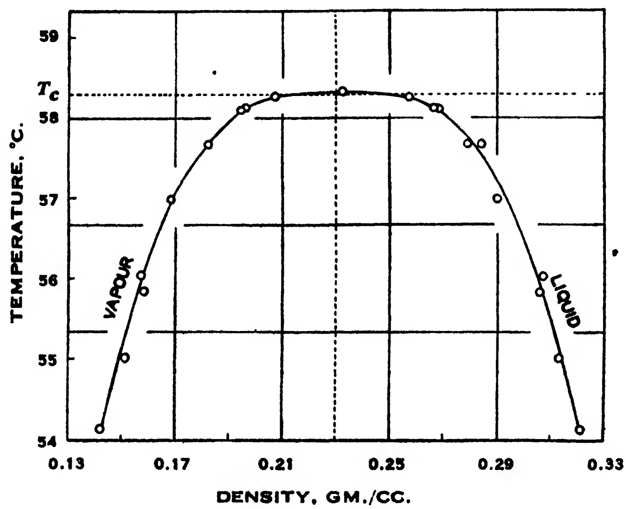

FIG. 3. *Plot of the density of the co-existing vapour and liquid phases in the critical temperature region.*

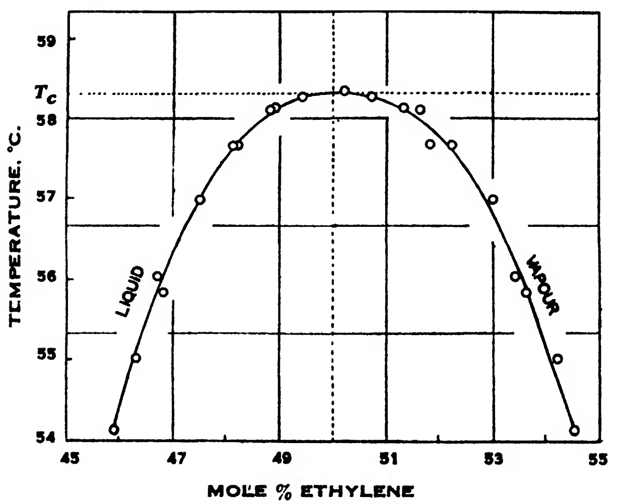

FIG. 4. *Curve showing the phase compositions of the co-existing vapour and liquid phases plotted against temperature in the critical temperature region.*

Discussion

The phase compositions obtained at each temperature are considered to represent true equilibrium conditions. The time of thermostating as well as the rate of stirring were ample to allow equilibrium to be attained. With the same rate of stirring in the glass bombs, the liquid phase was found to appear and disappear within a range of 0.01° C. at the critical temperature; this indicated a rapid establishment of equilibrium under these conditions. Finally, it has been demonstrated (Expt. no. 11, Table III) that the same equilibrium state is obtained when the system is first heated above the critical temperature, as when it is brought from a lower temperature and thermostated at the chosen temperature. The equilibrium is thus reversible with respect to temperature.

Although the meniscus behaviour in the equilibrium bomb could not be observed directly, it was possible to obtain fairly convincing evidence that a liquid phase was present in the equilibrium bomb at a temperature as high as 58.28° C. by the sound of the glass stirrer moving up and down in the metal bomb. In the absence of liquid (i.e., above the critical temperature) the noise of the stirrer moving up under the magnetic field and striking the bottom when the field was off was somewhat muffled, whereas in the presence of liquid the noise was particularly audible. By holding the ear close to the top metal support of the bomb a characteristic "swishing" of the liquid could be heard while it was being stirred.

The results of Table III indicate that the experimentally measured compositions as well as the densities of the vapour and liquid phases become uniform at the critical temperature. In this respect the results are in apparent disagreement with those of Winkler and Maass (20) who found a density discontinuity to persist in a one component system at the critical temperature when the medium was stirred. The stirring in the present work however is believed to be much more vigorous and efficient, and might be expected to favour a mutual dispersion of the liquid and vapour phases near the critical temperature, so that a density discontinuity is not detectable. Experimental evidence of a vapour-liquid dispersion at the critical temperature has been obtained by several investigators in this laboratory (1, 8, 9, 10, 13, 14). It was postulated that a liquid structure persists at the critical temperature, and since the surface tension of the liquid becomes zero at this temperature (14), the liquid phase will become dispersed, partially or completely with the vapour phase, depending on the degree of stirring or agitation. This hypothesis readily explains the relatively flat portion of the phase-density–temperature curve (Fig. 3) at the critical temperature, where in the presence of stirring a rapid mutual dispersion of the vapour molecules and liquid groups may be expected, causing the measured phase densities to become rapidly equalized. It may be argued that a similar flat portion at the critical temperature should occur in the composition-temperature curve (Fig. 4) as a result of the mutual dispersion of the persistent liquid and vapour phases, which, corresponding to the unequal phase densities just below the critical temperature, may differ

appreciably in composition at the critical temperature. To explain the actual curve obtained, the mutual solubility of the two components at the critical temperature must be considered to be either complete, or to be nearly complete and the present method to be incapable of detecting the exact behaviour. In the light of experimental evidence already accumulated on the critical temperature phenomena the present results can be most conveniently interpreted by supposing liquid groups, containing on the average an equal number of molecules of each component, to persist at the critical temperature, and to become mutually dispersed with vapour molecules, the dispersion being complete as a result of stirring of the system. While it is true that the results could, on the other hand, be explained simply by assuming the principle of continuity of state at the critical temperature, an exceedingly rapid change of phase density with temperature at the critical point would have to be postulated to explain the density-temperature curve. Accurate density measurements in a one component system in the absence of stirring (6, 11, 18, 20) have shown however that the change of phase density with temperature at the critical temperature is not as rapid as demanded by the theory of continuity of state, but that the change is much more gradual, corresponding to a gradual breaking-up of liquid structure which was found to persist over a finite temperature interval above the critical temperature.

References

1. Dacey, J., McIntosh, R., and Maass, O. Can. J. Research, B, 17 : 206-213. 1939.
2. Edwards, J. and Maass, O. Can. J. Research, B, 13 : 133-139. 1935.
3. Holder, C. H. and Maass, O. Can. J. Research, B, 18 : 293-304. 1940.
4. Kuenen, J. P. Z. physik. Chem. 24 (4) : 667-696. 1897.
5. Maass, O. Chem. Rev. 23 (1) : 17-28. 1938.
6. Maass, O. and Geddes, A. L. Trans. Roy. Soc. (London) A, 236 : 303-332. 1937.
7. Marsden, J. and Maass, O. Can. J. Research, B, 14 : 90-95. 1936.
8. Mason, S. Ph.D. Thesis, McGill Univ. 1939.
9. Mason, S. G., Naldrett, S. N., and Maass, O. Can. J. Research, B, 18 : 103-117. 1940.
10. McIntosh, R. L., Dacey, J. R., and Maass, O. Can. J. Research, B, 17 : 241-250. 1939.
11. McIntosh, R. L. and Maass, O. Can. J. Research, B, 16 : 289-302. 1938.
12. Morris, H. E. and Maass, O. Can. J. Research, 9 : 240-251. 1933.
13. Naldrett, S. N. and Maass, O. Can. J. Research, B, 18 : 118-121. 1940.
14. Pall, D. Ph.D. Thesis, McGill Univ. 1939.
15. Pall, D. B., Broughton, J. W., and Maass, O. Can. J. Research, B, 16 : 230-241. 1938.
16. Pickering, S. F. Bur. Standards, Sci. Papers, 21 : 597-629. (Sci. Paper 541). 1926.
17. Podbielniak, W. J. Ind. Eng. Chem. Anal. Ed. 5 : 119-142. 1933.
18. Tapp, J. S., Steacie, E. W. R., and Maass, O. Can. J. Research, 9 : 217-239. 1933.
19. Vaughan, W. E. and Graves, N. R. Ind. Eng. Chem. 32 (9) : 1252-1256. 1940.
20. Winkler, C. A. and Maass, O. Can. J. Research, 9 : 613-629. 1933.

THE DEVELOPMENT OF A PRESERVATIVE FOR GILL NETS[1,2]

By G. Cave-Browne-Cave[3] and R. H. Clark[4]

Abstract

In a search for an adequate preservative for gill nets many attempts were made to synthesize a plastic in the fibres of the twine. The resulting strands in no case possessed such requisite properties as sufficient flexibility and wearing qualities. Strands, treated with a solution of chlorinated pale crepe rubber, to which a plasticizer, dibutyl phthalate, and a bactericide were added, were found, by tensile strength measurements, to prolong the life of the twine in the sea. The strands had the necessary degree of flexibility, and their wearing quality was improved greatly.

Tests made by commercial fishermen on sections of net, treated according to the formula recommended, confirm in large measure the laboratory and sea immersion experiments. They report, among other findings, that the net was easier to handle, remained clean, caught an equal catch of fish as the untreated sections, and that the knots did not slip. The strength of the treated net after a summer's fishing, the fishermen found, was only slightly greater than that of the untreated net. This result was not at all in accord with the laboratory tensile strength measurements made on twine after several weeks of sea immersion. An examination of the knots revealed that this difference is due undoubtedly to the fact that the preservative did not penetrate sufficiently into the knots. Nets are now being manufactured from the treated twine; this is expected to overcome the difficulty and increase considerably the life of the net under fishing conditions.

Introduction

The need for a satisfactory gill net preservative has existed since this method of fishing began. The need is world-wide. Carter and Charnley (1) have written as follows:—

> ". . . . In British Columbia alone during 1933 the value of gear in use was over $1,625,000, representing about 14% of the total value of the fish landed in the province for that year. The annual depreciation of some types of gear is very considerable, particularly in the case of salmon gill nets. In certain localities such nets costing from $100 to $150 apiece often last for only 4 to 8 weeks during a fishing season, although some serve for a season of 8 to 10 weeks' duration, and even for a part of the next season. In other localities an average of two seasons' use is obtained."

The present war has markedly aggravated the need, so that the present paper seems timely.

Causes of Rotting of Nets in Sea Water

Bacterial action appears to be the dominant cause (2, 3, 4). That bactericides such as copper sulphate, copper oleate, and copper naphthenate are

[1] *Manuscript received May 23, 1941.*

Contribution from the Department of Chemistry, The University of British Columbia, Vancouver, B.C.

[2] *The Fisheries Research Board of Canada, by resolution, has recommended the publication of this paper.*

[3] *At the time, Postgraduate Student. At present, Chief Analyst, Department of Mines, Victoria, B.C.*

[4] *Professor of Chemistry.*

widely used net preservatives supports the above statement. Mechanical wear on a net during fishing operations reduces the life of the net, and it is of special importance in that if a method of materially retarding bacterial action can be found, mechanical wear may then determine the life of the net. Both oxidation of the cellulose and the effect of sunlight on the cellulose contribute to the deterioration of the net. They are, however, of less importance than bacterial action.

Desirable Properties of a Preservative and of a Treated Net

The preservative itself should be either transparent or of a colour acceptable to fishermen. It must be easy to apply to the net. The weight of the net should not be unduly increased by the application of a preservative. In the net, bacterial action should be materially retarded; the treated net should have greater resistance to mechanical wear than the untreated net; oxidation of the cellulose should be retarded; and the harmful effect of sunlight should be minimized. Moreover, the knots of the treated net should not slip under tension before breakage occurs; the treated net must have the desired degree of flexibility. The net should be easy to handle. Finally, it must catch fish, a property not always possessed by nets treated with certain preservatives.

No commercially available preservative appears to possess, or to produce in a net, to a marked degree all these desired properties. Here, on the Pacific Coast, copper sulphate, linseed oil, and copper naphthenate are in constant use, but almost all Pacific Coast fishermen are still seeking an adequate preservative. With this need in mind the Department of Chemistry of the University of British Columbia instituted several years ago a research the object of which was to find such a gill net preservative. The problem was attacked from an angle heretofore neglected, viz.: to coat the fibres of the net twine with a plastic. Tyner and Fisher (6) experimented with several of the new plastic ingredients, synthesizing the plastic actually in the fibres of the net twine. They found that in almost all cases a net so treated was too stiff to use, but that chlorinated rubber offered promise owing to the flexibility of the treated net. The present paper records the results of a research whose object was a thorough investigation of chlorinated rubber as a preservative for gill nets.

Experimental Methods

Linen gill net twine (5/40), from which most good nets are woven, was used exclusively. For brevity the word "strands" will be used in place of the phrase "length of twine".

Method of Applying Preservative

Chlorinated rubber was dissolved in benzene and a plasticizer added. Strands were soaked in this solution for a definite period of time then hung up to dry for one week, after which they were ready for the various tests.

Methods of Determining the Value of a Preservative

The rate at which the tensile strength of a treated strand decreases while immersed in the sea is a useful index of the value of the preservative. In this work the chief method of evaluating a preservative consisted in immersing treated strands in sea water (Coal Harbour, Vancouver) and measuring the tensile strengths of the treated strands after various immersion periods. Six-foot lengths of treated strands were suspended in sea water from a floating plank.

Tensile Strength Measurements

By tensile strength in this paper is meant the force in pounds necessary to break the strand, the force being increased slowly and steadily to the breaking point of the strand. Unless stated otherwise, all strands were broken, while wet, after being soaked for at least 12 hr. in water. The tensile strength was measured on a standard instrument made by Henry L. Scott and Company, the drums around which the strand was wound being 9 in. apart.

Wearing Quality Measurements

Taylor and Wells (5) tried various materials against which to test the wearing quality of treated strands, e.g., wood, iron, glass, and hard rubber. The most satisfactory method was to rub the strand against itself at an acute

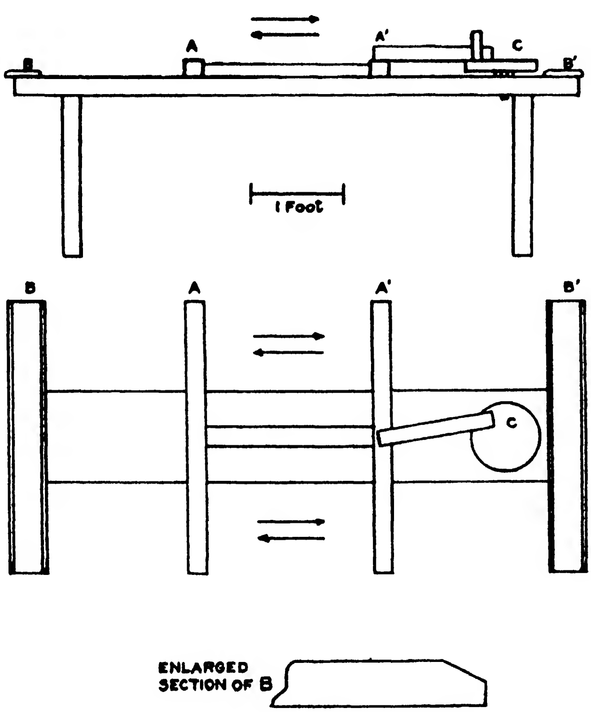

FIG. 1. *Wearing quality apparatus.*

angle and under tension. In the present investigation it was found that a rubbing surface of bevelled glass plate provided sufficiently significant results to warrant its use. Fig. 1 illustrates the design of the instrument used. Twelve treated strands were tied to cross-pieces A and A' and suspended over the bevelled glass plates B and B'. To the free end of each strand was tied a 500 gm. weight. Wheel C was turned by hand at a rate of one revolution per second, causing cross-pieces A and A' to move in approximately simple harmonic motion, in the direction of the arrows. The strands thus wore against the glass edges. The number of revolutions of wheel C was noted each time a strand broke. The wearing quality of a strand was defined as the number of revolutions of wheel C necessary to cause the strand to break through wear. An average of 48 measurements was taken as the wearing quality of a strand.

Flexibility Measurements

Tyner and Fisher (6) used no apparatus for their flexibility estimations. Taylor and Wells (5) devised an instrument by means of which a quantitative determination of flexibility may be made. Their method consists in measuring the energy dissipated when the strand bends through a definite angle. One end of the strand is attached to the end of a brass plummet. The other is held rigid. This, then, constitutes a pendulum. A definite initial phase is specified, and the number of oscillations to reduce the angle of the initial phase to one-half is taken as a measure of the flexibility. Such a method has, obviously, disadvantages. These are recorded by Taylor and Wells (5), who correct for the errors. Probably the greatest disadvantage is the large number of measurements that must be averaged in order to obtain a figure of significance.

To enable a significant measure of the flexibility of a strand to be made with as few measurements as possible, a new instrument was devised by the authors (Fig. 2).

Procedures for the operation of the flexibility instrument: One of several can be used, the choice being dependent on the time available and on the accuracy required. Below is given the procedure worked out and adopted in this investigation.

A strand was selected for a preliminary test. Ten grams was added to each scale pan. To one pan a weight (W_2) was added, the weight being such as to cause the pan to fall approximately 3 cm. in 25 sec. Next was selected a weight (W_1) necessary to cause the pan to fall approximately 3 cm. in 10 sec. Finally, a weight (W_3) necessary to cause the pan to fall approximately 3 cm. in 40 sec. was selected. These preliminary tests gave the weights W_1, W_2, and W_3, to be used in the actual determination. The procedure used in the actual determination follows:—

A new strand was selected and 10 gm. added to each pan. To one pan was added, in addition, W_1 gm. The length of strand chosen was such that when one pan was near the pulleys, the other almost touched the base of the

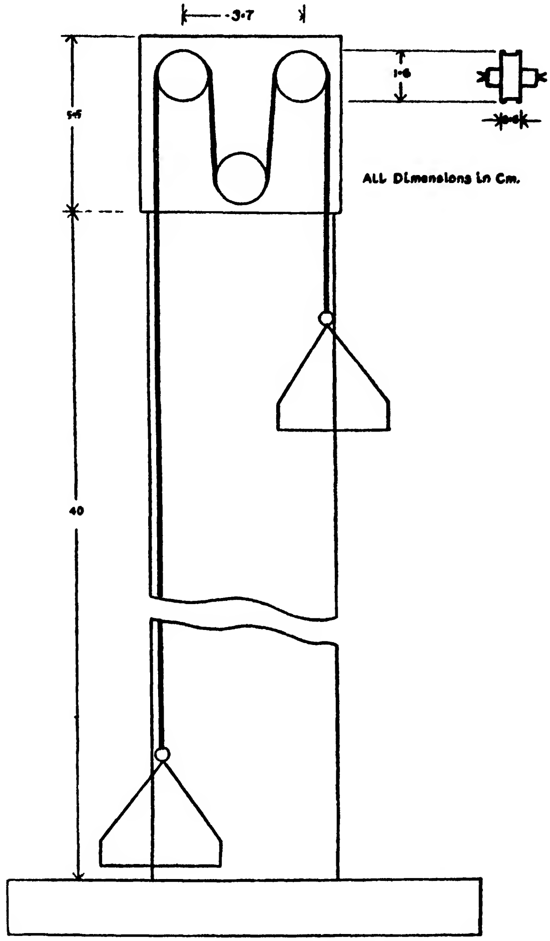

FIG. 2. *Flexibility instrument.*

instrument. The pans were kept from moving by a slight pressure of the finger on one pulley. The finger was now released, allowing the pans to accelerate, and the stopwatch was started. The pan was allowed to fall exactly 3 cm., the watch was stopped, and coincidently the pan stopped by pressing against the pulley. The time for a 3 cm. fall was recorded (T_1 sec.). The above procedure was repeated exactly, using W_2 gm. instead of W_1, and the time for a 3 cm. fall was recorded (T_2). The above procedure was repeated exactly, using W_3 gm. instead of W_2, and again the time for a 3 cm. fall was recorded (T_3). By this time, 9 cm. of strand had been used. Thus, there were three sets of values, namely, (W_1, T_1), (W_2, T_2), and (W_3, T_3). Weight W_3 now rested on the scale pan; it was replaced by W_1 and the entire procedure given above was duplicated. This gave three more sets of values (W_1, T_1), (W_2, T_2), and (W_3, T_3). The above procedure was used over and over again using new samples of strand when necessary, until 10 sets of values of (W_1, T_1), 10 of (W_2, T_2), and 10 of (W_3, T_3) were obtained. W was

then plotted against T. From this graph there was read off the value of W corresponding to $T=25$ sec. This interpolated value of W was arbitrarily defined to be the average flexibility of the strand.

The merits of the above described apparatus are obvious. A fairly large sample can be used for measurement. Moreover, a given length of strand is bent only six times. This virtually eliminates the error likely to be caused by a variation of flexibility with the number of times the strand is bent.

Preparation of Chlorinated Rubbers

The gum chicle, gutta percha, or pale crepe was dissolved in carbon tetrachloride. The pale crepe was first depolymerized by heating in air at 90° C. for four hours, and disaggregated with a high-speed stirrer during solution. Chlorine gas was passed through the continuously stirred solution for a definite length of time and at a definite temperature. The chlorinated rubber was then separated from the carbon tetrachloride by steam distillation. Steam was passed into the flask containing the product until, after frequently changing the condensed water in the flask, this water gave a pH reading of 5.5 or higher. The product was then crushed and dried. Some products containing a small amount of chlorine were somewhat elastic; those containing a large amount were fibrous.

Results

Effect of Solvent on Tensile Strength of Twine

Preliminary experiments showed that benzene, toluene, and xylene had no effect on the tensile strengths of strands immersed for six hours in each of these solvents.

Relative Preservation Qualities of Various Chlorinated Rubbers

Fifteen different chlorinated rubbers were prepared from gum chicle, gutta percha, and pale crepe, by chlorinating solutions of these for various lengths of time and at various temperatures. In addition to these products, three samples of a commercially available chlorinated rubber, "Parlon", were secured from the manufacturers, the Hercules Powder Company, Incorporated, Wilmington, Delaware, U.S.A. These samples were of viscosity types 6, 8, and 20 centipoises. Benzene solutions (20%) of each of these 18 products were prepared, dibutyl phthalate being added as a plasticizer in such concentrations as to produce treated strands of the same degree of flexibility. Sea immersion tests over a period of four weeks showed that whereas all strands treated with chlorinated gum chicle and chlorinated gutta percha were almost completely rotted after four weeks' immersion, the strands treated with chlorinated pale crepe and those treated with Parlon still had average tensile strengths of about 20 lb. Further, Parlon was as effective a preservative as the best of the chlorinated pale crepe products, but not more so. Therefore, it was concluded that Parlon was the most suitable product for commercial use, and it was used exclusively in all later measurements.

Extent of Knot Slippage

It was important to be sure that the treatment of a net with a solution containing Parlon produced no tendency for the knots to slip. A number of benzene solutions of Parlon plus dibutyl phthalate were prepared in which the concentrations of both Parlon and dibutyl phthalate were varied. Tests were made on the water-soaked treated sections of net. It was found that there is no knot slippage in nets treated with those preservative solutions that would be of practical use. Slippage occurred only when the concentration of plasticizer became so great that the nets would be useless owing to stickiness.

TABLE I

EFFECT OF VARIOUS PLASTICIZERS

In each experiment a solution of 20 gm. of Parlon (15 centipoises) was dissolved in 100 gm. of benzene, and the amount of plasticizer noted in Column 2 was added

Plasticizer	Ml. of plasticizer	Tensile strength, lb. (broken wet)		
		Before immersion in sea	Immersed in sea 4 weeks (March)	Immersed in sea 7 weeks (March–April)
Santiciser *M* 17	11.4		24.9	0.0
	14.0		40.8	15.0
	16.5		28.4	5.0
Dow No. 5	11.4		19.3	0.0
	14.0		31.5	5.0
	16.5		30.1	5.0
	19.0		37.1	17.3
	21.5		39.7	17.2
	24.1		27.7	5.0
Aroclor No. 1242	7.6	59.1	28.9	25.7
	10.1	58.6	Lost	30.6
	14.0	57.7	39.7	32.3
	19.0	58.1	46.0	28.1
	21.5	55.6	36.1	23.3
	24.1	52.6	35.0	20.0
Tricresyl phosphate	5.1	8.0	8.0	0.0
	10.1	17.0	17.0	5.0
	12.7	24.1	17.0	5.0
	15.2	37.6	37.6	5.0
	17.7	19.8	19.8	4.0
	20.3	10.7	10.7	0.0
n-butyl stearate	5.1		8.7	0.0
	7.6		16.3	0.0
	10.1		16.6	0.0
	11.4		19.0	0.0
	12.7		14.0	0.0
Dibutyl phthalate	8.9	59.1	41.0	27.6
	10.1	57.2	45.0	36.0
	11.4	58.3	50.6	45.1
	12.7	55.9	39.1	33.7
	13.9	52.7	32.1	30.2
	15.2	49.3	30.8	11.5
Untreated strand		52.0	0.0	

Dibutyl phthalate was found to be the best plasticizer for this particular purpose.

Effect of the Plasticizer on the Preservative Properties of the Parlon Film

In order to treat a net so that it has, after treatment, the requisite degree of flexibility, it is necessary to incorporate a plasticizer with the Parlon. Preliminary work showed that not only does the flexibility of a treated net vary with the ratio of plasticizer to Parlon, but that the life of the treated net in the sea is also a function of this ratio. An investigation was therefore undertaken to determine both the best plasticizer to use and the best ratio of plasticizer to Parlon.

Many plasticizers were investigated, including several commercial products sold under trade names. In Table I are given the results obtained with a few of the plasticizers tried in this work.

In Fig. 3 the concentration of dibutyl phthalate is plotted against the average tensile strengths of treated strands after four and after seven weeks' immersion in the sea. The data are taken from Table I. It is clear from this graph that there is an optimum concentration of dibutyl phthalate, namely about 11.5 ml. per 100 gm. of benzene in which 20 gm. of Parlon are dissolved. By optimum concentration is meant that concentration producing greatest longevity of strands in the sea. Further, all plasticizers investigated exhibited optimum concentrations. The reason for this optimum concentration was not investigated, but a possible explanation is that if the concentration of plasticizer falls below the optimum, the Parlon film shrinks and cracks, owing to its inelasticity, while, if the concentration of plasticizer is greater than the optimum, the porosity of the film may increase.

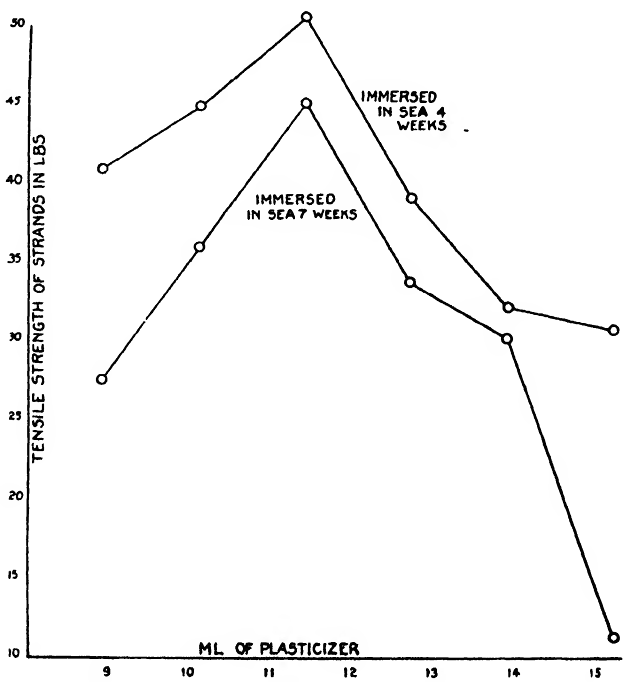

FIG. 3

Further Investigation of Dibutyl Phthalate as Plasticizer

Parlon is manufactured in several viscosity types. For example, viscosity type 10 centipoises means that a 20% solution in toluol at 25° C. has a viscosity of 10 centipoises. Viscosity types up to 20 centipoises were found to give solutions of viscosities low enough to be of use as gill net preservatives. Tests were therefore made to find if one viscosity type was superior to another. Since the linear density of a treated strand, and hence the film thickness, increases as the viscosity of the Parlon solution increases, the concentrations in benzene of the two types of Parlon used were not made the same, but were so chosen that the linear densities of the strands treated with the two types of Parlon were as nearly the same as possible. The results are given in Table II.

TABLE II

EFFECT OF VISCOSITY TYPE OF PARLON

Viscosity type Parlon, centipoises	Grams of Parlon per 100 gm. of benzene	Ml. of dibutyl phthalate per 100 gm. of benzene	Linear density of treated strand, gm. per metre	Tensile strength, lb. (broken wet)	
				Immersed in sea 3 weeks (April)	Immersed in sea 7 weeks (April–May)
7	20.0	8.0	0.66	30.8	5.0
7	20.0	11.0	0.66	39.3	18.4
7	20.0	13.0	0.66	38.8	18.0
7	20.0	14.0	0.66	37.2	18.1
7	20.0	16.0	0.66	28.0	15.7
13	19.8	8.0	0.65	35.5	5.0
13	19.8	11.0	0.65	46.3	28.4
13	19.8	12.9	0.65	44.2	26.2
13	19.8	14.0	0.65	35.5	23.1
13	19.8	16.0	0.65	33.1	20.6
Untreated strand			0.44	0.0	

In Fig. 4, concentration of plasticizer is plotted against average tensile strength of treated strands after seven weeks' immersion. The data are taken from Table II.

From the figure it is clear that 13 centipoises type Parlon is superior to 7 centipoises type. Further, from this, and additional data not given, for 7 centipoises type Parlon the optimum concentration of dibutyl phthalate is 11.5 ml. per 100 gm. of benzene containing 20 gm. of Parlon, while for 13 centipoises type Parlon the optimum concentration of dibutyl phthalate is 11.1 ml. per 100 gm. of benzene containing 19.8 gm. of Parlon. It is interesting to note that the optimum concentration of dibutyl phthalate is in agreement with that recorded in Table I.

Effect of the Length of Time of Immersion in Parlon Solution on the Life of the Treated Strand in the Sea

Strands were soaked in Parlon solutions (20 gm. of Parlon, 11.5 ml. dibutyl phthalate, 100 gm. of benzene) for periods of time ranging from two minutes to six hours. Both 7 and 13 centipoises types Parlon were used. Sea immersion

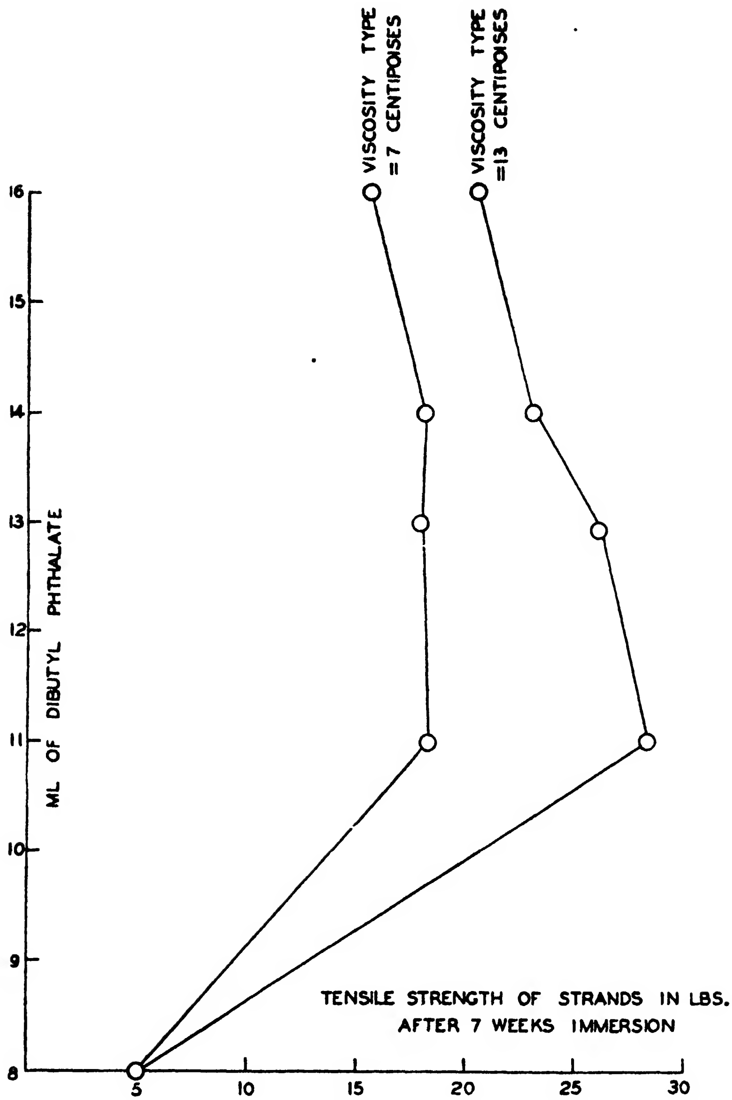

FIG. 4

tests showed that time of immersion of strand in impregnating solution has no perceptible effect on the life of the treated strand in the sea, strands soaked for two minutes in Parlon solution being as strong after seven weeks' sea immersion as those soaked for six hours. Further, this conclusion is valid for both 7 and 13 centipoises types Parlon. These data are given in Table III.

It should be noted that the above conclusion holds for twine, and not necessarily for nets. It is probable that the life of the net in the sea is a function of length of time of immersion in impregnating solution, since in a net there are knots to be impregnated.

TABLE III

EFFECT OF TIME OF IMMERSION IN PARLON SOLUTIONS

Viscosity type Parlon, centipoises	Grams of Parlon per 100 gm. of benzene	Ml. of dibutyl phthalate per 100 gm. of benzene	Time of immersion of strand in Parlon solution	Tensile strength, lb. (broken wet)	
				Immersed in sea 3 weeks (April)	Immersed in sea 7 weeks (April–May)
7	20.0	13.0	2 min.	40.6	21.4
7	20.0	13.0	10 min.	40.0	Lost
7	20.0	13.0	30 min.	38.3	17.7
7	20.0	13.0	2 hr.	38.1	16.7
7	20.0	13.0	6 hr.	37.6	18.7
13	19.8	12.9	2 min.	45.8	31.3
13	19.8	12.9	10 min.	44.0	26.2
13	19.8	12.9	30 min.	43.4	26.5
13	19.8	12.9	2 hr.	41.6	18.8
13	19.8	12.9	6 hr.	45.4	29.2

Effect of Concentration of Parlon Solutions on the Life of the Strand in the Sea

Impregnating solutions consisted of mixtures of Parlon, dibutyl phthalate, and benzene. Two viscosity types, 7 and 13 centipoises, of Parlon were used. In all impregnating solutions listed in Table IV, the ratio of Parlon to dibutyl phthalate was constant.

TABLE IV

EFFECT OF CONCENTRATION OF PARLON SOLUTIONS

Viscosity type Parlon, centipoises	Grams of Parlon per 100 gm. of benzene	Ml. of dibutyl phthalate per 100 gm. of benzene	Linear density of treated strands, gm. per metre	Tensile strength, lb. (broken wet)	
				Immersed in sea 3 weeks (April)	Immersed in sea 7 weeks (April–May)
7	10	6.5	0.55	29.1	0.0
7	15	9.8	0.59	32.1	18.1
7	20	13.0	0.66	37.9	24.0
7	25	16.3	0.74	39.9	31.0
7	30	19.5	0.84	46.5	32.0
13	8	5.2	0.46	27.4	0.0
13	14	9.2	0.59	35.1	25.5
13	19	12.4	0.62	44.1	32.5
13	24	15.7	0.67	46.1	40.2
13	28	18.3	0.80	45.4	39.2
Untreated strand			0.44	0.0	

In order to evaluate the results of Table IV, linear density was plotted against tensile strength of strand after sea immersion (Fig. 5).

Fig. 5 shows that over the entire range of linear densities used, 13 centipoises type Parlon is superior to the 7 centipoises type. The two types must of course be compared at the same linear density.

Fig. 5 is of considerable value when it is wished to decide what concentration of Parlon to use. This choice of concentration of Parlon solution cannot, however, be decided solely from Fig. 5. Factors such as cost and ease of penetration of the Parlon solution into the knots of a net must also be considered.

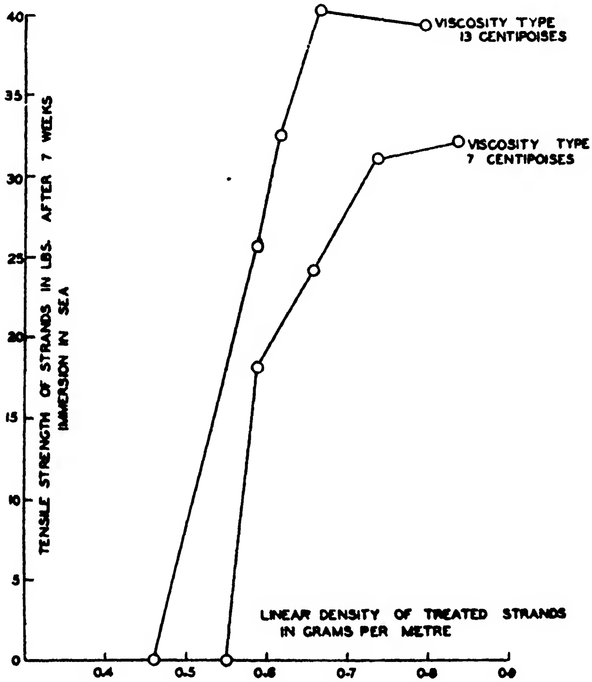

FIG. 5

Effect of Impregnating Strands with Bactericides

Since bacterial action is usually the most destructive force acting on gill nets immersed in the sea, it seemed natural that impregnation of the strands with a bactericide, followed by a coating of Parlon, should prove more effective in preventing rotting in the sea than a coating of Parlon alone. Further, the Parlon coating should retard the rate of washing away of the bactericide.

In most cases the strands were soaked for 30 min. in an aqueous solution of a toxic salt, dried, then soaked in a Parlon solution having the following composition: 20 gm. of 16 centipoises Parlon, 11.4 ml. of dibutyl phthalate, 100 gm. of benzene. In a few cases the toxic salt was dissolved in the Parlon solution.

The following bactericides were tried in various concentrations; silver nitrate, silver chloride, silver ammonium chloride, copper sulphate, mercuric chloride, mercurous chloride, silver sulphide, colloidal silver, mercurous sulphide, copper naphthenate, and silver naphthenate. Results of sea immersion tests on strands treated with some of the above-named salts are recorded in Table V.

TABLE V

EFFECT OF BACTERICIDES

All strands coated with Parlon except where noted

Description of toxic salt treatment (N = normality of solution)	Tensile strength, lb. (broken wet)		
	Before immersion in sea	Immersed in sea 5 weeks (Jan.–Feb.)	Immersed in sea 10 weeks (Jan.–Feb.–Mar.)
0.01 N silver nitrate	55.8	42.7	35.3
0.1 N copper sulphate	56.3	40.8	21.9
1.0 N copper sulphate	54 1	51.5	21.6
0.01 N mercuric chloride	54.6	47.7	37.2
0.01 N silver nitrate, silver precipitated by tannin solution	51 4	56.7	49 2
10% copper naphthenate in benzene No Parlon coating	51 7	5.0	0.0
30% copper napthenate in benzene No Parlon coating	55 0	24.0	0.0
10% copper naphthenate	54 8	57 6	45 5
1% copper naphthenate in Parlon solution	56 3	56.1	54 8
10% copper naphthenate in Parlon solution	57.0	53.4	38.4
1% silver naphthenate in Parlon solution	55.2	57.0	50.1
Parlon coating only. No toxic salt	58.8	48.4	29.2
Untreated strand	51.9	0.0	

Several important conclusions can be drawn from Table V. First, treatment of strands with copper sulphate solution followed by a Parlon coating gives less effective preservation than a Parlon coating alone. The reason is probably that hydrolysis of copper sulphate occurs, and the acid formed attacks the cellulose. Second, all preservative treatments given in the table are more effective than a 30 or a 10% benzene solution of copper naphthenate with no Parlon coating. This result indicates that copper naphthenate is not as effective a preservative as its wide use indicates. It should be noted, however, that these results were obtained with twine and not with nets. Third, the most effective preservative found was a solution of 1 gm. of copper naphthenate, 20 gm. of 13 centipoises Parlon, 11.4 ml. of dibutyl phthalate in 100 gm. of benzene. Strands treated with this preservative underwent virtually no change in tensile strength after 10 weeks' sea immersion. Further, no fading of the green colour of the film could be observed. The fact that 1% of copper naphthenate in Parlon solution proved a better preservative than 10% copper naphthenate in Parlon, is interesting. The reason may be that with the higher copper naphthenate concentration some of the salt washed out of the Parlon film, leaving pores.

Some of the results given in Table V are plotted in Fig. 6. This graph illustrates in a striking way the effectiveness of the preservative consisting of 1 gm. of copper naphthenate, 20 gm. of 13 centipoises Parlon, 11.4 ml. of dibutyl phthalate, in 100 gm. of benzene.

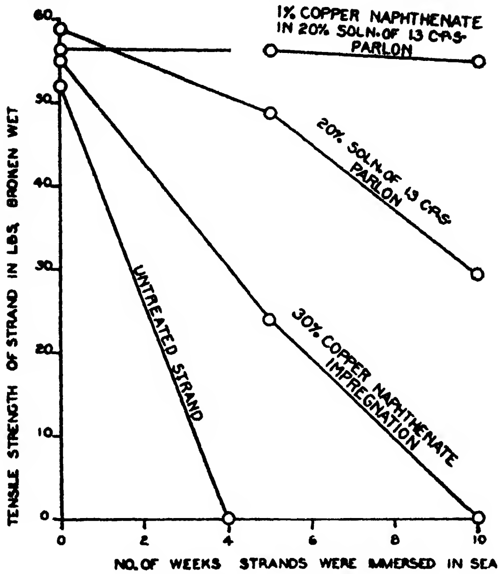

FIG. 6

Wearing Quality of Treated Strands

Though the thickness of the Parlon film on the strand will be a factor determining the wearing quality of the strand, it was thought unnecessary to determine the relation between these two variables. The concentration of plasticizer in the Parlon film should also affect the wearing quality of the treated strand. The relation between these two variables is not easy to predict and therefore quantitative measurements on them were made.

Table VI shows the compositions of the Parlon solutions used to treat the strands. All treated strands were dried one week and the wearing quality

TABLE VI

WEARING QUALITY OF STRANDS

Grams of 12 centipoises Parlon	Grams of benzene	Ml. of Aroclor No. 1242*	Wearing quality (No. of revolutions)	Increase in wearing quality due to Parlon film, %
Untreated strand			21.3	
20	100	6	30.0	40.8
20	100	9	48.2	126.3
20	100	12	58.6	175.1
20	100	15	52.5	146.5
20	100	18	51 2	140.3

*"*Aroclor No. 1242" is a trade name of a product manufactured by the Monsanto Chemical Company, St. Louis, U.S.A.*

determinations made on the dried strands. Strands were not immersed in the sea. The measurements were made with the instrument illustrated in Fig. 1.

While Aroclor No. 1242 was used as a plasticizer here, it is doubtless true that very similar results would be found using dibutyl phthalate. It has been shown elsewhere in this paper that a proportion of 11.4 ml. of dibutyl phthalate to 20 gm. of 13 centipoises Parlon gave a film on the strand possessing maximum preservative quality. From the results of Table VI it is safe to conclude that such a concentration of dibutyl phthalate would produce a film having nearly optimum wearing quality.

Flexibility of Treated Strands

The apparatus and procedure used are described elsewhere in this paper.

Table VII records not only the compositions of the impregnating solutions, but also the experimental results necessary for the calculation of flexibilities of treated strands. Treated strands were dried one week and the flexibilities determined on dry strands not immersed in the sea.

TABLE VII

FLEXIBILITY OF STRANDS

Cc. of dibutyl phthalate per 100 cc. of Parlon solution	Weights (W_1, W_2, W_3), gm.	Time for pan to fall 3 cm. (T_1, T_2, T_3), sec.
7	W_1 = 75	T_1 = 17.0
7	W_2 = 70	T_2 = 25.5
7	W_3 = 65	T_3 = 32.2
8	W_1 = 70	T_1 = 12.0
8	W_2 = 65	T_2 = 27.0
8	W_3 = 60	T_3 = 40.5
9	W_1 = 57	T_1 = 8.5
9	W_2 = 50	T_2 = 15.8
9	W_3 = 42	T_3 = 43.0
10	W_1 = 42	T_1 = 10.7
10	W_2 = 37	T_2 = 20.1
10	W_3 = 42	T_3 = 47.5
11	W_1 = 33.0	T_1 = 9.0
11	W_2 = 30.0	T_2 = 22.2
11	W_3 = 27.0	T_3 = 50.0

Taking weight as ordinate and time as abscissa, the points (W_1, T_1), (W_2, T_2), (W_3, T_3) were plotted for each of the five solutions of Column 1, Table VII. Five curves were obtained (see Fig. 7). On each of these five curves the weight W_{25}, corresponding to $T = 25$ sec., was read. This interpolated weight, W_{25}, has been arbitrarily defined to be the average flexibility of the treated strand. In Table VIII, Column 2, are given these average flexibilities for the five strands treated.

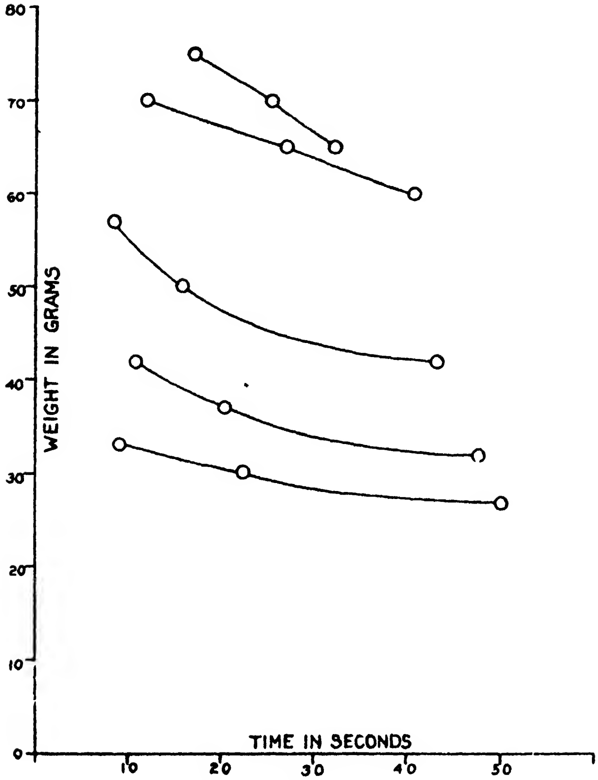

FIG. 7

TABLE VIII

AVERAGE FLEXIBILITY OF STRANDS

Cc. of dibutyl phthalate per 100 cc. of Parlon solution	Average flexibility (W_{25}) at T = 25 sec., gm.	Cc. of dibutyl phthalate per 100 cc. of Parlon solution	Average flexibility (W_{25}) at T = 25 sec., gm.
7	70.1	10	35.4
8	65.8	11	29.5
9	45.2		

The concentration of plasticizer (dibutyl phthalate) was plotted against average flexibility (see Fig. 8). The value of this graph lies in our ability to determine from it the concentration of plasticizer required to produce any desired degree of flexibility.

Sea immersion tests showed that 9 cc. of dibutyl phthalate per 100 cc. of Parlon solution produces a preservative giving the treated strand a maximum life in the sea. Commercial fishermen have examined strands treated with the solution of 9 cc. of dibutyl phthalate per 100 cc. of Parlon solution, and

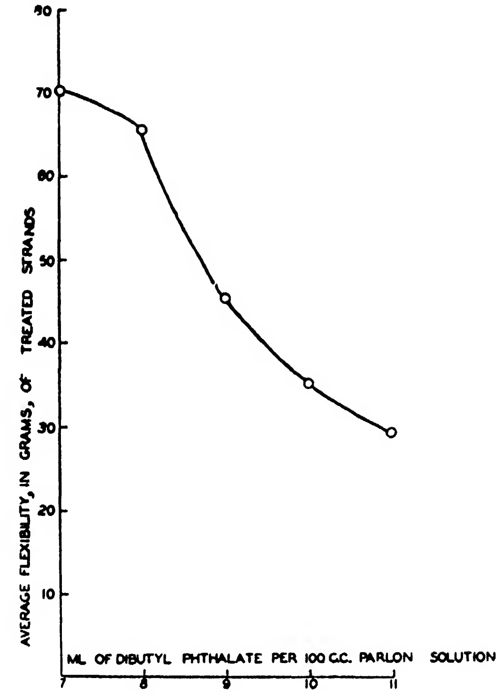

FIG. 8

are of the opinion that it is flexible enough for gill nets. From the graph it is seen that this concentration of plasticizer produces an average flexibility of $W_{25}=45.3$. Until the preservative has been tested under actual fishing conditions, it seems advisable to work with a preservative producing a flexibility of about 45. It is quite likely that tests to be made in the future under fishing conditions will show that somewhat greater flexibility will be necessary. Such increase of flexibility must, unfortunately, be made at the expense of the length of life of the treated net in the sea.

Treated Nets in Commercial Use

While sea immersion tests of twine treated with preservatives are convenient, simple, and economical, they are at best useful for weeding out relatively poor preservatives from those showing promise. Such tests do not give any indication of important requisites such as fishability of treated nets. Hence it was decided to impregnate sections of gill net and have them sewed on to gill nets to be fished with for a season by commercial fishermen. Only in this way could the real value of the various treatments be estimated, and unforeseen flaws be noticed.

Several commercial fishermen volunteered to sew into their nets sections of treated gill net. The sections of gill net were identical in nature with the main net to which they were sewn. The sections varied in size but an average one was 13 fathoms stretched and 50 meshes deep. The type of gill net varied from 4/40 to 5/50.

The section was soaked for 30 min. in a solution of 15 gm. of 20 centipoises Parlon, 8.5 ml. of dibutyl phthalate (technical grade), 0.75 gm. of copper naphthenate per 100 gm. of benzene. Excess solution was then drained off and the section was spread out to dry, by suspending it from short wooden stakes for 24 hr. It was found important to spread out the treated section immediately after taking it from the Parlon solution, since the Parlon film soon becomes temporarily sticky and separation of the strands becomes difficult. Rubber gloves should be worn to prevent the hands from being coated with the sticky, but harmless, solution. The treated sections of net were then sewn on to the regular nets by the fishermen, who fished with them in the Pacific Coast waters during the summer of 1940. The fishermen treated the main body of their nets with various preservatives, chief of which was copper naphthenate.

The fishermen filled in questionnaires at the end of the 1940 season. For brevity, their reports are summarized. By "treated section" shall be meant the section of gill net treated with Parlon; by "regular net" shall be meant the main body of the gill net to which the treated section was sewn.

All found the treated section easier to handle than the regular net; the treated section was generally considered to remain quite clean and easy to wash; all reported an equal catch of fish per unit area for treated section and regular net; only one fisherman desired greater flexibility of treated section. In no particular respect was the treated section considered inferior to nets impregnated with other commonly used preservatives, but rather the fishermen were definitely pleased with the treatment. The strength of the treated section was judged to be only slightly greater than that of the regular net after a summer's fishing. Measurements made by the authors confirmed this conclusion of the fishermen.

The above summary enables two very important conclusions to be drawn. First, a net treated with Parlon solution has several attractive properties possessed in a much lesser degree by a net treated with the commonly used preservatives, cutch, linseed oil, and copper naphthenate. Second, the Parlon treatment as it now stands does not retard rotting of a net to a much greater degree than copper naphthenate, a result not at all in agreement with the laboratory tensile strength measurements on treated twine. This was undoubtedly due to the fact that the Parlon solution did not penetrate into the knots sufficiently. This drawback probably can be overcome by treating the twine prior to weaving the net, and this method of treatment is now under study. Together with this investigation, there is being studied a promising method of actually increasing penetration of the Parlon solution into the knots of the net. In this latter investigation sea immersion tests are being conducted on sections of treated gill net, instead of twine. A solvent very much cheaper than benzene is also being investigated. Large-scale tests by fishermen will then be made.

Cost of Treating a Net with Parlon Solution

With benzene as a solvent, it costs between $12 and $14 to treat a complete net, using a solution of 15 gm. of 20 centipoises Parlon and 8.5 ml. of dibutyl phthalate per 100 gm. of benzene—approximately 10% of the prewar price of the net.

Summary

(1) A new instrument for measuring flexibility of strands has been devised.

(2) Several organic solvents have been shown to be without effect on the tensile strength of strands of 5/40 linen.

(3) Gum chicle, gutta percha, and pale crepe were chlorinated. Products containing various amounts of chlorine were obtained, by chlorinating for different periods of time, and at different temperatures. These products were used as preservatives of 5/40 linen twine. Parlon, the commercially produced chlorinated rubber, was also tested, simultaneously. The tensile strengths of the treated strands, after several weeks' immersion in the sea, showed all products from chlorination of gum chicle and gutta percha to be useless as preservatives, and the product of the chlorination of pale crepe to be as effective, but not more so, than Parlon.

(4) The addition of a plasticizer to the chlorinated rubber was found to be essential, in order that the treated strand would have the necessary degree of flexibility. After a strand of 5/40 linen, impregnated with Parlon plasticizer (dibutyl phthalate), had been immersed in the sea for several weeks its tensile strength was found to be a function of the concentration of plasticizer. An optimum concentration of plasticizer exists, at which concentration the life of a strand in the sea is greatest.

(5) For all concentrations of Parlon in benzene, and for all concentrations of plasticizer (dibutyl phthalate) of any practical value, no knot slippage occurs.

(6) The most effective preservative found consists of an impregnating solution with the composition:—

Parlon (13 centipoises)	20 gm.
Dibutyl phthalate	11 to 11.5 cc.
Benzene	100 gm.
Copper naphthenate	1 gm.

Stated more generally, the ratio of number of cubic centimetres of dibutyl phthalate to grams of Parlon is 0.56 for 13 centipoises Parlon. This ratio most probably applies to Parlon of viscosity 10 to 20 centipoises.

(7) Tests were conducted under actual fishing conditions. Sections of treated net were sewn with regular nets and fished with for a season. Results show that the Parlon preservative has many attractive features, but that further work is required in order to ensure greater penetration of the Parlon solution into the knots of the net.

Acknowledgments

It is a pleasure to acknowledge the assistance given by the following: The Canadian Fishing Company, Vancouver, for the use of their tensile strength machine; the Physics Department of this University for constructing the flexibility apparatus; the Hercules Powder Company, Inc., Wilmington, Delaware, U.S.A., for furnishing samples of Parlon. To many fishermen especial thanks are due for their suggestions and co-operation in large-scale tests on treated sections of net.

References

1. CARTER, N. M. and CHARNLEY, F. Biol. Board Can. Progress Rept. Pacific Biol. Sta. and Pacific Fisheries Exptl. Sta. No. 25 : 3-8. 1935.
2. DORÉE, C. Biochem. J. 14 (6) : 709-714. 1920.
3. FLEMING, N. and THAYSEN, A. C. Biochem. J. 14 (1) : 25-28. 1920.
4. ROBERTSON, A. C. Ind. Eng. Chem. 23 (10) : 1093-1098. 1931.
5. TAYLOR, H. F. and WELLS, A. W. U.S. Bur. Fisheries, Fisheries Document 947. 1923.
6. TYNER, R. V. and FISHER, J. H. Thesis, Univ. British Columbia. 1938.

Canadian Journal of Research

Issued by THE NATIONAL RESEARCH COUNCIL OF CANADA

VOL. 19, SEC. B. NOVEMBER, 1941 NUMBER 11

REACTION RATES OF THE OXIDATION OF LIQUID ACETALDEHYDE[1]

BY A. H. HEATLEY[2]

Abstract

In the commercial process for producing acetic anhydride and acid by the oxidation of acetaldehyde the observed concentrations of anhydride could not be accounted for till allowance was made for an important side reaction. The paper gives the differential equations based on the suggested mechanism; their solution is shown for certain limiting values of the reaction velocity coefficients, but in the general case numerical methods are required. Calculated and observed values are compared. Continuous operation of the process is also studied briefly.

Symbols Used

(Some symbols used only for a few times are not included)

a—$\frac{1}{2}(k_3K_4)^{\frac{1}{2}}$,

$(\quad)_a$—An equation that is approximate, rather than exact,

k_1, k_2, k_4, k_6, k_7—Coefficients of reaction velocity,

k_3—Fraction of Reaction B that yields anhydride,

k_5—Coefficient of variation of k_4,

t—Time,

p, w, x, y, z—Concentrations of acetaldehyde, peracetic acid, acetic anhydride, water, and acetyl peroxide, respectively, as mole fractions,

A, B, C—Integration constants,

$D(x)$—$I_{1/3}(x)/I_{-1/3}(x)$,

$E(x)$—$I_{-2/3}(x)/I_{2/3}(x)$,

$I_n(x)$—Modified Bessel function of the first kind and the n^{th} order,

$K_n(x)$—Modified Bessel function of the second kind and the n^{th} order,

K_2, K_4, K_6, K_7—k_2/k_1, k_4/k_1, etc.,

K_{62}—$K_6/2K_2$,

$Q(x)$—$I_{2/3}(x)/I_{-1/3}(x)$,

R—Ratio of t to the total time required for the reaction,

S—Moles of acetaldehyde per mole of oxygen (input in continuous operation).

χ—$1/x$

θ—$1 + k_5R$

κ—$(k_3K_4)^{\frac{1}{2}}/3k_5$

μ—$K_2/8$

ρ—$1 - R$

ω—$w + \rho/2$

[1] *Manuscript received in original form March 13, 1941 and as revised, July 10, 1941. Contribution from the Research Laboratories, Shawinigan Chemicals, Limited, Shawinigan Falls, Que.*

[2] *Research Chemist.*

Introduction

A commercial process for producing acetic anhydride by the oxidation of acetaldehyde has been described by Benson (1). The concentrations of the anhydride present during the oxidation are of importance commercially, and an explanation of their variation was sought by the consideration of the consecutive and side reactions believed to occur.

Prior to the development of this process the oxidation of acetaldehyde was generally believed to follow the course:—

$$CH_3CHO + O_2 \rightarrow CH_3COOOH$$
$$CH_3COOOH + CH_3CHO \rightarrow 2CH_3COOH,$$

although it was recognized that there were intermediate stages in the reactions, at least under some conditions (2, 3, 4, 8, 10, and others). With the discovery of the formation of acetic anhydride a different set of equations was suggested:

$$CH_3CHO + O_2 \rightarrow CH_3COOOH \qquad ; k_1 \qquad (A)$$
$$CH_3COOOH + CH_3CHO \rightarrow (CH_3CO)_2O + H_2O \quad ; k_3k_2 \qquad (B)$$
$$\searrow 2CH_3COOH \qquad (1 - k_3)k_2$$
$$(CH_3CO)_2O + H_2O \rightarrow 2CH_3COOH \qquad ; k_4(1 + k_5R) \qquad (C)$$

In addition there may be side reactions:

$$(CH_3CO)_2O + CH_3COOOH \rightarrow (CH_3CO)_2O_2 + CH_3COOH \; ; k_6 \qquad (D)$$
$$(CH_3CO)_2O_2 + H_2O \rightarrow CH_3COOOH + CH_3COOH \; ; k_7 \qquad (E)$$

The *problem* was to determine whether experimental data could be explained by the comparatively simple mechanism of Equations A, B, C, and, if not, whether the assumption of the side reactions D and E (for which there was some chemical evidence) could account for the observed trends of the anhydride concentration.

The *method*, briefly stated, was (*a*) to set up the system of differential equations corresponding to Equations A to E, (*b*) to calculate from these the values of anhydride concentration at various times (expressed as time ratio), using various assumed values of the rate constants, and (*c*) to compare these calculated values with those observed in experiments.

The complete solution of the system of differential equations was not achieved, but, for the data under consideration, certain approximations valid over a wide range lead to considerable simplification. The solutions* are given for several limiting cases because they may be of interest to those studying similar reactions, and because they assist in making preliminary estimates of the constants involved in the present work. The expressions for the concentrations of peracetic acid and of acetyl peroxide and a brief discussion of the continuous process are also given for the sake of completeness.

* *It must be emphasized that though these results involve mathematical functions rare in chemical work they should neither be feared nor respected more than the simple exponential function in the results for a reaction of the first order. These functions merely enable us to obtain the logical consequences of the assumptions involved in equations A to E in numerical form, so that they may be compared with experimental data.*

The Differential Equations and Their Solution

The condition considered in these computations is the addition of oxygen to the system at a uniform rate which, owing to its instantaneous reaction with the acetaldehyde, determines the rate of formation of peracetic acid (k_1 mole fraction per hour). Let t be the time at any instant, and R the ratio of t to the total time required (at the constant rate specified) to add the oxygen equivalent to all the aldehyde; since this total time is obviously $1/2k_1$, $R = 2k_1t$. Let p, w, x, y, and z be the concentrations in mole fractions of acetaldehyde, peracetic acid, acetic anhydride, water, and acetyl peroxide, respectively; the concentration of acetic acid is then $1 - (p + w + x + y + z)$. The reaction velocity coefficients are shown to the right of the various reactions to which they apply; the fraction k_3 of Reaction B yields the anhydride, the fraction $1 - k_3$ yields the acid. Experiments undertaken without reference to the oxidation reaction have indicated that the velocity coefficient for reaction C increases* as the aldehyde decreases. It is assumed that the variation is linear with respect to R:—** Velocity coefficient for $C = k_4(1 + k_5R)$.

The concentration of the various substances then follows the equations below, derived from Equations A to E.

$$\frac{dp}{dt} = -k_1 - k_2pw, \tag{1}$$

$$\frac{dw}{dt} = k_1 - k_2pw - k_6wx + k_7yz, \tag{2}$$

$$\frac{dx}{dt} = k_3k_2pw - k_4(1 + k_5R)xy - k_6wx, \tag{3}$$

$$\frac{dy}{dt} = k_3k_2pw - k_4(1 + k_5R)xy - k_7yz, \tag{4}$$

$$\frac{dz}{dt} = k_6wx - k_7yz. \tag{5}$$

It is more convenient to work in terms of R, the time ratio, and for convenience we write K_2 for k_2/k_1, K_4 for k_4/k_1, etc. With these changes we have

$$2\frac{dp}{dR} = -1 - K_2pw, \tag{6}$$

$$2\frac{dw}{dR} = 1 - K_2pw - K_6wx + K_7yz, \tag{7}$$

$$2\frac{dx}{dR} = k_3K_2pw - K_4(1 + k_5R)xy - K_6wx, \tag{8}$$

$$2\frac{dy}{dR} = k_3K_2pw - K_4(1 + k_5R)xy - K_7yz, \tag{9}$$

$$2\frac{dz}{dR} = K_6wx - K_7yz. \tag{10}$$

* *Plyler and Barr have also noted a variation in this reaction coefficient (12).*

***See also Appendix C.*

By inspection we note that

$$dp - dw - dz = -dR; \quad p - w - z = 1 - R, \tag{11}$$

$$dx - dy + dz = 0; \quad y = x + z. \tag{12}$$

Evaluation of w and z

The further solution of these equations obviously is quite impractical until it is noted that certain approximations are available owing to our knowledge of some of the experimental results. The values of w and of z are very low, except perhaps as R approaches unity; therefore K_2 is large. Whence we may say:—

from Equation (11) $p \approx 1 - R$; then $dp/dR = -1$ $\qquad (13)^{*}_{a}$

from Equation (6) $K_2pw = 1; \quad w = 1/K_2(1 - R).$ $\qquad (14)^{**}_{a}$

Since z is small, $dz/dR \approx 0$, whence

from Equation (10) $K_6wx - K_7(x + z)z = 0,$ $\qquad (15)_a$

then $z \approx (K_6/K_7)w = K_6/K_2K_7(1 - R).$ $\qquad (16)_a$

A rough value of the error of these approximations may be obtained as follows. By definition, let

$$w = \frac{1 + \Delta w}{K_2(1 - R)} \text{ and } z = (1 + \Delta z)(K_6w/K_7). \tag{17}$$

From Equation (11)

$$p = 1 - R + (w + z) \approx 1 - R + w(1 + K_6/K_7). \qquad (18)_a$$

From Equation (18)

$$\frac{dp}{dR} \approx -1 + (1 + K_6/K_7) \cdot \frac{1 + \Delta w}{K_2(1 - R)^2}. \qquad (19)_a$$

From Equation (6)

$$\frac{dp}{dR} = -\tfrac{1}{2} - \frac{K_2}{2}wp = -\tfrac{1}{2} - \frac{1 + \Delta w}{2(1 - R)}\{1 - R + w(1 + K_6/K_7)\}. \qquad (20)_a$$

Equating the right sides of Equations (19) and (20) and solving we have

$$\Delta w = \frac{-3(1 + K_6K_7)}{K_2(1 - R)^2 + 4(1 + K_6/K_7)}. \qquad (21)_a$$

From Equation (10)

$$2\frac{dz}{dR} = K_6wx - K_7xz - K_7z^2. \tag{22}$$

From Equation (17)

$$2\frac{dz}{dR} \approx 2(1 + \Delta z)\frac{K_6}{K_7}\frac{(1 + \Delta w)}{K_2(1 - R)^2}. \qquad (23)_a$$

Equating the right sides of these equations we have

$$\Delta z = -\frac{2K_2 + K_6}{2K_2 + 2K_6 + K_2K_7x(1 - R)}. \qquad (24)_a$$

* *Equations involving an approximation will be designated by a subscript "a". The $\approx$ sign will be used only the first time a new approximation is introduced.*

** *When z is zero and $K_2 = 8000$, this approximation is about 0.15%, 0.24%, 0.41%, and 0.94% high at $R = 0.5$, 0.6, 0.7, and 0.8. respectively. When corrected by Equation (21) it is about 1% low at $R = 0.94$ and more accurate at all lower values of R. These data are based on Equation (32). When z is not zero but does not exceed w, a careful estimate indicates that Equation (14) is not more than 1.2% high at $R = 0.8$, so that we are justified in using this approximation up to $R = 0.8$, as we do later in this paper.*

The approximations for w and z given in Equations (14) and (16) even when modified by the corrections in Equations (17), (21), and (24) are obviously inapplicable when R is nearly zero or unity. However, *when K_6 is zero*, i.e., when no acetyl peroxide is formed, the exact value of w can be found. Equation (7) reduces to

$$2\frac{dw}{dR} = 1 - K_2pw. \tag{25}$$

Since z is zero, $p = w + 1 - R$. Now put

$$\rho = 1 - R \qquad \text{and} \qquad \omega = w + \rho/2. \tag{26}$$

Then

$$\frac{d\omega}{d\rho} - \frac{K_2}{2}\omega^2 = -\frac{K_2}{8}\rho^2. \tag{27}$$

The solution of this equation is given in Appendix A.

$$\omega = -f(\mu,\rho)\cdot\rho/2, \tag{28}$$

where

$$f(\mu,\rho) = \frac{I_{-3/4}(\mu\rho^2) - CI_{3/4}(\mu\rho^2)}{I_{1/4}(\mu\rho^2) - CI_{-1/4}(\mu\rho^2)}, \tag{29}$$

and $\mu = K_2/8$. Reverting to the original variable,

$$w = \omega - \rho/2 = \{-f(\mu,\rho) - 1\}\rho/2. \tag{30}$$

When $R = 0$ and $\rho = 1$, $w = 0$ and therefore $f(\mu,\rho) = -1$ whence

$$C = \frac{I_{1/4}(\mu) + I_{-3/4}(\mu)}{I_{3/4}(\mu) + I_{-1/4}(\mu)}. \tag{31}$$

For convenience of form we write

$$w = \{U(\mu,\rho) - 1\}\rho/2, \tag{32}$$

where

$$U = \frac{I_{-3/4}(\mu\rho^2) - CI_{3/4}(\mu\rho^2)}{CI_{-1/4}(\mu\rho^2) - I_{1/4}(\mu\rho^2)}.$$

As $R \to 1$, $\rho \to 0$, the I functions of positive order become zero, and

$$w\,(\text{at } R = 1) = \frac{\rho}{2}\left\{\frac{(-\frac{1}{4})!}{\rho C(-\frac{3}{4})!}\left(\frac{2}{\mu}\right)^{\frac{1}{2}} - 1\right\} = \frac{0.6760}{CK_2^{\frac{1}{2}}}. \tag{33}$$

Evaluation of x

To proceed to the evaluation of x, we insert the approximate values of p, w, and y from Equations (12) to (14) in Equation (8) and obtain

$$2\frac{dx}{dR} = k_3 - K_4(1 + k_5R)x^2 - \frac{K_6}{K_2(1 - R)}x. \tag{34}_a$$

A solution of this equation has not been obtained, except for particular cases.

When k_5 is zero, put $\rho = 1 - R$, then $d\rho = -dR$. Write K_{62} for $K_6/2K_2$.

$$\frac{dx}{d\rho} = -\frac{k_3}{2} + K_{62}\cdot\frac{x}{\rho} + \frac{K_4}{2}x^2. \tag{35}_a$$

Now put

$$x = -\frac{K_{62} + 1}{K_4\rho} - \frac{2}{K_4t}\frac{dt}{d\rho}. \tag{36}_a$$

Then

$$\frac{dx}{d\rho} = \frac{K_{62} + 1}{K_4\rho^2} - \frac{2}{K_4t}\frac{d^2t}{d\rho^2} + \frac{2}{K_4t^2}\left(\frac{dt}{d\rho}\right)^2. \tag{37}_a$$

Equating the right sides of Equations (35) and (37) we have

$$\frac{d^2t}{d\rho^2} + \frac{1}{\rho}\frac{dt}{d\rho} - \left\{\frac{k_3K_4}{4} + \left(\frac{K_{62}+1}{2}\right)^2 \cdot \frac{1}{\rho^2}\right\} t = 0. \qquad (38)_a$$

This is the well known Bessel equation whose solution is

$$t = AI_n(a\rho) + BK_n(a\rho) \quad (n \text{ is an integer}), \qquad (39)_a$$

$$t = AI_n(a\rho) + BI_{-n}(a\rho) \quad (n \text{ is not an integer}), \qquad (40)_a$$

where $n = \frac{1}{2}(K_{62} + 1)$ and $a = \frac{1}{2}(k_3K_4)^{\frac{1}{2}}$. Reverting to the original variable

$$x = \frac{2a}{K_4} \cdot \frac{CK_{n-1}(a\rho) - I_{n-1}(a\rho)}{CK_n(a\rho) + I_n(a\rho)} \quad (n \text{ integral}) \qquad (41)_a$$

Since $y = 0$ when $\rho = 1$, $C = I_{n-1}(a)/K_{n-1}(a)$. Alternatively

$$x = \frac{2a}{K_4} \cdot \frac{-I_{n-1}(a\rho) + C'I_{-n+1}(a\rho)}{I_n(a\rho) - C'I_{-n}(a\rho)} \quad (n \text{ not integral}). \qquad (42)_a$$

Since $y = 0$ when $\rho = 1$, $C' = I_{n-1}(a)/I_{-n+1}(a)$.
When $K_6 = 2K_2$, $K_{62} = 1$, $n = 1$, and

$$x = \frac{2a}{K_4} \cdot \frac{CK_0(a\rho) - I_0(a\rho)}{CK_1(a\rho) + I_1(a\rho)}, \qquad (43)_a$$

where $C = I_0(a)/K_0(a)$. When $K_6 = K_2$, $K_{62} = \frac{1}{2}$, $n = \frac{3}{4}$ and

$$x = \frac{2a}{K_4} \cdot \frac{C'I_{1/4}(a\rho) - I_{-1/4}(a\rho)}{I_{3/4}(a\rho) - C'I_{-3/4}(a\rho)}, \qquad (44)_a$$

where $C' = I_{-1/4}(a)/I_{1/4}(a)$. When $K_6 = \frac{2}{3}K_2$, $n = \frac{2}{3}$ and

$$x = \frac{2a}{K_4} \cdot \frac{I_{1/3}(a\rho) - D(a)I_{-1/3}(a\rho)}{D(a)I_{2/3}(a\rho) - I_{-2/3}(a\rho)}, \qquad (45)_a$$

where $D(a) = I_{1/3}(a)/I_{-1/3}(a)$. When $K_6 = 0$, $n = \frac{1}{2}$ and

$$x = \frac{2a}{K_4} \cdot \frac{C''I_{\frac{1}{2}}(a\rho) - I_{-\frac{1}{2}}(a\rho)}{I_{\frac{1}{2}}(a\rho) - C''I_{-\frac{1}{2}}(a\rho)}, \qquad (46)_a$$

where $C'' = I_{-\frac{1}{2}}(a)/I_{\frac{1}{2}}(a)$. Since $I_{\frac{1}{2}}(a\rho)/I_{-\frac{1}{2}}(a\rho) = \tanh a\rho = \tanh(a - aR)$

$$x = \frac{2a}{K_4} \tanh aR \qquad (47)_a$$

In order to ascertain the effects of various changes in the coefficients upon the results, we now consider the case in which k_2 *is infinite* and k_6 *is zero*. w and z become zero, p becomes exactly $1 - R$ and the differential equation for x collapses to

$$2\frac{dx}{dR} = k_3 - K_4(1 + k_5R)x^2. \qquad (48)$$

To get this equation in workable form we put

$$\theta = 1 + k_5R \quad \text{and} \quad \chi = 1/x. \qquad (49)$$

Then we have the Riccati equation

$$\frac{d\chi}{d\theta} + \frac{k_3}{2k_5}\chi^2 = \frac{K_4}{2k_5}\theta. \qquad (50)$$

This corresponds to Equation (1) in Appendix A and the solution is given there in Equation (11), the corresponding symbols being χ, u; θ, x; $k_3/2k_5$, b; $K_4/2k_5$, c; 1, m. We write at once

$$x = \frac{1}{\chi} = \left(\frac{k_3}{K_4\theta}\right)^{\frac{1}{2}} \cdot \frac{I_{1/3}(\kappa\theta^{3/2}) - D(\kappa)I_{-1/3}(\kappa\theta^{3/2})}{I_{-2/3}(\kappa\theta^{3/2}) - D(\kappa)I_{2/3}(\kappa\theta^{3/2})}, \tag{51}$$

where $D(\kappa) = I_{1/3}(\kappa)/I_{-1/3}(\kappa)$ and $\kappa = (k_3K_4)^{\frac{1}{2}}/3k_5$.

When k_5 is zero, Equation (48) becomes

$$2\frac{dx}{dR} = k_3 - K_4x^2, \tag{52}$$

whence

$$x = (2a/K_4) \tanh aR, \tag{53}$$

If Equation (52) is integrated between the limits x_1 and x_2, R_1 and R_2, instead of between zero and x or R, we have

$$x_2 = \frac{x_1 + (2a/K_4) \tanh a\Delta R}{1 + x_1(K_4/2a) \tanh a\Delta R}. \tag{54)*$$

Note that Equation (53) is the same as the approximate equation (47). For the former, K_2 is large; for the latter, K_2 is infinite. Likewise Equation (51) gives an approximate value of x when K_2 is large but not infinite (and K_6 is zero).

For convenience of reference Table I indicates the various combinations of restrictions on the constants that have been studied and gives the number of the important equations that correspond.

TABLE I

EQUATIONS CORRESPONDING TO VARIOUS RESTRICTIONS ON THE CONSTANTS

K_2	k_5	K_6	Equation numbers
Large	N.r.	N.r.	13, 14, 16, 21, 24, 34
Large	N.r.	0	32, 33
Large	0	$2K_2$	43
Large	0	K_2	44
Large	0	$2K_2/3$	45, 71
Large	0	0	47
∞	N.r.	0	51, 72
∞	0	0	53, 54

NOTE 1. *N.r. means no restrictions.*

NOTE 2. *There are no restrictions on k_3, K_4. K_7 has no meaning when K_6 is zero.*

Continuous Operation

This reaction is carried out as a continuous process by adding acetaldehyde and oxygen at a uniform rate and withdrawing an equivalent amount of the reaction liquid, which is kept homogeneous by mixing. The calculations below refer to the steady state. It is assumed that the input of acetaldehyde

* *Theoretically, the integration of other equations in this paper could also be done between limits neither of which is zero; practically, it is impossible owing to the complicated form of the constants of integration.*

is S moles per mole of oxygen, and, since the fraction $(1 - p)$ of acetaldehyde reacts with the oxygen and the peracetic acid and the balance, p, flows out unchanged with the effluent, its net input is $S(1 - p)$ moles per mole of oxygen. Similarly a correction term is added to the equations for the other constituents. The variation factor for k_5 is also changed to be (approximately) equal to $(1 - p)$ as before. Then

$$\frac{dp}{dt} = -k_1 - k_2pw + Sk_1 - pSk_1 = 0, \tag{55}$$

$$\frac{dw}{dt} = +k_1 - k_2pw - k_6wx + k_7yz - wSk_1 = 0, \tag{56}$$

$$\frac{dx}{dt} = k_3k_2pw - k_4\{1 + 2k_5/S\}xy - k_6wx - xSk_1 = 0, \tag{57}$$

$$\frac{dy}{dt} = k_3k_2pw - k_4\{1 + 2k_5/S\}xy - k_7yz - ySk_1 = 0, \tag{58}$$

$$\frac{dz}{dt} = k_6wx - k_7yz - zSk_1 = 0. \tag{59}$$

From Equations (55), (56), and (59)

$$dp - dw - dz = -2k_1 + Sk_1\{1 - (p - w - z)\} = 0 \tag{60}$$

$$\therefore S = \frac{2}{1 - (p - w - z)}, \tag{61}$$

$$p \approx (S - 2)/S \tag*{(62)$_a$}$$

From Equations (57), (58), and (59)

$$dx - dy + dz = Sk_1(x - y + z) = 0, \tag{63}$$

$$\therefore x - y + z = 0; \qquad y = x + z. \tag{64}$$

From Equations (55) and (62)

$$K_2pw = S - pS - 1 \approx 1, \tag*{(65)$_a$}$$

$$p = \frac{S - 1}{K_2w + S}. \tag{66}$$

Solving Equations (62) and (66)

$$w = \frac{S}{K_2(S - 2)}. \tag*{(67)$_a$}$$

From Equation (59)

$$z = \frac{K_6wx}{K_7y + S} \approx \frac{K_6}{K_7}w. \tag*{(68)$_a$}$$

From Equations (57), (65), and (67)

$$k_3 - K_4\left(1 + \frac{2k_5}{S}\right)x^2 - \frac{K_6Sx}{K_2(S-2)} - Sx = 0. \tag*{(69)$_a$}$$

Then

$$x = \frac{-b + (b^2 + 4rk_3)^{\frac{1}{2}}}{2r}, \tag*{(70)$_a$}$$

where

$$b = \frac{K_6S}{K_2(S - 2)} - S; \; r = \frac{K_4(S + 2K_5)}{S}.$$

A higher yield of anhydride is obtained if an inert diluent is continuously added with the acetaldehyde (1), and calculations like the above have been made for this case. However, since they involve the rather bold assumption that the various reaction coefficients are the same as before, the results are not given.

Computation of Data

Most of the data to be computed require the use of functions not well known. Tables of tanh x (Equations (47), (53), and (54)) are available in many chemical handbooks and in books of mathematical tables. Excellent tables of quarter-integral (Equations (32) and (44)) and third-integral (Equations (45) and (51)) Bessel functions I are now being computed (14). No quarter-integral I tables are now available and the only tables of third-integral I functions (9, p. 285) cannot be used for interpolation, so that modification of the equations is necessary. Equation (45) is rewritten in the form—

$$x = \frac{2a}{K_4} \cdot \frac{\{1 - D(a\rho)\} - \{1 - D(a)\}}{Q(a\rho)[\{E(a\rho) - 1\} + \{1 - D(a)\}]}, \tag{71}_a$$

and Equation (51) is given the form

$$x = \left(\frac{k_8}{K_4\theta}\right)^{\frac{1}{2}} \cdot \frac{\{1 - D(\kappa)\} - \{1 - D(\kappa\theta^{3/2})\}}{Q(\kappa\theta^{3/2})\,[\{1 - D(\kappa)\} + \{E(\kappa\theta^{3/2}) - 1\}]} \tag{72}$$

where

$$D(x) = I_{1/3}(x)/I_{-1/3}(x), \quad Q(x) = I_{2/3}(x)/I_{-1/3}(x)$$

and

$$E(x) = I_{-2/3}(x)/I_{2/3}(x).$$

Tables of the functions $Q(x)$, $1 - D(x)$, and $E(x) - 1$ are given in Table II; the methods of computation are given in Appendix B. Tables of the Bessel functions I and K of the zero and first orders (Equation (43)) are available (13, Table II, pages 698–713) and (5). They are interpolable.

Several methods are available for the numerical evaluation of x from Equation (34), no solution of which could be found. For the data given below, Ford's method was used (6). Since the last term of Equation (34) is an approximation that becomes too inaccurate for reliable results when R exceeds 0.8 (for the value of constants used in these calculations), further values could be obtained only by reverting to the set of Equations (6) to (10), a very laborious task that has not been undertaken.

Owing to the increase of weight, the relation between the mole fraction and the percentage by weight varies during the reaction. The molecular weight at the beginning is 44 (acetaldehyde); the average molecular weight at the end, i.e., when $R = 1$, is 60. Whence we have the relation

$$\text{Percentage by weight} = \frac{\text{mole fraction} \times \text{molecular weight}}{44 + 16R} \times 100\%$$

For continuous operation, the denominator of the above expression becomes $44 + 32/S$.

TABLE II

VALUES OF FUNCTIONS USED IN EQUATIONS (71) AND (72)

x	$Q(x)$	$1 - D(x)$	$\log 1 - D(x)$	$\Delta \log$	$E(x) - 1$	$\log E(x) - 1$	$\Delta \log$
0.0	0.0000	1.000	0.0000	−1703	∞	—	—
.2	.1486	6.756×10^{-1}	$\bar{1}.8297$	1340	6.4367	0.8087	−4751
.4	.2897	4.963	.6957	1368	2.1557	.3336	3188
.6	.4169	3.621	.5589	1428	1.0346	.0148	2586
.8	.5267	2.607	.4161	1488	5.704×10^{-1}	$\bar{1}.7562$	2278
1.0	0.6182	1.850	$\bar{1}.2673$	1542	3.376	$\bar{1}.5284$	2101
.2	.6920	1.297	.1131	1586	2.081	.3183	1989
.4	.7505	9.005×10^{-2}	$\bar{2}.9545$	1621	1.317	.1194	1917
.6	.7961	6.200	.7924	1647	8.47×10^{-2}	$\bar{2}.9277$	1874
.8	.8315	4.243	.6277	1667	5.50	.7403	1834
2.0	0.8587	2.891	$\bar{2}.4610$	1684	3.605	$\bar{2}.5569$	1811
.2	.8799	1.962	.2926	1694	2.376	.3758	1795
.4	.8963	1.328	.1232	1704	1.571	.1963	1783
.6	.9091	8.970×10^{-3}	$\bar{3}.9528$	1710	1.042	.0180	1773
.8	.9192	6.050	.7818	1715	6.929×10^{-3}	$\bar{3}.8407$	1767
3.0	0.9274	4.077	$\bar{3}.6103$	1720	4.613	$\bar{3}.6640$	1762
.2	.9341	2.744	.4383	1721	3.075	.4878	1758
.4	.9395	1.846	.2662	1725	2.051	.3120	1755
.6	.9442	1.241	.0937	1726	1.369	.1365	1752
.8	.9481	8.339×10^{-4}	$\bar{4}.9211$	1727	9.148×10^{-4}	$\bar{4}.9613$	1751
4.0	0.9514	5.603	$\bar{4}.7484$	1729	6.113	$\bar{4}.7862$	1748
.2	.9543	3.763	.5755	1729	4.087	.6114	1748
.4	.9569	2.527	.4026	1731	2.733	.4366	1746
.6	.9591	1.696	.2295	1731	1.828	.2620	1746
.8	.9612	1.139	.0564	1732	1.223	.0874	1745
5.0	0.9629	7.642×10^{-5}	$\bar{5}.8832$	1731	8.183×10^{-5}	$\bar{5}.9129$	1744
.2	.9646	5.130	.7101		5.476	.7385	
.4	.9660						
.6	.9675						
.8	.9686						
6.0	0.9698						
.4	.9718						
.8	.9737						
7.2	.9753						
.6	.9767						
8.0	.9779						

Calculated and Observed Data

In the case of reactions of low order as usually studied one determines the reaction coefficients by relatively simple calculations direct from the experimental data. In the present case this method is limited to the determination of k_1, known from the oxygen input, and k_6, k_7 known roughly from the concentration of the corresponding chemicals, which the analytical methods do not sharply distinguish. For the remaining k's the only available method is to reproduce the experimental graph of x *versus* R by a suitable combination of k's and K's. Some economy of effort is achieved by first using Equation

(53), the simplest of all, to obtain a rough idea of some of the constants, and then proceeding to drop the simplifying assumptions.

Fig. 1 shows the experimental data for the concentration of anhydride, x, *versus* the time ratio, R, for several runs, using various conditions, and those calculated by means of several equations, the values of the constants being selected to give the closest possible approach to the general form of the observed curves, but no attempt being made to duplicate closely any of them. It is obvious that only Curve 4 or minor modifications of it can duplicate the observed data; thus the constants used in making that curve are the required reaction coefficients; a reaction mechanism excluding the side reactions (D) and (E) would be inadequate.

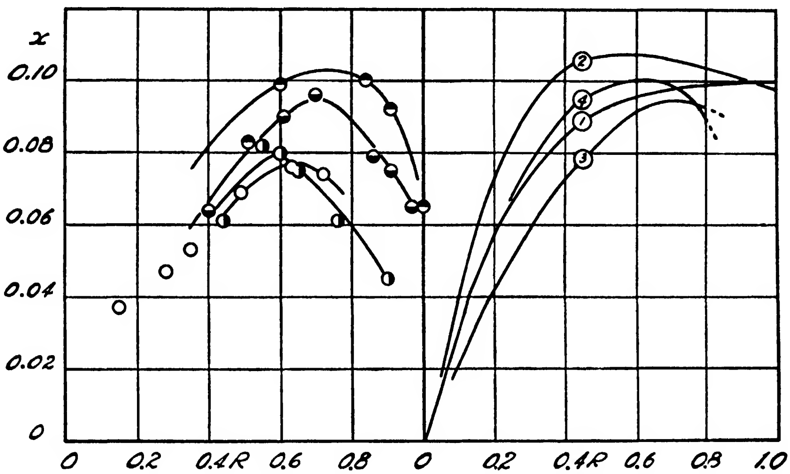

Curve	Equation	K_2	k_3	K_4	k_5	K_6
1	53	∞	0.64	64	0	0
2	51, 72	∞	0.81	44	1	0
3	45, 71	8000	0.44	20	0	5333
4	34	8000	0.64	25	1	8000

FIG. 1. *Acetic anhydride mole fraction, x, vs. time ratio, R. Left observed; right, calculated.*

It should be noted that the reaction proposed by Bowen and Tietz (4) as the source of acetyl peroxide, namely

$$CH_3COOOH + CH_3COOH \rightarrow (CH_3CO)_2O_2 + H_2O \qquad (F)$$

is highly improbable, for if it replaces reaction (D) in the mechanism, there is no K_6 in the differential equation for x; and it has just been seen that the experimental graph for x cannot be duplicated without assigning a substantial value to K_6.

The data for continuous operation using the reaction coefficients of Curve 4 above are given in Table III, as well as the corresponding data for batch operation. These show clearly that the advantages of the continuous process are offset by a greatly decreased yield of x, acetic anhydride, the more valuable

product. In practice this disadvantage is reduced by the use of an inert diluent (1).

TABLE III

VALUES OF x FOR VARIOUS TIME RATIOS (BATCH) AND INPUT RATIOS (CONTINUOUS)

R	x	S	x
0.0	0.000	2.4	0.058
.2	.058	2.8	.069
.4	.091	3.2	.072
.5	.098	3.6	.073
.6	.100	4.0	.073
.7	.099	4.8	.071
.8	.089		

Acknowledgment

This problem was suggested by Mr. G. Benson, Assistant Director of the Plant Research Department, to whom grateful acknowledgment is made for helpful discussion of much of the material presented.

References

1. BENSON, G. Chem. Met. Eng. 47 : 150-151. 1940; U.S. Patent, 2,170,002. Aug. 22, 1939.
2. BODENSTEIN, M. Sitzber. preuss. Akad. Wiss. 3 : 73-88. 1931.
3. BODENSTEIN, M. Z. physik. Chem. B, 12 : 151-164. 1931.
4. BOWEN, E. J. and TIETZ, E. L. J. Chem. Soc. 132 : 234-243. 1930.
5. BRITISH ASSOCIATION FOR THE ADVANCEMENT OF SCIENCE. Mathematical tables, Vol. 6, Part I. Cambridge University Press. 1937.
6. FORD, L. R. Differential equations, Chap. VII. McGraw-Hill Book Company, New York. 1933.
7. FORSYTH, A. R. Treatise on differential equations. 5th ed. The MacMillan Company, New York and London. 1921.
8. HATCHER, W. H., STEACIE, E. W. R., and HOWLAND, F. Can. J. Research, 7 : 149-161, 1932.
9. JANHKE, E. and EMDE, F. Tables of functions with formulae and curves. G. E. Stechert & Company, New York. 1933.
10. KAGAN, M. Y. and LUBARSKII, G. D. J. Phys. Chem. 39 : 837-857. 1935.
11. PEIRCE, B. O. A short table of integrals. 3rd ed. No. 83. Ginn & Company, Boston. 1929.
12. PLYLER, E. K. and BARR, E. S. J. Chem. Phys. 3 : 679-682. 1935.
13. WATSON, G. N. Treatise on the theory of Bessel functions. Cambridge University Press. 1922.
14. WORKS PROJECTS ADMINISTRATION OF NEW YORK CITY. Project for the computation of mathematical tables. Announcement, Dec. 1, 1940, and private communication from the project Supervisor, Dr. A. N. Lowan.

Appendix A

THE SOLUTION OF THE RICCATI EQUATION

Cf. Equations (27) and (50)

In the Riccati Equation

$$\frac{du}{dx} + bu^2 = cx^m, \tag{1}$$

put

$$u = \frac{1}{bv} \cdot \frac{dv}{dx} \, . \tag{2}$$

Then

$$\frac{d^2v}{dx^2} - bcvx^m = 0. \tag{3}$$

Now put

$$w = \frac{2}{m+2} x^{\frac{m+2}{2}}. \tag{4}$$

Then

$$\frac{d^2v}{dw^2} + \frac{m}{m+2} \cdot \frac{dv}{wdw} - bcv = 0. \tag{5}$$

Next put

$$v = rw^{\frac{1}{m+2}}. \tag{6}$$

Then

$$\frac{d^2r}{dw^2} + \frac{1}{w} \cdot \frac{dr}{dw} - \left\{ bc + \left(\frac{1}{m+2}\right)^2 \frac{1}{w^2} \right\} r = 0, \tag{7}$$

which is the well known Bessel Equation. If bc is positive the solution is

$$r = AI_p(w\sqrt{bc}) + BI_{-p}(w\sqrt{bc}) \tag{8a}$$

when $p = 1/(m+2)$ is not an integer or zero; or

$$r = AI_p(w\sqrt{bc}) + BK_p(w\sqrt{bc}) \tag{8b}$$

when p is an integer or zero. I_p and K_p are modified Bessel* functions of the first and second kind respectively. Reverting to the variables v and x, and taking the case when p is not integral or zero,

$$v = x^{\frac{1}{2}}\{AI_p(gx^{\frac{1}{2p}}) + BI_{-p}(gx^{\frac{1}{2p}}) \tag{9}$$

$$\frac{dv}{dx} = (bc)^{\frac{1}{2}}x^{\frac{m+1}{2}}\{AI_{p-1}(gx^{\frac{1}{2p}}) + BI_{-p+1}(gx^{\frac{1}{2p}}), \tag{10}$$

where $g = 2p(bc)^{\frac{1}{2}} = 2(bc)^{\frac{1}{2}}/(m+2)$. Then from Equation (2)

$$u = \frac{(bc)^{\frac{1}{2}}}{b} x^{\frac{m}{2}} \frac{I_{p-1}(gx^{\frac{1}{2p}}) + CI_{-p+1}(gx^{\frac{1}{2p}})}{I_p(gx^{\frac{1}{2p}}) + CI_{-p}(gx^{\frac{1}{2p}})}. \tag{11a}$$

The corresponding equation when p is an integer or zero is

$$u = \frac{(bc)^{\frac{1}{2}}}{b} x^{\frac{m}{2}} \frac{I_{p-1}(gx^{\frac{1}{2p}}) - CK_{p-1}(gx^{\frac{1}{2p}})}{I_p(gx^{\frac{1}{2p}}) + CK_p(gx^{\frac{1}{2p}})}. \tag{11b}$$

The constant C is to be determined from the boundary or initial conditions applying to the differential equation.

The above development follows that given by Forsyth (7, pp. 195, 196) who, however, proceeds only as far as the equivalent of the writer's Equation (8).

Appendix B

Computation of Table II, Page 270.

From $x = 0$ to 8.0, $Q(x)$ was computed from the tabulated values of $I_{2/3}(x)$ and $I_{-1/3}(x)$. For higher values of x the difference between $I_{1/3}(x)$ and $I_{-1/3}(x)$ is negligible and $Q(x)$ may be computed from the approximate formula

$$Q(x) \approx \frac{1 - \frac{7}{72x} - \frac{7}{72x}\cdot\frac{65}{144x} - \frac{7}{72x}\cdot\frac{65}{144x}\cdot\frac{209}{216x} - \cdots}{1 + \frac{5}{72x} + \frac{5}{72x}\cdot\frac{77}{144x} + \frac{5}{72x}\cdot\frac{77}{144x}\cdot\frac{221}{216x} + \cdots},$$

* *Bessel functions of various kinds are much used by physicists and electrical engineers, but as far as the author is aware, they have not hitherto appeared in chemical problems.*

which is derived from the asymptotic formulae for the I functions. For values of $x > 10$ this may be replaced by

$$Q(x) \approx 1 - \frac{1}{6x} - \frac{5}{72x^2},$$

with an error not exceeding 1 in 5000.

Because the functions $1 - D(x)$ and $E(x) - 1$ are not suitable for interpolation, their logarithms and logarithmic differences are tabulated. The computation of the former was based on the right-hand expression in

$$1 - D(x) = \frac{I_{-1/3}(x) - I_{1/3}(x)}{I_{-1/3}(x)} = \frac{(\sqrt{3}/\pi)e^x K_{1/3}(x)}{e^x I_{-1/3}(x)}.$$

The values of $e^x K_{1/3}(x)$ were taken from Watson (13, Table III, pages 714–29). Since there is no published table of $K_{2/3}(x)$, the same method cannot be used for $E(x) - 1$. From $x = 0$ to 1.8, $E(x)$ was computed as indicated by its definition Equation (72) page 269, and then $\log \{E(x) - 1\}$ was taken from tables. From $x = 2.0$ to 5.2, the computation was made in the same way using tables to nine significant figures kindly supplied in advance of publication by Dr. A. N. Lowan (14). Apart from these entries, the table is believed to be reliable to only 1 part in 1000 owing to unreliable final digits in the Jahnke-Emde table (9, p. 285). Several erronous values in their table were recomputed.

Appendix C

The result given below is not used in the present paper but is so closely related that it is desirable to record it here.

If the reaction velocity coefficient of reaction C is a linear function of x instead of R, Equation (48) becomes

$$2\frac{dx}{dR} = k_3 - K_4(1 + k_8 x)x^2 = k_3 - K_4 x^2 - K_4 k_8 x^3. \tag{C1}$$

The maximum value of x is now found by equating the right side of Equation (C1) to zero, using the actual numerical values of the various constants. Let h be this maximum value of x. Then

$$\frac{dx}{dR} = \frac{k_3}{2h}(h - x)\left(1 + \frac{x}{h} + \frac{K_4 k_8 h x^2}{k_3}\right). \tag{C2}$$

Rearranging and integrating, we have

$$R = \frac{2h}{k_3}\int_0^x \frac{dx}{(h - x)f(x)}, \tag{C3}$$

where $f(x) = 1 + x/h + K_4 k_8 h x^2/k_3$. The value of this integral may be taken from Peirce's table (11). Inserting the values at the two limits we have

$$R = \frac{h}{2k_3 + h^3 K_4 k_8}\left\{2.3026 \log \frac{f(x)}{(1 - x/h)^2} + \right.$$

$$\left. \frac{2}{\sqrt{q}}(2K_4 k_8 h^2/k_3 + 1/h)\left(\tan^{-1}\frac{2K_4 k_8 h x/k_3 + 1/h}{\sqrt{q}} - \tan^{-1}\frac{1}{h\sqrt{q}}\right)\right\}, \tag{C4}$$

where $q = 4K_4 k_8 h/k_3 - 1/h^2$.

CONTRIBUTION TO THE STUDY OF *CIS-TRANS* ISOMERS DERIVED FROM 3,3-DIPHENYL-1-HYDRINDONE. SYNTHESIS OF 3,3-DIPHENYLHYDRINDENE AND SOME OF ITS DERIVATIVES[1]

BY PAUL E. GAGNON[2] AND LS. PHIL. CHARETTE[3]

Abstract

Cis-trans isomers were obtained by condensation of 3,3-diphenyl-1-hydrindone with benzaldehyde or its *o*- and *m*-methyl-, *o*- and *p*-methoxy-, *o*-ethoxy, *o*- and *p*-chloro-derivatives, and by conversion of the condensation products by treatment with acetic acid.

3,3-Diphenyl-1-hydrindone was reduced to 3,3-diphenylhydrindene, and the condensation products of that ketone with the above mentioned aldehydes to derivatives of 3,3-diphenylhydrindene.

The methods of preparation of *trans*- and *cis*-3,3-diphenyl-2-benzylidene-1-hydrindone and of 3,3-diphenylhydrindene have been improved and the following compounds are described, as far as the authors are aware, for the first time: *trans*- and *cis*-3,3-diphenyl-2-(*o*-methylbenzylidene)-1-hydrindone, *trans*- and *cis*-3,3-diphenyl-2-(*m*-methylbenzylidene)-1-hydrindone, *trans*- and *cis*-3,3-diphenyl-2-(*o*-methoxybenzylidene)-1-hydrindone, *trans*- and *cis*-3,3-diphenyl-2-(*p*-methoxybenzylidene)-1-hydrindone, *trans*- and *cis*-3,3-diphenyl-2-(*o*-ethoxybenzylidene)-1-hydrindone, *trans*- and *cis*-3,3-diphenyl-2-(*o*-chlorobenzylidene)-1-hydrindone, *trans*- and *cis*-3,3-diphenyl-2-(*p*-chlorobenzylidene)-1-hydrindone, 3,3-diphenyl-2-benzyl-hydrindene, 3,3-diphenyl-2-(*o*-methylbenzyl)-hydrindene, 3,3-diphenyl-2-(*m*-methylbenzyl)-hydrindene, 3,3-diphenyl-2-(*o*-methoxybenzyl)-hydrindene, 3,3-diphenyl-2-(*p*-methoxybenzyl)-hydrindene, 3,3-diphenyl-2-(*o*-ethoxybenzyl)-hydrindene, 3,3-diphenyl-2-(*o*-chlorobenzyl)-hydrindene,3,3-diphenyl-2-(*p*-chlorobenzyl)-hydrindene.

Introduction

In previous work, one of the present authors (7) succeeded in isolating the two isomeric forms of 3,3-diphenyl-2-benzylidene-1-hydrindone (III), (IV), by condensation of 3,3-diphenyl-1-hydrindone (I) with benzaldehyde. The same author (7) prepared 3,3-diphenyl-hydrindene (II) from 3,3-diphenyl-1-hydrindone by Wolff's method (14), which consists in heating the hydrazone or the semicarbazone of the carbonyl compound with sodium ethoxide to about 170 to 180° C.

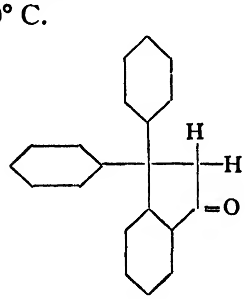

(*I*)

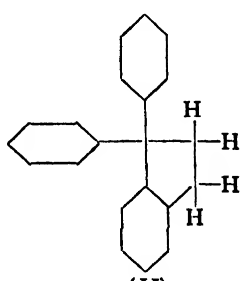

(*II*)

[1] *Manuscript received in original form April 9, 1941, and as revised, August 12, 1941. Contribution from the Department of Chemistry, Laval University, Quebec, Que.*

[2] *Professor of Chemistry.*

[3] *Graduate student, and holder of Studentships (1939–1941) under the National Research Council of Canada.*

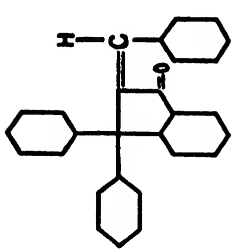

(III)

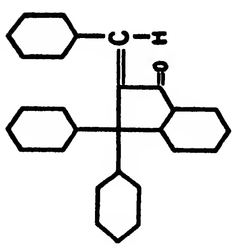

(IV)

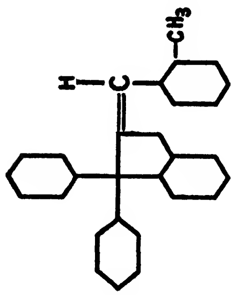

(V)

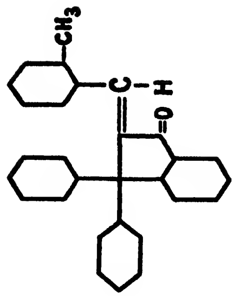

(VI)

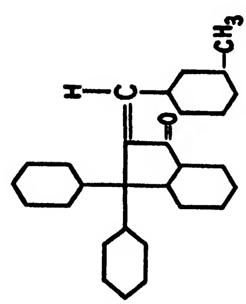

(VII)

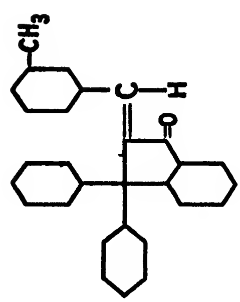

(VIII)

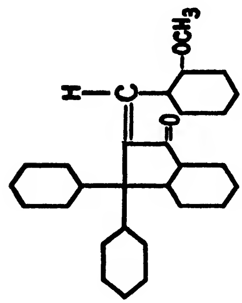

(IX)

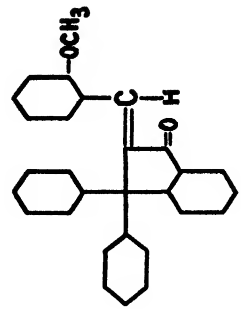

(X)

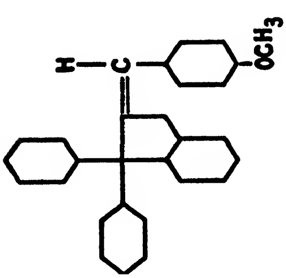

(XI)

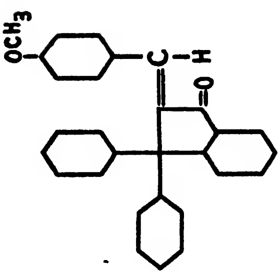

(XII)

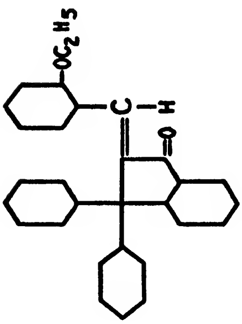

(XIII)

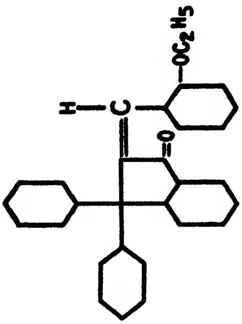

(XIV)

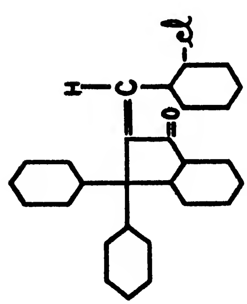

(XV)

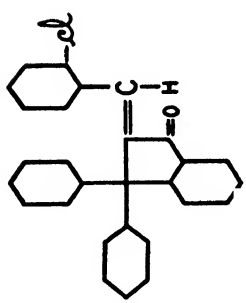

(XVI)

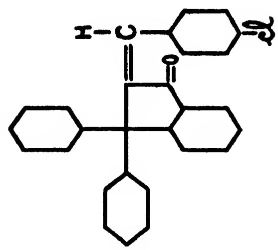

(XVII)

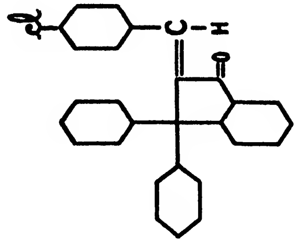

(XVIII)

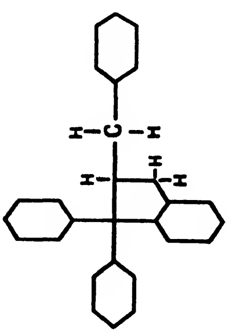

(XIX)

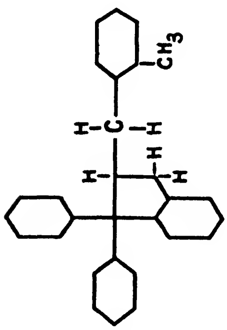

(XX)

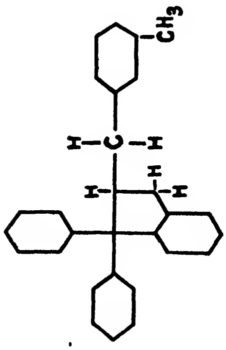

(XXI)

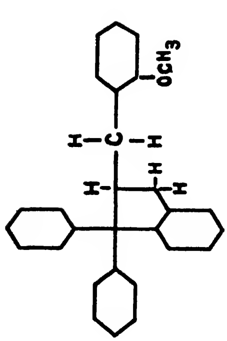

(XXII)

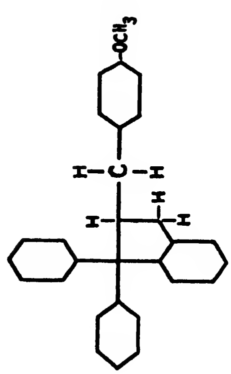

(XXIII)

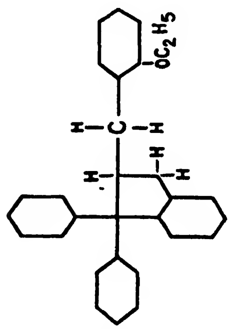

(XXIV)

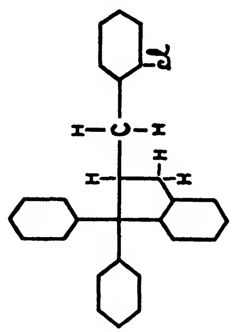

(XXV)

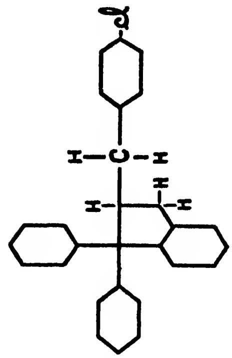

(XXVI)

The main object of the present work was to obtain, by condensation of 3,3-diphenyl-1-hydrindone with benzaldehyde and its derivatives, the isomeric compounds predicted by theory and to reduce them to 3,3-diphenylhydrindene derivatives.

The method used by Gagnon (7) for the condensation of 3,3-diphenyl-1-hydrindone with benzaldehyde consisted in adding, at room temperature, alcoholic potash to a solution of the ketone in benzaldehyde. The mixture was left standing and, two days later, a mixture of crystals of different colour was obtained. By very slow evaporation of a benzene solution of this mixture and sorting by hand, the two isomers were separated, one canary-yellow melting at 192° C. and the other pale yellow melting at 172° C.

The same compounds were prepared in this work by a slightly different method. The ketone and benzaldehyde were dissolved in boiling methyl alcohol and alcoholic potash was added. After about three hours of subsequent boiling, not a mixture, but only one canary-yellow compound melting at 192° C., which is the *trans*-form of 3,3-diphenyl-2-benzylidene-1-hydrindone (III), was obtained. By means of boiling glacial acetic acid it was converted into its isomer melting at 172° C. (IV).

By condensing, in the presence of alcoholic potash, 3,3-diphenyl-1-hydrindone with benzaldehyde derivatives and treating the condensation products with glacial acetic acid, similar results were obtained, except in the case of *o*-ethoxybenzaldehyde where the reaction product was almost only the *cis*-form. In this way were obtained:

the canary-yellow *trans*-3,3-diphenyl-2-(*o*-methylbenzylidene)-1-hydrindone melting at 190° C. (V) and its white *cis*-isomer melting at 176° C. (VI);

the nearly white *trans*-3,3-diphenyl-2-(*m*-methylbenzylidene)-1-hydrindone melting at 175° C. (VII) and its canary-yellow *cis*-isomer melting at 104° C. (VIII);

the white *trans*-3,3-diphenyl-2-(*o*-methoxybenzylidene)-1-hydrindone melting at 216° C. (IX) and its canary-yellow *cis*-isomer melting at 182° C. (X);

the nearly white *trans*-3,3-diphenyl-2-(*p*-methoxybenzylidene)-1-hydrindone melting at 163° C. (XI) and its canary-yellow *cis*-isomer melting at 133° C. (XII);

the canary-yellow *cis*-3,3-diphenyl-2-(*o*-ethoxybenzylidene)-1-hydrindone melting at 153° C. (XIII) and its darker *trans*-isomer melting at 161° C. (XIV);

the canary-yellow *trans*-3,3-diphenyl-2-(*o*-chlorobenzylidene)-1-hydrindone melting at 197° C. (XV) and its white *cis*-isomer melting at 151° C. (XVI);

the pale yellow *trans*-3,3-diphenyl-2-(*p*-chlorobenzylidene)-1-hydrindone melting at 201° C. (XVII) and its canary-yellow *cis*-isomer melting at 176° C. (XVIII).

It is generally known that there is a surprising regularity in the differences in physical properties between the *cis*- and *trans*-forms. The *cis*-form usually

has the lower melting point, the greater solubility in inert solvents, and is the labile form. This enables us to distinguish the *cis*-forms from the *trans*-forms (Table I).

TABLE I

SOLUBILITY OF *cis-trans* ISOMERS IN 100 ML. OF 95% ETHYL ALCOHOL AT 78.5° C.

Isomers	M.p., °C.*	Solubility, gm.
trans-3,3-Diphenyl-2-benzylidene-1-hydrindone	192	0.5
cis-3,3-Diphenyl-2-benzylidene-1-hydrindone	172	1.5
trans-3,3-Diphenyl-2-(*o*-methylbenzylidene)-1-hydrindone	190	0.5
cis-3,3-Diphenyl-2-(*o*-methylbenzylidene)-1-hydrindone	176	2.0
trans-3,3-Diphenyl-2-(*m*-methylbenzylidene)-1-hydrindone	175	0.9
cis-3,3-Diphenyl-2-(*m*-methylbenzylidene)-1-hydrindone	104	2.5
trans-3,3-Diphenyl-2-(*o*-methoxybenzylidene)-1-hydrindone	216	0.4
cis-3,3-Diphenyl-2-(*o*-methoxybenzylidene)-1-hydrindone	182	0.6
trans-3,3-Diphenyl-2-(*p*-methoxybenzylidene)-1-hydrindone	163	1.0
cis-3,3-Diphenyl-2-(*p*-methoxybenzylidene)-1-hydrindone	133	1.7
trans-3,3-Diphenyl-2-(*o*-ethoxybenzylidene)-1-hydrindone	161	1.2
cis-3,3-Diphenyl-2-(*o*-ethoxybenzylidene)-1-hydrindone	153	1.4
trans-3,3-Diphenyl-2-(*o*-chlorobenzylidene)-1-hydrindone	197	0.5
cis-3,3-Diphenyl-2-(*o*-chlorobenzylidene)-1-hydrindone	151	3.0
trans-3,3-Diphenyl-2-(*p*-chlorobenzylidene)-1-hydrindone	201	0.5
cis-3,3-Diphenyl-2-(*p*-chlorobenzylidene)-1-hydrindone	176	1.0

* *The melting points are uncorrected.*

As previously stated, by condensing 3,3-diphenyl-1-hydrindone with benzaldehyde or its derivatives, in each experiment as reaction product only one isomer was obtained except in the case of *o*-ethoxybenzaldehyde, which will be discussed later in this paper. The other isomer was obtained by treatment with acetic acid. Since the latter isomer is more soluble and melts at the lower temperature, it was named the *cis*-form and the former, the *trans*-form.

Moreover, it was observed that the *trans*-form was really the stable one. In fact, when 3,3-diphenyl-1-hydrindone was condensed with benzaldehyde or its *o*- and *m*-methyl-, *o*- and *p*-methoxy-, *o*- and *p*-chloro-derivatives, only the *trans*-form melting at the higher temperature was obtained. On boiling this *trans*-form in glacial acetic acid and by fractional crystallization the *cis*-form was obtained. The product from the first crystallization was not the pure *cis*-form, but a mixture of the two forms: the melting point of this mixture was intermediate between those of the *trans*- and *cis*-forms. The pure *cis*-form was obtained only after the second crystallization. Apparently an equilibrium is established during the conversion. On heating the *trans*-form at a temperature a little higher than its melting point, a mixture of the two isomers was obtained. On the other hand, on boiling the *cis*-form in methyl

alcohol in the presence of potash, it was completely converted into its *trans*-isomer. According to these observations, the *trans*-form melting at the higher temperature is the stable one.

In the condensation of 3,3-diphenyl-1-hydrindone with *o*-ethoxybenzaldehyde, the *cis*-form melting at 153° C. was the first to be obtained. The filtrate was then left standing for several hours. The *trans*-form, melting at 161° C., crystallized. The ratio of the *cis*- to the *trans*-form was 11 to 2. On boiling the *cis*-form in glacial acetic acid, it was completely converted into its *trans*-isomer. The same result was obtained when heating the *cis*-form to about 165° C. for a few seconds. This explains the fact that the melting point of the mixture of the two isomers is 161° C., the same as that of the *trans*-form. Here also the *cis*-form melting at the lower temperature is the labile one. The two isomers have virtually the same melting points; this is in agreement with the fact that they have nearly the same solubility and colour.

It was intended to apply the reduction method of Wolff to the condensation products, as Gagnon (7) did in the case of 3,3-diphenyl-1-hydrindone. However, on account of the decrease of reactivity of the CO group caused by replacement of the hydrogen atoms of the neighbouring CH_2 group by a benzylidene group, it was impossible to obtain the hydrazones of the condensation products by the method used for the preparation of the hydrazone of 3,3-diphenyl-1-hydrindone (7, 10). The authors then tried Clemmensen's method (3, 4, 5), which enabled them to obtain directly, from the carbonyl compounds, 3,3-diphenylhydrindene and the following derivatives:

3,3-diphenyl-2-benzylhydrindene (XIX),
3,3-diphenyl-2-(*o*-methylbenzyl)-hydrindene (XX),
3,3-diphenyl-2-(*m*-methylbenzyl)-hydrindene (XXI),
3,3-diphenyl-2-(*o*-methoxybenzyl)-hydrindene (XXII),
3,3-diphenyl-2-(*p*-methoxybenzyl)-hydrindene (XXIII),
3,3-diphenyl-2-(*o*-ethoxybenzyl)-hydrindene (XXIV),
3,3-diphenyl-2-(*o*-chlorobenzyl)-hydrindene (XXV),
3,3-diphenyl-2-(*p*-chlorobenzyl)-hydrindene (XXVI).

This paper is divided into two parts. In the first, the condensation products of 3,3-diphenyl-1-hydrindone with benzaldehyde or its derivatives, and also the isomers of these condensation products are described. The second part deals with 3,3-diphenylhydrindene and some of its derivatives.

As all the condensation products and their isomers were prepared by the same general method, the preparation of the first will be described in detail. Only the quantities of materials and any differences in experimental conditions and procedure will be given in the case of the others. The same applies to the derivatives of 3,3-diphenyl-1-hydrindene.

PART I

Condensation Products of 3,3-Diphenyl-1-hydrindone with Benzaldehyde or Its Derivatives, and Their Isomers

3,3-Diphenyl-1-hydrindone (I)

According to the methods of Fosse (6) and Hellerman (8), triphenylcarbinol (2400 gm.) was condensed with malonic acid (1560 gm.) in the presence of acetic anhydride (960 ml.) and, by elimination of water and carbon dioxide, triphenylpropionic acid was obtained. Yield, 2700 gm. (96.8%).

Several methods of preparation of 3,3-diphenyl-1-hydrindone by cyclization of triphenylpropionic acid are described. The process used by Moureu, Dufraisse, and Dean (9) and improved by Gagnon (7) eliminates a molecule of water from triphenylpropionic acid by means of concentrated sulphuric acid. Bergmann and Weiss (2) obtain the ketone by elimination of hydrochloric acid from triphenylpropionyl chloride. Unger (13) treated triphenylpropionic acid with monochloracetic anhydride. He pointed out that the melting point of 3,3-diphenyl-1-hydrindone was 121° C. By the method of Moureu, Dufraisse, and Dean, a large quantity of 3,3-diphenyl-1-hydrindone melting at 131° C. and not at 121° C., as stated by Unger, was prepared. The results obtained are in agreement with the data of the previously mentioned authors, except Unger, and also with those of Auwers and Hügel (1), who prepared this ketone by a different method, by cyclization of β-chloro-*trans*-cinnamyl chloride.

3,3-Diphenyl-2-benzylidene-1-hydrindones (7), (III), (IV)

By condensing 3,3-diphenyl-1-hydrindone with benzaldehyde, *trans*-3,3-diphenyl-2-benzylidene-1-hydrindone melting at 192° C. was obtained. This ketone was then converted into its *cis*-isomer melting at 172° C.

(a) Preparation of Isomer Melting at 192° C. (III)

In a round bottomed flask (1000 ml.) fitted with a reflux condenser, 3,3-diphenyl-1-hydrindone (15 gm.) and benzaldehyde (10 ml.) were dissolved in boiling absolute methyl alcohol (300 ml.). The mixture was kept boiling and, through the condenser, 100 ml. of alcoholic potash (300 gm. of potassium hydroxide in 1000 ml. of absolute methyl alcohol) was slowly added. After three and a half hours of subsequent boiling, the mixture was allowed to cool, and it was then filtered. The yellow crystalline product, washed with water and ethyl alcohol, was crystallized from benzene; m.p. 192° C. The compound separated from ethyl alcohol in hexagonal prisms. Yield, 15.7 gm. (80%). This canary-yellow compound was identified as 3,3-diphenyl-2-benzylidene-1-hydrindone (7) by a mixed melting point determination. Soluble in hot glacial acetic acid, it is almost insoluble in methyl and ethyl alcohols.

(b) Preparation of Isomer Melting at 172° C. (IV)

A concentrated solution of *trans*-3,3-diphenyl-2-benzylidene-1-hydrindone in glacial acetic acid was boiled for 14 hr. and then left standing at room

temperature. After several hours, a mixture of products melting at 167 to 187° C. was separated. From the filtrate another product, pale yellow and more soluble, crystallized. After recrystallization from benzene this product melted at 172° C. The compound separated from alcohol in pyramid-shaped crystals. It was identified as 3,3-diphenyl-2-benzylidene-1-hydrindone (7) by a mixed melting point determination. On boiling a methyl alcohol solution of this compound in presence of potash, its *trans*-isomer was obtained.

3,3-Diphenyl-2-(o-methylbenzylidene)-1-hydrindones (V), (VI)

By condensing 3,3-diphenyl-1-hydrindone with *o*-tolualdehyde, *trans*-3,3-diphenyl-2-(*o*-methylbenzylidene)-1-hydrindone melting at 190° C. was obtained. This ketone was then converted into its *cis*-isomer melting at 176° C.

(a) Preparation of Isomer Melting at 190° C. (V)

3,3-Diphenyl-1-hydrindone (10 gm.), *o*-tolualdehyde (7 ml.), absolute methyl alcohol (200 ml.), alcoholic potash (70 ml.); boiling time, 4 hr.

The canary-yellow product, washed with water and ethyl alcohol, was crystallized from glacial acetic acid; m.p. 189° C. Yield, 12 gm. (87.6%). Recrystallized from ethyl alcohol, in which it is very slightly soluble, this compound melts at 190° C. It separated from ethyl alcohol in needle-shaped crystals. It is soluble in hot benzene, very slightly soluble in methyl alcohol, but insoluble in ether and petroleum ether. Calc. for $C_{29}H_{22}O$: C, 90.16; H, 5.7%. Found: C, 89.42; H, 5.78%.

(b) Preparation of Isomer Melting at 176° C. (VI)

trans-3,3-Diphenyl-2-(*o*-methylbenzylidene)-1-hydrindone treated in the manner described above yielded a yellow product melting at 163 to 186° C. From the filtrate, another product crystallized. It was recrystallized, perfectly white, from ethyl alcohol; m.p. 176° C. The compound separated from ethyl alcohol in needle-shaped crystals (cluster of needles). This compound is more soluble in the usual solvents than its isomer melting at 190° C. Calc. for $C_{29}H_{22}O$: C, 90.16; H, 5.70%. Found: C, 88.9; H, 5.8%.

3,3-Diphenyl-2-(m-methylbenzylidene)-1-hydrindones (VII), (VIII)

By condensing 3,3-diphenyl-1-hydrindone with *m*-tolualdehyde, *trans*-3,3-diphenyl-2-(*m*-methylbenzylidene)-1-hydrindone melting at 175° C. was obtained. This ketone was then converted into its *cis*-isomer melting at 104° C.

(a) Preparation of Isomer Melting at 175° C. (VII)

3,3-Diphenyl-1-hydrindone (15 gm.), *m*-tolualdehyde (10 ml.), methyl alcohol (300 ml.), alcoholic potash (100 ml.); boiling time, 2 hr.

The pale yellow product, washed with water and ethyl alcohol, was crystallized from glacial acetic acid; m.p. 172° C. Yield, 16.5 gm. (81%). Recrystallized from ethyl alcohol, in which it is very slightly soluble, it melts at 175° C. The compound separated from ethyl alcohol in elongated prisms. It is white, and is soluble in hot benzene, and very slightly soluble in methyl

alcohol and ether. Calc. for $C_{29}H_{22}O$: C, 90.16; H, 5.70%. Found: C, 89.60; H, 5.79%.

(b) Preparation of Isomer Melting at 104° C. (VIII)

trans-3,3-Diphenyl-2-(*m*-methylbenzylidene)-1-hydrindone treated in the usual manner yielded a yellow product melting at 157 to 172° C. From the filtrate, another canary-yellow product crystallized. It was recrystallized twice from ethyl alcohol; m.p. 104° C. The compound separated from ethyl alcohol in small hexagonal prisms. This compound is more soluble in the usual solvents than its isomer melting at 175° C. Calc. for $C_{29}H_{22}O$: C, 90.16; H, 5.70%. Found: C, 89.50; H, 5.78%.

3,3-Diphenyl-2-(o-methoxybenzylidene)-1-hydrindones (IX), (X)

By condensing 3-3-diphenyl-1-hydrindone with *o*-methoxybenzaldehyde, *trans*-3,3-diphenyl-2-(*o*-methoxybenzylidene)-1-hydrindone melting at 216° C. was obtained. This ketone was then converted into its *cis*-isomer melting at 182° C.

(a) Preparation of Isomer Melting at 216° C. (IX)

3,3-Diphenyl-1-hydrindone (12 gm.), *o*-methoxybenzaldehyde (6 ml.), absolute methyl alcohol (240 ml.), alcoholic potash (80 ml.); boiling time, 3 hr.

The product, washed with water and ethyl alcohol, was crystallized, perfectly white, from benzene; m.p. 216° C. It separated from ethyl alcohol in small elongated prisms. Yield, 12 gm. (90%). This compound is soluble in hot glacial acetic acid, but almost insoluble in methyl and ethyl alcohols, ether, and petroleum ether. Calc. for $C_{29}H_{22}O_2$: C, 86.56; H, 5.47%. Found: C, 86.35; H, 5.53%.

(b) Preparation of Isomer Melting at 182° C. (X)

trans-3,3-Diphenyl-2-(*o*-methoxybenzylidene)-1-hydrindone yielded a yellow product melting at 168 to 214° C. From the filtrate, another canary-yellow product crystallized. It was recrystallized from ethyl alcohol; m.p. 182° C. The compound separated from ethyl alcohol in needle-shaped crystals. It is more soluble in the usual solvents than its isomer melting at 175° C. Calc. for $C_{29}H_{22}O_2$: C, 86.56; H, 5.47%. Found: C, 83.6; H, 5.5%.

3,3-Diphenyl-2-(p-methoxybenzylidene)-1-hydrindones (XI), (XII)

By condensing 3,3-diphenyl-1-hydrindone with *p*-methoxybenzaldehyde, *trans*-3,3-diphenyl-2-(*p*-methoxybenzylidene)-1-hydrindone melting at 162° C. was obtained. This ketone was then converted into its *cis*-isomer melting at 133° C.

(a) Preparation of Isomer Melting at 163° C. (XI)

3,3-Diphenyl-1-hydrindone (20 gm.), *p*-methoxybenzaldehyde (10 ml.), absolute methyl alcohol (400 ml.), alcoholic potash (140 ml.).

After three hours of boiling, the reflux condenser was replaced by another condenser, the alcohol distilled off, and the residue dissolved in benzene. The solution was washed with water, dried over anhydrous sodium sulphate, and completely evaporated. On cooling, a red solid product was obtained which, after several washings with ether and crystallizations from glacial acetic acid and ethyl alcohol, became almost white; m.p. 163° C. The compound separated from ethyl alcohol in elongated prisms. Yield, 5 gm. (17.7%). It is soluble in hot benzene, and slightly soluble in methyl and ethyl alcohols. Calc. for $C_{29}H_{22}O_2$: C, 86.56; H, 5.47%. Found: C, 86.46; H, 5.41%.

(b) Preparation of Isomer Melting at 133° C. (XII)

trans-3,3-Diphenyl-2-(*p*-methoxybenzylidene)-1-hydrindone yielded a yellow product melting at 150 to 161°. From the filtrate, another canary-yellow product crystallized. It was recrystallized from ethyl alcohol; m.p. 133° C. The compound separated from ethyl alcohol in rectangular prisms. It is more soluble in the usual solvents than its isomer melting at 163° C. Calc. for $C_{29}H_{22}O_2$: C, 86.56; H, 5.47%. Found: C, 84.7; H, 5.5%.

3,3-Diphenyl-2-(o-ethoxybenzylidene)-1-hydrindones (XIII), (XIV)

By condensing 3,3-diphenyl-1-hydrindone with *o*-ethoxybenzaldehyde, *cis*-3,3-diphenyl-2-(*o*-ethoxybenzylidene)-1-hydrindone melting at 153° C. was obtained. This ketone was then converted into its *trans*-isomer melting at 161° C.

(a) Preparation of Isomer Melting at 153° C. (XIII)

3,3-Diphenyl-1-hydrindone (10 ml.), *o*-ethoxybenzaldehyde (6 ml.), absolute methyl alcohol (200 ml.), alcoholic potash (70 ml.); boiling time, 5 hr.; flask, 500 cc.

The canary-yellow product, washed with water and ethyl alcohol, was crystallized from glacial acetic acid; m.p. 153° C. Yield, 12.2 gm. From the original filtrate, another dark yellow product crystallized; m.p. 161° C. The mixed melting point was 161° C. Total yield, 13.7 gm. (94%). Soluble in cold benzene, the compound melting at 153° C. is but slightly soluble in methyl and ethyl alcohols, ether, and petroleum ether. It separated from ethyl alcohol in elongated prisms. Calc. for $C_{30}H_{24}O_2$: C, 86.54; H, 5.77%. Found: C, 86.03; H, 5.85%.

(b) Preparation of Isomer Melting at 161° C. (XIV)

cis-3,3-Diphenyl-2-(*o*-ethoxybenzylidene)-1-hydrindone in glacial acetic acid was treated in the usual manner. After a few hours, the solution was filtered and the dark yellow product crystallized from ethyl alcohol; m.p. 161° C. By heating the *cis*-isomer melting at 153° C. to about 165° C. for a few seconds it was converted into the other form melting at 161° C. This compound melting at 161° C. is darker than its *cis*-isomer, but has about the same solubility in the usual solvents. The compound separated from ethyl alcohol in elongated prisms. Calc. for $C_{30}H_{24}O_2$: C, 86.54; H, 5.77%. Found: C, 85.72; H, 5.80%.

3,3-Diphenyl-2-(o-chlorobenzylidene)-1-hydrindones (XV), (XVI)

By condensing 3-3-diphenyl-1-hydrindone with *o*-chlorobenzaldehyde, *trans*-3,3-diphenyl-2-(*o*-chlorobenzylidene)-1-hydrindone melting at 197° C. was obtained. This ketone was then converted into its *cis*-isomer melting at 151° C.

(a) Preparation of Isomer Melting at 197° C. (XV)

3,3-Diphenyl-1-hydrindone (15 gm.), *o*-chlorobenzaldehyde (7 ml.), absolute methyl alcohol (300 ml.), alcoholic potash (100 ml.); boiling time, 3 hr.

The canary-yellow product, washed with water and ethyl alcohol, was crystallized from benzene; m.p. 197° C. The compound separated from ethyl alcohol in needle-shaped crystals. Yield, 20 gm. (90%). It is soluble in hot glacial acetic acid, but almost insoluble in methyl and ethyl alcohols, ether, and petroleum ether. Calc. for $C_{28}H_{19}OCl$: Cl, 8.73%. Found: Cl, 8.81%.

(b) Preparation of Isomer Melting at 151° C. (XVI)

trans-3,3-Diphenyl-2-(*o*-chlorobenzylidene)-1-hydrindone yielded a yellow product melting at 170 to 195° C. By diluting the filtrate with water, another product was precipitated. It was crystallized, perfectly white, from ethyl alcohol; m.p. 151° C. The compound separated from ethyl alcohol in hexagonal prisms. It is more soluble in the usual solvents than its isomer melting at 197° C. Calc. for $C_{28}H_{19}OCl$: Cl, 8.73%. Found: Cl, 8 72%.

3,3-Diphenyl-2-(p-chlorobenzylidene)-1-hydrindones (XVII), (XVIII)

By condensing 3,3-diphenyl-1-hydrindone with *p*-chlorobenzaldehyde, *trans*-3,3-diphenyl-2-(*p*-chlorobenzylidene)-1-hydrindone melting at 201° C. was obtained. This ketone was then converted into its *cis*-isomer melting at 176° C.

(a) Preparation of Isomer Melting at 201° C. (XVII)

3,3-Diphenyl-1-hydrindone (10 gm.), *p*-chlorobenzaldehyde (6 gm.), absolute methyl alcohol (200 ml.), alcoholic potash (70 ml.); boiling time, 3 hr.; flask, 500 cc.

The pale yellow product, washed with water and ethyl alcohol, was crystallized from glacial acetic acid; m.p. 201° C. The compound separated from ethyl alcohol in irregular prisms. Yield, 13 gm. (91%). This compound, soluble in cold benzene, is almost insoluble in methyl and ethyl alcohols, ether, and petroleum ether. Calc. for $C_{28}H_{19}OCl$: Cl, 8.73%. Found: Cl, 8.92%.

(b) Preparation of Isomer Melting at 176° C. (XVIII)

From *trans*-3,3-diphenyl-2-(*p*-chlorobenzylidene)-1-hydrindone a yellow product melting at 180 to 197° C. was obtained. From the filtrate, another canary-yellow product crystallized. It was recrystallized from ethyl alcohol; m.p. 176° C. The compound separated from ethyl alcohol in elongated prisms. It is more soluble in the usual solvents than its isomer melting at 201° C. Calc. for $C_{28}H_{19}OCl$: Cl, 8.73%. Found: Cl, 8.74%.

PART II

3,3-DIPHENYLHYDRINDENE AND ITS DERIVATIVES

The reduction of 3,3-diphenyl-1-hydrindone and its condensation products with aldehydes was carried out by Clemmensen's method (3, 4, 5).

3,3-Diphenylhydrindene (II)

The amalgamated zinc was prepared in a round bottomed flask (500 ml.) by covering granulated zinc (50 gm.) with a 5% aqueous solution of mercuric chloride (100 ml.). After standing for one hour, the solution was poured off and 3,3-diphenyl-1-hydrindone (5 gm.), dissolved in glacial acetic acid (125 ml.), was added to the amalgamated zinc. The mixture was brought to boiling and, drop by drop, concentrated hydrochloric acid (150 ml.) was added. After one hour, the mixture was allowed to cool. The upper oily layer, which consisted of 3,3-diphenylhydrindene, was removed from the reaction mixture by dissolving in petroleum ether. The ether solution was washed with sodium bicarbonate solution and water and dried over anhydrous sodium sulphate. The ether was distilled off and the residue taken up with methyl alcohol and decolorized with charcoal. The alcohol was evaporated, whereupon a white product crystallized. Yield, 4 gm. (84%). Recrystallized from methyl alcohol, it melts at 67° C. It was identified as 3,3-diphenylhydrindene (7) by a mixed melting point determination.

3,3-Diphenyl-2-benzylhydrindene (XIX)

Into a round bottomed flask (500 ml.) fitted with a reflux condenser and containing amalgamated zinc (50 gm.), was poured a solution of *trans*-3,3-diphenyl-2-benzylidene-1-hydrindone (2.5 gm.) in glacial acetic acid (100 ml.). The mixture was brought to boiling and, drop by drop, concentrated hydrochloric acid (100 ml.) was added. A light coloured crystalline product formed on the surface. After one hour, the mixture was allowed to cool, and it was then filtered. This reduction process was repeated twice. The final product was recrystallized, perfectly white, from glacial acetic acid; m.p. 179° C. Yield, 1.7 gm. (70%). It is soluble in hot benzene, but is almost insoluble in methyl and ethyl alcohols, ether, and petroleum ether. Calc. for $C_{28}H_{24}$: C, 93.33; H, 6.67%. Found: C, 92.1; H, 6.6%.

3,3-Diphenyl-2-benzylhydrindene (XIX)

cis-3,3-Diphenyl-2-benzylidene-1-hydrindone (3.5 gm.), glacial acetic acid (100 ml.), amalgamated zinc (50 gm.), concentrated hydrochloric acid (100 ml.); flask, 1000 ml.

A light-coloured crystalline product formed on the surface. After one hour, the mixture was allowed to cool, and it was then filtered. The reduction was complete. The product, washed with water and ethyl alcohol, was crystallized, perfectly white, from benzene; m.p. 179° C. Yield, 2.5 gm. (74%). It was identified as 3,3-diphenyl-2-benzylhydrindene by a mixed melting point determination. The *cis*-isomer was reduced much more easily and quickly than

the *trans*. Paal and Schiedewitz (11, 12) made the same observations when reducing some *cis*- and *trans*-acids.

3,3-Diphenyl-2-(o-methylbenzyl)-hydrindene (XX)

trans-3,3-Diphenyl-2-(*o*-methylbenzylidene)-1-hydrindone (6 gm.), glacial acetic acid (200 ml.), amalgamated zinc (50 gm.), concentrated hydrochloric acid (150 ml.); flask, 1000 ml.

A light-coloured crystalline product formed on the surface. After one hour and a half, the mixture was allowed to cool, and it was then filtered. The purification of the product required four crystallizations from glacial acetic acid; m.p. 132° C. Yield, 4 gm. (69%). The compound is white, is soluble in cold benzene and ether, but is almost insoluble in methyl and ethyl alcohols. Calc. for $C_{29}H_{26}$: C, 93.05; H, 6.95%. Found: C, 92 49; H, 6.93%.

3,3-Diphenyl-2-(m-methylbenzyl)-hydrindene (XXI)

trans-3,3-Diphenyl-2-(*m*-methylbenzylidene)-1-hydrindone (5 gm.), glacial acetic acid (200 ml.), amalgamated zinc (50 gm.), concentrated hydrochloric acid (150 ml.); flask, 1000 ml.

A light-coloured crystalline product formed on the surface. After one hour and a half, the mixture was allowed to cool, and it was then filtered. The product, washed with water and ethyl alcohol, was crystallized, perfectly white, from glacial acetic acid; m.p. 149° C. Yield, 4.2 gm. (78%). It is soluble in cold benzene and ether, but is almost insoluble in hot methyl and ethyl alcohols and petroleum ether. Calc. for $C_{29}H_{26}$: C, 93.05; H, 6.95%. Found: C, 92.0; 6.9%.

3,3-Diphenyl-2-(o-methoxybenzyl)-hydrindene (XXII)

trans-3,3-Diphenyl-2-(*o*-methoxybenzylidene)-1-hydrindone (3 gm.), glacial acetic acid (125 ml.), amalgamated zinc (25 gm.), concentrated hydrochloric acid (125 ml.).

A white crystalline product formed almost immediately. After 30 min., the mixture was allowed to cool, and it was then filtered. The product, washed with water and ethyl alcohol, was crystallized, perfectly white, from glacial acetic acid; m.p. 176° C. Yield, 2.6 gm. (90%). The compound is soluble in hot benzene, but is insoluble in methyl and ethyl alcohols, ether and petroleum ether. Calc. for $C_{29}H_{26}O$: C, 89.23; H, 6.67%. Found: C, 88.75; H, 6.65%.

3,3-Diphenyl-2-(p-methoxybenzyl)-hydrindene (XXIII)

trans-3,3-Diphenyl-2-(*p*-methoxybenzylidene)-1-hydrindone (5 gm.), glacial acetic acid (200 ml.), amalgamated zinc (25 gm.), concentrated hydrochloric acid (150 ml.); flask, 1000 ml.

A white crystalline product formed rapidly on the surface. After one hour, the mixture was allowed to cool, and it was then filtered. The product, washed with water and ethyl alcohol, was crystallized, perfectly white, from glacial acetic acid; m.p. 178° C. Yield, 4.1 gm. (85%). Soluble in hot benzene, this compound is insoluble in methyl and ethyl alcohols, ether, and petroleum ether. Calc. for $C_{29}H_{26}O$: C, 89.23; H, 6.67%. Found: C, 88.0; H, 6.6%.

3,3-Diphenyl-2-(o-ethoxybenzyl)-hydrindene (XXIV)

cis-3,3-Diphenyl-2-(*o*-ethoxybenzylidene)-1-hydrindone (5 gm.), glacial acetic acid (125 ml.), amalgamated zinc (25 gm.), concentrated hydrochloric acid (150 ml.).

A white crystalline product formed immediately on the surface. After 30 min. the mixture was allowed to cool, and it was then filtered. The product, washed with water and ethyl alcohol, was crystallized, perfectly white, from glacial acetic acid; m.p. 170° C. Yield, 4.4 gm. (90%). It is soluble in cold benzene, but insoluble in methyl and ethyl alcohol, ether, and petroleum ether. Calc. for $C_{30}H_{28}O$: C, 89.10; H, 6.93%. Found: C, 88.53; H, 6.91%.

3,3-Diphenyl-2-(o-chlorobenzyl)-hydrindene (XXV)

trans-3,3-Diphenyl-2-(*o*-chlorobenzylidene)-1-hydrindone (6 gm.), glacial acetic acid (210 ml.), amalgamated zinc (50 gm.), concentrated hydrochloric acid (200 ml.); flask, 1000 cc.

A crystalline product formed on the surface. After one hour and a half, the mixture was allowed to cool, and it was then filtered. The product, washed with water and ethyl alcohol, was crystallized, perfectly white, from glacial acetic acid; m.p. 160° C. Yield, 4.7 gm. (80%). Soluble in cold benzene and ether, this compound is insoluble in methyl and ethyl alcohols and petroleum ether. Calc. for $C_{28}H_{23}Cl$: Cl, 8.99%. Found: Cl, 9.08%.

3,3-Diphenyl-2-(p-chlorobenzyl)-hydrindene (XXVI)

trans-3,3-Diphenyl-2-(*p*-chlorobenzylidene)-1-hydrindone (5 gm.), glacial acetic acid (200 ml.), amalgamated zinc (50 gm.), concentrated hydrochloric acid (100 ml.).

A white product formed rapidly on the surface. After one hour, the mixture was allowed to cool, and it was then filtered. The purification of the product required three crystallizations from glacial acetic acid; m.p. 156° C. Yield, 4 gm. (82.5%). It is white, and is soluble in cold benzene and ether, and slightly soluble in methyl and ethyl alcohols. Calc. for $C_{28}H_{23}Cl$: Cl, 8.99%. Found: Cl, 9.07%.

References

1. AUWERS, K. v. and HÜGEL, R. J. prakt. Chem. 143 : 157-173. 1935.
2. BERGMANN, E. and WEISS, H. Ann. 480 : 49-59. 1930.
3. CLEMMENSEN, E. Ber. 46 : 1837-1843. 1913.
4. CLEMMENSEN, E. Ber. 47 : 51-63. 1914.
5. CLEMMENSEN, E. Ber. 47 : 681-687. 1914.

6. FOSSE, R. Compt. rend. 145 : 196-198. 1907.
7. GAGNON, P. Ann. chim. (Sér. 10) 12 : 296-343. 1929.
8. HELLERMAN, L. J. Am. Chem. Soc. 49 : 1735-1742. 1927.
9. MOUREU, C., DUFRAISSE, C., and DEAN, P. M. Bull. soc. chim. (Sér. 4) 43 : 1367-1371. 1928.
10. MOUREU, C., DUFRAISSE, C., and GAGNON, P. Compt. rend. 189 : 217-219. 1929.
11. PAAL, C. and SCHIEDEWITZ, H. Ber. 60 : 1221-1228. 1927.
12. PAAL, C. and SCHIEDEWITZ, H. Ber. 63 : 766-768. 1930.
13. UNGER, F. Ann. 504 : 267-286. 1933.
14. WOLFF, L. Ann. 394 : 86-108. 1912.

Canadian Journal of Research

Issued by THE NATIONAL RESEARCH COUNCIL OF CANADA

VOL. 19, SEC. B DECEMBER, 1941 NUMBER 12

CHEMOTHERAPEUTIC STUDIES IN THE THIOPHENE SERIES

I. THE SYNTHESIS OF 2-SULPHANILAMIDO-THIOPHENE[1]

BY C. VON SEEMANN[2] AND C. C. LUCAS[3]

Abstract

A method is described for the synthesis of (1-acetylaminobenzene-4-sulphonamido)-2-thiophene and of (1-aminobenzene-4-sulphonamido)-2-thiophene, also called 2-sulphanilamido-thiophene. The acute toxicity of the above compounds has been determined and an evaluation made of their chemotherapeutic activity in experimental infections of white mice with Pneumococcus Type I; 2-sulphanilamido-thiophene shows no chemotherapeutic activity.

Introduction

In the course of a series of chemotherapeutic studies carried out in this laboratory it was thought advisable to study some thiophene derivatives. As is now well known from the fundamental work of Victor Meyer (3)*, which was extended by Steinkopf** and his collaborators, thiophene and a large number of its derivatives are closely similar to the analogous compounds of the benzene series. The reported comparative absence of toxicity of thiophene (2), which was confirmed in this laboratory, made it all the more interesting to investigate the chemotherapeutic properties of thiophene derivatives. The marked anti-bacterial activity of 2-sulphanilamido-pyridine and -thiazole suggested that the study be begun by preparing the hitherto unknown 2-sulphanilamido-thiophene.

The extreme instability of 2-aminothiophene in air presented considerable difficulty. All reactions had to be carried out in an inert atmosphere. A special apparatus was finally evolved by which the difficulties could be overcome. It allowed the reaction to be carried out in three successive steps and with complete exclusion of oxygen throughout. A yield of about 8% of 2-sulphanilamido-thiophene was obtained based upon the amount of stannic chloride salt of 2-aminothiophene hydrochloride used.

Toxicity tests carried out by Dr. P. H. Greey of the Department of Pathology and Bacteriology showed that 2-sulphanilamido-thiophene as well as its

[1] *Manuscript received August 4, 1941.*
Contribution from the Department of Medical Research, Banting Institute, University of Toronto, Toronto, Ont.

[2] *Research Assistant.*
[3] *Associate Professor.*

* *And numerous papers, mainly in "Berichte der deutschen chemischen Gesellschaft".*
** *More than 50 papers, mainly in "Liebig's Annalen".*

acetylated product had no toxic effect upon white mice in single doses up to 50 mg. Chemotherapeutic tests on white mice infected with Pneumococcus Type I showed that 2-sulphanilamido-thiophene had no curative properties in such infections. Details of the testing and further results will be published shortly by Dr. Greey.

Grateful acknowledgment is made to the Banting Research Foundation for a grant to the Department of Medical Research which supported this work.

Experimental*

I. Preparation of Thiophene

Thiophene was prepared from disodium succinate and phosphorus trisulphide according to a modification of the method of Volhard and Erdmann (7) quoted in Organic Syntheses, Vol. XII, p. 72.

II. 2-Nitrothiophene

The preparation of this substance was carried out according to the method of V. S. Babasinian (1). The purified product (yield, 88%) had a melting point of 42° C.**

III. Reduction of 2-Nitrothiophene

This procedure was carried out according to the method of Steinkopf (5) using tin filings (freshly prepared) and hydrochloric acid as the reducing agent. The resulting compound, which according to Stadler (4) has the composition: $2C_4H_5NS + 2HCl + SnCl_4$, was obtained in 78% yield.

IV. Preparation of Free 2-Aminothiophene and Condensation with 1-Acetylaminobenzene-4-Sulphonyl Chloride

A modification of the method given by Steinkopf (5) was used for the preparation of 2-aminothiophene. Owing to the great instability of 2-aminothiophene, which leads it to react with oxygen with the almost immediate formation of resinous products of polymerization, the above two steps were carried out in quick succession in the apparatus shown in Fig. 1.

The apparatus consists of two separatory funnels of 500 and 50 ml. capacity respectively (*A* and *B* in Fig. 1) and of an Erlenmeyer flask of 250 ml. (*C*). Separatory funnel *A* carries a rubber stopper with three holes through which are introduced a separatory funnel, *B*, carrying stopcock *S* 4, the gas inlet tube *G*, reaching to the bottom of funnel *A*, and the connecting tube carrying stopcock *S* 1. The connecting tube protrudes 5 mm. into the interior of *A*. The Erlenmeyer flask, *C*, carries also a rubber stopper with three holes through which the connecting tube and the two outlet tubes carrying stopcocks *S* 2 and *S* 3 extend into the interior of the flask. The connecting tube and the outlet carrying stopcock *S* 2 reach to the bottom of the Erlenmeyer flask,

* *After the present paper had been prepared for publication an article appeared (R. W. Bost and Chas. F. Starnes, J. Am. Chem. Soc. 63: 1885–1886. 1941.) describing the preparation of 2-sulphanilamido-thiophene by a slightly different method.*

** *Melting points are corrected.*

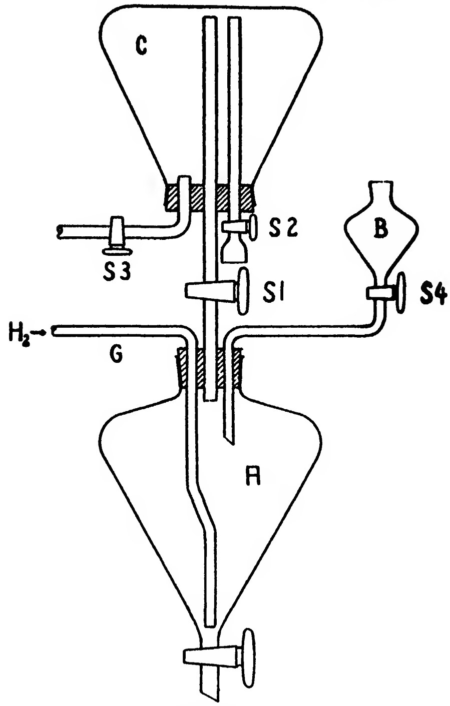

FIG. 1. *Diagram of apparatus.*

while the outlet carrying stopcock *S* 3 extends only a few millimetres into the interior. The apparatus is filled and assembled in the following way:

1-Acetylaminobenzene-4-sulphonyl chloride (4.66 gm., 0.02 mole), prepared according to Stewart's method (6), are dissolved in 50 ml. of purified acetone and the solution is introduced into the Erlenmeyer flask *C*. The stopper carrying the connecting tube and the two outlet tubes is then inserted and made secure with wire. It is essential that the three stopcocks *S* 1, *S* 2, and *S* 3 should be closed before the introduction of the stopper in order to prevent any solution from entering the tubes. The Erlenmeyer flask is then inverted and the rubber stopper on the other end of the connecting tube is closely fitted into the separatory funnel *A*, which has previously been charged with a solution of 5.4 gm. of the stannic chloride salt of thiophenine hydrochloride (equivalent to 0.02 mole of thiophenine) in 25 ml. of water and with 100 ml. of carefully purified ether. The completely assembled apparatus is then suspended on a ring stand at a suitable height and the separatory funnel *A* is submerged in an ice-bath. A two-litre beaker is especially suitable for that purpose because the reaction can be observed without interruption of the cooling. Stopcocks *S* 1 and *S* 2 are then opened while *S* 3 and *S* 4 remain closed and a vigorous current of hydrogen is introduced through the gas inlet tube, *G*. After complete elimination of the air inside the apparatus a solution of 5*N* sodium hydroxide is introduced drop by drop through the funnel *B* (with constant shaking and cooling and introduction of hydrogen)

until the precipitate initially formed has completely dissolved. The aqueous layer in separatory funnel *A* is then drawn off through the stopcock at the bottom and discarded. The ether layer containing the free thiophenine is washed with 50 ml. of water which is added in three portions through separatory funnel *B* and subsequently withdrawn at the bottom of *A* and discarded. Virtually no formation of polymerized thiophenine occurs in this process if the sodium hydroxide is added very carefully and if both the cooling and the agitation through shaking and through the rapid introduction of hydrogen are sufficient. If, however, a small amount of polymerized thiophenine should have been formed it can easily be disposed of by making it adhere to the wall of the separatory funnel *A*. Being of a very viscous nature it is readily eliminated in this way.

After having thus obtained a clear ethereal solution of thiophenine which has been freed from drops of water as thoroughly as possible, stopcock *S* 2 is closed without interrupting the current of hydrogen and the whole apparatus is rapidly and completely inverted. The Erlenmeyer flask *C* will now be at the bottom and separatory funnel *A* at the top, and as soon as stopcock *S* 3 is opened, in order to permit the escape of hydrogen, the ethereal solution of thiophenine in *A* will start running through the connecting tube into the sulphonyl chloride solution in *C* under the combined effects of gravity and hydrogen pressure. The current of hydrogen, which effects a quick mixing of the two solutions, is then interrupted for a moment, 1 ml. of pyridine is introduced into *C* through *S* 2 and the current of hydrogen is turned on again. The whole apparatus is left standing overnight at room temperature while a constant slow current of hydrogen is being maintained.

A considerable amount of a crystalline colourless substance separates. This substance is soluble in water, does not give a Beilstein reaction, and melts at 114° C. after previous slight sintering. It does not, however, contain any thiophenine, as it could be obtained from 1-acetylaminobenzene-4-sulphonyl chloride, dissolved in 1 : 1 ether-acetone with pyridine alone. The nature of this substance has so far not yet been established beyond doubt but we suppose that it is a salt-like combination of 1-acetylaminobenzene-4-sulphonic acid and pyridine. The identity of the substance obtained from the reaction mixture with that produced by mixing the sulphonyl chloride solution with pyridine in the absence of thiophenine was established by the mixed melting point which showed no depression.

The mother liquors from these crystals are then drawn off through *S* 3 into a 300 ml. flask connected with a reflux condenser by means of ground glass joints and previously swept out with hydrogen. This operation was carried out under complete exclusion of air by attaching the flask and condenser to the outlet *S* 3 by means of a Y-shaped connecting piece, using the waste hydrogen from *S* 3 to sweep out the flask, and then inclining the whole apparatus sufficiently to allow the solution to be forced by the hydrogen pressure from *C* through *S* 3 into the attached flask. The solution is then boiled under reflux and with constant introduction of hydrogen for three

hours, after which it is concentrated in a current of hydrogen to about 25 ml. The resulting dark brown solution is then dissolved in one litre of ether and transferred to a separatory funnel. The ether solution is shaken with 500 ml. of water in five portions in order to eliminate pyridine and the substance mentioned above, of which a small amount could be isolated from the water washings. The ether is then dried with sodium sulphate, filtered, and concentrated *in vacuo* to about 100 ml. After standing overnight, a considerable amount of acetylated 2-sulphanilamido-thiophene has separated and is filtered off. Further concentration of the mother liquors yields a second crop of crystals showing the same melting point as the first fraction. The substance is purified by recrystallization from acetone-ether and finally by continuous extraction with ether alone. The pure product is insoluble in water, slightly soluble in benzene and ether, very soluble in acetone and alcohol. It crystallizes from ether or acetone-ether in rhombic platelets and melts at 195° C.

The compound was recrystallized for analysis three times from acetone-ether and finally extracted with ether alone. It was dried at 60° C. and 0.1 mm. over phosphorus pentoxide, sodium hydroxide, and paraffin. Calc. for $C_{12}H_{12}O_3N_2S_2$ (mol. wt. 296.23): N, 9.46%. Found: N, 9.50, 9.44, 9.40%.

V. 2-Sulphanilamido-thiophene

Two hundred milligrams of (1-acetylaminobenzene-4-sulphonamido)-2-thiophene are dissolved in 20 ml. of 2 *N* sodium hydroxide and held in the boiling water-bath for 30 min. The clear solution is cooled with ice and carefully neutralized (litmus) with dilute hydrochloric acid. The precipitate formed crystallizes upon rubbing with a glass rod (colourless needles, which sometimes reach several millimetres in length) and is filtered after standing for some time in the refrigerator. Recrystallized from water, the substance melts at 155° C. Yield, 150 mg. = 87%. It is very soluble in alcohol and acetone, soluble in ether, insoluble in benzene. The substance is purified for analysis by dissolving in dilute sodium hydroxide, filtering, and carefully precipitating with hydrochloric acid. This process is repeated a second time and then followed by one recrystallization from water. The substance is dried at 60° and 0.1 mm. over phosphorus pentoxide and sodium hydroxide. Calc. for $C_{10}H_{10}O_2N_2S_2$ (mol. wt. = 254.22): N, 11.02%. Found: N, 11.05, 11.12%.

References

1. Babasinian, V. S. J. Am. Chem. Soc. 50 : 2748-2753. 1928.
2. Heffter, A. Arch. Physiol. 39 : 420-425. 1886.
3. Meyer, V. Die Thiophengruppe, Friedr. Vieweg und Sohn, Braunschweig. 1888.
4. Stadler, O. Ber. 18 : 1490-1492. 1885.
5. Steinkopf, W. Ann. 403 : 17-44. 1914.
6. Stewart, J. J. Chem. Soc. 121 : 2555-2561. 1922.
7. Volhard, J. and Erdmann, H. Ber. 18 : 454-455. 1885.

ON 4-(OR 5-) AMINOGLYOXALINE (IMINAZOLE)[1]

By G. Hunter[2] and J. A. Nelson[3]

Abstract

The dihydrochloride and sesquipicrate salts of 4-(or 5-)aminoglyoxaline have been prepared in the pure state for the first time. Previous attempts to isolate the substance have failed largely because insufficient allowance was made for the instability of the substance in aqueous media. The new glyoxaline is highly reactive and has unusual properties for a glyoxaline. It has certain properties like those of 4-(or 5-)guanidinoglyoxaline, being here proved to be a hydrolysis product of guanine.

The observation of Hunter (6), subsequently confirmed by Mohr (11), that guanine on hydrolysis yields significant amounts of 4-(or 5-)guanidinoglyoxaline,

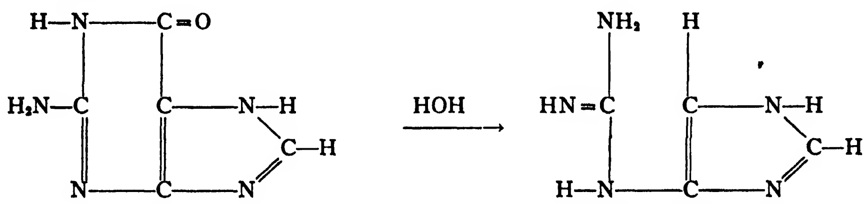

Guanine 4-(or 5-)Guanidinoglyoxaline

in a manner closely analagous to the conversion of uric acid to allantoin, raises a number of points of both chemical and physiological interest.

It was expected on the analogy of the hydrolysis of arginine to ornithine that 4-(or 5-)guanidinoglyoxaline on further hydrolysis would yield urea and 4-(or 5-)aminoglyoxaline,

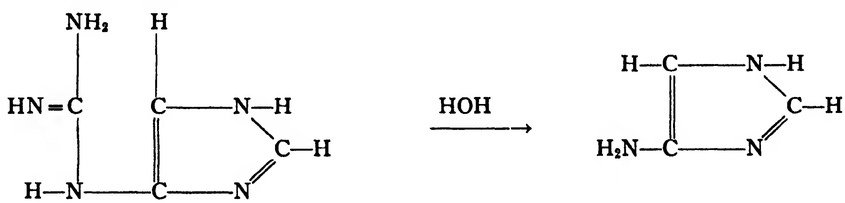

4-(or 5-)Guanidinoglyoxaline 4-(or 5-)Aminoglyoxaline

but the actual product obtained by Hunter (7) was the intermediate 4-(or 5-) carbamidoglyoxaline.

[1] *Manuscript received September 13, 1941.*
Contribution from the Department of Biochemistry, University of Alberta, Edmonton Alta.

[2] *Professor of Biochemistry.*

[3] *Research Assistant, now in Department of Chemistry, Macdonald College, McGill University, Montreal, Que.*

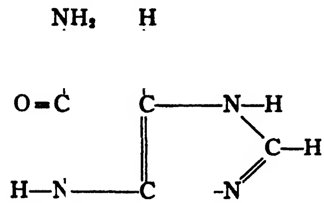

4-(or 5-)Carbamidoglyoxaline

However, in the products of hydrolysis of guanine, of 4-(or 5-)guanidinoglyoxaline, and of 4-(or 5-)carbamidoglyoxaline certain colour tests indicated the presence of another substance, which was probably 4-(or 5-)aminoglyoxaline. This compound has been sought by various workers, notably by Fargher and Pyman (5), Fargher (4), and Balaban (1), but it has not hitherto been isolated. Hunter and Hlynka (8) though also failing to isolate the substance were nevertheless successful in synthesizing 4-(or 5-)carbamidoglyoxaline by the addition of cyanic acid to a solution of 4-(or 5-)nitroglyoxaline reduced by sodium amalgam.

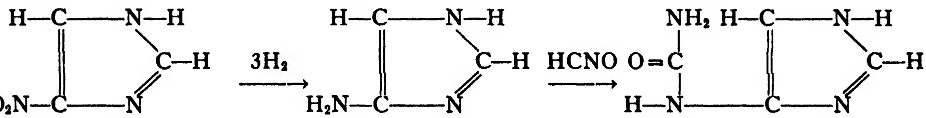

4-(or 5-)Nitroglyoxaline — 4-(or 5-)Aminoglyoxaline — 4-(or 5-)Carbamidoglyoxaline

This synthesis confirmed the existence of 4-(or 5-)aminoglyoxaline.

Because of the interest attached to this substance it was decided to make further attempts to isolate it. It was thought that it might readily be obtained from its acetyl derivative, which the writers found could be prepared by reducing 4-(or 5-)nitroglyoxaline with stannous chloride in the presence of acetic anhydride. The acetyl derivative, however, on hydrolysis with acids underwent fission of the glyoxaline nucleus, and hydrolysis with base led to similar results, though in the latter case traces of the aminoglyoxaline were detectable in the hydrolysate.

Recourse was thus made to the original line of attack. The writers were satisfied that the sodium amalgam method of reduction of the nitroglyoxaline gave good yields with minimum decomposition of the product. The solution of the problem seemed to lie in maintaining conditions during the isolation such as would avoid destruction of this very unstable glyoxaline.

As observed by Hunter and Hlynka (8), reduced solutions of the nitroglyoxaline gave a characteristic methylene-blue-like colour with the diazo reagent of Koessler and Hanke (10). The only other substance recorded as giving such a diazo test is 4-(or 5-)guanidinoglyoxaline. It might be expected that the amino- and the guanidino-substituents in the 4-(or 5-) position of the glyoxaline nucleus would have a like effect on the colour obtained in the diazo test. It was virtually certain at this stage that the diazo test

could be used to follow the synthesis or destruction of 4-(or 5-)amino-glyoxaline in solutions. Thus it was soon observed that the substance rapidly disappeared from aqueous solutions especially in the presence of acid. It was more stable in alkaline solution and seemed to hydrolyse readily in the presence of water. Accordingly, the reduction and isolation procedure was designed to maintain anhydrous conditions. The new base has been prepared as the dihydrochloride and as the sesquipicrate.

The properties of the substance are described and discussed later.

The writers failed to prepare the free base. The preparation of the salts described below is not unattended with difficulty and some uncertainty. The preparation should be carried through as expeditiously as possible.

Experimental

Synthesis of 4-(or 5-)Acetylaminoglyoxaline

4-(or 5-)Nitroglyoxaline (1 gm.), prepared according to the method of Fargher and Pyman (5), was suspended in 50 ml. of acetic anhydride and 20 ml. of glacial acetic acid and run slowly from a dropping funnel into a cold solution of 12 gm. of stannous chloride dihydrate in 40 ml. of acetic anhydride and 20 ml. of concentrated hydrochloric acid (37%). The reaction was carried out in an atmosphere of nitrogen. As the 4-(or 5-)nitroglyoxaline suspension was added, the temperature rose to about 90° C., at which temperature it was kept until the reaction was complete (usually 1.25 hr.) as judged by the diazo test.

When the reaction was complete the straw yellow solution was cooled to 0° C. and neutralized with 10 N sodium hydroxide, 2.5 N sodium hydroxide being used as the end-point was approached. The precipitated tin hydroxides were centrifuged off and washed five times with 150 ml. portions of distilled water.

The clear supernatant solution and washings were slightly acidified with sulphuric acid. To the acid solution was added just sufficient 25% aqueous mercuric acetate solution to react with all the compounds in solution. The solution was then brought to neutrality with barium hydroxide and the precipitate removed by centrifugation. After washing the mercury precipitate several times with water it was suspended in 200 ml. of 0.05 N sulphuric acid and treated with hydrogen sulphide. The mercuric sulphide was centrifuged off and washed with water saturated with hydrogen sulphide at least four times, using 150 ml. each time. The supernatant solution and washings were concentrated *in vacuo* to about 500 ml.

This solution was treated with 10% silver nitrate in slight excess as shown by the formation of silver oxide when a drop of the filtrate was made alkaline with barium hydroxide. The precipitate, mainly silver chloride, was centrifuged off and washed with 100 ml. portions of water four times. The supernatant and washings were made distinctly alkaline with barium hydroxide to precipitate the glyoxaline silver salt. This second precipitate was centri-

fuged off and washed with four 100 ml. portions of 0.05 *N* barium hydroxide. The silver precipitate was suspended in 150 ml. of 0.1 *N* sulphuric acid and treated with hydrogen sulphide. The silver sulphide was centrifuged off and washed four times with hydrogen sulphide water, using 100 ml. each time. The supernatant and washings were combined and concentrated to about 50 ml. *in vacuo*.

The concentrated solution was then treated with cold saturated barium hydroxide to just free the solution of sulphate ions.

The neutral solution was concentrated *in vacuo* to 10 to 15 ml. and bleached with charcoal. On further concentration of the solution to a volume of about 2 ml. the 4-(or 5-)acetylaminoglyoxaline crystallized out as white needles. This was purified, not very satisfactorily, by recrystallization from 97% dioxane. Crude yield; 50% of the theoretical. M.p. 226° C. (uncorrected). Found (micro-analysis): H, 5.70; C, 48.77; N, 34.32%. Calc. for $C_5H_7N_3O$: H, 5.64; C, 48.00; N, 33.59%.

An acetyl determination was carried out on the material using the method of Pregl for micro N-acetyl determinations. It was found that the results were twice too high for those required by the formula $C_5H_7N_3O$. This is explained from the fact that formic acid is formed through fission of the glyoxaline nucleus during hydrolysis. The presence of this acid was confirmed and it was determined quantitatively with alkaline potassium permanganate.* On making the residue from the hydrolysis alkaline with 10 *N* sodium hydroxide, ammonia was also distilled over and determined quantitatively. The final residue after the removal of the acetic acid, formic acid, and ammonia was tested for the presence of glycine by the method of Engel (3) using phenol and sodium hypochlorite. Glycine was found to be present. The following results were obtained from the hydrolytic determinations: acetic acid as CH_3CO, 33.71%; formic acid as $\equiv$C—H, 10.7%; ammonia as N_2H, 24.2%. The formula $C_5H_7N_3O$ requires: acetic acid, 34.4; formic acid, 10.4; ammonia, 24.2%. These figures give the hydrolytic products as 1 mole of acetic acid, 1 mole of formic acid, 2 moles of ammonia, and 1 mole of glycine, as expected from the following scheme (see Hunter (6)).

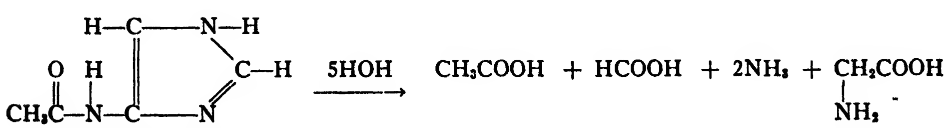

4-(or 5-)Acetylaminoglyoxaline Acetic Formic Glycine

* *Formic acid was determined quantitatively as follows. The distillate from the acetyl determination was made alkaline with 5 ml. of 5 N sodium hydroxide, and an excess of 0.02 N potassium permanganate was added. This solution was heated to 90° C. and kept at this temperature for 15 min. At the end of this time the solution was neutralized with sulphuric acid and 5 ml. of 10 N sulphuric acid added in excess. To this was added a slight excess of 0.02 N sodium oxalate and this was back titrated with the standard potassium permanganate. By the use of sodium oxalate in an acid solution a more sensitive end-point can be obtained.*

4-(or 5-)Acetylaminoglyoxaline readily forms a crystalline picrate in the form of needles, m.p. 208° C., and a flavianate of diamond-shaped crystals, m.p. 260° C.

The acetylaminoglyoxaline is easily soluble in water and slightly soluble in methanol. It is insoluble in ethanol, diethyl ether, acetone, and dioxane.

A minute amount of the substance gives an immediate and intense red colour with the diazo test. The nitroprusside test is entirely negative. A speck of the material on heating with ninhydrin and pyridine gives a garnet colour. Ferric chloride in acetic acid gives an orange colour. Treatment with bromine in alkali gives a brownish colour.

Preparation and Isolation of 4-(or 5-)Aminoglyoxaline Dihydrochloride

4-(or 5-)Nitroglyoxaline (1 gm.) was suspended in 150 ml. of methanol and cooled to 0° C. in an ice-bath. Nitrogen was bubbled through the solution to remove oxygen, then 3 gm. of 3% sodium amalgam was added. The suspension was then stirred vigorously to prevent the amalgam from settling to the bottom of the flask. When reduction was complete (usually 15 min.) as judged by the diazo test, the dirty bluish solution was decanted off and the remaining amalgam was washed three times with 15 ml. portions of methanol.

To the alkaline solution was added just enough mercuric acetate in methanol for complete precipitation. The precipitate was centrifuged off and washed with 200 ml. of water. This removed more of the impurities than washing with alcohol alone, and, as the mercury salt, the 4-(or 5-)aminoglyoxaline is relatively stable in water. The precipitate was washed with three 150 ml. portions of methanol after which it was assumed that all the water had been washed out. The precipitate was then suspended in methanol, and dry hydrogen chloride was bubbled in until the suspension tended to settle out rapidly. The mercury was then removed as the sulphide. During this treatment with hydrogen chloride and hydrogen sulphide the material was immersed in an ice-bath. The mercuric sulphide was centrifuged off and washed three times with 150 ml. portions of methanol. The solution was then concentrated *in vacuo* to about 20 ml. and filtered into a 3 cm. side-arm tube through a sintered glass funnel. The dark brown solution was then concentrated to 5 to 6 ml. *in vacuo* and treated with dry hydrogen chloride at 0° C. until precipitation was complete. The crystalline material was collected in a Schwinger vacuum filter and washed with several small portions of cold methanol and finally with cold pure diethyl ether.

The crude 4-(or 5-)aminoglyoxaline dihydrochloride was purified by dissolving it in a minimum volume of cold methanol and reprecipitating it with an equal volume of cold pure diethyl ether. The grey crystalline material was collected in a Schwinger vacuum filter and washed with several 0.5 ml. portions of 1 : 1 ether-methanol solution and then with pure diethyl ether. A second crop was obtained by adding an equal volume of diethyl ether to the filtrate and washings. Crystals, quadratic plates, m.p. 184° C. (uncor-

rected). Purified yield, 30% of the theoretical. Found: N, 26.83; Cl, 45.47%. Calc. for $C_3H_5N_3 . 2HCl$: N, 26.93; Cl, 45.48%. Amino nitrogen (Van Slyke):

I. 3.42 mg. substance gave 0.63 ml. of nitrogen at 25° C. and 703 mm. pressure, equals 9.72% amino N.

II. 4.34 mg. substance gave 0.74 ml. of nitrogen at 25° C. and 703 mm. pressure, equals 9.01% amino N.

The formula $C_3H_5N_3 . 2HCl$ requires 8.97% amino N.

Synthesis of 4-(or 5-)Aminoglyoxaline Sesquipicrate

4-(or 5-) Nitroglyoxaline (1 gm.) was reduced and the product precipitated with mercuric acetate as for the formation of the dihydrochloride. After washing the precipitate as above it was suspended in 150 ml. of methanol, and 3 gm. of purified picric acid was added. The glyoxaline was then freed of mercury with hydrogen sulphide and the mercuric sulphide formed was removed by centrifugation and washed with four 150 ml. portions of methanol.

The supernatant and washings were combined and evaporated *in vacuo* to 20 ml. This was transferred to a side-arm tube and evaporated further to the point at which fine needles just began to form. The solution was then filtered and washed with two 1 ml. portions of methanol. The precipitate here was discarded. The filtrate was further concentrated to about 0.5 ml. and was filtered into a sintered glass funnel. The crystals were washed with several portions of benzene to remove the excess picric acid and then with two 1 ml. portions of cold ethanol.

The material was redissolved in cold ethanol and evaporated *in vacuo* to about 0.5 ml. The crystals thus formed were collected in a sintered glass funnel and washed with two 1 ml. portions of cold ethanol. Yield of the pure picrate was 25% of the theoretical; m.p. 194° C. (uncorrected). Picric acid determinations were carried out on this material by the nitron method of Busch (2). Found: picric acid, 57.88%. Calc. for $(C_3H_5N_3)_2 . C_6H_3N_3O_7$: picric acid, 58.1%.

4-(or 5-)Aminoglyoxaline dihydrochloride and picrate are soluble in water, ethanol, and methanol. They are insoluble in benzene, acetone and diethyl ether.

Further Properties, Colour Tests, and Reactions of 4-(or 5-)Aminoglyoxaline

4-(or 5-)Aminoglyoxaline behaves as a typical glyoxaline in being precipitated by salts of mercury, silver, and by phosphotungstic acid. It gives a white precipitate with neutral ammoniacal silver solution which on warming rapidly darkens.

The base is unstable in aqueous media. A little of the dihydrochloride in water decomposes with the formation of brown and black pigments. In the presence of acids at room temperatures the glyoxaline ring suffers fission, as can readily be determined by the diazo test.

Diazo test. The substance (0.01 mg.) added to 7.5 ml. of diazo reagent gives an immediate methylene-blue-like colour, as described for guanidinoglyoxaline (6). On acidification the colour changes to a purplish-red.

Sodium nitroprusside test, as carried out by Rothera (12), is almost as sensitive as the diazo test. A blue-violet colour is obtained similar to that given by cysteine. This test, found to be given by the hydrolysates from both the guanidino- and the carbamidoglyoxaline, was thought by Hunter (7) to be more probably attributable to the presence of 4-(or 5-)hydroxyglyoxaline than to the aminoglyoxaline. The isolation of the aminoglyoxaline now settles this point and provides an explanation for other colour tests noted by Hunter (7) in the earlier work.

Ninhydrin test. When a speck of the substance is dissolved in a little water and ninhydrin and a drop of pyridine added, a grass-green colour develops slowly in the cold, and very rapidly on slight warming. The solution soon becomes brownish with a blue-green precipitate. The precipitate when separated and washed with water is soluble in alkali and reprecipitated by acid.

This test, which is quite distinct from the ninhydrin test typical of the amino acids, has previously been noted by Hunter (7) as given by the hydrolytic product of guanidino- and carbamidoglyoxalines.

Nitrous acid. As observed above, the 4-(or 5-)aminoglyoxaline yields its NH_2 nitrogen normally in the Van Slyke method. Under the Van Slyke conditions the glyoxaline ring is also broken. However when a speck of material is dissolved in a few drops of dilute acetic acid, the solution cooled in ice, and a drop of 0.5% sodium nitrite added, a faint passing green colour is observed. If a drop of this solution is quickly added to 1.1% sodium carbonate a slight greenish colour develops. If a drop is added to a mixed diazo reagent an unstable dull red colour appears; if a drop is added to 2.5 *N* sodium hydroxide a brown colour immediately appears, becoming bluish later; if a drop is added to 2.5 *N* sodium hydroxide in the presence of a little β-naphthol the colour is the same as for 2.5 *N* sodium hydroxide.

The significance of the blue colour with the nitrous acid and the red diazo test are dealt with more fully by Hunter and Hlynka (9). The fact that there is no coupling with β-naphthol indicates that the 4-(or 5-) carbon atom of the 4-(or 5-)aminoglyoxaline is not benzoid in character.

Ferric chloride in the presence of acetic acid gives a purple colour with 4-(or 5-)aminoglyoxaline.

Bromine in acid solution is absorbed by solutions of 4-(or 5-)aminoglyoxaline with fission of the glyoxaline nucleus. If, however, a speck of substance is dissolved in 2.5 *N* sodium hydroxide and a little bromine water added, a clear blue colour is produced. This is further discussed by Hunter and Hlynka (9).

Potassium permanganate. Solutions of the substance in the presence of sulphuric acid rapidly absorb potassium permanganate, with the production of a brown colour. This test is not typical of the glyoxaline nucleus. It is possibly indicative of the tautomeric change as indicated

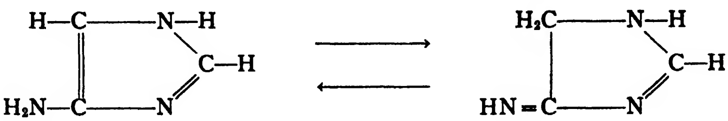

4-(or 5-)Aminoglyoxaline 4-(or 5-)Iminoglyoxylidine

In alkaline solution, potassium permanganate gives a bright green colour with 4 - (or 5 -) aminoglyoxaline, 4 - (or 5 -)acetylaminoglyoxaline, or with histidine. This is typical of the behaviour of glyoxalines with alkaline potassium permanganate.

Cupric carbonate. When a little of the substance is heated with cupric carbonate a dirty blue solution is obtained. If the bluish precipitate is separated, washed, the copper removed as cupric sulphide, and the hydrogen sulphide removed from solution with nitrogen, a lemon-yellow solution results. On making this alkaline, a blue colour rapidly develops. This test is discussed more fully by Hunter and Hlynka (9).

The high reactivity of 4-(or 5-)aminoglyoxaline is illustrated by the following tests:

A little of the dihydrochloride is put in a dry test-tube and two drops of acetic anhydride is added. On grinding with a glass rod, fine white crystals of 4-(or 5-)acetylaminoglyoxaline appear. A diazo test will show a bright red colour as described above for this derivative.

A little of the dihydrochloride dissolved in methanol with a drop of glacial acetic acid and a little potassium cyanate soon shows evidence, when left at room temperature, of the synthesis of 4-(or 5-)carbamidoglyoxaline. After a day or so, a drop of the solution will give a clear red diazo test indicative of the conversion of the amino- to the carbamidoglyoxaline (8).

Acknowledgments

The writers are indebted to Dr. Stanley Cook of Ayerst, McKenna and Harrison, Montreal, for microanalysis.

Most of the 4- (or 5-) nitroglyoxaline used in the research was prepared by Mr. T. H. Evans.

Mr. M. M. Pechet assisted in the preparation of the 4-(or 5-) acetylamino-glyoxaline.

This work was assisted by a grant from the Associate Committee on Medical Research of the National Research Council.

References

1. Balaban, I. E. J. Chem. Soc. 268-273. 1930.
2. Busch, M. Ber. 38 : 861-866. 1905.
3. Engel R. As quoted in J. Chem. Soc. Ab. 28 : 885. 1875.
4. Fargher, R. G. J. Chem. Soc. 117 : 669-680. 1920.
5. Fargher, R. G. and Pyman, F. L. J. Chem. Soc. 115 : 217-260. 1919.
6. Hunter, G. Biochem. J. 30 : 1183-1188. 1936.
7. Hunter, G. Biochem. J. 30 : 1189-1201. 1936.
8. Hunter, G. and Hlynka, I. Biochem. J. 31 : 488-489. 1937.
9. Hunter, G. and Hlynka, I. Can. J. Research, B, 19(12) : 305-309. 1941.
10. Koessler, K. K. and Hanke, M. T. J. Biol. Chem. 39 : 497-519. 1919.
11. Mohr, M. Z. Physiol. Chem. 249 : 57-64. 1937.
12. Rothera, A. C. H. J. Physiol. 37 : 491-494. 1909.

ON A NEW INDIGOID FORMED FROM THE GLYOXALINE (IMINAZOLE) NUCLEUS[1]

By G. Hunter[2] and I. Hlynka[3]

Abstract

Among the products of reduction of 4-(or 5-)nitroglyoxaline, formation of a blue pigment has been observed by various workers. The authors regard this pigment as a diglyoxalone containing the characteristic indigoid group, —CO . C=C . CO—. Its formation is dependent on the existence of 4-(or 5-) hydroxyglyoxaline, formed by deamination of the corresponding amino- compound. The hydroxyglyoxaline readily tautomerizes to the glyoxalone, which on oxidation condenses to form the pigment in question.

Fargher and Pyman (4) observed that when 4-(or 5-)nitroglyoxaline was reduced with alkaline sodium hyposulphite the liquors, on exposure to air, turned blue, and on acidification gave a blue precipitate. This formation of blue pigment had been previously noted by Behrend and Schmitz (1) and subsequently by others, but no one, to the writers' knowledge, has provided an explanation for its formation.

From the reduction products of 4-(or 5-)nitroglyoxaline Fargher (3) isolated glycine, and to account for it formulated the following likely chain of reactions:

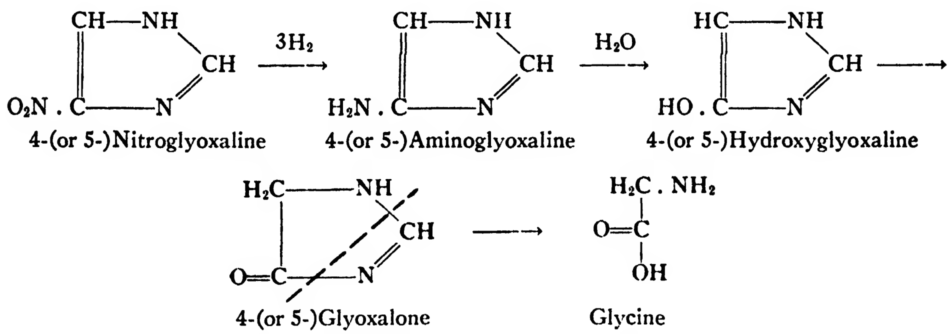

4-(or 5-)Nitroglyoxaline 4-(or 5-)Aminoglyoxaline 4-(or 5-)Hydroxyglyoxaline

4-(or 5-)Glyoxalone Glycine

assuming the glyoxalone ring to break in the manner indicated.

From the observation of Pyman (8) of amidine formation another possible mechanism of degradation of 4-(or 5-)aminoglyoxaline is:

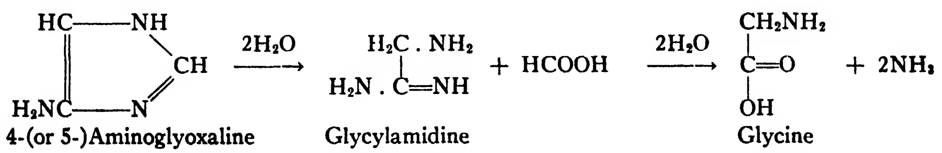

4-(or 5-)Aminoglyoxaline Glycylamidine Glycine

If glycine can be formed only through the intermediary amidine, then the hypothetical hydroxyglyoxaline and glyoxalone of Fargher become open to

[1] *Manuscript received September 13, 1941.*
Contribution from the Department of Biochemistry, University of Alberta, Edmonton, Alta.

[2] *Professor of Biochemistry.*

[3] *Research Assistant; now in Division of Dairy Research, Ottawa.*

question. The significance of glycine as an end-product of the degradation of certain glyoxalines has already been discussed by Hunter (5). It has been shown by Hunter and Nelson (7) to arise from 4-(or 5-)acetylaminoglyoxaline, and it can readily be shown to arise from 4-(or 5-)aminoglyoxaline by a variety of treatments, all fundamentally hydrolytic.

The above question can, however, be answered with the deaminised product of 4-(or 5-)aminoglyoxaline. This has been proved by Hunter and Nelson to deaminate quantitatively in the van Slyke machine. The product of deamination can be shown to yield glycine, so that, whether or not glycine may arise from its amidine, it can also arise through the mechanism suggested by Fargher. The probability of the existence of the hydroxyglyoxaline and glyoxalone is thus increased. The writers propose to examine other evidence for the existence of those substances, upon which is based their explanation of the blue pigment in question.

The following tests on 4-(or 5-)aminoglyoxaline dihydrochloride shed some light on the problem.

A little of the substance was treated in the cold with somewhat more than the theoretical amount of sodium nitrite in dilute acetic acid. A greenish colour appeared in the solution. Portions of it were tested as follows:

(*a*) Added to 2.5 *N* sodium hydroxide solution a dirty blue colour was formed.

(*b*) Added to 2.5 *N* sodium hydroxide solution in presence of β-naphthol a similar colour appeared, indicating absence of diazo linkage.

(*c*) On addition of one drop to the diazo reagent an immediate clear red colour, though rather faint, appeared. This indicates complete deamination and the probable presence in solution of 4-(or 5-)hydroxyglyoxaline.

(*d*) Ninhydrin test negative, thus absence of glycine at this stage.

The above solution was made about 0.1 *N* with sodium hydroxide and kept at boiling point for about 10 min. It was then cooled and made just acid with acetic acid. Portions of this were tested as follows:

(*e*) Diazo test entirely negative, indicating complete fission of all glyoxaline nuclei.

(*f*) Nessler's solution indicated mere trace of ammonia.

(*g*) Ninhydrin test, deep blue, indicative of glycine.

Thus the writers conclude that glycine is formed from 4-(or 5-)hydroxyglyoxaline, or more probably from the glyoxalone. From the faint red diazo test it would appear that 4-(or 5-)glyoxalone, which would not give a diazo test, is rapidly formed from 4-(or 5-)hydroxyglyoxaline. In presence of oxygen in alkaline solution blue pigment is produced.

Furthermore, Hunter (6) observed that the alkaline hydrolysates of both guanidino- and carbamidoglyoxalines when exposed to air rapidly turn blue. Hunter and Nelson have observed that the barium hydroxide hydrolysate of

4-(or 5-) acetylamino- and of 4-(or 5-)aminoglyoxaline behave similarly. So it is apparent that the blue pigment is formed from the glyoxaline nucleus, and the guanidino-, carbamido- or amino- group have no part in its production.

The work of Davidson and Baudisch (2) on urindigo, the first member of a new class of indigoids derived from pyrimidines, suggested that the blue pigment we were studying might be an indigoid derived from 4-(or 5-)glyoxalone in the following manner.

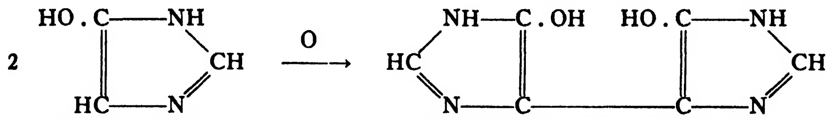

5-Hydroxyglyoxaline 5,5′-Hydroxydiglyoxaline-4 (leuco form)

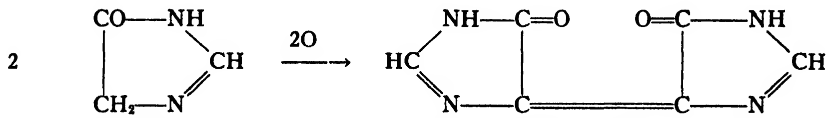

5-Glyoxalone 5,5′Diglyoxalone-4 (blue)

In the Experimental Section are described two preparations that the writers regard as corresponding to the leuco and blue forms of the pigment.

There may be mentioned a number of other reactions, whose mechanisms are less clear, but which probably give rise to the same blue pigment.

If a speck of 4-(or 5-)aminoglyoxaline dihydrochloride is dissolved in 2.5 *N* sodium hydroxide and a little bromine water added, a clear deep blue colour appears.

When dissolved in a little acetic acid the substance yields a purple colour with ferric chloride.

When boiled with cupric carbonate in sodium carbonate solution as described below, a blue pigment is formed.

Experimental

Preparation of 5,5′-Hydroxydiglyoxaline-4

Guanidinoglyoxaline dihydrochloride (0.5 gm.) was heated on a water-bath for seven minutes with two equivalents of freshly prepared cupric hydroxide suspended in 45 ml. of 1.1% sodium carbonate. The dark blue precipitate of copper salts that formed was separated by centrifugation and the supernatant fluid discarded. The copper salt, washed once, was suspended in water, acidified with glacial acetic acid and freed from Cu^{++} with hydrogen sulphide in the usual way. The resulting solution was freed from hydrogen sulphide by bubbling carbon dioxide rapidly through it.

The solution so obtained was lemon yellow in colour and contained about 50% of the original guanidinoglyoxaline together with the oxidation product. On addition of a drop of alkali to a test portion of the solution an immediate blue colour was produced.

The lemon yellow solution was made definitely acid to Congo red with glacial acetic acid, and an excess (about 3 ml.) of 10% silver nitrate was added. The yellow precipitate formed in acid solution was removed by centrifugation and washed with a small amount of 0.1 N acetic acid. It was then suspended in 5 ml. of 0.1 N acetic acid and Ag^+ was removed with hydrogen sulphide. The resulting solution, freed from hydrogen sulphide, was reduced to a small volume *in vacuo* and glacial acetic acid was added. It was then further evaporated to a volume of 0.5 ml. A lemon yellow precipitate was obtained by further addition of 5 ml. of glacial acetic acid. The solution and the precipitate were quickly transferred to a small test-tube, avoiding oxidation as much as possible, the test tube stoppered, and centrifuged. The supernatant was decanted and the precipitate washed twice with glacial acetic acid. The final precipitate was dried in a vacuum desiccator.

If care is not taken to avoid oxidation, the substance may turn red or blue, or may decompose, at any stage. The yield is very small, about 16 mg.

This is a crude preparation of what the writers regard as 5,5'-hydroxydiglyoxaline-4. It gives a number of colour reactions, already described. With sodium hydroxide, barium hydroxide, or ammonium hydroxide a blue colour is produced. With ferric chloride or bromine water a blue colour is also obtained. The substance is very unstable in solution but may be kept for long periods of time if dry.

Preparation of 5,5'-Diglyoxalone-4

It is possible to prepare the blue pigment, which the writers formulate as 5,5'-diglyoxalone-4, from guanidino- or carbamidoglyoxaline by the procedure just described, and by converting the leuco form to the blue pigment. The following alternative and more economical method has been used.

Nitroglyoxaline (1 gm.) suspended in 100 ml. of methanol was reduced with 50 gm. of 3% sodium amalgam in the usual manner. The alcoholic mixture was then acidified with nitric acid and the insoluble pigment was removed by centrifugation. The supernatant fluid was evaporated to dryness, the residue taken up in 25 ml. of water and a second insoluble residue was removed by centrifugation. The supernatant was made just neutral with sodium hydroxide and boiled on a water-bath for three minutes with two equivalents of cupric hydroxide in 45 ml. of 1.1% sodium carbonate. It was then centrifuged and the supernatant and washings were discarded. The precipitate was suspended in 15 ml. of water, acidified with sulphuric acid and Cu^{++} removed with hydrogen sulphide. The clear lemon yellow supernatant and washings from cupric sulphide was freed from hydrogen sulphide by bubbling through it carbon dioxide. Excess solid barium hydroxide was added. The solution acquired a deep blue colour on being shaken with air. After a half-hour it was neutralized with sulphuric acid and the barium sulphate precipitate washed until the extraneous pigment was removed. The blue pigment was then extracted from the barium sulphate precipitate with small portions of water to which a drop of 2.5 N sodium hydroxide was

added. The extraction was continued until all the pigment was removed. It was then precipitated by the addition of a slight excess of sulphuric acid. The pigment so obtained is contaminated with a large amount of barium sulphate, which is very difficult to remove completely. It was redissolved in water containing a minimum amount of 2.5 *N* sodium hydroxide. The solution was centrifuged at high speed to remove as much of the barium sulphate as possible, and the pigment was again reprecipitated with sulphuric acid. This procedure was repeated until the barium sulphate was removed. The pigment was finally washed with water, then alcohol, and dried *in vacuo*. The particles were too fine to be caught on a filter, and were removed by centrifugation. Yield, 7 mg. Found: N, 35.65, 34.32, 34.21%. Calc. for 5,5′-diglyoxalone-4: N, 34.15%. On the evidence of the nitrogen determination, and previous considerations as already given, it is formulated as 5-5′-diglyoxalone-4.

Acknowledgments

Acknowledgment is made to the Associate Committee on Medical Research of the National Research Council for a grant in aid of this work.

The writers would thank Mr. J. A. Nelson, for some technical assistance in the later stages of this research.

References

1. Behrend, R. and Schmitz, J. Ann. Chem. 277 : 310-339. 1893.
2. Davidson, D. and Baudisch, O. J. Biol. Chem. 64 : 619-623. 1925.
3. Fargher, R. G. J. Chem. Soc. 117 : 668-680. 1920.
4. Fargher, R. G. and Pyman, F. L. J. Chem. Soc. 115 : 217-260. 1919.
5. Hunter, G. Biochem. J. 30 : 1183-1188. 1936.
6. Hunter, G. Biochem. J. 30 : 1189-1201. 1936.
7. Hunter, G. and Nelson, J. A. Can. J. Research, B. 19(12) : 296-304. 1941.
8. Pyman, F. L. J. Chem. Soc. 121 : 2616-2626. 1922.

ON THE DETERMINATION OF URINARY GLYOXALINES (IMINAZOLES)[1]

By G. Hunter[2] and T. M. Raragosky[3]

Abstract

A method is described for the estimation of urinary glyoxalines that has certain advantages over the Koessler and Hanke method, though based on the same principles of urinary fractionation by basic lead acetate and employing the Koessler and Hanke diazo reagent. It is found that normal individuals commonly excrete 200 mg. of urinary glyoxalines, though some excrete less than half this amount, and others two or three times this amount in the course of 24 hr. Urine glyoxalines are thought to be largely of endogenous metabolic origin.

That glyoxaline derivatives are present in human urine was first proved by Engeland (4), who in 1908 isolated from it histidine and two other unidentified glyoxalines, one of which appeared to be glyoxaline amino acetic acid. Histidine has subsequently been isolated from human urine by Hunter (5), Armstrong and Walker (2), and Ackermann and Fuchs (1). Kapeller-Adler (8) has recently isolated small amounts of histamine from urines of pregnant women with eclampsia. Ackermann and Fuchs (1) had shortly before succeeded in isolating only 0.9 mg. of histamine dipicrate from 1000 litres of normal urine. It is unlikely that histamine constitutes a significant part of the glyoxalines present in urine.

In recent years interest in urinary glyoxalines has been increased by the claims notably of Kapeller-Adler (8) that histidine excretion is increased during pregnancy. The evidence of Kapeller-Adler is based largely on the finding that the urines of pregnant women give a positive Knoop test that is not found in the urine of men or of non-pregnant women. It has been suggested that there is a relationship between the excretion of histidine and the urinary gonadotropins.

The need for a method for determining urinary glyoxalines is obvious on wider considerations. Little is yet known of the metabolism of the glyoxaline nucleus, present in the essential amino-acid histidine, and in the dipeptide carnosine, found abundantly in certain mammalian muscles. On the evidence to date it is likely that much of the glyoxaline nuclear material ingested suffers fission during metabolism. Koessler and Hanke (11) and Lélu (12) have found some increase in urinary glyoxaline following high protein diets, but the increase was insufficient to account for the extra histidine intake. According to Kapeller-Adler the excretion of histidine in the urine is dependent on the presence of an enzyme, histidinase, in the liver. However, as Engeland has already indicated, histidine is not the only glyoxaline present in human urine. For a closer study of such problems the writers have elaborated the

[1] *Manuscript received September 13, 1941.*
Contribution from the Department of Biochemistry, University of Alberta, Edmonton, Alta.
[2] *Professor of Biochemistry.*
[3] *Research Student in the Faculty of Medicine.*

present method for the determination of urinary glyoxalines. The method may be regarded as a modification of that of Koessler and Hanke (11).

Two main colour tests are available for measuring urinary glyoxalines: the Knoop test (9) and the diazo test. When bromine is added to an acid solution of histidine in very slight excess, and the solution warmed, a brown colour is produced. This is the Knoop test. It is rather highly specific for histidine, but not very sensitive, and the colour obtained is subject to variation by a variety of interfering substances. There are certain glyoxalines apparently present in urine that do not respond to the test. It will not be considered further.

The diazo test employed here depends on the fact that most glyoxalines present in biological material couple in a weakly alkaline solution with diazotized sulphanilic acid to give orange or red coloured azo products. One notable exception is anserine, in which there is a CH_3- group in the 1-position of the glyoxaline ring. The diazo test is relatively sensitive and in suitable solutions of glyoxaline gives strict proportionality between colour produced and amount of reactant present. However, when coupling takes place in an alkaline medium, the diazo test is not highly specific. Phenols, for example, couple quantitatively like glyoxalines, and numerous substances interfere with colour development. Among these may be mentioned sulphides, ammonia, purines, acetone, acetoacetic acid, and certain chromogens found in urine: see Koessler and Hanke (11) and Hunter (6). In presence of a critical concentration of an interfering substance the azo colour produced, for example, from histidine, will be yellow, or orange, instead of a clear pink, and the proportionality between histidine present and colour produced ceases to hold. In the relevant range this linear proportionality serves as the best criterion of the reliable determination of glyoxalines by azo colorimetry.

The diazo test was first applied to urine by Ehrlich (3) in 1882, as a means for detecting a substance, not yet isolated, present in typhoid and certain other febrile conditions. As it is most probably not a glyoxaline it will not be further discussed here. Ehrlich's observation, however, led to a copious literature on "the diazo reaction of urine", which has been discussed in its essentials by Hunter (6). Not till Engeland's isolation of histidine from urine, however, was it recognized that glyoxaline derivatives probably contributed largely to the diazo reaction of normal urine.

When urine is mixed with the diazo reagent the yellow or orange colour produced is never proportional to the amount of urine used, as there are always substances present that interfere with colour development. This was realized by Weiss (14) who first recognized that by treating urine with basic lead acetate, phenolic and other substances are precipitated, while the glyoxalines appear in the filtrate. The diazo reagent of Pauly (13) used by Weiss was, however, not suitable for quantitative colorimetry, as the investigations of Weiss were more concerned with the constituents of the lead precipitate than with those of the filtrate. It thus remained for Koessler and Hanke (11), with the use of their own diazo reagent (10), to elaborate a method that may

be regarded as the first with any claim to accuracy for the estimation of urinary glyoxalines.

Experimental

Preparation of Glyoxaline Fraction from Urine

Five ml. of urine is placed in a 15 ml. centrifuge tube, followed by 4.0 ml. of 40% normal lead acetate $[Pb(CH_3COO)_2 . 3H_2O]$, with shaking. Four ml. of 2.0 *N* sodium hydroxide is then added and the contents thoroughly mixed. The tube is then centrifuged until the precipitate is well packed (two to five minutes). The supernatant fluid is poured off through a small filter paper, to remove floating particles of the lead precipitate, into a 50 ml. centrifuge tube. The drained lead precipitate is well suspended in 3.0 ml. of water and the tube again centrifuged. The supernatant fluid is filtered as before. The washing is repeated and the lead precipitate is discarded.

The filtrate should be as clear and colourless as water, slightly alkaline, and contain a trace of lead. The lead is precipitated by the addition of a few drops of 20% disodium hydrogen phosphate solution. The latter should be in slight excess to insure that all lead is removed at this stage.

The supernatant fluid from the centrifuged solution is decanted into a 125 ml. Erlenmeyer flask. The tube and lead phosphate precipitate are washed with a little water.

The flask is now placed on a temperature controlled hot plate at about 110° C., and the contents gently boiled to dryness. The white crystalline residue is now dissolved in a little water, transferred to a 10 ml. volumetric flask, and made up to the mark with washings. The glyoxaline fraction, now ready for colorimetry, has thus twice the volume of the native urine.

In the copious lead precipitate discarded in the method described above, there are present lead salts of such inorganic radicals as phosphate, carbonate, sulphate, and sulphide; such organic materials as sugars, acetone bodies, phenols, and purines; and such pigments as urochrome, urobilin, and their chromogens, as well as other chromogens and pigments, as bilirubin. The writers have tested urines containing glucose and giving a strong test for acetone bodies with ferric chloride, and found the lead filtrate quite free from these substances. When there is a high proportion of glucose present there is of course a larger lead precipitate.

There is no appreciable glyoxaline occluded in the lead precipitate. Koessler and Hanke (11) showed that glyoxaline acetic acid added to urine can be recovered quantitatively, and we have found that added histidine can be likewise recovered.

Evaporation to dryness of the faintly alkaline solution serves to get rid of ammonia and certain other materials potentially interfering with the subsequent determination. Glyoxalines present in human urine appear to be very stable to heat in presence of weak base. If, at the final stage, water is added and the drying repeated there is no less azo colour produced in the subsequent determination.

The method described here has several advantages over the Koessler and Hanke technique. A smaller amount of urine is used, vacuum distillation is dispensed with, and much time is saved by the use of a greater excess of lead acetate with a constant amount of standard sodium hydroxide.

Diazo Reagents

The diazo reagent according to Koessler and Hanke (10) is made from two stock solutions.

A. Nine gm. of sulphanilic acid with 90 ml. of 37% hydrochloric acid is made up to 1 litre with water.

B. Fifty gm. of 90% sodium nitrite is made up to 1 litre with water. This is best kept in a refrigerator.

The reagent is prepared by placing in a 50 ml. volumetric flask, immersed in ice-water, 1.5 ml. of solution *A* along with 1.5 ml. of solution *B*. After five minutes 6.0 ml. of solution *B* is added, and after five minutes more the flask is filled to the 50 ml. mark with cold water. The glass stopper is inserted, and the contents is thoroughly mixed. After 15 min. the reagent is ready for use. It is good for at least 24 hr. if kept cold.

A freshly prepared 1.1% solution of best quality anhydrous sodium carbonate is used to alkalinize the acid diazo reagent for each test. When thus mixed, the solution should remain perfectly clear and colourless for about 30 min.

Colour Standards

For measurement of the colour produced by the test solution, it is convenient to use an artificial comparison standard. Koessler and Hanke have shown that mixtures of Congo red and methyl orange make suitable stable standards for various glyoxalines. A standard suitable for the azo colour produced by histidine has been described by Hunter (7). It is important that the dyes be pure. This standard is suitable for the measurement of the azo colours produced by urine glyoxalines and is made as follows from two stock solutions.

Stock methyl orange. This consists of 0 1 gm. of pure methyl orange made up to 100 ml. with water.

Stock Congo red. This consists of 0.2 gm. of pure Congo red made up to 100 ml. with water.

The solutions should be kept in Pyrex glass.

Colour Standard for Histidine

About 80 ml. of distilled water is taken in a 100 ml. volumetric flask and 0.40 ml. of stock Congo red solution is added. After mixing, 0.06 ml. of stock methyl orange solution is added, the flask is filled to the mark with water, and the contents thoroughly mixed.

This colour standard is suitable for the measurement of glyoxalines in urine. Some of the above is poured into the right-hand cup of a semi-micro colorimeter of the Duboscq type.

Into the other cup is placed 2.5 ml. of 1.1% sodium carbonate solution along with 1.0 ml. of diazo reagent, and the time noted. The cup is agitated to mix. One minute later 0.5 ml. of the urinary glyoxaline fraction is added. The cup is quickly placed in the colorimeter and the contents mixed by raising and lowering the plunger several times. The plunger is then set at a depth of 10 mm. This is referred to as the *test solution*.

The colour in the test solution is at first yellow, then orange, and usually after three to four minutes, a clear pink. The standard solution plunger is moved to match. Several readings are taken between two and five minutes after mixing the test solution. Maximum readings are usually obtained at three to four minutes. Thereafter the colour gradually fades. The average of several maximum readings is recorded.

Under the above conditions, i.e., when the test solution is set at a depth of 10 mm., 0.01 mg. of histidine gives a reading of 7.4 mm. depth of standard, so that 1 mm. of standard is equivalent to 0.001352 mg. of histidine.

The volume of the test solution must be kept at 4 ml. Thus, if it is desired to use 0.1 ml. of the glyoxaline fraction above, 0.4 ml. of water should be added, before the reagents, to the colorimeter cup.

All determinations are carried out with at least two quantities of the solution under examination, and entered thus:

	Standard, mm.	Test, mm.
0.1 ml. of solution	7.1	10
0.2 ml. of solution	14.0	10

Here the proportionality is satisfactory.

The findings however might be:

0.1 ml. of solution	7.1	10
0.2 ml. of solution	11.5	10

Here the proportionality is not satisfactory, which means that the solution under test has not been adequately freed from substances that interfere with colour development. Of course the reading with the smaller quantity of glyoxaline solution will be nearer the true value than that from the greater quantity, but without linear proportionality in at least two readings, one cannot depend on the smaller quantity yielding the true reading.

From the evidence in the literature, noted above, and from our own observations (unpublished), histidine is not the only glyoxaline present in human urine. However, as histidine is probably the most constant and abundant glyoxaline present, we have expressed the urinary glyoxaline in terms of histidine.

Another consideration arises in this regard. It is well known that the azo-colours derived from different glyoxalines differ in shade and rate of colour

development. Thus the readings obtained would not always be strictly proportional, and the method might be expected to be approximate rather than precise. In practice, however, urinary glyoxalines can, in nearly all urines, be measured with a fair approach to precision. There are occasional urines from which the lead filtrates prepared as above still seem to retain substances interfering with colour development. When histidine is added to such a urine, the recovery may be greater than 100%.

Recovery of Added Histidine

To normal urine *(a)*, histidine was added in one case to the amount of 104 mg. per litre *(b)*, in the second case to the amount of 208 mg. per litre *(c)*. The three urines were treated in duplicate as described above. The detailed results are shown below.

Urine		Solution used, ml.	Reading of test, mm.	Reading of standard, mm.	Glyoxaline as histidine, mg./litre urine	Expected histidine, mg./litre urine
a	(1)	0.10	10	9.6		
		0.05	10	4.8		
	(2)	0.10	10	9.5		
		0.05	10	4.6	256.8	—
b	(1)	0.10	10	13.4		
		0.05	10	6.8		
	(2)	0.10	10	13.0		
		0.05	10	6.8	359.6	360.8
c	(1)	0.10	10	16.7		
		0.05	10	8.5		
	(2)	0.10	10	17.5		
		0.05	10	8.8	465.2	464.8

In the above the histidine values are obtained from the average of the four readings of the standard solution, and using 1 mm. of standard as equivalent to 0.001352 mg. of histidine.

The above experiment shows that histidine added to urine is fully recovered in the fractionation procedure described above.

Results

The 24-hr. urinary glyoxaline output has been determined in about one hundred normal individuals, mostly students. In Table I are the day and night excretions, in terms of histidine, for individuals where several samples were studied.

TABLE I

URINARY GLYOXALINE, AS HISTIDINE

Subjects (all men)	No. of 24-hr. samples	Average day excretion, mg.	Average night excretion, mg.	Average 24-hr. excretion, mg.
T.M.R.	17	157.8	154.8	312.6
W.L.D.	2	130.7	86.3	217.0
G.A.L.	3	369.3	344.5	713.8
J.G.R.	2	223.0	184.3	407.3

In Table II are the results from three classes of medical students. In the groups of 42 and 35 students, the urines were collected according to the directions for the Mosenthal kidney function test. In the class of 46 students, the urines were collected under ordinary conditions of diet for vitamin C determination.

TABLE II

URINARY GLYOXALINE, AS HISTIDINE, IN THREE GROUPS OF STUDENTS

No. in group (nearly all men)	Average 24-hr. excretion, mg.	Variation in 24-hr. excretion, mg./24 hr.	Average glyoxaline, mg./litre	Variation in glyoxaline, mg./litre
42	181.0	80–340	128	47–263
46	227.3	113–426	161	71–533
35	226.0	78–447	163	48–319

From Table II it may be concluded that the normal adult individual on a mixed diet commonly excretes in the urine about 200 mg. of glyoxaline, expressed as histidine, in the course of 24 hr. The daily output commonly varies from about 80 to 450 mg., although as seen from Table I (G.A.L.) more than 700 mg. may be excreted by the healthy male.

As seen from Table I, the day and night outputs of glyoxaline are not markedly different in amounts. This would suggest that urinary glyoxalines are mainly of endogenous origin.

The writers' findings suggest that the level of glyoxaline excretion is to some extent a characteristic of the individual.

Acknowledgments

The writers are indebted to Mr. J. A. Nelson for the incorporation of some of his analyses, and to Miss Sybil Fratkin for technical assistance.

This work was assisted by a grant from the Associate Committee on Medical Research of the National Research Council.

References

1. Ackermann, D. and Fuchs, H. G. Z. physiol. Chem. 259 : 32-34. 1939.
2. Armstrong, A. R. and Walker, E. Biochem. J. 26 : 143-146. 1932.
3. Ehrlich, P. Z. Klin. Med. 5 : 285-288. 1882.
4. Engeland, R. Z. physiol. Chem. 57 : 49-66. 1908.
5. Hunter, G. Brit. Med. J. 751-752. 1922.
6. Hunter, G. Biochem. J. 19 : 25-33. 1925.
7. Hunter, G. Biochem. J. 19 : 42-46. 1925.
8. Kapeller-Adler, R. Biochem. J. 35 : 213-218. 1941.
9. Knoop, F. Hofmeisters Beiträge. 11 : 356. 1908.
10. Koessler, K. K. and Hanke, M. T. J. Biol. Chem. 39 : 497-519. 1919.
11. Koessler, K. K. and Hanke, M. T. J. Biol. Chem. 59 : 803-834. 1924.
12. Lélu, P. Bull Soc. Chim. Biol. 17 : 637-656. 1935.
13. Pauly, H. Z. physiol. Chem. 42 : 508-518. 1904.
14. Weiss, M. Biochem. Z. 102 : 228. 1920.

A FURTHER MODIFICATION OF THE SKRAUP SYNTHESIS OF QUINOLINE[1]

BY RICHARD F. H. MANSKE[2], FRANK LEGER[2], AND GEO. GALLAGHER[3]

Abstract

It has been found that recent modifications of the Skraup quinoline synthesis can be further improved as to yield and ease of operation by substituting acetylated amines for the free bases.

In the course of the preparation of a series of substituted quinolines in this laboratory, it was necessary to prepare and purify the required primary amines via their acetyl derivatives. It was considered probable that these derivatives could be used directly in the Skraup reaction, thus avoiding the necessary loss of time and material consequent upon their separate hydrolysis. Since there seems to be no previous record in which an acetylated amine has been used in the Skraup synthesis, some experiments using the cheaper acetanilide for the preparation of quinoline were carried out. The methods of Cohn (2) and of Clarke and Davis (1) (yielding 47 gm. and 41 gm. of quinoline respectively from 53.5 gm. of aniline) were used as standard procedures. In parallel experiments the aniline was replaced by an equivalent amount of acetanilide, and in either case the yield was 67 gm. Not only had the yield been substantially increased but the violence of the reaction—always serious in the Skraup synthesis—had been reduced to the point where its inception was difficult to observe. The amount of by-product tars usually obtained was also greatly reduced, presumably owing to the increased yield of quinoline.

A detailed outline of an experiment following the Cohn "Boric Acid Method" is given.

Experimental

To 20 gm. of powdered crystalline ferrous sulphate in a five litre flask, there was added in the order named, 77.6 gm. of acetanilide, 42 gm. of nitrobenzene, a solution of 35.5 gm. of boric acid in 216 gm. of glycerol, and 182 gm. of concentrated sulphuric acid, with shaking. The solution was then heated gently under a reflux condenser until it began to simmer. Mild heat was applied for one-half hour, at the end of which time the heat was increased for a further three hours.

The solution was then cooled slightly and to it was added 300 cc. of water, and the mixture was steam distilled to remove the excess nitrobenzene (about 10 gm.). The solution was then cooled and to it was added a solution of 340 gm. of sodium hydroxide in 1 litre of water. Steam distillation served

[1] *Manuscript received October 20, 1941.*

Contribution from the Division of Chemistry, National Research Laboratories, Ottawa, Canada. Issued as N.R.C. No. 1026.

[2] *Chemist.*

[3] *Voluntary Research Assistant.*

to remove the quinoline. The aqueous layer that separated in the distillate was further concentrated by steam distillation.

To the final combined distillate was added 70 gm. of concentrated sulphuric acid, and the resulting solution was diazotized at 8° C., with an excess of aqueous sodium nitrite. One to two grams was sufficient. The diazotized solution was heated on the steam-bath for 30 min., then steam distilled to remove volatile impurities. A solution of 100 gm. of sodium hydroxide in 400 cc. of water was added to the residual solution and the mixture was again steam distilled. The aqueous layer in the distillate was again concentrated as described above, and the quinoline was extracted from the combined distillates by means of benzene. Upon removal of the benzene and distillation of the residue under reduced pressure, there was obtained 67 gm. of water-white quinoline.

When the Clarke and Davis modification (1) was used (no boric acid) the yield of quinoline was 67 gm. When N-acetyl-*o*-anisidine was used as a starting material, with picric acid as the oxidizing agent, a good yield of 8-methoxy-quinoline was obtained. The use of 4-acetylamino-diphenyl gave a good yield of 6-phenyl-quinoline.

References

1. Clarke, H. T., and Davis, Anne W. Org. Syntheses, 2 : 79-83. 1928.
2. Cohn, E. W. J. Am. Chem. Soc., 52 : 3685-3688. 1930.

SECTION B

INDEX TO VOLUME 19

Authors

SECTION B

INDEX TO VOLUME 19

Subjects